CONFIDENTIAL

X62-10303

Copy No. 5

Issue Date: 18 April 1962

(Unclassified Title)

DESIGN STUDY OF A LARGE UNCONVENTIONAL LIQUID PROPELLANT ROCKET ENGINE AND VEHICLE

CCN

Prepared by

AEROJET-GENERAL CORPORATION
Liquid Rocket Plant
Sacramento 9, California

Final Report
Report No. LRP 257

Volume 2: Engine Concepts Considered

Contract NAS 5-1025

Prepared for

OFFICE OF LIQUID ROCKETS
NASA HEADQUARTERS
Code MLPL (Mr. H. Burlage)
400 Maryland Avenue, S. W.
Washington 25, D. C.

CLASSIFICATION CHANGE
TO = UNCLASSIFIED
By authority of T.D. No. 24-235
Changed by CONFIDENTIAL
Date 3/22/64

EXCLUDED FROM AUTOMATIC REGRADING, DOD DIR 5200.10 DOES NOT APPLY

THIS DOCUMENT CONTAINS INFORMATION AFFECTING THE NATIONAL DEFENSE OF THE UNITED STATES WITHIN THE MEANING OF THE ESPIONAGE LAWS, TITLE 18, U. S. C., SECTIONS 793 AND 794. THE TRANSMISSION OR THE REVELATION OF ITS CONTENTS IN ANY MANNER TO AN UNAUTHORIZED PERSON IS PROHIBITED BY LAW.

DOWNGRADED FROM TOP SECRET GDS

Aerojet-General® CORPORATION

LIQUID ROCKET PLANT • SACRAMENTO, CALIFORNIA

THE GENERAL TIRE

(NASA-CR-137269) DESIGN STUDY OF A LARGE UNCONVENTIONAL LIQUID PROPELLANT ROCKET ENGINE AND VEHICLE. VOLUME 2: ENGINE CONCEPTS (Aerojet-General Corp., Sacramento, Calif.) 500 p

N74-74177

Unclas
00/99 33232

TABLE OF CONTENTS

		PAGE NO.
I.	INTRODUCTION	I-1
II.	CONCEPTS CONSIDERED	II A-1
III.	BASES FOR EVALUATION	III A-1
IV.	BEST UNCONVENTIONAL SYSTEM	IV-1
V.	GROUND SUPPORT EQUIPMENT	V-1
VI.	FACILITIES	VI-1

TABLE OF CONTENTS

PAGE NO.

I. INTRODUCTION I-1

I. INTRODUCTION

Task 1, which is summarized in this volume, commenced on 1 May 1961, the contract initiation date. It was completed as scheduled on 25 August 1961.

This phase of the contractual effort encompassed the following:

A. Establishing a reasonably optimum launch design using conventional design concepts (gimbaled De Laval nozzle engines) and current technology wherever possible. This design included estimates of weight and cost. It became the basis for comparison with the unconventional concepts.

B. All known unconventional liquid propellant rocket engine configurations were considered (Section II of this volume). Suitable associated vehicle designs were prepared, incorporating unusual vehicle construction that minimized structural complexity and cost. The resulting array of engine-vehicle combinations was analyzed with respect to feasibility, performance, cost, and reliability. Assumptions, upon which these studies were based, were documented.

C. Research and development costs were estimated. The costs of test and production facilities needed to develop and produce the system were established. These estimates were based upon quantity productions of the system in the order of 25, 100, and 400 to be manufactured over a six-year period (not to be construed as expected launching rates). A plot of unit cost in relationship to production quantity was also established.

Section III of this volume discusses the bases used for evaluation and Section IV details the best unconventional system.

TABLE OF CONTENTS

		PAGE NO.
II.	CONCEPTS CONSIDERED	
A.	INTRODUCTION	II A-1
B.	VEHICLE CONCEPTS	II B-1
C.	CLUSTERING	II C-1
D.	PRESSURE-FED ENGINES	II D-1
E.	PUMP-FED ENGINE CYCLES	II E-1
F.	ENGINE CONFIGURATIONS	II F-1
G.	THRUST VECTOR AND ROLL CONTROL	II G-1
H.	PRESSURIZATION SYSTEM	II H-1
I.	THRUST CHAMBER CONCEPTS	II I-1
J.	TURBOPUMPS	II J-1
K.	JET PUMPS	II K-1
L.	ENGINE CONTROL CONCEPTS	II L-1
M.	AIRFRAME AND TANKAGE	II M-1
N.	AIR-BREATHERS	II N-1

TABLE LIST

	TABLE NO.
Engine Performance Degradation	II E-1
Weight Summary for Various Propulsion Systems	II F-1
Forced Deflection Engine Characteristics	II F-2
Plug Nozzle Engine Characteristics	II F-3
Comparison of Tankage Fabrication Costs	II M-1
Comparison of Tankage Weights	II M-2

FIGURE LIST

	FIGURE NO.
Vehicle Cost and Payload Variations with Size	II B-1
Propellant Comparison and Conventional Configurations (Man-Rated)	II B-2
Propellant Comparison for Conventional	II B-3
Recovery Method Comparison and Configurations (Man-Rated)	II B-4
Recovery Method Cost Comparisons	II B-5
Staging Methods, Configurations	II B-6
Staging Methods Cost Comparison	II B-7
Cost Factor vs Payload per Flight (100 Operational Launches)	II C-1
Ratio of Production Cost of Clusters to the Production Cost of Single Units vs Number of Units Clustered for an 85% Learning Curve	II C-2
Ratio of Production Cost of Clusters to the Production Cost of Single Units vs Number of Units Clustered for Various Percent Learning Curve	II C-3

FIGURE LIST (cont.)

	FIGURE NO.
Cost Factor vs Number of Operational Launches	II C-4
Booster, Pressure-Fed	II D-1
Schematic, LO_2/LH_2 Engine, Plug Nozzle	II D-2
Propulsion Cost-per-lb of Payload	II D-3
G-Fed Rocket Idealized Geometry	II D-4
Tank Configurations	II D-5
GΔP Rocket	II D-6
300-nm Payload Versus Thrust Chamber Pressure for Various Engine Cycles	II E-1
Gas Generator Cycle, Parallel Turbines	II E-2
Gas Generator Cycle, Series Turbines	II E-3
Staged Combustion Cycle, Fuel-Rich Gas Generator System, Series Turbines	II E-4
Staged Combustion Cycle, Fuel-Rich Gas Generator System, Parallel Turbines	II E-5
Staged Combustion Cycle, Fuel-Rich Plus Oxidizer-Rich Gas Generators	II E-6
Schematic--Staged Combustion Cycle, Fuel-Rich Gas Generators, H_2 Coolant Flow in Series with Gas Generator	II E-7
Schematic--Staged Combustion Cycle, Fuel-Rich Gas Generators, H_2 Coolant Flow in Parallel with Gas Generator	II E-8
Schematic--Staged Combustion Cycle, Fuel-Rich Gas Generators, Dual Hydrogen Turbopumps	II E-9
Schematic--Staged Combustion Cycle, Fuel-Rich Gas Generators, Multiple Thrust Chambers	II E-10
Schematic--Staged Combustion Cycle, Fuel-Rich and Oxidizer-Rich Gas Generators	II E-11
Schematic--Staged Combustion Cycle, Fuel-Rich and Oxidizer-Rich Gas Generators, Multiple Thrust Chambers	II E-12
Heated-H_2 Bleed Cycle, Parallel Turbines	II E-13

FIGURE LIST (cont.)

	FIGURE NO.
Heated-H_2 Bleed Cycle, Series Turbines	II E-14
Heated-H_2 Bleed Cycle, Series Turbines with Bleed Flow Booster Pump	II E-15
Heat Exchanger Design Requirements for Heated-H_2 Cycle	II E-16
8-Chamber Heated-H_2 Cycle, Forced Deflection Engine, Baffle-Type Heat Exchanger	II E-17
Heated-H_2 Topping Cycle, Parallel Turbines	II E-18
Heated-H_2 Topping Cycle, Series Turbines	II E-19
Chamber Bleed Cycle, Heat Exchanger, Cooled Gas	II E-20
Chamber Bleed Cycle, Diluted Gas	II E-21
Chamber Bleed-Off Method	II E-22
Third Fluid Turbine Drive Cycle, Open Cycle	II E-23
Third Fluid Turbine Drive Cycle, Closed Cycle	II E-24
Third Fluid Cycle Component Weights Versus Thrust Chamber Pressure	II E-25
Delivery Feed Cycle, Continuous Feed	II E-26
Performance Comparison of Gas-Generator and Afterburner Cycles	II E-27
Engine Vacuum I_s Versus Thrust-Chamber Pressure for Various Engine Cycles--De Laval Nozzle	II E-28
Engine Vacuum I_s Versus Thrust-Chamber Pressure for Various Engine Cycles--Altitude-Compensating Nozzles	II E-29
Engine Sea Level I_s Versus Thrust Chamber Pressure for Various Engine Cycles--De Laval Nozzle	II E-30
Engine Sea Level I_s Versus Thrust-Chamber Pressure for Various Engine Cycles--Altitude-Conpensating Nozzles	II E-31
Area Ratio Versus Thrust-Chamber Pressure	II E-32
Pump Discharge Requirements for Various Engine Cycles	II E-33
Engine Weight Versus Thrust-Chamber Pressure, De Laval Nozzle	II E-34

FIGURE LIST (cont.)

	FIGURE NO.
Engine Weight Versus Thrust-Chamber Pressure, Altitude-Compensating Nozzles	II E-35
Engine Mixture Ratio Versus Thrust-Chamber Pressure for Various Engine Cycles--De Laval Nozzle	II E-36
Engine Mixture Ratio Versus Thrust-Chamber Pressure for Various Engine Cycles--Altitude-Compensating Nozzles	II E-37
Four 500 K De Laval Chambers, One Turbopump	II F-1
Rocket Engine, Forced-Deflection Gas Generator Cycle, 2,000,000-lb Thrust	II F-2
Controls Schematic, 2,000,000-lb Thrust Rocket Engine, Forced Deflection	II F-3
Plug-Nozzle Rocket Engine, 2,000,000-lb Thrust, Gas Generator Cycle	II F-4
Plug-Nozzle Engine Controls Schematic, 2,000,000-lb Thrust	II F-5
Reverse-Flow Engine, Annular Chamber	II F-6
Reverse-Flow Engine, Eight Discrete Chambers	II F-7
Characteristic Duty Cycle with Maximum Wind Loading, Trajectory, and Jet Stream Loading	II G-1
Stored Gas (Helium)	II H-1
Stored Gas (Nitrogen)	II H-2
Stored Gas and Heat Exchanger (Helium), Standard Vehicle	II H-3
Stored Gas and Heat Exchanger (Nitrogen)	II H-4
Heated Oxygen	II H-5
Bipropellant Gas Generator	II H-6
Solid Propellant Gas Generator (Sodium Azide)	II H-7
Vapor-Pressurized System (VāPak)	II H-8
Step Nozzle Contour	II I-1
Mechanical Means of Varying Exit Area	II I-2

FIGURE LIST (cont.)

	FIGURE NO.
Expandable Nozzle Before and After Testing	II I-3
Annular External Expansion Nozzles	II I-4
Discrete-Throat Forced-Deflection Nozzle Schematics	II I-5
Truncated Isentropic Plug-Nozzle Performance Obtained from Flow Tests	II I-6
Nozzles with Flow Process Depicted	II I-7
Nozzle-Control Surfaces and Parameter for Performance and Design Analysis	II I-8
Vacuum Thrust Coefficient	II I-9
Optimum Exit-Length Ratio	II I-10
Optimum Exit-Radius Ratio	II I-11
Optimum Exit Angles	II I-12
Optimum Vacuum Thrust Coefficient	II I-13
Total Heat Flux vs Chamber Pressure	II I-14
Ablative Chamber	II I-15
Effect of L* Upon Injector Performance	II I-16
Spherical Centrifugal Combustor	II I-17
Pumping System Wet Weight Versus Engine Thrust	II J-1
Relative Pumping System Production Cost Versus Engine Thrust	II J-2
Wet Weight Versus Net Positive Suction Pressure for 2$\bar{m}$-lb-Thrust O_2 Turbopump	II J-3
Wet Weight Versus Net Positive Suction Pressure for 2$\bar{m}$-lb-Thrust H_2 Turbopump	II J-4
Flow Schematic (Turbopump with Inducer Stage)	II J-5
Equivalent Wet Weight Versus Net Positive Suction Pressure for 2$\bar{m}$-lb-Thrust O_2 Turbopump	II J-6
Equivalent Wet Weight Versus Net Positive Suction Pressure for 2$\bar{m}$-lb-Thrust H_2 Turbopump	II J-7

FIGURE LIST (cont.)

	FIGURE NO.
Equivalent Wet Weight Versus Maximum Tank Pressure for 2m-lb-Thrust Oxygen Turbopump with O_2 Tank above Hydrogen Tank	II J-8
Equivalent Wet Weight Versus Maximum Tank Pressure for 2m-lb-Thrust Oxygen Turbopump with O_2 Tank below Hydrogen Tank	II J-9
Equivalent Wet Weight Versus Maximum Tank Pressure for 2m-lb-Thrust H_2 TPA	II J-10
Weight of O_2 Tank and Pressurization System Versus Maximum Tank Pressure	II J-11
Weight of H_2 Tank and Pressurization System Versus Maximum Tank Pressure	II J-12
Combined Equivalent Weight Versus Maximum Tank Pressure for 2m-lb-Thrust O_2 System with O_2 Tank above H_2 Tank	II J-13
Combined Equivalent Weight Versus Maximum Tank Pressure for 2m-lb-Thrust O_2 System with O_2 Tank below H_2 Tank	II J-14
Combined Equivalent Weight Versus Maximum Tank Pressure for 2m-lb-Thrust H_2 System with Tank at Either Top or Bottom	II J-15
Suction Line Wet Weight at Burnout Versus O_2 Liquid Elevation above Pump Inlet at Burnout	II J-16
Pump Discharge Pressure Versus Thrust Chamber Pressure for Various Engine Cycles	II J-17
Pump Discharge Pressure Versus Thrust Chamber Pressure for a Staged Combustion Cycle	II J-18
Turbopump Wet Weight Versus Pump Discharge Pressure	II J-19
Turbine Weight Flow Versus Pump Discharge Pressure	II J-20
Relative Turbopump Production Unit Cost Versus Pump Discharge Pressure	II J-21
H_2 Turbopump Wet Weight Versus Bearing Rubbing Velocity	II J-22
H_2 Pump Efficiency Versus Bearing Rubbing Velocity	II J-23
H_2 Turbopump with Four Hydraulically Balanced Discharge Outlets	II J-24
O_2 Turbopump with Four Hydraulically Balanced Discharge Outlets	II J-25

FIGURE LIST (cont.)

	FIGURE NO.
Specific Impulse Versus Chamber Pressure	II J-26
Turbine Equivalent Weight Versus Turbine Exhaust Pressure for an H_2 Turbopump	II J-27
Turbine Equivalent Weight Versus Turbine Bucket Pitch Line Velocity for an H_2 Turbopump	II J-28
Turbine Equivalent Weight Versus Turbine Exhaust Pressure for an O_2 Turbopump	II J-29
Turbine Equivalent Weight Versus Turbine Bucket Pitch Line Velocity for an O_2 Turbopump	II J-30
Overall Cost Comparison--Single-Stage Turbine Versus Two-Stage Turbine for an H_2 Turbopump	II J-31
Gear Drive Dry Weight Versus Low Speed Shaft Torque for 3:1 Speed Ratio Gearbox	II J-32
Specific Weight Versus Volumetric Flow Rate for Flightweight Reciprocating Machinery	II J-33
Oxidizer Jet Pump (clustered) for 6-Million-lb-Thrust O_2/Hydrocarbon Booster	II K-1
Oxidizer Jet Pump for 6-Million-lb-Thrust O_2/Hydrocarbon Booster	II K-2
Fuel Jet Pump for 6-Million-lb-Thrust O_2/Hydrocarbon Booster	II K-3
Weight Comparison of Three Types of Gimbal Actuators	II L-1
Pump-Mounted Gate Valve	II L-2
Ring Gate Valve	II L-3
Butterfly Valve	II L-4
Gate Valve	II L-5
Spring Valve	II L-6
Plug Valve	II L-7
Ball Valve	II L-8
Valve Diameter vs Weight for Ring Gate Valve	II L-9
Valve Size vs K_w for Ring Gate Valve	II L-10
Horsepower vs Diameter for Ring Gate Valve (for a 1.0 sec Opening Time)	II L-11

FIGURE LIST (cont.)

	FIGURE NO.
Torque vs Diameter for Ring Gate Valve	II L-12
Hot Gas Control for Secondary Injection Butterfly Valve Principle	II L-13
Hot Gas Control for Secondary Injection Jet Pipe Principle	II L-14
Electric Control LH_2 Cooled and Pressurized	II L-15
Gimbal Actuation System-Electric	II L-16
Gimbal Actuation System-Power Take Off, Direct Mechanical Control	II L-17
Gimbal Actuation System-Hydraulic	II L-18
Servo Actuator-3 Stage Hydraulic	II L-19
Multiple Piston Hydraulic Pump	II L-20
Pneumatic Gear Motor	II L-21
Schematic of Turbine Speed Control for Hydrogen Cycle	II L-22
Tankage Weight vs Configuration	II M-1
Toroidal Tank Configuration, 6-Million-lb-Thrust	II M-2
Tandem Sphere Tank Configuration, 6-Million-lb-Thrust	II M-3
Clustered Sphere Tank Configuration, 6-Million-lb-Thrust	II M-4
Tandem Sphere Tank Configuration, 2-Million-lb-Thrust	II M-5
Wall Thickness vs Length-to-Radius Ratio for Lighter-than-Air Hydrogen-Filled Steel Cylinder	II M-6
Wall Thickness vs Length-to-Radius Ratio for Lighter-than-Air Hydrogen-Filled Aluminum Cylinder	II M-7
Wall Thickness vs Length-to-Radius Ratio for Lighter-than Air Hydrogen-Filled Beryllium Cylinder	II M-8
Standard Vehicle Tank Configuration	II M-9
Single-Stage-to-Orbit Tank Configuration	II M-10
Clustered Cylindrical Tank Configuration	II M-11
Clustered Booster	II M-12

FIGURE LIST (cont.)

	FIGURE NO.
Isometric of Clustered Booster	II M-13
Liquid Oxygen/RP-1 Tankage	II M-14
Air-Breathing Devices	II N-1
Comparative Models	II N-2
Drag Coefficient for Model A	II N-3
Drag Coefficient for Model B	II N-4
Drag Coefficient for Model A and B	II N-5
Ramjet Flow Model	II N-6
Combustion Temperature vs C_p for H_2-Air at Stoichiometric Mixture Ratio and Preheated to 1,000°R	II N-7
Trajectory	II N-8

II. CONCEPTS CONSIDERED

A. INTRODUCTION

Rocket engine and vehicle concepts considered during Task 1 of this investigation are evaluated in this section. Throughout, the objective was to find significant cost savings and increases in reliability

In evaluating these concepts, the major considerations were payload, cost-per-pound of payload, reliability, adaptability to recovery methods, and mission flexibility. Of these, only payload can be accurately calculated and relative costs can only be estimated Evaluation of the other factors is largely upon a subjective basis.

As discussed in Section III, C, payload comparisons are adequate in cases where the vehicle configuration is not changed significantly. Consequently, the evaluation of the engine cycles at various thrust chamber pressures upon the basis of single-stage vehicle payload is fully adequate. In comparing staging methods, numbers of stages, and propellants, it becomes necessary to introduce cost considerations into the evaluation.

II, Concepts Considered (cont.)

B. VEHICLE CONCEPTS

1. General

a. Summary

In this section various vehicle concepts are reviewed and evaluated. The propellant combinations considered are O_2/H_2 and O_2/hydrocarbons. Vehicles of one, two, and three stages for orbit and escape missions are compared. The best propellants for the booster are then selected. Booster recovery methods are reviewed and the potential payoff shown. Several methods for vehicle staging are also evaluated and reviewed.

It is concluded that the best conventional vehicle is an O_2/H_2 orbital booster with a second stage for escape missions.

Significant cost savings are possible with booster recovery for programs with a large number of flights. With the orbital booster recovery the greatest cost savings is offered.

b. Bases for Evaluation

The following three bases were used in evaluating the vehicles considered: cost-per-pound of payload, reliability, growth potential.

Methods used in evaluating each vehicle within these areas are explained below. Combining these ratings to select the best vehicle was accomplished on a subjective basis as discussed in the appropriate subsections.

II, B, Vehicle Concepts (cont.)

(1) Cost-per-Pound of Payload

The basic cost model, described in Section III, D, was used in evolving the costs for each vehicle. Best staging for minimum cost-per-pound of payload was determined by using this cost model in conjunction with the vehicle-design computer program (Section III, D).

Two missions were considered: a 300-nm circular orbit and escape. The best staging for one mission rarely corresponds to the best staging for another mission, however, in every case considered, it was possible to select ideal velocity increments that were within 2% of minimum cost-per-pound of payload for both missions. In most cases, the best staging for the escape mission was adequate for the orbit mission.

As discussed in Section III, D, vehicle cost-per-pound of payload becomes less as the vehicle size increases. This is illustrated in Figure II B-1, which is a plot showing the variation of payload delivery cost with size for vehicles of the same type as the conventional O_2/H_2 two-stage vehicle. Therefore, the vehicle cost comparisons presented are, in all cases, for vehicle sizes that provide the following payloads: 300-nm circular-orbit payload of 120,000 lb, escape payload of 48,500 lb These payloads correspond to those of the conventional two-stage vehicle with O_2/H_2 propellants in both stages (Figure II B-2).

All cost comparisons are relative to the conventional O_2/H_2 two-stage vehicle. Costs are normalized as shown (the best conventional is rated as 1.0). This was done to avoid difficulties that would result from different ratios of orbit-to-escape payload for all of the vehicles.

II, B, Vehicle Concepts (cont.)

Only vehicles with turbopump-fed engines are considered conventional. Therefore, all vehicles discussed in this section are turbopump-fed engines.

In all of the comparisons, it was assumed that upper stages need not be developed. In most cases, the Saturn S-IV stage or Saturn S-II stage could be adapted with minor modifications to the 2,000,000-lb-thrust booster. At higher thrust levels, this may not be so; therefore, the effect of adding this second stage development cost is discussed and shown in Figure II B-3. Obviously, this assumption would not be valid at much higher thrust levels and is further discussed under growth potential.

(2) Reliability

All of the vehicles considered in this section are conventional and it must be assumed that each can be developed to a high reliability. There is no data showing reliability to be a function of physical size or thrust level; therefore, reliability was assumed to be a function of the number of stages only. Thus, the reliability number represents the number of stages. For vehicles with a different number of stages for orbit and escape, one-half reliability factors are used. For example the best conventional two-stage vehicle has a booster with substantial single-stage-to-orbit capability; therefore, its overall reliability rating would be 1-1/2. Obviously, the smaller the number, the higher the reliability. Hence, this number is referred to as the unreliability number in the comparison.

II, B, Vehicle Concepts (cont.)

Reliability effects were not included in the cost analysis because this inclusion would have required establishing a base reliability.

(3) Growth Potential

Each vehicle analyzed required a different second stage. At the first-stage thrust level considered (2, 000, 000 lb), stages being developed for Saturn could be adapted to these vehicles with minor modifications Therefore, no second-stage development cost was charged in any of the vehicles analyzed. However, in Figure II B-3, the effect of this assumption is shown. Note that when second-stage development cost is included, vehicle cost is increased by 50% at 25 flights. Even at 400 flights, the cost is still 10% greater. This example shows clearly that vehicles requiring second-stage development would be much costlier than vehicles not requiring second-stage development.

Although basic investigation involves 2, 000, 000-lb thrust, higher thrust levels (up to 24, 000, 000 lb) are also considered. At high thrust levels, assuming no second-stage development cost is invalid. At intermediate thrust levels, second-stage development is necessary for some vehicles but not for others. The maximum payload deliverable, using a given vehicle type with a new booster and a developed second stage, is important because for greater payload, second-stage development cost must be added. The best vehicle type is that for which this maximum payload is greatest. To rate vehicle types upon this basis, a measure of the maximum payload achievable with a developed second stage is required.

II, B, Vehicle Concepts (cont.)

Propellant tanks can be lengthened fairly easily to increase propellant capacity in the currently developed stages. Therefore, propellant tank volume modification was not considered significant from a development-cost standpoint. Thrust increases generally require an extensive redesigning of engine, stage structure, and subsystems. Therefore, the payload-per-pound of stage thrust was considered the significant parameter in measuring growth potential when no stage development was assumed. By using this parameter, it is also possible to estimate the highest payload (when no second-stage development cost is necessary) if developed-stage thrust level is known. An example is presented in the following section (the maximum payload of two-stage vehicles with Saturn S-II stage for a second stage is given).

Thrust levels for the upper stages of the vehicles compared were selected upon the basis of maximum payload for a gravity turn trajectory. Therefore, the payload-per-pound-of-thrust values shown are lower than they would be if suitable angle programs were used. However, the payload-to-stage-thrust-level comparisons shown are valid for comparing vehicles on a relative basis.

2. Vehicle and Propellant Comparison

The two combinations, O_2/H_2 and O_2/hydrocarbons, were analyzed in vehicles of one, two, and three stages to determine the best conventional vehicle for comparison with vehicles incorporating unique concepts. RP-1 was selected as being representative of the hydrocarbon group.

II, B, Vehicle Concepts (cont.)

Initially, vehicles were considered with the stage propellants in the following tabulation:

PROPELLANTS

STAGE

1	2	3
O_2/H_2	O_2/H_2	O_2/H_2
O_2/H_2	O_2/H_2	NONE
O_2/H_2	NONE	NONE
O_2/RP-1	O_2/RP-1	O_2/RP-1
O_2/RP-1	O_2/RP-1	NONE
O_2/RP-1	NONE	NONE
O_2/RP-1	O_2/RP-1	O_2/H_2
O_2/RP-1	O_2/H_2	O_2/H_2
O_2/RP-1	O_2/H_2	NONE

Optimum staging at minimum cost for each of the vehicles was determined for the orbit and escape mission, and the costs were calculated. In all cases, the three-stage vehicles were shown to be more expensive payload carriers than the two-stage vehicle. Three-stage vehicles are also less reliable than the two-stage vehicles. In addition, the three-stage vehicles were inferior on the basis of payload-per-pound of second-stage thrust; therefore, the three-stage vehicles promised less growth potential than the two-stage vehicles. Three-stage vehicles were consequently eliminated, and subsequent analysis was devoted to one- and two-stage vehicles. These remaining vehicles are shown in Figure II B-2.

II, B, Vehicle Concepts (cont.)

It was recognized that the single-stage vehicles would require a second stage for the escape mission. Therefore, the two-stage vehicles were designed for the escape mission and the first stages adapted for the orbit mission, which results in a somewhat higher thrust-to-weight ratio for the single-stage vehicles than for the two-stage vehicles. However, as pointed out in the Boeing study (Volume 5), this higher ratio is probably better.

a. Cost

Figure II B-3 was prepared to show the relative costs of these vehicles for the orbit and escape missions. The single-stage $O_2/RP-1$ vehicle had so little payload that it was not considered practical and is not shown. There is little difference between the remaining vehicles on the basis of cost alone, although the two-stage O_2/H_2 vehicle has a slight edge. The single-stage O_2/H_2 vehicle (the first stage of the two-stage O_2/H_2 vehicle) shows a 12% advantage over the others at the four-hundredth unit.

b. Reliability

For reliability, the two-stage O_2/H_2 vehicle is best because the booster can be used by itself for the orbit mission.

c. Growth Potential

The ratio of payload to second-stage thrust level is shown in Figure II B-2 which indicates that the two-stage O_2/H_2 vehicle is superior to others. The importance of this parameter in measuring growth potential is shown in the following examples:

II, B, Vehicle Concepts (cont.)

The effect of including second-stage development cost is shown in Figure II B-3. Note the significant difference in cost; at 25 missions, the second-stage development increases the payload delivery cost by 50%. Even at 400 missions, the cost is 10% higher than for the same vehicle with an existing stage.

An example was prepared to show the maximum payloads that could be expected from vehicles that differed in first-stage propellants, with both vehicles using the Saturn S-II for the upper stage. By using the value of 800,000-lb thrust for this stage and the values of escape payload-per-pound of second-stage thrust, it can be shown that the O_2/RP-1 boosted vehicle will require a new second stage for payloads above 62,500 lb. With the O_2/H_2 booster, a payload of 184,000 lb can be attained without requiring additional second-stage development. As previously discussed in Section II, B, 1, only the relative payloads are significant. Therefore, it would be better to state that the assumption of no second-stage development cost is valid for the O_2/H_2 booster vehicle for three times the payload for which the same assumption would be applicable with the O_2/RP-1 boosted vehicle.

d. There is little difference in cost between the three vehicles, except at 400 flights (at this point the single-stage-to-orbit vehicle begins to show a significant advantage over the other vehicles). The two-stage O_2/H_2 vehicle with a booster of single-stage-to-orbit capability is thus more favorable. The vehicle is also better than the other vehicles because of reliability and growth potential. Therefore, the use of O_2/H_2 propellants for future boosters is recommended.

II, B, Vehicle Concepts (cont.)

3. Recovery Methods

In this section, the recovery methods discussed in Section III, E are applied to the best conventional vehicle (two-stage O_2/H_2 vehicle) to determine possible cost advantages. No recovery-system development or production cost was included in this comparison.

Three types of recovery were considered: recovery from low burnout velocities (7,000 ft/sec), by methods such as parachute, retro-rockets, dive brakes, or combinations of these; recovery from intermediate burnout velocities (approximately 15,000 ft/sec) by installation of wings and suitable propulsion for returning to the landing site; recovery from orbit velocities by applying the subsystems discussed in Section III, E.

Each of these recovery methods is detailed in Section III, E, in which basic assumptions and weight penalties are evolved. The vehicles and these recovery methods are shown in Figure II B-4.

a. Cost Comparison

The total program cost at 400 flights is in excess of 2-billion dollars. Here, a 25% savings represents 500-million dollars. This sum appears to be adequate for recovery system development and still show some program cost savings. However, at a lower number of flights, it would be difficult to show this. Therefore, the cost comparison at 400 flights or more is of most interest (Figure II B-5).

II, B, Vehicle Concepts (cont.)

The comparison of the three methods at 400 flights is presented in the following tabulation. A cost factor of 1 is equivalent to the best two-stage conventional vehicle cost.

RECOVERY METHODS	COST FACTORS		
	Orbit	Escape	Average
Low velocity	0.74	0.91	0.825
High velocity	0.75	0.75	0.75
Recovery from orbit	0.83	0.66	0.745

It can be seen from Figure II B-5 that recovery from orbit shows the most rapid improvement as the number of flights is increased. Therefore, as the number of flights increases beyond 400, the orbit-recovery method becomes superior to the others

b. Reliability

The recovery from orbit is best for reliability because this method requires only one stage for the orbit mission. All others require two stages for all missions.

c. Growth Potential

The growth potential factors, payload-per-pound of second-stage thrust level, are shown in Figure II B-4. The recovery-from-orbit method is best for growth potential.

II, B, Vehicle Concepts (cont.)

d. Best Recovery Method

There is little cost difference between the three recovery methods. However, for reliability and growth potential, the recovery-from-orbit method is best. Therefore, this recovery method is considered the most promising one for future boosters.

4. Vehicle Staging Concepts

a. General

Several staging methods are considered in this section. These are:

(1) Tandem staging
(2) Staging of engines only
(3) Staging of tanks only
(4) Complete parallel staging of engine-tank modules.

Complete parallel staging of engine-tank modules was not analyzed in detail because this method has, as a minimum, all of the clustered booster disadvantages for reliability. In addition, clustering of booster modules was shown to provide insignificant cost savings even with the optimistic assumptions presented in Section II C.

Vehicles with parallel staging of engines or parallel staging of tanks also require an additional stage to accomplish the escape mission and in reality become two-and-a-half stage vehicles. Therefore, for reliability, they cannot be superior and may actually be inferior to the two-stage tandem-staged vehicle for that type of mission.

II, B, Vehicle Concepts (cont.)

The tandem-staged vehicle used for comparison is the best conventional vehicle (described in Section II, B). The first stage of this vehicle has substantial single-stage-to-orbit payload capability. Payload capability of vehicles incorporating the parallel staging of engines or parallel staging of tanks was compared to the single-stage-to-orbit payload capability of the first stage of the best conventional vehicle.

Also, on the basis of results described in Section II, B, use of O_2/H_2 propellants only was considered in this discussion.

Stage-mass drop parameters are based on the assumptions in Section III, B. No weight penalty was included for the staging system of vehicles on which engines only or tanks only are staged. Therefore, the results are optimistic in favor of these vehicles.

The vehicle configurations considered are shown in Figure II B-6. Cost comparison of the system is shown in Figure II B-7. Assumptions used in arriving at relative costs are discussed in Section III, D. Specific cost assumptions required to modify the cost model for staging methods other than tandem staging were necessary. These assumptions are discussed in a following paragraph.

The relative unreliability of each vehicle shown in Figure II B-6 is based upon one unit for a stage with a single engine and single airframe. Modification of this is required for clusters and partially staged vehicles. The following ground rules were established for evaluating unreliability of the staging methods considered.

II, B, Vehicle Concepts (cont.)

No unreliability was assumed for the staging operation of any of the vehicles. Of the total stage unreliability of 1, the engine was assumed to contribute one-third, the remaining stage components two-thirds. Because the vehicle which stages engines only has three engines and one airframe, it has an unreliability factor of 1-2/3. Except for tankage, the clustering of other airframe components would not be necessary for the vehicle which stages tanks only. Because the major airframe unreliability is associated with components other than tanks, no unreliability besides the stage unreliability of 1 was charged to this system.

b. Evaluation

The evaluation of the staging methods are shown in Figures II B-6 and II B-7.

(1) Staging of Engines Only

The vehicle staging engines only is the least costly of the three vehicles considered because of the lower engine development costs. This results from using three engines, each supplying one-third of the total thrust. The apparent advantage dwindles for a large number of flights when compared to the single-stage-to-orbit vehicle and a vehicle with parallel staging of tanks. For reliability, this staging method is inferior to the other two methods because of the multiple engines having an unreliability factor of 1-2/3 as compared to an unreliability factor of 1 for the other staging methods. Because there appears to be no net significant gain, this staging method was eliminated from further consideration in this investigation.

II, B, Vehicle Concepts (cont.)

(2) Staging of Tank Only

The vehicle staging tanks only is the most costly of the three vehicles considered. This cost results from high airframe development and production costs, however, in 400 flights the vehicle becomes competitive with the other two vehicles. Reliability for this vehicle is equal to that for the single-stage vehicle. The vehicle staging tanks only appears to be an attractive alternative for a large number of flights, however, within the scope of this investigation, it did not offer advantages over the single-stage vehicle.

c. Bases for Cost Analysis

The vehicle costs are based upon the vehicle cost model described in Section III, D with the following exceptions. None of the costs for these vehicles is affected by the selection of staging point, except as staging point affects size. Therefore, vehicle staging is based upon maximum payload considerations.

Reliability effects are excluded from the cost analysis.

(1) Staging of Engines Only

(a) The number of engines before and after staging were selected on the basis of maximum payload-per-pound of takeoff weight. This resulted in the selection of three engines, two of which are simultaneously jettisoned during flight.

II, B, Vehicle Concepts (cont.)

(b) Specific impulse values are consistent with those used for the standard vehicle. For the engines that are jettisoned, a value of 411 sec is used. For the remaining engine, a value of 426 sec is used.

(c) Engine development and production costs are based upon the use of three engines, each supplying one-third of the total thrust.

(d) Airframe development cost was increased by 20% for the additional development of systems required for staging of the two engines.

(2) Staging of Tanks Only

(a) The number of tanks before and after staging were selected on the basis of maximum payload. This resulted in the selection of five tanks, four of which are simultaneously jettisoned during flight.

(b) Specific impulse is based on that for the standard vehicle booster described in Section III, B.

(c) Payload was calculated on the assumption that the propellants in the jettisoned tanks are expelled into the nonjettisoned tank before staging. Therefore, the nonjettisoned tank is full just before staging.

II, B, Vehicle Concepts (cont.)

(d) Airframe development cost was increased by 20% to account for additional propellant feed systems and staging development.

(e) Airframe production was based on that for a single-tank stage. This cost was then increased by 50% to account for the added expense of fabrication and system checkout.

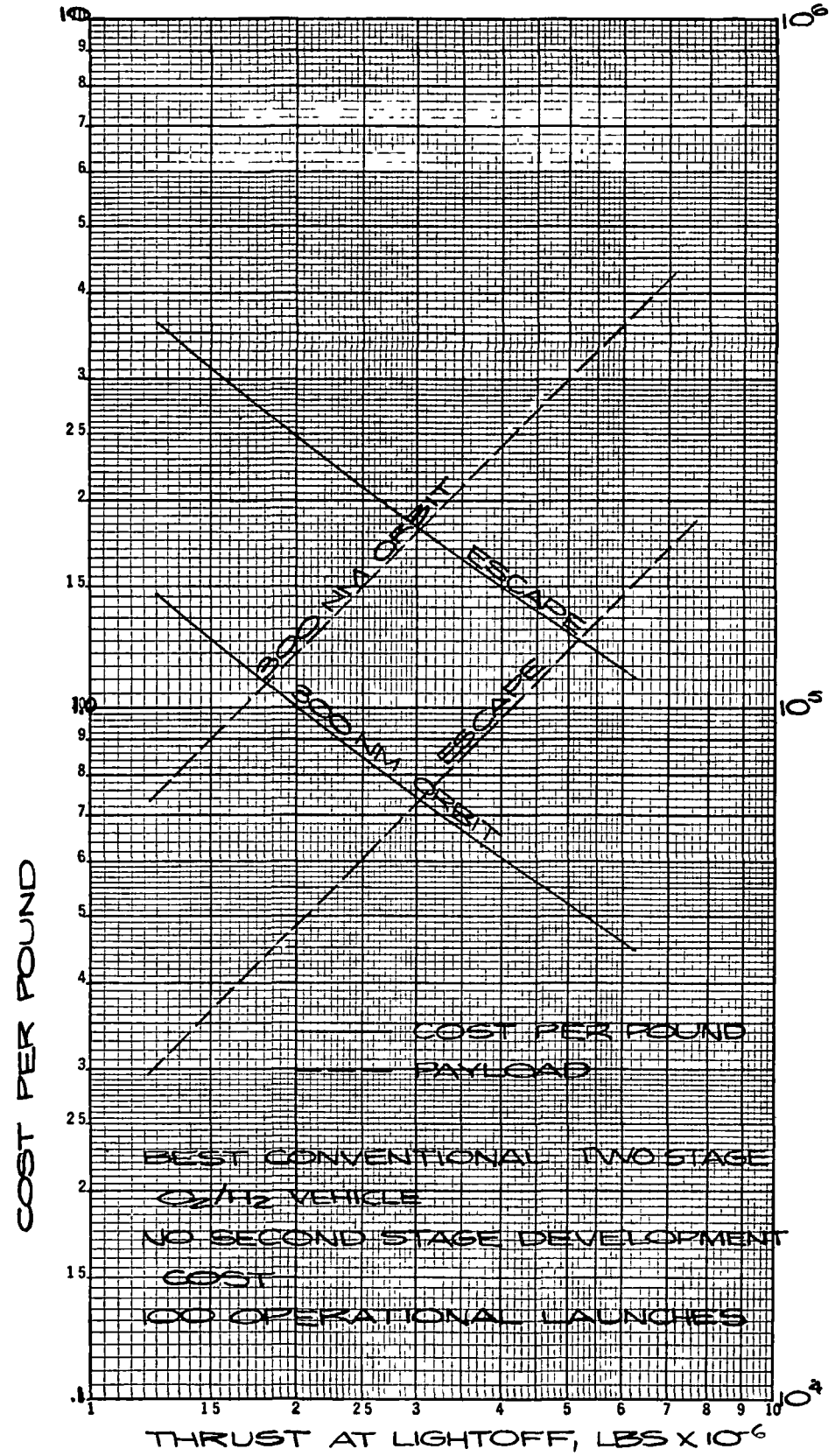

Vehicle Cost and Payload Variations with Size

Figure II B-1

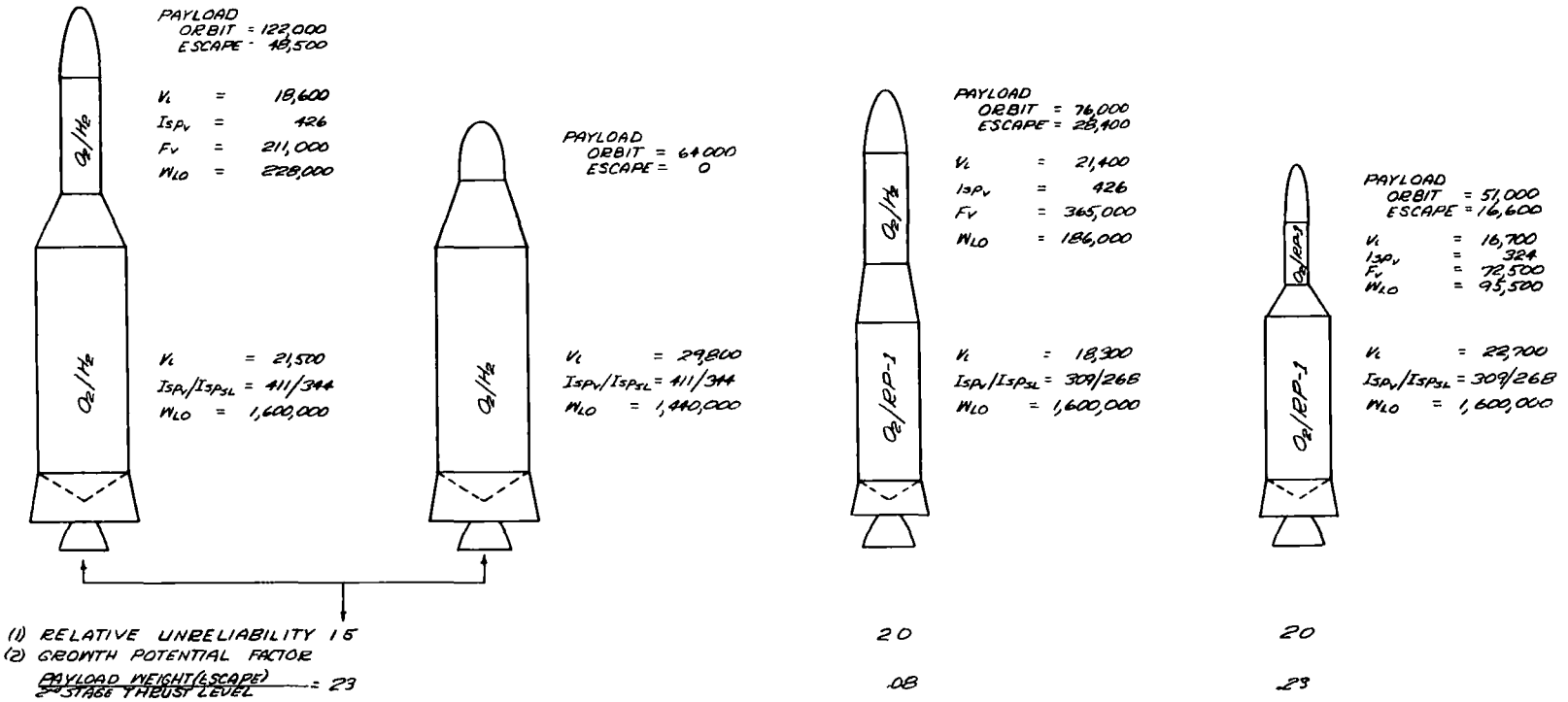

Figure II B-2

Propellant Comparison and Conventional Configurations (Man-Rated)

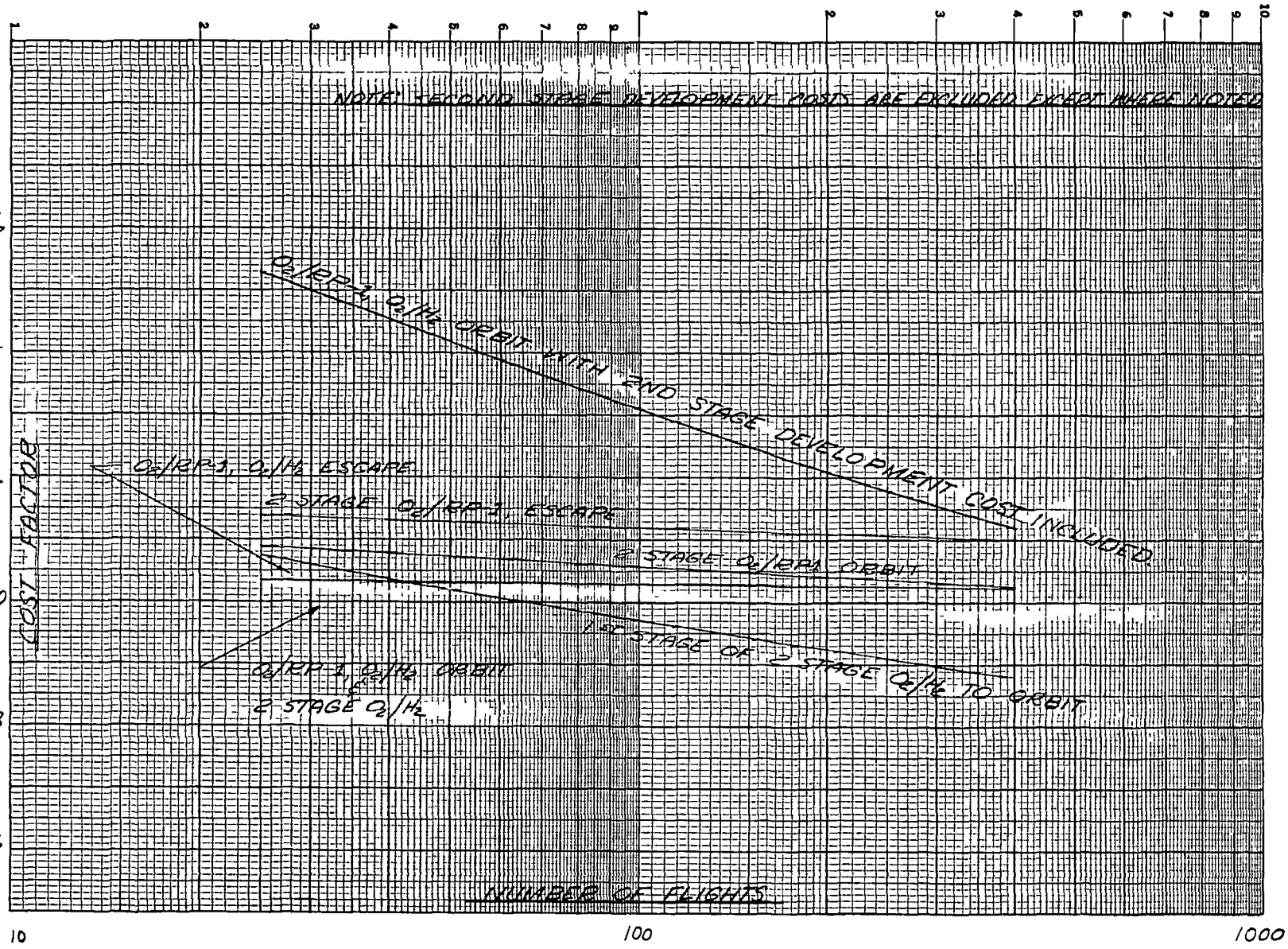

Figure II B-3

Propellant Comparison for Conventional Systems

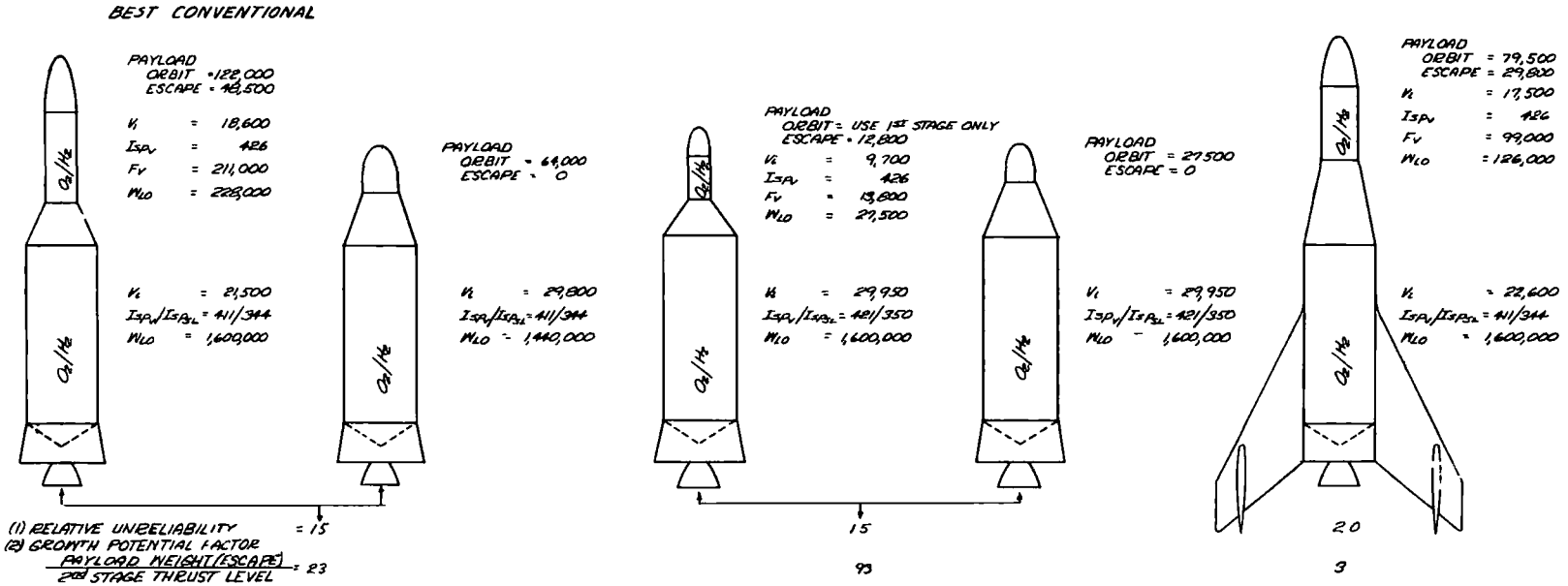

NOTES PAYLOAD, LIGHTOFF WEIGHT AND THRUST ARE IN LB., IDEAL VELOCITY INCREMENT IN Ft/SEC., VELOCITY INCREMENTS ARE FOR ESCAPE MISSION; SPECIFIC IMPULSE IN SEC

Figure II B-4

Recovery Method Comparisons and Configurations (Man-Rated)

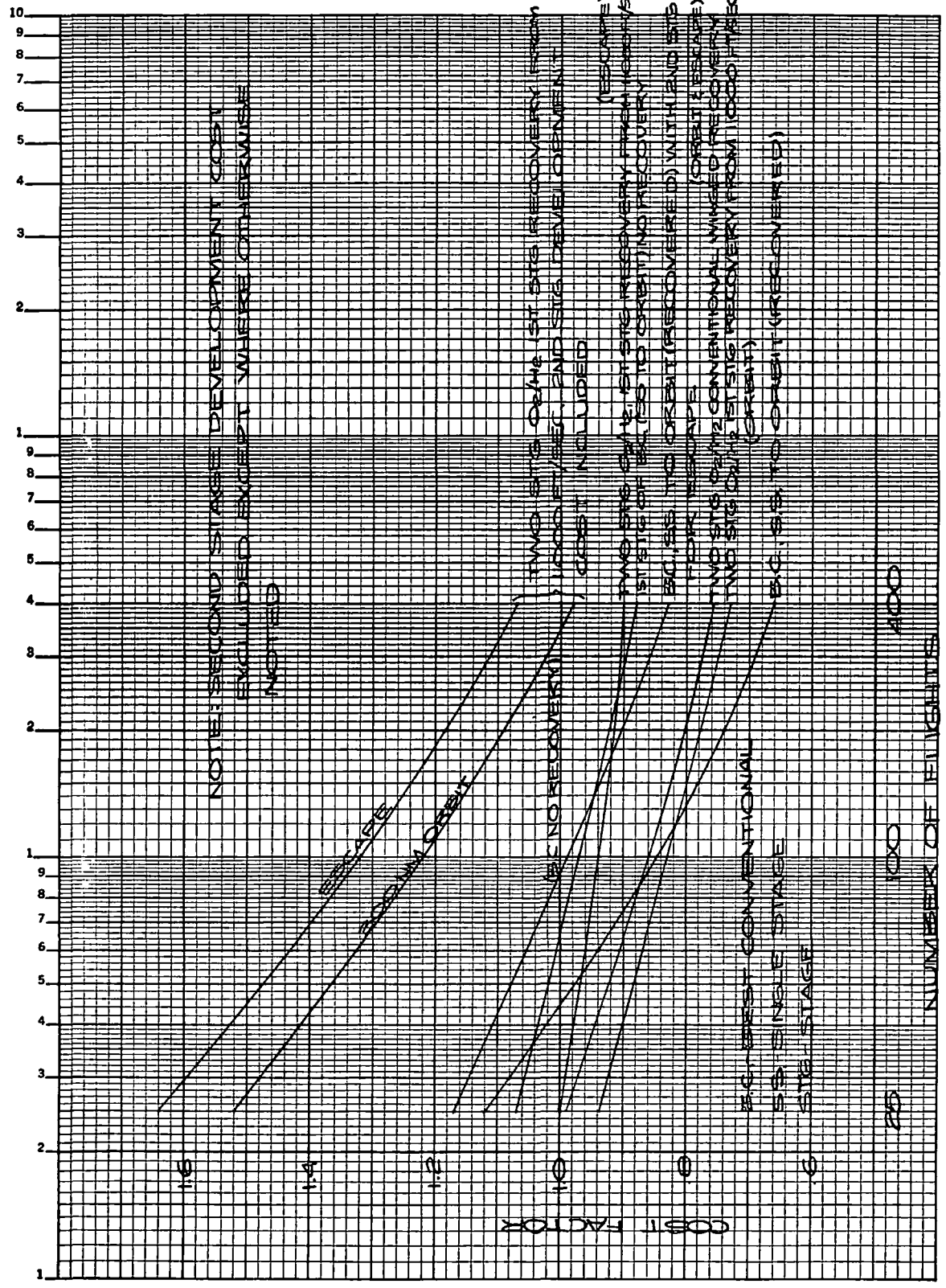

Figure II B-5

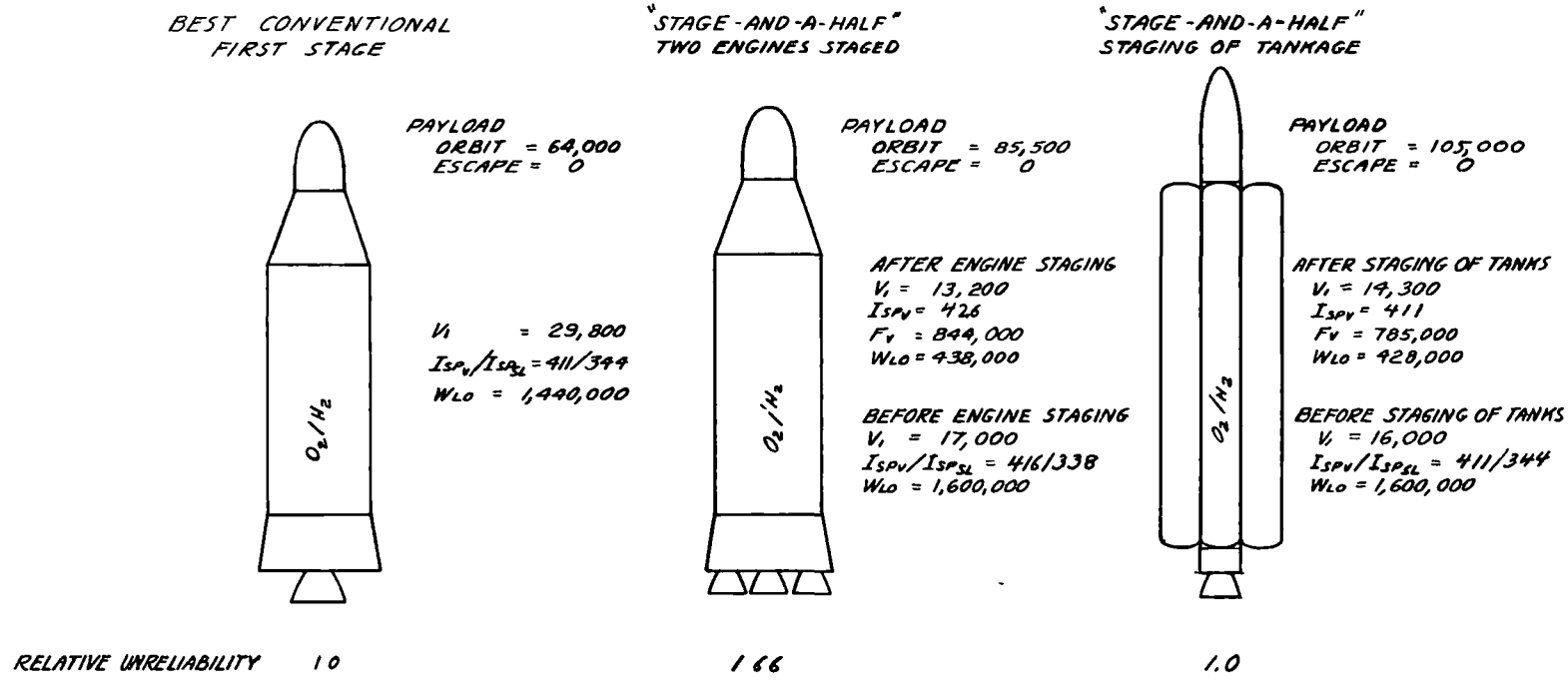

NOTES PAYLOAD, LIGHTOFF WEIGHT, AND THRUST ARE IN LB., IDEAL VELOCITY INCREMENT IN FT/SEC; VELOCITY INCREMENTS ARE FOR ESCAPE MISSION; SPECIFIC IMPULSE IN SEC

Figure II B-6

Staging Methods, Configuration

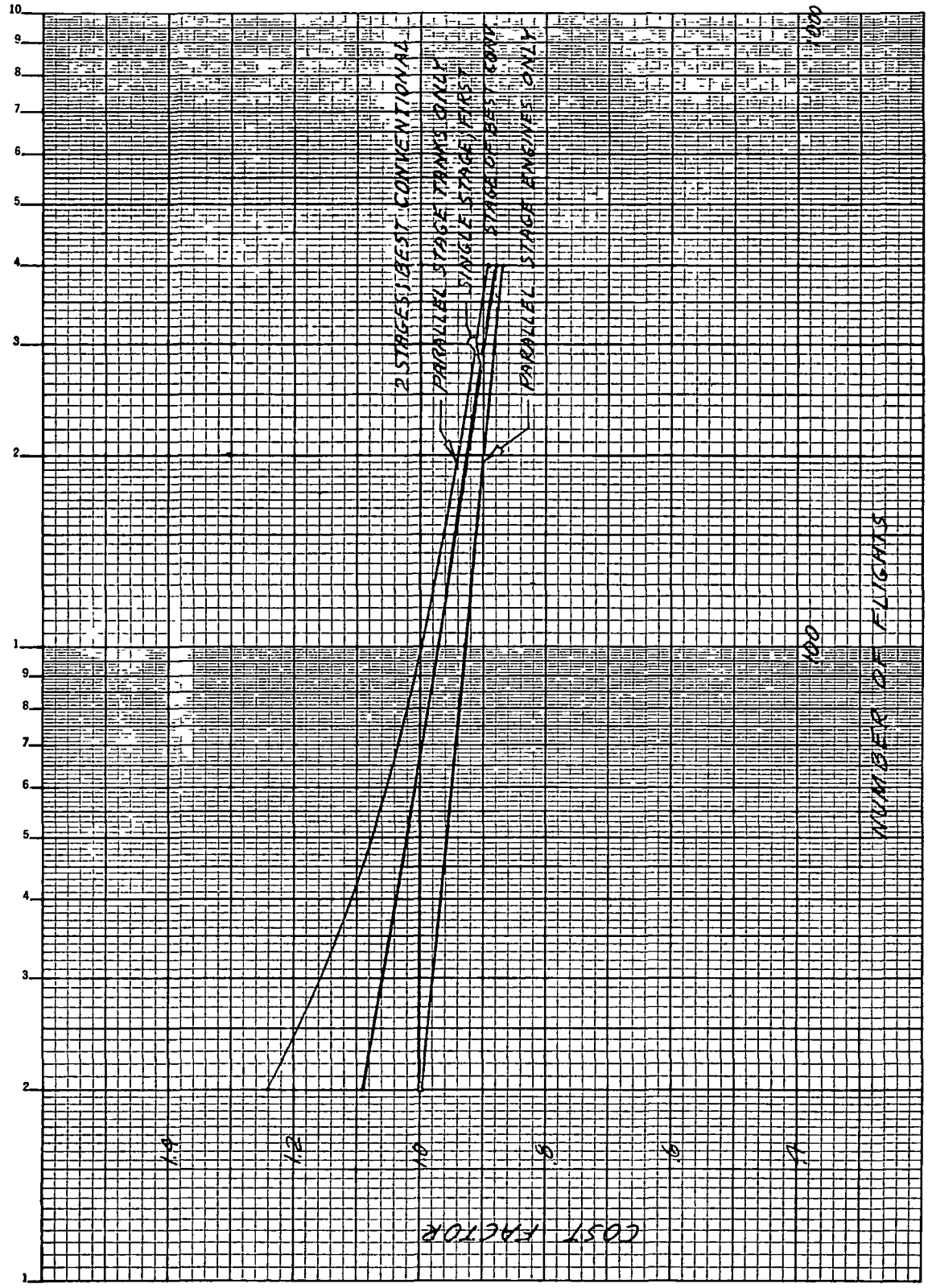

Staging Methods Cost Comparison

Figure II B-7

II, Concepts Considered (cont.)

C. CLUSTERING

Clustering is normally proposed for four reasons: (1) The development of one basic "building block" can be applied to solving a multitude of payload and mission requirements; (2) to avoid problems, such as tooling limitations, which could occur if components become very large, (3) to achieve low cost through large-quantity production of many small units; and (4) to obtain reliability through the use of major component redundancy. The methods for clustering are numerous. Clustering of various numbers of engines, propellant tanks, turbopumps, combustors, small control components, and various combinations of these components has been suggested.

1. Building-Block Concept

In the building-block concept, one basic engine and tank configuration (module) is used for the significant portion of all missions. The first stage is generally made up of three or more modules, with the upper stages composed of one or more modules. The exact number used in each stage would be selected on the basis of resultant minimum cost. Modified building block concepts would include clustering various numbers of engines on a single tank. Cylindrical sections could be removed for second-stage use or for missions requiring less than design payloads.

Clustered tanks and single engines constitute another concept that could be classified with these modular concepts.

All of these concepts are similar enough in nature so that analysis of one should show if significant advantages exist for any of them.

II, C, Clustering (cont.)

The complete modular unit was selected for preliminary analysis because it is sufficiently representative of these concepts to indicate whether any promise of significant cost reduction exists

The best conventional vehicle described in Part III and shown in Figure III C-1 was selected as the basis for comparisons.

The modular concept analyzed incorporates four units in the booster and one unit in the second stage, thus for every vehicle, five units are produced Hence, production quantities are five times those for the best state-of-the-art configuration. However, the size of each unit is considerably smaller and, as detailed in Paragraph II, C, 3, this results in higher production costs.

An advantage for the modular approach is the lower development cost Also, for missions requiring less than design payload, modules can be eliminated, thereby providing a cost savings

The modules have to be structurally connected, but this was ignored in the analysis. Therefore, the cost-per-lb of payload values presented will be slightly optimistic in favor of the modular concept.

Figure II C-1 shows the cost-per-lb of payload factor plotted as a function of payload for the modular approach as well as for the best conventional vehicle for 100 operational launches. Discontinuties in the curve for the modular concept represent the effect of using less modules upon cost when payload is reduced. The discontinuity for the best conventional vehicle curve represents the effect on cost at a payload where the first stage alone is adequate for payload delivery. It is interesting to note that only at very low payloads is

II, C, Clustering (cont.)

there any cost advantage shown for the modular approach. Over most of the payload range, the best conventional vehicle is superior. The major feature of this curve is that the cost differences are insignificant.

Reliability would favor the best conventional vehicle because there are fewer major components. In view of the fact that structure weight and cost for mutually attaching the modules were ignored, the comparison shown is biased in favor of the modular configuration.

Based on these results, the modular approach delineated was eliminated from further consideration in this study.

2. Tooling Limits

Much effort was expended both prior to and during this investigation to determine if any size limits were being approached which would favor clustering because of tooling considerations. It is concluded (and later supported in Task 4) that no limits exist up to at least 24,000,000 lb of thrust.

3. Mass Production Economy

One advantage for clustering is that producing large quantities would give lower costs because of production learning effects. However, as a result of this investigation it was determined that as size increases, cost-per-lb of components is reduced. Another effect is that development cost would be less for smaller units that are used in a cluster.

II, C, Clustering (cont.)

The analysis that follows compares single to clustered units. Production cost effects are analyzed first and then the development cost effects are incorporated.

Investigations have shown that the production cost of rocket vehicle components varies approximately linearly with size when plotted using logarithmic coordinates. Therefore, the production cost of rocket vehicle components can be written as a function of size as follows:

$$C_p = KS^a \qquad \text{(Eq. 1)}$$

where,

C_p = Component Production Cost

K = Constant

S = Measure of Size (Thrust, Volume, etc.)

a = Slope of the Production Cost vs Size Curve.

Equation 1 is useful for determining the production cost of a unit if production quantity is fixed. However, as more units are produced the production cost of each successive unit is decreased by the effect of the manufacturing learning curve. Hence, the production cost of a unit, N, is equal to a learning curve factor multiplied by the first unit production cost. The learning curve factor also varies linearly with the number of units produced, when plotted using logarithmic coordinates. Variation in the learning curve factor can be

II, C, Clustering (cont.)

shown by the following relationship

$$LCF = N^b \qquad \text{(Eq. 2)}$$

LCF = Learning Curve Factor
N = Number of Units Produced
b = Slope of the Learning Curve

The production cost of the Nth unit can, therefore, be expressed by the following relationship.

$$C_p = K (S)^a (N)^b \qquad \text{(Eq. 3)}$$

If Equation 3 is used to express the production cost of single units, then the production cost of clustered units can be expressed as follows:

$$C_{pc} = nK \left(\frac{S}{n}\right)^a (nN)^b \qquad \text{(Eq. 4)}$$

C_{pc} = Production Cost of Clustered Units
n = Number of Units Clustered

Dividing Equation 4 by Equation 3 results in the following relationship.

$$\frac{C_{pc}}{C_p} = n^{(1 - a + b)} \qquad \text{(Eq. 5)}$$

Equation 5 shows that the ratio of the production cost of clustered units to the production cost of single units is only dependent upon the number of units clustered, the slope of the production cost versus size curve and the slope of the learning curve.

The variation of the slope of the learning curve, b, with the percent learning curve is tabulated below.

II, C, Clustering (cont.)

Learning Curve (%)	Slope of the Learning Curve
95	-0.0740
85	-0.2345
75	-0.4150
65	-0.6215

Equation 5 is plotted in Figure II C-2 for an 85% learning curve and various slopes of production cost in relationship to size curves. Figure II C-2 shows that, if the production of clusters is greater than the production cost of a single unit for a cluster of two units, then the production cost of clustered units will remain greater and increase with the number of units clustered. Only if the slope of the production cost as compared with the size curve is between 0.75 and 1.0, would it be economical to cluster. As shown in Part III, D, the production cost for all major rocket vehicle components varies with size to a power between one-half and two-thirds. Figure II C-2 shows this for an 85% learning curve. Clustering does not show an economical advantage on a production cost basis. This is shown by the shaded area in Figure II C-2.

Equation 5 was also plotted in Figure II C-3 for variations in the percent learning curve and the assumption that production cost varies as the two-thirds power of size. Figure II C-3 shows that it is not economical to cluster on a production cost basis unless a learning curve of less than 80% can be achieved. Learning curves most generally used in estimating cost vary between 80% and 90%. This is shown by the shaded area in Figure II C-3. If a slope of one-half for the variation of production cost with size was assumed to establish Figure II C-3, clustering would show even a greater disadvantage on a production

II, C,, Clustering (cont.)

cost basis.

Based on Figures II C-2 and II C-3, it can be concluded that clustering does not offer any significant production cost advantages.

One major factor favoring component clustering is the decreased development cost for clusters. Investigations have shown that development cost also varies linearly with size, if plotted using logarithmic co-ordinates. The development cost for single units and clusters can be expressed as follows.

$$C_D = K (S)^d \qquad \text{(Eq. 6)}$$

$$C_{DC} = K \left(\frac{S}{n}\right)^d \qquad \text{(Eq. 7)}$$

C_D = Development Cost of Single Units

C_{DC} = Development Cost of Clustered Units

K = Constant

S = Measure of Size

n = Number of Units Clustered

d = Slope of the Development Cost vs Size Curve

Dividing Equation 7 by Equation 6 results in the following relationship.

$$\frac{C_{DC}}{C_D} = n^{-d} \qquad \text{(Eq. 8)}$$

As expected, it is obvious from Equation 8 that the development cost for clustered units is always less than the development cost of single units and will decrease as the number of units clustered is increased. Only if the value of d is

II, C, Clustering (cont.)

negative, that is if the development costs decrease with increasing size, would the development costs of single units be less.

To determine the combined effect of production and development cost on the single and clustered unit comparison, an analysis was performed for the standard O_2/H_2 vehicle defined in section III, A of this report. In this analysis, the single engine used in the standard vehicle was replaced by four engines, each developing 500,000 lb of thrust at sea-level. Component costs used to determine vehicle cost factors are discussed in Part III, D. Vehicles are compared on the basis of the 300-nm orbit mission as a function of the number of flights. In addition, engine weight differences, except for the structural weight necessary to join the cluster, were accounted for. Results of this analysis are presented in Figure II C-4. In this figure, the base cost factor of one was selected for 25 missions using the standard O_2/H_2 vehicle. The cost factors for other launch rates and for the cluster of four engines are compared against this base. Figure II C-4 shows that for 400 launches no cost savings result from clustering, and at 25 launches, a cost saving of approximately 5% results from the clustering of four engines. However, cost and weight penalties associated with assembling a cluster were excluded from the analysis, therefore, the cost factors for the vehicle with clusters are slightly optimistic.

Based on this analysis, clustering is not shown to be undersireable but neither has the analysis shown that clustering can significantly reduce costs, which is the basic study objective. Therefore, clustering was not considered further as a means for significantly reducing costs.

4. Reliability

Clustering has been suggested as a possible means for increasing reliability in high thrust rocket vehicles. Presently, there is no evidence that high

II, C, Clustering (cont.)

thrust level has any degrading effect upon inherent rocket engine reliability. Therefore, if higher reliability is to be attained through clustering, redundant engines must be incorporated.

It is a simple matter to show that the use of spare engines in a cluster can theoretically result in higher net reliability for the cluster as compared to individual engines in the cluster. However, as the problem is more minutely examined, reliability degrading effects are found which lower cluster reliability. These reliability degrading effects result because:

a. Destructive malfunctions within any engine of the cluster will abort the flight.

b. A control system is needed that would be capable of detecting impending malfunction and shutting the engine down. Very little confidence exists that such a system could be developed which would be error-free. Typical of this type of error are shutdown of functioning engines, failure to shutdown malfunctioning engines, shutting down too many engines, and failure to make necessary thrust-vector corrections to compensate for the shutting down of an engine. Hence, unreliability is associated with the control system.

Analyses that include the indicated considerations are heavily loaded with assumptions based on empirical data only. Results from several analyses of this type have shown that when these effects are included, the probability of cluster failure is comparable with the probability of single-engine failure. Typical results from such an analysis are tabulated below. The analysis was obtained with unit engine reliability of 95%, and it was assumed that 10% of these failures resulted in a stage abort because of explosion or control system malfunction. Also, 19% of the failures occur at start and 11% at shutdown.

II, C, Clustering (cont.)

These assumptions were based upon a study of Titan testing history.

No. of Engines Clustered	No. of Spare Engines	Overall Reliability	Flight Reliability*
1	0	.9500	.9615
4	0	.8145	.9544
4	1	.9190	.9641
8	0	.6634	.7291
8	1	.8337	.9162
8	2	.8575	.9425

The reliability numbers presented are based upon the assumption that spare engines are not started unless they are needed.

It should be noted from the above table that no clear reliability advantage is gained from clustering. Conversely, there is no clear loss in reliability from clustering provided that the proper number of spare engines are used.

* Flight reliability does not include failures before liftoff if nondestructive shutdown can be accomplished.

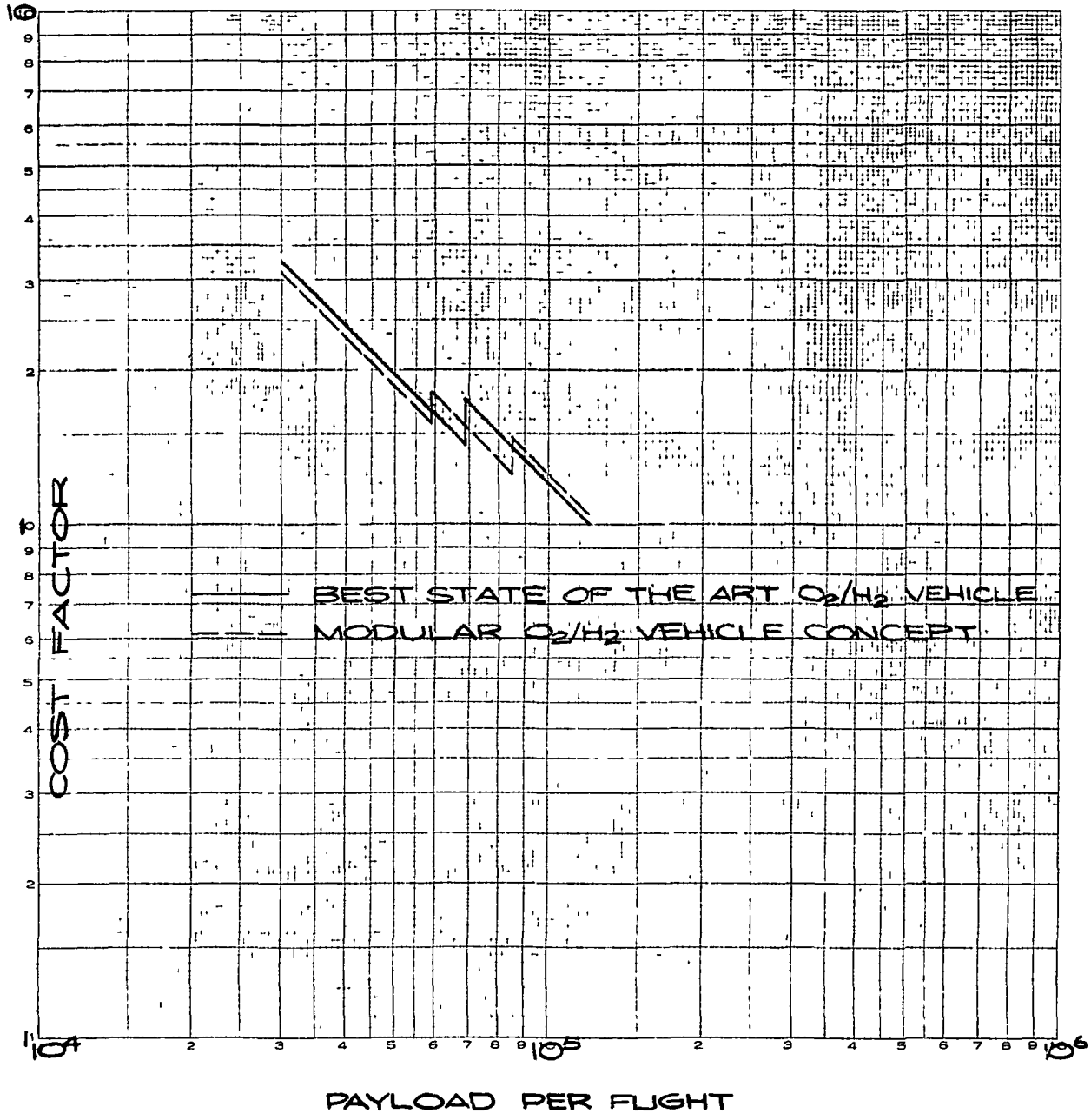

Cost Factor vs Payload per Flight (100 Operational Launches)

Figure II C-1

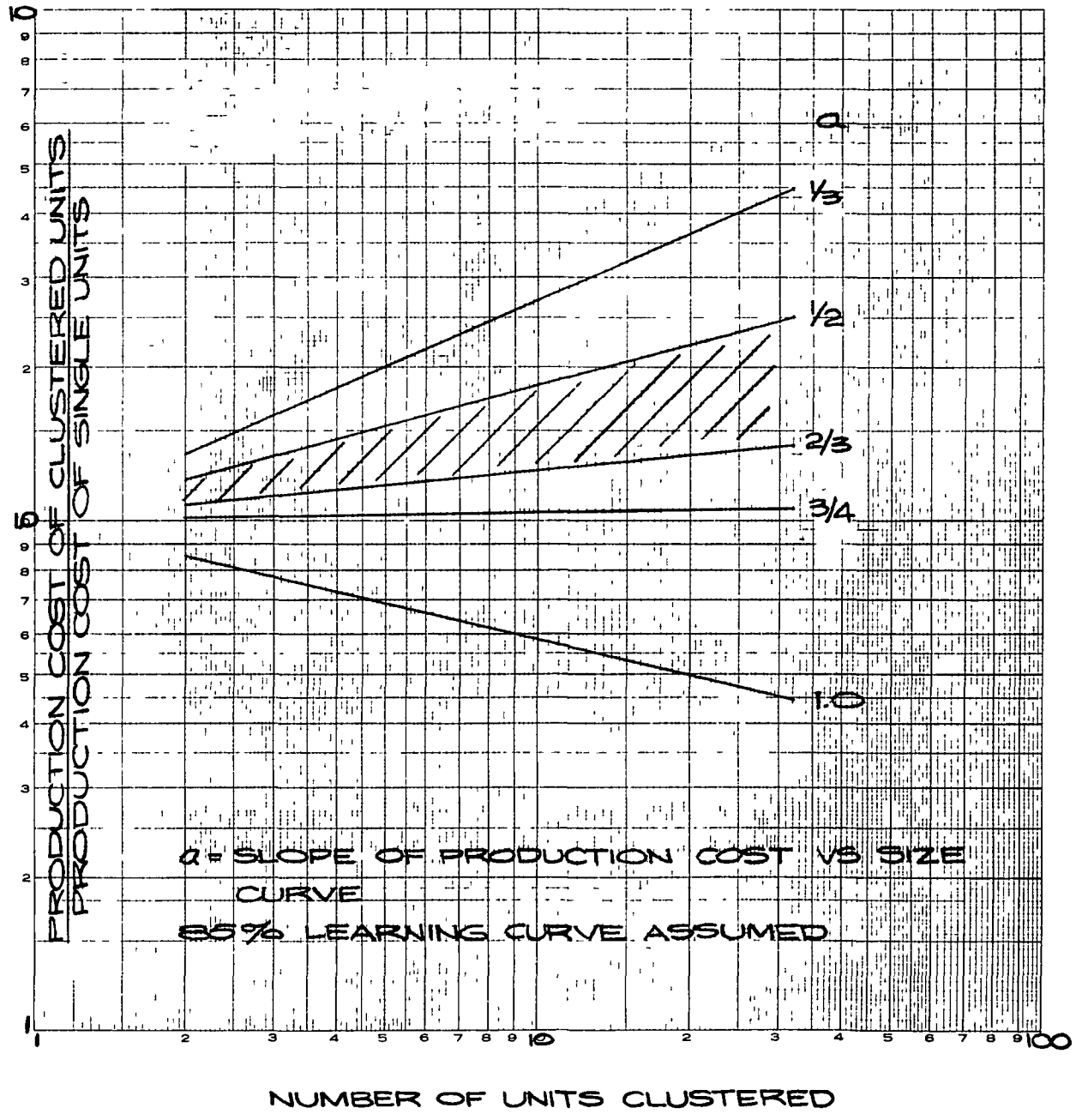

Ratio of Production Cost of Clusters to the Production Cost of Single Units vs Number of Units Clustered for an 85% Learning Curve

Figure II C-2

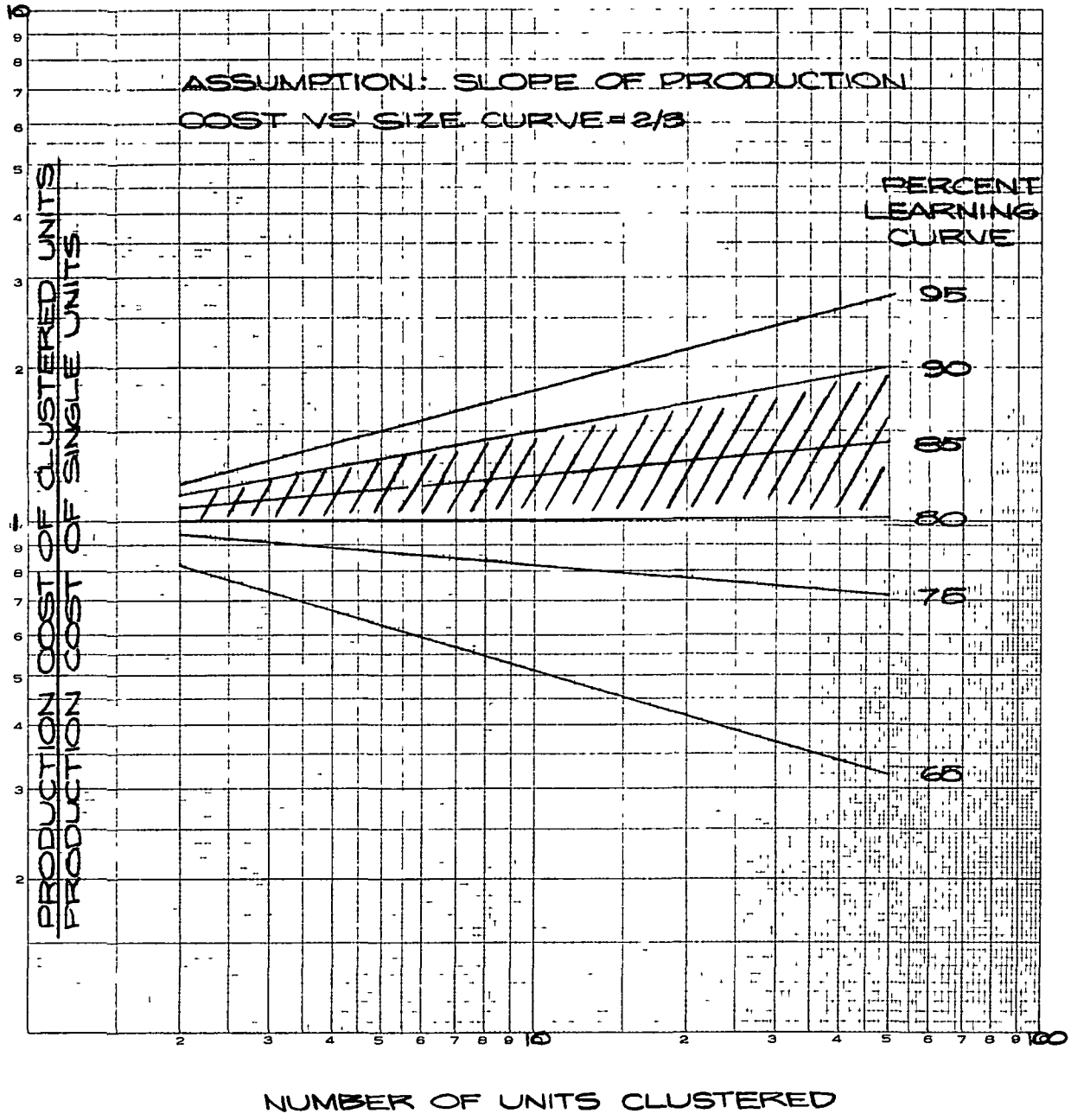

Ratio of Production Cost of Clusters to the Production Cost of Single Units vs Number of Units Clustered for Various Percent Learning Curve

Figure II C-3

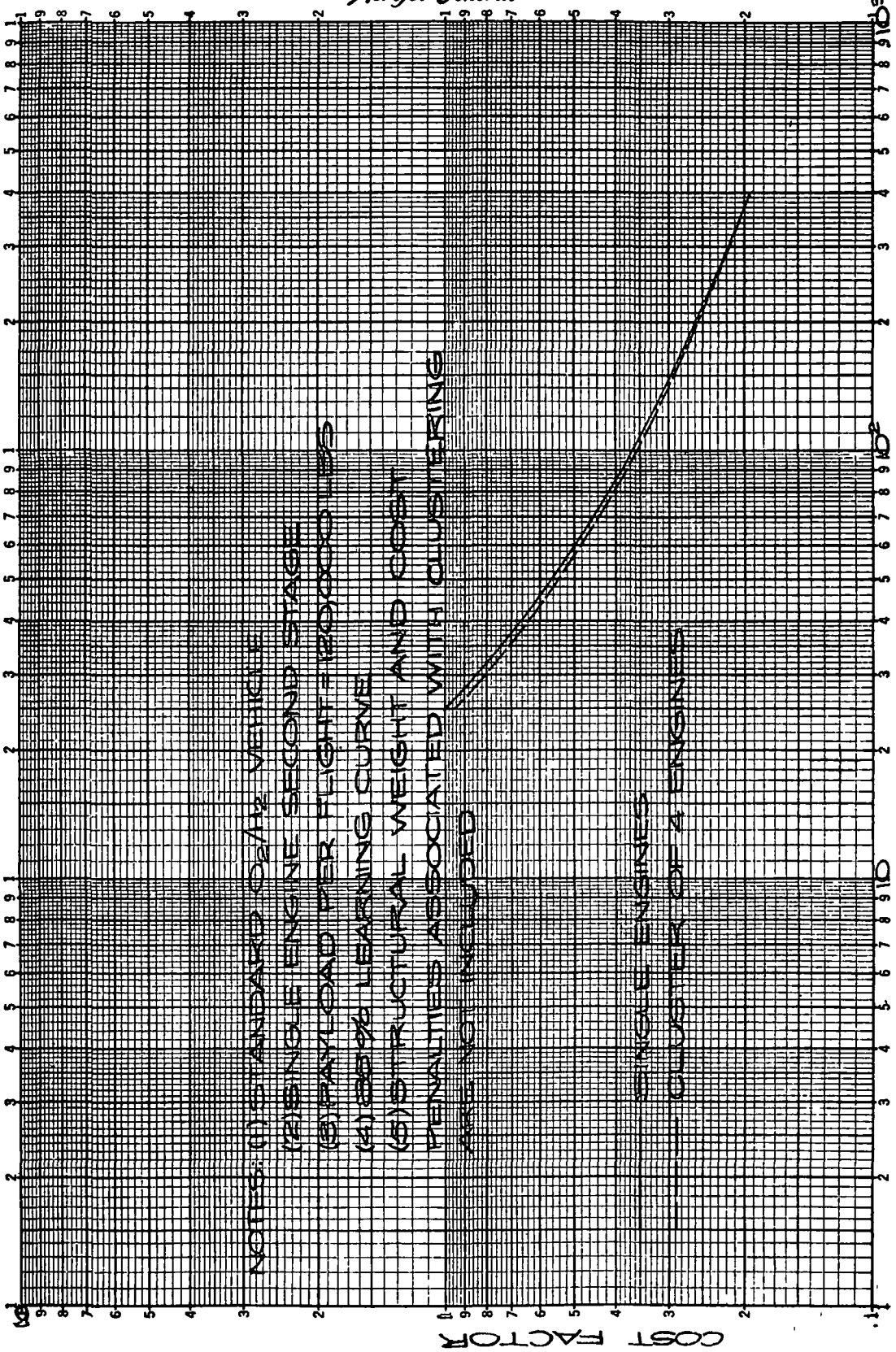

Cost Factor vs Number of Operational Launches

Figure II C-4

II, Concepts Considered (cont.)

D. PRESSURE-FED ENGINES

Propellant pumps and their appurtenant equipment are considered complex; therefore, the concept of building large booster vehicles using tank pressurization for supplying both fuel and oxidizer directly to the engines was investigated. While it appeared that major gains could be made in simplifying the booster, with resultant increases in reliability, the factors which tend to work against such gains are the increase in weights and the inherently lower performance of a pressure-fed booster. A number of different possibilities exist for supplying pressure to such a booster, and for the sake of throughness, they were all investigated. These systems are: stored gas pressurization; VāPak; the gravity and acceleration fed; and GΔP. They are discussed as follows:

1. Stored Gas Pressurization System

This system depends upon a supply for its pressurant. The gas is stored in a separate tank unless one of the propellants is used for pressurization. Gas is passed through a heat exchanger before being introduced into the propellant tank.

A previous company-sponsored investigation of a large pressure-fed booster stage (Appendix H) provided the design data used in making comparisons with competitive systems. The pressure-fed booster configuration evolved is pictured in Figure II D-1 and II D-2. It was selected as the standard pressure-fed configuration after integrating the results of vehicle and subsystem tests and analyses. These investigations included: trajectory analysis; booster performance analysis; engine design; propellant tankage and structure design; propellant tank pressurization system design; thrust-vector and roll control system design and

II, D, Pressure-Fed Engines (cont.)

analysis; and propellant loading system design. Various booster studies previously conducted by the Aerojet-General Corporation as well as by other companies were reviewed and evaluated. The Cosmos Booster study was particularly useful because of the similarity in booster design requirements. Because of the time and cost limitations, the booster resulting from this investigation was redesigned and used as the 6,000,000-lb-thrust standard, against which the pressure-fed system was evaluated.

This pressure-fed booster was designed to boost the same stage payload at an ideal velocity increment of 10,000 ft/sec as the indicalect 6,000,000-lb-thrust pump-fed booster. Although the velocity increment is not optimum for a pump-fed system, it is near optimum for this configuration.

This pressure-fed booster has a plug nozzle engine which develops 6,700,000 lb of thrust at sea-level, with liquid oxygen and liquid hydrogen as propellants. A plug-nozzle configuration was selected for the engine because of its altitude compensation capability. After an extensive investigation, the final design has 32 individual pen-shaped thrust chambers located around the engine expansion cone's circumference. These chambers are operated at a chamber pressure of 250 psia and a mixture ratio of 6:1. Maximum expansion ratio is 19:1 and effective I_s, is 364 sec. The low chamber pressure permits film cooling.

Propellants are contained in spherical tanks, with the oxidizer tank located above the fuel tank. The oxidizer tank is pressurized by helium gas, which is heated by a heat exchanger located on the engine plug. Fuel tank pressurization is provided by hydrogen stored in liquid form in a separate tank and heated in another heat exchanger. Heated helium gas is used to provide the pressure head for this second hydrogen tank. The additional tank is required to overcome the pressure drop in the system.

II, D, Pressure-Fed Engines (cont.)

Thrust-vector control is obtained by chamber pressure modulation. The main propellant valves throttle propellants to obtain the necessary turning moment. Roll control is provided by two small auxiliary nozzles located above the main engine 180° apart.

This pressure-fed booster was compared with the pump-fed booster for a 200-nm orbit payload when used in two-stage vehicles. Both used pump-fed O_2/H_2 second stages. Trajectory calculations were performed with an IBM-7090 computer and established the 200-nm circular-orbit payload capability as 250,000 lb. (Later company-sponsored studies have shown that this estimate was slightly pessimistic because of jettison-mass parameters assumed in determining payload.) Further evaluation of the jettison-mass parameters show that the payload capability of this vehicle should be 288,000 lb. This, however, in no way effects the vehicle comparisons discussed in following paragraphs because the payload capabilities of all vehicles would be increased 38,000 lb. For example, a 4,800,000-lb sea-level-thrust O_2/H_2 vehicle will deliver approximately 288,000 lb to a 300-nm orbit. This thrust-to-payload ratio is consistent with the standard O_2/H_2 vehicle. The vehicle with an O_2/H_2 pressure-fed booster was then compared to a two-stage pump-fed O_2/H_2 vehicle designed to deliver a 250,000-lb payload to a 300-nm orbit. Sea-level thrust in this case was determined to be 4,800,000 lb. These vehicles are compared in Figures II D-3.

Figure II D-3 shows that the relative cost-per-lb of payload for the O_2/H_2 pressure-fed booster would be approximately 92% greater than the cost of the two-stage pump-fed vehicle. Therefore, further company-sponsored effort was conducted to examine other pressure-fed booster concepts to ascertain if cost could be reduced significantly. These concepts are also shown in Figure II D-3. Of the concepts investigated, only the modular VāPak concept with high-density

II, D, Pressure-Fed Engines (cont.)

propellants and fiber-glass tankage seems to have any merit. Even with the light weight tanks and the cost reduction associated with modular tanks, the cost-per-lb of payload for this system is still approximately 64% greater than the two-stage pump-fed vehicle.

The symbols used in Figures II D-3 and II D-4 are as follows:

W_{lo}	=	Stage lightoff weight, lb
F_v	=	Engine vacuum thrust, lb
F_{sl}	=	Engine sea-level thrust, lb
V_i	=	Stage ideal velocity increment, ft/sec
Isp_v	=	Engine vacuum specific impulse, sec
Isp_{sl}	=	Engine sea-level specific impulse, sec

After comparing these pressure-fed boosters with the pump-fed system having the same payload capability, it was concluded that while the pressure-fed booster has some merit because of simplicity, it is heavier and inferior in performance; therefore, it was not given any further consideration in this investigation.

2. The VāPak System

Another pressure-fed variation is the VāPak system, evaluated in Figure II D-3, which depends upon the vapor pressure of the propellants themselves for its pressurization.

II, D, Pressure-Fed Engines (cont.)

Under equilibrium conditions, the pressure of the vapor for any given propellant is a function of the nature of the substance and its temperature. If no other gas is present, this vapor pressure is the total pressure in the container.

If an attempt is made to lower the pressure by draining-off either liquid or gas (vapor), the vapor-liquid equilibrium will be upset and liquid will vaporize, creating additional gas, thereby tending to counteract the reduction in pressure. In the absence of an external source, heat to vaporize the gas comes from that stored in the body of the liquid. The temperature of the liquid will then fall, and so will the equilibrium vapor pressure.

The magnitude of the decrease in pressure is a function of the proportion of liquid drained-off, the specific heat of the liquid, its latent heat of vaporization, the specific volume of the liquid, the specific volume of the vapor, and the vapor pressure-temperature relationship.

These relationships have been investigated for a number of possible rocket propellants. It was concluded that while there was a possibility that such a method of tank pressurization might be of some value for use in a small rocket vehicle (i.e., rockets designed to carry weather measuring instrumentation), its inherently low performance level removes it from serious consideration for large space boosters.

3. Gravity and Acceleration-Fed Systems, and the GAP System

Several possibilities exist for pressurization, at least in theory, without the use of the stored-gas or VaPak-type systems. One of these possibilities uses the static head of the fuel tanks and the acceleration of flight, while the other possibility uses combustion chamber gas to pressurize the tanks.

II, D, Pressure-Fed Engines (cont.)

As liquid storage tanks increase in height, the hydrostatic pressure in the tanks increases directly proportional to the depth of the fluid. Rockets that are several hundred feet long can develop pressures at the injector face capable of feeding propellants into the combustion chamber. These pressures result from the combination of propellant tank height and vehicle acceleration. Figure II D-4 is a schematic drawing of a G-Fed Rocket.

The weight of the smallest rocket for which G-feeding becomes feasible depends upon the fineness ratio of the tanks. If long slender tanks are acceptable from a structural (i.e., mass function) point of view, then it may be feasible to use the G-fed principle in rockets as small as 10,000,000 lb in weight. At conventional (10:1) fineness ratios, the weight is more nearly in the 100,000,000-lb category.

This type of booster suffers great performance losses because even with the very long tanks, combustion chamber pressures are low, and I_{sp} is correspondingly low. In one investigation, a booster 6,000,000-lb-thrust burning N_2O_4 and N_2H_4 required a fuel tank 10.6-ft diameter by 254 ft in length to achieve a chamber pressure of 110 psia and an expansion ratio of 3:1. Because of the severe performance loss, and such radical tank configurations (see Figure II D-5), the gravity and acceleration fed boosters were not considered further.

It is possible to modify the G-fed concept to the extent of not relying upon hydrostatic head for propellant feed during the entire period of engine operation. Instead, propellant tankage would provide a static head equal to the injector pressure drop, and supply combustion gas to the ullage spaces in the fuel and oxidizer tanks for missile pressurization. This system, the GΔP, shown in Figure II D-6, consists of fuel and oxidizer tanks, suitably proportioned and

II, D, Pressure-Fed Engines (cont.)

arranged vertically over a thrust chamber. They are connected to the chamber by means of propellant lines and thrust chamber valves. Combustion gas is bled from the thrust chamber and delivered through check valves into the ullage spaces above the fuel and oxidizer tanks. Temperature of the bled gas may be controlled by introducing excess fuel or oxidizer at the extraction ports, as appropriate.

Assuming the use of hypergolic, storable propellants, operation of this propulsion system requires filling of the fuel and oxidizer tanks only in preparation for launch. The system can be designed to be stand-loaded and made ready with any desired length of time between servicing and launching.

This system also requires very long, slender tankage, and while it provides somewhat more performance than the G-fed rockets, it is still a low performance system. Because of this, and its many structural difficulties, as well as its lack of performance gain, this sytem was also discarded.

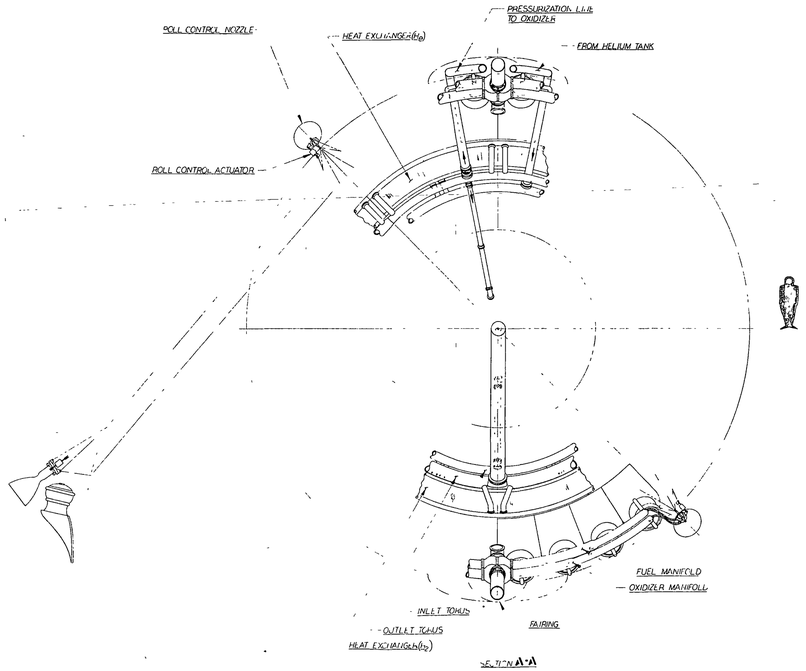

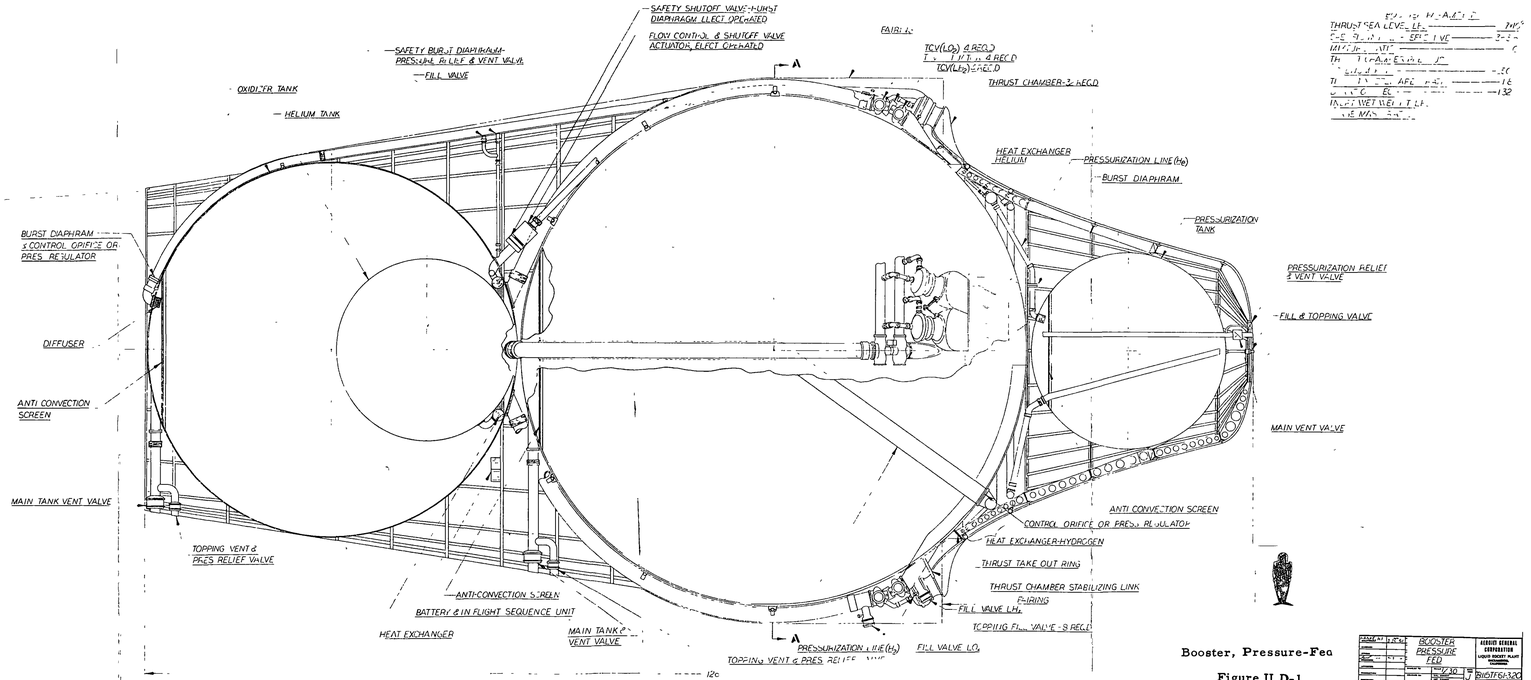

Booster, Pressure-Fed

Figure II D-1

		BOOSTER PRESSURE FED		AEROJET GENERAL CORPORATION LIQUID ROCKET PLANT SACRAMENTO	
		SIZE	CODE IDENT NO.	DRAWING NO.	
		SCALE	WEIGHT	SHEET	

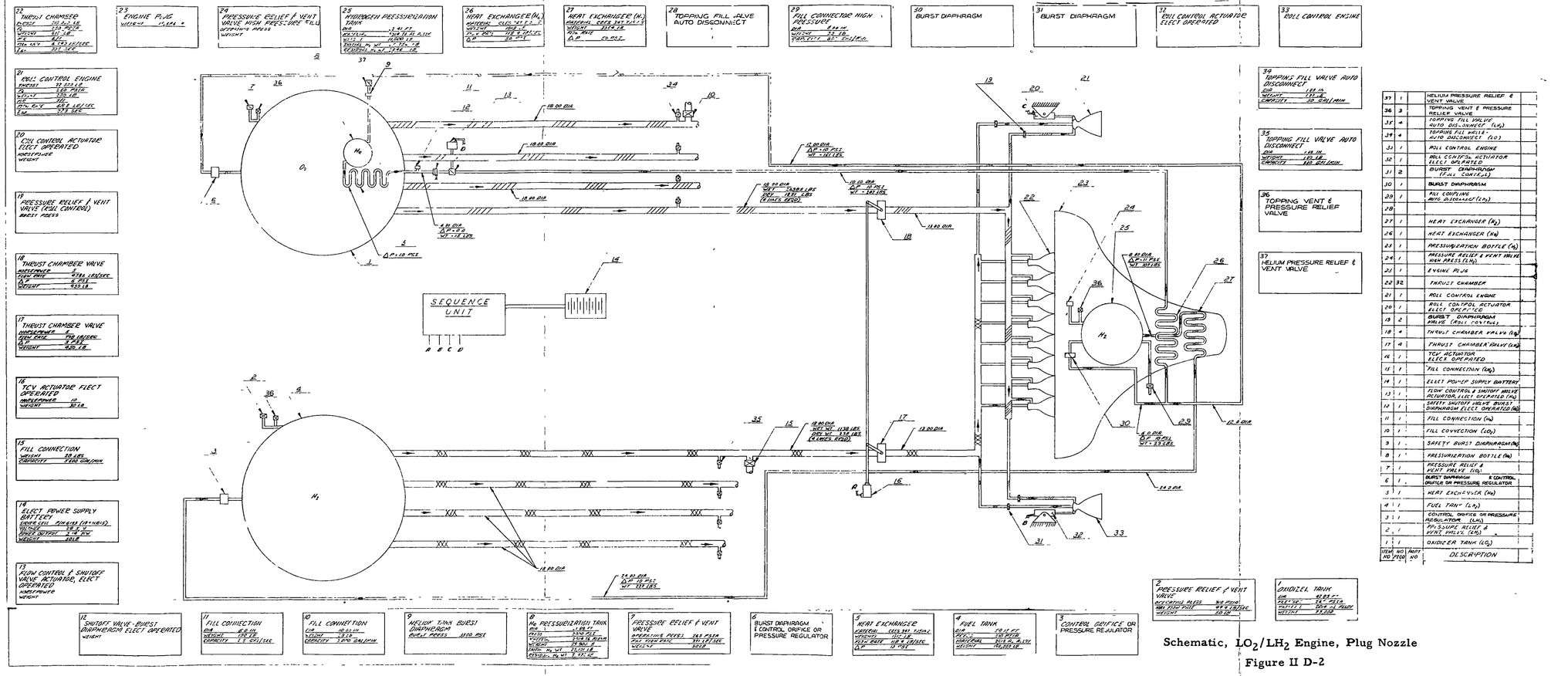
SEQUENCE UNIT
A B C D
O_2
H_2
H_1
18.00 DIA
15.00 DIA
13.00 DIA
12.00 DIA
14.00 DIA
4.80 DIA
6.40 DIA
8.40 DIA
ΔP=10 PSI
ΔP=10 PSI WT=181 LBS
ΔP=10 PSI WT=191 LBS
ΔP=10 PSI WT=197 LBS
ΔP=10 PSI WT=193 LBS
WT=188 LBS
WT=197 LBS
WT=1138 LBS (NO. WT. 138 LBS. EACH)
WT=1138 LBS (NO. WT. 138 LBS. EACH)
WT=1138 LBS (NO. WT. 138 LBS. EACH)

100%

STAGE II

W_{LO}	LBS	956,000
F_V	LBS	1,360,000
V_I	FT/SEC	15,100

	WEIGHT LBS	COST %
STAGE	685,000	26.5
ENGINE	8,300	11.0
AIRFRAME	33,250	07.9
PROPELLANTS	630,000	02.3
TEST & %	X	05.3

STAGE I

W_{LO}	LBS	3,850,000
F_{SL}	LBS	4,800,000
V_I	FT/SEC	15,200

	WEIGHT LBS	COST
STAGE	2,830,000	73.5
ENGINE	35,100	24.7
AIRFRAME	138,000	24.7
PROPELLANTS	2,600,000	09.4
TEST & %	X	14.7

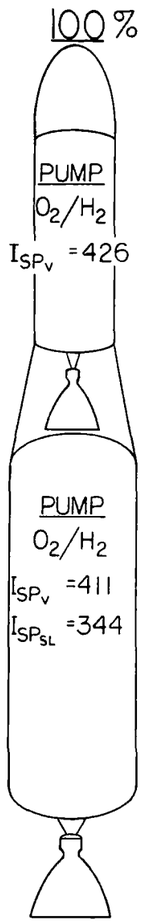

STAGE II

W_{LO}	LBS	1,870,000
F_V	LBS	3,210,000
V_I	FT/SEC	21,200

	WEIGHT LBS	COST %
STAGE	1,619,000	48.0
ENGINE	20,000	18.0
AIRFRAME	79,600	15.0
PROPELLANTS	1,487,000	05.4
TEST & %	X	09.6

STAGE I

W_{LO}	LBS	5,360,000
F_{SL}	LBS	6,700,000
V_I	FT/SEC	9,950

	WEIGHT LBS	COST
STAGE	3,491,000	144.3
ENGINE	57,000	38.9
AIRFRAME	428,000	65.7
PROPELLANTS	2,960,000	10.7
TEST & %	X	29.0

SCALE

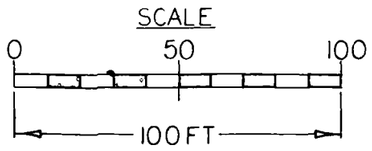

192.3%

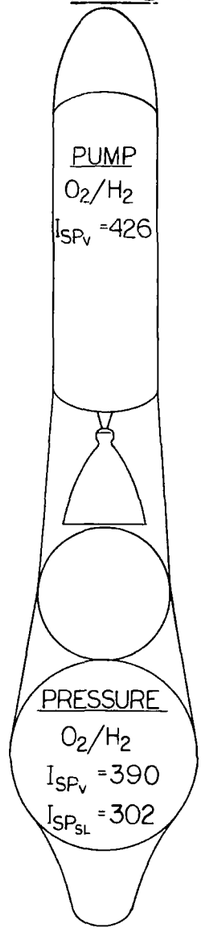

STAGE III

W_{LO}	LBS	985,000
F_V	LBS	1,340,000
V_I	FT/SEC	15,700

	WEIGHT LBS	COST %
STAGE	735,000	27.6
ENGINE	8,400	08.6
AIRFRAME	35,100	11.0
PROPELLANTS	677,000	02.5
TEST & %	X	05.5

STAGE II

W_{LO}	LBS	2,290,000
F_V	LBS	4,170,000
V_I	FT/SEC	8,000

	WEIGHT LBS	COST
STAGE	1,300,000	80.4
ENGINE	27,900	27.4
AIRFRAME	160,000	33.0
PROPELLANTS	1,088,000	03.9
TEST & %	X	16.1

STAGE I

W_{LO}	LBS	5,260,000
F_{SL}	LBS	8,470,000
V_I	FT/SEC	8,000

	WEIGHT LBS	COST
STAGE	2,980,000	137.0
ENGINE	56,700	40.0
AIRFRAME	365,000	60.5
PROPELLANTS	2,510,000	09.0
TEST & %	X	27.5

245%

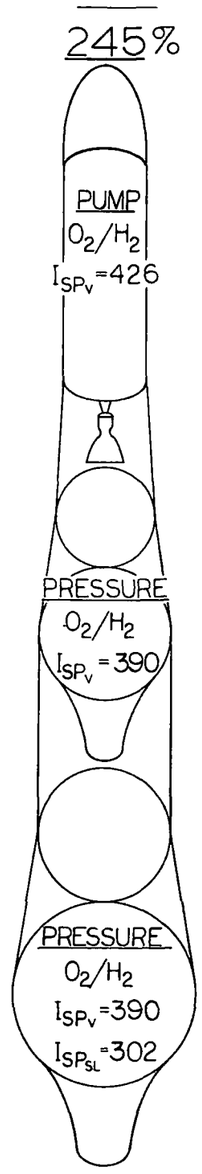

Propulsion Cost-per-lb of Payload

Figure II D-3
Sheet 1 of 2

248.6%

STAGE III

W_{LO} LBS 882,000
F_V LBS 1,200,000
V_I FT/SEC 14,500

	WEIGHT LBS	COST
STAGE	632,000	25.1
ENGINE	7,500	10.5
AIRFRAME	30,600	07.5
PROPELLANTS	582,000	02.1
TEST & %	X	05.0

STAGE II

W_{LO} LBS 2,898,000
F_V LBS 5,290,000
V_I FT/SEC 8,000

	WEIGHT LBS	COST
STAGE	2,020,000	70.0
ENGINE	33,800	22.2
AIRFRAME	158,000	28.7
PROPELLANTS	1,770,000	05.1
TEST & %	X	14.0

STAGE I

W_{LO} LBS 9,350,000
F_{SL} LBS 11,700,000
V_I FT/SEC 8,000

	WEIGHT LBS	COST
STAGE	6,450,000	153.5
ENGINE	87,400	37.5
AIRFRAME	500,000	69.0
PROPELLANTS	5,700,000	16.3
TEST & %	X	30.7

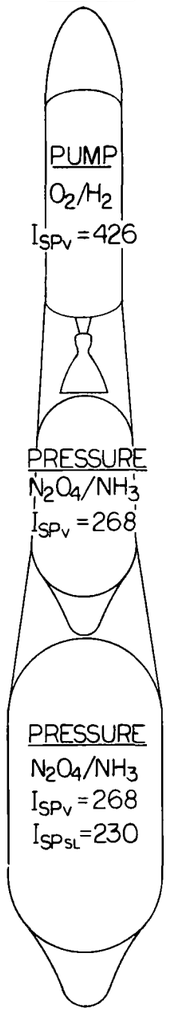

STAGE III

W_{LO} LBS 882,000
F_V LBS 1,208,000
V_I FT/SEC 14,500

	WEIGHT LBS	COST
STAGE	632,000	25.1
ENGINE	7,550	10.5
AIRFRAME	30,600	07.5
PROPELLANTS	582,000	02.1
TEST & %	X	05.0

STAGE II

W_{LO} LBS 2,623,000
F_V LBS 4,800,000
V_I FT/SEC 8,000

	WEIGHT LBS	COST
STAGE	1,740,000	715
ENGINE	30,700	212
AIRFRAME	119,000	239
PROPELLANTS	1,550,000	121
TEST & %	X	143

STAGE I

W_{LO} LBS 7,680,000
F_{SL} LBS 9,570,000
V_I FT/SEC 8,000

	WEIGHT LBS	COST
STAGE	5,050,000	152 8
ENGINE	73,000	344
AIRFRAME	399,000	524
PROPELLANTS	4,520,000	354
TEST & %	X	306

SCALE
0 50 100FT

249.4%

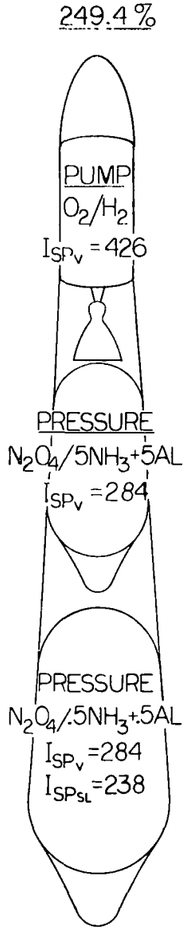

STAGE III

W_{LO} LBS 755,000
F_V LBS 913,000
V_I FT/SEC 12,900

	WEIGHT LBS	COST
STAGE	503,000	21.7
ENGINE	5,700	09.0
AIRFRAME	24,000	06.7
PROPELLANTS	464,000	01.7
TEST & %	X	04.3

STAGE II

W_{LO} LBS 2,130,000
F_V LBS 2,850,000
V_I FT/SEC 8,300

	WEIGHT LBS	COST
STAGE	1,380,000	285
ENGINE	18,100	89
AIRFRAME	68,500	38
PROPELLANTS	1,290,000	101
TEST & %	X	57

STAGE I

W_{LO} LBS 7,650,000
F_{SL} LBS 9,560,000
V_I FT/SEC 10,000

	WEIGHT LBS	COST
STAGE	5,520,000	113.7
ENGINE	72,400	35.3
AIRFRAME	274,000	15.2
PROPELLANTS	5,140,000	40.4
TEST & %	X	22.8

163.9%

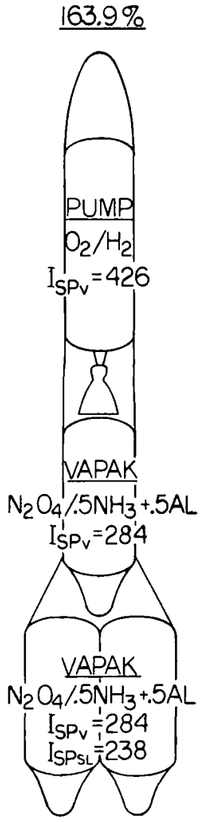

Propulsion Cost-per-lb of Payload

Figure II D-3
Sheet 2 of 2

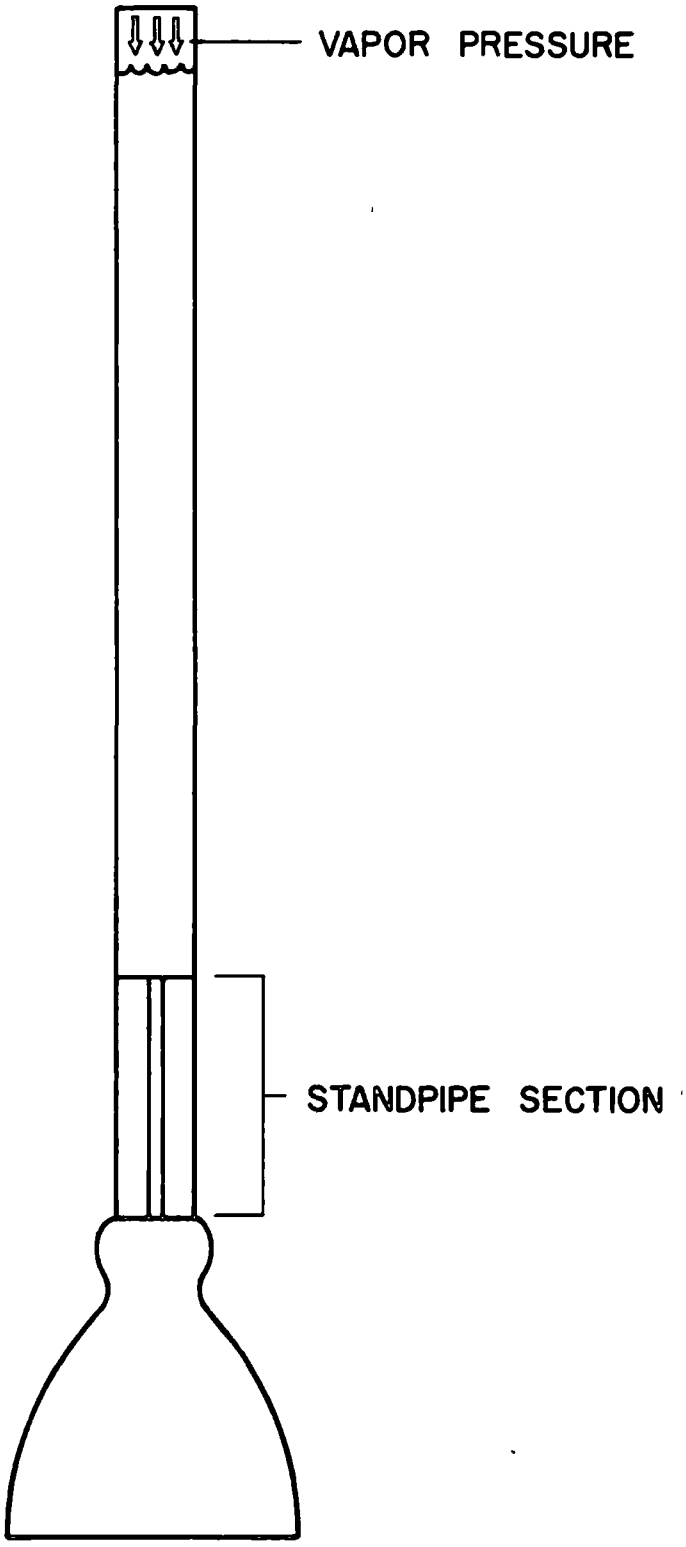

G-Fed Rocket Idealized Geometry

Figure II D-4

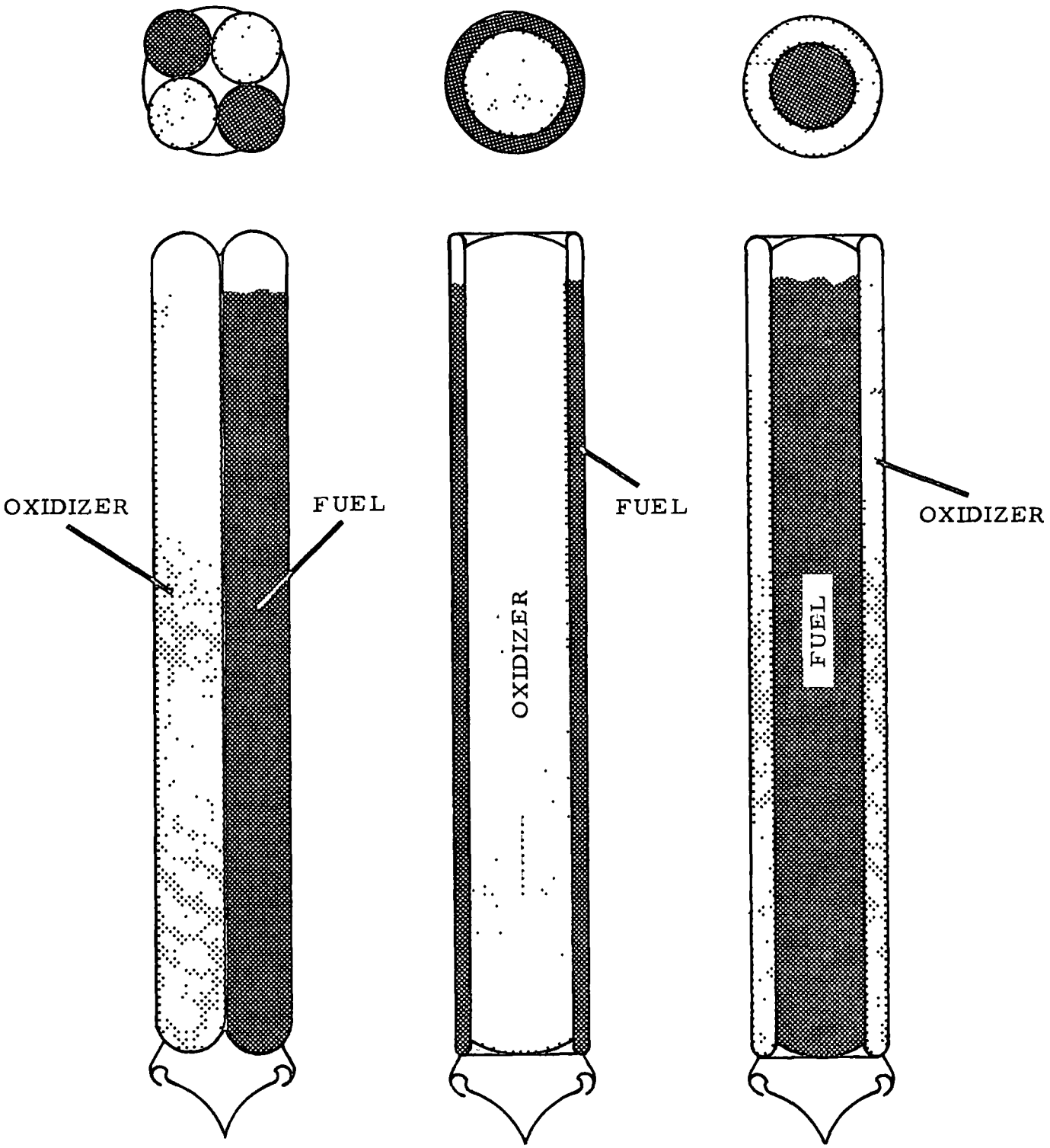

Tank Configurations

Figure II D-5

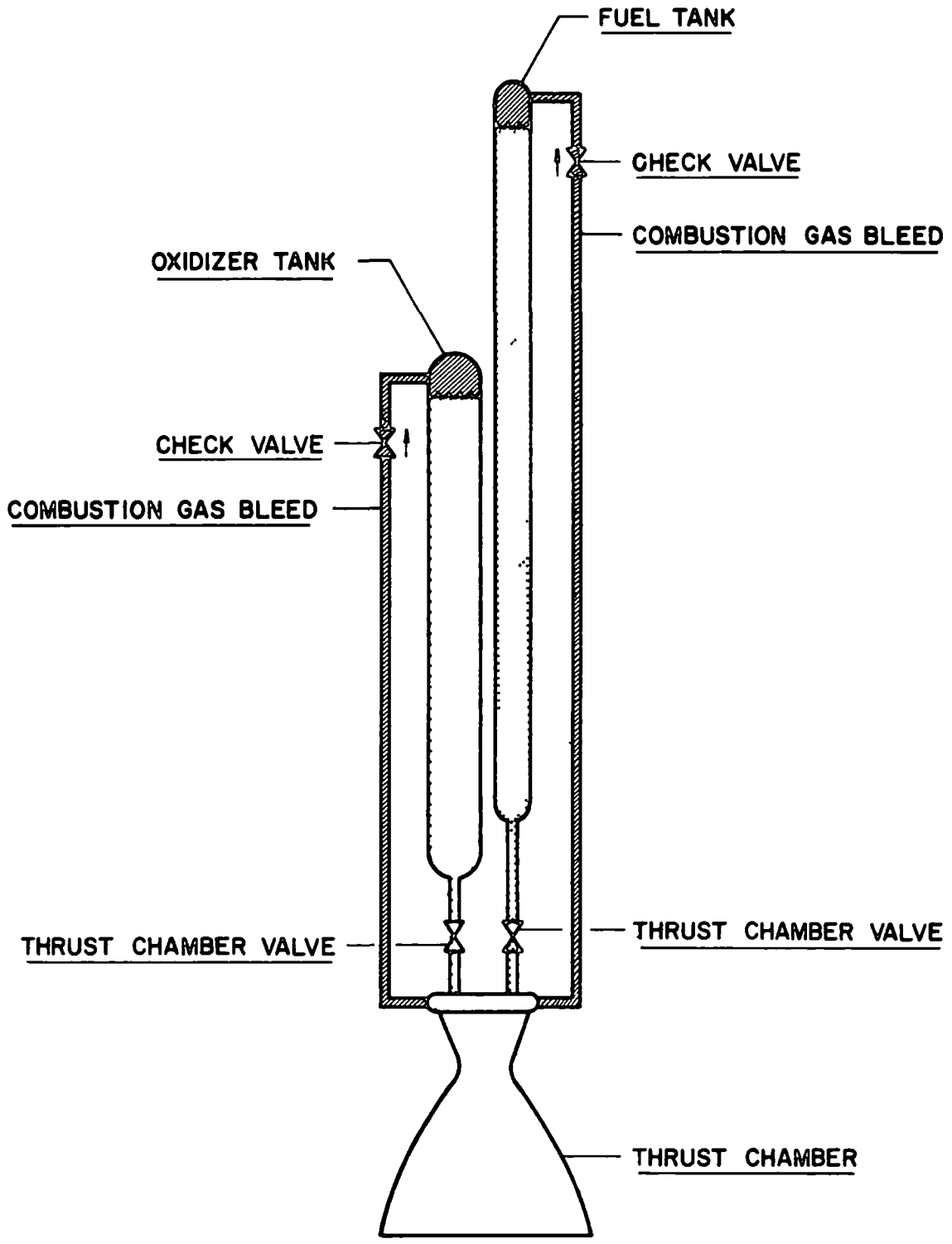

GΔP Rocket

Figure II D-6

II, Concepts Considered (cont.)

E. PUMP-FED ENGINE CYCLES

1. Introduction

An investigation was made to determine if a significant advantage can be realized through use of an engine cycle other than the conventional gas generator cycle. Emphasis was placed upon cycles offering increased reliability through system simplification, increased engine performance, or both. The latter gain becomes very significant if the performance is improved to a point where single-stage-to-orbit vehicles become practical.

The cycles investigated that seemed to offer potential simplification included the heated-H_2 cycle and the thrust-chamber-bleed cycle. In both cycles, the conventional gas generator is eliminated.

Parameter studies have indicated that chamber pressures higher than the conventional offer substantial performance increase. However, raising chamber pressure for the gas-generator cycle results in a degradation of engine specific impulse and increases the difference between engine and thrust chamber mixture ratio because of the required increase in turbine propellant flow rates. This partially offsets the gain in thrust chamber specific impulse. It is desirable to minimize the differences between engine and thrust-chamber mixture ratio because this minimizes the propellant tankage size for a given thrust-chamber mixture ratio. These effects become more significant with increasing chamber pressure. Therefore, new engine cycles were evolved for evaluation that offered the performance increase associated with increased chamber pressures without the losses incurred in the gas-generator system.

II, E, Pump-Fed Engine Cycles (cont.)

The staged-combustion cycle with two fuel-rich gas generators is a cycle in which the specific impulse and mixture ratio for the thrust chamber and engine are identical. A variation of this cycle using a fuel-rich and oxidizer-rich gas generator offers similar advantages and also provides a potential cost saving through simplified injector design. In both cycles, the pump discharge pressure, and hence the pumping system weight, increases exponentially with higher chamber pressure. This is the basic disadvantage of staged combustion cycles.

The closed third fluid cycle was then considered in an effort to find a cycle which provided increased performance without having to substantially increase pump discharge pressure above chamber pressure. This closed cycle does this, but requires a relatively complex feed system and condensing equipment, thereby introducing what could be a limiting factor in the system.

Two other types of cycles were considered. The first is a delivery feed pumping cycle. In this cycle, the work involved in pressurizing the propellants is eliminated, and if practical would raise over-all system performance. The other cycle is designated as a gas generator with afterburner, and is identical to the standard gas generator cycle, except that turbine exhaust gases are augmented with O_2 and then afterburned at thrust-chamber mixture ratio.

To facilitate proper evaluation, all cycles were classified. The source and flow of pumping system drive fluid differentiates cycles. All cycles for pump-fed engines were classified as follows:

II, E, Pump-Fed Engine Cycles (cont.)

a. Gas-Generator Cycle: Gas-generator-supplied turbine-drive fluid flows parallel to thrust chamber flow

b. Staged Combustion Cycle. Gas-generator-supplied turbine-drive fluid flows in series ("topping" flow) with thrust chamber flow

(1) Fuel-rich gas generator system

(2) Fuel-rich plus oxidizer-rich gas generators

c. Heated Hydrogen Bleed Cycle: Parallel turbine and thrust chamber flow

d. Heated Hydrogen Topping Cycle: Series or "topping" flow through turbine then thrust chamber

e. Chamber Bleed Cycle:

(1) Heat-exchanger-cooled gas

(2) Diluted gas

f. Third Fluid Turbine Drive Cycle:

(1) Open cycle

(2) Closed cycle

II, E, Pump-Fed Engine Cycles (cont.)

g. Delivery Feed Cycle:

(1) Continuous feed

(2) Intermittent feed

(3) Intermittent feed; pump-assisted

h. Gas Generator with Afterburner Cycle:

These cycles are described and technically evaluated in the following discussion.

As discussed in Section III, C, the evaluation of these cycles on the basis of payload is fully adequate. The final selection of chamber pressure will consider development difficulty and cost. These cycles were applied to a single-stage vehicle because it is with this vehicle that the best advantage of increased performance is shown.

The single-stage-to-orbit vehicle requires a reduction in thrust during flight to limit burnout accelerations. The manner in which this is achieved with the best engine cycles is discussed herein.

2. Summary of Results

Results of the integrated analysis (detailed in Section II, E, 4, below) are shown in Figure II E-1. Based upon this analysis, the best engine for a single stage O_2/H_2 orbital vehicle would use an intermittent feed-pump assisted

II, E, Pump-Fed Engine Cycles (cont.)

cycle and an altitude-compensating nozzle, and operate at 6,000-psia thrust-chamber pressure. This engine increases the single-stage vehicle payload capability 48% over a vehicle with an engine using a conventional gas-generator cycle, a De Laval nozzle, and operating at 1,000 psia thrust-chamber pressure. However, the final practical feasibility evaluation of this cycle has not been concluded. Therefore, an engine using a staged-combustion cycle, an altitude-compensating nozzle and operating at approximately 2,000 to 3,000 psi is considered a more practical choice. A vehicle with this engine will deliver 40% more payload than the conventional, 1,000 psia thrust chamber pressure, De Laval-nozzle engine.

Hence it was recommended that effort with altitude-compensating nozzles and the staged combustion cycle be continued during Task 2.

3. Engine Cycles Considered

a. Gas-Generator Cycles

(1) Description

The oxidizer- and fuel-turbopump assemblies are driven by a single bipropellant gas generator. The gas generator uses the same propellants as the thrust chamber. These propellants are tapped from the main-pump discharge lines. Propellants are injected into the generator and burned. The resultant combustion gases are proportioned to the oxidizer and fuel turbo-pump assemblies, as required, to obtain the desired engine mixture ratio. After

II, E, Pump-Fed Engine Cycles (cont.)

passing through the turbines, the gases are expanded in a nozzle to atmosphere, providing additional thrust. A schematic of the engine cycle is shown as Figure II E-2.

(2) Summary

The single bipropellant gas generator cycle is considered the standard conventional one. It is incorporated into both the first- and second-stage engines of the standard vehicle and is used as a basis for comparison with all of the other cycles considered in this study.

The major advantages of the gas generator cycle are that it gives good performance at normal thrust-chamber operating pressures and is fully developed and proved. Virtually all of the present-day, large, pump-fed rocket engines use this cycle. Therefore, much of the accumulated development experience can be applied to new, large, booster engines, which should result in a development cost savings.

The major disadvantage of the cycle is that, at high chamber pressures, which are desirable because of the increase in thrust chamber performance, engine performance degradation associated with lower gas-generator specific impulse and lower engine-mixture-ratio becomes very significant. It is mainly for this reason that other cycles were investigated.

(3) Technical Discussion

There are several undesirable characteristics associated with the gas generator cycle.

II, E, Pump-Fed Engine Cycles (cont.)

First, thrust chamber specific impulse is greater than engine specific impulse. This difference becomes larger with increasing chamber pressure. This performance degradation is not large at normal operating pressures, but at high chamber pressures becomes very significant Figures II E-28 through II E-31 show this relationship for both conventional deLaval and altitude-compensating nozzles. Using a deLaval nozzle, engine specific impulse at 1,000 psi chamber pressure is only 3 sec below thrust-chamber specific impulse, but this difference increases to 5.5 and 9.5 sec at 2,000 and 3,000 psi, respectively.

Second, mixture ratio is not equal to thrust chamber mixture ratio, and increasingly diverges with increasing chamber pressure. Figures II E-36 and II E-37 show the change in engine mixture ratio with thrust chamber pressure. The effect of this is that, for a given thrust chamber mixture ratio, the size and weight of the propellant tankage are increased. This results from the very low density of hydrogen.

Third, the gas generator requires a separate ignition system because the propellants are not hypergolic. This is a reliability consideration which cannot be overlooked when comparing cycles.

Control of the main propellant flow may be accomplished with valves located in the pump discharge lines or pump suction lines. Discharge line valves are conventional. For certain engine configurations (e.g., one with a single turbopump and multiple combustors) the use of suction line valves or a pump-integrated single discharge valve eliminates the multiple valving otherwise required. Using suction valves may present transient control problems because the turbopumps cannot be precooled or bled in. These problems are discussed in the sections pertaining to specific engine configurations and controls components.

II, E, Pump-Fed Engine Cycles (cont.)

Propellants for gas generator operation can be tapped either upstream or downstream of the main propellant (discharge) valves. Both methods are considered current technology and they are being used in the Titan I and Titan II, respectively.

Engines using the gas-generator cycle can be started in a variety of ways; therefore, starting is not considered a major problem. Starting by ground-supplied propellants, stored gas, solid cartridge, auxiliary pump-drive assembly, and propellant tank head are all considered proved current methods.

The gas-generator cycle is easily adaptable to either chamber pressure or propellant utilization control, if required. Chamber pressure can be effectively controlled by regulating the liquid flow to the gas generator (used on Titan I). A study of a 200,000-lb-thrust LO_2/LH_2 engine indicated that mixture ratio control for a propellant utilization system is feasible by using a throttling valve located in the oxidizer pump discharge line.

All cycles must be analyzed for application to engine configurations that use secondary injection for vector control. In the gas generator cycle, the turbine exhaust gas is available for hot-gas injection. No other practical hot-gas source exists which can be utilized without either greatly affecting engine steady-state operation or reducing over-all engine performance. Turbine exhaust gas is sufficient to provide the necessary control for vehicle configurations possessing nearly neutral aerodynamic stability. For unstable vehicles, additional control may be required for brief periods. This can be provided by supplementary liquid injection of hydrogen from pump discharge. Engine performance will shift during the brief period that liquid is being used, but it is anticipated that satisfactory engine operation can be sustained.

II, E, Pump-Fed Engine Cycles (cont.)

An engine cycle variation with individual gas generators for each turbopump was also investigated. For very large engines, an integrated gas generator-turbopump design is attractive for some configurations. A complete steady-state analysis was performed with this system for a 6-million-lb-thrust LO_2/LH_2 engine. The effects of vehicle flight and engine tolerances were included. Also, control systems for chamber pressure control and propellant utilization were evaluated. The report of this investigation is included as Appendix G.

A modification of the gas-generator cycle described above consists of operating the oxidizer and fuel turbopumps in series instead of in parallel (Figure II E-3). Use of flow circuit results in slightly more efficient use of the gas-generator gases, reducing the gas flow rate required. Therefore, the mixture ratio and specific impulse degradation associated with gas generator operation is reduced. After reviewing all aspects of the cycle, it was decided that, for the purpose of this study, both series- and parallel-turbines operations offer approximately the same over-all potential as engine cycles. Analysis of the parallel-turbine cycle is also applicable to the series-turbine cycle.

b. Staged-Combustion Cycles

(1) Description

The staged-combustion cycle (several variations are shown schematically in Figures II E-4, II E-5, and II E-6) consists of gas-generator-driven turbines with the turbine exhaust injected into the thrust chamber. In this cycle, oxidizer and fuel turbopump flows may be in series or parallel, as shown schematically in Figures II E-4 and II E-5.

II, E, Pump-Fed Engine Cycles (cont.)

Another version of the cycle has a fuel-rich fuel turbopump gas generator and an oxidizer-rich oxidizer turbopump gas generator. Turbine exhaust flows are injected separately into the thrust chamber giving completely gaseous main chamber injection. This cycle is illustrated schematically by Figure II E-6.

(2) Advantages and Disadvantages

These cycles offer high payloads for single-stage-to-orbit missions because they are well-suited to high-thrust-chamber-pressure applications. High chamber pressures yield the necessary exhaust velocities to achieve significant load-carrying capability with a single-stage-to-orbit vehicle. The staged-combustion cycle is well-suited to high-pressure engines because, in this cycle, engine mixture ratio equals thrust-chamber mixture ratio, which minimizes fuel tankage size, weight, and cost. Also, engine specific impulse equals thrust-chamber specific impulse, which reduces both fuel and oxidizer tankage size, weight, and cost. The performance of this cycle is shown in Figures II E-28 through II E-31. Another advantage is that no main chamber ignition is required.

The high-pressure, large-turbine exhaust flow rate provides an ample gas source to give vehicle thrust-vector control by injecting turbine exhaust into selected quadrants of the thrust-chamber skirt. This feature is important because, for a large, high-pressure engine, thrust-vector control by secondary gas injection is simpler and lighter than a vector control system which moves the thrust chamber.

II, E, Pump-Fed Engine Cycles (cont.)

The two primary versions of this cycle offer the above advantages. A cycle having separate oxidizer-rich and fuel-rich gas-generator systems has a completely gaseous main-chamber injection system, which permits a simple, inexpensive injector arrangement. However, the oxidizer-rich gas generator must operate at extremely high mixture ratios (110 for O_2-H_2) to satisfy turbine maximum allowable temperature requirements. Design of ignition systems and a reaction product mixing device for the high-mixture-ratio O_2-H_2 gas generators must be developed and demonstrated before this version of the cycle may be considered feasible.

The most important disadvantage of all staged-combustion cycles is that a relatively high pump-discharge pressure must be generated to yield a given chamber pressure, which increases pumping system cost and weight.

(3) Summary

The most promising version of this cycle has separate fuel-rich gas generators driving the oxidizer and fuel turbopumps in parallel. Thrust chamber fuel coolant flow is passed directly from pump discharge into the chamber coolant tubes, then injected into the thrust chamber.

Thrust-vector control is obtained by selectively valving turbine exhaust gas flow to one or two of the four secondary gas injection nozzles located in the lower portion of the thrust-chamber skirt. Roll-control flow requirements are also furnished by turbine exhaust. Engine mixture ratio control, propellant utilization control, and vehicle acceleration control, if required, are effected by modulating gas generator valves. Single-stage-to-orbit

II, E, Pump-Fed Engine Cycles (cont.)

payloads for vehicles with engines with this cycle and either conventional deLaval or altitude-compensating nozzles are shown in Figure II E-1. The staged-combustion cycle is compared to other engine cycles in Section II, E, 4.

(4) Technical Discussion

Because the maximum payload capability of the staged combustion cycle is given with a thrust chamber pressure in the 2,000 to 4,000 psia range, basic cycle variations with chamber pressures of approximately 2,000 psia were analyzed to select the most promising cycle variation.

Fuel-rich gas generator cycle analyses are shown schematically in Figures II E-7 through II E-10. In all cases, parallel gas generator flow through the separate oxidizer turbopump and fuel turbopump turbines is shown. Because of the relatively low pressure ratios of this cycle, turbine efficiencies for parallel turbines are high and very little improvement in turbine performance could be effected by series flow through the two turbopump turbines. Figures II E-7 and II E-8 show alternative means of ducting fuel coolant flow through the thrust-chamber-coolant jacket.

In the cycle shown as Figure II E-7, fuel passes in series through the coolant jacket, the gas generators, the turbines, then to the chamber injector. For a 3,000 psi hydrogen pump discharge pressure, chamber pressure is 1,800 psi. In the alternative cycle, Figure II E-8, approximately 10% of the fuel passes directly from pump discharge through the chamber coolant tubes, and is then injected into the chamber. The remainder of the fuel flows through the gas generators and turbines. This cycle yields 2,200 psia chamber pressure for a 3,000 psia pump discharge pressure. It is selected over the series

II, E, Pump-Fed Cycles (cont.)

coolant flow variation because, for a given chamber pressure, it requires a lighter, less-expensive pumping system. Hydrogen coolant flow, after being heated to inner coolant tube wall temperature in the coolant jacket, will have a characteristic exhaust velocity similar to the reaction products, therefore, no significant specific impulse degradation is caused by the parallel coolant flow. Figure II E-9 shows an alternative component arrangement for the parallel coolant flow cycle which features a dual, fuel turbopump instead of a single staged unit. This arrangement may have packaging or production advantages, but it offers no significant cost or payload change.

In addition to the two gas generator valves, there is a valve in the fuel-coolant-jacket line and a valve in the thrust-chamber oxidizer line. Start energy is furnished by tank head. The start sequence consists of supplying energy to the gas generator igniter, and simultaneously opening gas generator valves, then, after a timed delay, opening the thrust-chamber oxidizer valve, followed by opening the thrust-chamber fuel-coolant-flow valve. Shutdown is effected by closing the gas generator valves, followed by a scheduled closing of the thrust chamber oxidizer valve and the thrust chamber fuel-coolant valve.

II, E, Pump-Fed Engine Cycles (cont.)

The above described fuel-rich gas generator, staged-combustion engine with a De Laval thrust nozzle is compared to engines of other cycles in Section II, E, 4.

A cycle analysis for the cycle version having separate oxidizer-rich and fuel-rich gas generator systems is schematically shown in Figure II E-11. As previously explained, this version was not selected because of the required feasibility demonstration of suitable oxidizer-rich gas generator ignition and gas mixing systems. Furthermore, there is not a sufficien difference in cost or performance between these cycle variations to motivate this feasibility demonstration.

The staged-combustion cycle is also adaptable to altitude-compensating thrust devices, such as forced-deflection nozzles, which give a significant single-stage-to-orbit payload increase over noncompensating nozzles. Cycle analyses for both the fuel-rich gas generator cycle and the combined fuel-rich gas generator plus oxidizer-rich gas generator cycle are presented in Figures II E-10 and II E-12. Here again, the fuel-rich cycle was selected because of the required oxidizer-rich gas generator feasibility demonstration.

II, E, Pump-Fed Engine Cycles (cont.)

This altitude-compensating, staged-combustion engine is compared to engines of other cycles in Section II, E, 4.

c. Heated-Hydrogen Bleed Cycle

(1) Description

Engine turbopumps may be powered by heated H_2. Figures II E-13, II E-14, and II E-15 are schematics of heated-H_2 bleed-cycle variations. High-pressure LH_2 is tapped from the fuel-pump discharge, passed through the thrust chamber walls, where it picks up heat while cooling the walls, and is used to drive the engine turbines. The exhaust from the turbines is expanded through nozzles for additional thrust.

(2) Summary

The investigation of the heated-H_2 bleed cycle indicated that performance is lower than that of the standard gas-generator cycle. This system is also limited to chamber pressures below 1,000 psi, unless special complex baffled thrust chambers are used, because increasing chamber pressure reduces the effective heating area available to generate H_2. Engine mixture ratio is lower than thrust-chamber mixture ratio, and decreases rapidly with increased chamber pressures because of the increase in hydrogen flow required to supply the higher pumping energy.

II, E, Pump-Fed Engine Cycles (cont.)

The main attraction of this cycle is the system simplification resulting from elimination of the gas generator and associated controls and subsystems. However, the loss in over-all system performance overrrides the gas generator elimination. Therefore, the cycle offers no over-all advantage when compared with the gas-generator cycle.

(3) Technical Discussion

The hydrogen bleed cycle was evaluated to determine the technical feasibility and steady-state operating point. Emphasis was placed upon determining if adequate heating surface is available on the thrust chamber walls to produce sufficient high-quality hydrogen gas for turbine drive. The complete heat transfer analysis is given in Appendix A of this report. The forced-deflection nozzle contour shown in Figure II E-16 was used.

It was found that 15% of the total hydrogen flow (at 1,000°R) is needed to feed the turbines for a 2-million-lb-thrust, 1,000 P_c engine. At higher chamber pressures, the cycle is unfeasible unless baffles are incorporated into the combustion chamber and nozzle to provide additional heat transfer area. Such a design is shown in Figure II E-17.

Once the required turbine flow rates were determined, an over-all vehicle performance analysis of the cycle was made. The results are presented in Figure II E-1 and show vehicle payload in relation to chamber pressure for this cycle. It can be seen that the cycle is inferior to the gas-generator cycle at all chamber pressures.

II, E, Pump-Fed Engine Cycles (cont.)

d. Heated-H_2 Topping Cycle

(1) Description

Engine turbopumps can be driven by an H_2 topping turbine system. Figures II E-18 and II E-19 are schematics of the basic topping cycle with parallel or series turbines. Total engine hydrogen flow is used to regeneratively cool the combustion chamber. It is then expanded through the turbines to develop pump shaft horsepower. This expanded hydrogen is then ducted to the thrust chamber, where it is combusted with LO_2 to produce the required engine thrust.

(2) Summary

Major advantages in this system are the elimination of a separate gas generation system and the inherent increase in vehicle performance by making engine mixture ratio equal to chamber mixture ratio as well as engine I_s equal to chamber I_s Its major disadvantage is that it is chamber-pressure limited. This cycle was completely analyzed during a previous study of a 200,000-lb-thrust LO_2/LH_2 engine.* Although this thrust level was considerably lower than the range considered in this investigation, the technical analysis is applicable to these higher thrust levels. It was found that the cycle is limited to chamber pressures below 500 psi. Even at this pressure there was a specific impulse penalty of 4 sec as compared with a conventional engine configuration. At 200,000 lb, an estimated chamber-length increase of 50 to 80 in. (corresponding to a characteristic length of 145 to 245 in) would be required

* See Aerojet-General Report No. LR60033, 200,000-lb-thrust Hydrogen/Oxygen Rocket Engine, Vol. II, Part 2, Appendix B, March 1960

II, E, Pump-Fed Engine Cycles (cont.)

to operate the topping cycle at a chamber pressure of 600 psia with a specific impulse equal to that of the conventional gas generator design.

Topping turbine operation is limited primarily by the heat-transfer capability of the coolant jacket and the thrust-chamber plenum (at fuel-pump discharge pressures). As chamber pressure increases, the heat-transfer area decreases, therefore, characteristic chamber length would have to become greater

It is concluded that H_2 topping cycles are not feasible at chamber pressures above 500 psia. The investigation delineated in Section III, C, showed that the objectives of low cost and increased reliability are achieved through the use of orbital booster vehicles having high-performance engines. Because high-performance is obtained mainly from increased engine chamber pressure, the H_2 topping cycle was eliminated from further consideration.

e. Chamber Bleed Cycles

(1) Description

Gas bled from the main combustion chamber may be used to drive the engine turbopumps. Figures II E-20 and II E-21 are schematics of two methods for utilizing chamber gas to drive turbines.

The first method is by bleeding gas from the chamber at a mixture ratio of 6.0:1 and cooling this gas in an H_2 heat exchanger to a temperature acceptable at the turbines. The gas discharged from the turbines would be further expanded through nozzles to obtain additional thrust.

II, E, Pump-Fed Engine Cycles (cont.)

The second method is to bleed gas from the main chamber at a mixture ratio of 6.0:1 and add sufficient H_2 to reduce the turbine inlet temperature by dropping the mixture ratio to 1.0:1.

(2) Summary

The chamber bleed cycles offered no significant advantage over the conventional cycle, therefore, no further comparison with the other cycles was made.

The cooled-gas version of this cycle was studied at 1,000 psia chamber pressure. Turbine flow was ten times that required for the standard cycle because of the low specific impulse of the cooled combustion gases. As chamber pressure increases, this condition degenerates further. Because this cycle was unfeasible at 1,000-psia chamber pressure, no further calculations were made.

The diluted chamber bleed cycle has the same relative performance as the gas generator cycle (Section II, E, 3, a).

(3) Technical Discussion

(a) Cooled-Gas Cycle

The chamber bleed cycle using cooled gas at chamber mixture ratio has two advantages over the standard gas generator cycle. It eliminates the gas generator, and engine mixture ratio is equal to thrust chamber mixture ratio. Major disadvantages, however, include engine I_s not equal

II, E, Pump-Fed Engine Cycles (cont.)

to chamber I_s (I_s of the turbine exhaust is only 160 sec) and the required weight flow bled from the chamber is 1,200 lb/sec. (A standard gas generator cycle for a chamber pressure of 1,000 psia requires 123 lb/sec.) A heat exchanger to cool the chamber gas is not feasible.

After a comparative analysis, it was concluded that the chamber bleed cycle with cooled chamber gas as a turbine drive fluid offers no significant advantages over the standard gas generator cycle. It was therefore eliminated from further study.

(b) Diluted-Gas Cycles

The chamber bleed cycle, with H_2 used to dilute chamber gas at a mixture ratio of 6.0:1 to a mixture ratio of 1.0.1, has no basic advantages over the standard gas generator cycle. In essence, the bleed port coupled with the diluent system forms a gas generator. Figure II E-22 shows a method for obtaining H_2 coolant directly from the cooling jacket The bleed ports are between each tube of the chamber wall, and orifices located at these ports provide the proper mixture ratio. A separate ignition system is not required, because the gas is in an ignited state. The major disadvantage with this cycle is the design of the tap-off system, which will be susceptible to burn-out. Also, chamber I_s and mixture ratio are not equal to engine I_s and mixture ratio. The technical analysis of this cycle is the same as that of the gas generator cycle. No additional study was warranted because there is no significant advantage over the standard cycle.

II, E, Pump-Fed Engine Cycles (cont.)

f. Third-Fluid Turbine-Drive Cycles

(1) Open Cycle

(a) Description

Gas for turbine operation is obtained from a third fluid (i.e., not one of the main propellants). This fluid is stored in liquid form in a separate container, converted to the gaseous phase, and passed through the turbine at high pressure to provide the turbine power source. After passing through the turbines, the gas is exhausted through a nozzle to atmosphere, providing addition engine thrust.

A representative third-fluid open-cycle system is shown schematically in Figure II E-23.

(b) Summary

Third-fluid open cycles appear to offer no advantage over the conventional gas generator cycle. The turbine exhaust performance obtainable with practical third fluids is considerably less than that of the conventional cycle, resulting in reduced over-all engine performance. Addition of the third-fluid system causes an increase in weight and complexity over the conventional system.

A questionable advantage of these systems is the isolation of the pump-drive system from the main propellant system. Also, by using an inert third fluid (i.e., water, nitrogen, or helium) base-recirculation adverse effects and fire danger in the engine compartment can be

II, E, Pump-Fed Engine Cycles (cont.)

minimized. However, it seems doubtful that these considerations alone would dictate the choice of this engine cycle. For these reasons, third-fluid open cycles were eliminated from further study.

(c) Technical Discussion

Third-fluid open cycles can be grouped into two categories; reactant fluid systems and inert fluid systems. Representative systems in each category include the following:

1. Reactant Fluid Systems
   - a. Hydrazine monopropellant gas generator
   - b. Hydrogen peroxide monopropellant gas generator
   - c. Thrust chamber gases diluted with water
   - d. Bipropellant gas generator using propellants other than the main propellants.
2. Inert Fluid Systems
   - a. Steam, generated by heating water in the thrust chamber assembly

II, E, Pump-Fed Engine Cycles (cont.)

b Heated nitrogen

c Heated helium

d Heated hydrogen

One of the main interests in pursuing engine cycles other than the conventional gas generator cycle is to increase over-all engine performance by eliminating the lower-performing turbine exhaust gas, or by using an exhaust gas equal in performance to that of the thrust chamber. Per pound of fluid flow, the energy of any turbine drive fluid is proportional to the spouting velocity ($E = mv$). From the expressions for spouting velocity and specific heat, it is found that the spouting velocity of any fluid is roughly proportional to the square root of the gas temperature divided by its molecular weight, i.e., $V = f(\sqrt{\frac{T}{mw}})$. The maximum gas temperature is dictated by the turbine design and is roughly constant for all fluids. Therefore, the molecular weight of any candidate fluid must be less than that of the H_2/O_2 exhaust of the standard gas generator cycle ($mw = 4.0$ at M.R. = 1) if it is to have higher performance capability.

On the basis of performance, all reactant fluid systems are eliminated because of the relatively high molecular weights of the fluids. These systems were examined for other potential advantages, such as system simplification, but none were found to make any one system attractive.

The inert fluid systems are similar in nature to the H_2 bleed cycle, in that they are heated by the walls of the thrust chamber. The inert fluid of lowest molecular weight is most desirable for the reasons discussed above. Helium has the lowest molecular weight of all inert fluids.

II, E, Pump-Fed Engine Cycles (cont.)

However, its molecular weight is twice that of H_2. Therefore, the performance degradation for an engine using heated helium, or any other inert fluid, for turbine drive is greater than for the H_2 cycle previously discussed.

It was concluded that third-fluid open cycles offer no significant advantages over the standard gas generator cycle, therefore, no further evaluation of these cycles was performed.

(2) Closed Cycle

(a) Description

Gas for turbine operation is obtained from a third fluid, which recirculates through a closed loop. The cycle evaluated has water as the third fluid and operates as a conventional steam-turbine cycle. This water is raised to high pressure by an auxiliary pump, geared from the main oxidizer pump. High-pressure fluid is then passed through the thrust-chamber regenerative-coolant tubes to provide cooling for the chamber while raising the fluid to a superheated state. The resulting high-pressure, high-temperature steam is then expanded through the main turbines to low pressure, providing the pumping energy to the main propellants. Turbine exhaust gas is passed through a condenser and integrated into the fuel discharge line, where it condenses the steam to a liquid for pumping purposes.

(b) Summary

The primary advantage of the third-fluid closed cycle is that high engine performance and mixture ratio can be achieved without incurring the disadvantage of relatively high pump discharge pressures,

II, E, Pump-Fed Engine Cycles (cont.)

along with the associated turbopump weight increase of the staged-combustion cycle. Engine specific impulse is near the theoretical maximum and engine mixture ratio equals thrust chamber mixture ratio.

This cycle, however, requires auxiliary equipment not needed in the other cycles. The weight of this equipment and the associated increased complexity have degrading effects upon over-all vehicle performance and reliability.

Investigation disclosed that the cycle may not be practical because of severe design integration problems associated with the boiler and condenser. However, cycle performance is sufficiently high so that it was compared with other cycles to determine if further design analysis need be made (Section II, E, 4).

(c) Technical Discussion

1 Turbine Working Fluid

An evaluation of various third fluids for turbine operation was made. Its purpose was to determine the suitability of various fluids with respect to a turbine drive fluid and compatibility with the closed cycle operations. The following properties were examined for various fluids:

a Molecular Weight

A low molecular weight is desired because it results in high spouting velocities.

II, E, Pump-Fed Engine Cycles (cont.)

b Heat of Vaporization

Low heat of vaporization reduces the condenser size.

c Freezing and Boiling Points

A low freezing point and high boiling point minimize freezing problems in the condenser.

No fluid was found to possess all of the desired characteristics. Water was selected as being the most practical of the fluids evaluated. It may be possible that other fluids not considered would prove better. However, the relative merits of this cycle can be compared using water.

2 Flow-Cycle Analysis

A thermodynamic balance of the cycle was computed for an engine operating at 1,000 psi chamber pressure. The third fluid is stored in the liquid state at 20 psi. Its pressure is raised to 1,000 psi by an auxiliary pump operating off the main oxidizer turbopump. The fluid at this pressure passes through the thrust chamber coolant tubes and injector baffles, providing the required chamber cooling, and is raised to a superheated condition (1,960°R). Thrust-chamber tubes are ceramic-coated to allow for higher wall temperatures, lowering the required fluid velocity and associated pressure drop. The superheated steam is expanded through the main turbines (in series) at a total pressure ratio of 50:1, removing a great portion of the available energy at 60% efficiency. Exhaust conditions are 20 psi and 950°F. Heat of vaporization is removed at constant pressure in the condenser, returning the fluid to the liquid state. Final temperature of the liquid is dependent upon the condenser design.

II, E, Pump-Fed Engine Cycles (cont.)

3 Performance

Because there is no overboard discharge of turbine exhaust in this cycle, thrust-chamber specific impulse is equal to engine specific impulse. However, the energy exchanges in the boiler, condenser, and turbine result in a degradation from the maximum theoretical thrust chamber specific impulse (assuming no pumping losses). This degradation over a range of operating chamber pressures is shown in Figures II E-28 and II E-30. The cycle is limited to some maximum chamber pressure because the heat transfer area of the thrust chamber (boiler) decreases as the area of the thrust chamber pressure increases, whereas the requirement for heat exchange increases. However, sufficient area appears to be available within the pressure range considered, providing baffles are used in the nozzle area.

Higher chamber pressure requires higher pumping energy. To supply this energy, the third-fluid flow rate increases, thus increasing the required heat-injection rate in the condenser. This results in increased condenser weight, size, and main propellant pressure drop. It has an over-all degrading effect upon system performance.

Engine mixture ratio is equal to thrust chamber mixture ratio, which minimizes propellant tankage weight and increases payload capability.

4 Auxiliary Equipment Required

As chamber pressure increases, the size and weight of the auxiliary pumping system and condenser increase. These effects

II, E, Pump-Fed Engine Cycles (cont.)

were computed and are shown in Figure II E-25. Note that the condenser weight is large and rises rapidly with chamber pressure. It is mainly this weight that degrades the engine cycle as regards over-all vehicle performance. Also note in Figure II E-1 that maximum payload occurs at 3, 500 to 4, 000 psi. At higher chamber pressures, the high system weight has a greater degrading effect than the increased performance inherent with higher chamber pressures.

g. Delivery-Feed Cycles

(1) Continuous-Delivery Feed Cycle

(a) Description

In the continuous-delivery feed cycle (Figure II E-26), propellants are conveyed to the thrust chamber at tank pressure via a positive displacement delivery pump. The propellant is transferred from the pump into the chamber by gravity. Chamber pressure (which is considerably higher than tank pressure) is generated by reaction of the propellants. An auxiliary drive, typically a gas-generator-driven turbine, is used to power the delivery pump, which is restricted to delivery only and requires no energy for pressurization. Reaction products conveyed from the thrust chamber in the feed mechanism are vented overboard.

(b) Summary

The chief advantage offered by this cycle is that high thrust-chamber pressure may be attained without applying the work of pressurization to the propellants. However, this cycle has several disadvantages

II, E, Pump-Fed Engine Cycles (cont.)

that elminate it from serious consideration as a practical power plant. The most pronounced drawback is that thrust-chamber pressure is higher than propellant-feed pressure, which means that reaction products will leak back into the feed system, creating a hazardous condition.

This cycle has further disadvantages in that it provides no energy for propellant mixing and performance is degraded because the delivery-feed mechanism conveys a volume of reaction products from the chamber that is equal to the volume of liquid propellant delivered.

h. Intermittent-Delivery Feed Cycle

(1) Description

The intermittent-delivery feed cycle is characterized by periodic operation and is somewhat analogous to the pulse-jet principle. Propellant feed to the thrust chamber is periodic and the chamber pressure oscillates from extremely high pressures (20, 000 to 40, 000 psia) to low pressures (500 to 5, 000 psia). The sequence of operation follows:

(a) Propellant is delivered to the chamber at low pressure

(b) A check valve in the feed line is closed, preventing reverse flow

(c) The propellant mixes and explodes, providing high pressure.

(d) Chamber pressure then drops because of the gases expanding through the nozzle.

II, E, Pump-Fed Engine Cycles (cont.)

The cycle is then repeated.

Two versions of this system have been considered. The first, without a pump, feeds the chamber with propellant pressurized by tank head and tank pressurization. The second version uses a pump assist and appears to be the more practical, as will be shown.

The pump-assist cycle is visualized as having two or more thrust chambers fed from a single pumping system. Propellant flow is diverted from one chamber to the other, thus keeping pump flow rate approximately uniform while thrust-chamber flow rate is intermittent. Injection is accomplished in each chamber while at low pressure, allowing use of a low-pressure pump. (Low pressure refers to chamber pressures of 500 to 5,000 psia.) Average chamber pressure over one complete cycle is considerably above the injection chamber pressure and may be between 2,000 and 10,000 psia, depending upon system design. The combustion chamber for this cycle must be designed for extremely high pressures and consequently becomes a heavy component. For example, this cycle might have an average chamber pressure of 4,000 psia with a minimum pressure during injection of 1,000 psia and a maximum pressure of 24,000 psia. All system components operate at the low pressure except the combustion chamber, injector, and check valves. The check valves are located near the injector to prevent peak pressure from being transmitted up the propellant lines. This cycle, operating with a mean chamber pressure of 4,000 to 6,000 psia, appears to offer greater I_s and payload increases than any other cycle considered.

II, E, Pump-Fed Engine Cycles (cont.)

(2) Summary

(a) Advantages

The basic advantage of this system is low engine weight for high effective chamber pressure. In a single-stage-to-orbit mission, this engine offers I_s and payload increases greater than the other systems considered (Figure II E-1 and II E-28 through II E-31).

(b) Disadvantages

Disadvantages of this system stem primarily from design and development problems. System components must accomplish intermittent propellant feed to the combustion chamber at high frequencies while maintaining proper mixture ratio. The injection period must be synchronized to occur when the oscillating chamber pressure is at a minimum. Injection and mixing of propellants will require special hardware and new concepts. A check valve allows lines and pumps to be designed for low pressure by limiting the high-pressure peak to the combustion chamber. This valve must be large and capable of operation in the high frequency range.

(c) Recommendations and Conclusions

Preliminary analysis of the intermittent feed cycle shows potential high performance. Realization of this potential is largely dependent upon new component concepts and development. Because of the apparent advantages of this system, further and more detailed analysis is recommended.

1. Gas Generator With Afterburner Cycle

(1) Description

This cycle is identical to the conventional gas generator cycle, except that the turbine exhaust gases are augmented with oxidizer to the extent that turbine-exhaust mixture ratio is equal to thrust-chamber mixture ratio. After mixing and further combustion is accomplished, the combustion gases are expanded through a nozzle to atmosphere, thereby providing a portion of the engine thrust.

II, E, Pump-Fed Engine Cycles (cont.)

(2) Summary

The gas generator afterburner cycle was conceived as a cycle thought to potentially offer the advantages of having engine mixture ratio equal to thrust chamber mixture ratio, as well as engine specific impulse competitive with other high-performance cycles, while still maintaining the conventional gas-generator-type cycle. Technical analysis showed, however, that the engine performance is not superior to the gas generator cycle in the pressure range of 1,000 to 3,000 psi. The advantages of the improved engine mixture ratio alone did not compensate for the low performance and the auxiliary engine required to afterburn the exhaust gases. Therefore, this cycle was eliminated from further study.

(3) Technical Discussion

The performance of the afterburner cycle was compared to the gas generator cycles at chamber pressures of 1,000 and 3,000 psi for two-stage and single-stage-to-orbit missions. Most practical application for this cycle was considered to be in a forced-deflection altitude-compensating engine. The augmented turbine exhaust would be expanded over a plug nozzle located in the center of the forced-deflection nozzle, just below the turbopump assembly. Ambient air is then present between the gas flow streams of both engines, providing altitude compensation.

Analysis showed that the augmented turbine exhaust flow was approximately 10% of the thrust-chamber flow. Assuming a pressure ratio of 10 across the turbines, the chamber pressure of the gas generator is approximately 10% of the thrust-chamber pressure. Therefore, the required throat area of the afterburner engine is about the same as that of the main engine ($A_t = \frac{(I_s)(w)}{(C_f)(P_c)}$). To physically locate the afterburner engine within the main engine,

II, E, Pump-Fed Engine Cycle (cont.)

the obtainable area ratio of the former is seriously limited. It was decided to first determine the performance aspects of the cycle, over a range of afterburner engine area ratios, and, if the results were favorable, to investigate practical design limitations.

A description of the engine configurations selected for comparison follows:

CHARACTERISTIC	STANDARD CYCLE		ENGINE WITH AFTERBURNER	
	1,000 P_c	3,000 P_c	1,000 P_c	3,000 P_c
Main Thrust Nozzle				
Altitude-compensating	Yes	Yes	Yes	Yes
Maximum area ratio	40	300	40	300
Mixture ratio	6.0	6.0	6.0	6.0
Gas Generator				
Mixture ratio	1.0	1.0	1.0	1.0
Turbine Exhaust Nozzle				
Altitude-compensating	No	No	Yes	Yes
Maximum area ratio	3	(see note)	5 to 20	40
Chamber pressure, psia	100	300	100	300
Mixture ratio	1.0	1.0	6.0	6.0

Note: Area ratios selected at max. effective C_f

II, E, Pump-Fed Engine Cycle (cont.)

The cycles were compared on the basis of engine effective specific impulse. Effective specific impulse is defined as follows:

Two-stage missions. $I_{s(eff)} = 0.7 I_{s(vac)} + 0.3 I_{s(sl)}$

Single-stage missions. $I_{s(eff)} = 0.9 I_{s(vac)} + 0.1 I_{s(sl)}$

Engine effective specific impulse is then calculated.

$$I_{s\ ENG} = \frac{I_{s\ TC(eff)} \dot{w}_{TC} + I_{s\ Te(eff)} \dot{w}_{Te}}{\dot{w}_{TC} + \dot{w}_{Te}}$$

The results of the comparison made for 1,000 psi chamber pressure are given in Figure II E-27. Turbine exhaust area ratios from 5 to 20 were included. It is seen that the engine specific impulse of the afterburner cycle is lower than that of the standard cycle up to a turbine exhaust area ratio of approximately 20·1 for both two-stage and single-stage missions.

A single point check was then made for an engine of 3,000-psi chamber pressure for single-stage-to-orbit missions to ascertain if the relative performance improved. A turbine exhaust area ratio (maximum) of 40 was assumed. Engine specific impulse for the afterburner cycle was 443.0, compared to 442.5 for the standard cycle.

Engine mixture ratios were computed for the standard cycle to compare with that of the afterburner cycle, which remained fixed at 6.0:1. The engine mixture ratios for 1,000- and 3,000-psi chamber pressure engines were 5.6:1 and 5.34:1, respectively.

II, E, Pump-Fed Engine Cycles (cont.)

It was concluded that the more favorable engine mixture ratio was the only advantage of this cycle. Because a second engine (in effect) would be required, and the over-all engine cycle performance is generally below that for the standard cycle, this one advantage does not offer a significant improvement over the standard cycle. Therefore, evaluation of the afterburner cycle was discontinued.

4. Comparative Evaluation

a. Discussion

This investigation was made to determine the best engine cycle and thrust chamber pressure for a 2-million-lb-thrust O_2/H_2 engine. A single-stage vehicle (300-nm circular earth orbit mission) was assumed in this analysis, but the relative comparison results are equally applicable to the booster of a two-stage vehicle. Both deLaval and altitude-compensating nozzles were considered.

The final selection of an engine cycle and optimum thrust-chamber pressure is based upon vehicle performance as measured by payload, cost-per-pound of payload, and reliability. As discussed in Section III, C, increases in inherent specific impulse and decreases in vehicle inert part weights are the major contributors to lower cost and higher reliability. These two factors vary significantly between various engine cycles. The combined effect of these variations can be measured by vehicle payload. Therefore, payload was selected as the basis for evaluating engine cycles and chamber pressures.

The engine cycles included in the comparative analysis were the gas generator, staged-combustion, heated-H_2-bleed, third-fluid

II, E, Pump-Fed Engine Cycles (cont.)

turbine-drive, and intermittent-delivery feed, pump-assisted. These cycles, described in the preceding section, were selected as the most promising of all considered. Cycles offering no apparent improvement over the standard gas generator cycle were not included.

The major effect tending to increase performance for all engine cycles is increased thrust chamber specific impulse resulting from increased chamber pressure. Higher chamber pressures increase the allowable nozzle area ratio that can be contained within a given vehicle diameter, which is the major contributor to the increased specific impulse.

The general effects tending to decrease performance with increasing thrust-chamber pressure were discussed in the technical discussions of the various cycles. A quantitative analysis of the integrated performance characteristics is given in the following section.

b. Analysis

The effects of increasing chamber pressure upon engine specific impulse, engine mixture ratio, and vehicle inert weight were determined for each cycle. Using both deLaval and compensating nozzles, it was found that nozzle type does not significantly affect the relative merits of an engine cycle. Therefore, the heated-H_2-bleed and third-fluid cycles were not compared for altitude-compensating nozzles. The results were then integrated with a trajectory analysis to make the final selection. Each of these factors is discussed in the following paragraphs.

II, E, Pump-Fed Engine Cycles (cont.)

(1) Specific Impulse

The variation of thrust-chamber specific impulse with chamber pressure is shown in Figures II E-28 through II E-31 for a thrust chamber mixture ratio of 6:1. Shifting equilibrium flow in the nozzle and values of λ (nozzle efficiency) and η_c (combustion efficiency) of 0.97 and 0.98, respectively, were assumed. For the deLaval nozzle, the variation of area ratio with thrust chamber pressure was determined so that the ratio of the atmospheric pressure to the engine exit pressure is equal to 4:1 at sea level. This was done to provide a maximum-area-ratio nozzle that would not allow exhaust gas separation at sea-level. The single-stage O_2/H_2 vehicle diameter was determined to be approximately 28 ft for a tank L/D of 4. This vehicle diameter was used to determine the engine exit area for an altitude-compensating nozzle operating at a thrust chamber pressure of 1,000 psia. This engine exit diameter was then used to determine the area ratios at other chamber pressures for an altitude-compensating nozzle. The variation of area ratio with thrust-chamber pressure for the deLaval and altitude-compensating nozzles used in this analysis is shown in Figure II E-32. This variation of area ratio with thrust-chamber pressure was used to establish the thrust chamber specific impulse values shown in Figures II E-28 through II E-31.

The method used to determine the variation of engine specific impulse with thrust-chamber pressure for the various engine cycles is given in the following paragraphs.

Performance of any rocket engine is directly dependent upon the particular cycle used to provide pumping energy. This loss of performance was analyzed for the cycles considered and is summarized in Table II E-1.

II, E, Pump-Fed Engine Cycles (cont.)

The following analysis was used to determine the amount of pumping energy required, based on I_s.

Specific impulse if defined as,

$$I_s = \frac{\lambda Ve}{g}$$

where, λ = Nozzle divergence coefficient
Ve = Exit velocity of the nozzle
g = Acceleration of gravity

The velocity of the combustion products is assumed uniformly distributed and the Bernoulli equation applied, yielding

$$Ve = \sqrt{2g\ J\ \Delta H}$$

Where. J = Conversion factor = 778 $\frac{\text{ft lb}}{\text{Btu}}$

ΔH = Hx - Hc

Hx = Enthalpy of exit products

Hc = Enthalpy of the products in the combustion chamber

Because the nozzle does not have an infinite pressure ratio, all the available energy is not turned into useful work. The isentropic cycle efficiency designates the amount of available energy used.

Isentropic efficiency, η,

$$= \frac{Hx - Hc}{Hae} = 1 - \left(\frac{Px}{Pc}\right)^{\frac{K-1}{K}}$$

II, E, Pump-Fed Engine Cycles (cont.)

Where: P_x = Exit pressure
P_c = Chamber pressure
K = Ratio of specific heats
H_{ae} = Available energy

Therefore,

$$\Delta H = \eta H_{ae}$$

$$\text{and } I_s = \lambda \sqrt{\frac{2 J \eta H_{ae}}{g}}$$

The first derivative

$$d I_s = \frac{\lambda}{2} \sqrt{\frac{2 J \eta}{g}} \left(\frac{dH}{\sqrt{H_{ae}}} \right)$$

Substituting $\frac{\Delta H}{\eta} = H_{ae}$

Then $$d I_s = \frac{\lambda}{2} \sqrt{\frac{2 J \eta^2}{g}} \left(\frac{dH}{\Delta H^{1/2}} \right)$$

This relationship gives the reduction in specific impulse ($d I_s$) resulting from the loss of energy (dH) used for pumping.

The primary difference between different cycle pumping energy requirements is the pump discharge pressure necessary to produce the required chamber pressure. This pressure, for the various cycles, is summarized in Figure II E-33.

II, E, Pump-Fed Engine Cycles (cont.)

(a) Staged Combustion

Because the removal of pumping energy from the chamber propellants is accomplished prior to injection, the degradation ($d I_s$) must be applied. The amount of pumping energy (dH) is determined from the discharge pressure requirement, shown in Figure II E-33 and shaft horsepower input. The resulting I_s degradations are shown in Table II E-1.

(b) Third Fluid

This cycle, operating on a slightly lower discharge pressure, has a smaller pumping energy (dH) requirement than the staged combustion. Results are shown in the comparison graphs and table.

(c) Gas Generator

The energy for pumping in this cycle is from a source other than the main chamber. Engine specific impulse is less than thrust chamber specific impulse because of the low-performance turbine exhaust. The exhaust nozzle pressure is determined on a pressure ratio of 10:1 across the turbine. Derivation of the resulting engine performance is accomplished from:

$$I_{s_{ENG}} = \frac{\text{Total Thrust}}{\text{Total Flow Rate}} = \frac{F_{TC} + F_{Te}}{\dot{w}_{TC} + \dot{w}_{Te}}$$

$$\text{or} \quad I_{s_{ENG}} = \frac{F_{TC}}{\dot{w}_{TC} + \dot{w}_{Te}} + \frac{F_{Te}}{\dot{w}_{TC} + \dot{w}_{Te}}$$

II, E, Pump-Fed Engine Cycles (cont.)

$$\text{and} \quad I_{s_{Te}} = \frac{F_{Te}}{\dot{w}_{Te}} \qquad \text{and} \quad I_{s_{TC}} = \frac{F_{TC}}{\dot{w}_{TC}}$$

$$\text{then} \quad I_{s_{Eng}} = \frac{\dot{w}_{TC} I_{s_{TC}}}{\dot{w}_{TC} + \dot{w}_{Te}} + \frac{\dot{w}_{Te} I_{s_{Te}}}{\dot{w}_{TC} + \dot{w}_{Te}}$$

Because $I_{s_{Te}} < I_{s_{TC}}$, the $I_{s_{Eng}}$ is reduced from the thrust chamber specific impulse. The resulting I_s degration is shown in Table II E-3.

(d) Delivery Feed Cycle (Intermittent-Pump Assisted)

Engine performance loss (dI_s) for this cycle is the same as that for the gas generator cycle because turbine-drive gas is expanded at low performance through the turbine exhaust nozzles. Resultant losses are less because of the low discharge pressure required to accomplish the mean chamber pressure.

(e) Heated-H_2 Topping Cycle

The pumping energy (dH) for this cycle is obtained from the heat transfer to the chamber coolant and results in a I_s degradation (dI_s). A further loss results from the expansion of this gas as turbine exhaust.

(2) Engine Effects

The variation of engine weight used in this analysis is shown in Figures II E-34 and II E-35. These engine weights include the variation of turbopump weight and thrust-chamber assembly weight with thrust-chamber

II, E, Pump-Fed Engine Cycles (cont.)

pressure. The engine weights shown in Figures II E-34 and II E-35 are according to preliminary weight estimates. Further investigation has shown that the deLaval engine weights should be 1,400 lb heavier and the forced-deflection engine weights (altitude-compensating nozzle) should be 1,600 lb lighter. This difference in engine weight was not accounted for in Figure II E-1, but would make altitude compensating nozzles even more desirable on a payload basis.

As the thrust chamber pressure increases, the required pump discharge pressure also increases, causing the turbopump to become heavier. Also, because of the increase in turbine-flow requirements with thrust-chamber pressure, the engine mixture ratio decreases for the gas generator, heated-H_2 bleed, and intermittent-feed engine cycles. These effects are shown in Figures II E-36 and II E-37. Also this causes the engine weight and turbine flow to change with mixture ratio. The effect was included in the analysis by assuming that the weight and turbine flow of each individual turbopump is proportional to the pump flow rate at a given chamber pressure. The turbopump weights and operating parameters for the various engine cycles are discussed in Section II, K.

Values of engine weight are shown for two different frequencies for the intermittent-feed cycle. A frequency of 100 cps was used in the analysis. If a frequency of 50 cps for this cycle appears to be more feasible, then a payload loss corresponding to the engine weight differences between the two frequencies would result.

(3) Airframe Effects

A propellant-tank weight-to-volume ratio of 0.623 lb/ft^3 was determined from a layout of propellant tankage for a 2-million-lb-thrust

II, E, Pump-Fed Engine Cycles (cont.)

single-stage O_2/H_2 vehicle with a tank L/D of 4. This tank weight-to-volume ratio was used to determine the variation of vehicle airframe weight with propellant consumption and engine mixture ratio. The same value was assumed for both the fuel and oxidizer tanks. Therefore, the vehicle airframe weights increase with decreasing engine mixture ratio because of the decrease in propellant bulk density.

(4) Trajectory Effects

The combined effect of the engine parameters discussed above upon vehicle performance was established through trajectory calculations performed with the IBM-7090 computer for each of the engine cycles discussed above.

The trajectory assumptions used in this evaluation are the same as discussed in Section III, B, of this volume.

During the ascent to orbit, the engine was assumed to be throttled back approximately two-thirds. The vacuum thrust then changes from approximately 2,400,000 lb to 800,000 lb. Time of throttle-back was adjusted for minimum required ideal velocity to orbit. For all cases, this time occurred at approximately 25,000 ft/sec ideal velocity. Throttle-back at this point in the trajectory limits the maximum g's-to-orbit to 5 or less.

In evaluating the 300-nm orbit payload for all the vehicles, an initial thrust-to-weight ratio of 1.25:1 was assumed. An analysis to determine the effect of initial thrust-to-lightoff weight upon the performance comparison was conducted. In this analysis, the maximum g's throughout flight were limited to 6. This analysis showed that some increase in payload (approximately 2-1/2%) could be achieved by launching at a thrust-to-weight ratio of

II, E, Pump-Fed Engine Cycles (cont.)

approximately 1.4:1. Higher thrust-to-weight ratios resulted in a decrease in vehicle payload capability. This analysis also showed that the initial thrust-to-weight ratio assumption does not affect the relative results of this high thrust chamber pressure and engine cycle evaluation because the payloads for all systems shown in Figure II E-1 would be raised approximately 2-1/2%. Boeing Report No. D2-12072 (see Volume 5, this report) also substantiates that an initial thrust to weight ratio of approximately 1.4 1 would probably be best for a single-stage-to-orbit vehicle.

c. Results

Integrated results of this study are shown in Figure II E-1, which shows the 300 nm-orbit payload capability of a single-stage O_2/H_2 vehicle as a function of thrust-chamber pressure for deLaval and altitude-compensating nozzles and various engine cycles. The best operating thrust-chamber pressures established in Figure II E-1 for the various engine cycles are tabulated as follows

Engine Cycle	Thrust Chamber Pressure (psia)
Gas generator	2,500
Heated-H_2 bleed	2,000
Third-fluid	3,500
Stage-combustion	3,000
Intermittent-pump-assisted	6,000

Figure II E-1 also shows that the nozzle type does not appreciably affect the best operating thrust chamber pressure.

II, E, Pump-Fed Engine Cycles (cont.)

Comparing the nozzles and cycles at the best thrust chamber pressure tabulated, it is seen that a payload increase of approximately 18% can be attained over the deLaval-nozzle, conventional-gas-generator-cycle engine by using an altitude-compensating, conventional-gas-generator-cycle engine. A further payload increase of approximately 8% can be achieved with an altitude-compensating stage-combustion engine. The single-stage payload capability can be increased still another 5% if an altitude-compensating, intermittent-feed cycle proves to be feasible.

Based on the results shown in Figure II E-1, it is concluded that significant payload increases can be attained with an altitude-compensating nozzle. Also, the potentially best engine cycle is the intermittent-feed, pump-assisted. However, if this cycle does not prove to be practical, significant payload increases can be attained over the conventional gas-generator cycle by using the staged-combustion-engine cycle.

(End II, E)

TABLE II E-1

ENGINE PERFORMANCE DEGRADATION

d(ISP) -- (SEC)

CYCLES	PRESSURE				
	1000	2000	3000	5000	10000
THIRD FLUID	1.0	12	1.5	2.7	5.3
TWO STAGE COMBUSTION	1.0	1.2	1.5	4.0	11.0
INTERMITTENT FEED	10	27	3.2	47	6.0
GAS GENERATOR	5.0	5.5	8.9	159	28.8
HEATED HYDROGEN	5.0	69	9.3	14.4	33.2

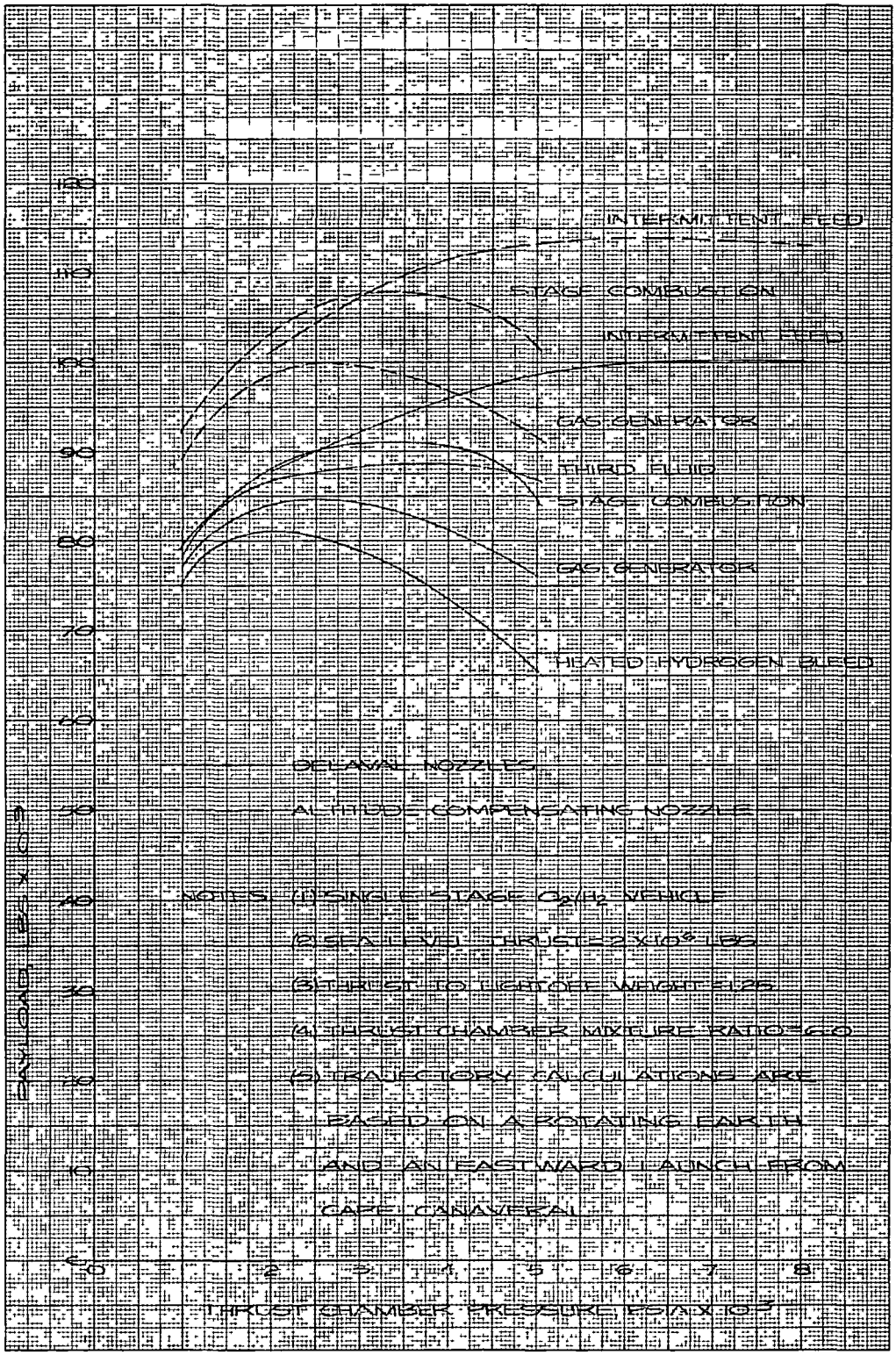

300-nm Payload vs Thrust Chamber Pressure for Various Engine Cycles

Figure II E-1

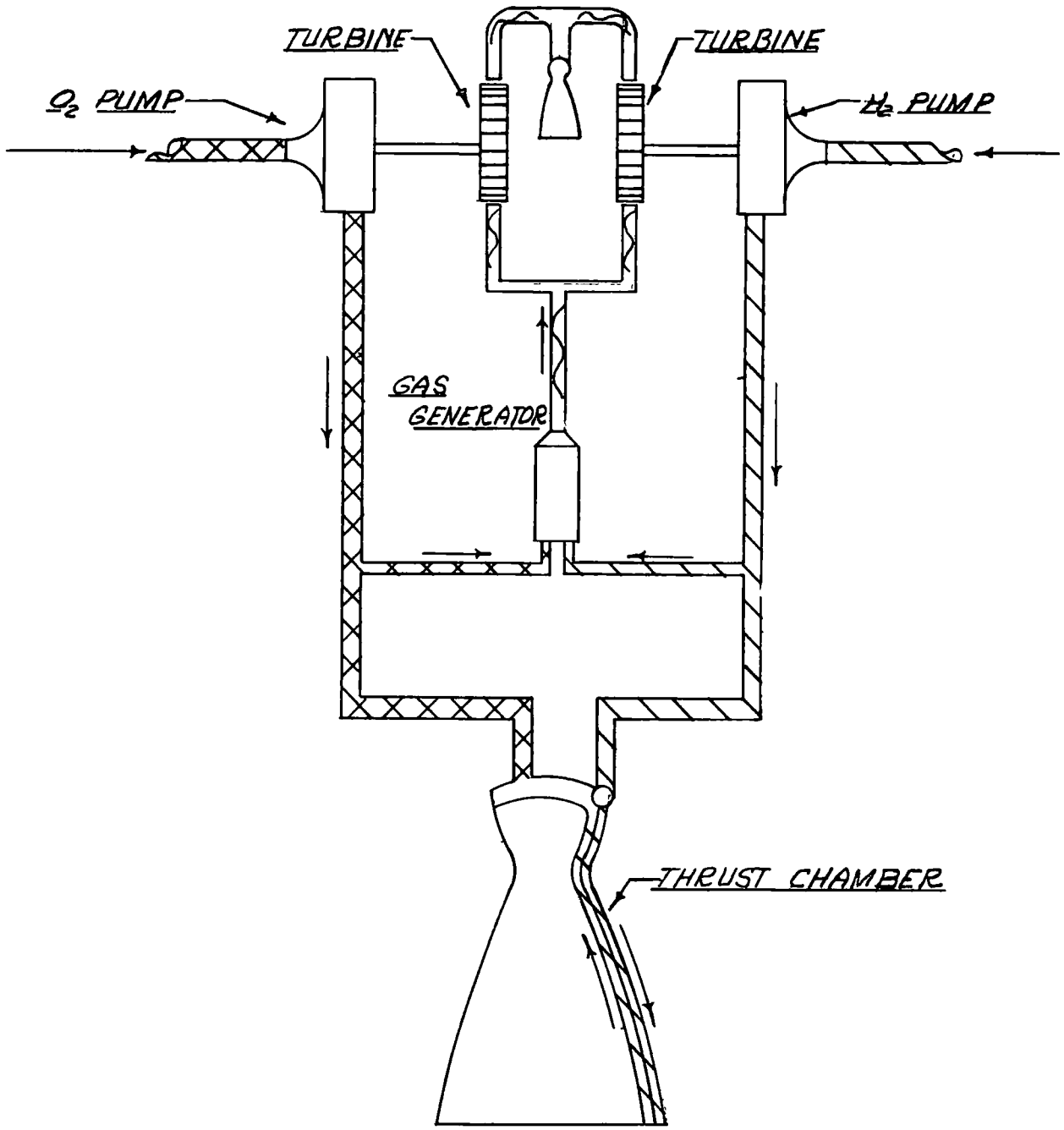

Gas Generator Cycle, Parallel Turbines

Figure II E-2

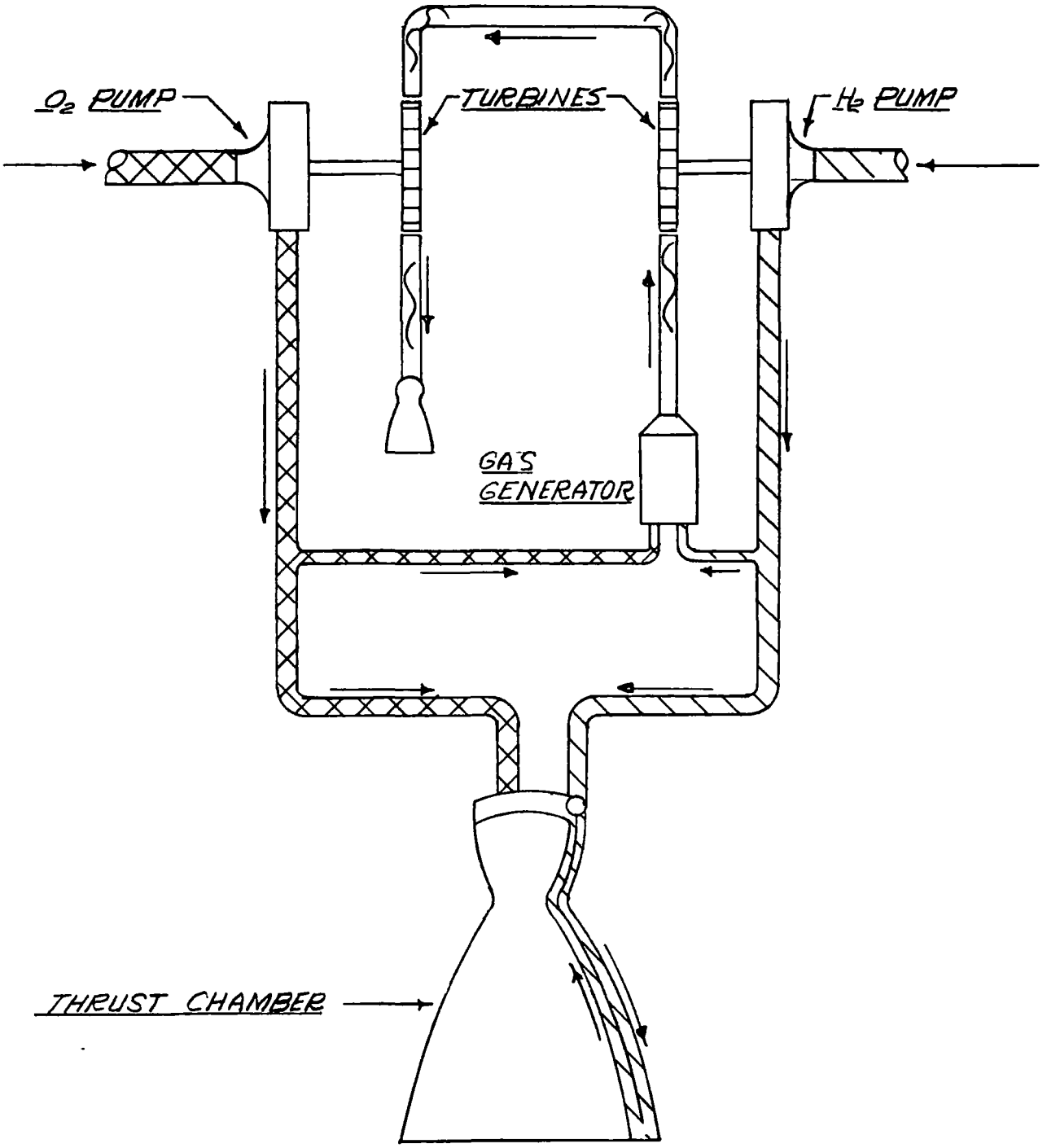

Gas Generator Cycle, Series Turbines

Figure II E-3

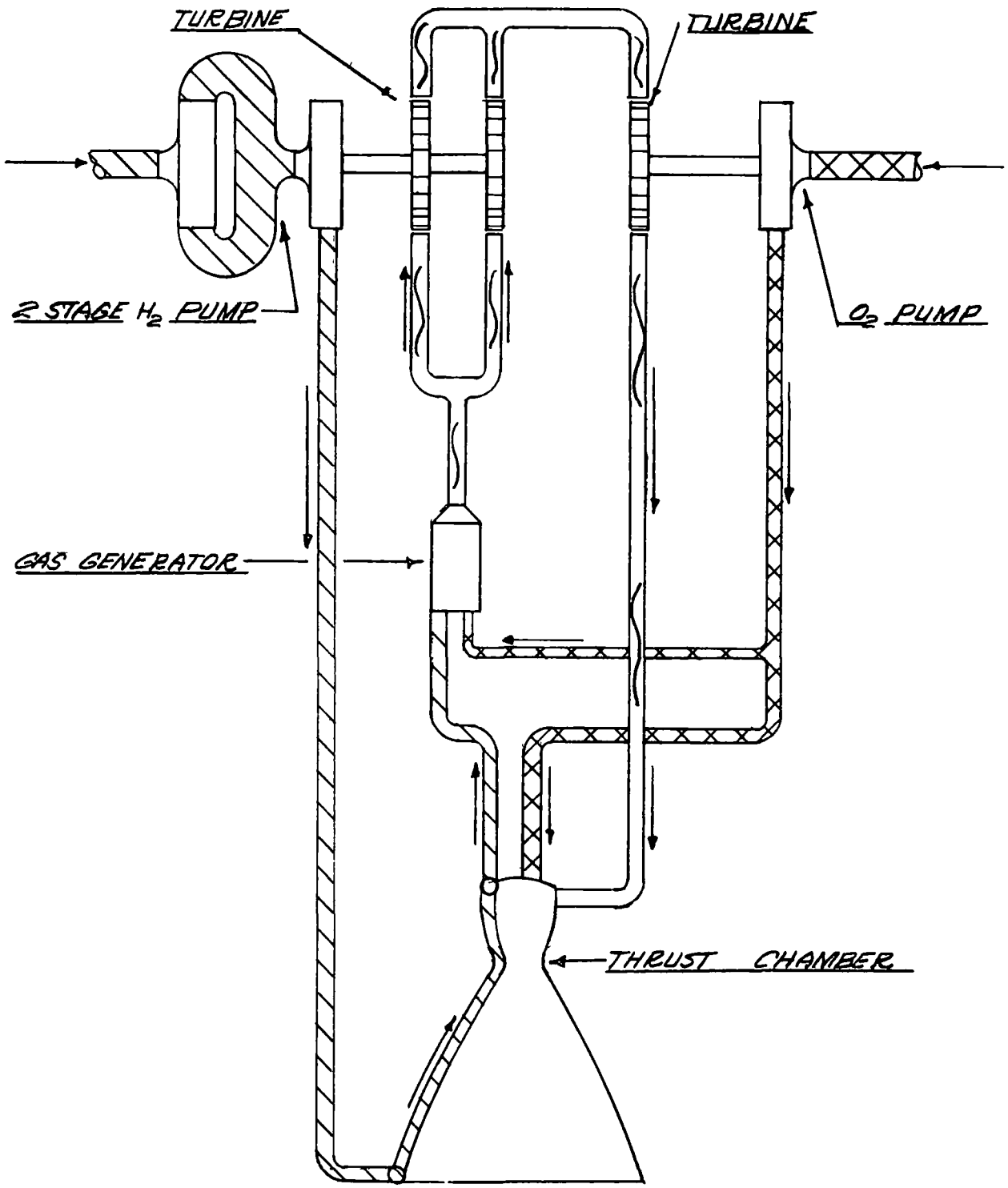

Staged Combustion Cycle, Fuel-Rich Gas Generator System, Series Turbines

Figure II E-4

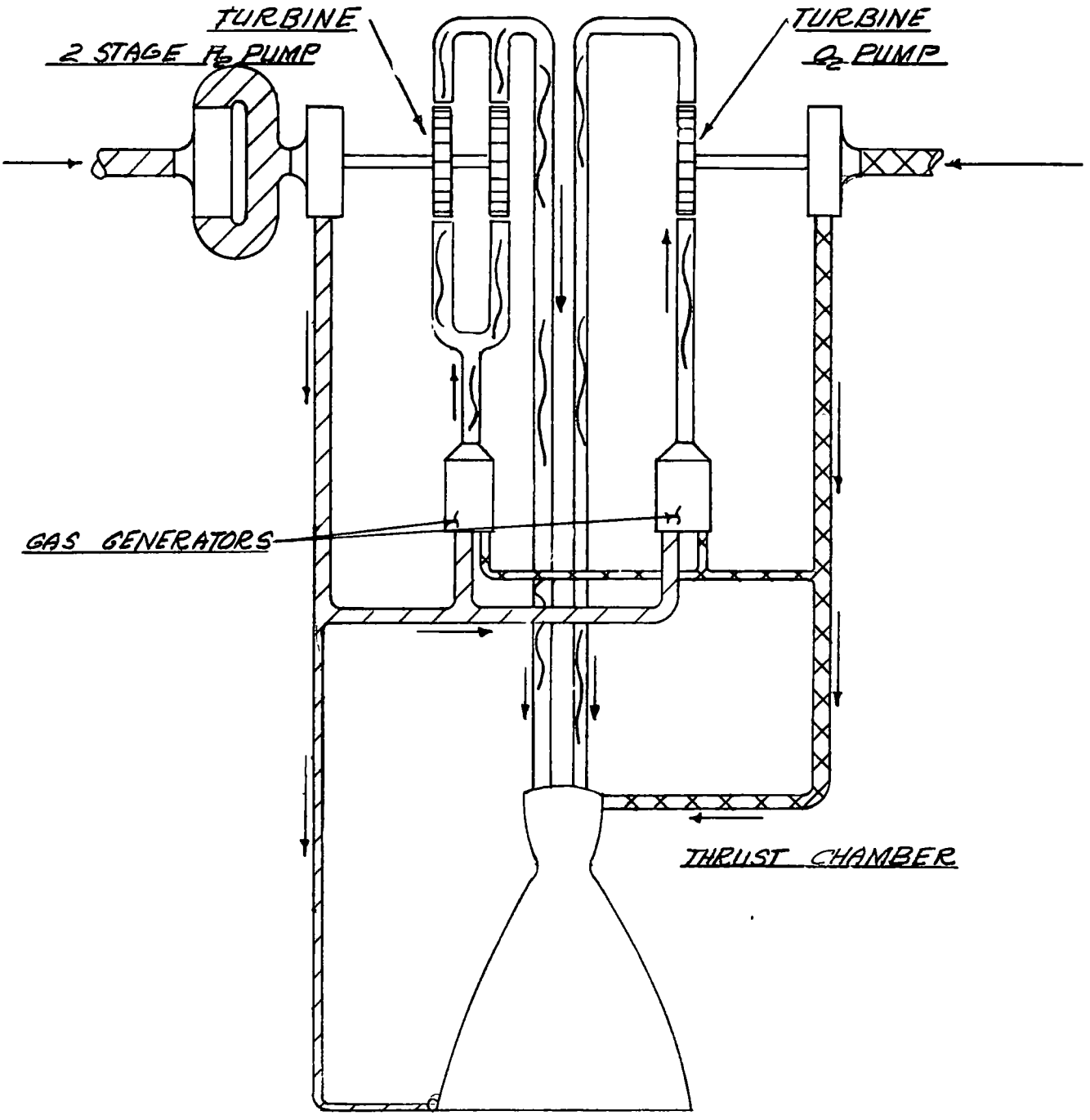

Staged-Combustion Cycle, Fuel-Rich Gas Generator System, Parallel Turbines

Figure II E-5

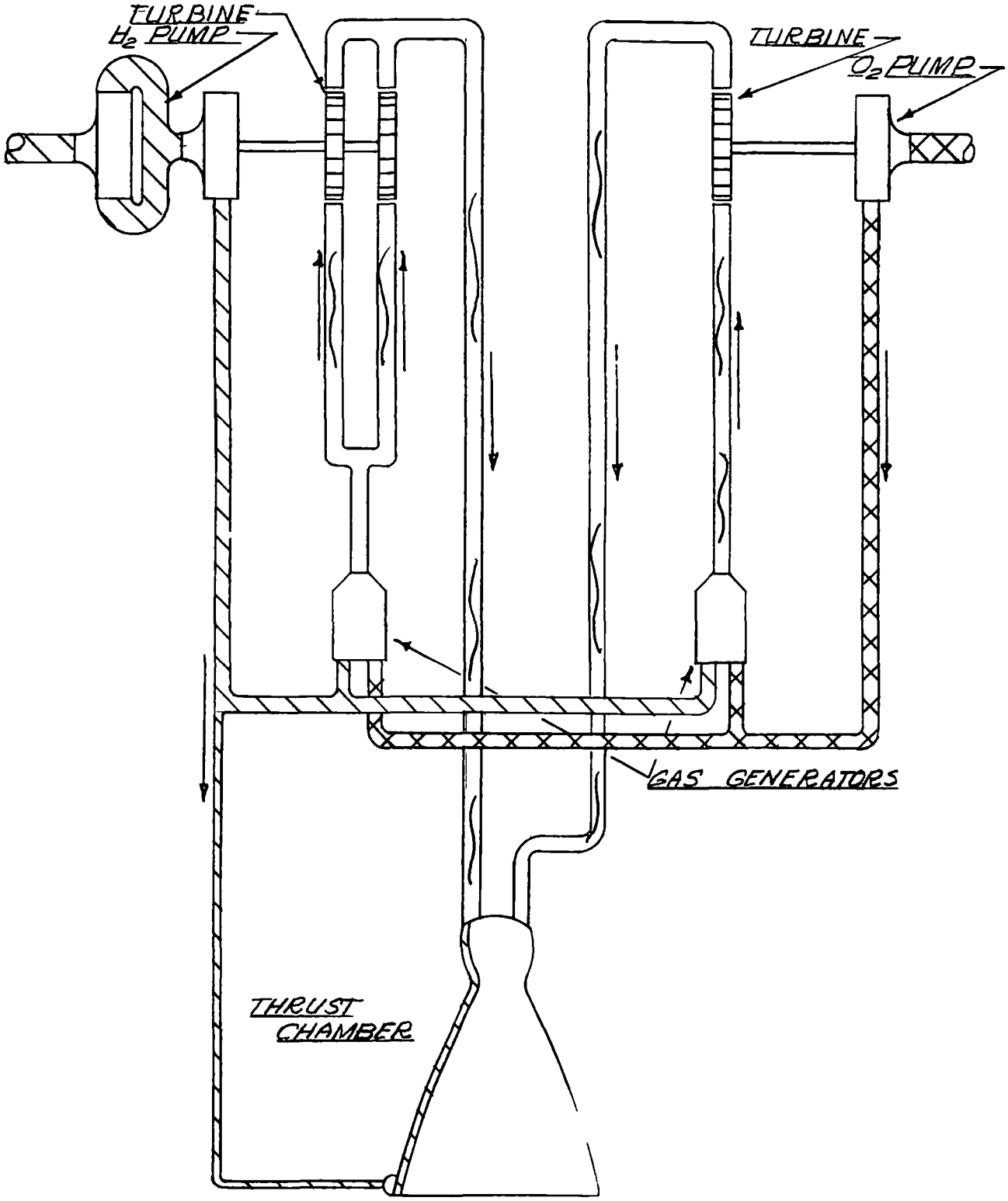

Staged Combustion Cycle, Fuel-Rich Plus Oxidizer-Rich Gas Generators

Figure II E-6

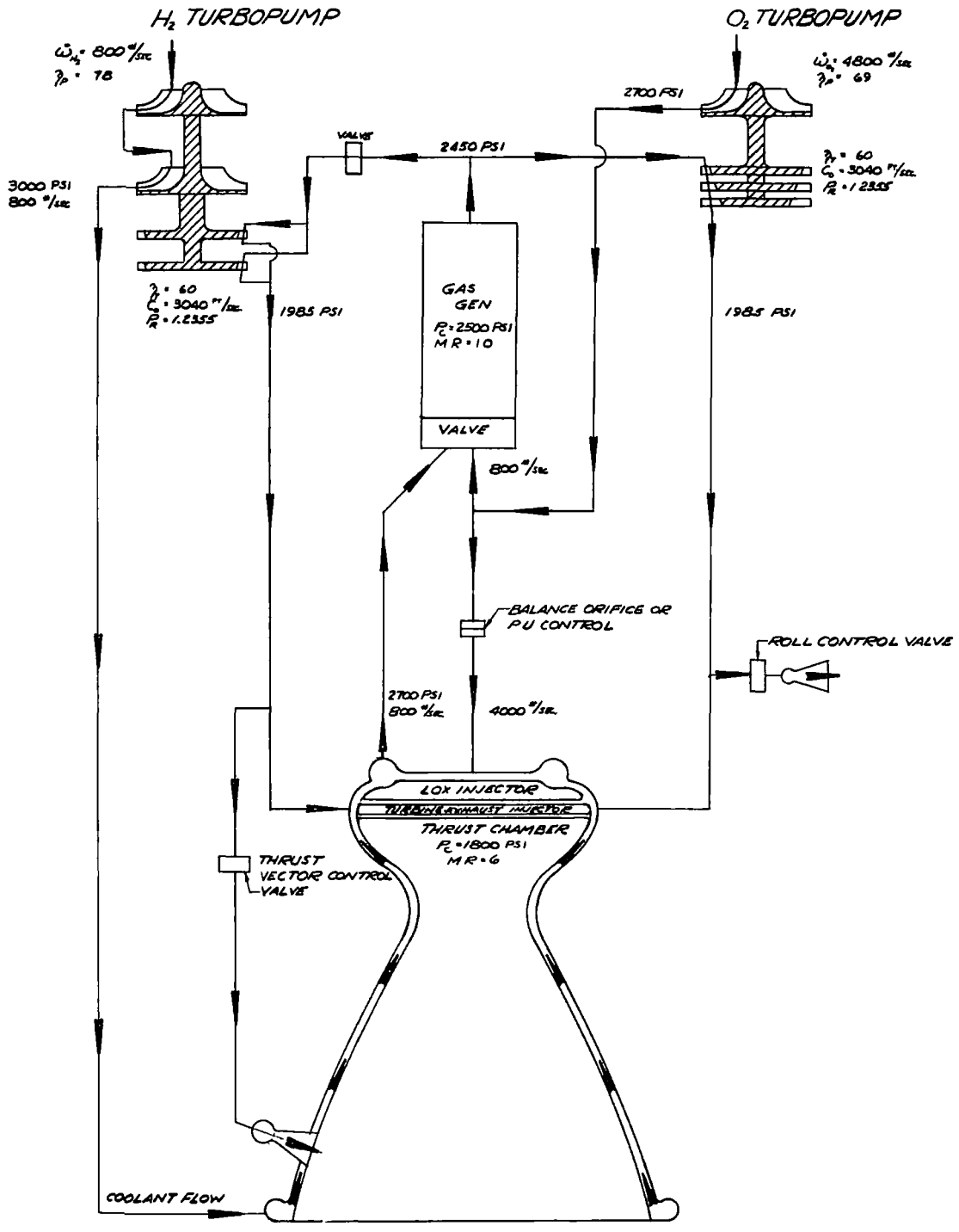

Schematic--Staged Combustion Cycle, Fuel-Rich Gas Generators, H_2 Coolant Flow in Series With Gas Generator

Figure II E-7

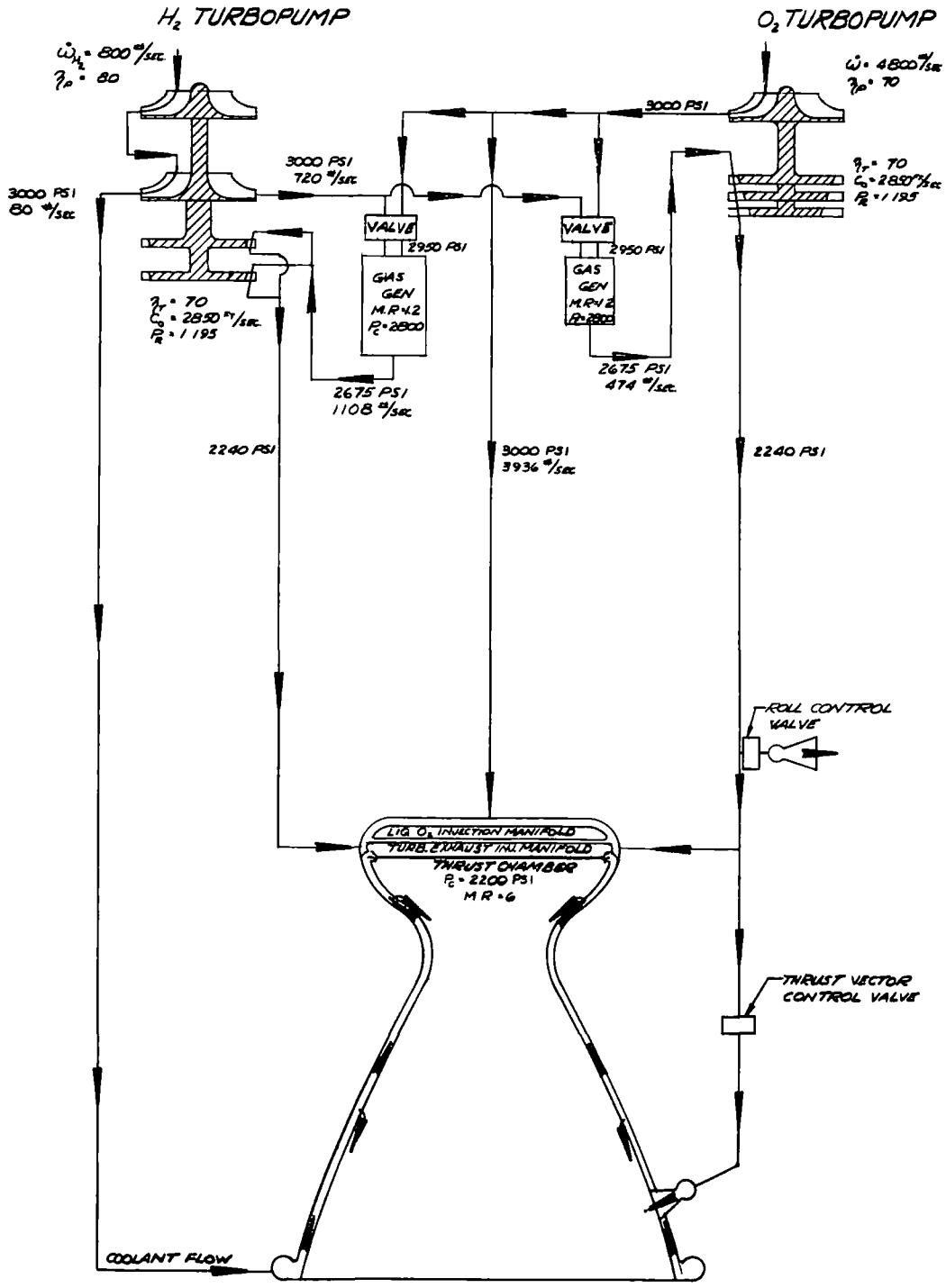

Schematic--Staged Combustion Cycle, Fuel-Rich Gas Generators, H_2 Coolant Flow in Parallel With Gas Generator

Figure II E-8

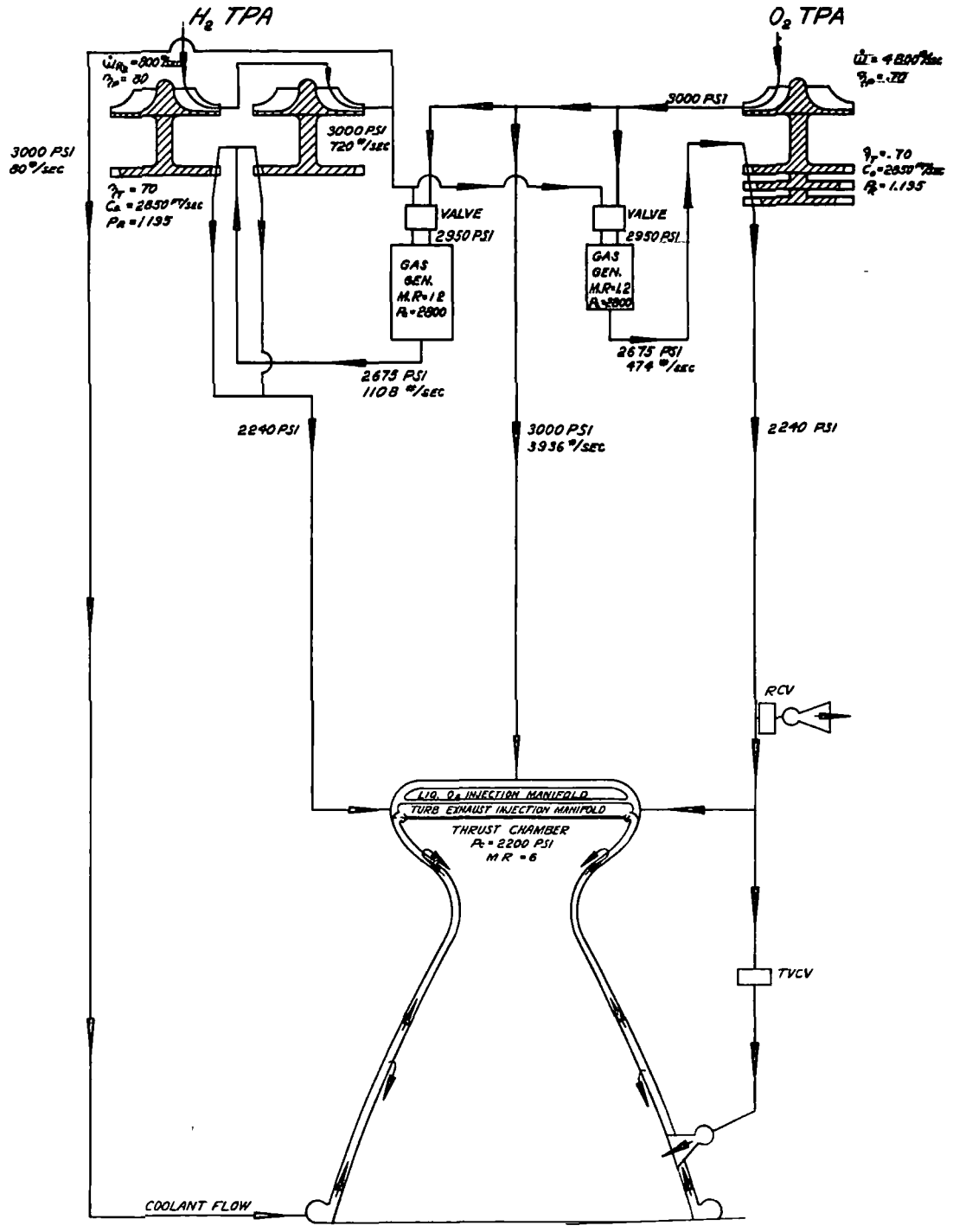

Schematic--Staged Combustion Cycle, Fuel-Rich Gas Generators, Dual Hydrogen Turbopumps

Figure II E-9

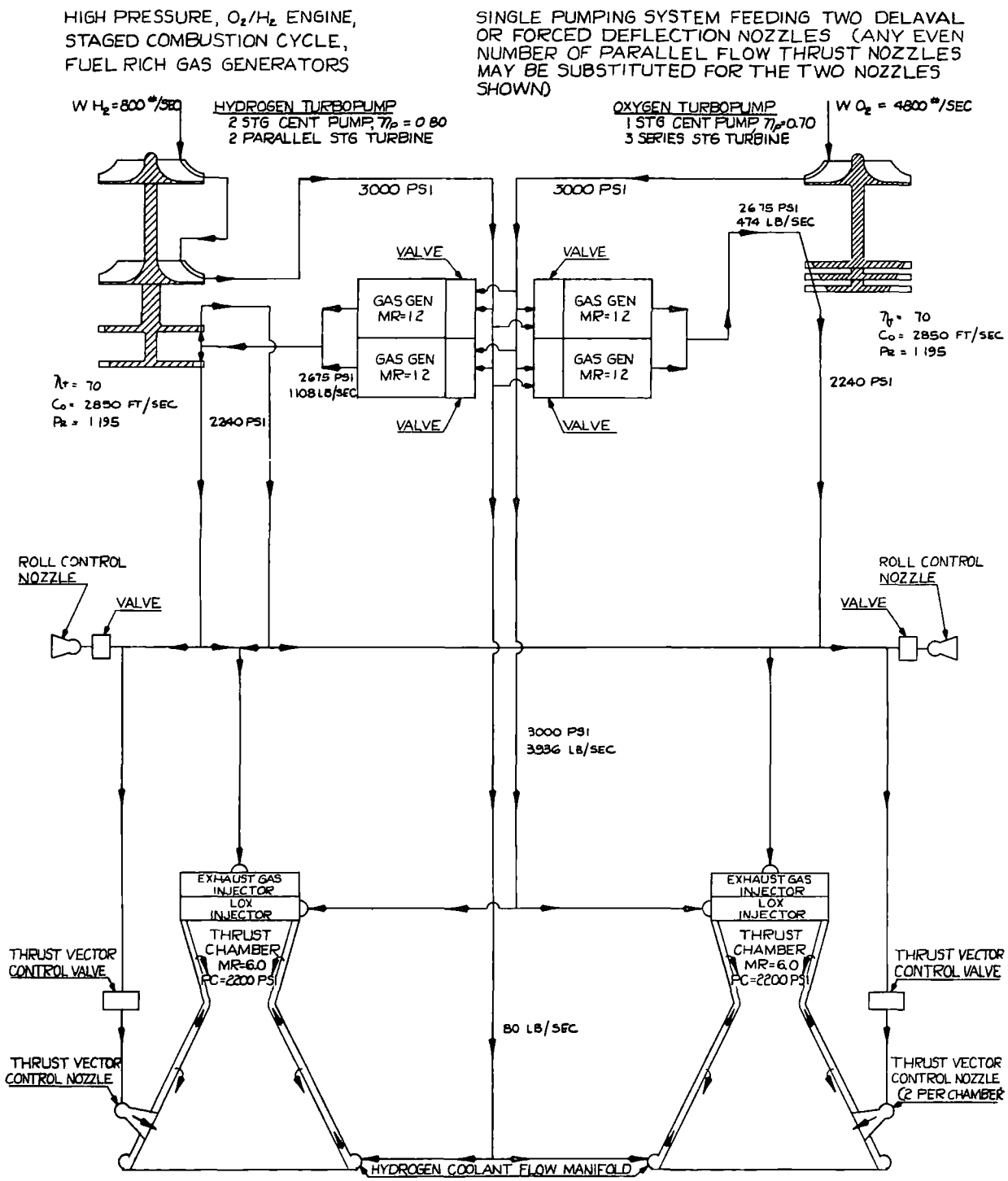

Schematic--Staged Combustion Cycle, Fuel-Rich Gas Generators, Multiple Thrust Chambers

Figure II E-10

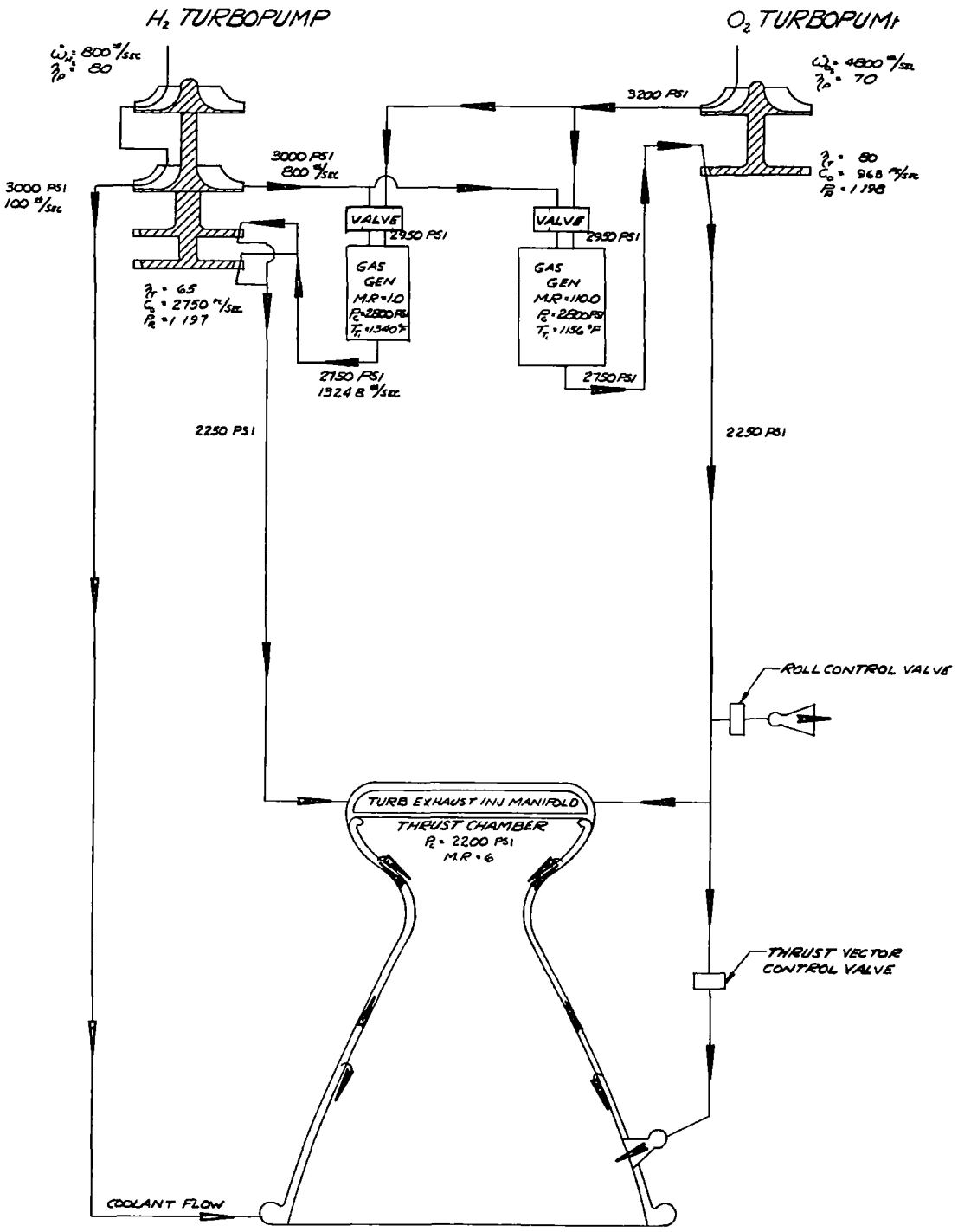

Schematic--Staged Combustion Cycle, Fuel-Rich and Oxidizer-Rich Gas Generators

Figure II E-11

HIGH PRESSURE, O_2/H_2 ENGINE, - STAGED COMBUSTION CYCLE, FUEL RICH FUEL TURBOPUMP GAS GENERATORS OXYGEN RICH OXYGEN TURBOPUMP GAS GENERATORS

2 $\overline{M}$ - SINGLE PUMPING SYSTEM FEEDING TWO DELAVAL OR FORCED DEFLECTION NOZZLES (ANY EVEN NUMBER OF PARALLEL FLOW THRUST NOZZLES MAY BE SUBSTITUTED FOR THE TWO NOZZLES SHOWN)

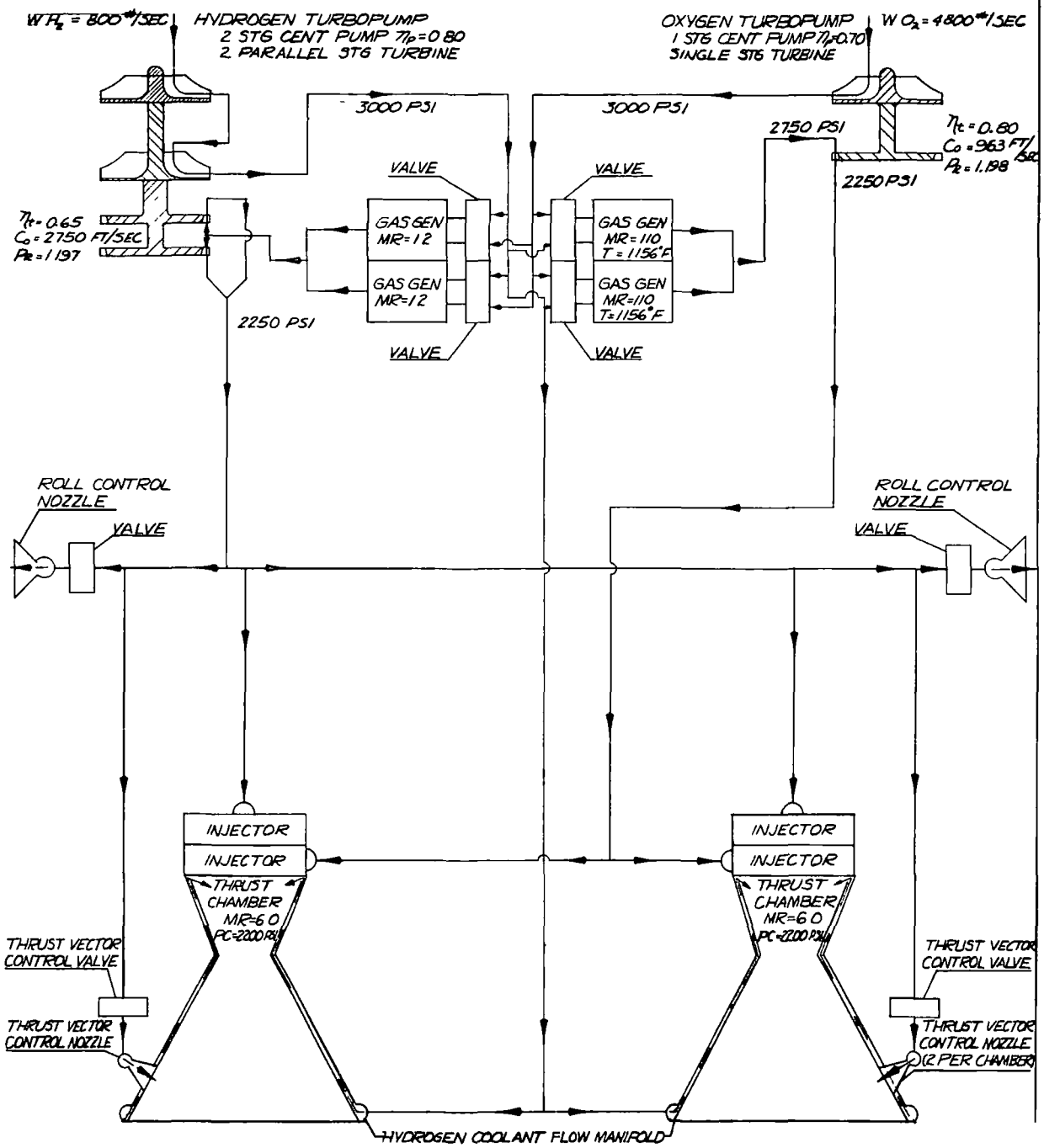

Schematic--Staged Combustion Cycle, Fuel-Rich and Oxidizer-Rich Gas Generators, Multiple Thrust Chambers

Figure II E-12

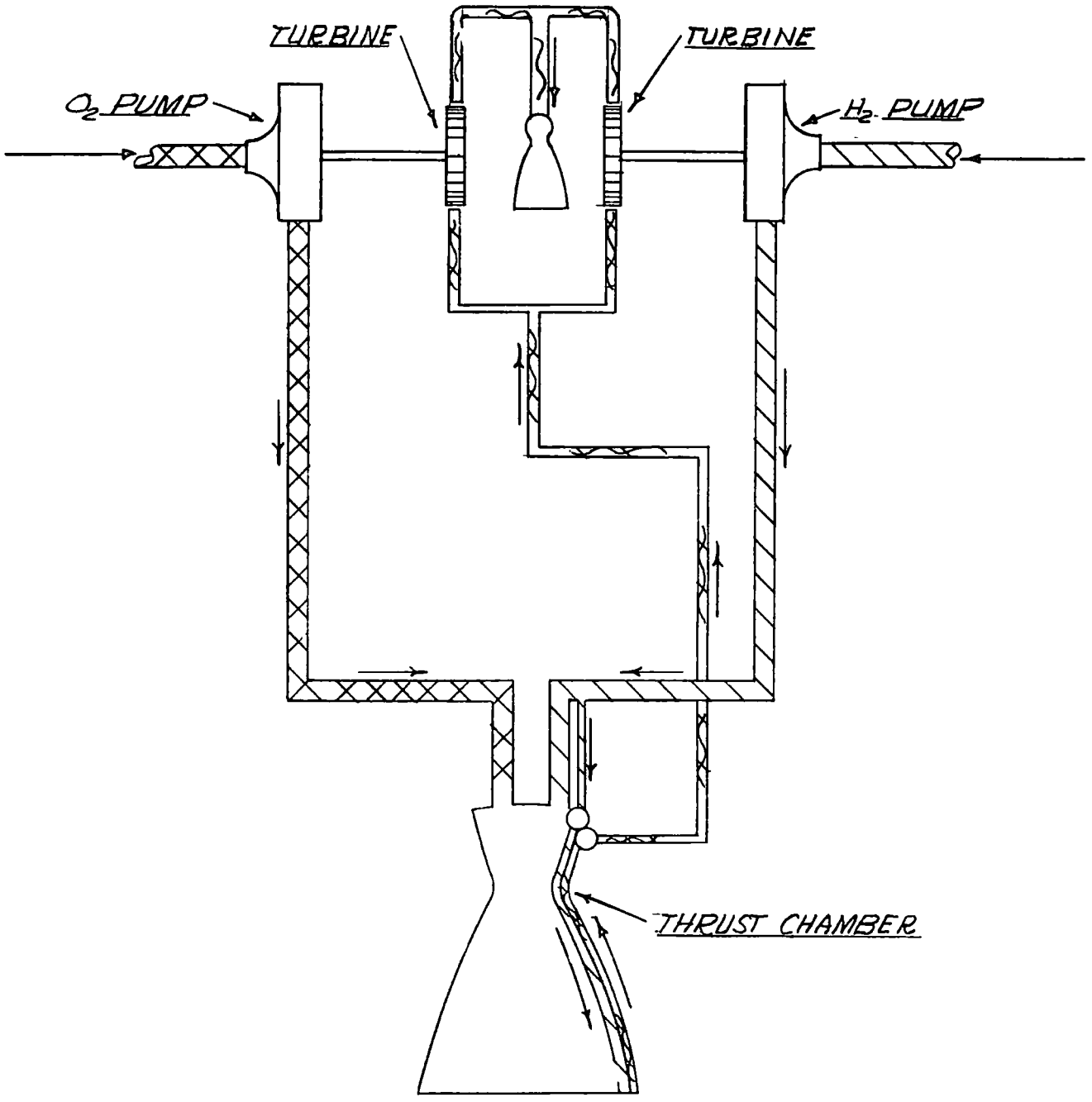

Heated-H_2 Bleed Cycle, Parallel Turbines

Figure II E-13

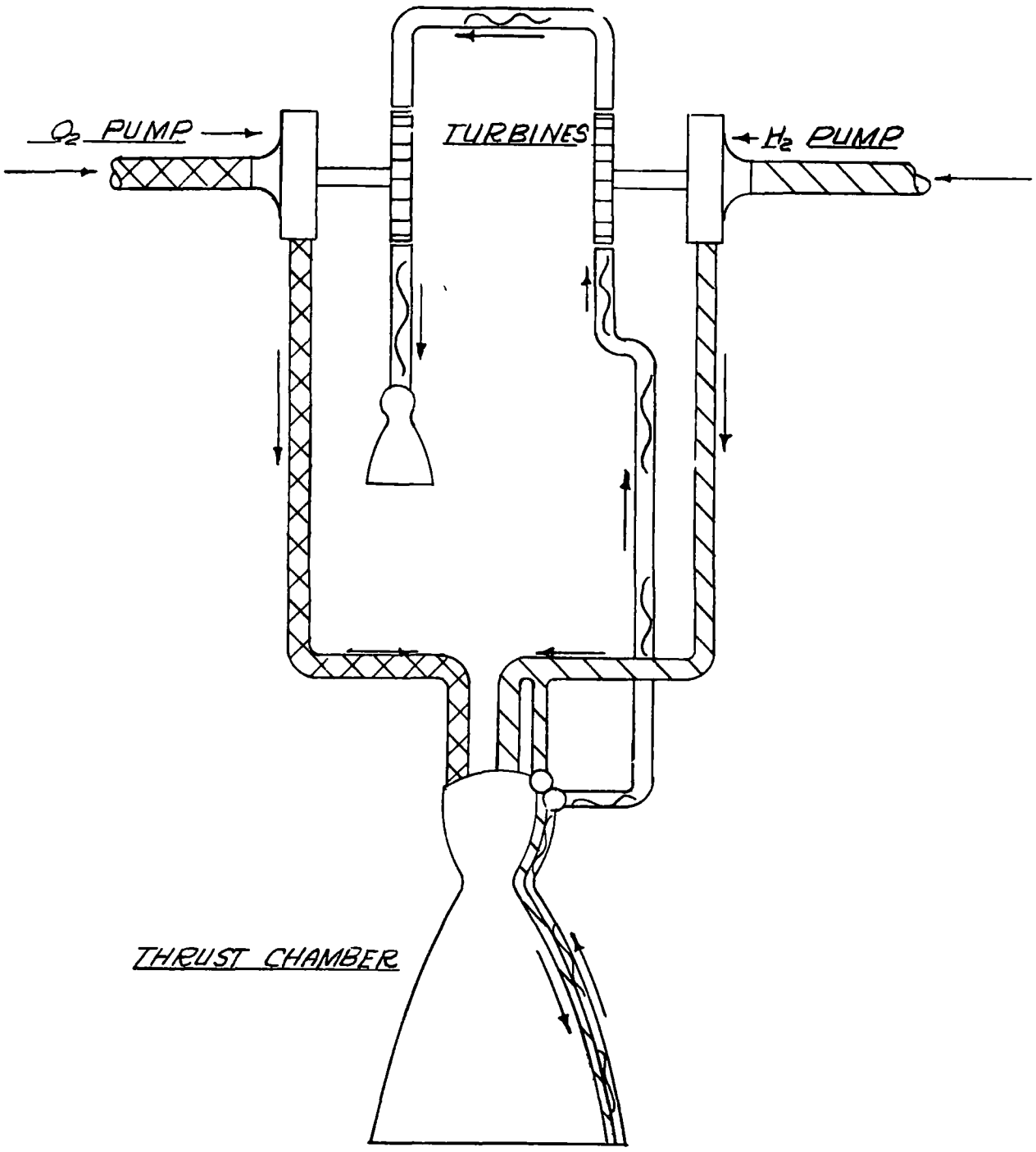

Heated-H_2 Bleed Cycle, Series Turbines

Figure II E-14

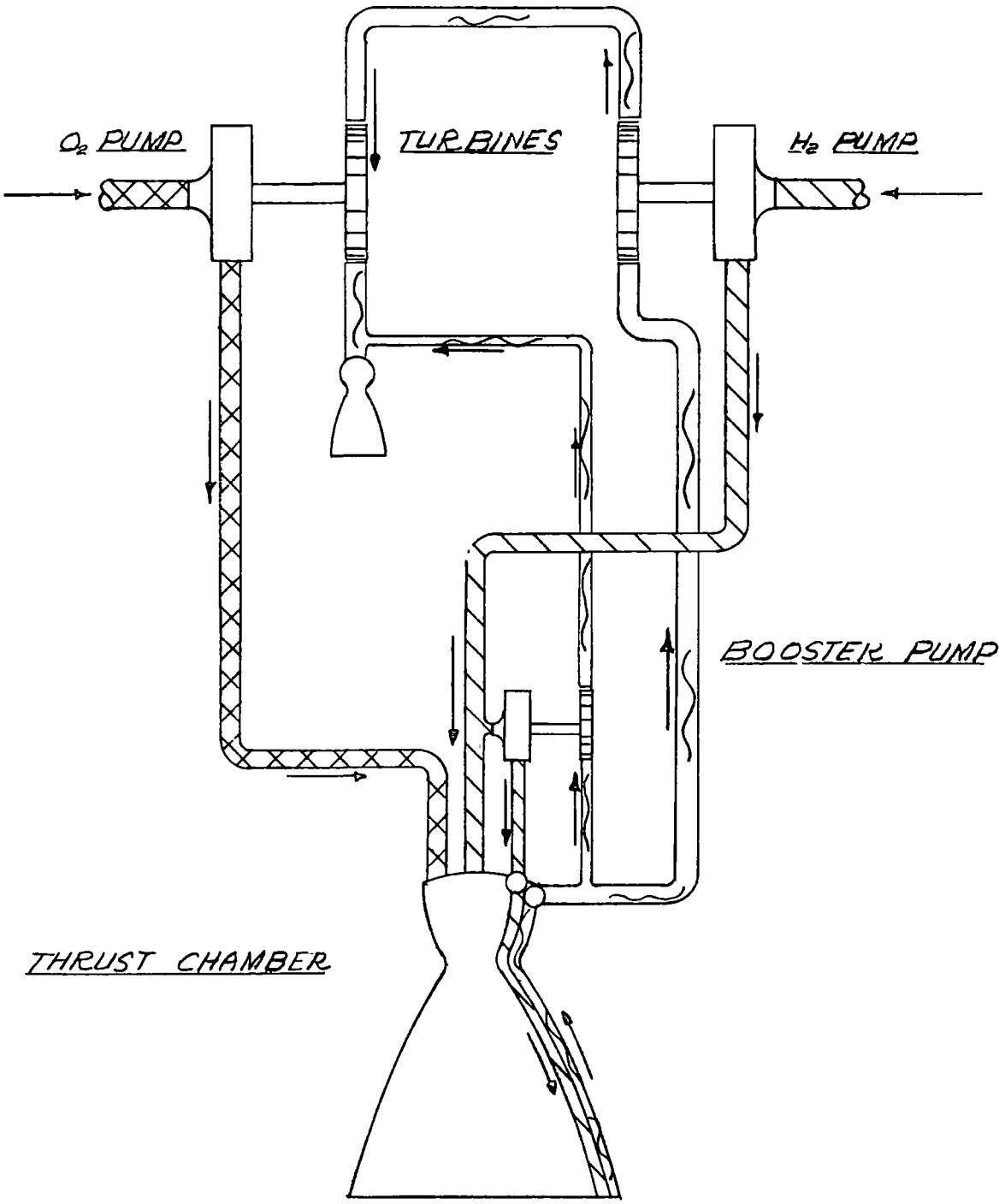

Heated-Bleed Cycle, Series Turbines with Bleed Flow Booster Pump

Figure II E-15

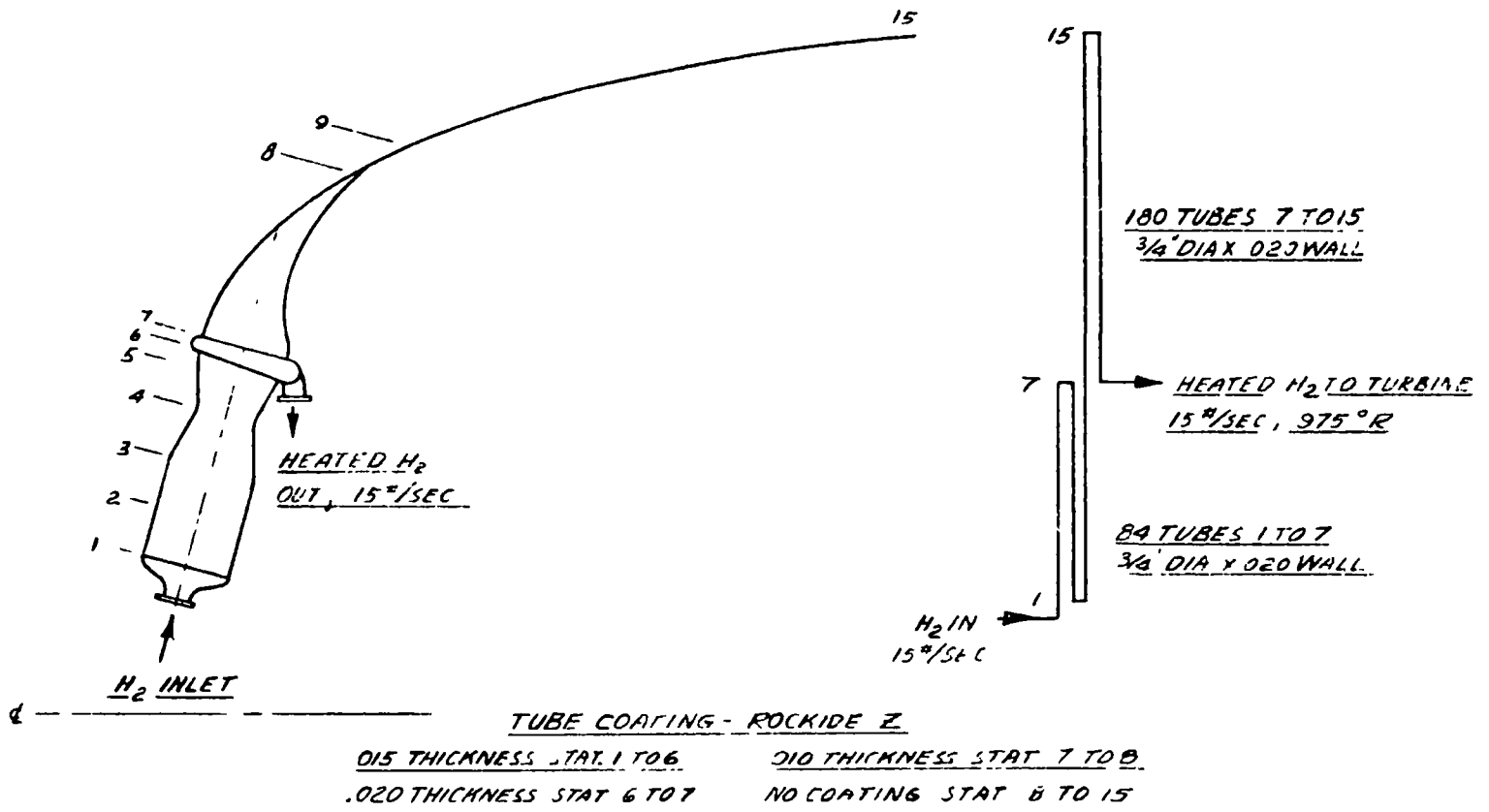

Figure II E-16

Heat Exchanger Design Requirements for Heated-H_2 Cycle

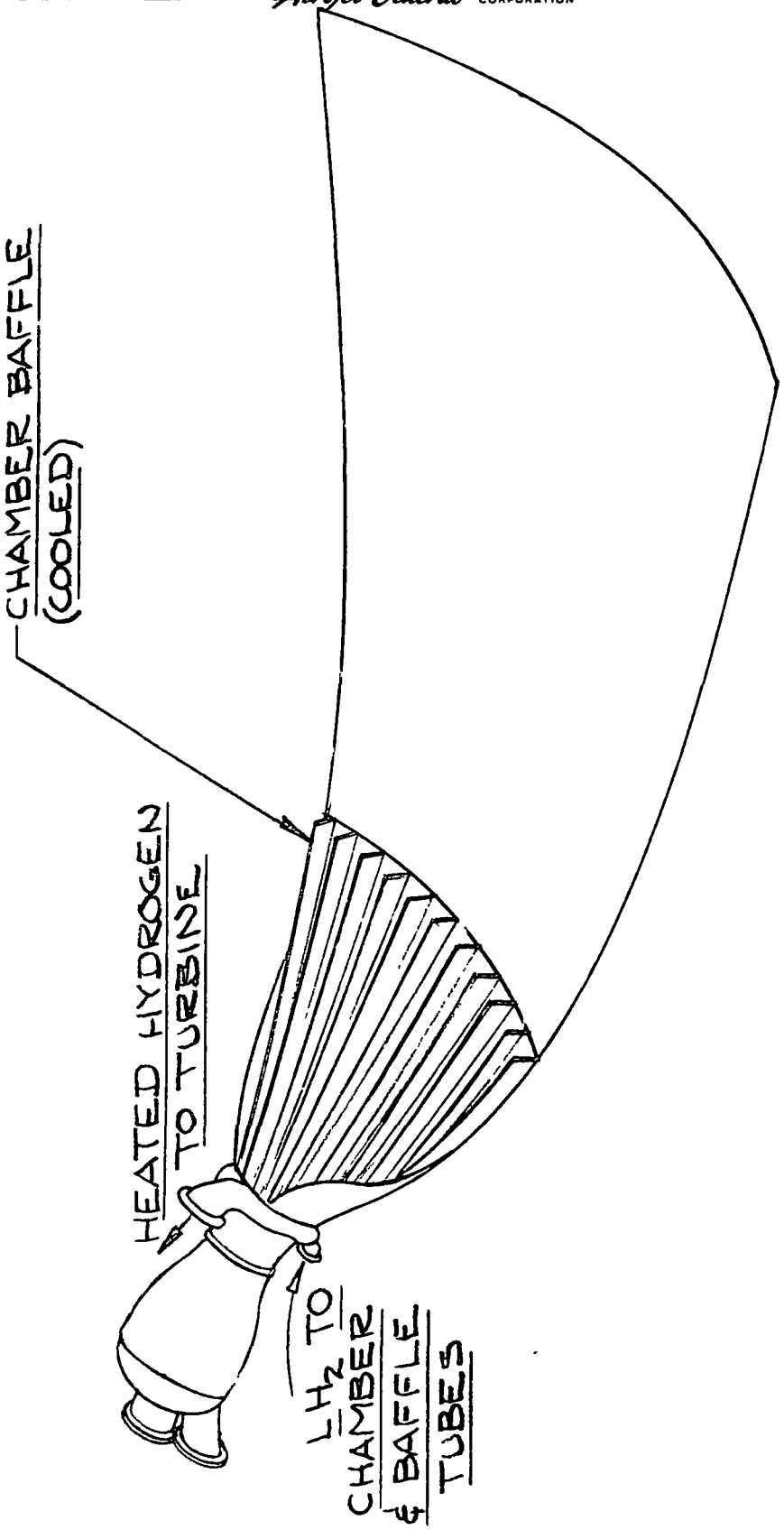

8-Chamber Heated-H_2 Cycle, Forced Deflection Engine,
Baffle-Type Heat Exchanger

Figure II E-17

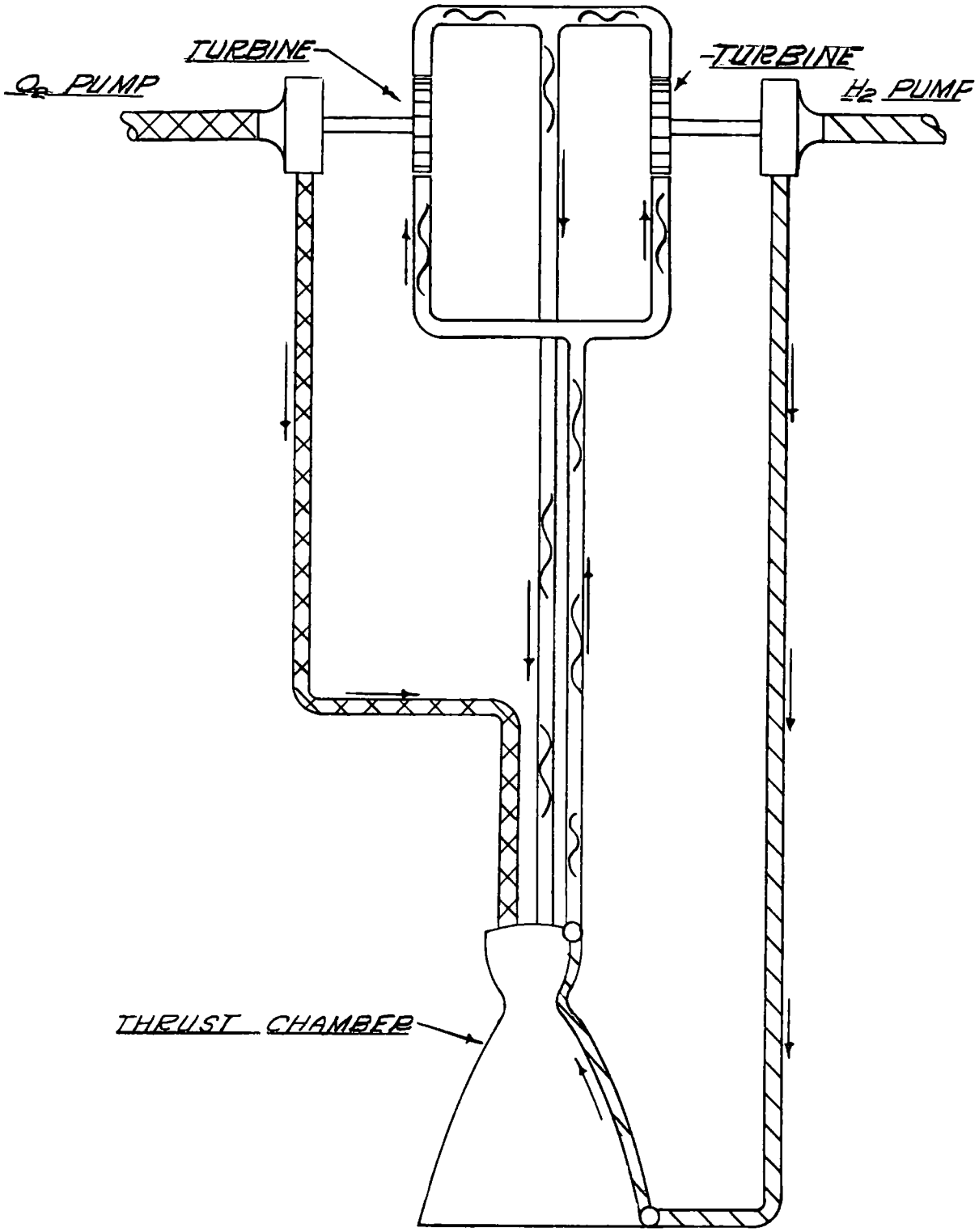

Heated-H_2 Topping Cycle, Parallel Turbines

Figure II E-18

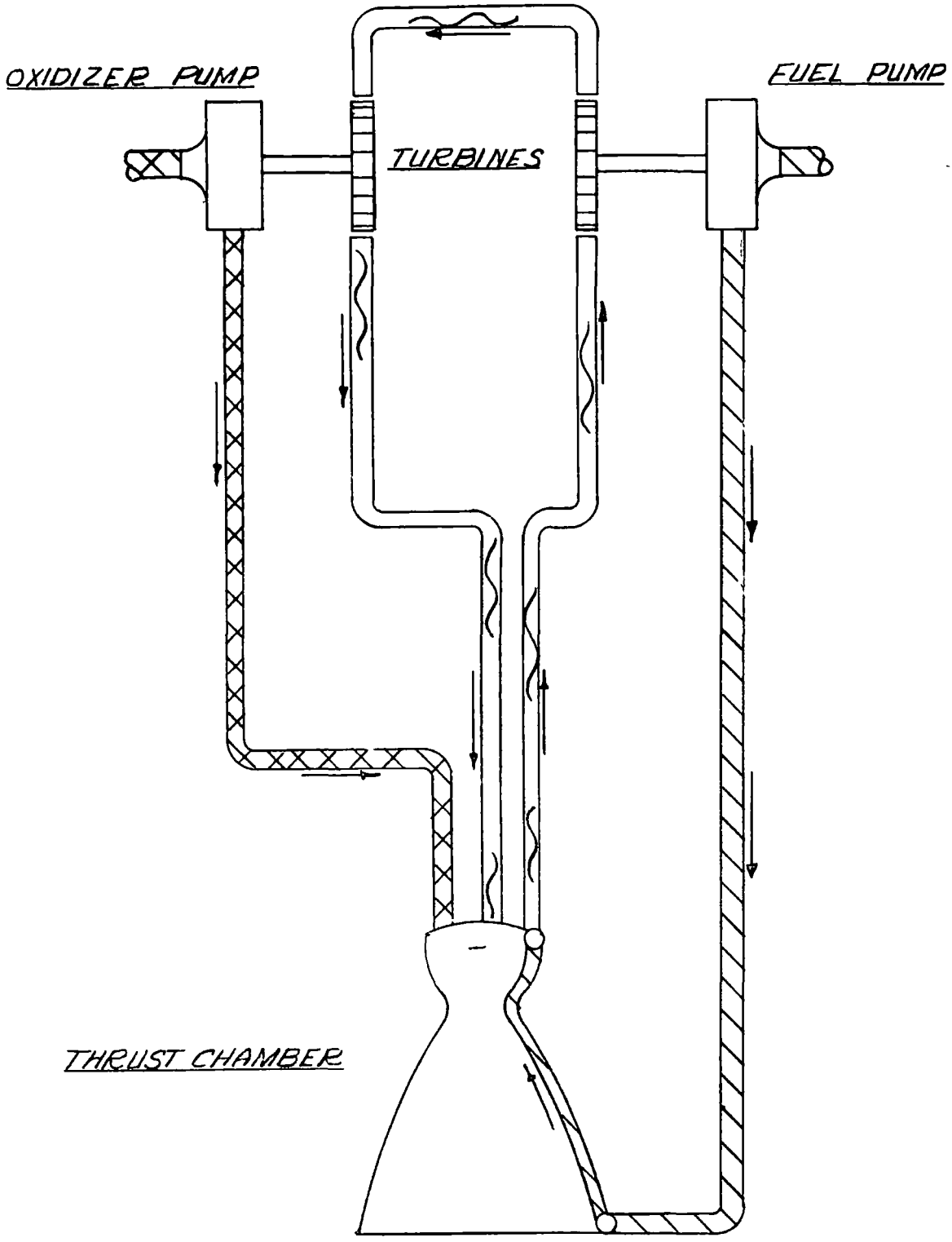

Heated-H_2 Topping Cycle, Series Turbines

Figure II E-19

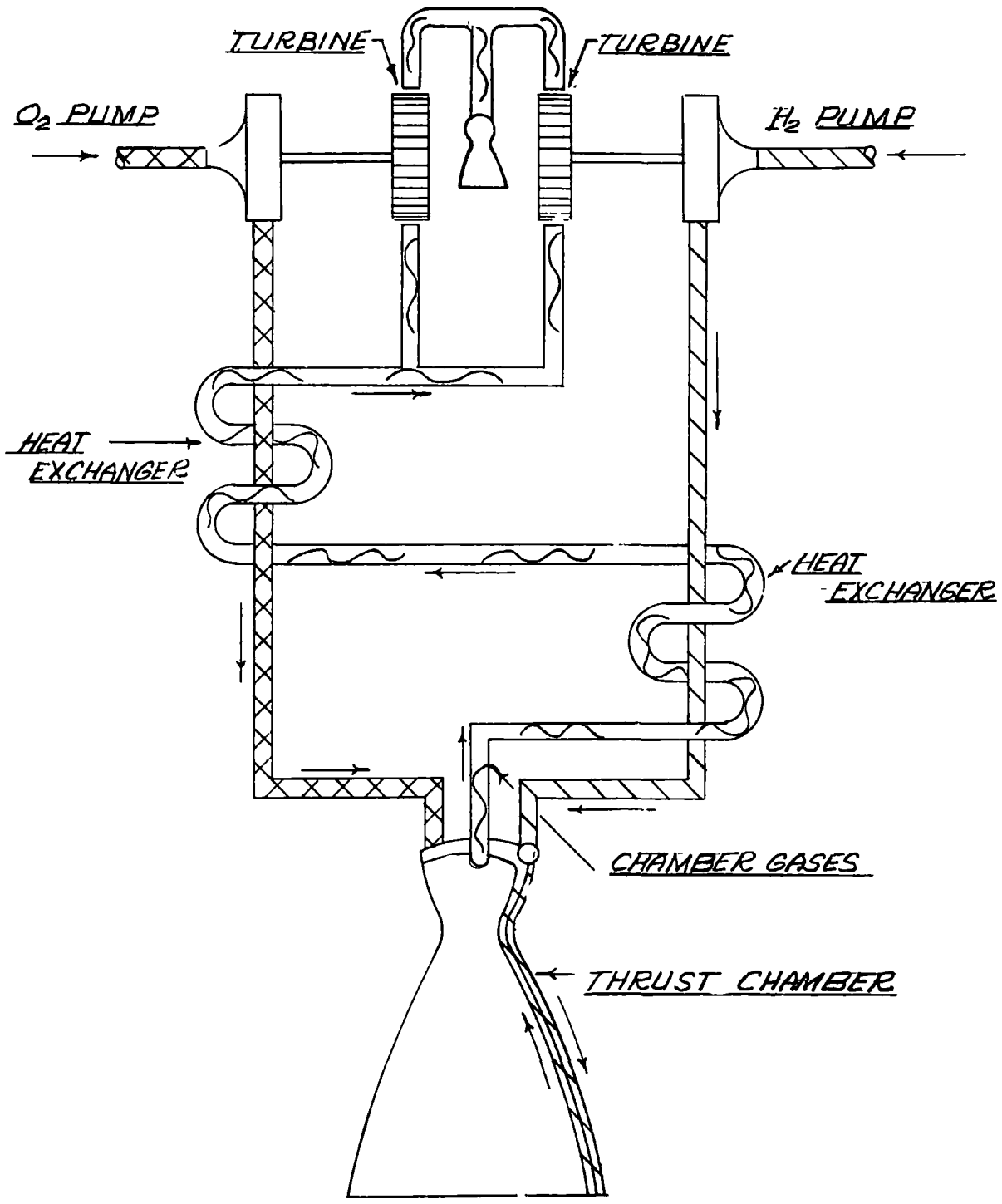

Chamber Bleed Cycle, Heat Exchanger, Cooled Gas

Figure II E-20

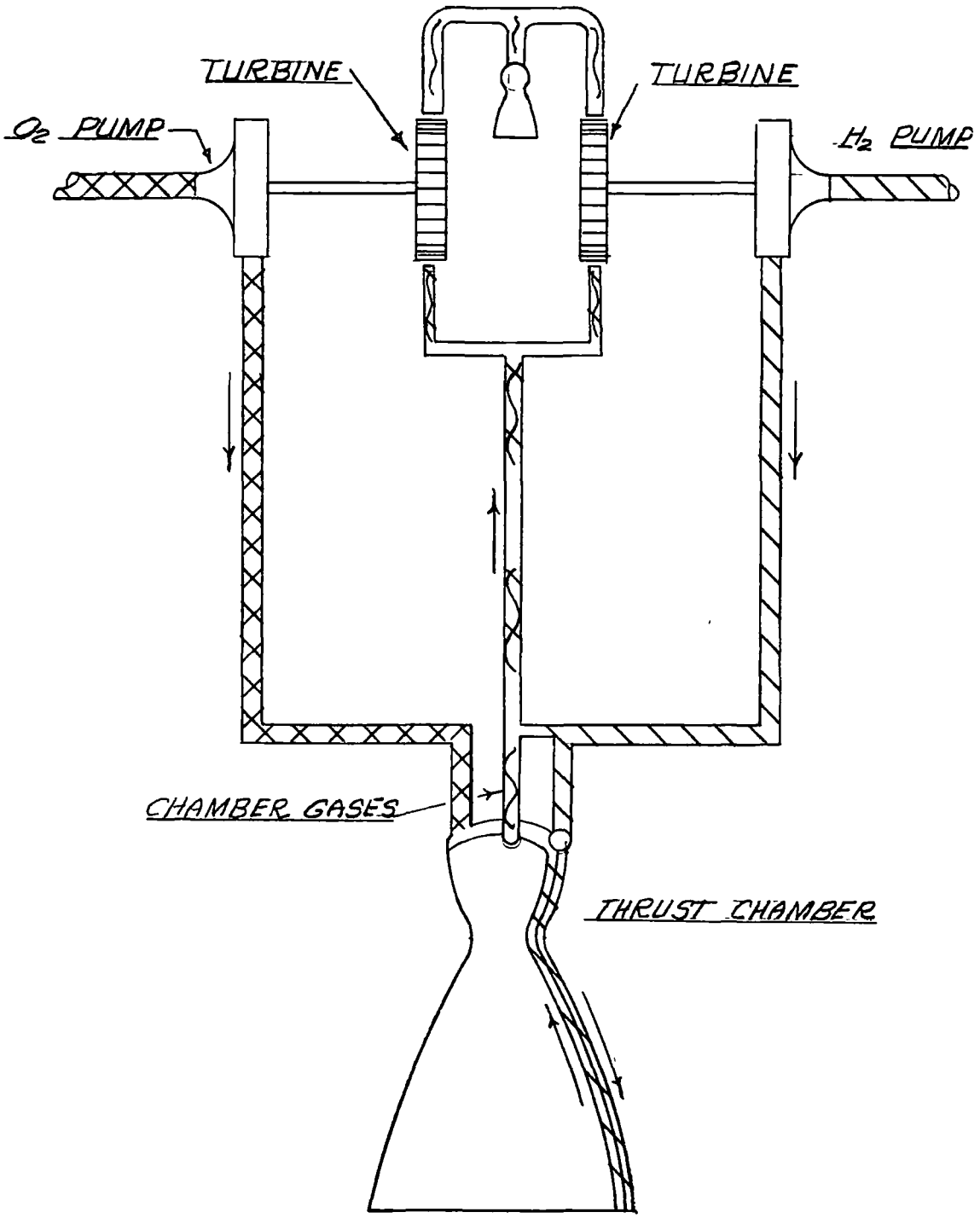

Chamber Bleed Cycle, Diluted Gas

Figure II E-21

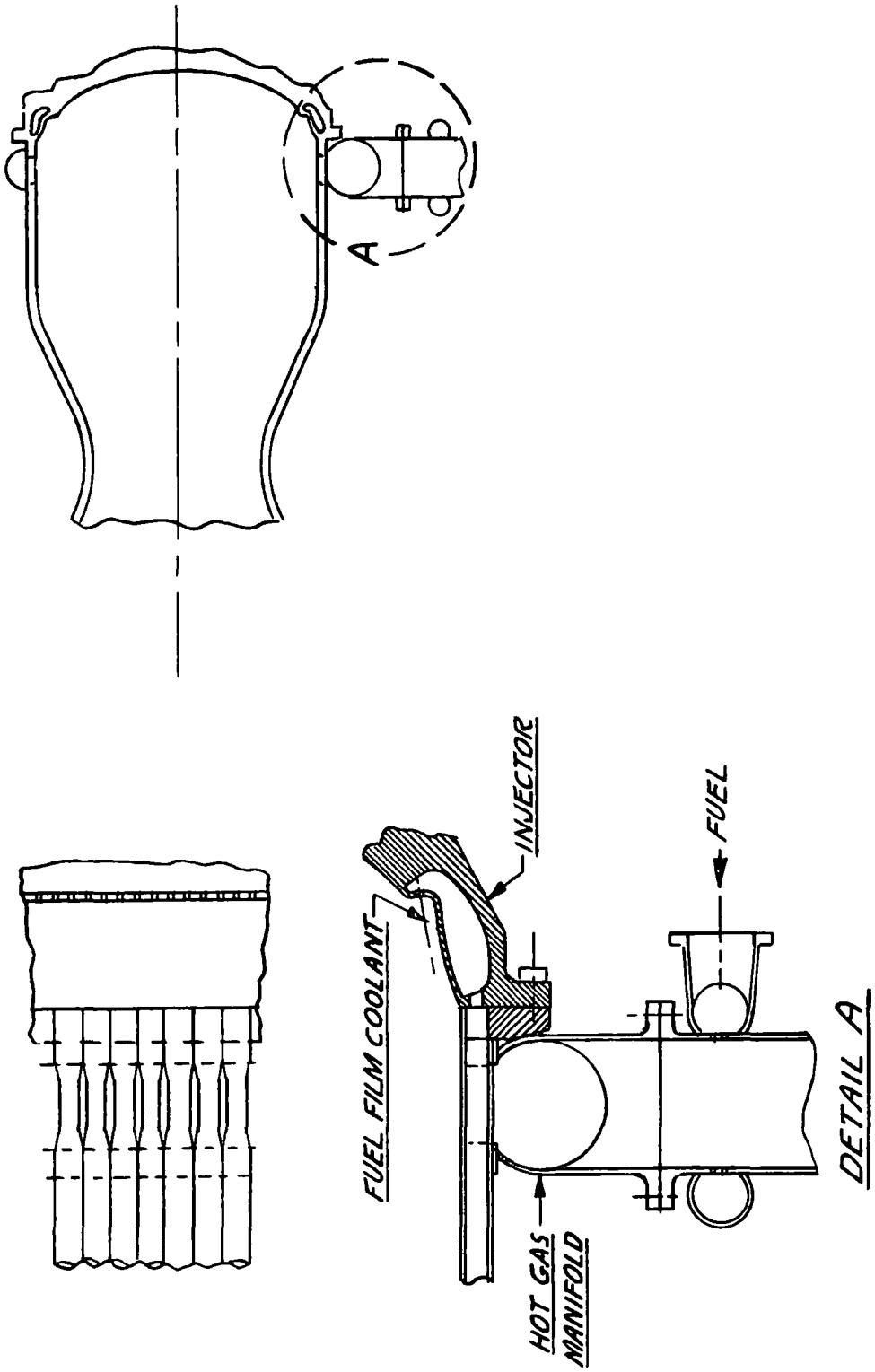

Chamber Bleed-Off Method

Figure II E-22

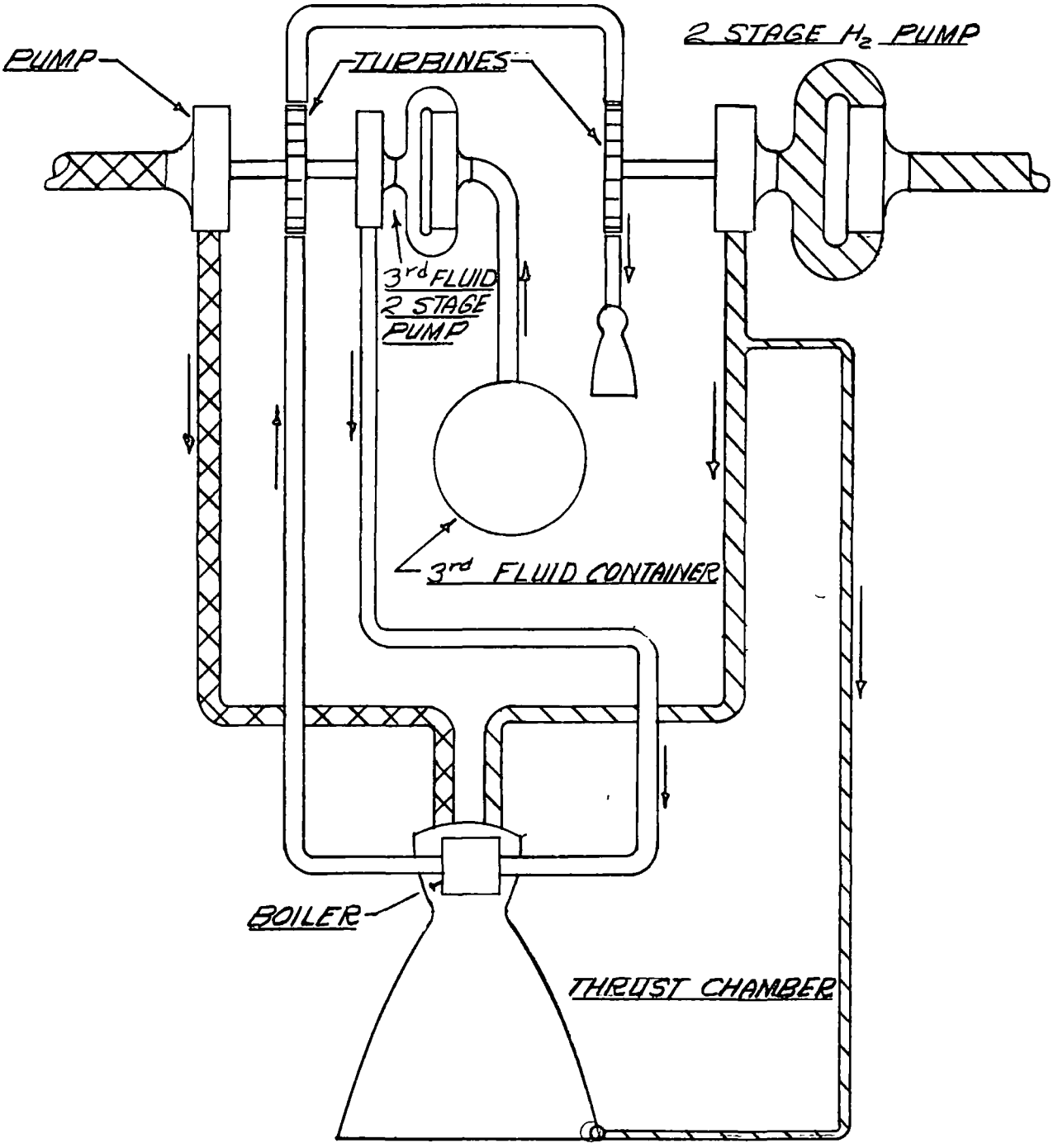

Third Fluid Turbine Drive Cycle, Open Cycle

Figure II E-23

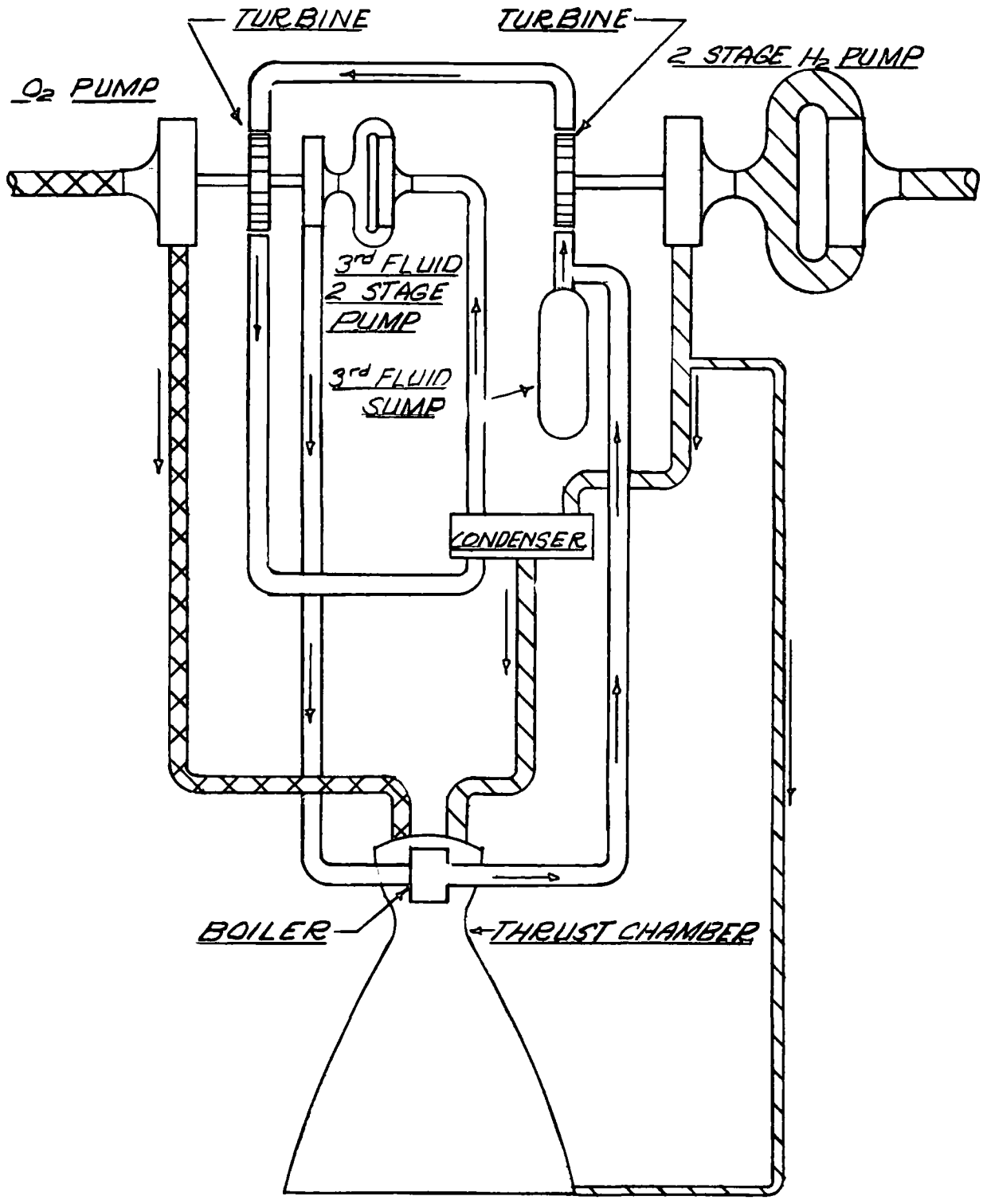

Third Fluid Turbine Drive Cycle, Closed Cycle

Figure II E-24

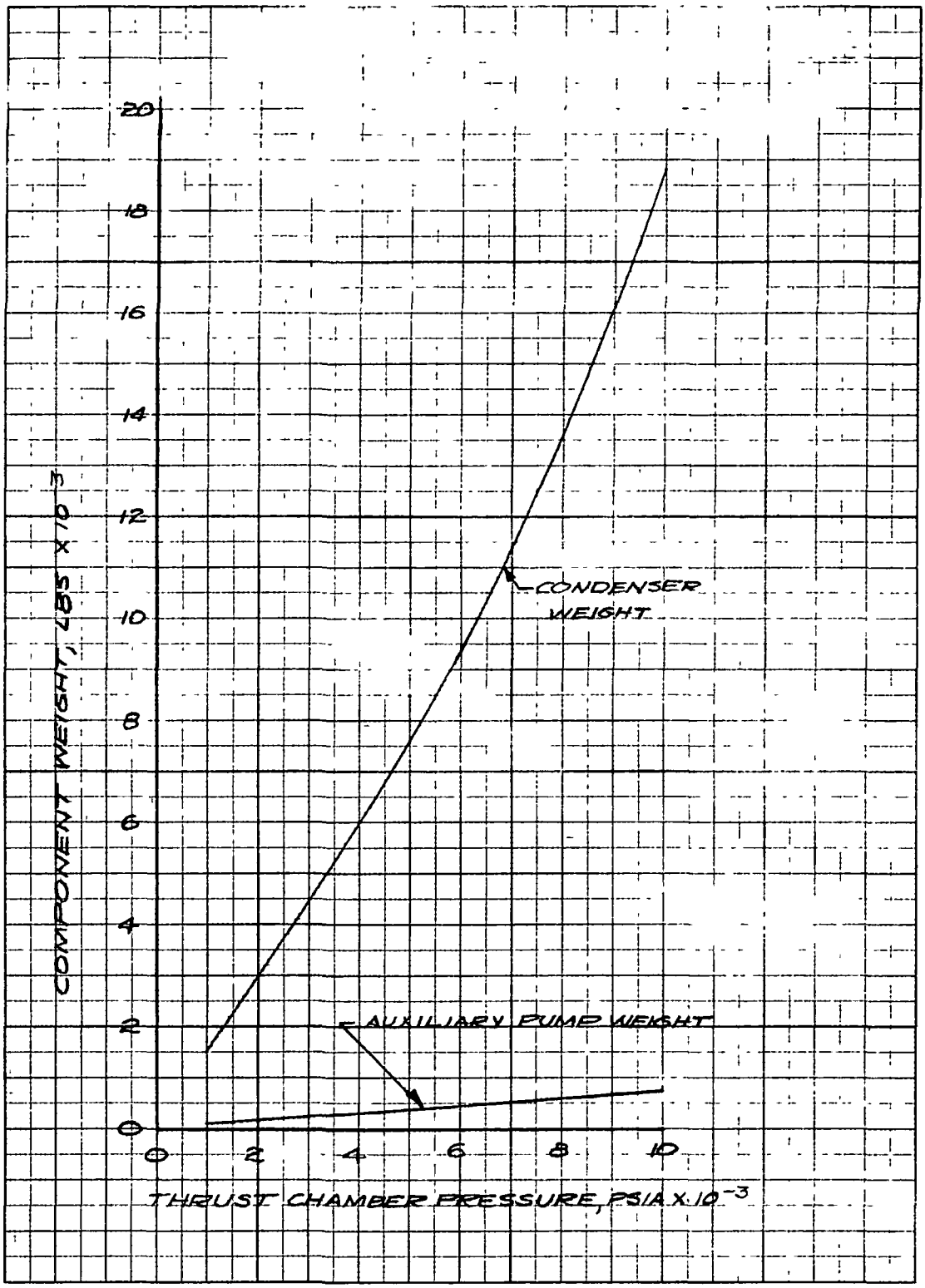

Third Fluid Cycle Component Weights Versus Thrust Chamber Pressure

Figure II E-25

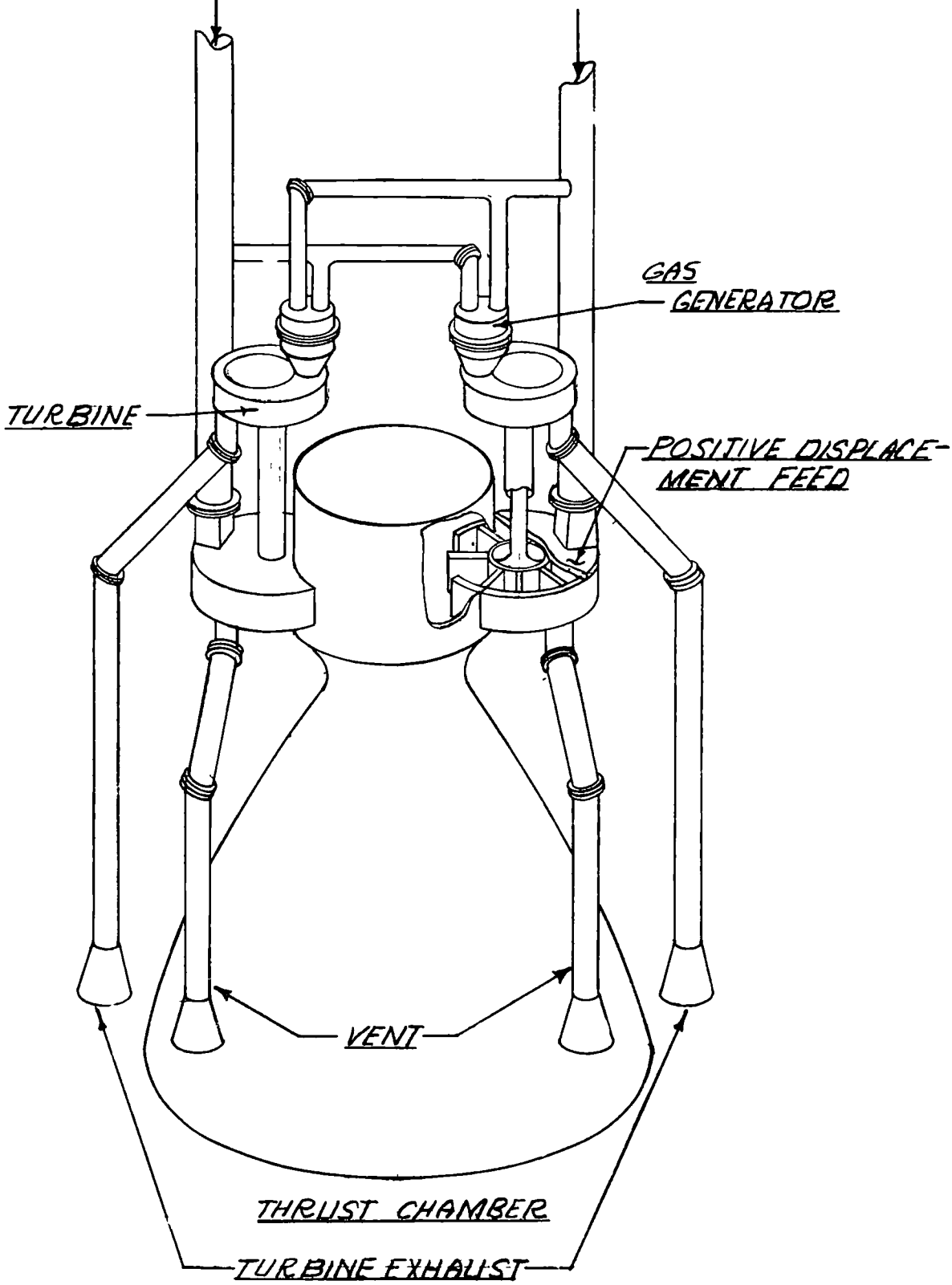

Delivery Feed Cycle, Continous Feed

Figure II E-26

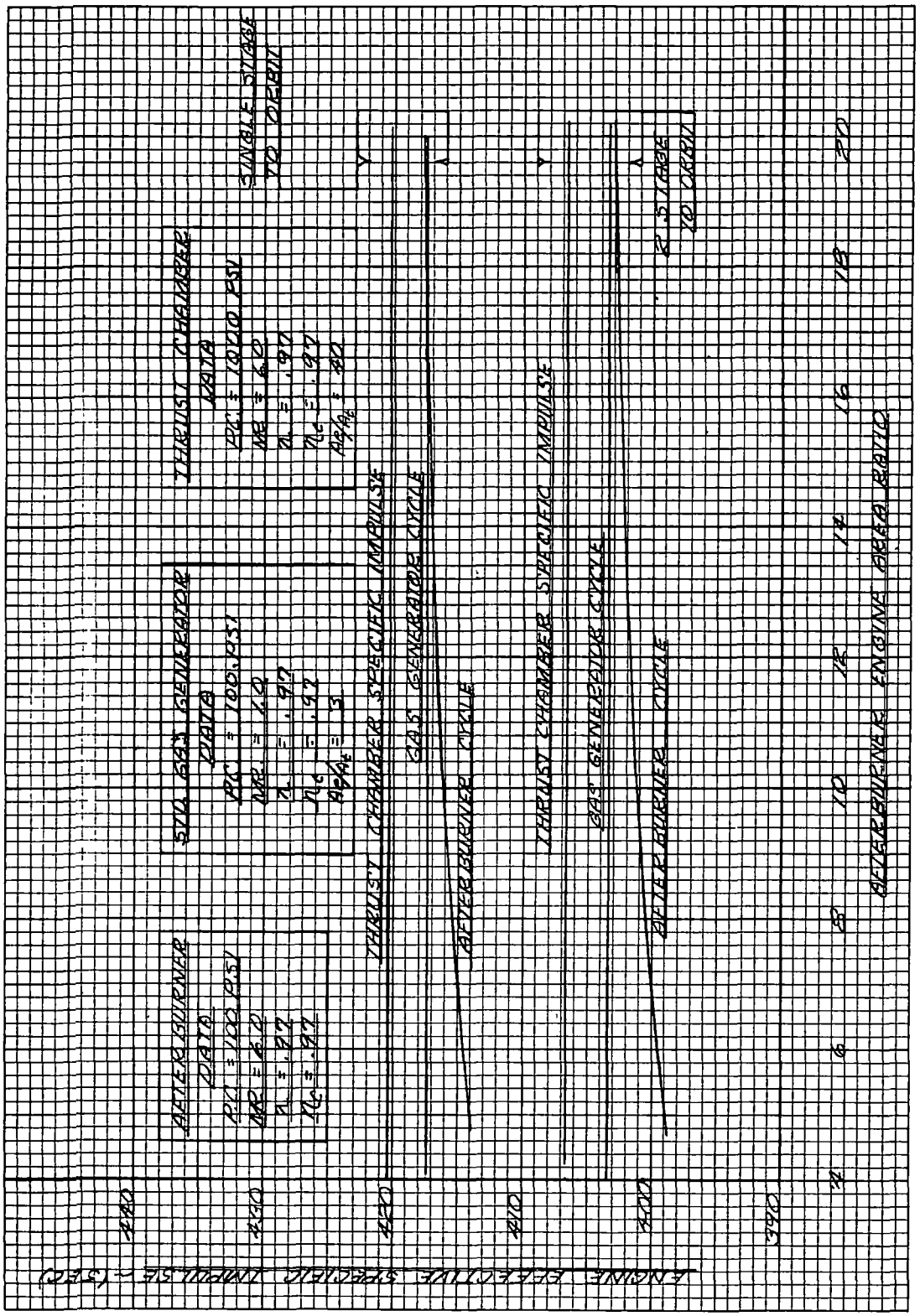

Figure II E-27

Performance Comparison of Gas-Generator and Afterburner Cycles

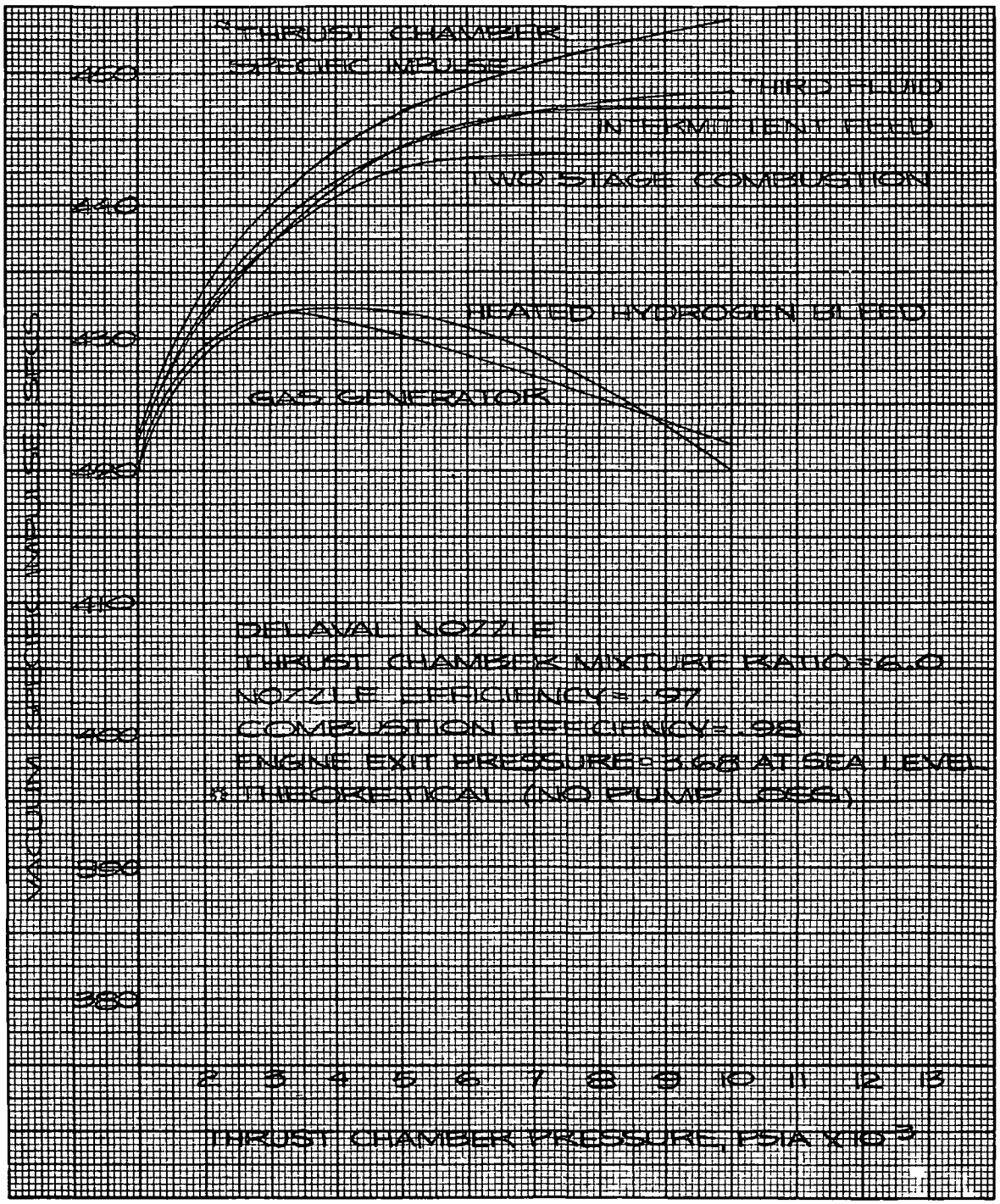

Engine Vacuum I_s versus Thrust-Chamber Pressure
for Various Engine Cycles--DeLaval Nozzle

Figure II E-28

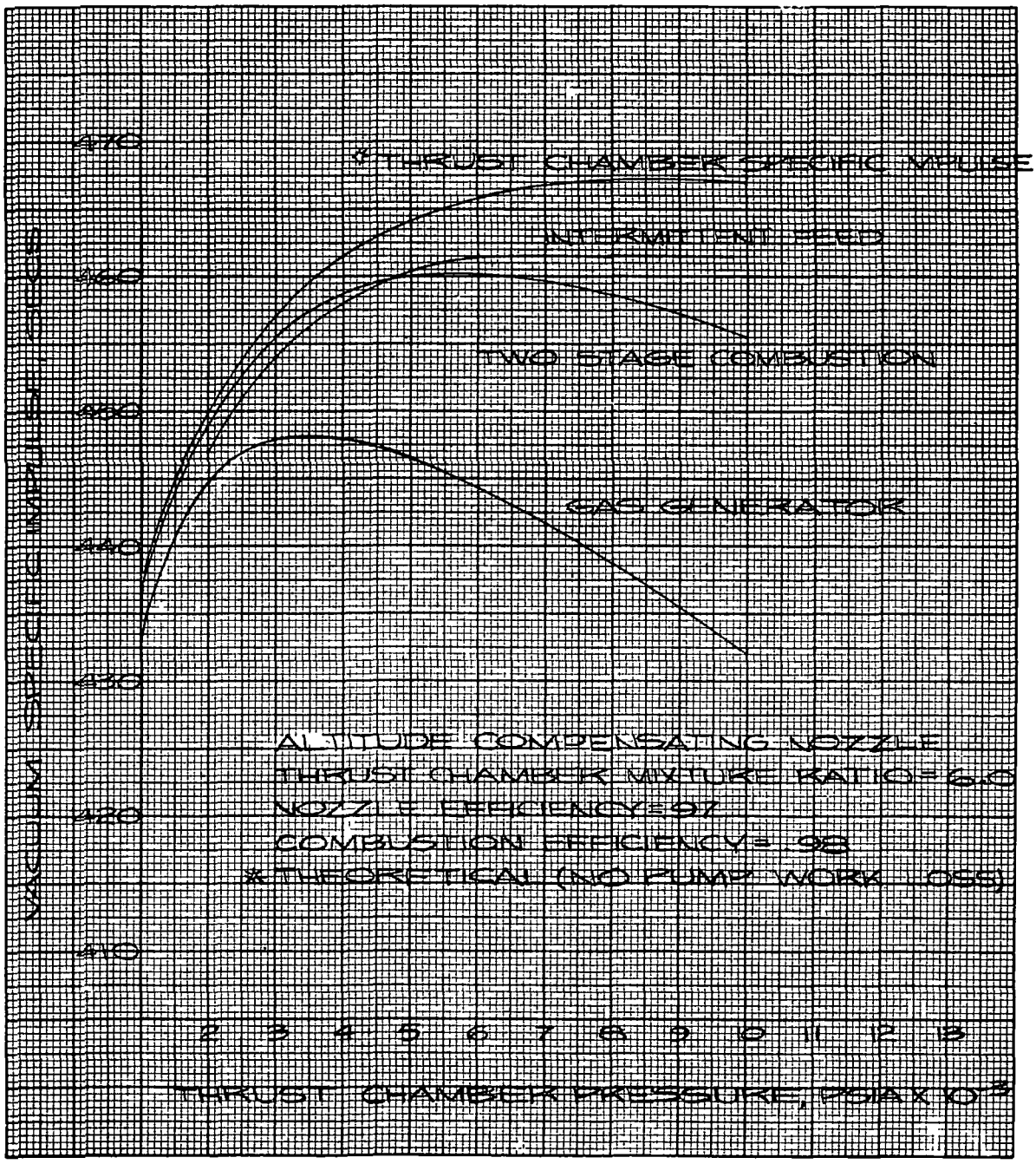

Engine Vacuum I_s versus Thrust-Chamber Pressure
for Various Engine Cycles--Altitude-Compensating Nozzles

Figure II E-29

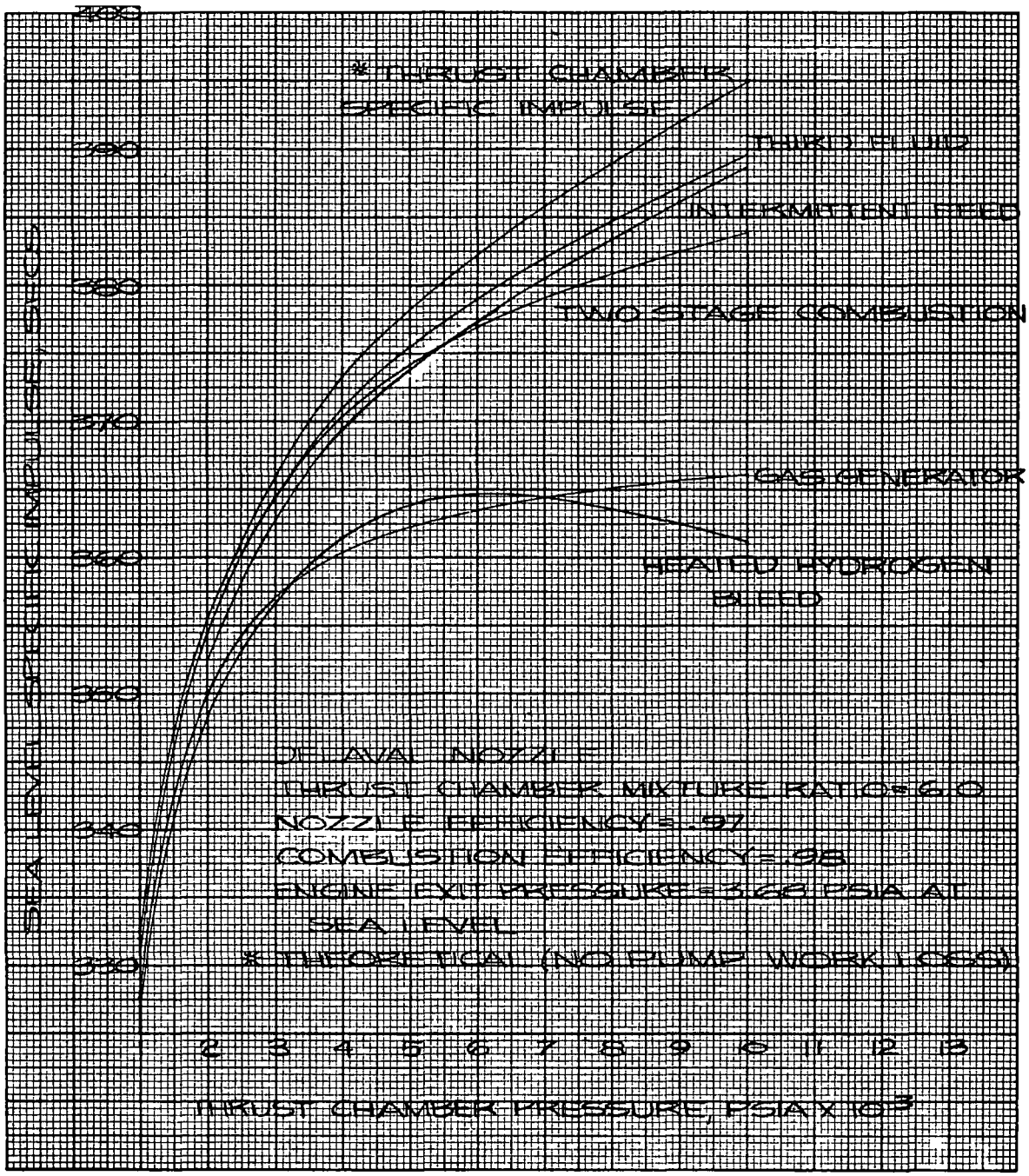

Engine Sea-Level I_s versus Thrust-Chamber Pressure for Various Engine Cycles--DeLaval Nozzle

Figure II E-30

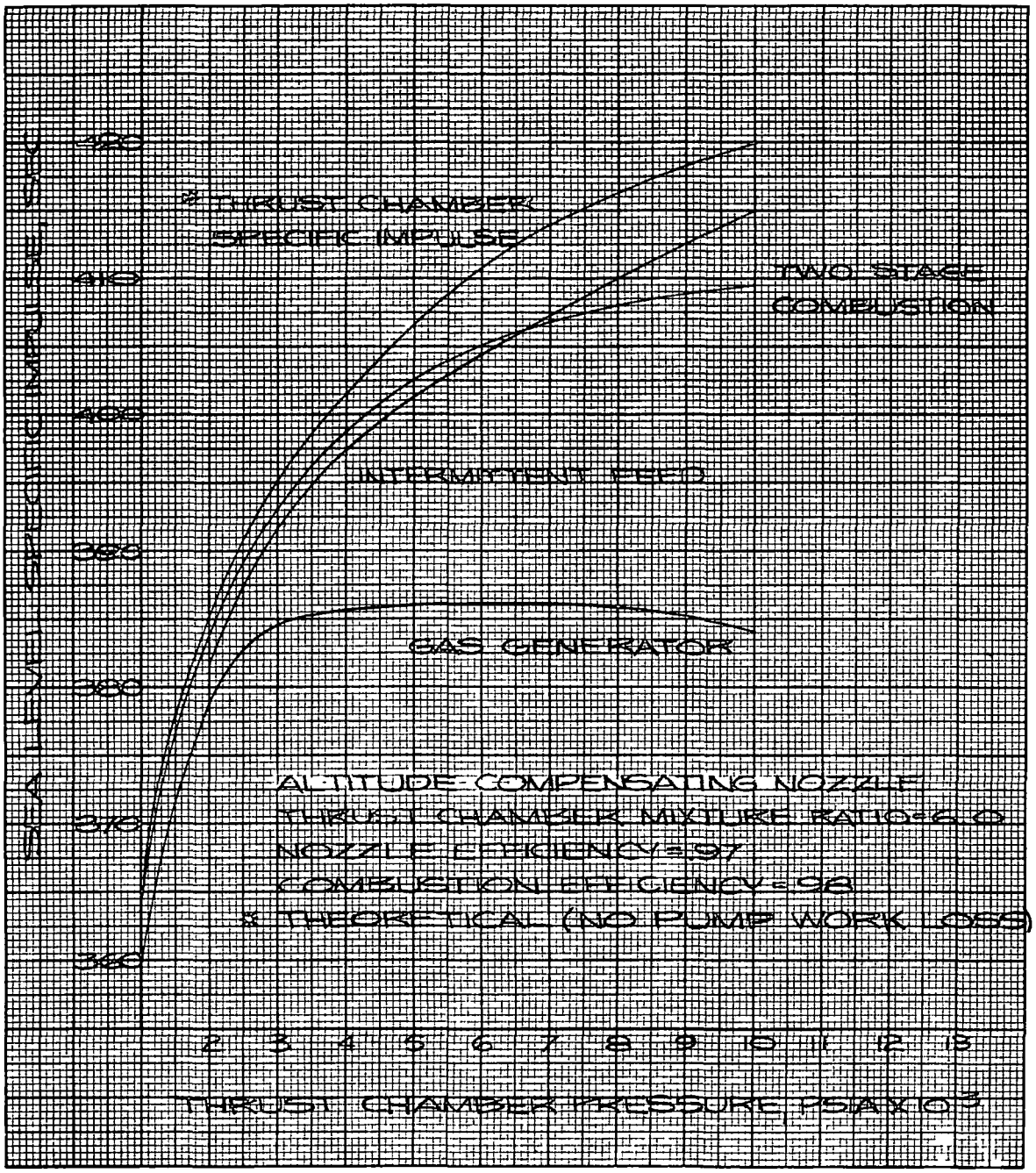

Engine Sea-Level I_s versus Thrust-Chamber Pressure for Various Engine Cycles--Altitude-Compensating Nozzles

Figure II E-31

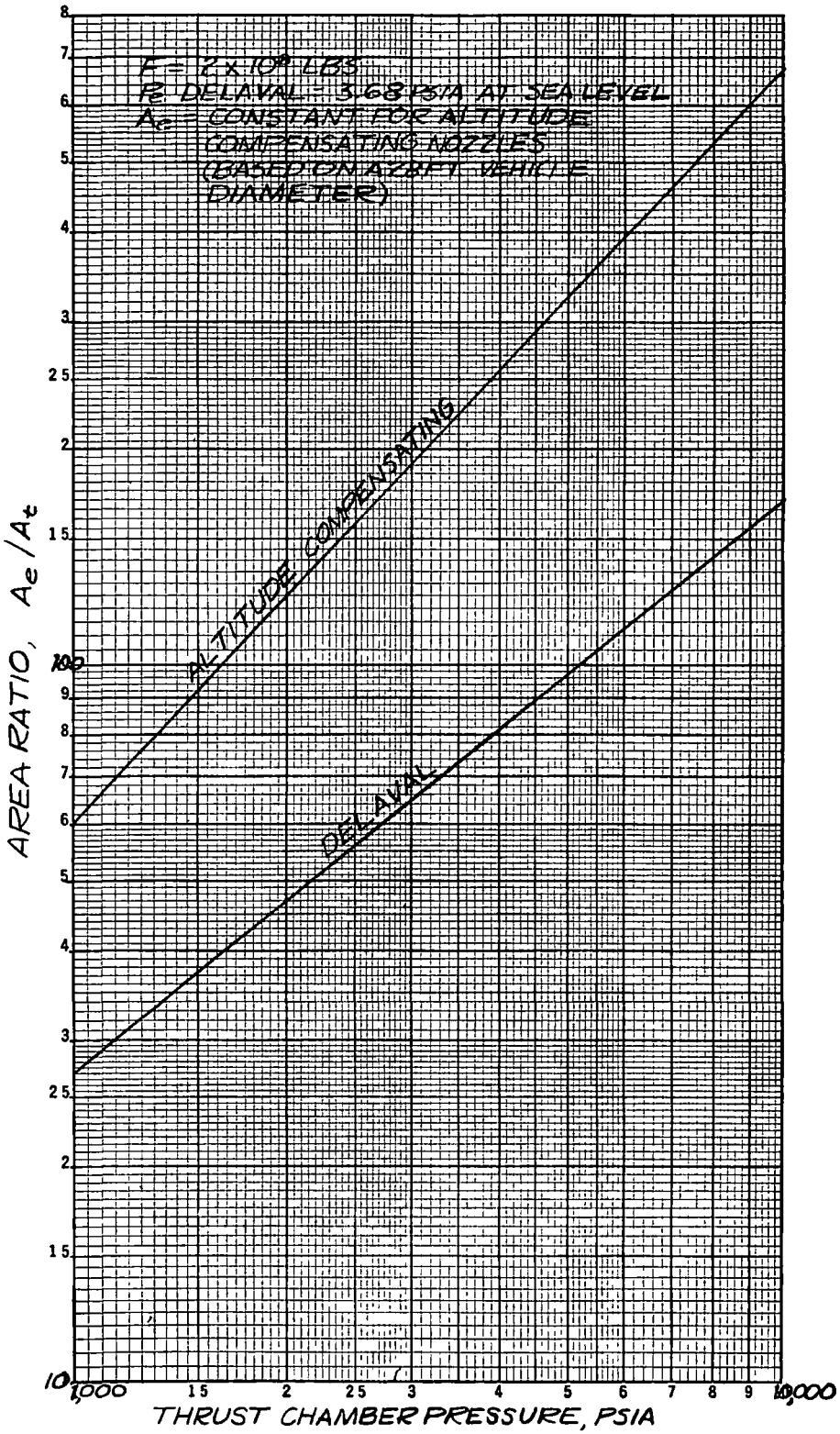

Area Ratio vs Thrust-Chamber Pressure

Figure II E-32

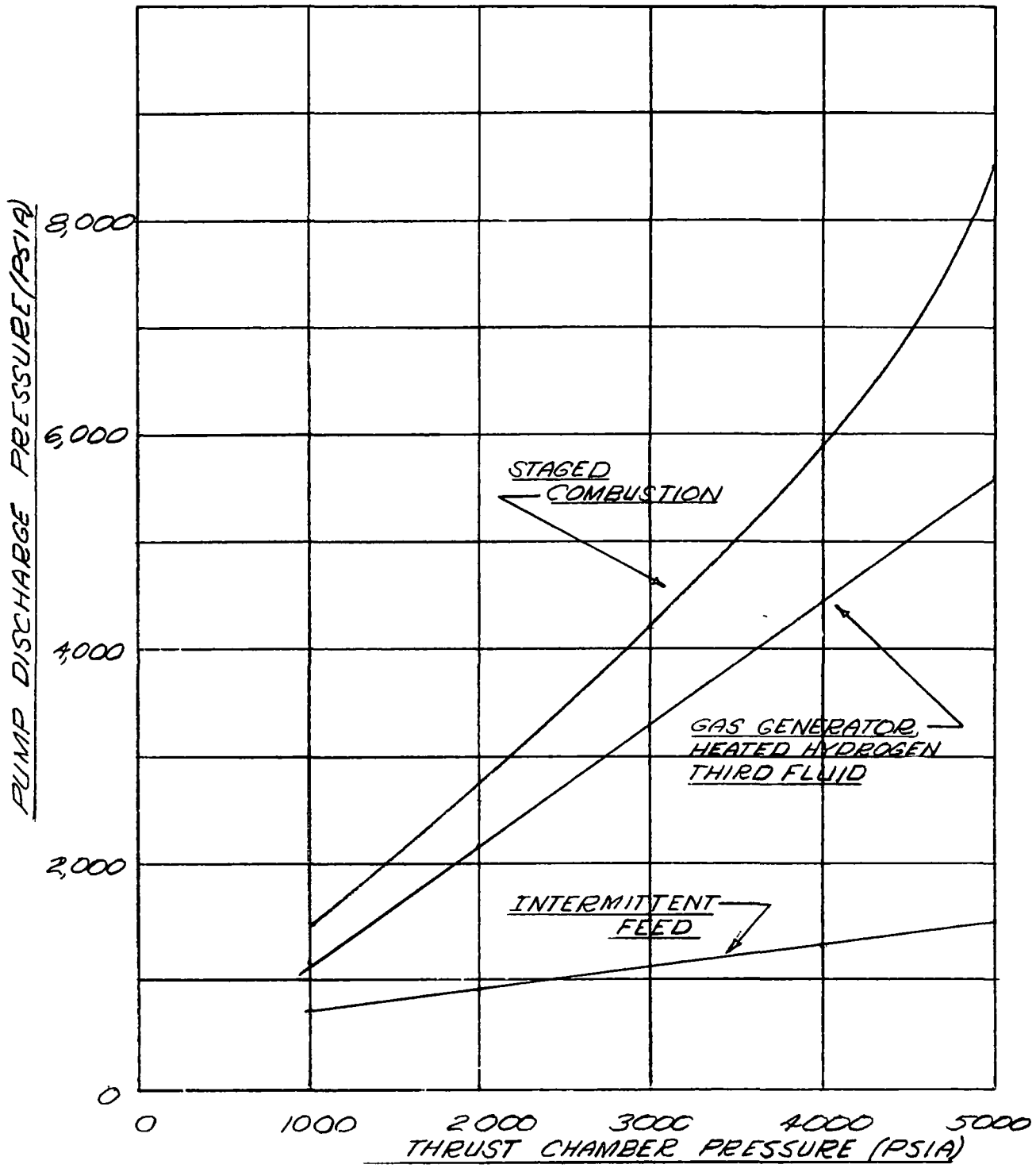

Pump Discharge Requirements for Various Engine Cycles

Figure II E-33

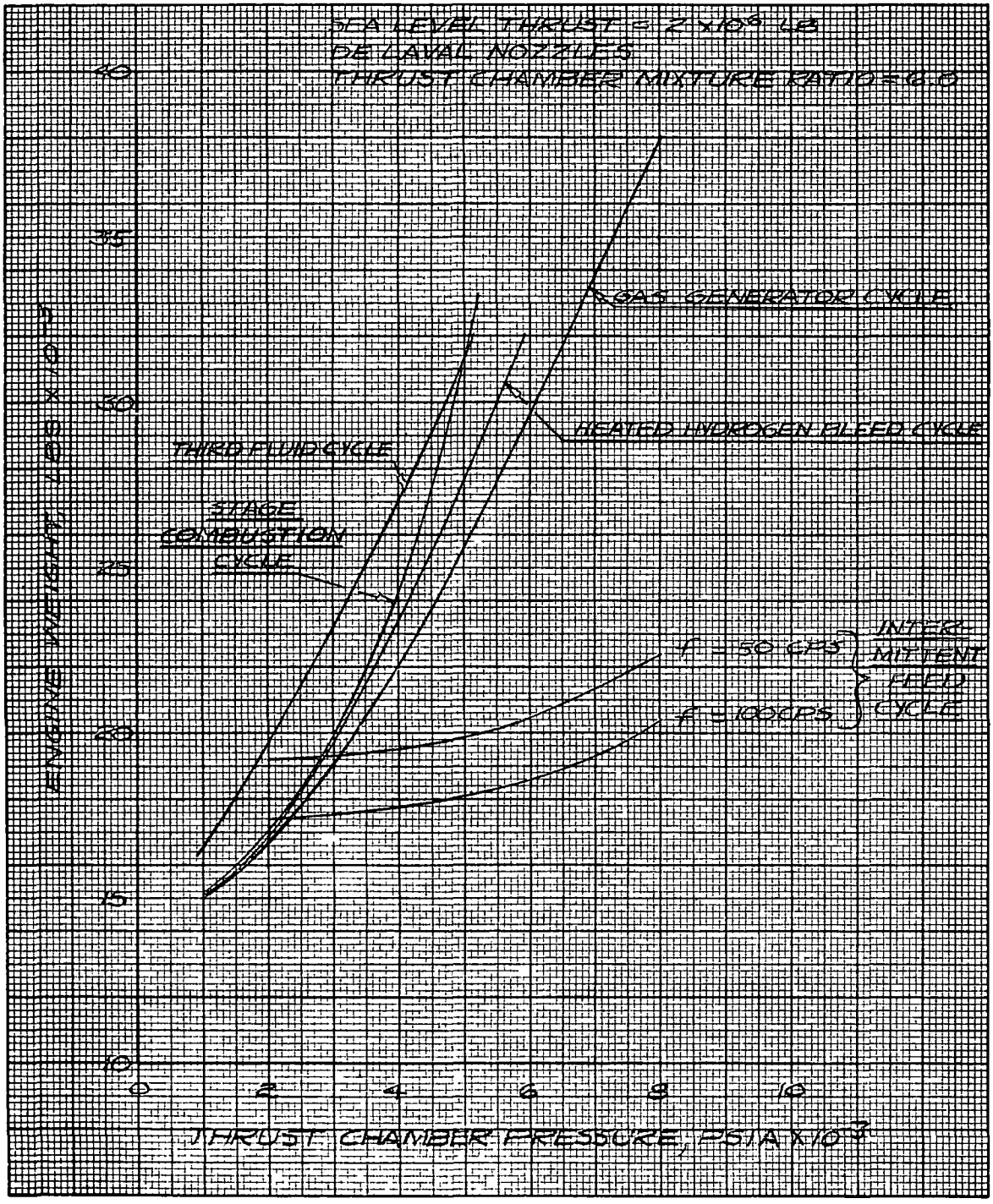

Engine Weight versus Thrust-Chamber Pressure, DeLaval Nozzle

Figure II E-34

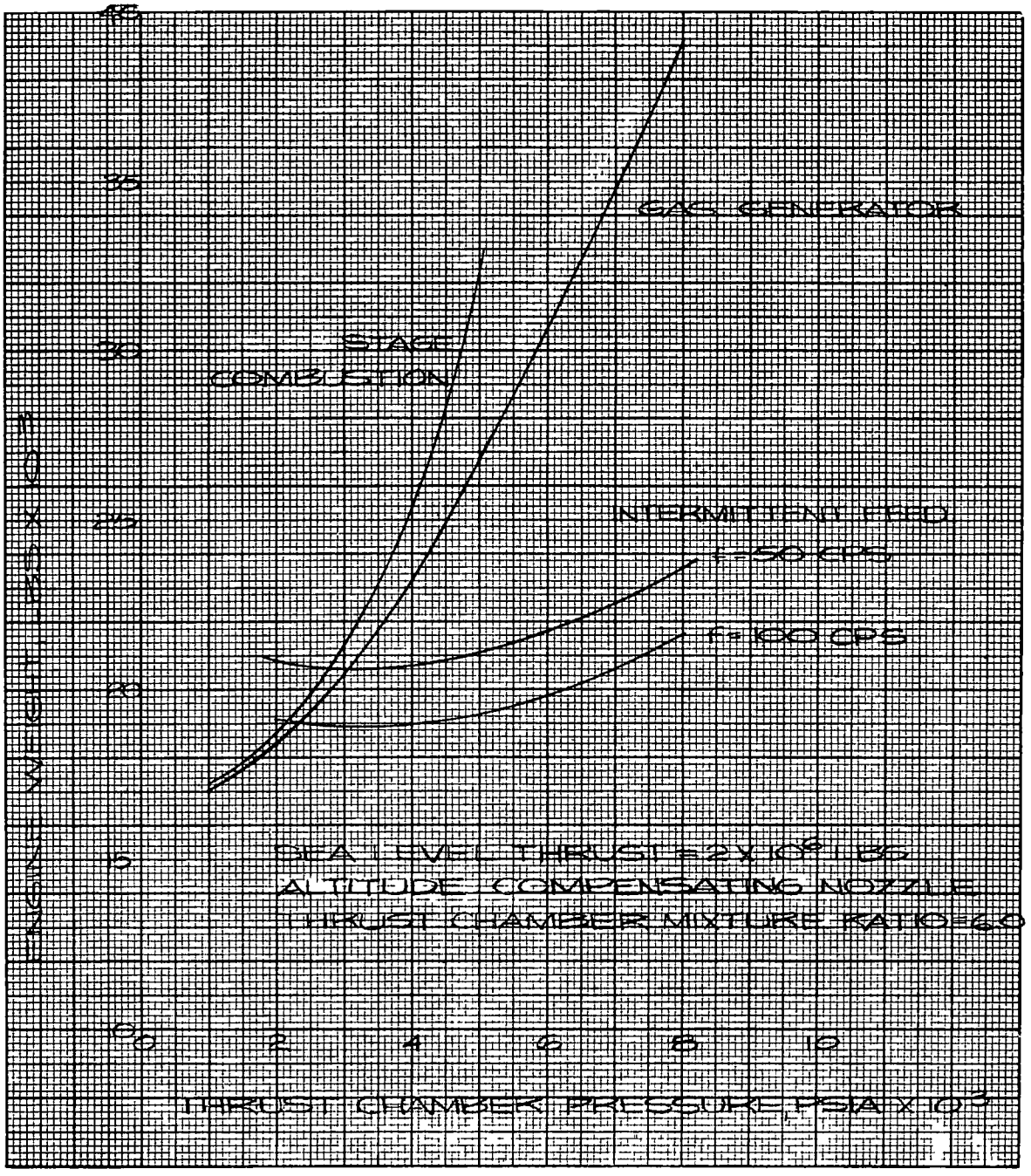

Engine Weight versus Thrust-Chamber Pressure,
Altitude-Compensating Nozzles

Figure II E-35

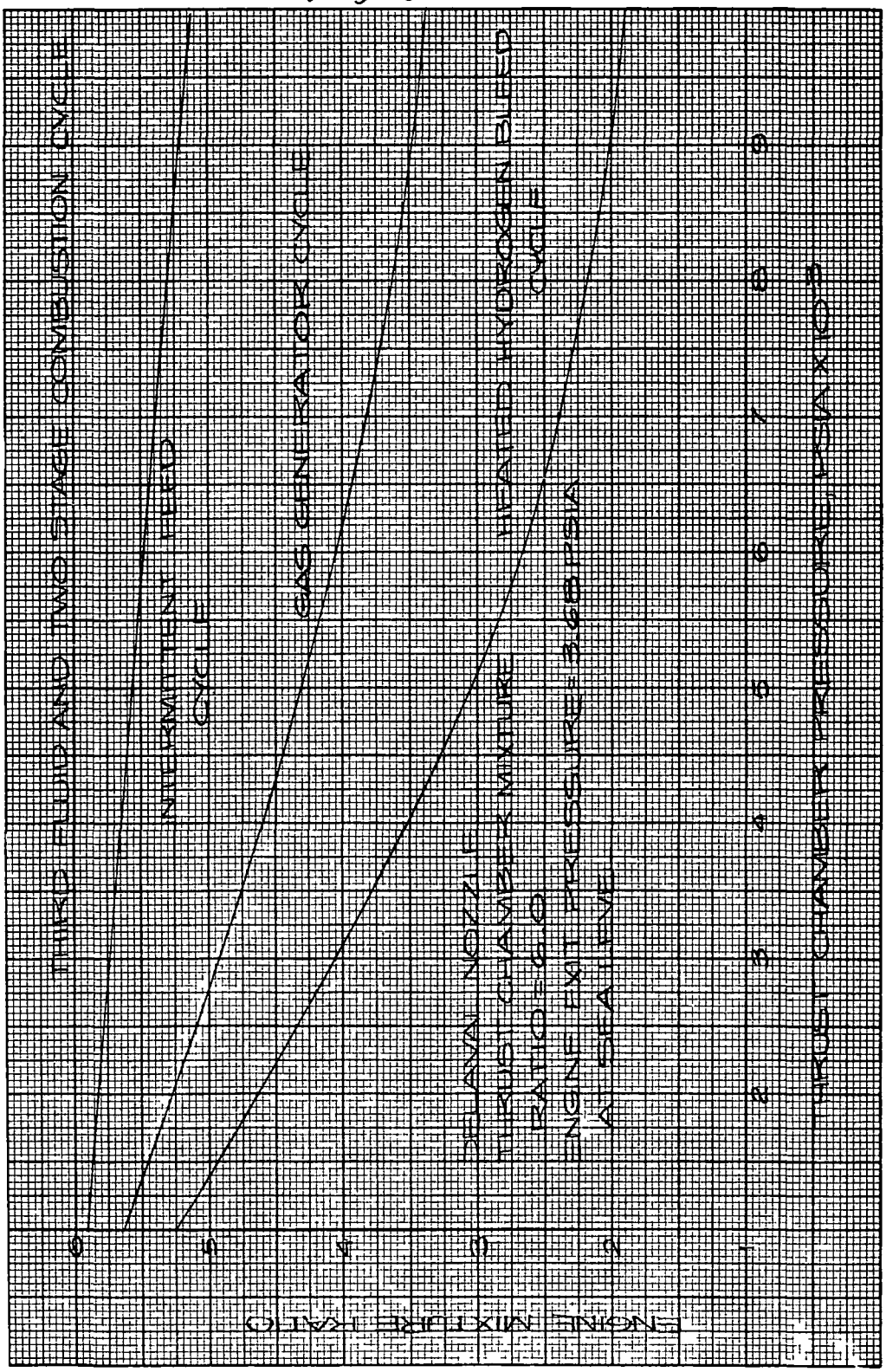

Engine Mixture Ratio versus Thrust-Chamber Pressure for Various Engine Cycles--DeLaval Nozzle

Figure II E-36

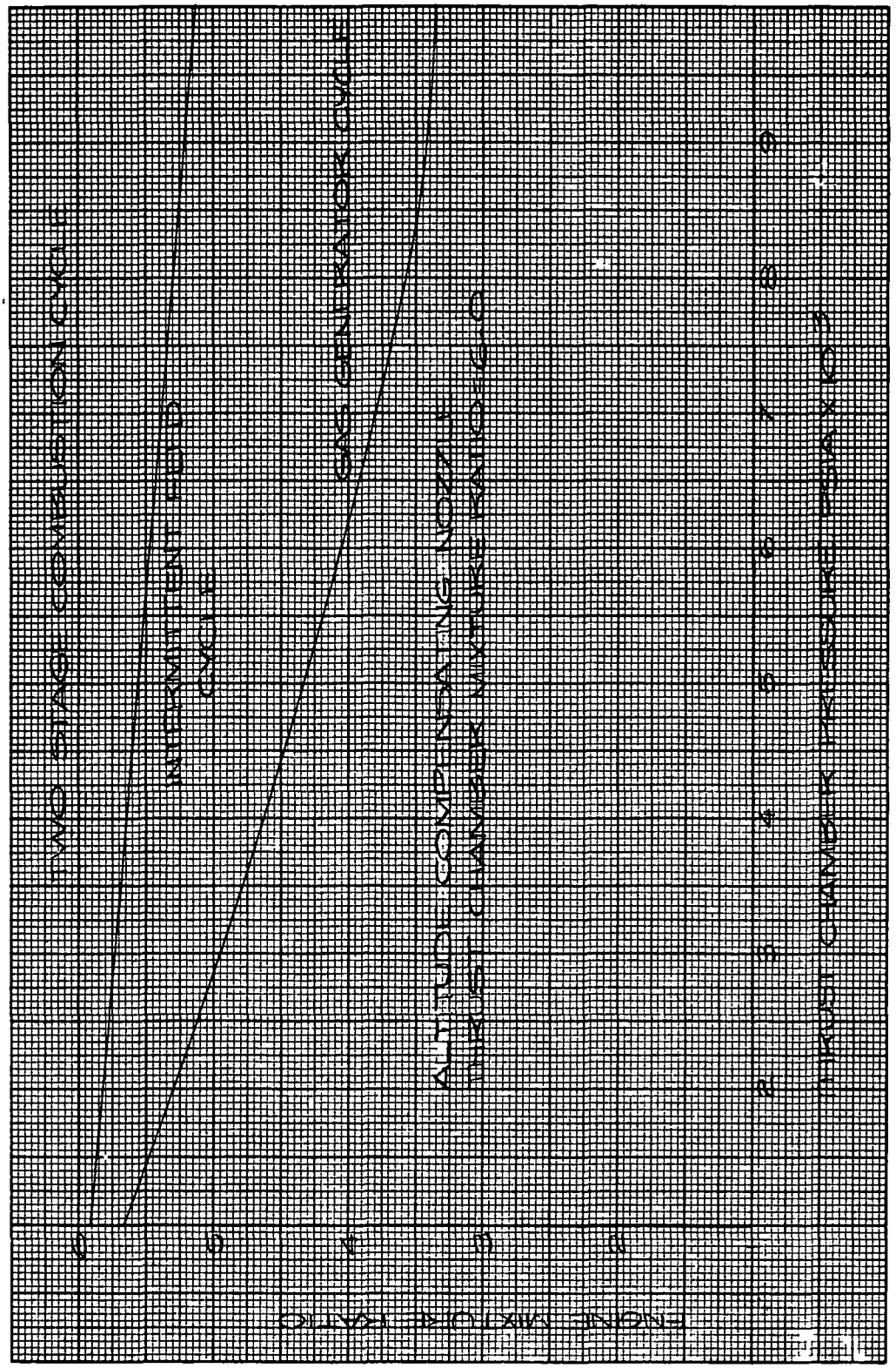
ENGINE MIXTURE RATIO
0
2
4
6
8
10
12
CHAMBER PRESSURE, PSIA
0
100
200
300
400
500
600
700
800
900
1000
1100
1200
1300
1400
1500
1600
1700
1800
1900
2000
2100
2200
2300
2400
2500
2600
2700
2800
2900
3000
3100
3200
3300
3400
3500
3600
3700
3800
3900

II, Concepts Considered (cont.)

F. ENGINE CONFIGURATIONS

1. Introduction and Summary

Various engine configurations were evaluated to determine if a significant increase in performance, greater reliability, decrease in weight, or reduction in cost could be attained over the standard De Laval configuration. The investigation of engine cycles showed that major payload increases are mainly reached by using engine configurations having altitude compensating nozzles and large maximum area ratios. Therefore, the major emphasis of the engine configuration investigation was placed upon engine designs having these features.

The nozzle concepts evaluated included the De Laval, forced-deflection, plug, and reverse flow Designs were generated to incorporate these nozzle concepts into integrated engine systems. To establish a basis for comparison, all initial engine designs incorporated the standard gas generator cycle operating at a thrust chamber pressure of 1,000 psi and a mixture ratio of 6:1. The engine configurations were then evaluated with respect to the various engine cycles discussed in Section II, E. The adaptability of the engine configurations to cluster applications was also included. A final comparison was made of the most promising combination of engine configurations and cycles. Results of this evaluation are presented in Section IV, which is a discussion of the best unconventional system.

The weight summary for the engine configurations evaluated, together with the propellant tankage and subsystems required for a complete stage, is shown in Table II F-1. Also included are several special adaptations of the engines to specific engine cycles, tankage, and single-stage-to-orbit vehicles. Standard booster tank volumes were used for all O_2/H_2 two-stage

II, F, Engine Configurations (cont.)

vehicles. The O_2/H_2 single-stage-to-orbit vehicle tankage was established for a 300-nm orbit by using a 2,000,000-lb thrust (sea level) booster and a 1.25:1 thrust-to-takeoff weight ratio. The O_2/RP-1 tankage was established for optimum staging based on maximum payload, using an O_2/H_2 second stage to deliver the same payload as the standard vehicle. Weights shown were used to establish mass drop parameters used in the trajectory calculations (see Section III, B).

The vented forced-deflection engine proved to be the best of all engine configurations. The altitude compensation feature provides near optimum performance throughout the vehicle trajectory. Engine weight is lower than all other altitude compensating designs evaluated, and the use of multiple combustors allows combustor development to be performed at a lower thrust level, thereby reducing development costs.

2. Configurations Considered

a. De Laval

A conventional De Laval engine configuration with a single thrust chamber was used as a basis for comparison with all other engine configurations evaluated in this study, and it was used in the engines of the standard vehicle. A complete engine description, together with physical and performance data, is given in the discussion of the standard vehicle (Section III, A of this volume).

In complying with the major objectives of this study, as generated from the over-all study philosophy, engine configurations offering higher performance, higher reliability, and lower development cost were of primary interest. Lower weight and reduced production cost were secondary

TABLE II F-1

WEIGHT SUMMARY FOR VARIOUS PROPULSION SYSTEMS

COMPONENT	STANDARD DELAVAL, A_e/A_t = 20 B11STF61-520 DRY	OXID	FUEL	WET	FORCED DEFLECTION, A_e/A_t = 60 B11STF61-547 DRY	OXID	FUEL	WET	PLUG NOZZLE, A_e/A_t = 54 B11STF61-519 DRY	OXID	FUEL	WET
W_2 GUIDANCE	——	——	——	——	——	——	——	——	——	——	——	——
W_3 TANKAGE & AIRFRAME	37,360	5000	——	42,360	34,785	5,000	——	39,785	37,630	5000		42,630
OXIDIZER TANK	5876	——	——	5876	5876	——	——	5876	5876	——	——	5876
FUEL TANK	25,468	——	——	25,468	22,468	——	——	22,468	23,520	——	——	23,520
FUEL TANK INSULATION	320	——	——	320	320	——	——	320	320	——	——	320
OXIDIZER SUCTION LINE	350	5,000	——	5,350	700	5,000	——	5700	700	5000	——	5700
ANTI SLOSH & VORTEX	1,000	——	——	1,000	1,000	——	——	1,000	1,000	——	——	1,000
ENGINE THRUST STRUCTURE	675	——	——	675	750	——	——	750	2,543	——	——	2,543
PRE VALVE (2)	100	——	——	100	100	——	——	100	100	——	——	100
TANK LEVEL SENSOR	50	——	——	50	50	——	——	50	50	——	——	50
ELECTRICAL & MISC	46	——	——	46	46	——	——	46	46	——	——	46
FAIRINGS & INTERSTAGE STRUCTURE	3445	——	——	3,445	3,445	——	——	3,345	3,445	——	——	3,445
FUEL SUCTION LINE	30	——	——	30	30	——	——	30	30	——	——	30
INTEGRATING STRUCTURE	——	——	——	——	——	——	——	——	——	——	——	——
W_4 ENGINE	13572	2624	211	16,407	12,227	3,006	156	15,389	17,823	4488	134	22,439
THRUST CHAMBER	7,195	304	116	7915	(1) 4,039	352	146	(1) 7,334	(1) 10,528	352	84	(1) 10,944
PUMPS	(10) 3,210	860	35	4105	(2) 4,465	944	10	(2) 5,419	(3) 4085	840	10	(3) 4,935
GAS GENERATOR	(4) 450	——	——	(4) 450	(5) ——	——	——	(5) ——	(5) ——	——	——	(5) ——
ADDITIONAL ENGINE COMPONENTS	2417	1,460	60	3937	924	1,710	——	2634	3230	3290	40	6,560
BATTERY	40	——	——	40	40	——	——	40	40	——	——	40
SEQUENCE UNIT	20	——	——	20	20	——	——	20	20	——	——	20
GIMBAL ACTUATORS	172	——	——	172	——	——	——	——	——	——	——	——
SUCTION LINE	500	1,30	50	1860	(6) 160	1,710	——	(6) 1,870	(6) 160	1710	——	(6) 1,870
DISCHARGE LINES	400	150	10	560	(7) ——	——	——	(7) ——	2275	1,580	40	3875
TURBINE EXHAUST	100	——	——	100	257	——	——	257	350	——	——	350
ELECTRICAL & CONTROL HARNESS	25	——	——	25	35	——	——	35	45	——	——	45
MISC	1070	——	——	1,070	——	——	——	——	——	——	——	——
ROLL CONTROL NOZZLE & ACTUATOR	90	——	——	90	90	——	——	90	90	——	——	90
VECTOR NOZZLES & MANIFOLD	——	——	——	——	322	——	——	322	250	——	——	250
W_5 PRESSURE SYSTEM	(8) 8443	——	——	(8) 8,443	(8) 8,443	——	——	(8) 8,443	(8) 8443	——	——	(8) 8,443
W_6 FILL & VENT SYSTEM	(9) 207	——	——	(9) 207	(9) 207	——	——	(9) 207	207	——	——	(9) 207
W_7 RECOVERY EQUIPMENT	——	——	——	——	——	——	——	——	——	——	——	——
W_8 UNUSEABLE PROPELLANT	——	1,860	330	2,190	——	1,860	330	2,190	——	1,860	330	2,190
W_9 EXPECTED PROPELLANT CONSUMPTION	——	930,825	164,426	1,095,251	——	930,825	164,426	1,095,251	——	930,825	164,426	1,045,251
TOTAL BOOSTER WEIGHT	59,582	940,309	164,967	1,164,858	55,662	940,691	164,912	1,161,265	64,103	942,107	164,840	1,171,160
STAGE MASS FRACTION				940				943				945

CONFIDENTIAL

TABLE II F-1 (cont.)

COMPONENT	REVERSE FLOW, A_e/A_t 60 8115TFG1-536 DRY	OXID	FUEL	WET	MODULAR BOOSTER 4-500K DELAVAL, A_e/A_t 20 8115TF61-560 DRY	OXID	FUEL	WET	SINGLE STAGE TO ORBIT VEHICLE TWO STAGE COMBUSTION-FF-0.3000 Pc 8115TFG-580 A_e/A_t = 190 DRY	OXID	FUEL	WET	2700 K THRUST STANDARD DE LAVAL - O_2/RP-1 A_e/A_t =16 DRY	OXID	FUEL	WET
W_1 GUIDANCE	—	—	—	—	—	—	—	—	—	—	—	—	—	—	—	—
W_2 TANKAGE & AIRFRAME	35,837	5,000	—	40,837	49,330	5,000	—	54,330	40,869	5,000	—	45,869	30,083	5,850	—	35,933
OXIDIZER TANK	5876	—	—	5876	6,310	—	—	6,310	7651	—	—	7651	9,699	—	—	9,699
FUEL TANK	23,520	—	—	23,520	28,660	—	—	28,660	26,587	—	—	26,587	14,773	—	—	14,773
FUEL TANK INSULATION	320	—	—	320	640	—	—	640	400	—	—	400	—	—	—	—
OXIDIZER SUCTION LINE	700	5,000	—	5,700	700	5,000	—	5,700	700	5,000	—	5,700	325	5,850	—	6,175
ANTI SLOSH & VORTEX	1,000	—	—	1,000	1000	—	—	1000	1100	—	—	1,100	800	—	—	800
ENGINE THRUST STRUCTURE	750	—	—	750	750	—	—	750	750	—	—	750	965	—	—	965
PREVALVE (2)	100	—	—	100	100	—	—	100	100	—	—	100	100	—	—	100
TANK LEVEL SENSOR	50	—	—	50	100	—	—	100	60	—	—	60	45	—	—	45
ELECTRICAL & MISC	46	—	—	46	35	—	—	35	46	—	—	46	46	—	—	46
FAIRINGS & INTERSTAGE STRUCTURE	3,445	—	—	3,445	6,250	—	—	6,250	3,445	—	—	3,445	3,300	—	—	3,300
FUEL SUCTION LINE	30	—	—	30	30	—	—	30	30	—	—	30	30	—	—	30
INTEGRATING STRUCTURE	—	—	—	—	1755	—	—	1755	—	—	—	—	—	—	—	—
W_4 ENGINE	12,027	2,917	209	15,153	13,974	1951	171	16,096	18341	3142	125	21,608	15,150	2776	2,940	20,866
THRUST CHAMBER	(1) 6,830	352	184	(1) 7,366	7,974	381	101	8456	9,809	182	105	10,096	7660	306	1160	9,126
PUMPS	(2) 1,085	840	10	(2) 1935	2,990	345	25	3,360	(10) 7,885	1250	20	(10) 9125	4570	1,160	830	6,560
GAS GENERATOR	(5) —	—	—	(5) —	—	—	—	—	—	—	—	—	450	—	—	450
ADDITIONAL ENGINE COMPONENTS	1,112	1725	15	2852	3,010	1,225	45	4,280	671	1,710	—	2,387	2,470	1,310	950	4,730
BATTERY	40	—	—	40	40	—	—	40	50	—	—	50	40	—	—	40
SEQUENCE UNIT	20	—	—	20	30	—	—	30	20	—	—	20	20	—	—	20
GIMBAL ACTUATORS	—	—	—	—	275	—	—	275	—	—	—	—	200	—	—	200
SUCTION LINE	180	1550	—	1730	750	1100	40	1890	(6) 160	1,710	—	(6) 1,870	500	1310	500	2,310
DISCHARGE LINES	125	175	15	315	600	125	5	730	(7) —	—	—	(7) —	400	—	450	850
TURBINE EXHAUST	300	—	—	300	200	—	—	200	—	—	—	—	125	—	—	185
ELECTRICAL & CONTROL HARNESS	35	—	—	35	45	—	—	45	35	—	—	35	25	—	—	25
MISC	—	—	—	—	1,070	—	—	1070	—	—	—	—	1070	—	—	1,070
ROLL CONTROL NOZZLE & ACTUATOR	90	—	—	90	—	—	—	—	90	—	—	90	90	—	—	90
VECTOR NOZZLES & MANIFOLD	322	—	—	322	—	—	—	—	382	—	—	382	—	—	—	—
W_5 PRESSURE SYSTEM	(8) 8,443	—	—	(8) 8,443	(8) 8,443	—	—	(8) 8443	(8) 8539	—	—	(8) 8539	(8) 7,069	—	—	(8) 7,069
W_6 FILL & VENT SYSTEM	(9) 207	—	—	(9) 207	(9) 207	—	—	(9) 207	(9) 207	—	—	(9) 207	(9) 208	—	—	(9) 208
W_7 RECOVERY EQUIPMENT	—	—	—	—	—	—	—	—	—	—	—	—	—	—	—	—
W_8 UNUSABLE PROPELLANT	—	1,860	330	2,190	—	1,860	330	2,190	—	2,450	350	2,800	—	2,140	892	3,032
W_9 EXPECTED PROPELLANT CONSUMPTION	—	930,825	164,426	1095,251	—	930,825	164,426	1,095,251	—	1226 490	175,210	1401, 700	—	1070,700	446,100	1,516,800
TOTAL BOOSTER WT	56,514	940,602	164,965	1,162,081	71,954	939,636	164,927	1,176,517	67956	1,233,082	175,685	1,480,723	52,510	1081,466	449938	1,583 908
STAGE MASS FRACTION				942				931				947				953

TABLE II F-1 (cont.)

(1) Weight (450 Lbs) of discharge valves included in pumps.

(2) Includes weight (345 Lbs) of thrust chamber injectors; pump discharge lines and oxidizer suction lines. The lines plus fluids amount to 471 lbs. Also includes weight of 450 lbs for discharge valves.

(3) Weight of thrust chamber injectors and pump discharge lines not included.

(4) Weight of start cartridge only. Weight (230 Lbs) of gas generator included in pump weights.

(5) Weight (230 Lbs) of gas generator included in pump weights.

(6) 47 Lbs included in pump weights.

(7) Entire weight included in pump as part of basic pump structure.

(8) Includes 1,330 lbs of hydrogen gas remaining at end of run.

(9) Tankage backfilled through oxid and fuel suction lines, therefore no additional weight allowance is required for these lines.

(10) Includes weight of 1,010 lbs for pump discharge pressure equalizing lines to balance radial hydraulic forces on pump impeller.

(11) Turbopump assembly weights do not include injector weight allowances.

II, F, Engine Configurations (cont.)

considerations. DeLaval engine configurations, other than the standard, were evaluated for potential improvements and are discussed as follows.

(1) Engines with DeLaval Altitude-Compensating Nozzle

Increased engine performance is achieved mainly by using altitude-compensating nozzles with large, maximum area ratios. Evaluation programs are currently underway for modifying the standard DeLaval nozzle design to incorporate altitude compensation. Such a nozzle would provide near-optimum performance at all altitudes and enable much larger maximum area ratios than normally obtainable. This is especially advantageous for single-stage-to-orbit missions. Several configurations have been conceived, including the stepped nozzle, a nozzle with a plug insert, and a nozzle with separation controlled by gas injection. These are detailed in the nozzle concepts discussion (Section II, I). If one of these nozzles proves technically and economically feasible, the altitude-compensated DeLaval engine may be competitive with other engine types conceived during this study at the lower thrust levels (up to 2,000,000 lb). The main limitation for such a configuration, as with any single combustor high thrust unit, is that scaling-up is very costly because of the required thrust chamber development.

(2) Clustered DeLaval Engines

A cluster of DeLaval engines to form a higher thrust unit offers no performance gain over a single DeLaval engine. Clustering studies showed that a slight cost advantage may result from developing a number of smaller units instead of a single unit. However, the cost difference is not significant. A detailed discussion of this subject is presented in Section II, C.

II, F, Engine Configurations (cont.)

Clustered engines are heavier than a single unit because of the structure required to connect them together and to the airframe. Also, utilization of the vehicle exit area is not as efficient because of the space between engines. This is important for larger thrust units, because the exit area of the engine nozzle varies as the two-thirds power of thrust (for given vehicle L/D). For example, at 1,000 P_c, the maximum area ratio which can be contained under the vehicle diameter is 66 (single chamber). At 6,000,000-lb thrust, this maximum area ratio is reduced to 40:1.

(3) Clustered DeLaval Thrust Chambers

An engine configuration using one set of turbopumps and four DeLaval thrust chambers (Figure II F-1) was evaluated. As with clustered engines, there was no performance gain with this engine. Furthermore, many long propellant lines are required, which is undesirable from the engine control and reliability aspects. It was concluded that this configuration offers no improvement over the standard engine.

b. Forced-Deflection Engine

(1) Description

The forced-deflection engine is an altitude-compensating engine that provides near-optimum expansion of the combustion gases within the atmosphere. This expansion takes place between a forced-deflection nozzle outer boundary and an ambient pressure core. Presence of atmospheric pressure within the nozzle provides an elastic wall, against which the gases expand. As ambient pressure decreases with altitude, the exhaust gases automatically vary their expansion ratio, maintaining a near-optimum rate of expansion from sea level to vacuum.

II, F, Engine Configurations (cont.)

Various design configurations of forced deflection nozzle engines were evaluated. Configurations of the major components were selected from the results of the component design studies (discussed in Section II, G through II, N of this volume) and their applicability to the over-all engine integration.

The engine consists of eight thrust chamber sub-assemblies circumferentially located around oxidizer and fuel turbopumps. Each turbopump is driven by its own single, bipropellant gas generator. The combustors are of conventional design to an area ratio of 2:1. A transition section follows until, at an area ratio of 20:1, the individual thrust chamber nozzle contours blend together to form a single skirt. This skirt extends out to the over-all area ratio of 60:1, coinciding with the vehicle diameter.

The engine is rigidly connected to the airframe, except for bellows in the pump suction lines to compensate for thermal expansion and engine misalignment. Thrust-vector control is obtained by secondary injection of turbine exhaust into the main thrust chamber nozzle. Roll control is provided by expanding a small amount of turbine exhaust gas through a two-way nozzle located on the base of the engine skirt.

The engine assembly and flow schematics are shown in Figure II F-2 and II F-3 respectively.

II, F, Engine Configurations (cont.)

(2) Summary

The forced-deflection principle offers four primary advantages over conventional DeLaval designs: (1) near-optimum performance throughout the flight is obtained, (2) the nozzle allows maximum utilization of area ratio without separation and low altitude performance losses, (3) the nozzle is shorter for a given area ratio than the DeLaval, and (4) structural requirements are reduced in comparison to the plug nozzle because the high pressure area occurs in the portion of the nozzle where the diameter is small, whereas the converse is true with the plug.

The discrete throat forced-deflection principle offers further advantages. The subassembly concept rather than one large diameter torus results in lower weight, improved combustion stability, and earier control of throat area. Multiple combustor designs are particularly advantageous for engines with greater than 2,000,000-lb thrust because development of the individual thrust chamber is completely within current technology and can be accomplished using available manufacturing facilities.

Another advantage of the proposed design is that the use of gas injection for thrust-vector control eliminates the gimbal and permits transmission of the thrust loads from each chamber directly to the tank bottom. This evenly distributed thrust takeout results in reduced frame weight.

II, F, Engine Configurations (cont.)

The major unknown design parameters of the forced-deflection nozzle include the required nozzle contour, the amount of vent area required to achieve maximum altitude compensation, and, if the discrete throat concept is used, the effect of the interactions between exhaust streams as they blend together. It is not anticipated that any of these parameters will cause performance losses that cannot be eliminated or reduced to a very low level during the development program.

(3) Technical Discussion

(a) Description of Major Components

1 Thrust Chamber Assembly

The thrust chamber assembly consists of eight independent subassemblies connected to a common expansion skirt (area ratio 60:1*). All subassemblies are of identical design. They are bolted together and to the skirt forming the complete thrust chamber assembly. Each module develops approximately 250,000 lb of thrust at sea level.

Component parts of each subassembly include the combustion chamber, adapting nozzle, and injector. The injector, combustion chamber, and nozzle (to an area ratio of 2:1) designs are identical to a conventional regeneratively cooled DeLaval engine. Each subassembly has

*For this engine concept, the exit area is defined as the projected arc of the external expansion portion of the nozzle on a plane normal to the center line of symmetry. Area ratio is, therefore, this projected area divided by the total area of the eight discrete throats.

II, F, Engine Configurations (cont.)

a conical combustion zone, a throat of circular cross section, and a conical expansion portion. The adapting nozzle section extends from an area ratio of 2:1 to an area ratio of 20:1. The eight circular exits flow to a common expansion skirt. This section is formed as a integral part of the combustion chamber and upper nozzle and uses the same regeneratively cooled steel tubes for construction. The tubes in this section are formed to smoothly adapt the chamber section to the skirt section.

The skirt section is constructed of 0.010-in. wall tapered tubes, furnace-brazed together and reinforced with bands located circumferentially around the back of the skirt. Turbine exhaust gases are introduced at the top of the skirt, are ducted down through the skirt tubes to provide cooling for the skirt, and are then collected and used for vector control by gas injection into the main gas stream. When vector control is not required, the gases expand to the atmosphere through a series of small nozzles located on the base of the skirt.

2 Turbopump Assemblies

The pumping system consists of separate fuel and oxidizer turbopumps centrally located in the engine. Each turbopump is driven by its own single bipropellant gas generator.

A further discussion of the turbopump is presented in Section II, K of this volume.

II, F, Engine Configurations (cont.)

3 Engine Controls

Engine control functions include initiation and termination of the main propellant flow, control of propellants into the gas generator, and ignition of propellants in the thrust chamber. A controls schematic of a representative control system is shown in Figure II F-3.

The physical configuration of the forced-deflection engine is particularly adaptable to engine control functions. The close coupling between the turbopump and thrust chamber assemblies results in minimum propellant discharge lines. Control of the main propellant flow can be accomplished by single valves located in each turbopump.

In the engine configuration shown, valves are located in the pump suction inlets and in the discharge lines. The section valves act as pre-valves and can be used in the engine control circuit if desired. Prior to engine start, these valves would be opened, allowing the turbopump to chill-down to cryogenic temperatures. At engine start, the discharge valves are opened, and the engine bootstraps to rated operation using tank head pressure. At engine shutdown, the suction valves are closed after the gas generator valves have started to close, terminating propellant flow. In this system, the shutdown valve does not have to close against high pressure, minimizing valve seal development. If this is not a problem, and pre-valves are not required, the suction valve can be eliminated.

II, F, Engine Configurations (cont.)

The gas-generator valves can be of the conventional butterfly, poppet, or ball valve types and can be currently used designs.

Controls are shown with electromechanical actuators. Because there are no high-power requirements (such as gimbal actuators) the weight penalty associated with electrical systems is not significant. Electrical power is supplied either by a battery or by a small alternator operating off the turbopump. A pneumatic system could also be used, operating on hydrogen tapped from the thrust chamber cooling jackets.

4 Thrust-Vector Control

Thrust-vector control is accomplished by secondary injection of turbine exhaust gas into the jet stream at the base of the main thrust chamber.

In secondary injection systems, a jet of fluid creates a side thrust by its own momentum and most significantly, by the deflecting of the flow of the main exhaust stream. Lateral thrust from the main stream gas flow results from the detached shock wave which forms as a result of the secondary fluid being discharged into the engine nozzle. This shock wave produces an altered boundary layer in front of the secondary jet source, which, in turn, produces a pressure increase over an area of the wall. It is this difference in pressure over that of the opposite nozzle wall that produces lateral thrust.

II, F, Engine Configurations (cont.)

The magnitude of side force is a function of the mass flow of the secondary jet, its specific impulse, and the angle it makes with the axis of the main nozzle. Of prime importance is the position of the detached shock wave.

An analytical study of this subject has been made.*

With the 2,000,000-lb thrust engine system, various means for obtaining fluid for secondary injection were evaluated. It was determined that the turbine exhaust gas is sufficient to provide the required control moment for vehicles which possess aerodynamic static stability. An effective gimbal angle of 1.8° in a plane 45° to the pitch or yaw plane, and an angle in the pitch or yaw plane of 2.5° can be obtained from turbine exhaust injection. If the vehicle is unstable, turbine exhaust gas is sufficient at all times, except during the period when the vehicle passes through excessively high cross winds such as those encountered in the jet stream. The turbine exhaust can be augmented by hydrogen or oxygen to satisfy these peak requirements. The physical design of the vector control system for stabilized vehicles is shown in an engine layout drawing (Figure II F-2).

The thrust-vector control system consists of four valved nozzles, equally spaced around the periphery of the main nozzle exit, to direct fluid into the thrust chamber at 90° to the gas stream. When thrust-vector control is not required, 20 relief valves are arranged around the bottom of the thrust chamber in a half torus section to vent turbine exhaust downward.

*Aerojet-General Corporation, Thrust-Vector Control for Plug Nozzles, Report No. LRP 210, March 1961

II, F, Engine Configurations (cont.)

Gas flow to the nozzles is controlled by an electrically actuated flapper valve. This flapper is located directly in the throat to ensure close flow control. For this application, small amounts of valve leakage will have negligible effects; therefore, no attempt will be made to obtain a perfect seal with the flapper valve.

The relief valves consist of a spring-loaded poppet and a 3:1 nozzle extension. Multiple valves were used instead of fewer larger valves to increase reliability (up to four valves can fail and the system will still operate satisfactorily) and for ease of development. They are made of temperature-resistant stainless steel and attach directly to the flat plate of the half torus placed around the main nozzle exit. Absolute sealing is not necessary for operation; therefore, no sealing is provided other than the metal poppet resting on the metal seat.

Roll control is provided by expanding a small portion of the turbine exhaust gas through a small two-way nozzle located on the base of the thrust chamber skirt. When roll control is not required, the gas flows through the relief valves.

5 Structure and Integration of Engine Components

The mounting structure for the forced-deflection engine is a cone which consists of stringers and sheet aluminum that carry the compression and shear loads.

II, F, Engine Configurations (cont.)

The engine is mounted to the cone at the torus on the thrust chambers where the thrust chamber skirt attaches. (see Figure II F-2). The thrust chambers support the turbopump in the center of the engine.

Thrust chambers are made of cast aluminum-backed stainless steel tubes that can carry the compression and bending loads induced by supporting the turbopump as well as the thrust loads.

The turbopump is attached to the oxidizer and fuel suction lines by flex sections.

An ablative heat shield completely encloses the bottom of the engine. This shield has removable manhole covers to permit easy access to the engine interior.

(c) Performance

Performance calculations for the LO_2/LH_2 propellant combination are based upon results from the thermo-chemical-data calculation program used in conjunction with the IBM-7090 automatic digital computer. Shifting equilibrium is assumed.

Sea-level performance is on the basis of optimum expansion conditions that correspond to an area ratio of 9.8:1 at 1,000-psia chamber pressure. Vacuum performance is the same as that of a standard DeLaval nozzle of corresponding area ratio.

II, F, Engine Configurations (cont.)

The turbopump assembly performance is discussed in Section II,K of this volume.

Engine performance and weight summary appears in Tables II F-2 and II F-1, respectively.

(d) Engine Cycles Applicable

To compare the forced-deflection nozzle engine to other engine configurations, a gas generator cycle has been used as a standard. However, the particular configuration of this nozzle lends itself to all cycles discussed under the engine cycle portion of this report (Section II,E).

(e) Cluster Applications

The forced-deflection nozzle engine lends itself to cluster applications as easily as the DeLaval. The only limitation for clustering is the large vehicle diameter required to cluster large-area-ratio nozzles. This diameter increase will make tank weight high because of low L/D ratio. It is recommended that in cluster applications, more subassemblies are added about a single turbopump for maximum utilization of available exhaust area.

c. Plug-Nozzle Engine

(1) Description

A plug-nozzle engine is defined as an engine in which the combustion gases are expanded externally over an exhaust cone, or plug, that

II, F, Engine Configurations (cont.)

is contoured to provide the desired expansion profile. These gases expand against the ambient atmosphere, which acts as an elastic wall to provide near-optimum expansion at all altitudes.

Various design configurations of plug type engines were evaluated. The configurations of the major engine components were selected from the results of the component design studies (discussed in Section II, G through II, N of this volume) and their applicability to the over-all engine integration. The final plug-nozzle engine design configuration is pictured in Figure II F-4.

The engine consists of eight thrust chamber assemblies, circumferentially located around the expansion plug. Oxidizer and fuel turbopump assemblies mounted inside the expansion plug supply both propellants to the thrust chambers. Turbine exhaust gases are passed through the expansion plug for cooling and exhausted to the atmosphere through a series of small nozzles to provide additional thrust.

Thrust-vector control is obtained by secondary injection of gas derived from gas generators located in each quadrant. Roll control is provided by expanding a small amount of the turbine exhaust gas through either one of two nozzles located at the base of the lower propellant tank.

(2) Summary

The main advantage of the plug nozzle engine, as with the force-deflection engine, is the performance gain from the altitude

II, F, Engine Configurations (cont.)

compensating nozzle and large engine area-ratios obtainable. Three significant disadvantages of plug nozzle configurations are evident, however, as seen upon examination of the design shown in Figure II F-4.

First, the maximum area ratio which can be contained within a given vehicle diameter is significantly less than with a forced deflection nozzle (34:1 as compared to 60:1 for the "standard" tankage configuration). Therefore, the performance is not as high as with the forced-deflection engines.

Secondly, the geometrical configuration and relative location of engine components require long propellant lines between the thrust chambers and turbopumps. This presents a problem of engine control, especially during transient periods when lines are being filled and emptied.

Thirdly, the plug nozzle is heavier than either the DeLaval or forced-deflection configurations. The geometrical shape, structure loads, and relatively large amount of plumbing required are principal contributors (see Section II, I).

It was concluded that the plug-nozzle engine is superior to the conventional DeLaval configuration because it has a compensated nozzle. However, the forced-deflection engine is thought to have the advantages of the plug nozzle without the disadvantages associated with it. Therefore, the plug configuration is not recommended as the best engine type.

II, F, Engine Configurations (cont.)

(3) Technical Discussion

(a) Description of Major Components

1 Thrust Chamber Assembly

The thrust chamber assembly consists of eight independent subassemblies attached to an external expansion cone via adjustable connections. The modules meet at an area ratio of 25:1 to form a continuous mating circle with the remainder of the truncated plug nozzle cone.

Each subassembly has a conical combustion zone, a throat of circular cross-section, and a conical nozzle entrance leading into a modified pen-shaped nozzle. The modified pen nozzle provides a transition from the circular nozzle position to the main expansion cone. Each is regeneratively cooled by fuel that enters at the pen exit and runs counter to the gas flow and directly into the injector. Thus, adequate cooling is obtained with a minimum of manifolding and the smallest possible pressure drop.

The thrust chambers are of cast aluminum-backed stainless steel tube construction. Thrust takeout is provided by a cone structure, in which the thrust chambers rest in saddles formed in the cone. The injector is stabilized by links attached to the thrust cone mounting ring.

The exhaust cone is truncated at approximately one-third of its full isentropic length. An investigation was made to determine the tradeoff point between nozzle performance and plug weight as a function of plug length. It was found that no significant gains can be obtained by using more than one-third of the total length. Use of a significantly greater

II, F, Engine Configurations (cont.)

portion of the plug increases the length of the vehicle greatly, and is not warranted. Truncating the plug results in a 1% specific impulse loss.

The truncated cone connects to the subassemblies at an area ratio of 25:1. The cone, exhaust gas-cooled and reinforced with honeycomb sandwich, attaches to the lightweight aluminum airframe forming eight identical sections. Turbine exhaust cooling is through 3/8-in. x 0.010-in. wall tubing formed to the prescribed plug-nozzle contour. A three-area-ratio flare is formed on the tube exits for thrust augmentation and partial reduction of base drag against the plug cap. The honeycomb sandwich is made of 2-in. honeycomb and two 0.020-in. aluminum sheets. The internal structure is of I-beam construction with aluminum vertical ties.

A detachable ablative cap is provided for access to the plug interior. This cap is structually reinforced by honeycomb sandwich.

An alterante design for the expansion cone is an ablative coating over the honeycomb. The turbine exhaust gas is then ducted through the ablative cap. No change in the inner frame is required.

2 Turbopump Assembly

The turbopumps incorporated in the engine design are essentially identical to the ones used in the forced-deflection engine.

II, F, Engine Configurations (cont.)

The gas-generator assembly also is identical in function and configuration to that used for the forced-deflection engine.

3 Engine Controls

Engine control functions include initiation and termination of the main propellant flow, control of propellants into the gas-generator, and ignition of propellants in the thrust chamber. A controls schematic of a representative control system is shown in Figure II F-5.

Control of the main propellant flow, particularly during the start and shutdown transients, presents more of a problem with plug nozzle engine configurations than with any of the other engine types considered. This is because of the inherently long propellant lines connecting the thrust chambers to the turbopump assembly. For the engine configuration shown in Figure II F-4, the oxidizer and fuel discharge lines to each chamber are 14.1 and 5.7-ft long x 6-in. diameter, respectively. The volume in these lines is 2.78 and 1.12 cu in. for each oxidizer and fuel line, respectively. This problem can can be minimized by using individual thrust chamber valve sets located at the entrance to each thrust chamber. However, the eight sets of valves required result in a large increase in functional engine components and potentially decreased engine reliability. If a single discharge valve is used upstream of the separate discharge lines, the propellant discharge lines must be filled during the engine start transient, which will result in a slow start transient and may make a smooth start difficult. A more detailed analysis is required to determine the most practical method.

II, F, Engine Configurations (cont.)

In the engine configuration shown, the same control system used in the forced-deflection design was incorporated. Included are suction and discharge propellant valves, conventional gas generator valves, and an electro-mechanical actuation system. The controls discussion for the forced-deflection engine is also applicable to this engine.

4 Thrust-Vector Control

Thrust-vector control for the plug-nozzle engine is obtained by secondary gas injection. Gas for injection is produced in generators located on the thrust chamber skirts in each of the four quadrants. Propellants are bled from the main pump discharge lines, passed through throttling valves, and ignited in the respective generators. The gas produced, injected into the flow stream at high velocity, results in obtaining the required side thrust for vector control. They system is shown schematically in Figure II F-5.

The control system consists of four separate closed-loop position-controlled valve assemblies. Each is designed to maintain a constant mixture ratio regardless of flow rate. In their closed position, the valves will produce enough leakage flow to maintain combustion during off control periods. This also prevents gas backflow from the main engine flow stream.

On the basis of an equivalent gimbal angle requirement of $\pm$ 3°, the maximum flow rate required in any plane was

II, F, Engine Configurations (cont.)

calculated to be 177 lb/sec for a 2,000,000-lb thrust engine. If simultaneous pitch and yaw are required, this flow rate is increased to 250 lb/sec. The flow ratios were computed using the following assumptions:

Engine chamber pressure	1,000 psi
Gas generator chamber pressure	1,000 psi
Gas generator mixture ratio	2:1
Engine pressure at point of injection	70 psi
Side jet thrust amplification factor (β)	2.25

A detailed investigation of vector control systems for plug nozzle engines was recently completed* The control system described above was found to be the most practical of all the systems considered. It provides easy control, has small interaction with the main engine, and is relatively light in weight. It does, however, require a supplemental roll control system.

Gimbaling is unattractive for plug configurations because of the large diameter at the top of the engine and the general geometrical shape of the engine. If stabilizing fins are used on the missile, thus lowering the vector control requirement, turbine exhaust can be used as the injectant fluid, eliminating the gas generators. The expansion cone would then have to be constructed of ablative material instead of being exhaust-cooled, increasing the cone weight approximately 25%. At high chamber pressures (over 2,000 psi) turbine exhaust gas flow rates are sufficiently high to provide the required control moment for aerodynamically unstable vehicles.

*Aerojet-General Corporation, Thrust Vector Control for Plug-Nozzle Engines, Report No. LRP 210, March 1961.

II, F, Engine Configurations (cont.)

5 Structure and Integration of Engine Components

The pump assembly is bolted to a ring on the bottom of the fuel tank as shown in Figure II F-4. The ring transmits the gyroscopic forces of the pump as well as the side loads and transient loads during start and shutdown to the tank bottom. These loads are transmitted to the side walls of the tank by radial ribs from the pump mounting ring.

The thrust chambers are mounted to the tank bottom by a conical thrust structure. This structure attaches to the thrust chambers at the transition section between the pen nozzles and the skirt. The nozzles rest in saddles formed in the cone. All of the thrust and vector control loads are taken by this structural cone.

The thrust cone is fabricated from sheet metal stampings which conform to the shape of the pen nozzle thrust chambers, forming the saddles in which they rest. These stampings are made of two embossed steel sheets which are spot welded together to form a rigid structure that will carry compression and bending loads. The area of the cone between thrust chambers is covered with heat-resistant ablative material. This cone structure seals off the interior of the engine from the thrust chambers heat and flame.

The vector control gas generators are attached to the fuel inlet torus on the bottom of the thrust chambers as shown in Figure II F-9. The gas-generator injector is supported by struts to the pump mounting ring.

II, F, Engine Configurations (cont.)

The turbine exhaust cooled plug assembly is attached to the thrust chambers by means of a bolted connection between the exhaust torus on the plug and the fuel torus on the bottom of the thrust chambers.

(b) Performance

The performance of the plug-nozzle engine is evaluated as having optimum expansion at all altitudes. At vacuum, the ambient pressure is zero and results in conventional vacuum performance. The method of performance computation is identical to that of the forced-deflection nozzle and all other altitude compensating nozzles.

Major engine and component operating parameters as well as engine weight are shown in Tables II F-3 and II F-1, respectively.

(c) Engine Cycles Applicable

To compare the plug engine to other engine configurations, it was designed with an engine system using the standard gas generator cycle. The plug configuration, however, is not restricted to this cycle and is compatible with most of the engine cycles considered in Section II, E.

The staged combustion, third fluid "open" chamber bleed, and delivery feed cycles (which do not require heat input for cycle operation) will be equally as applicable to plug configurations as to other engine types.

II, F, Engine Configurations (cont.)

(d) Cluster Applications

The plug-nozzle engine is not as suitable for cluster applications as the deLaval, forced-deflection, or reversed flow engine types. Performance of the plug nozzle depends upon the ambient air pressure surrounding the nozzle. If engines are used in clusters, ambient conditions at the inner portions of each engine would be severly disturbed during flight because of the interactions between the streams in that region. By moving the engines sufficiently far apart to eliminate all possibility of interactions, this problem can be eased; however, doing this makes inefficient use of the area under the tankage available for useful engine area ratio.

Another disadvantage in clustering plug configurations stems from the general shape of the engine, which results in a heavy structure when mounting engines in clusters. The plug engine, having its largest diameter at the top, is ideally suited for integration with the propellant tankage when used as a single unit. However, when used in clusters, each engine must be attached to a thrust cone which accepts the large diameter interface. The result is that the mounting structure is considerably heavier than one in which the engines are attached where the diameter is smaller.

d. Reverse-Flow Engine

The reverse-flow engine is a special version of the forced-deflection engine, in which the thrust chambers are designed so that the combustion gases expand through a very large turning angle. Two configurations of this engine were designed (Figures II F-6 and II F-7). The first uses a

II, F, Engine Configurations (cont.)

single thrust chamber with an annular throat, and the second has eight separate chambers, each with its own discrete throat.

The primary advantage of the reverse flow engine is that it is shorter and more compact than the standard forced-deflection engine. Performance and operating characteristics of the engines (for a given area ratio) are identical.

There are several disadvantages inherent in the configuration of the thrust chamber assembly. First, the high curvature of the nozzle causes an increase in local heat flux, which makes cooling of the nozzle more critical. Secondly, the vent area available for altitude compensation is reduced because of the more compact design. Because altitude compensation capability is a fundamental advantage of all forced-deflection engines, adequate vent area is an important consideration. Finally, the complex shape of the combustor and nozzle requires additional reinforcement over the simple tension structure of the standard forced-deflection engine.

Investigation for determining the optimum gas turning angle, with respect to over-all engine design integrity, has not been concluded. It appears that the design when made optimum will be closer to that of the forced-deflection engine than to the reversed flow configuration. However, final conclusion must be withheld pending further investigation.

TABLE II F-2

FORCED-DEFLECTION ENGINE CHARACTERISTICS

ENGINE	
Vacuum Thrust, lb	2.44×10^6
Sea Level Thrust, lb	2.03×10^6
Vacuum Specific Impulse, sec	433
Sea Level Specific Impulse, sec	360
Oxidizer Flow Rate, lb/sec	4783
Fuel Flow Rate, lb/sec	857
Mixture Ratio, O/F	5.59
Length, ft	16.16
Diameter, ft	25.8
THRUST CHAMBER ASSEMBLY	
Vacuum Thrust, lb	2.4×10^6
Sea Level Thrust, lb	2×10^6
Vacuum Specific Impulse, sec	437
Sea Level Specific Impulse, sec	364
Chamber Pressure, plenum, psia	1000
Chamber Pressure, injector face, psia	1052
Area Ratio, A_e/A_t	60
Mixture Ratio, O/F	6.0
Propellant Flow Rates, lb/sec	5500
Oxidizer	4720
Fuel	780
Characteristic Velocity, C^*, ft/sec	7450
Vacuum Thrust Coefficient, C_F	1.87
Sea Level Thrust Coefficient, C_F	1.57

TABLE II F-2 (cont.)

TURBOPUMPS	Oxygen	Hydrogen
Propellant Flow Rate (lb/sec)	5005	883
Pump Discharge Pressure (psia)	1300	1300
Pump Total Suction Pressure (psia)	73	29
Propellant Vapor Pressure (psia)	21	22
Turbine Inlet Total Pressure (psia)	1000	1000
Turbine Exit Static Pressure (psia)	100	1000
Turbine Total Flow Rate lb/sec	70	78
Total Exhaust Thrust (lb) sea-level	30,000	
Turbine Exhaust Thrust (lb) Vacuum	40,000	

GAS GENERATOR	
Mixture Ratio	1.0
Flow Rate	148
Chamber Pressure	1000
Gas Temperature	1800

TABLE II F-2 (cont.)

	Oxidizer	Fuel
PRESSURE SCHEDULE (PSIA)		
Propellant System		
Chamber, plenum	1000	1000
Chamber, Injector Face	1052	1052
△ P Injector	150	60
Injector Inlet	1202	1112
△ P Coolant Jacket		163
Coolant Jacket Inlet		1275
△ Line and Orifice	98	25
Pump Discharge	1300	1300
Turbine System		
Turbine Inlet	700	700
△ P Orifice and Ducting	150	150
Gas Generator Injector Face	850	850
△ P Injector	120	170
Injector Inlet	970	1020
△ P GGV	80	100
GGV Inlet	1050	1120
△ P Orifice and Line	130	135
GG Propellant Tap-Off	1180	1255

TABLE II F-3

PLUG NOZZLE ENGINE CHARACTERISTICS

ENGINE	
Vacuum Thrust, lb	2.391×10^6
Sea Level Thrust, lb	2.028×10^6
Vacuum Specific Impulse, sec	424
Sea Level Specific Impulse, sec	360
Oxidizer Flow Rate, lb/sec	4785
Fuel Flow Rate, lb/sec	855
Mixture Ratio, O/F	5.6
Length, ft	17.5
Diameter, ft	23.7
THRUST CHAMBER ASSEMBLY	
Vacuum Thrust, lb	2.35×10^6
Sea Level Thrust, lb	2.0×10^6
Vacuum Specific Impulse, sec	427
Sea Level Specific Impulse, sec	364
Chamber Pressure, plenum, psia	1000
Chamber Pressure, injector face, psia	1052
Area Ratio, A_e/A_t	34
Mixture Ratio, O/F	6.0
Propellant Flow Rates, lb/sec	5500
Oxidizer	4720
Fuel	780
Characteristic Velocity, C^*, ft/sec	7450
Vacuum Thrust Coefficient, C_F	1.83
Sea Level Thrust Coefficient, C_F	1.57

TABLE II F-3 (cont.)

TURBOPUMPS	Oxygen	Hydrogen
Propellant Flow Rate (lb/sec)	5005	883
Pump Discharge Pressure (psia)	1300	1300
Pump Total Suction Pressure (psia)	73	29
Propellant Vapor Pressure (psia)	21	22
Turbine Inlet Total Pressure (psia)	1000	1000
Turbine Exit Static Pressure (psia)	100	100
Turbine Total Flow Rate lb/sec	70	78
Total Exhaust Thrust (lb) sea-level	30,000	
Turbine Exhaust Thrust (lb) Vacuum	40,000	
GAS GENERATOR		
Mixture Ratio	1.0	
Flow Rate	148	
Chamber Pressure	1000	
Gas Temperature	1800	

TABLE II F-3 (cont.)

	Oxidizer	Fuel
PRESSURE SCHEDULE (PSIA)		
Propellant System		
Chamber, Plenum	1000	1000
Chamber, Injector Face	1052	1052
△ P Injector	120	60
Injector Inlet	1172	1112
△ P Coolant Jacket		140
Coolant Jacket Inlet		1252
△ P Line and Orifice	128	48
Pump Discharge	1300	1300
Turbine System		
Turbine Inlet	700	700
△ P Orifice and Ducting	150	150
Gas Generator Injector Face	850	850
△ P Injector	120	170
Injector Inlet	970	1,020
△ P GGV	80	100
GGV Inlet	1050	1120
△ P Orifice and Line	130	135
GG Propellant Tap-Off	1180	1255

TCA		PARAMETER	ENGINE	
SEA LEVEL	VACUUM		SEA LEVEL	VACUUM
2×10^6	2.55×10^6	THRUST	2.028×10^6	2.591×10^6
332	423	SPECIFIC IMPULSE	329	420
60	60	MIXTURE RATIO	5.55	5.55
1000	1000	THRUST CHAMBER PRESS	1000	1000
27	27	NOZZLE AREA RATIO	27	27
6030	6030	FLOW RATE LBS/SEC	6170	6170
		WET WEIGHT-LBS.	16096	

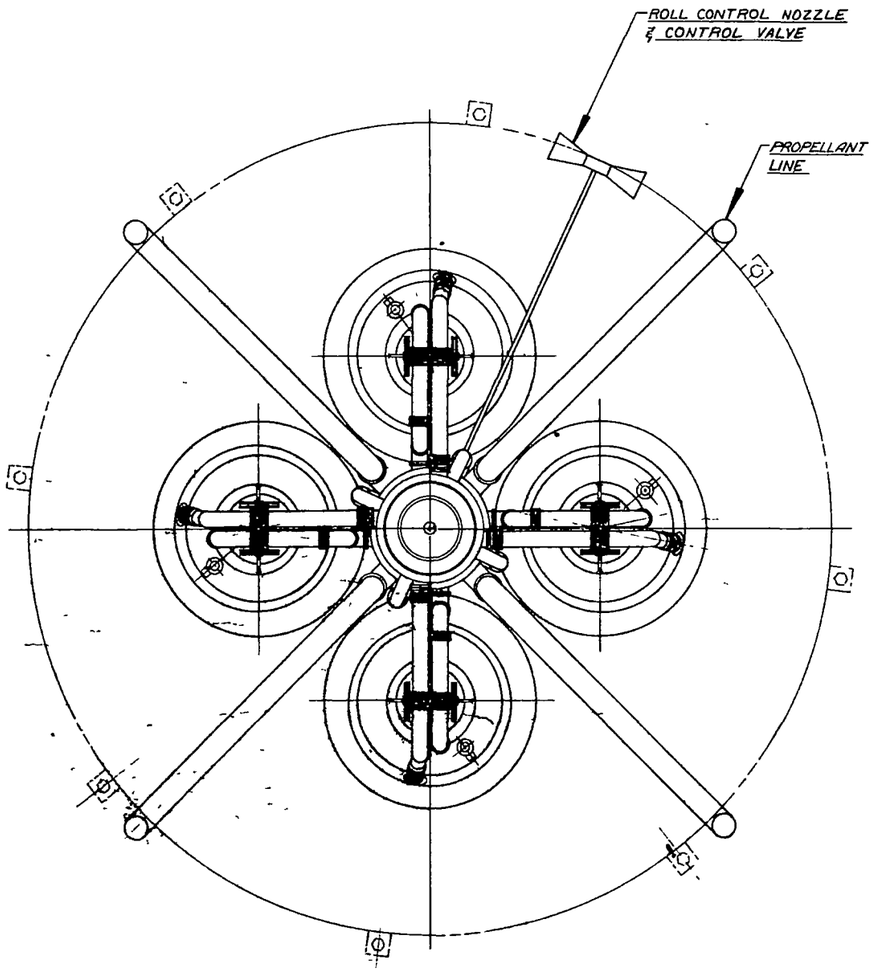

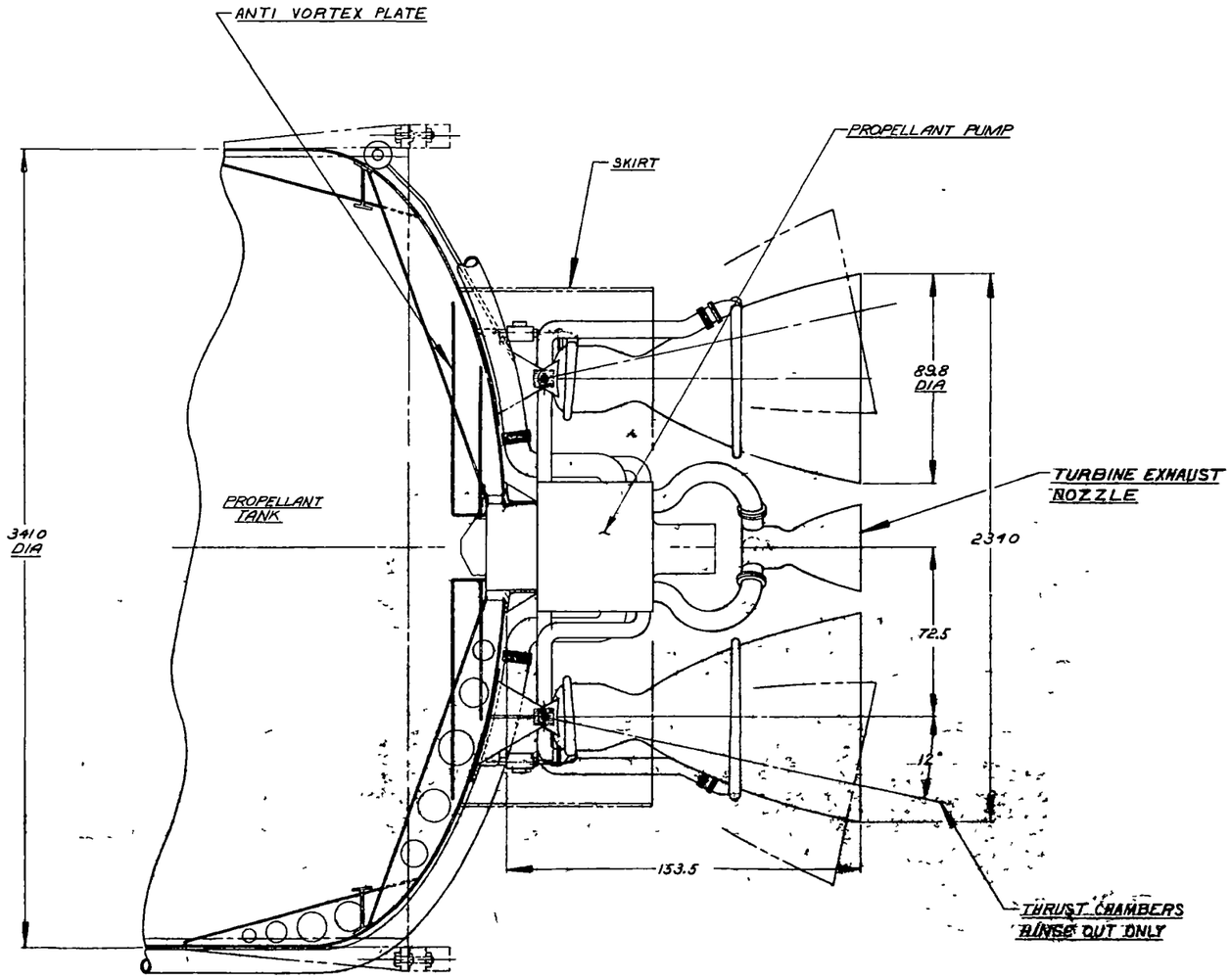

Four 500k De Laval Chambers, One Turbopump

Figure II F-1

TCA		PARAMETER	ENGINE	
SEA LEVEL	VACUUM		SEA LEVEL	VACUUM
2×10^6	2.4×10^6	THRUST	2.028×10^6	2.441×10^6
364	437	SPECIFIC IMPULSE	360	433
6.0	6.0	MIXTURE RATIO	5.59	5.59
1000	1000	THRUST CHAMBER PRESS	1000	1000
60	60	NOZZLE AREA RATIO	60	60
5500	5500	FLOW RATE LBS/SEC	5640	5640
		WET WEIGHT	15389 LB	

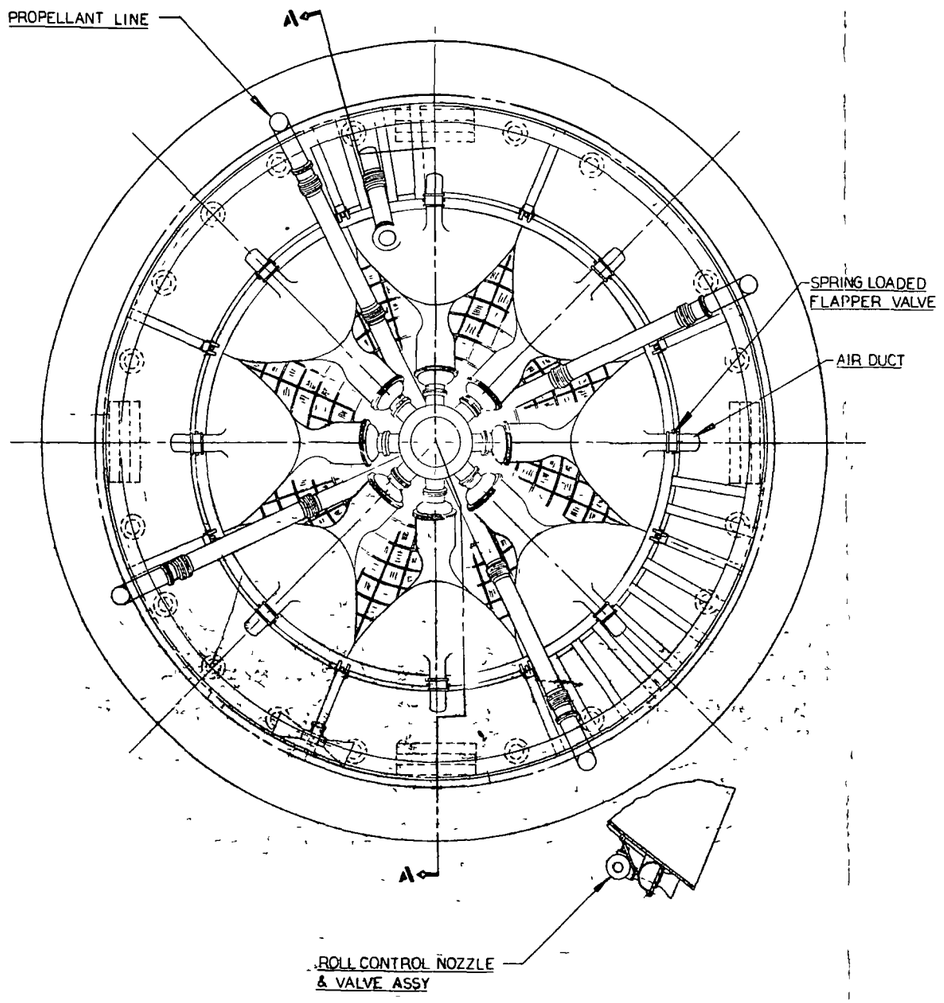

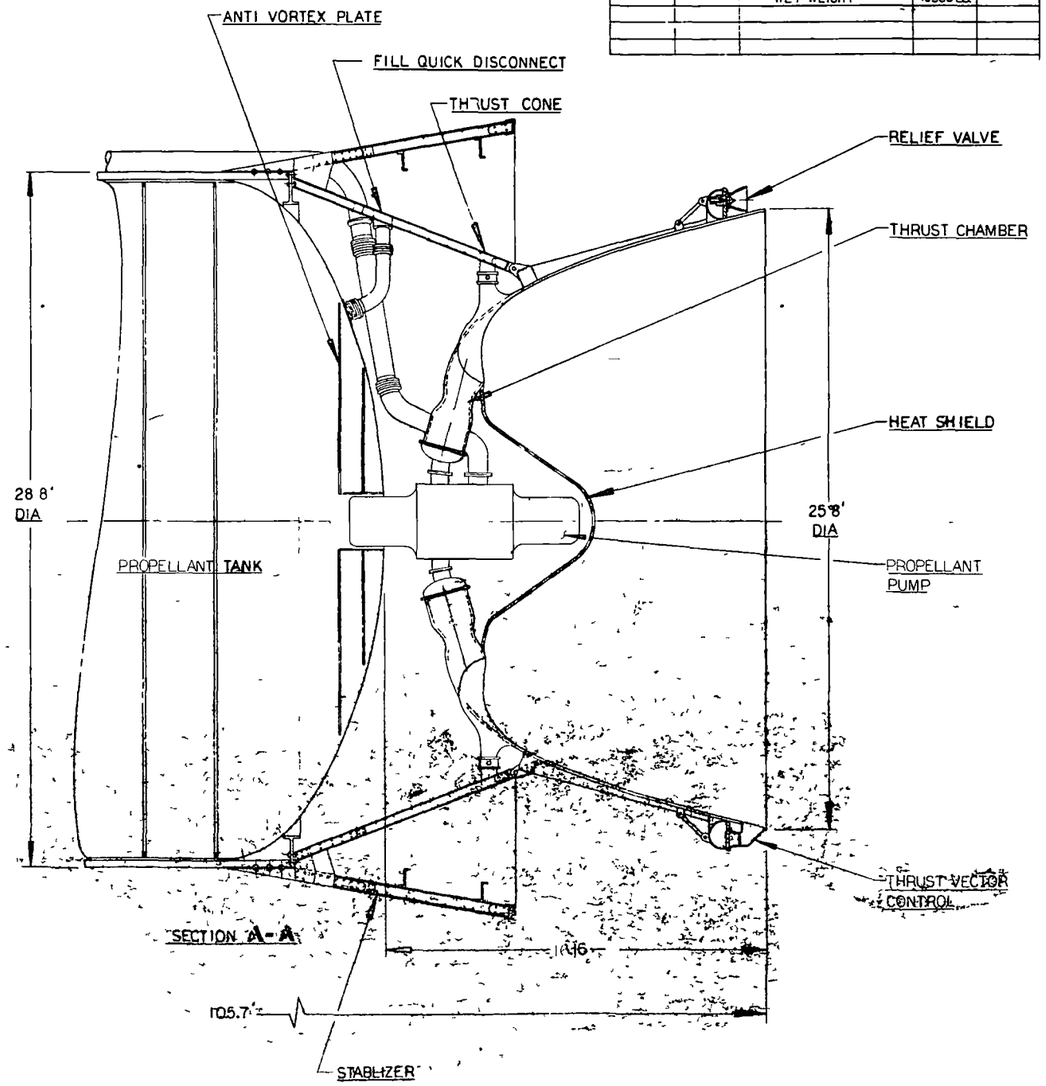

Rocket Engine, Forced-Deflection Gas Generator Cycle, 2,000,000-lb-Thrust

Figure II F-2

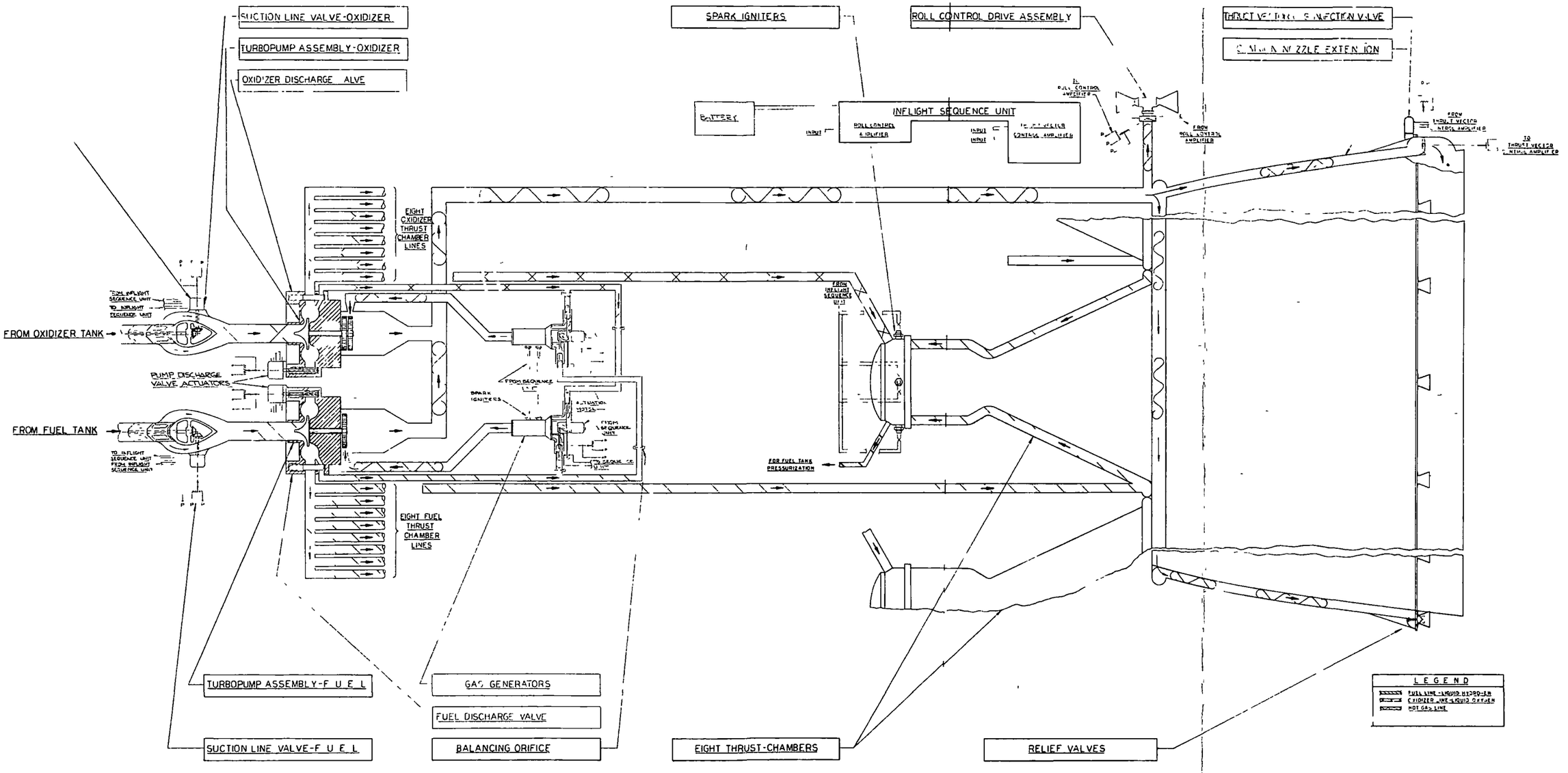

Controls Schematic, 2,000,000-lb-Thrust Rocket Engine, Forced-Deflection

Figure II F-3

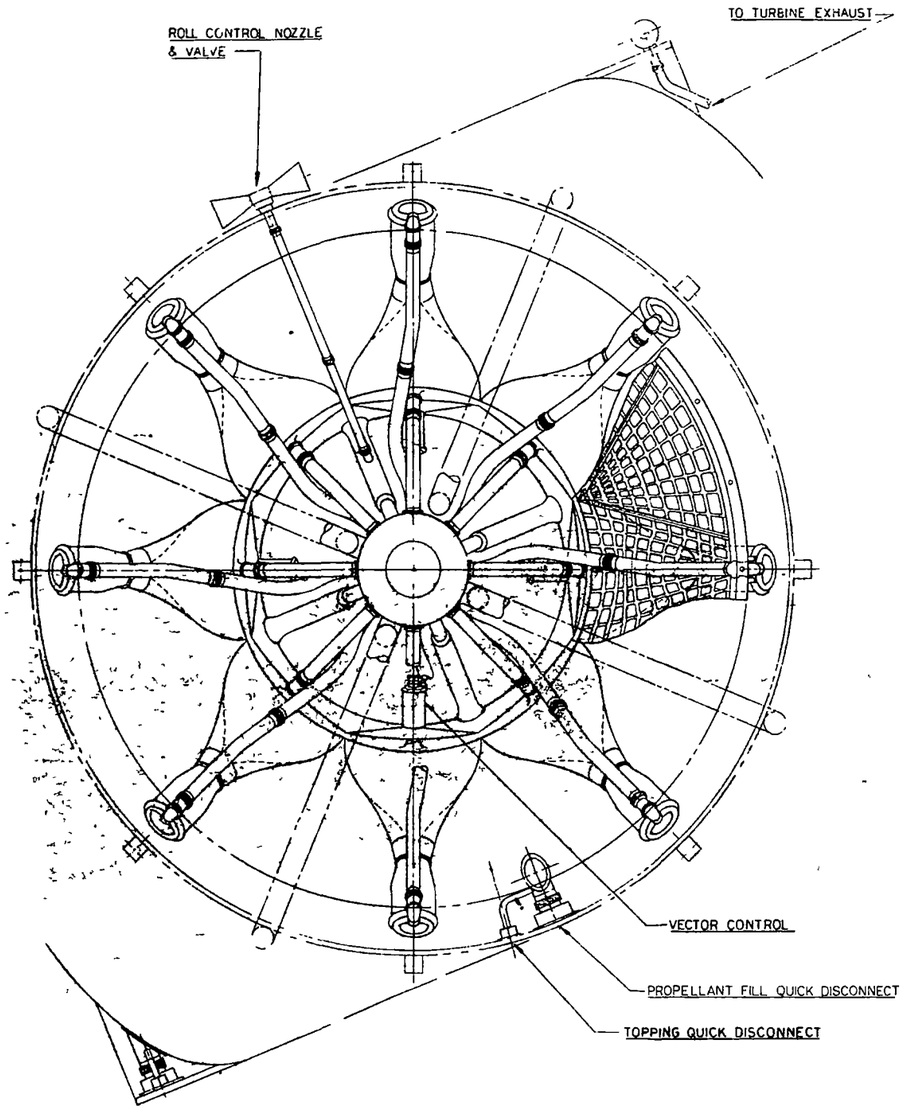

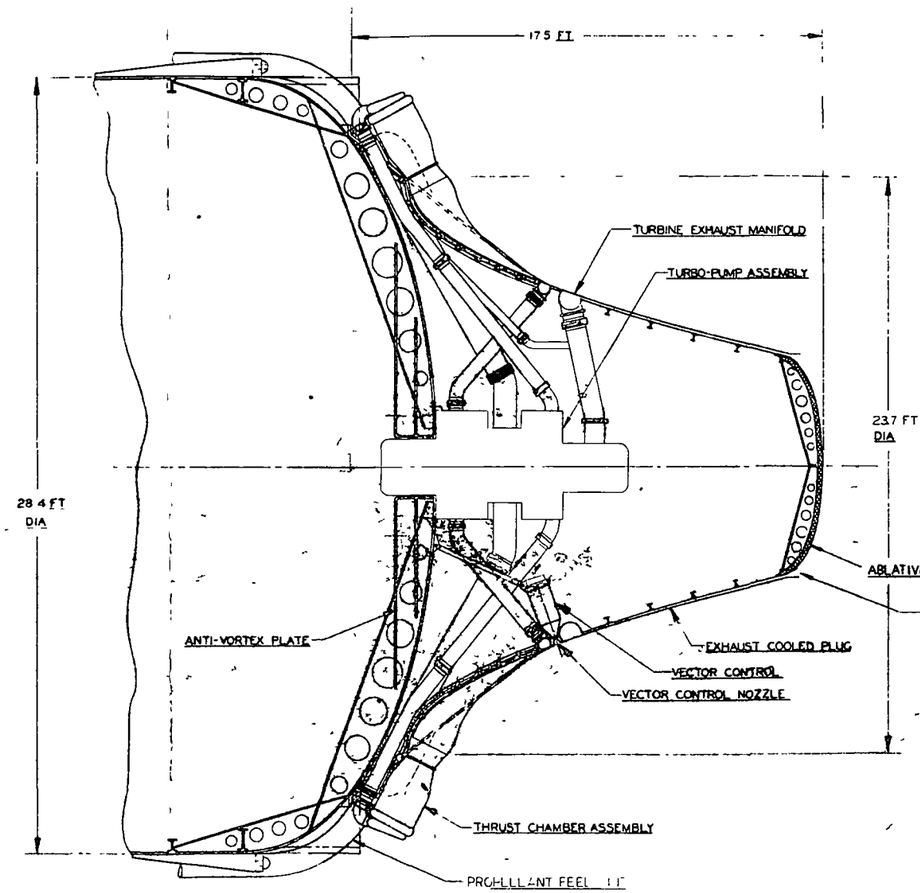

ROCKET ENGINE PARAMETERS	TCA	ENGINE
THRUST, SEA LEVEL, LB	2,000,000	2,028,000
THRUST, VACUUM, LB	2,350,000	2,391,000
SPECIFIC IMPULSE, SEA LEVEL, SEC	384	380
SPECIFIC IMPULSE, VACUUM, SEC	427	424
MIXTURE RATIO	6 0	5.8
THRUST CHAMBER PRESSURE PLENUM, PSIA	1,000	1,000
THRUST NOZZLE AREA RATIO	34	34
FLOW RATE, LB/SEC	5,500	5,640
WET WEIGHT, LB		22,438

Plug-Nozzle Rocket Engine, 2,000,000-lb-Thrust, Gas Generator Cycle

Figure II F-4

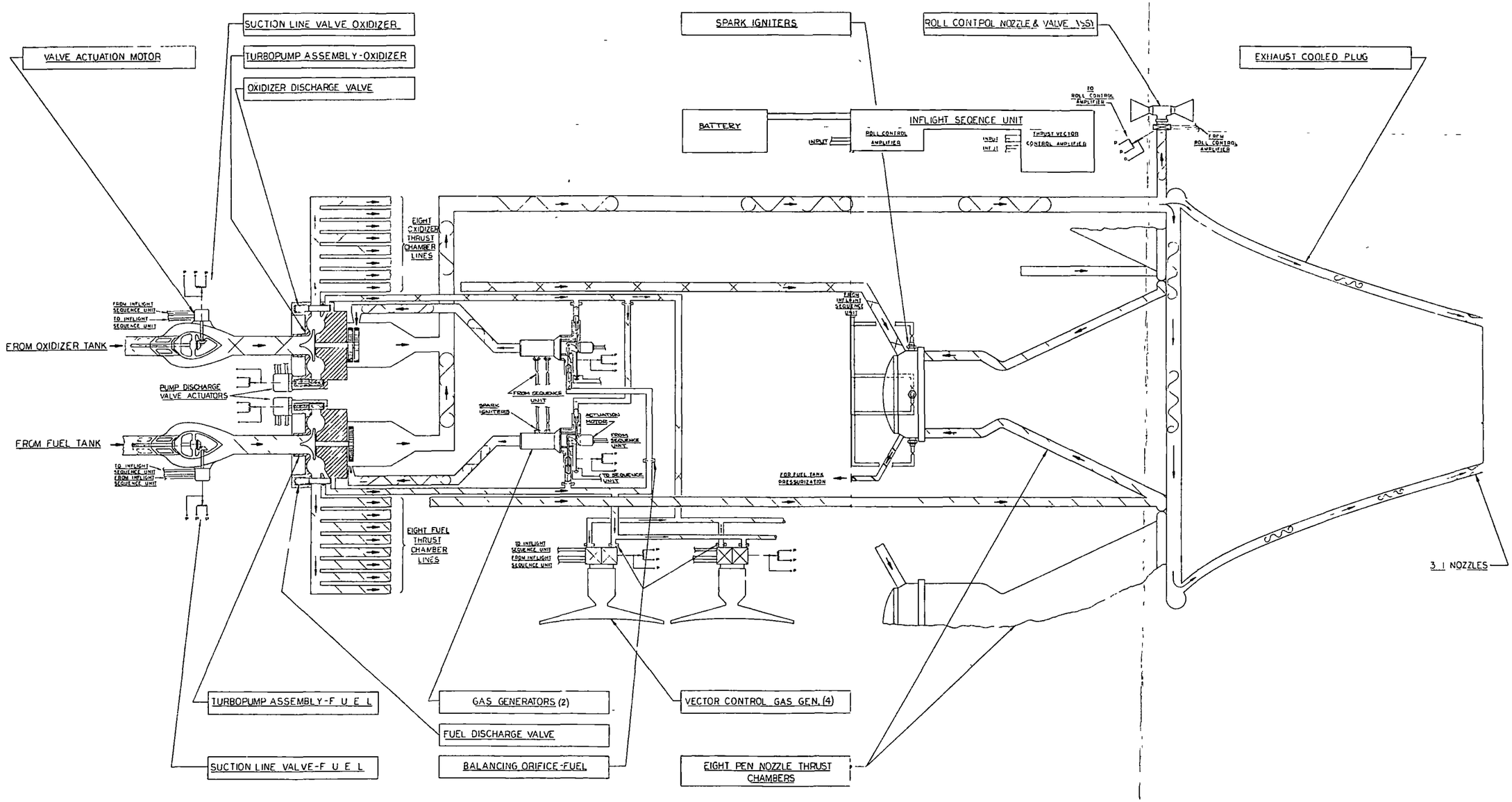

Plug-Nozzle Engine Controls Schematic, 2,000,000-lb-Thrust

Figure II F-5

BOOSTER PARAMETERS

	TCA	ENGINE
THRUST, SEA LEVEL, LB	2×10^6	$2\,028 \times 10^6$
THRUST, VACUUM, LB	$2\,4 \times 10^6$	$2\,441 \times 10^6$
CHAMBER PRESSURE, PSIA	1000	1000
SPECIFIC IMPULSE, S L, SEC	364	360
SPECIFIC IMPULSE, VAC, SEC	437	433
WEIGHT FLOW, LB/SEC	5640	5640
MIXTURE RATIO	6 0	6 0
NOZZLE AREA RATIO	60	60

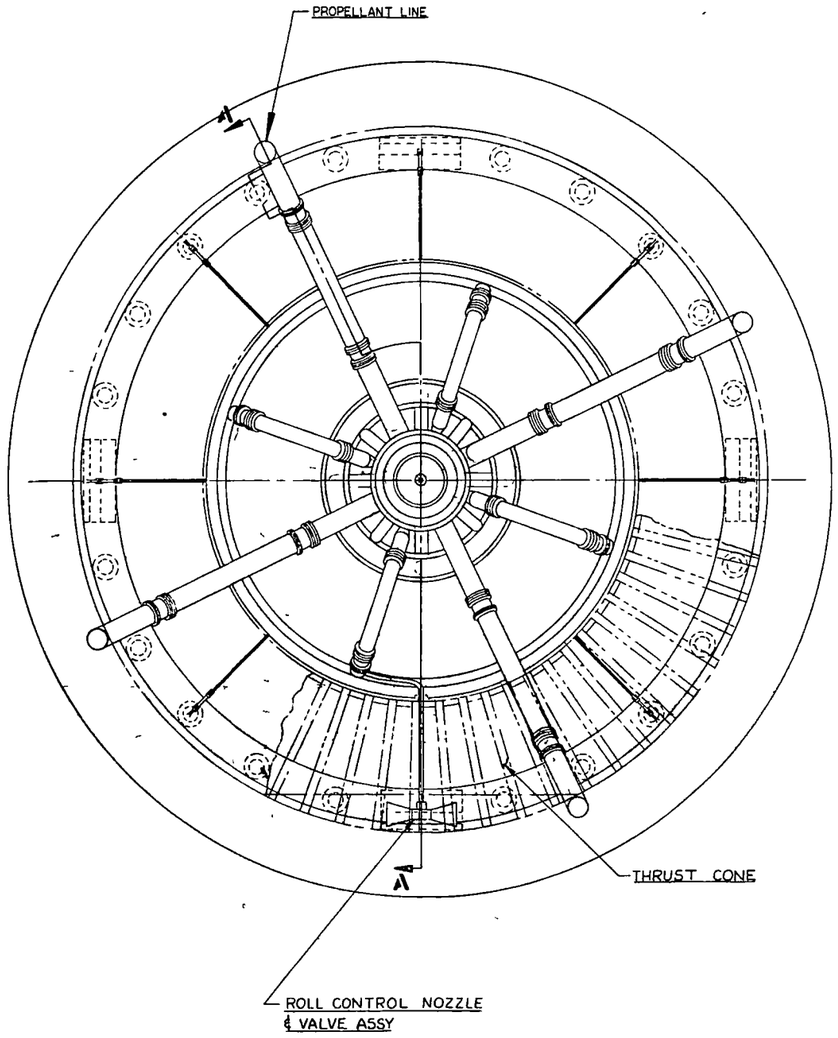

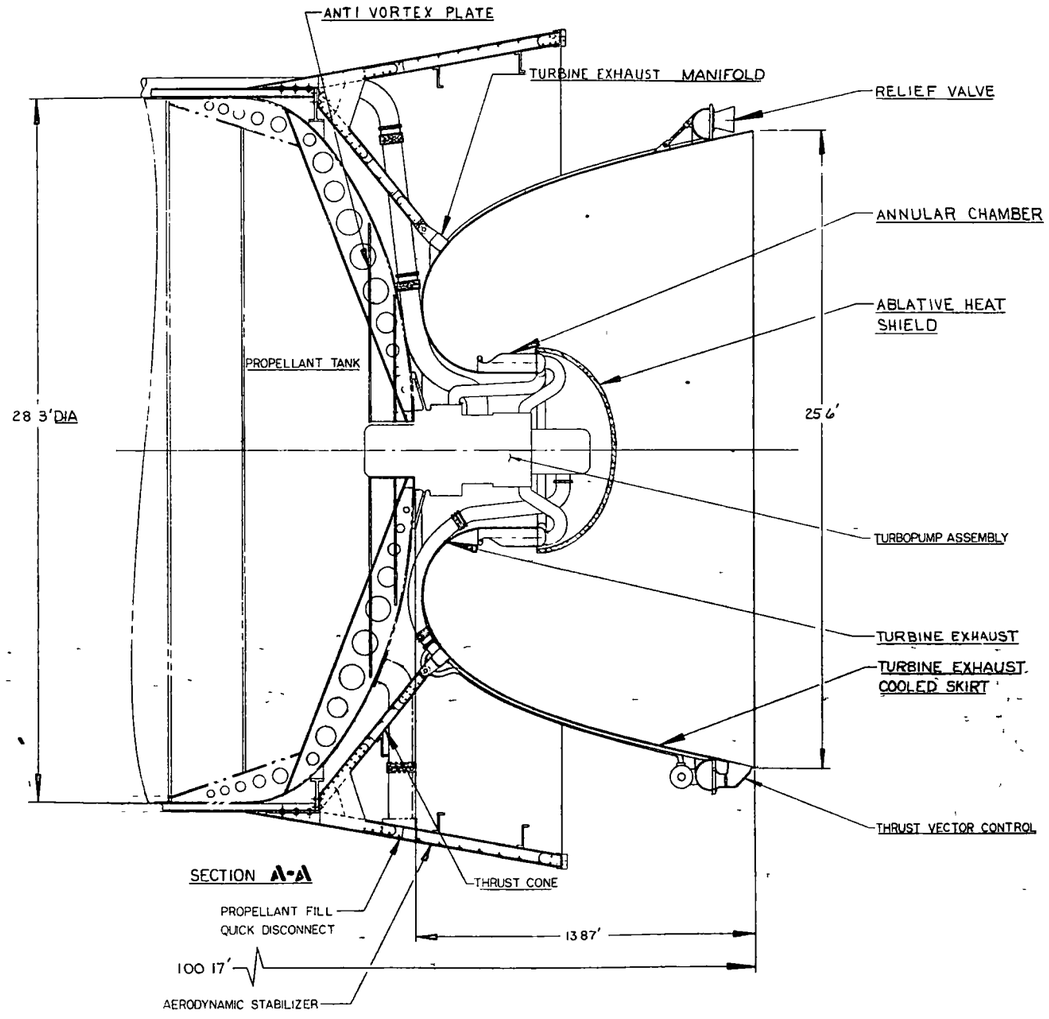

Reverse-Flow Engine, Annular Chamber

Figure II F-6

BOOSTER PARAMETERS

	TCA	ENGINE
THRUST, SEA LEVEL, LB	2×10^6	2.028×10^6
THRUST, VACUUM, LB	2.4×10^6	2.441×10^6
SPECIFIC IMPULSE (SEA LEVEL) SEC	364	360
SPECIFIC IMPULSE (VACUUM) SEC	437	433
CHAMBER PRESSURE, PSIA	1000	1000
TOTAL WEIGHT FLOW, LB/SEC	5640	5640
MIXTURE RATIO	6.0	5.6
NOZZLE AREA RATIO	60	60
ENGINE WET WEIGHT LBS		15153

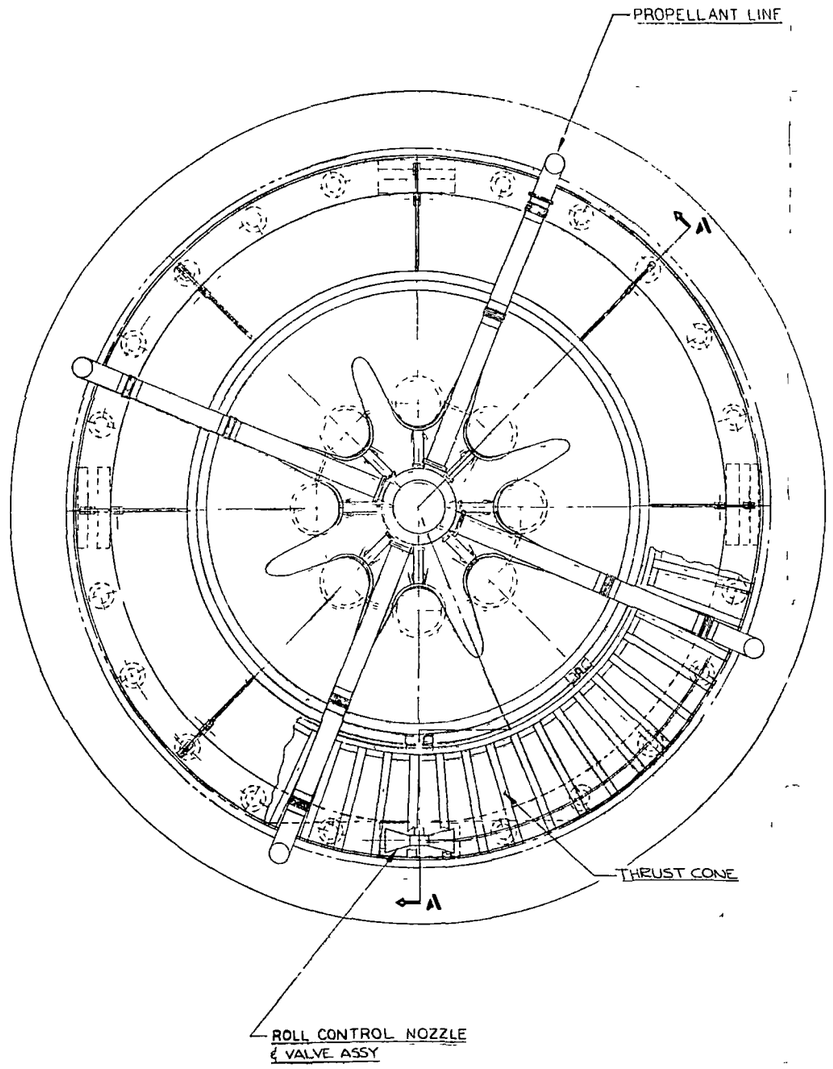

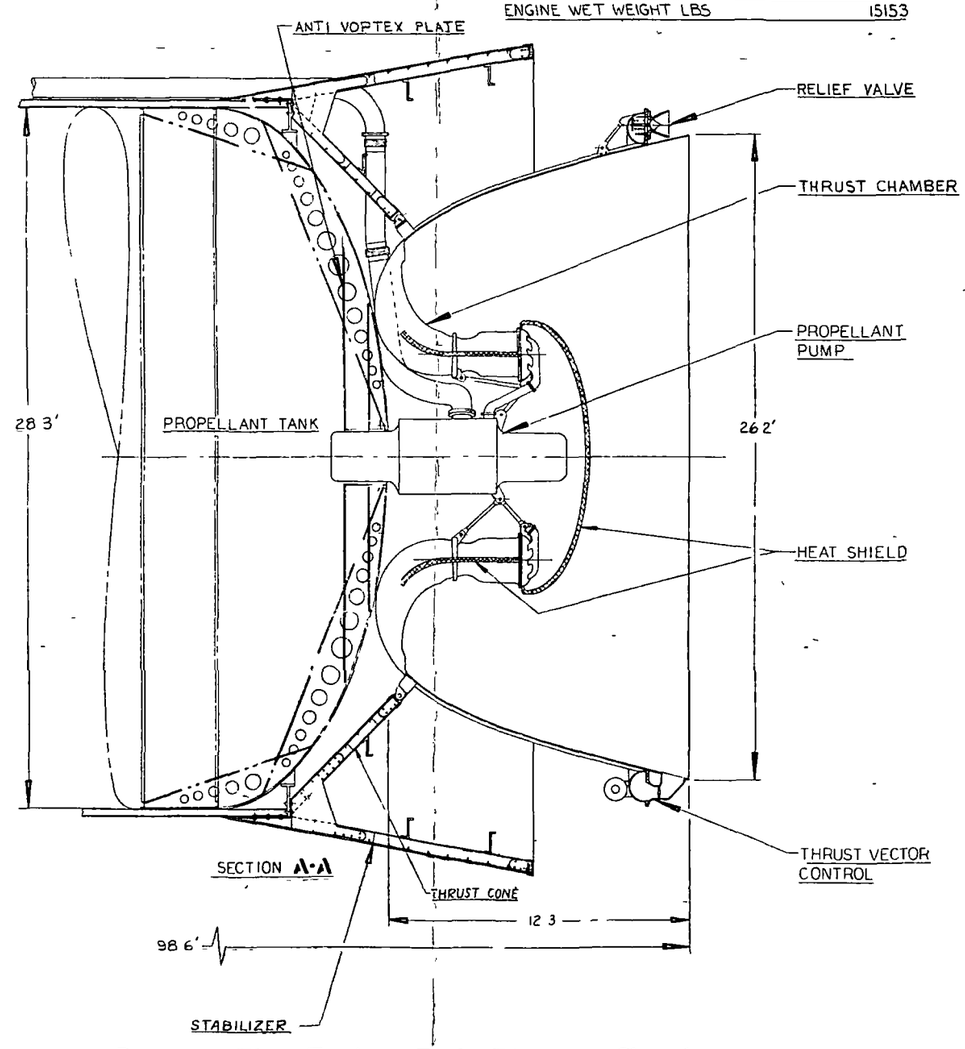

Reverse-Flow Engine, Eight Discrete Chambers

Figure II F-7

II, Concepts Considered (cont.)

G. THRUST VECTOR AND ROLL CONTROL

1. General

Three modes of control are required for rocket vehicles: pitch, yaw, and roll control. The pitch and yaw control moments are necessary to adjust the thrust-vector to compensate for wind loading, lateral misalignment of thrust, and trajectory. Roll control is needed to correct for aerodynamic asymmetrical loading, exhaust swirl, and vehicle orientation for guidance system orientation.

The roll control moment is small when compared to the pitch and yaw requirements. It can be supplied by a single nozzle, by swiveled nozzles, or by two fixed nozzles intermittently operated by turbine drive or exhaust fluid. These nozzles are very light in weight and require very little total flow. Only negligible improvements in vehicle performance or lessening of complexity is available by detailed design in this area; therefore, no further consideration was given to the roll control system during this investigation.

Necessary pitch and yaw control moments were assumed to be equal. Magnitude of the equivalent gimbal angle, determined from the standard vehicle dynamic stability study, was $\pm 2.5°$. These studies were on the basis of a rigid, aerodynamically stable body. No consideration was given to the vehicle natural bending frequencies because actual structural design is necessary to determine spring rates. By assuming characteristic requirements, a control frequency of 0.67 cps was obtained for the $\pm 2.5°$ vector deflection. It was assumed that these control requirements would be compatible with the vehicle system and would not excite the vehicle at its natural frequency. The inert hardware of the

II, G, Thrust Vector and Roll Control (cont.)

vector control system was evaluated on the basis of ±4°, to allow for error in the study; however, the characteristic duty cycle considered was similar to the results of the dynamic study. Figure II G-1 is a sketch of the duty cycle used.

Vector control, regardless of the method, causes a performance loss. For a conventional gimbaled engine, this loss is from the weight of the inert parts of the stage. Therefore, alternative methods for thrust vector control that would reduce this weight were sought. These methods include:

a. Jet vanes
b. Paddles
c. Spoilers
d. Hinged or gimbaled auxiliary nozzles
e. Jetavators
f. Thrust modulation (multiple chambers or engines)
g. Gimbaled main nozzles
h. Secondary fluid injection

Other methods for vehicle control (i.e., gimbaling the payload, warping the vehicle, aerodynamic control surfaces for systems operating in the atmosphere, and control jets in the forward portion of the vehicle) depend upon the vehicle design and are independent of the engine. Such systems offer no basic advantage for vector control and were not considered in this investigation.

Results of the thrust-vector control study indicated that secondary fluid injection offered a potential weight savings over other control methods and would result in a significant payload gain.

II, G, Thrust Vector and Roll Control (cont.)

2. Gimbaled Engine Thrust-Vector Control

Gimbaling the main engine or thrust chamber is the most common thrust-vector control method used with liquid rockets. It is necessary to ascertain the weight penalty associated with this conventional method before attempting to evaluate alternatives. To determine this, a stage equipped with a rigidly mounted engine without vector control capability was compared with a stage having a gimbaled engine. The forced-deflection nozzle engine configuration at 2,000,000 lb thrust was used for this comparison. Weight differences are tabulated below.

Thrust structure weight increase and heat shield	950 lb
Skirt weight increase	150 lb
Engine weight (thrust concentration structure)	1,020 lb
Gimbal bearing	300 lb
Gimbal actuators	300 lb
Flexible propellant supply lines (wet)	3,980 lb
TOTAL	6,700 lb

The thrust structure, skirt, and heat shield weights were obtained from the study conducted by The Boeing Company (see Volume 5). Additional engine weight results because all thrust loads must be transmitted to the center of the engine. The gimbal bearing is then used to transmit the thrust loads to the airframe. The actuator moves the engine in accordance with guidance system commands. Propellant line weight is the largest single penalty in the gimbaled engine. This weight results from providing necessary suction line flexibility to permit gimbaling. Nearly all of the weight consists of oxidizer remaining in the additional line length needed at the end of flight. A crossover manifold system similar to that used in the Titan was the basis for determining weight. More detailed design would result in a reduction of weight in this area.

II, G, Thrust Vector and Roll Control (cont.)

3. Evaluation of Alternative Thrust-Vector Control Methods

a. Jet Vanes, Paddles, Spoilers, Jetavators

Jet vanes, paddles, spoilers, and jetavators have all been tested and were found to offer no advantage over gimbaling for a liquid rocket engine. Therefore, no further effort was expended evaluating these concepts.

b. Movable Auxiliary Nozzles

The use of gimbaled or auxiliary nozzles offers no advantage over a completely movable engine. Necessary thrust structure, actuation system, control components, and flexible propellant lines decrease the advantage of movable auxiliary nozzles. Also, small thrust chambers require a higher angular deflection to net the same side thrust. This increases thrust structure complexity and induces high-temperature problems in the main engine because of the proximity of the combustion products. The same flow injected into the main nozzle (secondary injection) would net a higher side force because of the amplification factor. Therefore, this method was eliminated from further consideration.

c. Thrust Modulation

Thrust modulation as a vector control method may be considered for propulsion systems of more than one engine assembly, or a single pumping system with multiple thrust chambers. The basic problem of this method is the large change in thrust required to generate the necessary movement. The condition exists because the major effect upon the thrust vector is a lateral rather than an angular change.

II, G, Thrust Vector and Roll Control (cont.)

A study was made of vector control for a plug nozzle by chamber modulation (Contract Aerospace 60-102). Thrust was increased by 15% in one engine quadrant while it was reduced by 30% in the others, but even then insufficient vector deflection was obtained with the vehicle considered.

The penalty associated with this method of thrust-vector control includes increases in the weight of the support structure as well as the valves and manifold needed to control propellant flow to each combustion chamber. Because thrust must be increased over the normal operating level in one quadrant, the engine must be over designed accordingly. If an increase of 15% is required, the continuous operating point is only 85% of design, causing an equivalent weight penalty of approximately 3,000 lb for this effect alone. The other penalties would be of comparable magnitude. Therefore, no further consideration was given this system.

d. Secondary Injection

Fluid may be injected into the main engine nozzle to deflect the primary gas flow. This method of vector control is called secondary injection. Past studies indicated that there are three basic approaches to secondary injection: the injection of nonreactive liquid, reactive liquid, or gas. The injection of gas provides the highest possible efficiency with respect to the propellant required for vector control. This is the system that was evaluated.

Besides the primary rigid engine and system weights, the following weight is added:

II, G, Thrust Vector and Roll Control (cont.)

Secondary gas control units	340 lb
Chamber reinforcing to distribute side force	525 lb
Delivery gas ducts	920 lb
TOTAL	1,785 lb

In addition to the inert weight, the propellant required to effect control through flight must be evaluated. The following equation is used to determine the inert weight equivalent of the gas used:

$$\frac{Mpl}{M_{Ps}/g} = 1 - \frac{\dot{w}_{ENG}\left(t_{btot}-t_{bl}\right)}{M_{tol} - \dot{w}_{ENG}\, t_{bl}}$$

where: M_{pl} = change in payload mass

M_{ps}/g = mass of secondary injection gas used at a particular time

$\dot{w}_{ENG}$ = main engine flow rate

t_{btot} = total flight time

t_{bl} = time from start of flight to time of injection of the gas

M_{tol} = takeoff mass of the vehicle

Figure II G-1 was used to determine the weight of gas required and its equivalent payload penalty. A total gas weight of 4,141 lb was necessary, resulting in an equivalent weight of 1,065 lb, which was added to the system. The total weight penalty is 2,850 lb. This compares quite favorably with the gimbaled engine weight penalty of 6,760 lb discussed previously. A net weight savings of 3,910 lb is available by using secondary gas injection. Therefore, the secondary gas injection system was selected as the best method for vector control.

II, G, Thrust Vector and Roll Control (cont.)

4. Secondary Injection Design

Because secondary injection was shown superior to other thrust vector control methods, additional effort was initiated to determine design parameters.

a. The following relationships were used to describe the secondary injection method of control:

$$F_s = I_{ss}\,\dot{w}_s \qquad \text{(Eq. 1)}$$

where: F_s = the effective side thrust

I_{ss} = side jet I_s

$\dot{w}_s$ = side jet flow rate

K = amplification factor

This relationship was used in an analytical study of secondary injection control of a plug nozzle as part of Contract Aerospace 60-102. Liquid oxygen and liquid hydrogen where used in the engine as the propellants and secondary injection gas was at a gas generator mixture ratio. The amplification factor was found to be as high as 2.0 for optimum conditions. Another expression used to describe secondary injection during test programs is:

$$\frac{F_s}{F_a} = K\,\frac{\dot{w}_s}{\dot{w}_p}$$

where: F_s = the measured total side force, perpendicular to the axis of the nozzle

F_a = the measured axial main nozzle thrust

II, G, Thrust Vector and Roll Control (cont.)

$\dot{w}_s$ = side jet weight flow rate

$\dot{w}_p$ = the main chamber primary flow rate

K = amplification factor

b. A survey of secondary injection test reports was made. One report indicated that in cold flow tests, K varied from 1 to 2.2.[1] It was also found that K is a function of the following factors:

(1) Secondary jet location as a function of distance from the throat.

(2) Angle of injection with respect to the wall.

(3) Geometric configuration of the injection orifice and $\frac{\dot{w}_s}{\dot{w}_p}$ (i.e., ratio of relative flow rates).

All tests reviewed were made with sonic injection with no divergent nozzle section. However, Equation 1 indicates that a divergent section may be beneficial.

For optimum jet location, injection angle, and orifice geometric configuration, K varied from 1.8 to 2.2. At low flow ratios, the amplification factor is greatest and is relatively independent of orifice configurations (one hole, a series of holes, or slots). However, at high flow ratios, a series of holes (or slots) has an advantage over a single hole and will increase the wall force portion of the side force from 50 to 80%.

(1) JANAF Solid Propellant Conference, Bulletin of the 17th Meeting, Volume III, 1961

II, G, Thrust Vector and Roll Control (cont.)

The total side force can be described as follows:

F_s total = $F_r + F_w$

where: F_r = the side jet reaction force or momentum exchange

F_w = force attributable to increase in the chamber wall pressure in the boundary layer

(1) Optimum Geometric Injection

The tests reviewed were conducted with conical, De Laval, and inverse plug nozzles. It was found that data from the three different nozzles in cold flow testing was similar and the same amplification factors could be obtained. There was, however, a marked difference in the optimum point of injection for each injection port configuration considered.

A single round port had its highest effectiveness when located approximately 50% down the nozzle wall (from the throat) with its axis approximately 30° upstream (in relation to the nozzle wall). A series of round, closely spaced holes and a slot were found to have their optimum location near or at the exit point of the nozzle perpendicular to the nozzle axis. This relationship can be explained in two ways. The side force is a combination of the secondary jet reaction (momentum exchange) and the increase in wall pressure upstream of the injection port is caused by the stagnation of the main-nozzle-stream boundary layer. There is a low pressure area created below the secondary jet because of boundary layer separation. This reduction or negative effect of the low pressure is canceled out by the increase in wall pressure resulting from the impingement of the oblique shock wave upon adjacent areas. The slot and row of holes has the highest effective side force near the nozzle exit because the amount of wall area below the injection port exposed to the separated boundary

II, G, Thrust Vector and Roll Control (cont.)

layer is minimized. A slot produces a larger disturbance both upstream and downstream than a single hole for the same flow rate; however, the oblique shock wave does not cancel out all of the negative force produced by the boundary layer separation below the jet. By reducing the amount of wall area exposed to the low pressure, the negative side force is lessened, resulting in an increase in the effective side force.

(2) Optimum Injection Angle

The optimum injection angle is a function of nozzle contour and the location of the injection port. There is indication that the further the injection port is located from the throat, the less effect the injection angle has. This angle is considered in relation to the nozzle wall.

One hot flow test program[2] was conducted with the main engine using LOX/RP-1, and secondary warm gas (668°F to 1,760°F) of LOX/RP-1 at various mixture ratios. Tests were made with bell nozzles having expansion ratios of 16 to 1 and 25 to 1. Injection was at 12 to 1 and 14 to 1 with the 16 to 1 nozzle, and 15 to 1 for the 25 to 1 nozzle. Results of these tests indicated that the same general characteristics for port location, injection angle, and port configuration applied in the hot tests. However, there was a significant change in the amplification factor. The cold flow tests have indicated K factors of from 1 to 2.2, while K factors of 0.4 to 0.7 were measured in the hot flow tests. As the difference in temperature between the two impinging streams became greater, the amplification factor was reduced. The relationship is much more complex than is indicated, but the trend was obvious. A review was then made of tests conducted at Aerojet-General in which the secondary gas was bled from the combustion chamber. It was found that the K factor measured was the same as that determined in the cold flow program.

(2) Ibid.

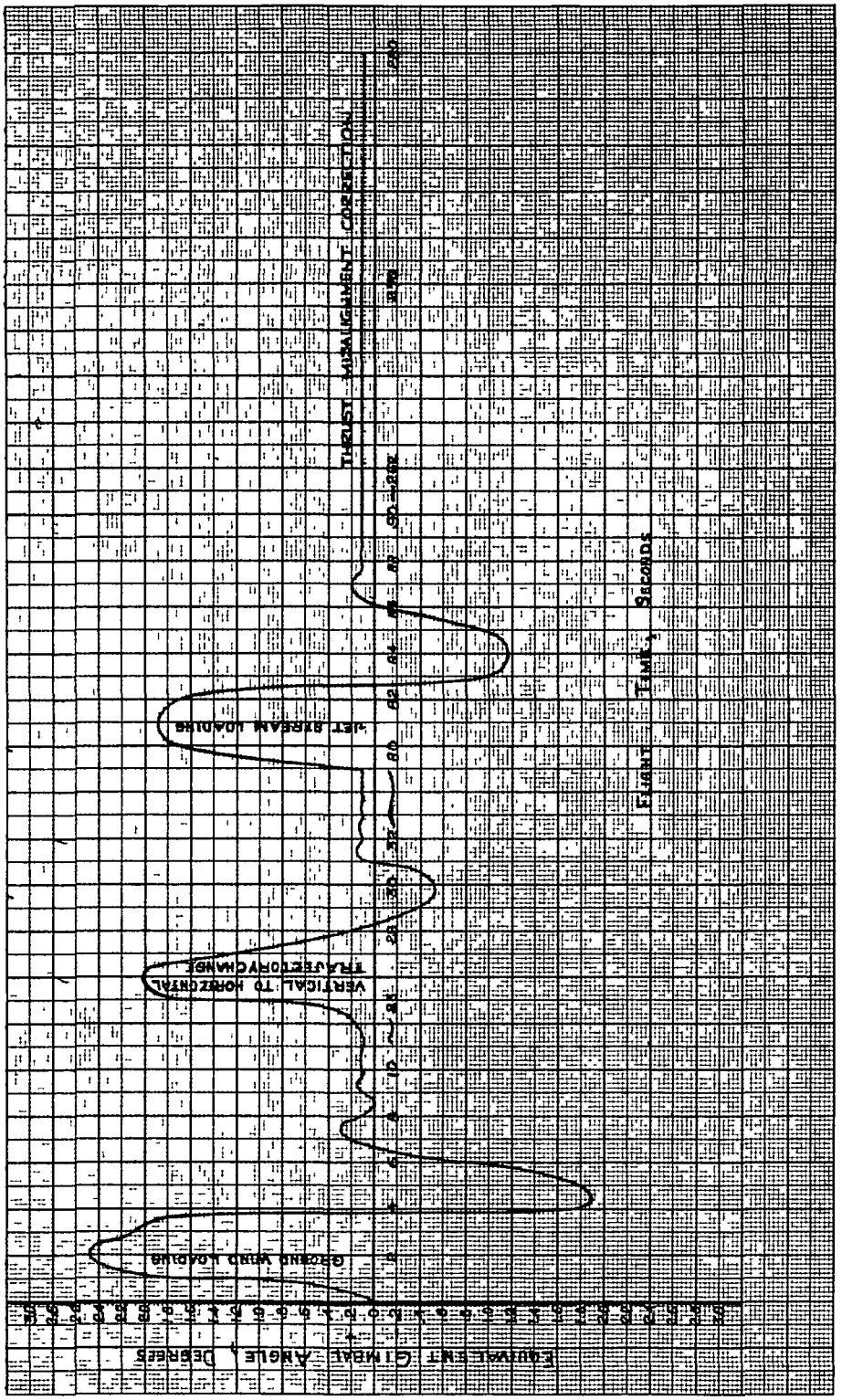

Characteristic Duty Cycle with Maximum Wind Loading, Trajectory, and Jet Stream Loading

Figure II G-1

II, Concepts Considered (cont.)

H. PRESSURIZATION SYSTEM

A complete investigation of propellant tank pressurization systems was completed. Some improvement over the standard configuration system is indicated; however, none of the systems considered shows outstanding gains. Each of these systems is briefly described and the weight of their major components are estimated. The effect of tank pressure upon vehicle payload is discussed in section II, K of this volume.

1. Basis of Comparison

For comparitive purposes, tank pressures were established at 4 psi above the vapor pressure of the propellant. All systems considered suppress boiling with the exception of the vapor pressurized (VāPak) system. Weight of the major components for each system and system complexity are used at the bases for comparison. Each propellant tank and the applicable pressurization systems are considered as independent of the other propellant tank. When establishing quantitative data, the standard vehicle is used as the system that requires tank pressurization.

2. Summary of Results

Hydrogen gas is the best for hydrogen tank pressurization because of its low density. The only recommended change to the standard vehicle hydrogen tank pressurization system is removal of the hydrogen heat exchanger from the turbine exhaust. This gives a slight over-all system weight saving of approximately 35 lb.

II, H, Pressurization System (cont.)

One system appears to offer some weight saving over the standard vehicle's oxygen tank pressurization system. This system incorporates an oxidizer-rich gas generator to supply pressurization gas to the oxygen tank at 1,150°F and offers an estimated 300-lb weight saving at the expense of increased complexity. Details of each of the above systems as well as others studied are discussed as follows.

3. System Descriptions

a. Hydrogen Tank

The standard vehicle hydrogen tank is pressurized with warm hydrogen gas. This gas is readily available in the standard engine cycle at approximately 1,100 psia and -420°F. The hydrogen is further heated to approximately -200°F in a heat exchanger located in the turbine exhaust. It is then passed through a regulator and used to pressurize the hydrogen tank. Both system weight and complexity are difficult to improve upon. The system weight is low because of the low density of warm hydrogen gas and system components consist of only lines, a heat exchanger, and a regulator.

No reduction in system weight resulting from the use of a different pressurization gas is foreseen. One possible modification of the standard hydrogen tank pressurization system is removal of the heat exchanger in the turbine exhaust, giving a weight saving of approximately 35 lb. Because of the increased collapse factor associated with the higher hydrogen gas temperature, little gas weight saving results from the higher temperature. It may also be desirable to have this turbine exhaust available for the oxygen tank pressurization system. No other improvement is foreseen for the hydrogen tank pressurization system.

II, H, Pressurization System (cont.)

b. Oxygen Tank

The oxygen tank of the standard configuration is pressurized with helium gas. Helium is initially stored at 3,000 psia in a sphere located in the oxygen tank. It is regulated and passed through a heat exchanger, where it is again regulated to 25 psia for oxygen tank pressurization. This pressurization system was compared with several others on the basis of weight and complexity. The systems considered were:

(1) Stored gas (helium or nitrogen)
(2) Stored gas with a heat exchanger
(3) Heated oxygen
(4) Bipropellant gas generation
(5) Solid gas generator
(6) VāPak (no pressurization system)

Each of these systems is summarized on the schematic diagrams that are indicated in the following discussions. Their advantages and disadvantages will be discussed.

(1) Stored Gas

(a) Helium (See Figure II H-1)

Gas stored at 3,000 psia and -297° F is allowed to expand through a two-stage pressure regulator to 25 psia. For computing gas weight, a collapse factor ($C.F. = \frac{\text{actual gas weight}}{\text{theoretical wt at inlet p and t}}$) of 1 was assumed conservative because of the low average inlet temperature of the gas, -355°F. This system, although simple, is considerably heavier than the corresponding system in the standard vehicles.

II, H, Pressurization System (cont.)

(b) Nitrogen (See Figure II H-2)

Nitrogen gas is initially stored at 3,000 psia and 70° F. It expands through a two-stage pressure regulator to 25 psia.

An assumed gas-collapse factor of 1.5 indicates that this system is much heavier than the standard configuration. The storage of nitrogen outside of the propellant tanks is a further disadvantage.

(2) Stored Gas with a Heat Exchanger

(a) Helium (Standard Configuration)(See Figure II H-3)

This system differs from that previously described because a heat exchanger has been added. This heat exchanger is located in the turbine exhaust and raises the temperature of the helium gas entering the oxygen tank to 40°F. Assumed collapse-factor of 1.5 results in a helium weight of 470 lb and a helium tank weight of 1,730 lb. The sum of these weights, 2,200 lb, is used as a standard of comparison for the other systems.

(b) Nitrogen (See Figure II H-4)

This system is identical to the previous one, except that nitrogen gas instead of helium is used as the pressurizing standard configuration.

II, H, Pressurization System (cont.)

(3) Heated Oxygen (See Figure II H-5)

This system uses high pressure liquid oxygen from the pump discharge as the pressurizing gas source. Using heat exchangers in both turbine exhausts of the standard configuration, the gas temperature is approximately 0° F. As assumed collapse-factor of 1.5 gives a gas weight of 3,210 lb; approximately 1,000 lb heavier than the standard vehicle.

(4) Bipropellant Gas Generation (See Figure II H-6)

This system appears to offer some weight savings over the standard system. Oxygen and hydrogen from the pump discharge are fed into a gas generator at a mixture ratio of 110.1. Gases generated at 1,150° F are fed directly into the oxygen tank. A gas-collapse factor of three gives a gas weight at the end of the run of 1,740 lb. This system, although slightly more complex than the standard system, does offer approximately 300 lb in weight saving. Justification for the use of this system is dependent upon a study of reliability degradation in relationship to decreased weight.

(5) Solid Gas Generator (See Figure II H-7)

The use of a solid propellant cartridge as a pressurization gas source was evaluated. For a sodium azide solid gas generator, it was assumed that the generated gas was nitrogen at 750° F. An assumed collapse-factor of 3 gives a gas weight of 2,200 lb and a solid propellant weight of 3,500 lb. This system does not appear to be advantageous in this application because of its weight.

II, H, Pressurization System (cont.)

(6) VāPak (Vapor Pressurized System) (See Figure II H-8)

The vapor pressurized system offers the ultimate in simplicity because it is essentially a non-pressurization system. The vaporization of propellants maintains tank pressure at a propellant vapor pressure corresponding to propellant temperature. This system does not suppress boiling at the surface of the liquid as do all the other systems considered. Suppression of boiling is desirable to assure that the pump does not receive vapor bubbles which may be drawn through the suction lines. In the absence of an analysis of the boiling depth problem, this system was shown to be disadvantageous from the weight standpoint, also. At the end of the run, the oxygen tank is filled with cold oxygen vapor weighing 4,680 lb. This is approximately 2,000 lb more than the standard system weight. It is concluded that the vapor-pressurized system is not advantageous for this application.

4. Discussion of Results

Several assumptions were made throughout the pressurization system study. The selection of a gas-collapse factor applicable to each of the systems considered was somewhat arbitrary. A complete heat flow analysis for each system considered was not within the scope of this study. Some experimental data was used in making the collapse factor estimate.

A more detailed design of any of the above systems requires a careful thermodynamic analysis, including the effects of all heat sinks, tank insulation, and propellant sloshing.

II, H, Pressurization System (cont.)

The problem of propellant boiling was encountered in the tank pressurization study. It was assumed that the acceleration head of the propellants was sufficient for the NPSH requirements of the pumps. This might indicate that no pressurization system is required. However, to assure that cavitation does not occur in the pumps, it was required that no vapor bubbles reach the pump. If boiling occurred at a significant depth in a nearly empty tank, it appears that vapor bubbles might be drawn into the suction line and the pump. Therefore, it was required that tank pressure suppress propellant boiling.

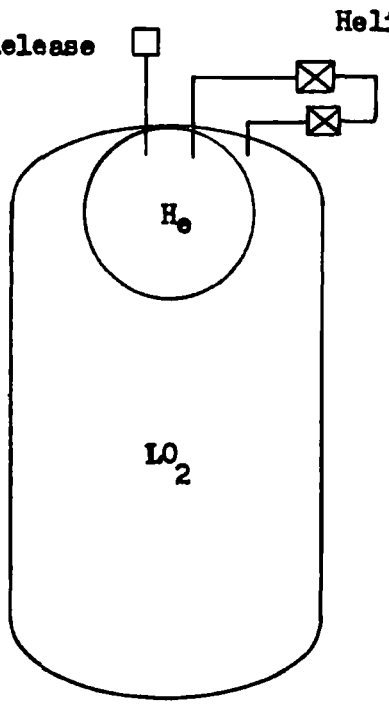

Initial He. Pressure	= 3,000 psia
Final He. Pressure	= 100 psia
LO_2 Tank Pressure	= 25 psia
Ave. Temperature of He. Entering Tank	= -355° F
Assumed Collapse Factor	= 1.0
Helium Tank Volume	= 272 ft^3
Helium Tank Weight	= 5,330 lbs
Helium Weight	= 1,440 lbs

System Components

- Helium Tank
- Lines
- 2 Stage Regulator
- Fill and Safety Release
- Helium Release Valve (Shut-Off)

Stored Gas (Helium)

Figure II H-1

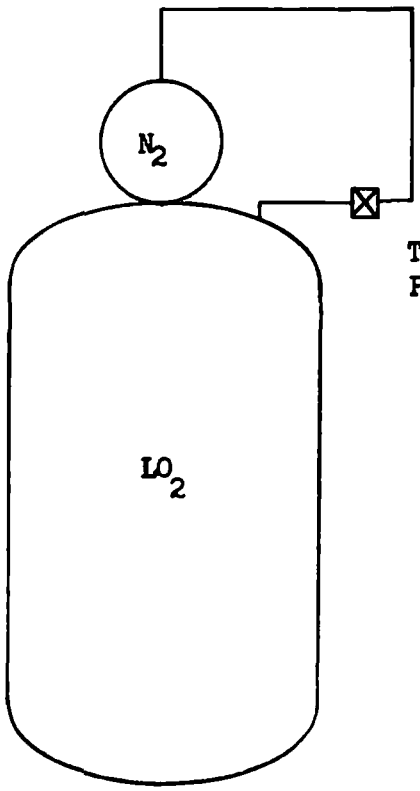

Two Stage
Pressure Regulator

Initial N_2 Pressure	= 3,000 psia
Final N_2 Pressure	= 100 psia
LO_2 Tank Pressure	= 25 psia
Average Temperature of N_2 Entering Tank	= -131° F
Assumed Collapse Factor	= 1.5
N_2 Tank Volume	= 320 ft^3
N_2 Tank Weight	= 6,280 lbs
N_2 Weight	= 4,480 lbs

System Components

Nitrogen Tank

Lines

Two Stage Pressure Regulator

Stored Gas (Nitrogen)

Figure II H-2

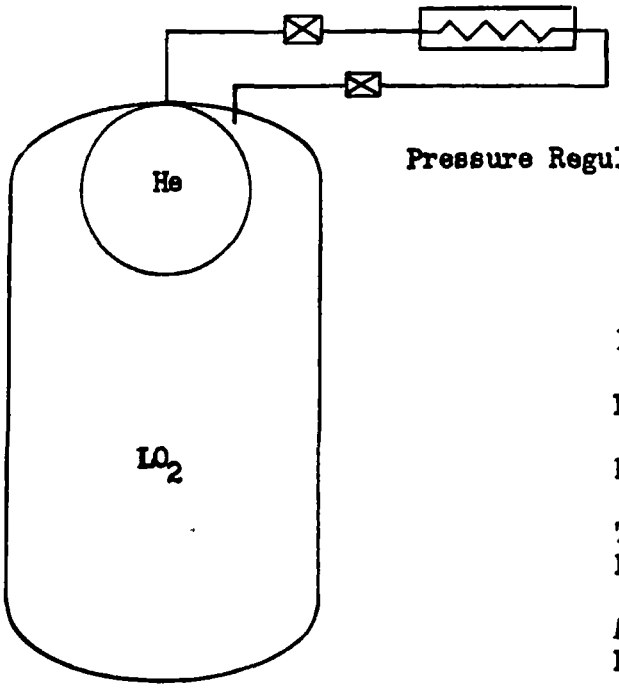

Initial He Pressure = 3,000 psia

Final He Pressure = 100 psia

LO_2 Tank Pressure = 25 psia

Temperature of He Entering Tank = 40° F

Assumed Collapse Factor = 1.5

Helium Tank Volume = 88.4 ft^3

Helium Tank Weight = 1,730 lbs

Helium Weight = 470 lbs

System Components

Helium Tank

Lines

Heat Exchanger

Pressure Regulators (2)

Stored Gas and Heat Exchanger (Helium), Standard Vehicle

Figure II H-3

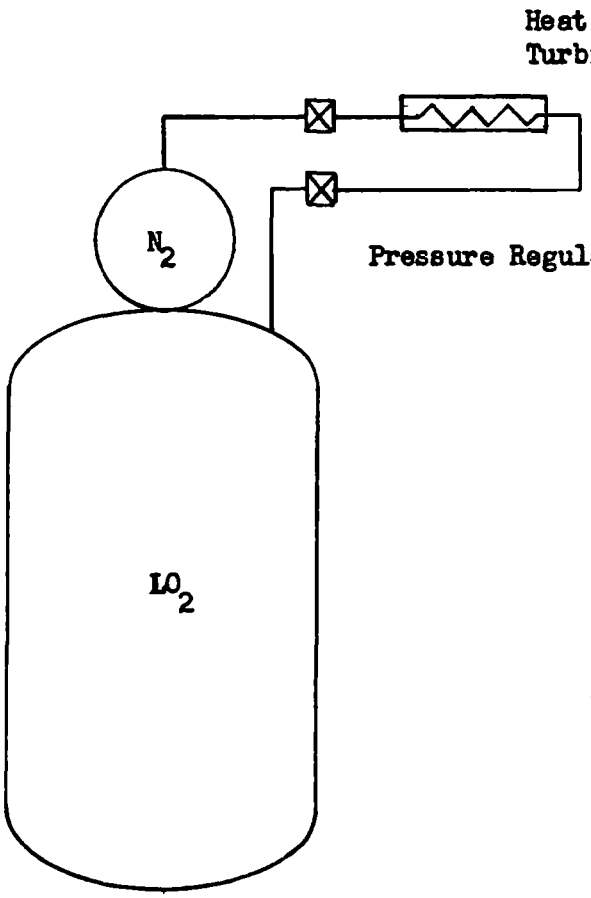

Initial N_2 Pressure	= 3,000 psia
Final N_2 Pressure	= 100 psia
LO_2 Tank Pressure	= 25 psia
Temperature of N_2 Entering Tank	= 40° F
Assumed Collapse Factor	= 2.0
N_2 Tank Volume	= 278 ft^3
N_2 Tank Weight	= 5,450 lbs
N_2 Weight	= 3,890 lbs

System Components

- Nitrogen Tank
- Lines
- Heat Exchanger
- Pressure Regulators (2)

Stored Gas and Heat Exchanger (Nitrogen)

Figure II H-4

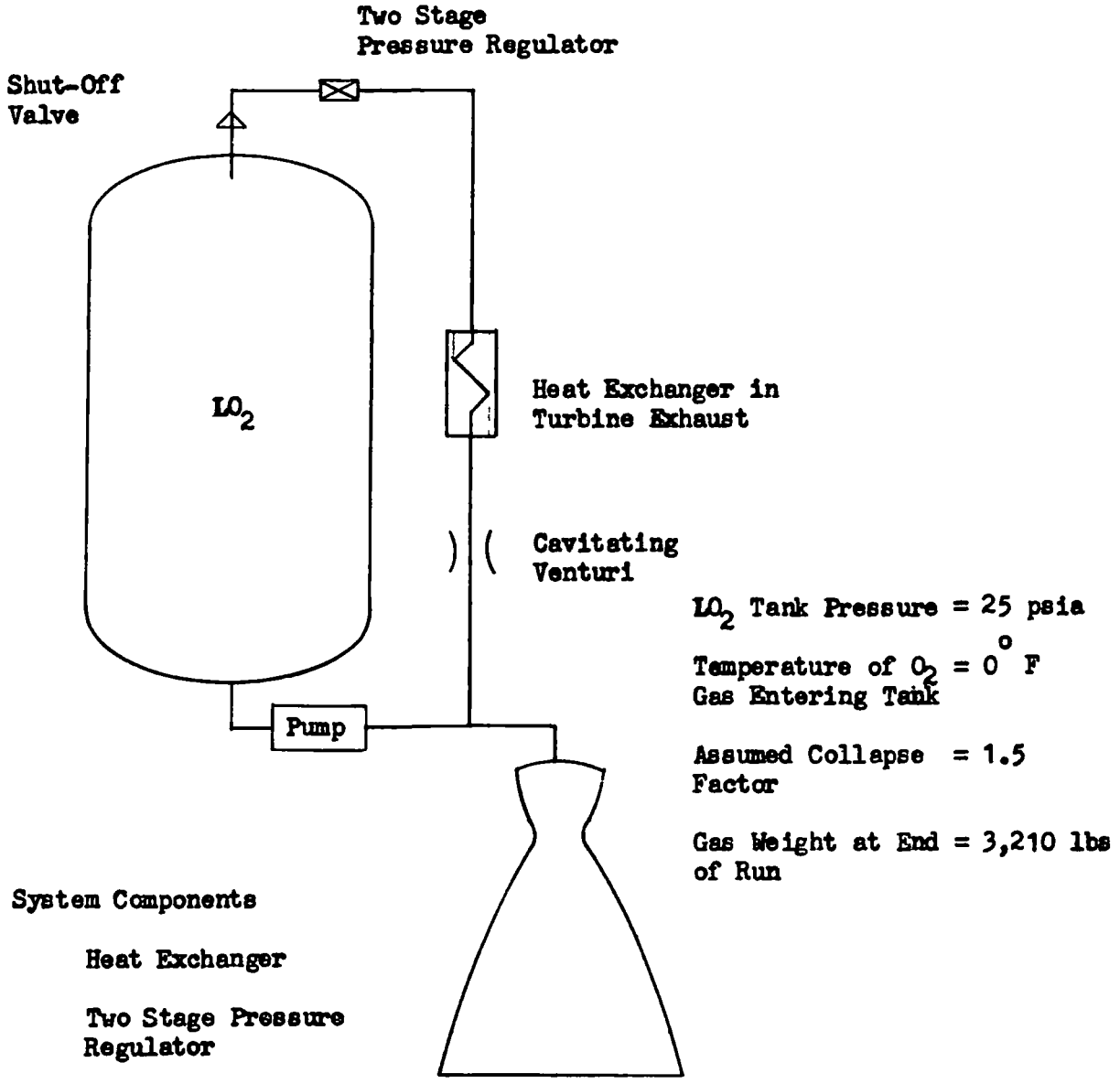

Heated Oxygen

Figure II H-5

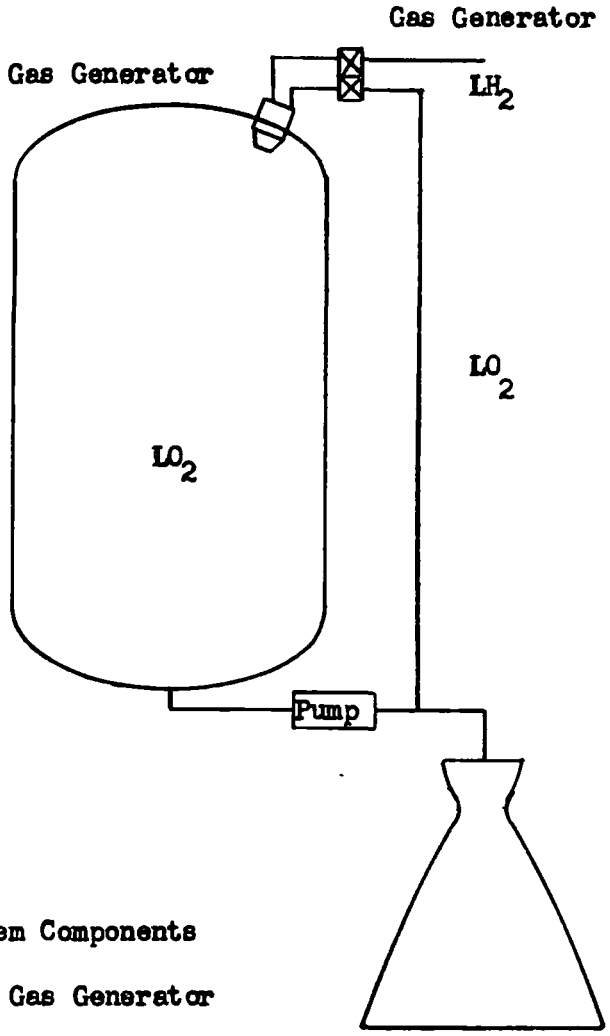

Mixture Ratio = 110

Gas Temperature = 1,150° F

LO_2 Tank Pressure = 25 psia

Assumed Collapse Factor = 3.0

Gas Weight at End of Run = 1,740 lbs

System Components

Gas Generator

Ignition System

Lines

G.G. Valves (Shut-Off + M.R. Control + Flow Control)

Bipropellant Gas Generator

Figure II H-6

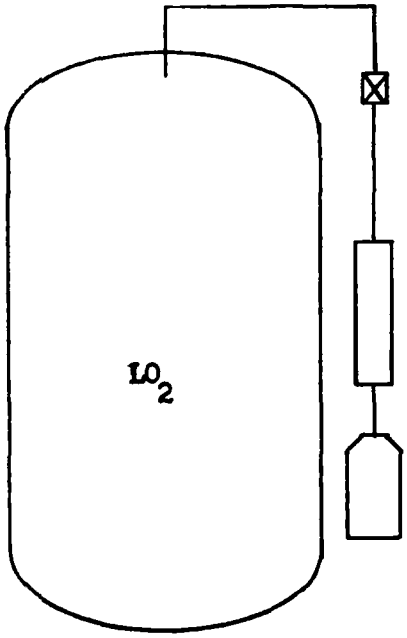

LO_2 Tank Pressure	= 25 psia
Gas Temp. Entering Tank	= 750° F
Assumed Collapse Factor	= 3
Solid Propellant Weight	= 3,500 lbs

System Components

- Solid Gas Generator
- Separator
- Ignition System
- Check Valve

Solid Propellant Gas Generator (Sodium Azide)

Figure II H-7

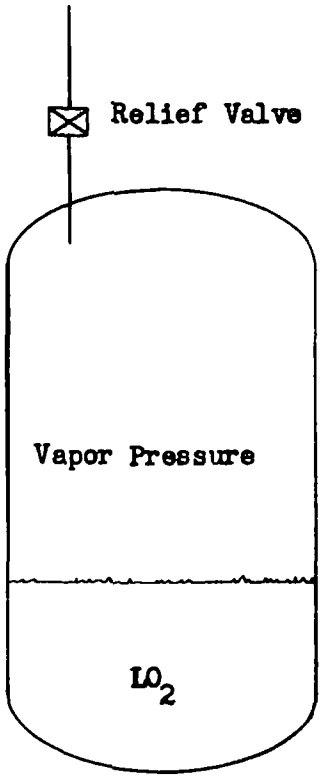

Initial Temperature = -282° F

Initial Pressure = 30 psia

Final Pressure = 20 psia

Final Temperature = -290° F

O_2 Vapor Weight at end of run = 4,680 lbs

System Components

Relief Valve

Vapor-Pressurized System (VāPak)

Figure II H-8

II, Concepts Considered (cont.)

I. THRUST CHAMBER CONCEPTS

1. General

The combustor and the nozzle comprise the thrust chamber. An injector and a combustion chamber make up the combustor in which propellants are combined and chemical energy is converted to heat energy. It is in the nozzle that this heat energy is converted to kinetic energy, thereby producing thrust. The efficiency with which these processes occur is influenced by thrust chamber design. As discussed in Section IV, C of this volume, the factors contributing most significantly to low cost and high reliability of vehicle payload delivery are high specific impulse, low weight of inert parts, and low development cost. It was toward these goals that the thrust chamber effort was directed and is reflected in the following discussion.

The chemical energy available from given propellants is fixed. Therefore, increased thrust chamber performance can only be attained by design changes in the thrust chamber.

Modern rocket engine combustors are highly efficient. It is relatively simple to produce efficiencies of 95% in the combustors and much higher efficiencies (as high as 98%) have been attained. Also, conventional combustors are quite light in weight. However, combustor development cost is high and it is in this area that significant progress towards program objectives can be made when considering combustor approaches that are not conventional. Also, there are certain desirable unconventional nozzle concepts that may dictate the use of non-conventional thrust chambers to best achieve program objectives.

II, I, Thrust Chamber Concepts (cont.)

Modern rocket nozzles are also quite efficient in converting available energy into kinetic energy at the designed pressure ratio. However, at other than the designed pressure ratio, the conventional De Laval nozzle is not so efficient. In altitude-compensating nozzles, efficient energy conversion is obtained at all altitudes where atmospheric pressure is greater than nozzle design pressure. Therefore, primary emphasis was placed upon nozzle concepts offering the altitude compensating feature.

In addition, a great deal of the heat energy produced in the combustion chamber is unavailable because of limited nozzle area ratio. Area ratio is selected for a rocket nozzle by trading weight and specific impulse so that maximum overall performance results. Adding more area ratio nets a greater gain in weight than in specific impulse. However, with higher thrust chamber pressure and greater optimum area ratio, there is an increase in overall performance. Figure II E-1 presents typical results from vehicle analyses showing the effect of chamber pressure upon vehicle performance. With these results, it is anticipated that chamber pressure of approximately 2, 500 psia will be of interest in future rocket engines. Hence, much of the discussion of combustors deals with this operating pressure.

It is expected that increased thrust chamber pressure will have little effect upon thrust chamber weight. This can be seen when the following factors are considered: In the combustion chambers, throat area is inversely proportional to combustor pressure, and provided characteristic length (L*) remains constant, combustor volume will be inversely proportional to combustor pressure. Therefore, it is concluded that pressure vessel criteria are satisfied in the combustor.

II, I, Thrust Chamber Concepts (cont.)

Injector considerations then follow. As pressure is increased, the injector can be made smaller in diameter provided injection density can be increased. Large element injection provides a means for increasing injection density. Although greater injector thickness may also result, there is high confidence that injector weight will not increase and may even decrease as pressure is increased.

With the nozzle, as thrust chamber pressure is increased, throat area is decreased but the physical dimensions of the nozzle change minutely except in a region very close to the nozzle. The assumption that these physical dimensions do not change with pressure changes is almost completely valid. Also, when thrust chamber pressure is increased, and constant nozzle exit area is maintained, nozzle exit static pressure also remains very nearly constant, as does the pressure at any given place across the nozzle. This is true except very close to the throat; therefore, the structure for supporting the internal nozzle pressure will not change significantly with increases in chamber pressures. This assumption is also valid for the stiffening structure of the nozzle.

Finally, the regenerative coolant tubes were considered. The thickness of these tubes is dictated by the cooling requirements. For the most effective cooling, minimum tube-wall thickness consistent with ease of fabrication is desired. This thickness must remain constant even if the pressure is increased. Therefore, as chamber pressure is increased the tube diameter must be decreased and the number of tubes must become greater. This increases pressure drops in the system but results in the same weight of the bundle of tubes.

Based on the preceding discussion, it appears justifiable to assume that thrust chamber and nozzle weight remains constant with changes in chamber pressure.

II, I, Thrust Chamber Concepts (cont.)

The remaining discussion is devoted to nozzle and combustor concepts. Because the nozzle type selected will strongly influence the combustor type, nozzle concepts are discussed first.

2. Nozzle Concepts

a. Introduction

The purpose of the rocket nozzle is to convert the thermal energy produced in the combustor into kinetic energy. This is accomplished with the highest efficiency when the nozzle exit pressure and the ambient pressure are approximately equal. With a conventional De Laval nozzle, this ideal condition exists only at one altitude. Thus, for a first-stage rocket engine, with a conventional De Laval nozzle, the nozzle design must be a compromise so that the loss in efficiency is minimized over the entire trajectory. This loss in performance is a significant disadvantage of the De Laval nozzle. Therefore, nozzle concepts were examined that would provide some means of altitude compensation.

There are concepts that provide partial altitude compensation for De Laval nozzles. Several of these are discussed briefly. However, the most promising altitude compensating nozzles are the plug and forced-deflection types. Hence, a major portion of the effort in this investigation was devoted to these. Nozzles of other than circular geometry were also considered, but no application was found for them. Consequently, no effort was made for further evaluation.

II, I, Thrust Chamber Concepts (cont.)

b. Conclusion

It is concluded that the most promising nozzle for application in an advanced rocket engine is the forced-deflection type. This nozzle is potentially the lightest in weight of all nozzle types considered and, theoretically, can provide nearly perfect altitude compensation up to its design pressure ratio.

c. Modified De Laval Nozzles

Modified De Laval nozzles include the stepped De Laval, gas-injected De Laval, plug insert in a De Laval, and the expandable nozzle. These methods, discussed below, are depicted in Figures II I-1 and II I-2.

(1) Stepped De Laval

The stepped De Laval nozzle is shown in Figure II I-1. The increase in the angle of the nozzle wall at the step is great enough so that at sea level, the gases will separate from the wall and not over-expand. When the ambient pressure is sufficiently decreased, the nozzle downstream of the step is filled. Several steps could be used.

Difficulties exist in arriving at a contour that will separate the gases from the wall at discrete intervals in a trajectory so as to realize a performance gain, without large losses caused by shocking at the steps. However, if these problems can be overcome, this nozzle would then show promise; therefore, Aerojet-General is exploring its potential, both analytically and in cold flow tests. Results from initial investigation indicate that high nozzle efficiency will be very difficult to obtain with such a configuration. Hence, it was eliminated from further consideration in this investigation.

II, I, Thrust Chamber Concepts (cont.)

(2) Gas-Injected De Laval

This concept would require gas injection orifices placed around the nozzle at a given area ratio. Injection of gas would cause enough distrubance to separate the gases from the nozzle wall and providing altitude compensation.

The major disadvantage of this concept is loss of performance attributable to the gas injected. Also, additional weight caused by the gas ducts and the mechanisms required for controlled injection. An alternative means for accomplishing this type of altitude compensation is shown in Figure III-2b. This figure shows slots that are opened to allow ambient air to enter the over-expanded nozzle region. Disadvantages of this concept include weight and nozzle cooling difficulties. Heavy weight results because of the activation mechanism and the added structure required for bridging the air slot. Also, regenerative cooling of the flaps and lower nozzle portion would be very difficult. Heat transfer analyses have shown that with oxygen/hydrogen propellants, radiation cooling in this region is inadequate. Therefore, a heavy ablative section would probably be required.

(3) Plug Insert

Another method for providing stepwise altitude compensation is with a plug insert (Figure III-2e). The plug is expelled at some given time during flight. If the proper moment is selected, when the C_f values of the plug and the nozzle are equal, considerable gain is made in performance.

II, I, Thrust Chamber Concepts (cont.)

Two or three plugs could be expelled, resulting in a stepwise approximation to an optimum C_f curve. As the number of plugs increases, the gain with each progressively decreases. The total number for any trajectory could be made optimum by comparison against the increased weight and complexity to be incurred. Major disadvantages of this scheme are the weight of the plug inserts and the actuation system required to jettison the plugs.

(4) Expandable Nozzle

Another means for compensating a De Laval nozzle is the expandable nozzle (Figure II I-2c and 2d). Models of these nozzles have been successfully tested at Aerojet-General (Figure II I-3). These expandable nozzles are capable of resisting internal but not external loads. Therefore, they collapse sufficiently to provide an optimum expansion ratio. At the present state of development, they are limited in application to relatively low chamber pressures because of heat transfer considerations.

d. External Expansion Nozzles

(1) General

Two of the most widely considered external-expansion nozzles, the plug nozzle and forced-deflection nozzle, are shown schematically in Figure II I-4. Both nozzles are axially symmetric; however, in the plug nozzle, the nozzle gases are expanded radially inward, while in the forced-deflection nozzle, the gases are expanded radially outward or away from the axis of symmetry. Therefore, the forced-deflection nozzle is, in principle, the

II, I, Thrust Chamber Concepts (cont.)

inverse of the plug nozzle. It is also possible to produce many external-expansion nozzle configurations by combinations of the plug and forced-deflection nozzle principles, but most combinations lead to complex engine systems. Normally, only one or the other nozzle is used.

(a) Annular Throat Nozzles

The completely annular forced-deflection or plug nozzle (annular throat, exit, and combustion chamber) has several serious disadvantages when compared to the conventional nozzle. The annular nozzle throat is an annular gap and has many times the peripheral area of a single circular throat for the same total throat area. The Reynolds number for the annular gap is smaller and results in a higher heat-transfer coefficient. The total heat transfer of the overall nozzle is increased by both effects. The total hoop stress of the annular combustion chamber is greater for the outer shell, and the inner wall must be prevented from buckling. Because of the higher structural loads, it becomes difficult to maintain the dimensional stability of the nozzle throat. Any asymmetry of the throat will result in a skew thrust vector for the engine.

(b) Discrete Throat Nozzles

The problems of an annular nozzle are eliminated or lessened to some extent by the use of several discrete circular throats rather than the continuous annular throat. Flow from the discrete throats is merged to form an annular flow at the exit of the transition sections so that good performance is realized and the advantage of external expansion is retained.

II, I, Thrust Chamber Concepts (cont.)

The use of discrete throats reduces the total area exposed to the maximum heat flux and results in decreased hoop stress in the nozzle near the throat. Discrete throats allow for multiple combustion chambers, allow scaling up on total thrust or expansion ratio without complete redevelopment, and provide for combustor and partial nozzle development at a fraction of total thrust.

Many types of discrete-throat nozzles are possible; however, some types offer distinct advantages in design and performance prediction (Figure II I-5). It is possible to produce very compact nozzle systems with the reverse-flow discrete-throat nozzle shown in Figure II I-5. This nozzle is similar to the discrete-throat nozzle with a wedge transition section (Figure II I-5). The flow in the transition section undergoes a supersonic turn as the flow expands internally. Some experimental work is necessary to achieve an efficient design, but may be minimized by using information that can be obtained from axisymmetric calculations of an equivalent nozzle. The wedge transition section is easily designed with existing analytical techniques and is further discussed in Section (4) following.

(2) Current Technology

The plug nozzle and the forced-deflection nozzles have been analytically and experimentally investigated at Aerojet-General. Both annular- and discrete-throat configurations were considered.

Nozzle design techniques were developed and several IBM-7090 computer programs are available for nozzle-contour design and performance prediction. These computer programs are not limited to design and analysis of external-expansion nozzles only, but may be applied to all classes of axisymmetric nozzles, either annular or circular in cross-section.

II, I, Thrust Chamber Concepts (cont.)

Cold-flow test programs have been conducted both at the Aerojet-General Sacramento test area and under sub-contract at the FluiDyne Engineering Corporation.

Hot-flow tests have been performed at Aerojet-General, Sacramento, with both plug nozzles and forced-deflection nozzles. These firings have included the use of both liquid- and solid-propellant combustion gases. Performance of the hot-flow models was successfully correlated with cold-flow and analytical results, thereby permitting confident use of cold-flow data to provide confirmation of proposed techniques for hot-flow design. This procedure can greatly reduce the number of hot-flow tests required during development.

Some typical data obtained by means of hot- and cold-flow testing for the plug nozzle is shown in Figure II I-6. These test nozzles were designed by the techniques described in Section (3) following. Test results confirmed the validity of the methods.

(3) External-Expansion Nozzle Theory

(a) External Expansion Compared to Internal Expansion

In the conventional converging-diverging nozzle, the expansion precess takes place on the internal side of the nozzle walls, but in the external-expansion nozzle, the expansion occurs on the external side of the nozzle walls. In Figure II I-7, the flow process for both internal- and external-expansion nozzles is shown schematically. Depending upon the pressure ratio, the nozzle gases are either under-expanded, over-expanded, or optimum expansion.

II, I, Thrust Chamber Concepts (cont.)

At under-expanded conditions, the nozzle gases are not fully expanded at the nozzle exit, with further expansion occuring after leaving the nozzle. The incomplete expansion results in lowered thrust efficiency for both the internal-expansion nozzle and the external-expansion nozzle (Figure II I-2).

At optimum expansion, the nozzle gases are fully expanded to the ambient pressure, which results in maximum thrust efficiency for internal- and external-expansion nozzles (Figure II I-7).

Over-expansion of the nozzle gases results when the gases are expanded to a pressure at the nozzle exit, which is lower than the ambient pressure. Over-expansion, like under-expansion, results in lowered thrust efficiency. Over-expansion takes place in a conventional nozzle as a result of the flow not being exposed to the ambient conditions until the nozzle exit is reached, and because the flow is supersonic, the ambient pressure cannot be propagated upstream. However, the ambient conditions can be propagated through the boundary layer, and where the pressure differences between nozzle exit and ambient are sufficiently high, the boundary layer can cause flow separation that will tend to decrease the extent of over-expansion losses. Shock waves necessarily accompany the flow separation and result in some loss of thrust efficiency.

In the over-expanded region of operation, the external-expansion nozzle characteristics differ from the converging-diverging nozzle characteristics. The flow in the external-expansion nozzle is continously exposed to ambient conditions from throat to exit, and as a result, the expansion can adjust to ambient pressure (Figure II I-7). It is this property of external-expansion nozzles that provides superior thrust efficiency when compared to

II, I, Thrust Chamber Concepts (cont.)

internal-expansion nozzles at over-expanded conditions. The external flow does not over-expand, but expands to ambient pressure only in the plug nozzle and to the nozzle base pressure for the forced-deflection nozzle. Ambient or base pressure is attained at some intermediate point on the nozzle surface. Beyond that point, the flow continues to be turned toward the axial direction by the nozzle contour. This turning, in the absence of expansion, causes the generation of distributed compression waves, consequently, the pressure upon the plug or shroud surface becomes higher than the ambient pressure. The increased surface pressure results from the recovery of some of the nonaxial momentum by the component that exists at the termination of the expansion (Figure II I-7).

Gas dynamics of the plug and forced-deflection nozzles are similar, with one exception. The gas boundary entirely exposed to ambient conditions occurs on the outer periphery of the jet for the plug nozzle, while the other boundary is enclosed by the flow field in the forced-deflection nozzle (Figure II I-4). To ensure that ambient pressure exists on the internal-flow boundary of the forced-deflection nozzle, it is necessary to provide an addquate flow area from the atmosphere. Although it is possible for ambient conditions to be felt through the central core of the gas stream under favorable conditions, it will not be possible under all operating conditions. In general, mass and momentum transfer will occur between the semistagnant gas of the central core and the high velocity exhaust stream, resulting in core pressure less than ambient, unless provision is made for flow from ambient conditions to the nozzle-plug base area. When the plug base or core pressure is less than

II, I, Thrust Chamber Concepts (cont.)

the ambient pressure, over-expansion of the nozzle gases occurs with the resultant loss in thrust efficiency. If the nozzle must operate in a range of pressure ratio that includes pressure ratios (P_c/P_a) less than the nozzle design point, then provision must be made to ensure that the plug base pressure is maintained near ambient; otherwise, the nozzle will not have improved performance when compared to the conventional De Laval nozzle.

(b) Gas Dynamic Model for External Expansion

In theory, the flow process of an external-expansion nozzle involves the same gas dynamic principles involved in the expansion process of conventional internal-expansion nozzles. The flow process involves transonic and supersonic flow in axisymmetric annular flow spaces. The perturbation techniques used by Sauer for solution for solution of the equations of motion for

II, I, Thrust-Chamber Concepts (cont.)

flow of a compressible fluid at velocities near Mach 1 are easily adapted to the annular flow space, while the method of characteristics for axisymmetric supersonic flow is used to solve the equations of motion at supersonic velocities. These analytical tools are available in IBM 7090 programs for use in nozzle design and performance prediction.

The exact techniques just discussed apply only to continuous annular flow fields, and consequently, only to nozzles having continuous annular throats. However, the flow fields of external expansion nozzles are significantly different from the flow field of a conventional nozzle and certain judicious assumptions may be made with surprising accuracy. These assumptions, in turn, permit a great reduction in the labor required for both design and evolving optimum external-expansion nozzles. These rapid methods are particularly useful in the design of discrete-throat nozzle configurations where the flow process can only be approximated by the axisymmetric flow relations because the flow is no longer axisymmetric.

The expansion process in the external-expansion nozzle originates as a Prandtl-Meyer expansion about the plug lip (Figure I-8). The entire flow field is asymetric with respect to the direction of flow, and the gas streamlines are monotonic curves from the throat to the nozzle exit. The IBM 7090 computer programs for the method of characteristics have been used for the design of external-expansion plug and forced-deflection nozzle contours. Exact solution of the gas dynamic equations has shown that the following assumptions may be made:

(1) The family of characteristics or Mach lines associated with the Prandtl-Meyer expansion may be assumed to lie straight and with uniform flow properties, V and θ.

II, I, Thrust Chamber Concepts (cont.)

(2) The flow properties may be determined by the two-dimensional Prandtl-Meyer relationship.

Using these assumptions, the nozzle contour may be determined from continutiy and axisymetric, geometric considerations. Both the resulting nozzle contour and calculated performance agree with that of the more laborious approach using numerical solution of the equations for axisymetric flow. These facts have been verified by cold-flow tests performed by the FluiDyne Engineering Corporation in the Aerojet-General contract. Cold-flow tests were performed with both plug and forced-deflection nozzles and the rapid design method has been completely verified.

c. Nozzle Contour and Performance Analysis

The expressions for thrust and mass flow from the nozzle are found from application of continuty and momentum considerations, respectively. To apply these principles, it is necessary to properly select a control surface, S, which completely encloses the rocket system,

Continuity

$$\dot{m} = \int_S \rho \vec{V} \cdot \vec{n} \, ds \qquad \text{(Eq 1)}$$

Momentum

$$F = \int_S \left[(\rho \vec{V} \cdot \vec{n}) \vec{V} + p\vec{n} \right] ds \qquad \text{(Eq 2)}$$

II, I, Thrust Chamber Concepts (cont.)

All gravitational, electrostatic, and aerodynamic flight forces are ignored.

When Equations 1 and 2 are applied to the specific control surfaces, S, for the external expansion nozzles (Figure I-8), the following relationships exist:

Plug nozzle,

$$\dot{m} = \int_{R_e}^{R_L} \rho_e \; V_e^{\,2} \left[\frac{\sin \alpha_e \, 2\pi R (-dR)}{\sin (\theta_e - \alpha_e)} \right] \qquad \text{(Eq 3)}$$

$$F = \int_{R_e}^{R_L} \left[\rho_e \; V_e^{\,2} \left(\frac{\sin \alpha_e \cos \theta_e}{\sin (\theta_e - \alpha_e)} \right) + (P_e - P_a) \right] (-dR) \qquad \text{(Eq 4)}$$

$$+ \int_{o}^{R_e} (P_b - P_a) \, 2\pi R dR$$

Forced deflection nozzle,

$$\dot{m} = \int_{R_p}^{R_e} \left[\rho_e \; V_e^{\,2} \left(\frac{\sin \alpha_e \, 2\pi R dR}{\sin (\theta_e + \alpha_e)} \right) \right] \qquad \text{(Eq 5)}$$

$$F = \int_{R_p}^{R_e} \left[\rho_e \; V_e^{\,2} \left(\frac{\sin \alpha_e \cos \theta_e}{\sin (\theta_e + \alpha_e)} \right) + P_e - P_a \right] 2\pi R dR \qquad \text{(Eq 6)}$$

$$+ \int_{o}^{R_o} \left[(P_b - P_a) \, 2\pi R dR \right]$$

II, I, Thrust Chamber Concepts (cont.)

where:

ρ	=	density of gas,	F	=	thrust
V	=	gas velocity,	C_F	=	thrust coefficient
p	=	static pressure,	ϵ	=	area ratio
n	=	unit vector, outer normal to S,			
S	=	control surface,			
α	=	Mach angle, $\sin^{-1}\left(\frac{1}{M}\right)$			
θ	=	flow angle,			
R	=	radial coordinate,			
$\dot{m}$	=	weight flow rate,			
M	=	gas mach number			

Subscripts,

e	=	exit
b	=	plug base,
L	=	nozzle lip.

Equations 3 and 5 may be used for computation of the nozzle contour by equating the mass flow through the control surface to the mass flow through the throat. The following relationships result,

Plug nozzle,

$$\left(\frac{R_i}{V_t}\right)^2 - \left(\frac{R_L}{V_t}\right)^2 = \left[\left(\frac{2}{\gamma+1}\right)\left(1+\left[\frac{\gamma-1}{2}\right]M_1^2\right)\right]^{\left(\frac{\gamma+1}{2(\gamma-1)}\right)} \sin(\theta_i - \alpha_i) \qquad \text{(Eq 7)}$$

Forced deflection nozzle,

$$\left(\frac{R_i}{V_t}\right)^2 - \left(\frac{R_p}{V_t}\right)^2 = \left[\left(\frac{2}{\gamma+1}\right)\left(1+\left[\frac{\gamma-1}{2}\right]M_1^2\right)\right]^{\left(\frac{\gamma+1}{2(\gamma-1)}\right)} \sin(\theta_1 + \alpha_i) \qquad \text{(Eq 8)}$$

II, I, Thrust Chamber Concepts (cont.)

Where the subscript, i, designates an i^{th} control surface an γ = ratio of specific heats, r_t = radius of equivalent circular throat = $\sqrt{\frac{At}{\pi}}$.

The flow properties along the i^{th} control surface are found from the two-dimensional Prandtl-Meyer relationship,

Plug nozzle,

$$\theta_i = \theta_e + \nu_e - \nu_i \qquad \text{(Eq 9)}$$

Forced-deflection nozzle,

$$\theta_i = \theta_e + \nu_e - \nu_i \qquad \text{(Eq 10)}$$

where,

ν = Prandtl-Meyer angle, and is defined by

$$\nu = \left(\sqrt{\frac{\gamma+1}{\gamma-1}}\right)\left[\tan^{-1}\sqrt{\left(\frac{\gamma-1}{\gamma+1}\right)\left(M^2-1\right)}\right] - \tan^{-1}\sqrt{M^2-1} \qquad \text{(Eq 11)}$$

Thus, once the nozzle exit conditions and lip or plug radius are known, the entire contour may be found through successive application of Equations 7 and 8 with the flow properties determined by Equations 9, 10, and 11.

The nozzle performance is found from Equations 4 and 6 for the plug nozzle and forced deflection nozzle After some manipulation Equations 4 and 6 are obtained in the form:

II. Thrust Chamber Concepts (cont.)

Plug nozzle,

$$C_F = \left(\frac{P_e}{P_c}\right) \epsilon_e \left[\gamma\left(\frac{M_e \cos \theta_e}{\sin(\theta_e - \alpha_e)}\right) + \left(-\frac{P_a}{P_e}\right)\right] + \left(\frac{P_b}{P_c} - \frac{P_a}{P_c}\right) \epsilon_b \qquad \text{(Eq 12)}$$

$$\epsilon_e = \left(\frac{R_e}{r_t}\right)^2 - \left(\frac{R_e}{r_t}\right)^2 \quad , \quad \epsilon_b = \left(\frac{R_e}{r_t}\right)^2$$

Inverse plug nozzle,

$$C_F = \left(\frac{P_e}{P_c}\right) \epsilon_e \left[\gamma\left(\frac{M_e \cos \theta_e}{\sin(\theta_e + \alpha_e)}\right) + 1 - \left(\frac{P_a}{P_e}\right)\right] + \left(\frac{P_b}{P_c} - \frac{P_a}{P_c}\right) \epsilon_p \qquad \text{(Eq 13)}$$

$$\epsilon_e = \left(\frac{R_e}{r_t}\right)^2 - \left(\frac{R_p}{r_t}\right)^2 \quad , \quad \epsilon_p = \left(\frac{R_p}{r_t}\right)^2$$

Equations 12 and 13 must be used with some reservation to obtain performance, because it has been assumed in the derivation that the exit flow from the nozzle is not affected by ambient conditions. The exit conditions for both the plug and forced-deflection nozzle remain unaffected by ambient conditions only in the region of under-expanded operation where, $P_e > P_a$.

The base pressure in the plug and forced-deflection nozzle is also affected by ambient conditions and does not remain constant until the design pressure ratio of the nozzle has been exceeded. Design pressure ratio is defined as the ratio of nozzle stagnation pressure to the ambient static pressure at which the ratio of nozzle thrust to ideal maximum thrust (thrust efficiency) is a maximum. In general, the design pressure ratio is somewhat greater than the exit pressure ratio,

II, I, Thrust Chamber Concepts (cont.)

$$\frac{P_c}{P_{(des)}} > \frac{P_c}{P_e}$$

and Equations 12 and 13 should only be used for near vacuum or vacuum performance conputations. It should also be pointed out that Equations 12 and 13 are for frozen equilibrium flow and some correction from thermo-chemical calculations for equilibrium performance is necessary to obtain an accurate estimate of real-gas nozzle performance.

d. Optimum Nozzle Contour

Techniques were derived in the previous section designing nozzle contours for both the plug nozzle and the forced-deflection nozzle. These techniques are applicable once the parameters R_p/r_t, M_e, and θ_e have been established (other nozzle parameters could be selected because only three independent conditions are necessary). In all cases, the optimum nozzle is, by definition, the nozzle system that results in maximum system burnout velocity unless some compromise between a variety of missions is necessary. The problem of optimum design of the plug and forced-deflection nozzles involves establishing the parameters R_p/r_t, M_e and θ_e for a particular application.

Most rocket-engine missions involve operation over wide ranges in ambient pressure and the optimum nozzle is a compromise because the nozzle cannot, in general, be designed for maximum performance at all pressure ratios. The optimum nozzle actually only produces maximum performance for its weight or length at one pressure ratio. In general, maximum thrust nozzles for a given nozzle weight are designed for vacuum operation and result in a unique relationship between expansion-area ratio or performance and nozzle weight. This

II, I, Thrust Chamber Concepts (cont.)

family of nozzles is then considered for operation over the entire mission and the nozzle providing maximum over-all performance is selected.

(1) Base Pressure Effect

The characteristics of the two nozzles, the plug and the forced-deflection nozzle, are quite different in optimum nozzle-contour design and require separate treatment. The significant difference is in the plug base pressure contribution to performance in Equations 12 and 13. Because of the nature of the two flow fields the plug base pressures are greatly different for the two nozzles at fully expanded flow conditions. In Figure 17, the flow fields of both the plug and forced-deflection nozzle are shown schematically. Pressure on the plug-nozzle plug base is maintained by the gases flowing around the plug and converging toward the nozzle axis. Some expansion occurs at the end of the plug so that $P_b < P_e$; however, P_b is generally on the order of 1/2 P_e. The base pressure for the forced-deflection nozzle is much less than P_e because the nozzle gases expand from θ_e at the nozzle exit to a direction toward the nozzle axis. This change in angle is much greater than for the plug-nozzle base, and for the forced-deflection nozzle P_b is on the order of 1/1,000 P_e. Thus, the contribution of base pressure to thrust can be ignored for the forced-deflection nozzle, while for the plug nozzle the base thrust is significant.

The base pressure for the plug nozzle cannot be computed accurately because of the lack of a theoretical model for flow in the base region. The phenomenon is similar to the base region of a blunt body in a supersonic stream; however, the flow approaching the base is not uniform or infinite in extent as it is for the blunt body in flight. Some work has been done by Korst for flow in the base region of supersonic vehicles where mixing occurs

II, I, Thrust Chamber Concepts (cont.)

between semistagnant and supersonic streams. These techniques are not sufficiently developed to permit accurate determination of P_b as a function of M_e, θ_e, and R_e/r_t.

(2) Optimum Plug Nozzle Design

A very inclusive cold-flow experimental program has been conducted at FluiDyne Engineering Corporation under Aerojet-General direction Results of this program provided empirical data for plug-nozzle performance, and verified the technique of nozzle design that will be described subsequently

An efficient plug-nozzle design results if an isentropic plug nozzle is designed to give uniform parallel flow at the exit This is commonly referred to as the "isentropic spike," and the plug may be truncated to less than one-third the spike length (Figure I-8). The performance of the nozzle at design pressure ratio and above, (P_c/P_a), remains essentially unaffected by plug truncation, although low pressure ratio performance is affected. Vehicle weight and performance trade-off studies must be performed to establish the optimum nozzle length and expansion ratio. The performance versus pressure ratio for operation at pressure ratios less than design must be obtained empirically.

The following relationships apply to the design of the isentropic spike:

$$\epsilon_e = \left(\frac{R_L}{r_t}\right)^2$$

II. I. Thrust Chamber Concepts (cont.)

where the exit Mach number is related to the expansion ratio by,

$$\epsilon_e = \left(\frac{2}{\gamma+1}\right)^{\left[\frac{\gamma+1}{2(\gamma-1)}\right]} \left(M_e\right)^{-1} \left(1 + \left[\frac{\gamma-1}{2}\right] M_e^2\right)^{\left[\frac{\gamma+1}{2(\gamma-1)}\right]} \qquad \text{(Eq 14)}$$

The exit Mach number must be found by iteration of Equation 14 for a specified ϵ_e. For these conditions, $R_e/r_t = 0$ (nozzle ends at the axis of symmetry). Equation 7 is used to solve for the radial contour coordinates.

$$\left(\frac{R_1}{r_t}\right)^2 = \left(\frac{R_L}{r_t}\right)^2 + \left\{\left(\frac{2}{\gamma+1}\right) \left(1 + \left[\frac{\gamma-1}{2}\right] M_1^2\right)\right\}^{\left[\frac{\gamma+1}{2(\gamma-1)}\right]} \sin\left(\theta_1 - \alpha_i\right) \qquad \text{(Eq 15)}$$

where $\theta_e = 0$

$$\theta_1 = \nu_1 - \nu_e,$$

and ν is the Prandtl-Meyer expansion angle that is a function of M.

The length coordinate of the point 1 is found by geometric consideration (Figure I-8).

$$\frac{L_1}{r_t} = \frac{\left(\frac{R_i}{r_t}\right) - \left(\frac{R_L}{r_t}\right)}{\tan\left(\theta_1 - \alpha_1\right)}$$

II, I, Thrust Chamber Concepts (cont.)

The Mach number is decreased in arbitrary increments to M = 1 to establish the entire contour and annular throat location

(3) Optimum Forced-Deflection Nozzle Design

Design of optimum forced-deflection nozzles may be accomplished analytically in a manner analogous to the technique used for optimum design of the conventional nozzle, because the thrust contribution resulting from P_b is very small and may be ignored for the purpose of analysis. The actual problem of involving an optimum configuration consists of establishing a maximum thrust nozzle for fixed weight and ambient conditions (or trajectory). Because nozzle weight is very difficult to express analytically, the assumption is made that weight is approximately proportional to nozzle length for a fixed value of R_p/r_t, so that the external problem may be formulated as: establish the nozzle for maximum performance with fixed length, ambient conditions (or trajectory), and R_p/r_t as constraints. The parameter R_p/r_t should also be allowed to vary for fixed weight optimums, however, this parameter is very closely allied with design and weight of the entire engine system and consequently must be considered carefully in connection with the over-all optimum engine

The performance of the forced-deflection nozzle is obtained from Equation 13 with $P_b/P_a = 0$

$$C_F = \left(\frac{P_e}{P_c}\right)\epsilon_e\left[\gamma\left(\frac{M_e \cos\theta_e}{\sin(\theta_e+\alpha_e)}\right)+1\right] - \left(\frac{P_a}{P_c}\right)(\epsilon_e+\epsilon_p) \qquad \text{(Eq 16)}$$

III, I, Thrust Chamber Concepts (cont.)

where

$$\epsilon_e = \left(\frac{R_e}{r_t}\right)^2 - \left(\frac{R_p}{r_t}\right)^2 \quad , \quad \epsilon_p = \left(\frac{R_p}{r_t}\right)^2$$

The constraint of fixed length is expressed by

$$\frac{L_e}{r_t} = \frac{\epsilon_e}{\tan(\theta_e + \alpha_e)} = \text{const.} \qquad \text{(Eq 17)}$$

One more relationship is obtained between θ_e, M_e and ϵ_e from continuity expressed by Equation 8.

$$\epsilon_e = \left[\left(\frac{2}{\gamma+1}\right)\left(1 + \left[\frac{\gamma-1}{2}\right] M_e^2\right)\right]^{\left[\frac{\gamma+1}{2(\gamma-1)}\right]} \sin(\theta_e + \alpha_e) \qquad \text{(Eq 18)}$$

The system of Equations 16, 17, and 18 may be solved for values of ϵ_e, M_e and θ_e because there are three independent constraints, Equation 17 and 18 combined with the requirement that

$$C_F = \max$$

Optimum nozzle parameters may be obtained by iteration because of the simplicity of the equations (direct differentiation of Equation 16 may be performed and a system of three simultaneous equations formed; however, the equations are nonlinear and solution is again only possible by iteration).

II, I, Thrust Chamber Concepts (cont.)

The results of an analysis for optimum forced-deflection nozzle contours are shown in Figure I-9, where the vacuum thrust coefficient is plotted as a function of the parameters L_e/r_t, θ_e, and M_e for $R_p/r_t = 2.5$. Maximum thrust nozzles are indicated by the dashed line forming the envelope of the curves for constant M_e. Properties of the family of optimum nozzles for a range of R_p/r_t are plotted in the Figures I-10, I-11, I-12 and I-13. These optimum nozzles are for a ratio of specific heats equal to 1.4 and a plug base pressure assumed to be negligibly small.

II, I, Thrust Chamber Concepts (cont.)

(4) Discrete-Throat External-Expansion Nozzles

(a) The external-expansion nozzles that have been considered, both plug and forced-deflection nozzles, have been treated as completely annular configurations from some point in the subsonic portion of the nozzle. This generally results in an annular throat of relatively small width. Although the complete annular nozzle is desirable from a gas dynamic standpoint, some practical problems arise:

1 The total surface area exposed to the high flux existing at the nozzle throat is greatly increased, which, in turn, increases the nozzle total cooling requirement. In general, the heat-transfer coefficient also is greater for an annular throat because of decreased length for boundary layer formation.

2 Structural problems also arise with annular throat nozzles because tolerances must be maintained closely as a result of the relatively small throat gap to control total throat area and throat symmetry.

These reasons, as well as development factors, have produced interest in external expansion nozzles which use a number of discrete circular throats rather than the annular throat. If discrete throats are used, a transition section is necessary to merge the discrete flows at some point in the nozzle to form a near-annular flow with the properties described previously for the external-expansion nozzle.

II, I, Thrust Chamber Concepts (cont.)

e. Evaluation of Nozzle Types

The simplest means for achieving altitude compensation is with the external-expansion-type nozzles. All methods for compensating De Laval nozzles result in decreased overall performance because of increased weight or decreased nozzle efficiency resulting from the necessary compromises in the aerodynamic liner of the nozzle. The plug and forced-deflection nozzles provide simple means for achieving nearly perfect altitude compensation. The forced-deflection nozzle is superior to the plug nozzle because of weight and engine integration. Therefore, the forced-deflection nozzle is selected as the most promising for application in the advanced engine.

3. Combustor Concepts

a. General

Combustor selection was based on a combination of features providing the highest performance, greatest reliability, lowest weight, and minimum overall cost.

In Section II, E, the staged combustion cycle was shown to be superior to the other engine cycles considered. Also engines operating at thrust chamber pressures between 2,000 and 3,000 psia offer significant performance advantage over engines operating at conventional pressures. The forced-deflection nozzle was selected as the most advantageous because of performance and engine integration. In this section emphasis is placed upon combustor design considerations compatible with these other findings. As a result of this investigation, the following conclusions were made:

II, I, Thrust Chamber Concepts (cont.)

(1) Configuration

Multiple circular combustors are best.

(2) Cooling

Regenerative cooling is most desirable. Film cooling can be used in high-heat flux regions to reduce wall temperatures required. Use of materials such as Inconel-X or molybdenum lessens film cooling requirements.

(3) Construction

The cast aluminum jacket over regenerative cooling tube bundle is best.

(4) Injector

A large element injector should be used.

(5) Combustion Zone

Use of baffles will ease combustor development.

(6) Ignition

Electric spark ignition is recommended in the gas generator. With the staged combustion cycle, probably no ignition device will be required in the main combustor.

The bases for each of these selections are discussed in the paragraphs that follow.

b. Combustor Configuration

Combustor configurations considered are multiple combustors with discrete circular throats, annular combustor and throat, and single chamber with circular discrete throat.

II, I, Thrust Chamber Concepts (cont.)

Multiple combustors with discrete throats have two advantages over annular combustor and throat combinations. First, the structural weight for high chamber pressures is lower for multiple combustors because of the difference in diameter between the individual combustors and the annular design. Secondly, the heat flux at the throat of an annular nozzle is higher as a result of the surface area exposed to the high temperature.

The ability to segment the annular nozzle for development purposes will establish development costs for both annular and multiple combustors at approximately the same level.

Multiple combustors with discrete throats have an advantage over the single chamber and nozzle type primarily in the cost required to develop the unit. Application of the wedge motor principle to the development of single chamber design reduces the cost of propellant and allows the use of facilities rated at a fraction of the ultimate design. However, the cost of a wedge thrust chamber may exceed that of the full combustor. There are some minor influences of the wedge side walls upon combustion dynamics and performance analysis that are not present in multiple combustors with discrete throats.

The advantage of multiple combustors with discrete throats may be summarized as resulting in lower development costs because of hardware size, coupled wity continuing experience in fabricating and testing components identical to those used in the final engine design.

II, I, Thrust Chamber Concepts (cont.)

c. Combustion Chamber Cooling

A major problem encountered in the design of higher pressure combustors is the rate of heat transfer. Figure II I-14 shows the increase of total heat flux as a function of chamber pressure. Combustors must be designed upon the basis of a practical union of materials and methods that will provide solutions to the heat-transfer problem. Combustor cooling is detailed in Appendix A.

The following alternative cooling techniques were considered and they are listed in the order of preference.

(1) The regeneratively cooled axial tube bundle with auxiliary fuel film cooling.

(a) Locally injected film coolant

(b) Transpiration film coolant

(2) Regeneratively cooled axial tube bundle

(3) Film cooled

(a) Locally injected film coolant

(b) Transpiration film coolant

(4) Ablation cooled

(5) Radiation cooled

The regeneratively cooled axial tube bundle with auxiliary fuel film cooling is the logical choice for this application because of development cost, fabrication cost, and proved ability to perform the task of containing the combustion energy.

II, I, Thrust Chamber Concepts (cont.)

Locally applied fuel film cooling minimizes the performance losses resulting from incomplete mixing in the combustor. Film coolant applied through local points of injection is preferred in the development phase because of the ease in adjusting flow rate at that point. When requirements are accurately defined, it is possible that further reduction in film coolant can be accomplished with porous walls in the high-heat flux areas.

For the selected engine concept, use of a straight regeneratively cooled axial tube bundle is limited to materials having higher operating temperatures or higher conductivities, or a combination of both. Currently, use of molybdenum or Inconel-X tubing appears feasible. The presence of high-temperature gases circulating within the combustor (in ways which have thus far defied analysis) can well dicatate the use of local film coolant for any known material having practical fabrication characteristics.

A combustion chamber of film cooled design is possible. Manifolding to distribute the film coolant will act as a regenerative coolant before entrance into the combustor. Application of transpiration cooling would constitute the ultimate design of this type for performance. The maximum performance attainable will be below that of any system in which there is less film cooling. Necessary film cooling would be minimized with a refractory material as the porous medium for injection of the transpiration coolant. While this concept is desirable from the standpoint of system simplicity, the problem of developing large curved surfaces with uniform porosity is formidable. Both the weight and development cost of such a system are estimated to exceed that of a tube bundle.

II, I, Thrust Chamber Concepts (cont.)

Combustion chambers with ablation cooling (Figure II I-15) are being developed at Aerojet-General. Satisfactory operation has been achieved with chambers operating at chamber pressures of 100 to 200 psia. The weight and unit cost of ablative combustion chambers are proportional to duration and chamber pressure. These factors combine to make the use of ablative chambers for chamber pressures above 2,000 psi and durations in the order of 250 sec a poor contender with the regeneratively cooled unit selected. An additional difficulty is the compounding of currently available ablative materials so that ablation takes place in the nozzle contour in a manner which would minimize losses resulting from a configuration change. However, with the continued development of new materials and processes, ablative cooling at some future date is entirely possible.

Radiation cooled chambers are limited to that combination of heat flux, chemical attack, and duration which lies within the limiting characteristics of the selected material. Currently, the radiation cooled chambers are useful for low chamber pressure applications as well as nozzle extensions. Continued development of thermal barrier materials and higher temperature alloys has some promise in the low to medium chamber pressure application with the high limit extended by film cooling to the point where performance loss makes this impractical.

The effects of chamber coatings and film cooling are discussed in Appendix A.

II, I, Thrust Chamber Concepts (cont.)

d. Combustion Chamber Construction

With the recommendation of a regenerative and partial film cooled combustion chamber, it is now necessary to consider the means of reinforcing the combustor and nonaxisymmetric internal expansion nozzle section. The following alternatives are listed in the order of their overall desirability:

(1) Cast aluminum jacket

(2) Brazed wire wrap

(3) Bonded wire wrap

(4) Filanent wound fiberglass

(5) Bolt-on jacket

An aluminum jacket is installed by first preparing the furnace-brazed tube bundle. Following a thorough cleaning, the tube bundle is sprayed with aluminum, after which the unit is installed in a mold and the jacket cast. Removal of the aluminum is accomplished by bringing the assembly to a temperature above the melting point of aluminum. When this is done, the aluminum bonds to the tubes supporting them against both external and internal loads. This jacket can be designed to provide structural attachment and reinforcement wherever required. Heat treatment of the unit develops the proper combination of tensile strength and elongation in the aluminum. The resultant assembly is structurally sound, relatively easy to manufacture and repair, as well as being capable of absorbing heat from outside the nozzle. Resistance to external heat is important during operations where some recirculation of exhaust gas in anticipated.

II, I, Thrust Chamber Concepts (cont.)

An alternative and somewhat more expensive process combines in a multiple braze cycle the basic tube bundle, a wire or strip wrap, and such structural reinforcements, including attachments, as necessary. One difficulty common to braze wire wrap, bonded wire wrap, and filament wound fiberglass is the difficulty in maintaining the proper tension throughout the process of wrapping a nonaxisymmetric nozzle. The principal advantage of the brazed wire wrap is that it may be able to withstand higher gas recirculation temperatures than the cast aluminum jacket.

The bonded wire wrap system is identical to the brazed wire wrap, except that plastic bonding agents are used in place of the brazing operations beyond the assembly of the tube bundle. Tolerance to high temperature gas and thermal radiation is lower for this design. Repair of damage is quite difficult because of the requirement that the entire wire wrap be removed before repairing the external surface of the tube bundle.

Filament wound fiberglass reinforcement is structurally appealing, except for the difficulty in providing structural attachments and resistance to thermal radiation as well as hot-gas recirculation. Again, repair is quite difficult because of the tendency to damage the tube bundle during removal of the reinforcement.

The bolt-on jacket or corset is easy to repair. However, it is difficult to obtain a good fit between the tube bundle and jacket. A satisfactory attachment between the tube bundle and the reinforcing jacket would make repair as difficult as for any of the other types. Fabrication of the jacket for a nonaxisymmetric nozzle is limited to casting or expensive machining operations. The joints required for installation will raise the weight of the system above that of a jacket cast in place.

II, I, Thrust Chamber Concepts (cont.)

e. Injector

The purpose of the injector is to inject propellants into the combustor. High performance is achieved by uniform mixing and combustion. Maximum performance is obtained when the mixture ratio throughout the combustion zone is equal to the mixture ratio of the design. For the selected engine cycle, liquid-gas injection is required. A gas-liquid propellant combination imposes additional restriction upon the selection of a design. The design selected is typical of a number of possible injection systems with large injector elements. Engine configuration is benefited from a small diameter combustor operating at high pressure. This combination of size and pressure renders the use of conventional multichannel injectors unusable because the total injection area required exceeds that obtainable with drilled orifices.

This injector is an annular large-thrust-per-element design with the elements forming a conical pattern in the combustion zone. There are two fuel passages impinging at 90°, bisected by one oxidizer passage. Radial baffles divide the combustor into equal parts and the number as well as arrangement of these baffles will vary with the configuration of the combustor. They will require verification by tests.

An annular element is located at the median radius providing equal volume outward and inward from the element. This design is being developed for a similar application with storable propellants.

Fuel is divided at the pump and directed to the regeneratively cooled surfaces and gas generator. This fuel is partly burned with oxidizer in the gas generator where it becomes the working fluid for the turbine.

II, I, Thrust Chamber Concepts (cont.)

The gasified fuel, mixed with the fuel heated in the nozzle and combustor cooling jackets, is then injected into the combustor. The oxidizer is heated slightly as it flows through the injector feed tubes and into the annular element. The baffles mentioned previously serve to support the oxidizer annule within the fuel stream.

Alternative injection techniques were considered. They include multiple-oxidizer elements intersecting at the center of the injector where a single fuel injection port is located; multiple large element units distributed around the injector head, and impinging like-on-like fans injecting oxidizer at right angles to the flow of fuel entering through an annulus at the median radius. Also of interest is an injector design with flameholder principles, with spokes feeding oxidizer to slots along the trailing edge of the spoke. A splash plate, suspended below the spoke, deflects the oxidizer into the fuel passing between adjacent spokes.

Results of the study of high-thrust-per-injector element systems are presented as Appendix D.

f. Combustor Development Problems

Combustor development problems fall into two main groups, problems for obtaining reliable operation, and those for obtaining high combustion efficiency. When performance is not considered, reliability becomes a matter of obtaining stable combustion. In the event very high combustion efficiency is required, program cost will be increased by a factor that becomes infinite as 100% of theoretical performance is approached. Approximately 97 to 98% theoretical characteristic velocity has been obtained previously. Therefore,

II, I, Thrust Chamber Concepts (cont.)

the greatest potential for cost savings is to design the complete missile with sufficient capacity to permit a specified performance of 93 to 94% of theoretical for liquid oxygen/hydrocarbon, and 94 to 95% of theoretical for liquid oxygen/liquid hydrogen. There is experimental evidence to show that a somewhat higher efficiency can be more readily obtained with LO_2/LH_2 than with other propellants.

From the point of view of performance development, a large characteristic length has an interesting implication. If the injection pattern is held fixed and the characteristic length is increased from a low value, the characteristic velocity increases rather rapidly to a maximum and then decreases slowly (Figure II I-16). An inherently higher performance injector will reach its maximum at lower characteristic length, while poor performing injectors reach maximum performance at high characteristic length. Excess characteristic length will be helpful during the early part of a development program and will cause a degradation in performance only when the system is highly developed.

g. Baffled Combustion Zone

Use of combustion zone baffles for the suppression of tangetial mode instability is a proved concept and use at the outset of a program will eliminate the most troublesome of all combustor development problems. However, development of these baffles will require separate consideration because only limited information is available as a basis for designing baffle configuration. A program now underway is expected to improve the technology for baffle-configuration design. Development of an adequate set of baffles is a problem because of the complex combustion dynamic problems involved.

II, I, Thrust Chamber Concepts (cont.)

Following the establishment of an adequate configuration, the development for optimum baffle designs is directed largely toward providing adequate cooling without performance loss. Regenerative cooling, film cooling, and the use of ablative materials appear practical. Further experimental evidence is required before one of the various techniques can be selected.

h. Pregasification of Propellants

Several of the engine cycles previously discussed result in the delivery of one or both of the propellants to the combustor in the gaseous stage. Gaseous propellants can be mixed by diffusion if the injection pattern is sufficiently fine. Heat transfer from combustion products to unburned propellants need be only sufficient to provide ignition. Thus, the combustion zone processes are reduced in number and complexity.

Ample experimental evidence exists to show that combustion tends to be more stable with both propellants or even one gaseous propellant than is the case if both propellants are injected in the liquid state.

Disadvantages of gaseous combustion are the requirement for somewhat larger injection areas which are of little significance at high pressure and the relatively low impendance in the propellant distribution system. The use of gaseous injection is not believed to be sufficiently advantageous from this point of view to justify the addition of components, such as heat exchangers for the purpose of gasification. However, an engine cycle providing gaseous propellant as a by-product should receive favorable considered.

II, I, Thrust Chamber Concepts (cont.)

1. Ignition

Proved ignition systems should be selected upon the basis of reliability. The placement of the selected ignition system is primarily a consideration of propellant accumulation before ignition.

Hard starts are the direct result of propellant accumulation caused by ignition delay time. Ignition delays of abnormal duration are invariably followed by pressure spikes that can be of such magnitude as to damage or destroy the combustion chamber.

Ignition of multichambered engines must occur within definite prescribed limitations. Under no circumstances should the interval of ignition delay extend beyond a point where unburned propellants exit from the combustor into the nozzle. The risk of external ignition of an unignited chamber presents a hazard which cannot be tolerated.

The various methods for achieving ignition follow.

(1) Ignition by Electrical Spark

Reliable ignition of engines with oxygen/hydrogen propellants has been accomplished by air-gap as well as by surface-gap plugs with equal success. The time required to develop a spark after excitation is approximately 10 millisec. Therefore, excitation should precede propellant entry into the chamber to minimize ignition delay. The sparking energy of each unit is 100 millijoules per plug. No problems are forseen in the application of these units for satisfactory ignition and no testing will be required.

II, I, Thrust Chamber Concepts (cont.)

(2) Ignition by Pilot Flame

A design has been completed for ignition of the main chamber by means of pilot flames from a small combustion chamber centrally located on the main injector. Ignition of the pilot chamber is accompliched by two-surface-gap igniters, each developing an ignition energy of 60 milijoules. The central ignition unit is operated at a mixture ratio of 1 to 1 to prevent damage to its film-cooled chamber walls. These units will require development testing and system analysis for phasing with the main chamber.

External sources of pilot flames can be used as a means of ignition. The units would consist of expendable plastic versions of the Bunsen burner and would use natural gas and air as the combustibles. The problems presented by hydrogen leaks necessitate that such a device by remotely lit before or after insertion into the chamber. Sufficient air must be available in the chamber to maintain the ignition flame.

(3) Ignition by Pyrotechnics

Pyrotechnics give the advantages of being highly reliable and being a ground support, high-energy method of ignition that contributes no weight penalty to the vehicle.

(4) Ignition by Hypergolic Additives

Ignition of liquid-oxygen and liquid-hydrogen mixtures by the addition of substances to the oxygen supply that react hypergolically with hydrogen is a new concept in ignition systems. The mechanism by which ignition is accomplished is as follows:

II, I, Thrust Chamber Concepts (cont.)

(a) Hydrogen enters the chamber in the gaseous phase just a few miliseconds ahead of the liquid oxygen that contains ozone difluoride.

(b) The exothermix reaction of hydrogen with the ozone difluoride produces enough heat to ignite the entire mass.

Studies indicate 0.1% by weight of ozone difluoride is necessary for reliable ignition. The saturation concentration is 1.1%.

The problems encountered in the consideration of such an ignition system are the ozone difluoride availability, storability, and compatibility with seals and tanks. Present production of ozone diflouride is simply on a laboratory level and facilities for generating as well as refrigerating would have to be designed and fabricated to meet these needs. The storability of ozone difluoride is poor. At liquid-oxygen temperatures, the decomposition is approximately 4% per day; however, methods of adding the hypergolic ozone difluoride during vehicle tank loading would assure the minumum 0.1% concentration and provide mixing directly in the tank fill lines. High reactivity of ozone difluiride would necessitate laboratory studies of its compatibility with the liquid-oxygen system components in the vehicle.

(5) Alternative Methods

Other ignition systems beyond practical consideration at this time are radiation capsules and adiabatic compression.

II, I, Thrust Chamber Concepts (cont.)

Certain radioactive materials such as Polonium 210 emit sufficient radiation to cause their encapsultating metals to glow. These capsules could be placed in strategic locations and would cause spontaneous ignition of the propellants upon contact.

The adiabatic-compression method would require an additional mechanism to compress gaseous propellants and release the combusting mixture during the transient flow conditions of the propellants into the chamber. This would call for excellent sequencing apparatus that, at this time, appears unnecessary in view of the abundance of suitable methods presently available for ignition.

j. Integration Effects

The arrangement of the engine and location of thrust take-out points has negligible effect upon the weight and cost of combustors, though the effect upon the overall vehicle may be considerable. Concepts that may seriously affect the combustor is the use of gases bled from the combustion zone for the purpose of driving turbine or for thrust-vector control.

k. Combustors with Fluctuating Chamber Pressure

If high mean chamber pressure can be obtained without increasing pump weight, substantial vehicle payload gains will be realized. The following cycle is an example of a method for reaching this high chamber pressure. This cycle is known as the "intermittent delivery feed cycle "

II, I, Thrust Chamber Concepts (cont.)

(1) Step 1

Propellants are delivered to an empty chamber at high flow rates against a low head.

(2) Step 2

Propellant flow ceases. Propellants mix, combustion begins, and the chamber pressure rises to the peak value.

(3) Step 3

Combustion continues. Combustion products flow through the nozzle at the rate at which they are produced. Specific impulse and thrust are constant.

(4) Step 4

Combustion ceases because of propellant exhaustion. Chamber pressure decays to a minimum value as the gases remaining in the chamber are discharged through the nozzle.

The four phases described will overlap somewhat in any practical system. Flow through the nozzle will begin as soon as any gas is produced. Upon initiation of combustion, the rate of the pressure rise will not be instantaneous.

A small thrust chamber incorporating this concept has been operated by Dr. R. B. Morrison and his associates at the University of Michigan. In their design, the combustion chamber is annular and propellants are supplied continuously at relatively low pressure. Upon ignition, a detonation wave is produced which is propagated around the annulus. Propellants admitted

II, I, Thrust Chamber Concepts (cont.)

between wave passages are ignited and burned as the wave passes. Products of combustion are discharged from the relatively high pressure region behind the wave front. While this technique shows some promise for future applications, it presents great practical difficulties and currently can be considered as little more than a laboratory demonstration.

1. Centrifugal Injection

Figure II I-17 shows a water-flow model of a spherical centrifugal combustor having an injector similar in principle to the high-thrust-per-element injectors discussed previously, except the propellants are injected tangentially against a spherical wall. Centrifugal force holds the propellants against the wall until vaporization is complete and keeps the wall cool at low pressure drop.

This injector concept has never been tested with reactive propellants because the turbulence of water flow was such as to suggest severe instability. The success of other types of high-thrust-per-element injectors exhibiting similar turbulent water flow patterns causes renewed interest in this injection system. The slow pressure-drop characteristics make it most attractive for pressure-fed systems, but the weight and cost are high in comparison with those shown in Appendix F.

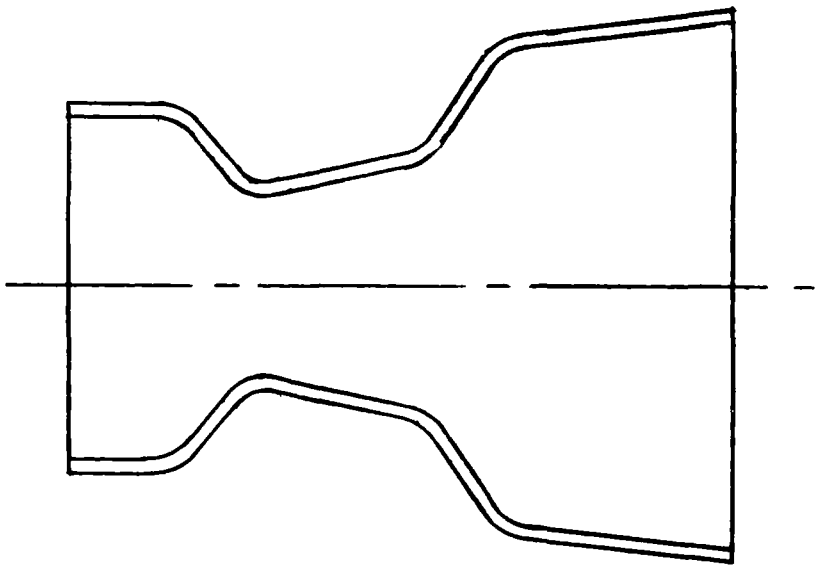

Step Nozzle Contour

Figure II I-1

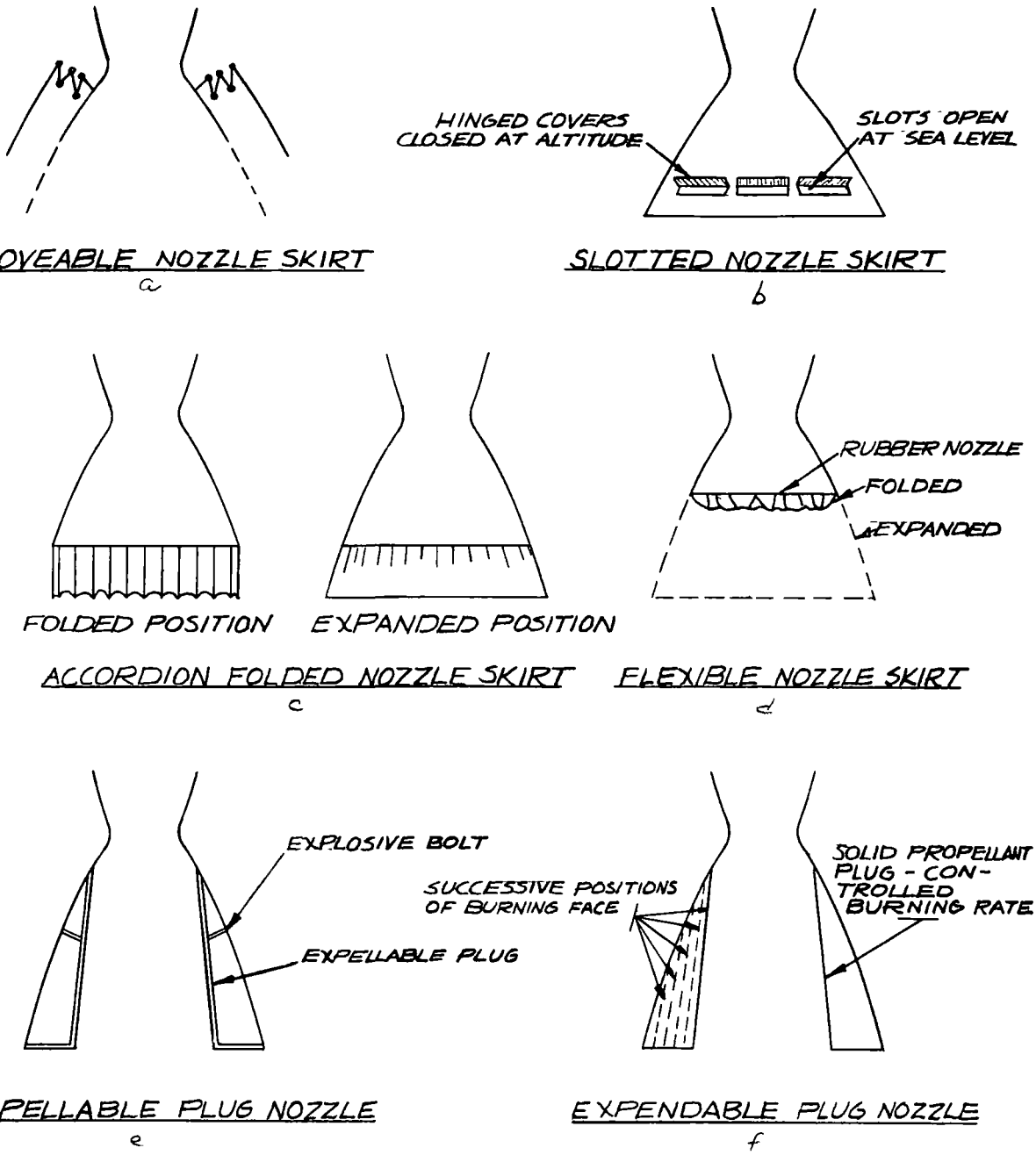

MOVEABLE NOZZLE SKIRT
a

SLOTTED NOZZLE SKIRT
b

ACCORDION FOLDED NOZZLE SKIRT
c

FLEXIBLE NOZZLE SKIRT
d

EXPELLABLE PLUG NOZZLE
e

EXPENDABLE PLUG NOZZLE
f

Mechanical Means of Varying Exit Area

Figure II I-2

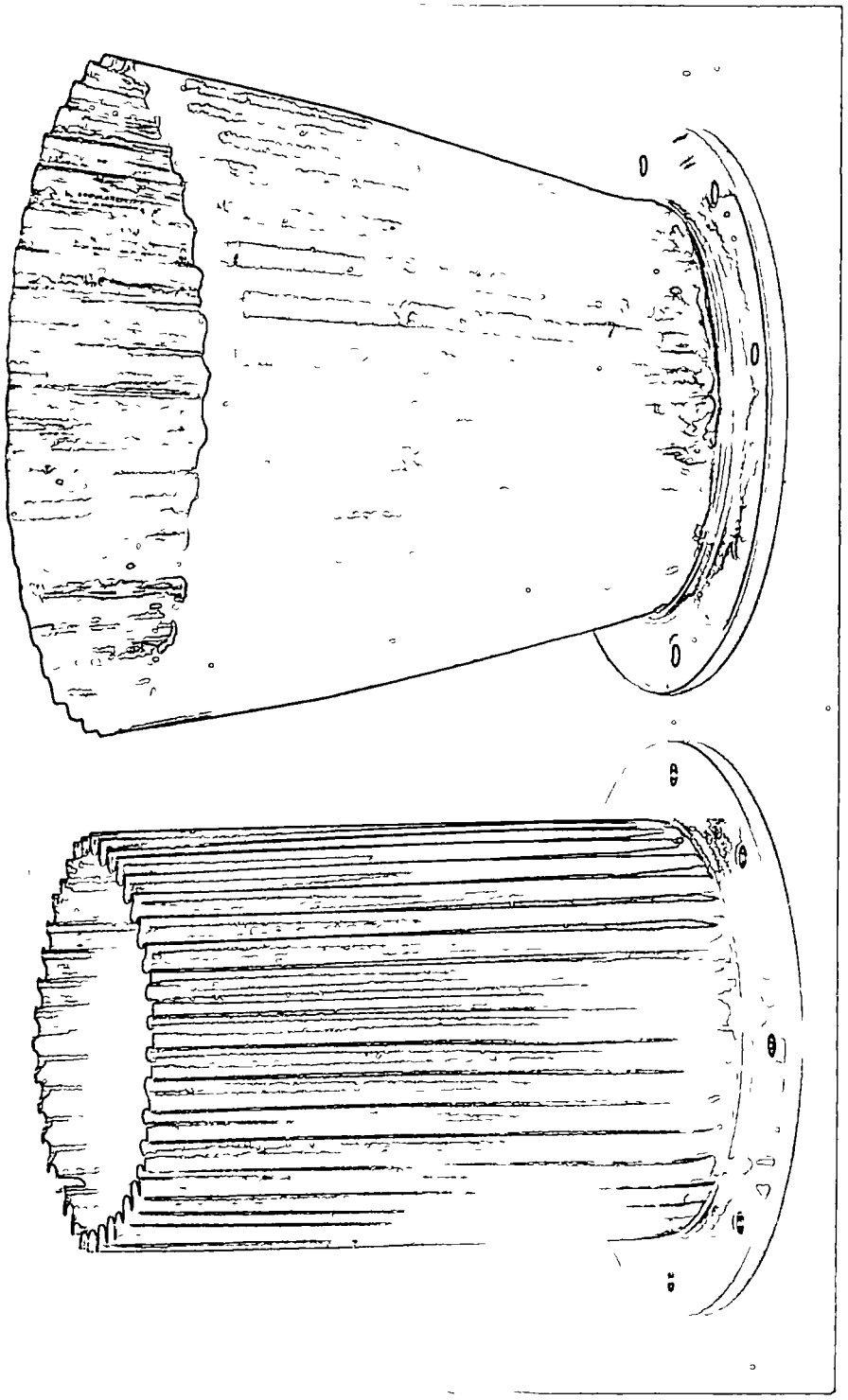

L860 1413

Expandable Nozzle Before and After Testing

Figure II I-3

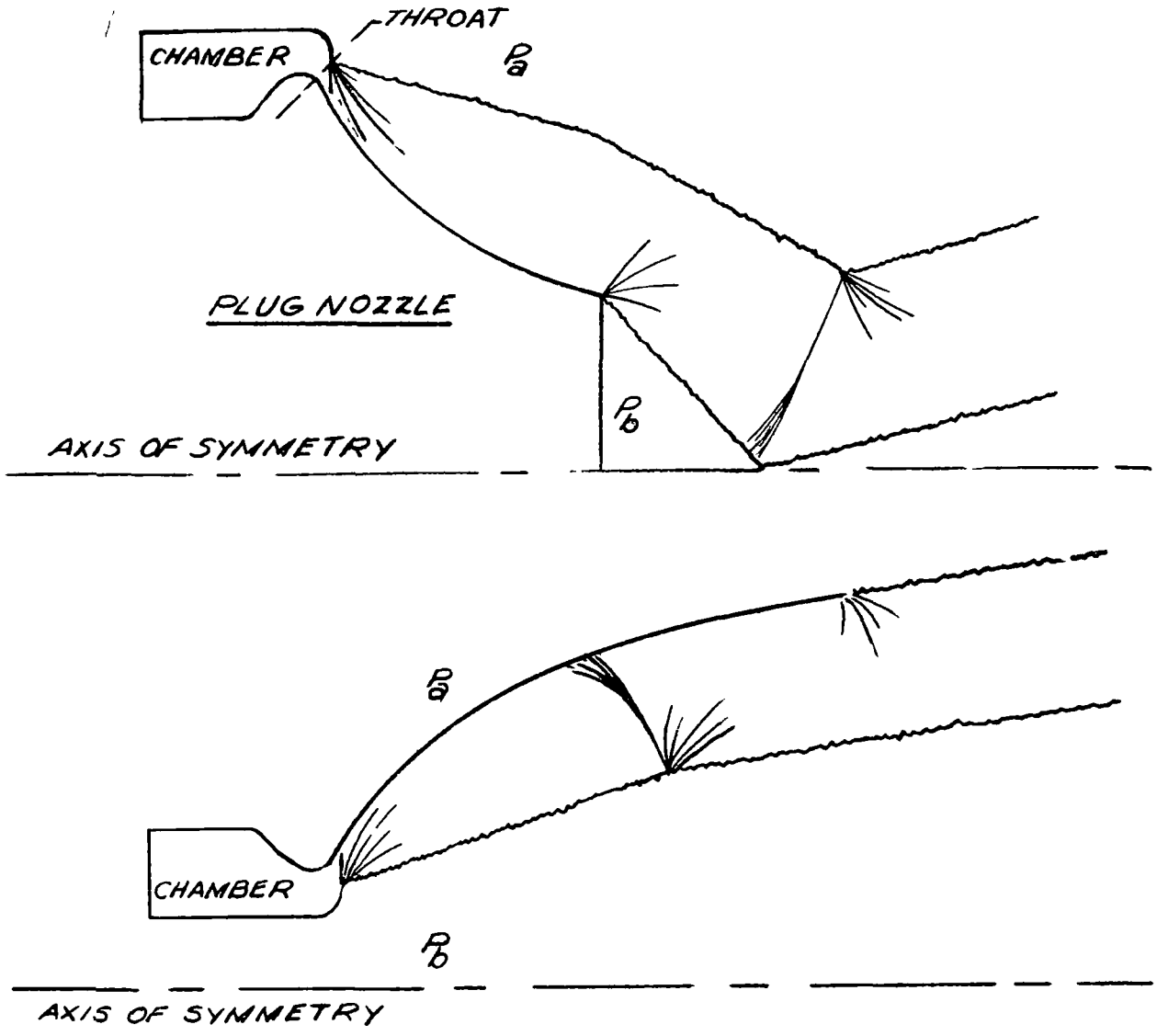

FORCED DEFLECTION NOZZLE

Annular External Expansion Nozzles

Figure II I-4

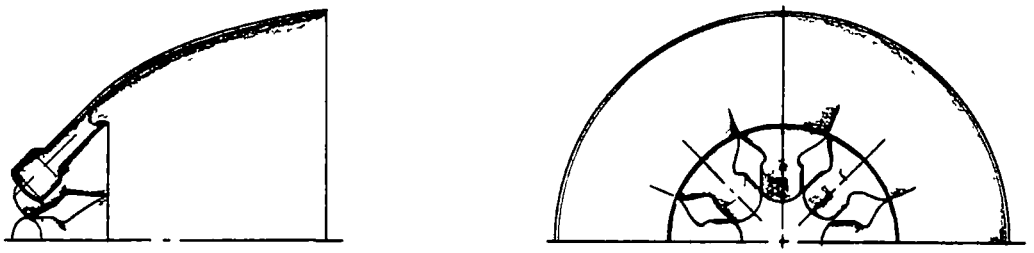

STRAIGHT WEDGE SECTIONS

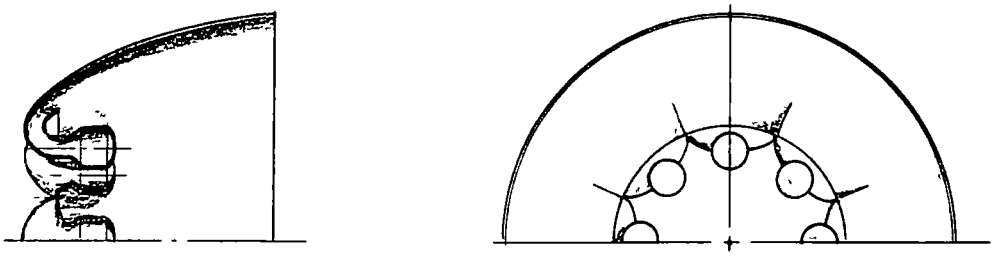

REVERSE WEDGE SECTIONS

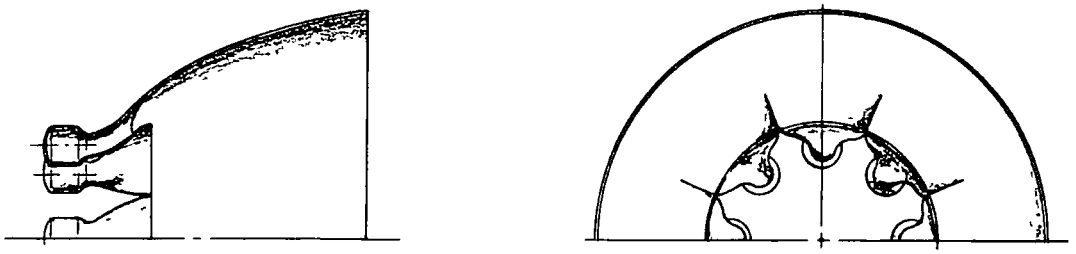

FORWARD WEDGE SECTIONS

Discrete-Throat Forced-Deflection-Nozzle Schematics

Figure II I-5

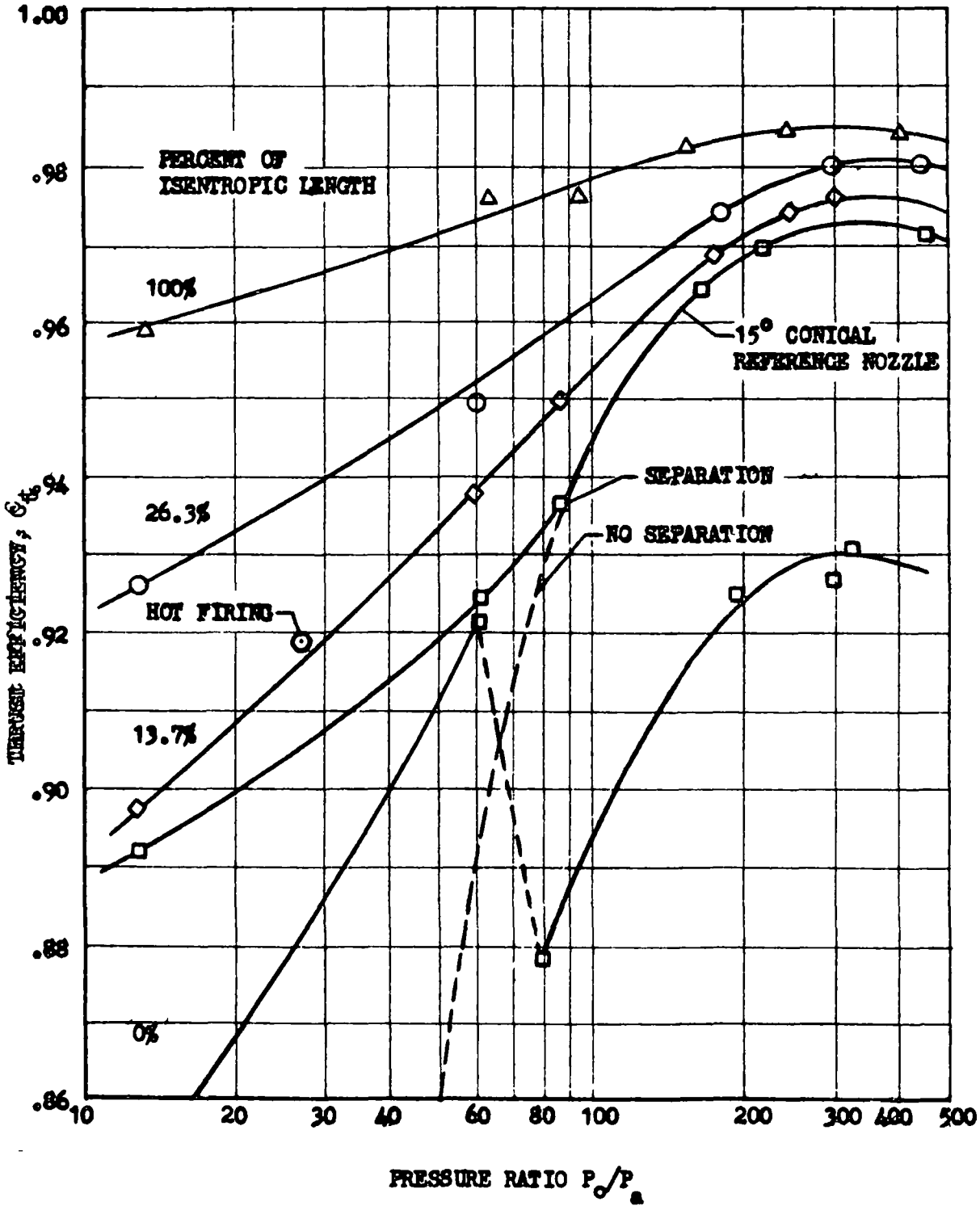

Truncated Isentropic Plug Nozzle Performance Obtained from Cold-Flow Tests

Figure II I-6

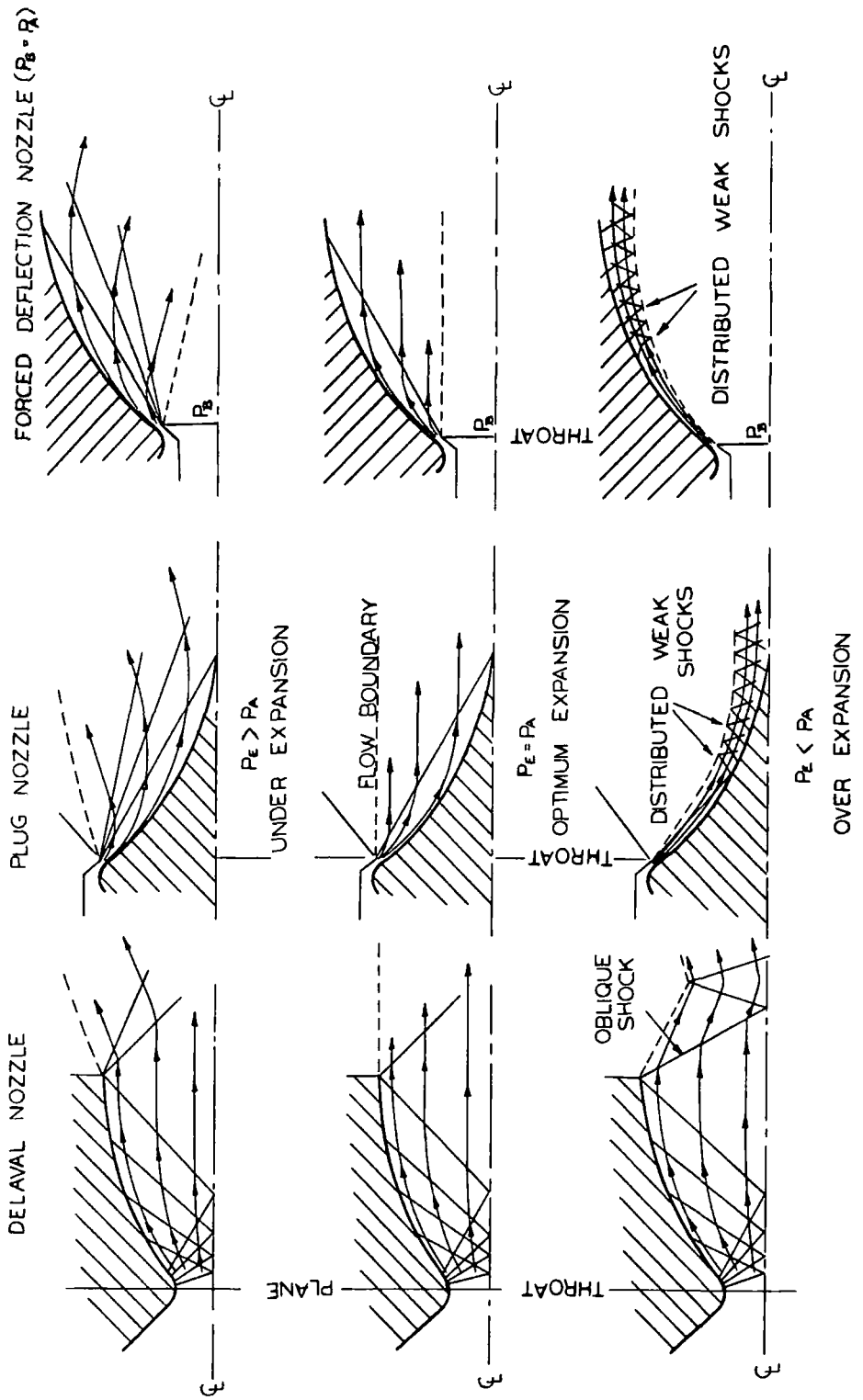

Nozzles with Flow Process Depicted

Figure II I-7

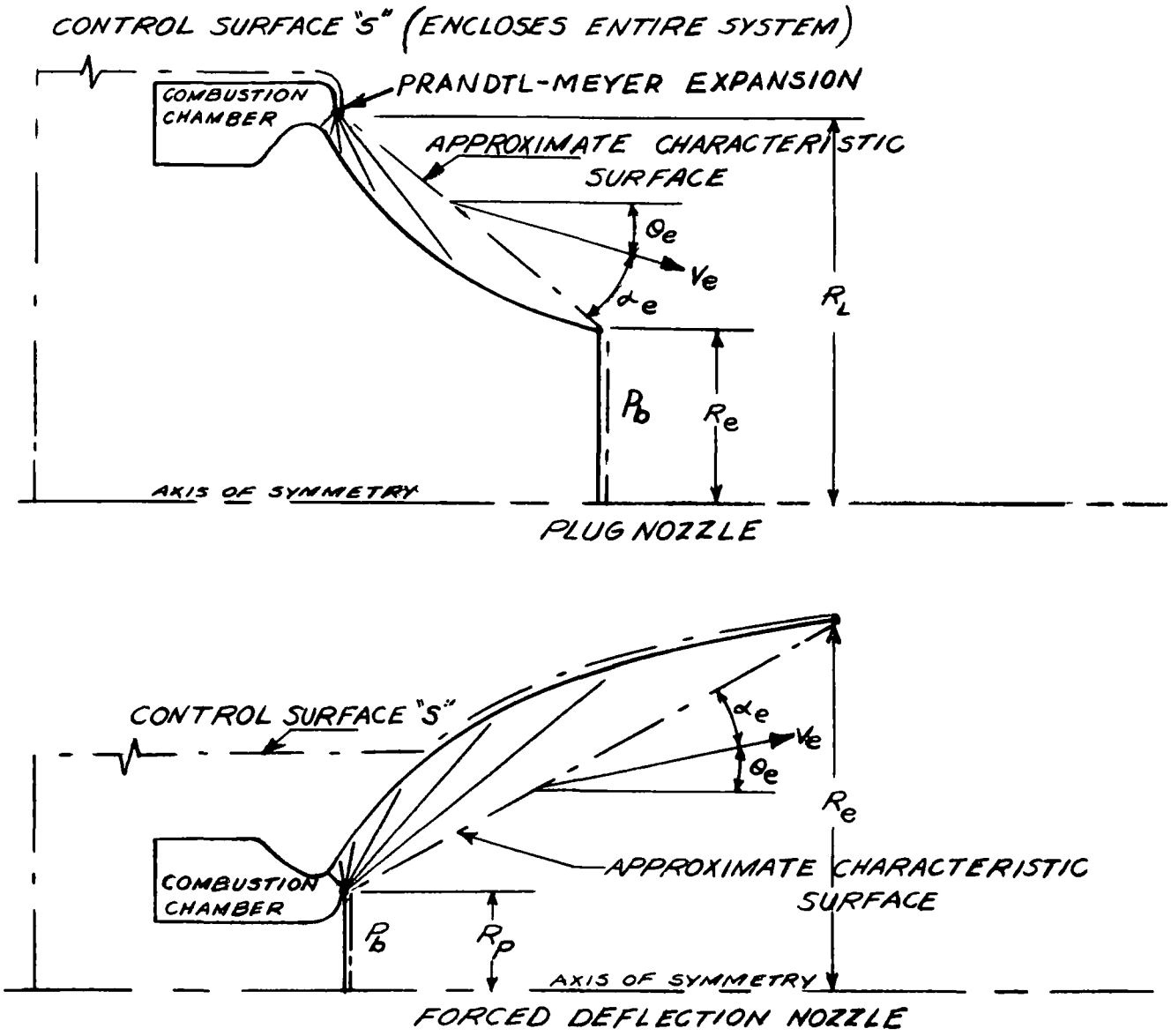

Figure II I-8

Nozzle-Control Surfaces and Parameter for Performance and Design Analysis

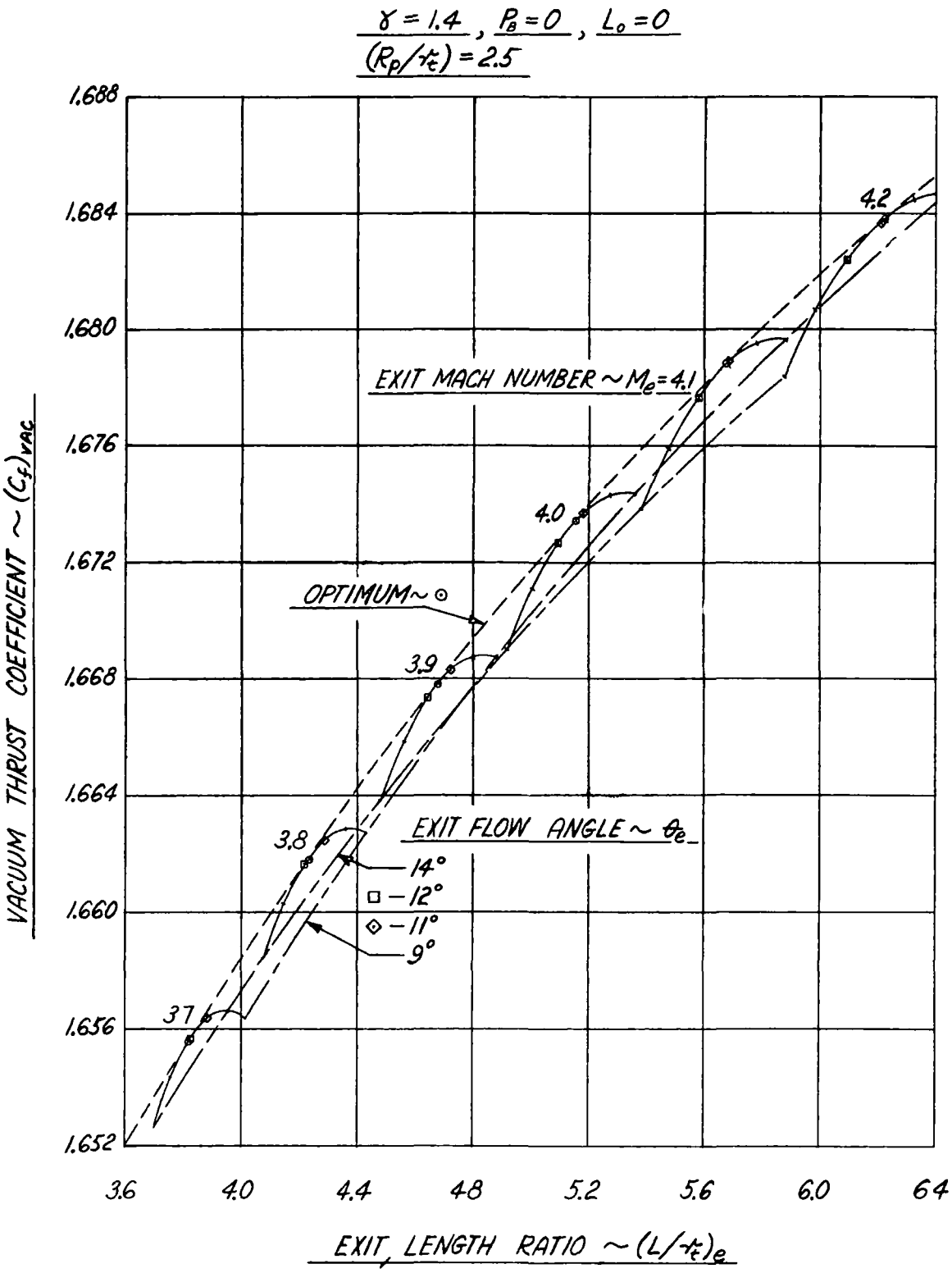

Vacuum Thrust Coefficient

Figure II I-9

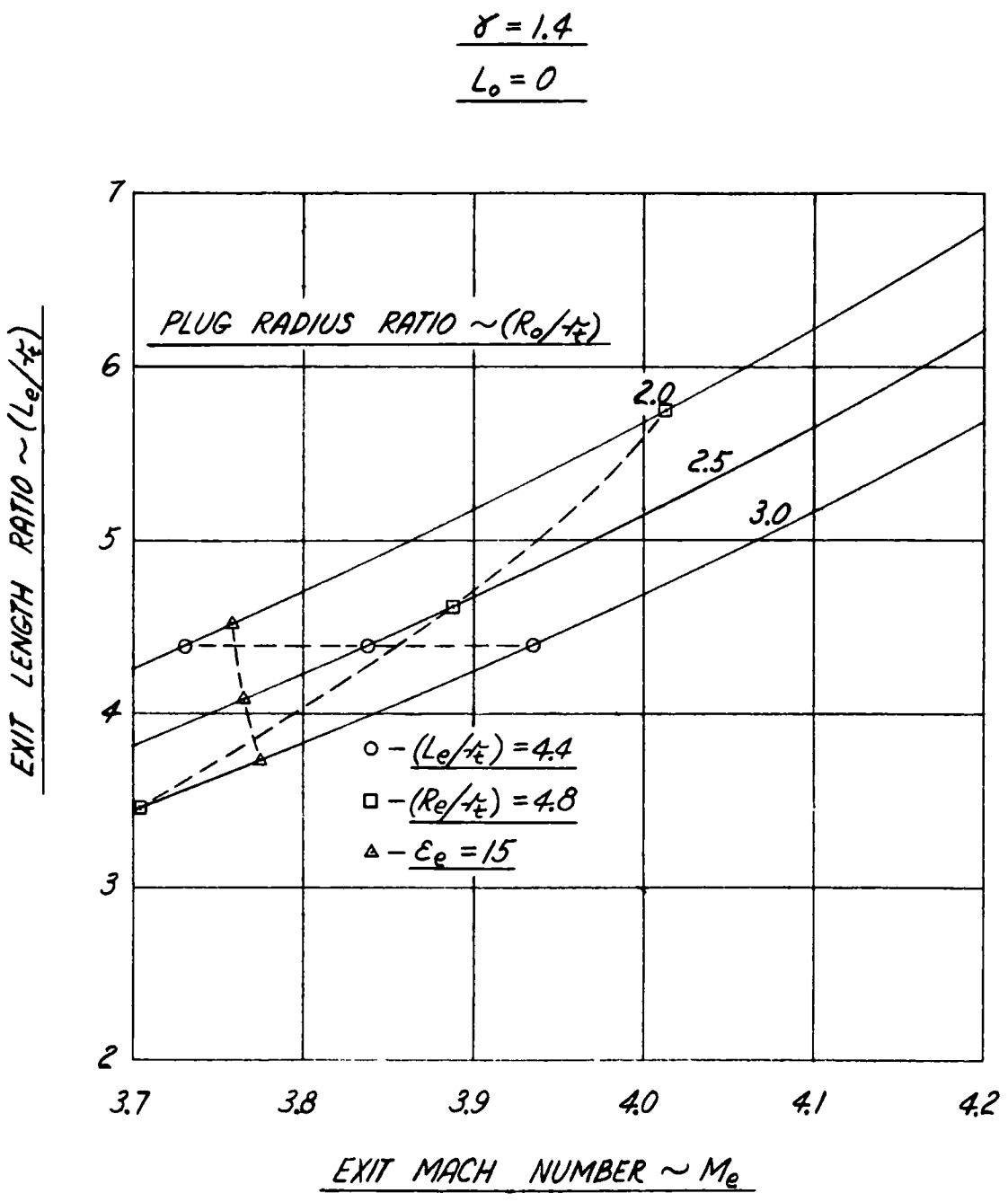

Optimum Exit-Length Ratio

Figure II I-10

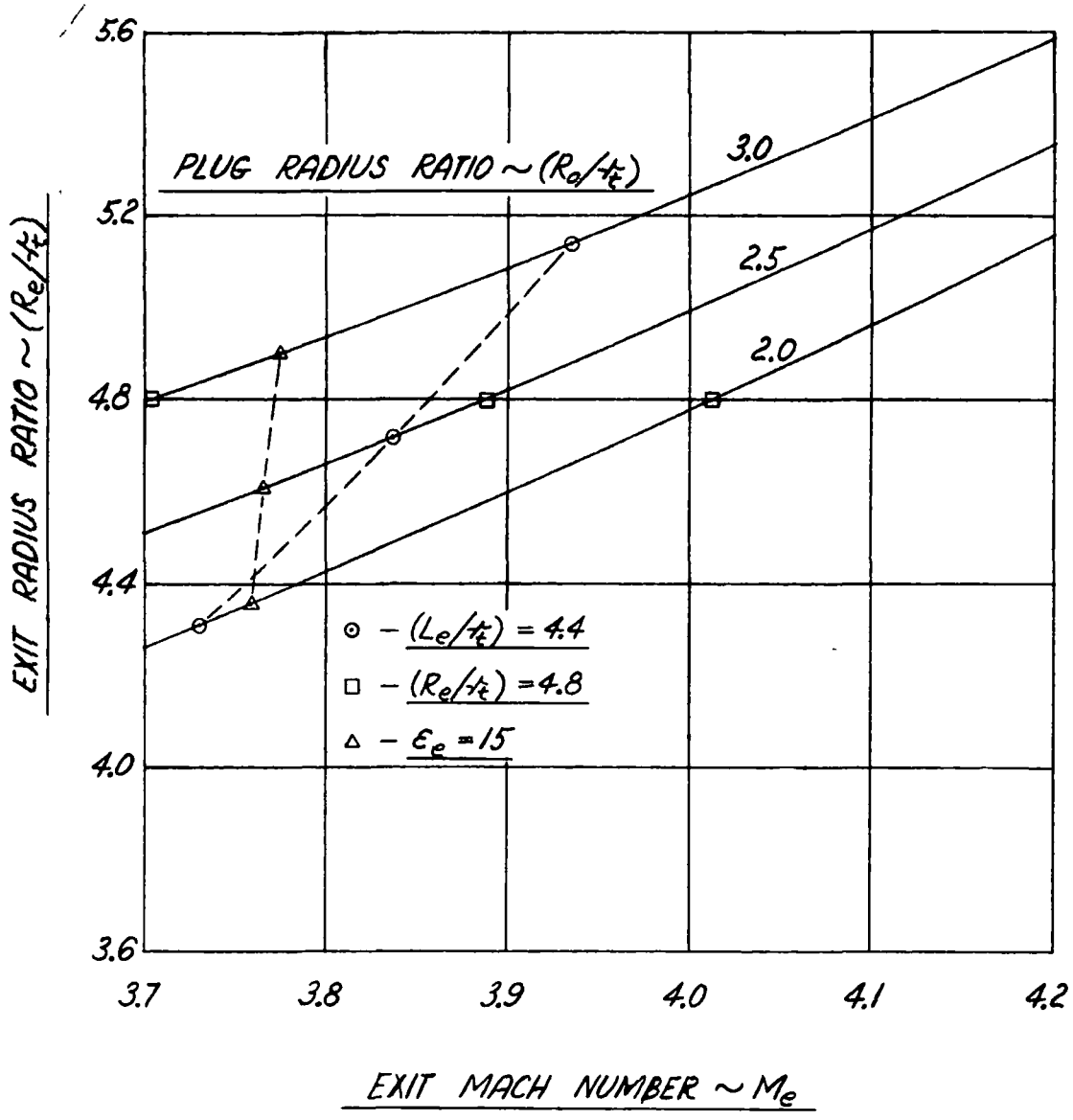

Optimum Exit Radius Ratio

Figure II I-11

$\gamma = 1.4$

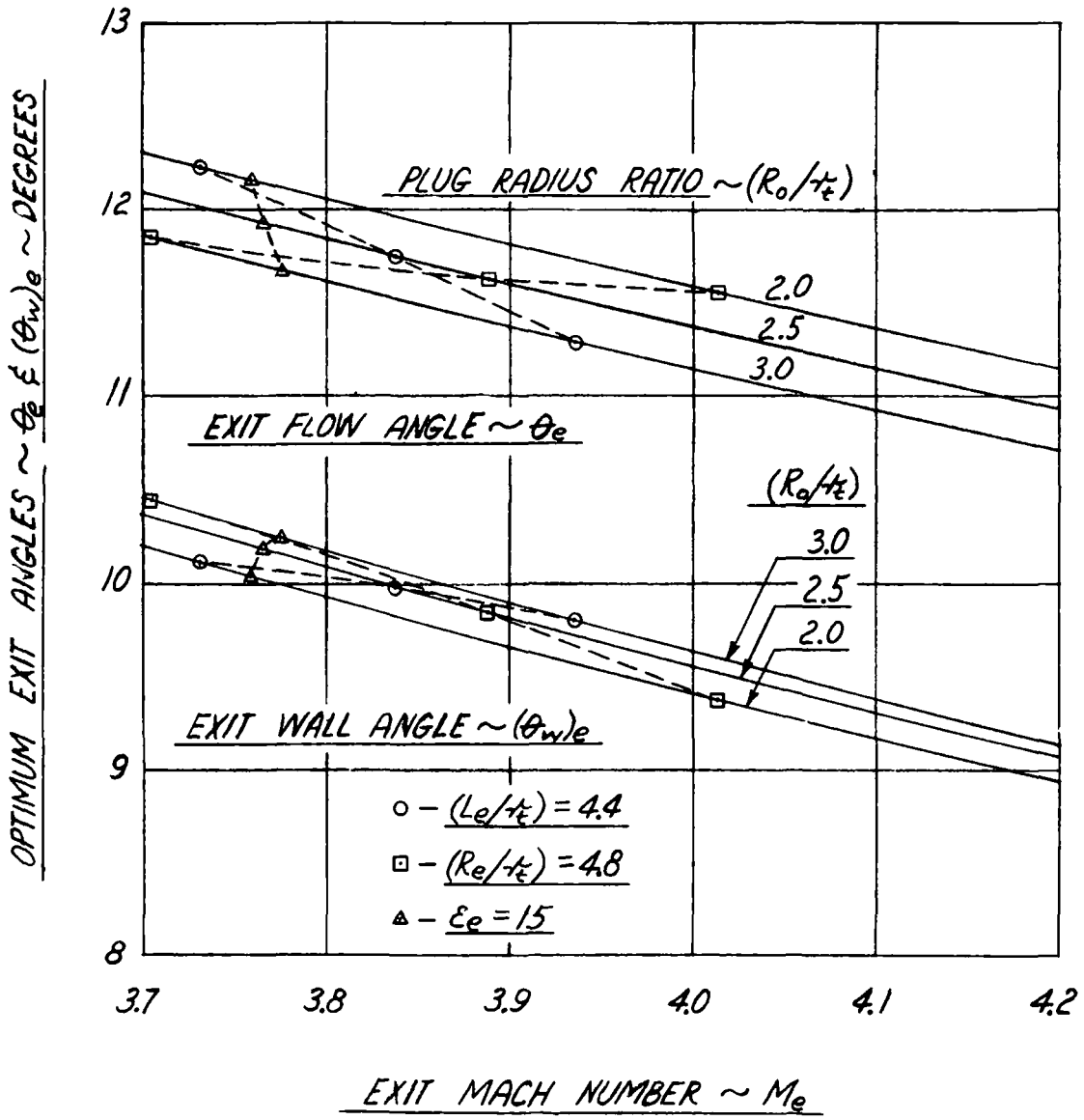

Optimum Exit Angles

Figure II I-12

$\gamma = 1.4$

$P_B = 0$

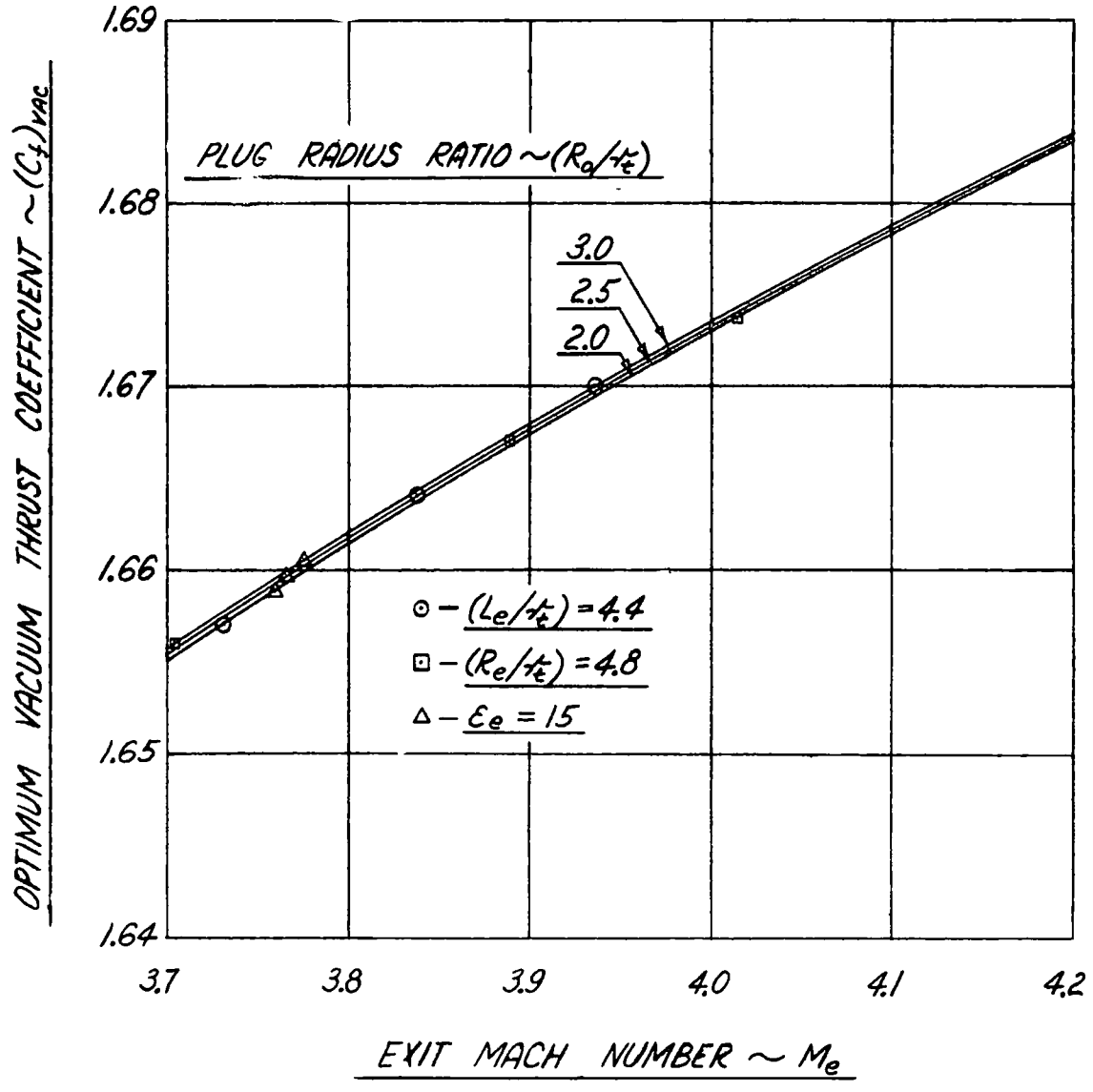

Optimum Vacuum Thrust Coefficient

Figure II I-13

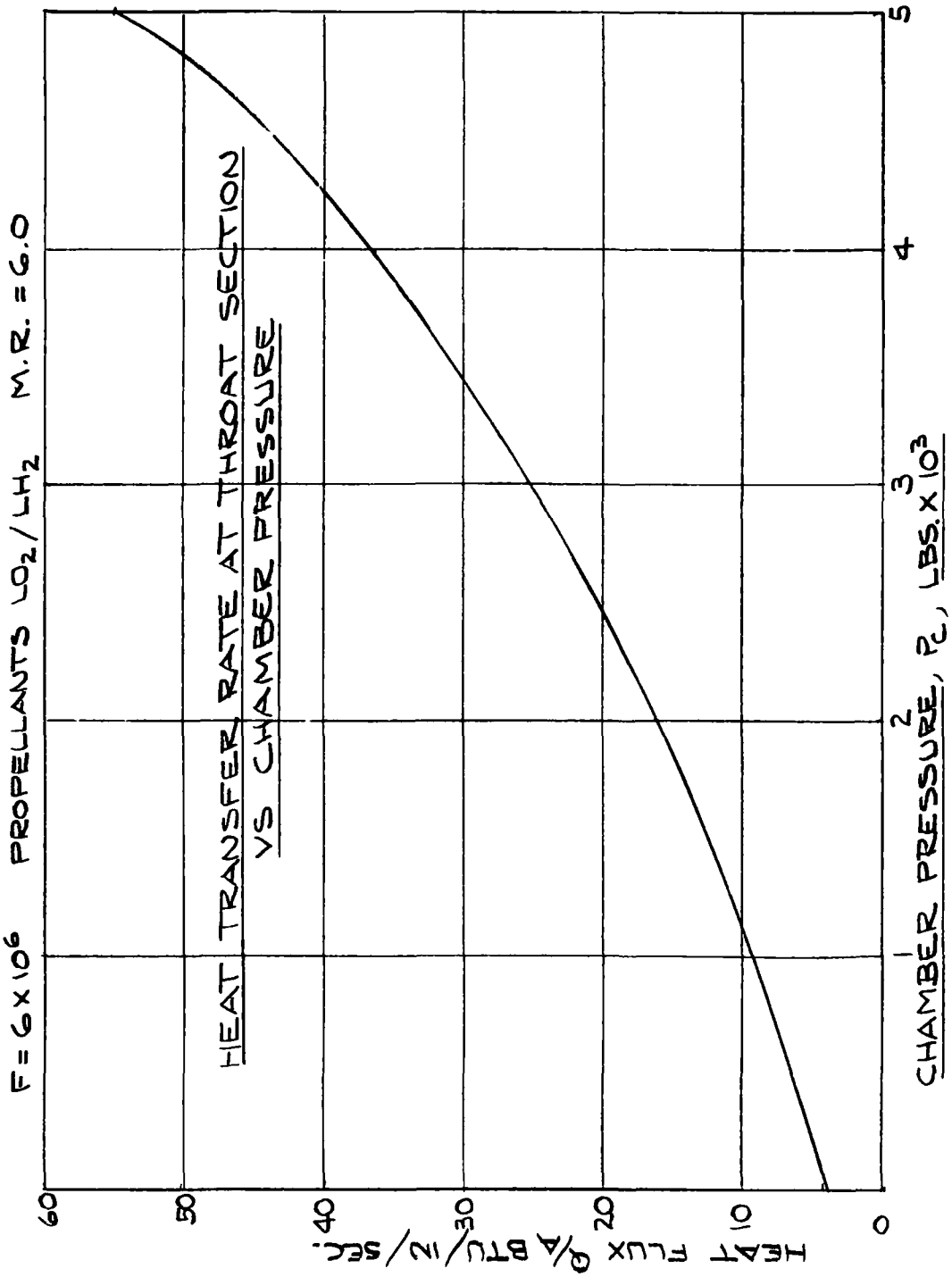

Total Heat Flux vs Chamber Pressure

Figure II I-14

a. Inlet Isometric

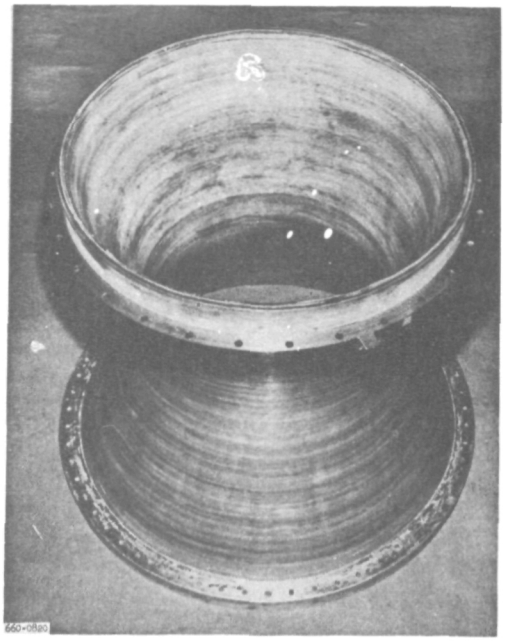

b. Inlet Isometric, Other Side

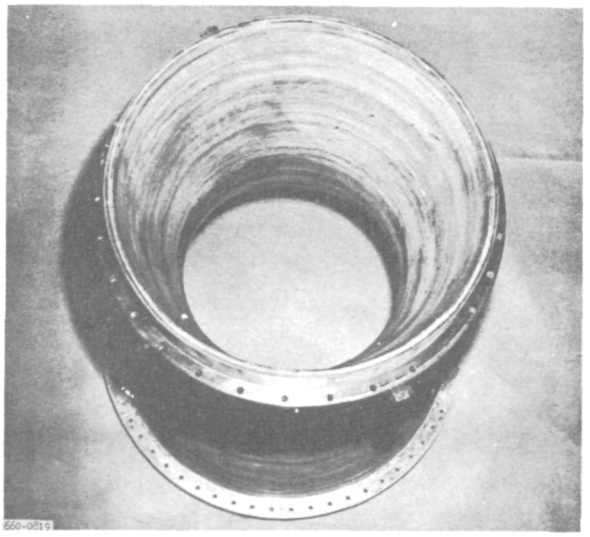

c. Inlet

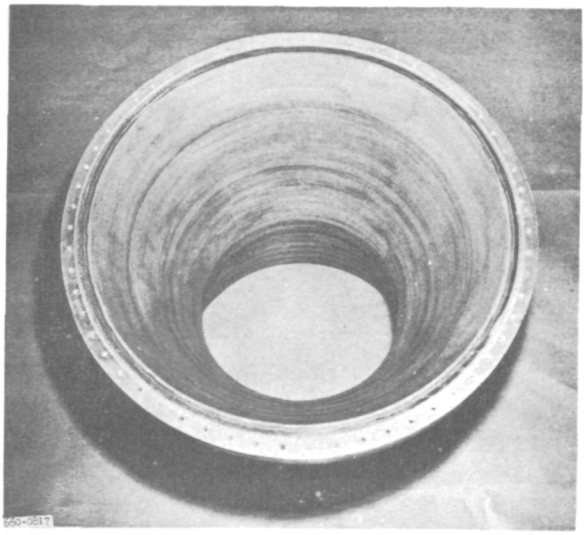

d. Exit

Ablative Chamber

Figure II I-15

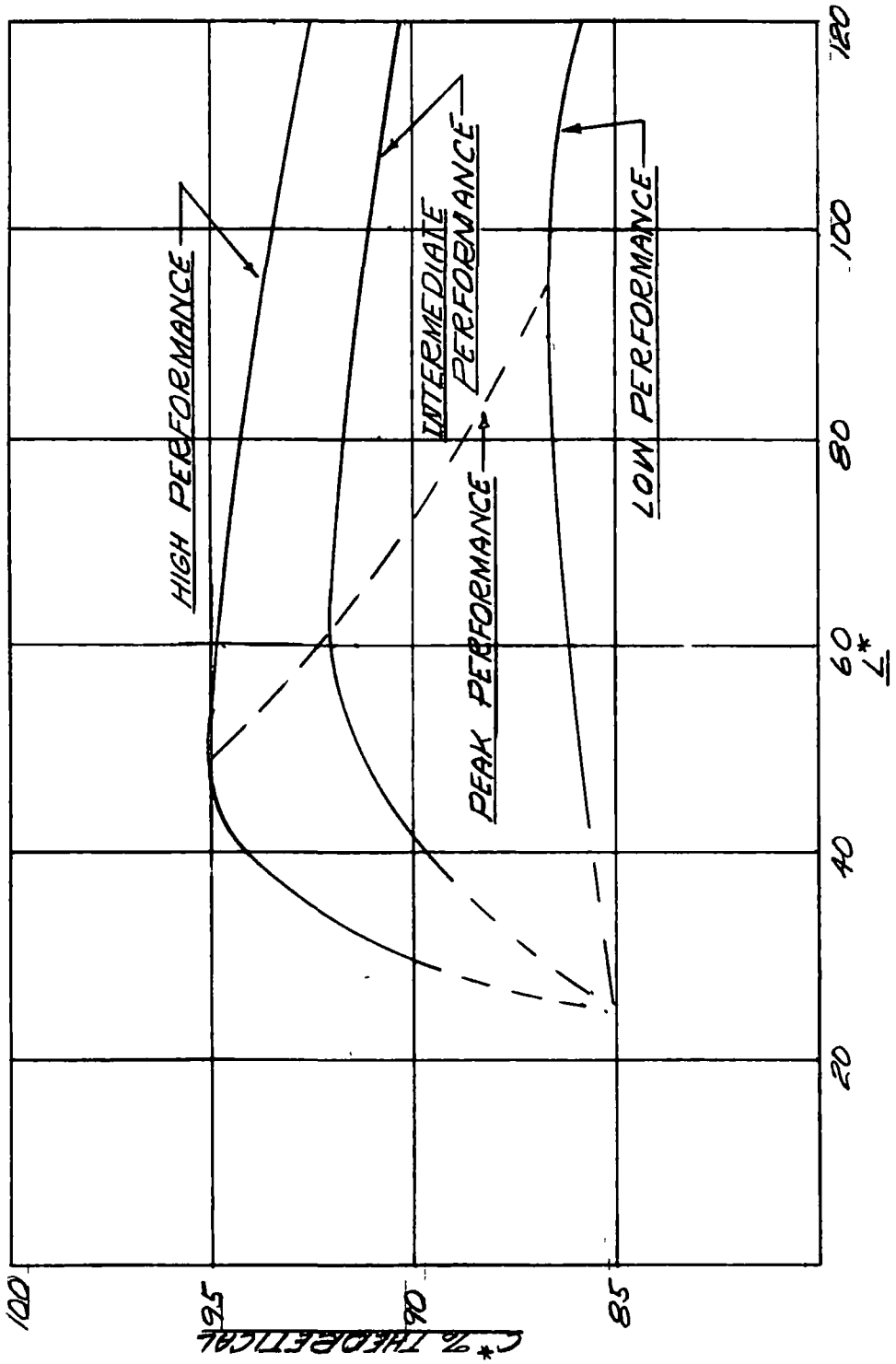

Effect of L* Upon Injector Performance

Figure II I-16

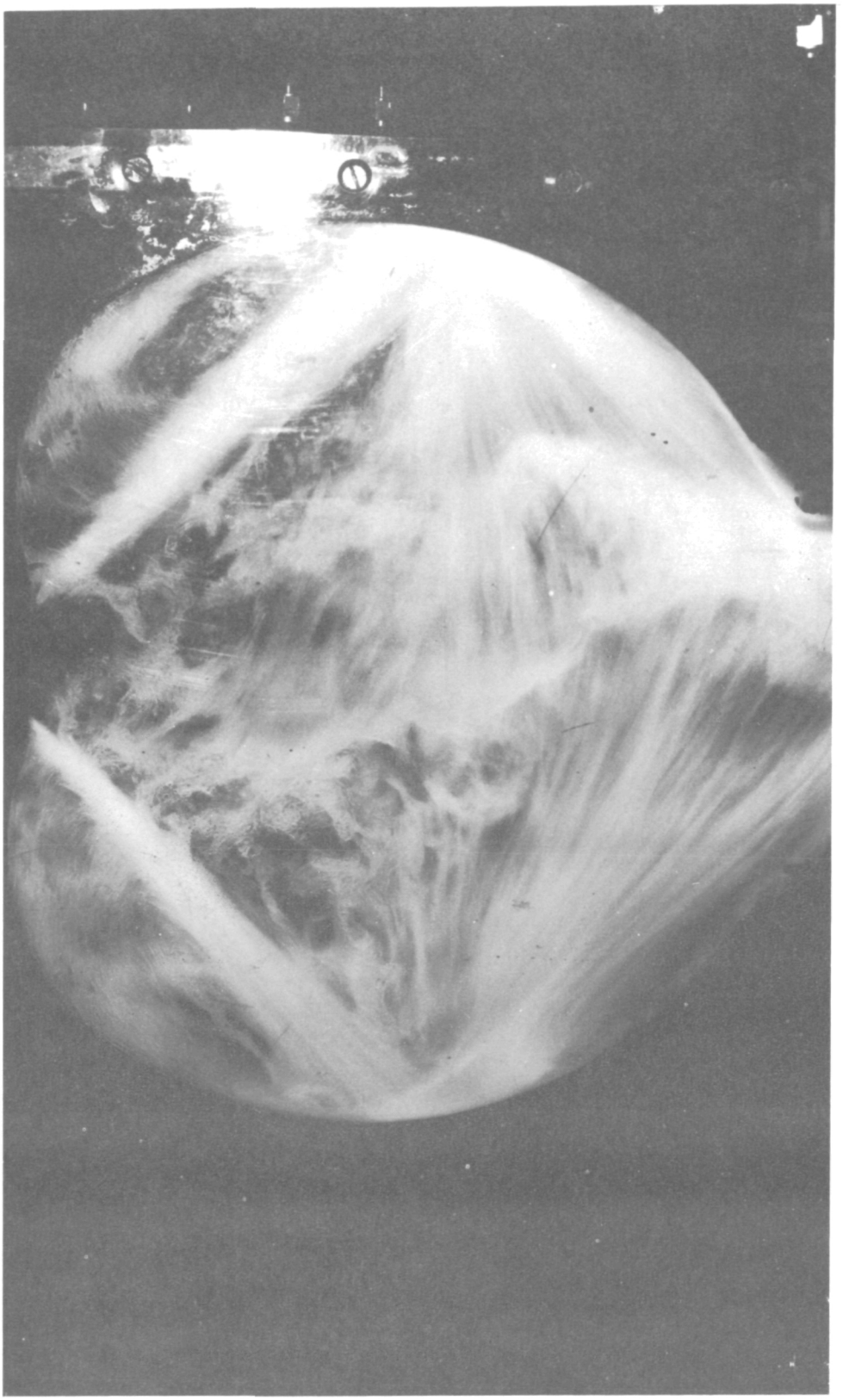

Spherical Centrifugal Combustor

Figure II I-17

II, Concepts Considered (cont.)

J. TURBOPUMPS

1. Introduction

The standard vehicle pumping requirements were specified at the outset of Task 1. Then, conventional turbopump configurations were selected; and weights, sizes, and performance values for these turbopumps were determined.

Next, effects of varying pumping requirements were analyzed and various alternative concepts evaluated. The following turbopump concepts and pumping requirements are discussed in this section.

a. Standard vehicle turbopumps

b. Effects of pump suction pressure

c. Low-speed inducer pump stage concepts

d. Suction-line propellant-utilization concept

e. Effects of thrust chamber pressure

f. High-head pump impeller concept

g. High-pressure H_2 turbopump concept for staged combustion cycle

h. High-pressure turbine inlet nozzle concept

II, J, Turbopumps (cont.)

i. Series turbopump turbine flow compared to parallel flow

j. Single turbopumps compared to clustered turbopumps

k. Pumping system concepts for engines having forced-deflection nozzles or plug nozzles

l. Turbine staging and back pressure selection

m. Gear-driven pumps compared to direct-driven pumps

n. Axial flow pumps compared to centrifugal flow pumps

o. Positive displacement pumps compared to centrifugal flow pumps

2. Standard Vehicle Turbopumps

The standard vehicle pumping system consists of single, separate, oxygen and hydrogen turbopumps, each having a single-stage, single-inlet, centrifugal-flow pump directly driven by a two-stage, axial-flow, gas turbine with shaft bearings located between the pump and turbine. Gas generator products flow in parallel through the separate turbine sets. Turbine exhaust gas is diffused, then expelled in converging-diverging nozzles located near the lower extremity of the thrust chamber.

Standard vehicle turbopump cost, size, and weight estimates are derived from designs of turbopumps in the 200,000- to 6-million-lb thrust range. Figure II J-1 presents turbopump wet weight in relation to engine thrust for tandem-tank, oxygen-hydrogen booster stages. These stages have the oxygen tank on top, 1,000-psia engine chamber pressure, and sufficiently

II, J, Turbopumps (cont.)

high pump inlet pressures so that oxygen-turbopump shaft speed is limited by oxygen-pump specific speed and hydrogen turbopump shaft speed is limited by bearing rubbing velocity. For the specified conditions of pump inlet and discharge pressure, the pump specific speed and bearing limitations are primary factors for turbopump size and weight. Figure II J-2 shows production unit cost trends in relation to engine thrust for this type of turbopumps.

Net positive pump inlet pressures for the standard vehicle turbopumps are 52 psi for O_2 and 7 psi for H_2. Pump inlet pressure has a pronounced effect upon the weights of the pumping system, tank, and tank pressurization system. The effects of varying pump inlet pressure and the selection of the best pump inlet pressure and pump system configuration, based on inlet pressure considerations, are discussed in this presentation.

Standard vehicle O_2 and H_2 pump discharge pressures are 1,300 psia each. Pump discharge pressure also predominately affects the turbopumps and various engine cycles.

To provide a fully adequate basis for estimating standard vehicle turbopump cost and weight, designs of the oxygen/hydrogen engine were made at the 6,000,000-lb and 800,000-lb thrust levels. These pumps deliver 1,000 psia chamber pressure and incorporate the gas generator cycle for turbine drive. All oxidizer turbopumps have an integral, low shaft speed, hydraulically-driven inducer stage with low pump inlet pressure.

II, J, Turbopumps (cont.)

These designs show that, up to 6-million-lb thrust, turbopump rotating parts would be no larger than the aircraft gas turbines now in use. This means that large turbopumps could be constructed without exceeding the limits of existing manufacturing facilities. Also, the designs show that turbopumps for large space-booster vehicles would be similar in design to the smaller turbopumps of intercontinental missiles in that they could be based on proved engineering practice and would have the same limits of stress, temperature, rubbing velocities, and performance values. Therefore, only a limited amount of feasibility effort is required prior to the actual design and construction of turbopumps in the size range of the standard vehicle and larger.

Beside the basic turbopump, the standard vehicle includes pump-discharge-pressure-equalizing lines, the wet weight of which adds approximately 1,000 lb to the basic turbopump wet weight (Figure II J-1).

Because it has been concluded from this study that major gains in cost and reliability can be achieved with a single-stage-to-orbit vehicle using O_2 and H_2 propellants, the concepts discussed in the following sections are limited to O_2 and H_2 turbopumps.

3. Effect of Pump Suction Pressure

Because of cavitation limitations, pumping system design is extremely dependent upon pump inlet conditions. Figures II J-3 and II J-4 show wet weight in relationship to net positive suction pressure for the

II, J, Turbopumps (cont.)

O_2 and H_2 turbopumps of a 2-million-lb-thrust, 1,000-psia chamber-pressure, gas generator cycle, O_2-H_2 engine. Curves are presented for turbopumps having single-inlet, single-stage, centrifugal-flow pumps directly driven by two-stage, axial-flow gas turbines with no separate low-shaft-speed inducer stages. Also, curves are shown for turbopumps that include a similar main-stage turbopump plus an integrally packaged, low-shaft-speed, hydraulically driven inducer stage.

In the turbopumps having inducer stages, propellant flows through the axial-flow-inducer impeller, then through a diffuser section where it is directed into the main-stage impeller. Flow is recirculated from the discharge housing of the main-stage pump through the hydraulic turbine and into the inducer diffuser stage to re-enter the main stage pump as illustrated in the flow schematic, Figure II J-5.

The inducer-stage impeller rotates on bearings supported by a stationary shaft attached to the diffuser housing. Hydraulic turbine buckets, formed in a single row, are machined from a peripheral ring which is an integral part of the inducer impeller. Turbine drive is accomplished via four, separate partial-admission flow passages. In two of these passages, fluid makes a single pass through the row of turbine buckets and re-enters the main stage pump inlet. In the other two passages, fluid passes through the turbine buckets twice. Fluid initially enters the row of buckets from the inlet nozzle, going to the opposing side, where it is redirected back through the buckets. Then it re-enters the main-stage pump inlet.

The turbine arrangement provides a turbine no-load shaft speed, or so-called runaway speed, which is less than the maximum allowable

II, J, Turbopumps (cont.)

pump shaft speed for cavitation limits. With this design, the maximum inducer-stage shaft speed is linked with the main-stage pump discharge pressure. This means that a turbopump with a hydraulically driven inducer has an anticavitation capability equal to a turbopump with a direct or gear-driven inducer when either propellant tank pressurant pressure is continuously below the allowable minimum or propellant bulk temperature is continuously above the maximum value In the event of a momentary excursion of either tank pressurant pressure or propellant bulk temperature, the turbopump with a hydraulically driven inducer stage would have superior anticavitation capability because the inducer stage could absorb momentary high-temperature or low-pressure propellant with only a slight increase in shaft speed. The inducer stage would be ready to receive normal-pressure-and-temperature propellant without cavitating Of course, if normal-pressure-and-temperature propellant flow did not recur quickly enough, the main-stage pump would cavitate and overspeed.

The weight savings potential of turbopumps with low shaft speed and inducer stages is apparent in Figures II J-3 and II J-4. Minimum turbopump weight with adequate suction pressure is limited in the case of the O_2 turbopump by the maximum allowable specific speed (i.e , impeller configuration index) for a mixed-flow, high-pressure-rise, single stage. For the H_2 turbopump, minimum weight is limited by maximum allowable bearing rubbing velocities. Turbine bucket root stresses may also impose shaft-speed limitations, but these stresses may be reduced to permissible values by appropriately changing turbine back pressure, nozzle angles, or both to shorten turbine buckets at the expense of increased turbine weight flow

II, J, Turbopumps (cont.)

As net positive suction pressure is decreased below the values at which pump specific speed or bearing rubbing velocities limit shaft speed, the cavitation conditions created by the lower suction pressures cause the turbopump design shaft speed to be reduced. With this reduced shaft speed, the pump impeller tip diameter must be larger, to generate the required pressure, as the optimum turbine diameter increases; thus turbopump size and weight become greater. However, if a low-shaft-speed inducer stage is added at values of low net positive suction pressure, the inducer-stage discharge pressure (which is equal to the main-stage inlet pressure) may be raised to the point that either pump specific speed or bearing rubbing velocities limit the main-stage shaft speed. Hence, main-stage turbopump shaft speed and wet weight would be very nearly equal to the weight of a turbopump with no inducer stage at high net positive suction pressures. (The slight difference is caused by the increase in main-stage pump flow rate resulting from the hydraulic turbine recirculating flow.) Thus, the wet weight of a turbopump with a hydraulic-driven turbine is equal to the minimum turbopump weight plus the weight of the inducer stage.

There are five basic methods of increasing turbopump shaft speed (thus decreasing turbopump weight) for given pump inlet conditions. They are:

a. Direct-driven inducer (i.e., an inducer section on inlet end of a main-stage impeller).

b. Hydraulic-turbine-driven, low-shaft-speed, inducer stage (previously described).

II, J, Turbopumps (cont.)

c. Gear-driven, low-shaft-speed, inducer stage.

d. Separate, low-shaft-speed, gas-turbine-driven booster pump.

e. Inducer jet pump with pump discharge pressure liquid drive.

The inducer jet pump is somewhat analogous to the hydraulic-driven, low-shaft-speed inducer stage in that both require a recirculating flow from the main-stage pump. Because the jet pump efficiencies are considerably lower than the hydraulic turbine inducer efficiencies, the inducer jet pump was eliminated.

The separate gas-turbine-driven booster pump has no significant weight advantage over either a gear- or hydraulic-driven inducer stage, yet it gives severe penalties in the form of control complexity, plus engine packaging and installation problems. A gas-turbine-driven booster pump does have application to vehicles where certain propellant tanks are jettisoned. However, vehicle configurations of this type have not shown promise; therefore, the gas-turbine-driven booster pump is eliminated.

An alternative form of the gas-turbine-driven booster pump is one in which the low-shaft-speed inducer pump is driven through a coaxial shaft within the main-stage turbopump shaft by a gas turbine located in the main-stage gas turbine exhaust stream. This arrangement is not suitable for an H_2 turbopump because the necessity for a hollow shaft would weaken the highly stressed turbine and pump discs. Also, in all cases, it would have the same control disadvantage mentioned in the preceding paragraph.

II, J, Turbopumps (cont.)

O_2 turbopumps with direct-driven, hydraulic-driven, and gear-driven inducers are compared, on an equivalent turbopump wet weight basis, in Figure II J-6 . Equivalent wet weight equals turbopump wet weight, plus the turbine weight flow, multiplied by an exchange ratio. This exchange ratio accounts for flight duration, the equivalent inert weight of propellant weight, the excess tankage weight for turbine propellant, and the ratio of turbine exhaust effective specific impulse to thrust chamber effective specific impulse.

The hydraulic-driven inducer adds less inert weight than a gear-driven inducer, but because of the inefficiency of the fluid transmission (main-stage pump efficiency, 0.70, hydraulic turbine efficiency, 0.35, to obtain a high ratio of design to no-load speed), the gas turbine weight flow for the hydraulic-driven inducer unit exceeds that of a gear-driven inducer unit. However, the gear-driven inducer unit offers a negligible equivalent wet weight improvement, and was, therefore, eliminated in favor of the simpler, less-expensive hydraulic drive. Gear weights are shown in Figure II J-33.

Figure II J-7 shows equivalent wet weights in relation to net positive suction pressure for hydrogen turbopumps, both with and without separate inducer stages.

To select the best tank pressure for a given pumping system, as well as compare competitive pumping systems on an over-all weight basis, effects of tank weight, tank pressurizing-system weight, and equivalent wet turbopump weight must be considered. A convenient means for evaluating these weights is to plot each weight in relation to maximum tank pressure, where maximum tank pressure is defined as nominal tank pressure plus nominal to maximum pressure regulator tolerance.

II, J, Turbopumps (cont.)

Turbopump equivalent wet weights have been shown in relation to net positive suction pressure. Minimum net positive suction pressure can be correlated to maximum tank pressure as follows:

Minimum net positive suction pressure equals maximum tank pressure, minus total pressure regulator tolerance, minus maximum vapor pressure, minus suction line frictional pressure drop, plus minimum liquid gravitational head pressure.

Assuming that large space-booster vehicles have fixed pressure-tank pressure regulators, then the minimum pump inlet liquid gravitational head occurs at the termination of a full-duration captive test. On the basis of these criteria, the equivalent turbopump wet weight (which is shown in Figures II J-6 and II J-7 versus net positive suction pressure) is shown in relation to maximum tank pressure in Figures II J-8 through II J-11.

O_2 turbopump equivalent weight for a tandem tank stage with the O_2 tank above the H_2 tank is shown in Figure II J-8. Figure II J-9 depicts the O_2 turbopump equivalent weight for the reversed tandem tank situation. The H_2 turbopump equivalent weight is shown in Figure II J-10 for either tandem tank arrangement. Location of the tank makes little difference because the increased liquid gravitational head with the tank on top is almost exactly offset by the increased suction line functional pressure drop.

O_2 and H_2 tank weights and tank pressurization-system weights in relation to maximum tank pressure for a 2-million-lb-thrust, 180-sec-duration, booster stage are shown in Figure II J-12 and II J-13. Heated helium and heated H_2 were selected as the pressurants for the O_2 and H_2 tanks, respectively, because they offer advantages in weight, simplicity, and development.

II, J, Turbopumps (cont.)

Summary curves of tank, tank-pressurizing system, and turbopump equivalent weights as a function of tank pressure are presented in Figures II J-13, II J-14, and II J-15. These curves show that pumping systems having hydraulic-driven inducer stages offer definite weight advantages. A 4,100-lb overall weight savings in the O_2 system is realized with the O_2 tank on top, and a 5,400-lb saving results when the oxygen tank becomes the bottom one. Hydrogen system weight savings would be 1,200 lb for either tank location. Thus, total weight savings realized by adding the inducer concept to the standard vehicle booster stage are 5,300 lb when the oxygen tank is on top and 6,600 lb when it is on the bottom. These curves also show that minimum overall weight is achieved with the oxygen tank on top. With separate inducer stages in both pumping systems, a vehicle with an upper O_2 tank in the booster stage is 2,000 lb lighter; and with no separate inducer-pump stages, the booster stage is 4,800 lb lighter with an upper O_2 tank.

The previously described figures provide a comprehensive comparison of the merits of pumping systems, both with and without separate inducer stages. However, to completely compare the advantages of locating the O_2 tank on the top or bottom of the stage, consideration must also be given to the factors of vehicle stability for man-rating, vehicle control requirements, and suction line wet weight at burnout. Locating the O_2 tank on top gives advantages in combined tank, tank pressurizing system, and turbopump equivalent weight as previously shown. It also provides gains for improving vehicle stability and minimizing control requirements. Its only, but significant, disadvantage is that at burnout the weight of oxygen in the suction line is high. For this reason, the concept of utilizing part of the suction-line O_2 is attractive.

II, J, Turbopumps (cont.)

Figure II J-16 shows suction line wet weight in relation to the elevation of liquid O_2 in the suction line at burnout. With the suction line full, the liquid level is 74 ft, and the combined weight of the four suction lines, plus propellant, is 13,200 lb. With no inducer stage, the suction line liquid level could be reduced to 24 ft at burnout, giving a potential savings of 6,800 lb. It should be noted, however, that not all of this weight could be saved, because during the draw-down of the suction line, a certain amount of additional O_2 would be vaporized and remain as unused propellant. During suction line draw-down, the upper layer of the liquid would be boiling. At burnout, it is required that the boiling layer does not penetrate below 24 ft for a pumping system without an inducer stage. Therefore, the effectivity of this concept depends upon the depth of a boiling layer of the O_2 column, which must be determined by experimentation. This concept presents two more problems, but these may be overcome as follows.

The first problem would occur if the suction line cavitated before all the liquid in the tank had entered this line. Elimination of this problem can be accomplished by funneling the uppermost section of the suction line so that the net positive suction head exceeds the velocity head until the liquid level reaches the suction line inlet.

The second problem would be to demonstrate the operation of the propellant-level cutoff sensor (located in the suction line) during captive tests. To draw-down the suction line during captive tests, tank pressure would have to be increased to prevent pump cavitation. This could be accomplished by adjusting the tank pressure regulator to give above-normal tank pressure. (Tank pressure can be adjusted up to 14.7 psi above normal without exceeding altitude differential pressure limits.)

II, J, Turbopumps (cont.)

As shown in Figure II J-16, a pumping system with an inducer stage may be used to further reduce unused suction-line O_2. The curve sharply increases at the lower end because, although the liquid level is lower, the required pump inlet diameter begins to increase with decreasing liquid level, causing a similar increase in suction line diameter.

The best use of the inducer stage for this concept would be to keep the burnout liquid level at a relatively high point (20 to 25 ft above the pump inlet) so that full-duration, captive-stage, propellant-exhaustion, oxygen-sensor cut-off tests may be conducted without altering tank-pressure-regulator settings.

4. Effect of Thrust Chamber Pressure Upon Various Engine Cycles

As discussed in section II, E, thrust chamber pressure is a major variable in the payload-carrying capability of a vehicle. It also has an important effect upon turbopump size and weight. However, pump-discharge pressure has a more direct effect upon turbopumps. Figure II J-17 shows pump discharge pressure for the direct-feed engine cycles, such as the gas generator cycle, the third fluid cycle, the heated-hydrogen bleed cycle, and the chamber bleed cycle. The difference between the pump discharge and the thrust chamber pressure allows for pressure drop in the distribution lines, valves, cooling jackets, and injectors.

In topping-type cycles, such as the staged combustion cycle, pump discharge pressure increases at a more rapid rate with increasing chamber pressure (Figure II J-18). In this cycle, the turbine pressure ratio adds to line, valve, and injector pressure drops to provide a higher pump discharge pressure for a given chamber pressure. For a given pump discharge

II, J, Turbopumps (cont.)

pressure, the turbine pressure ratio is determined primarily by the turbine inlet temperature, as well as the pump and turbine isentropic efficiencies. Because the turbine pressure ratios are comparatively low, the turbine-bucket-to-gas-stream-velocity ratio is favorable, and relatively high turbine efficiencies result.

Turbopump wet weight in relation to pump discharge pressure for various O_2-H_2 2-million-lb-thrust engine cycles is shown in Figure II J-19. Turbine weight flow rate versus discharge pressure for a gas generator cycle engine is presented in Figure II J-20. Figure II J-21 reflects turbopump production unit cost trends as functions of chamber pressure. Information from these figures was used for the engine cycle evaluations of Section II, E. Maximum pressure rise per turbopump was assumed to be 1, 300 psi for H_2 turbopump, and 5, 000 psi for an O_2 turbopump. High hydrogen pressures are achieved by operating multiple hydrogen turbopumps in series.

An investigation was made to determine whether it would be better to have a higher pressure rise per single H_2 pump stage. A high-head-rise impeller design was conceived which facilitates impeller stress analysis and offers manufacturing economies for a large-diameter impeller. Based on this impeller design, hydrogen pressure rises of 2, 600 psi/stage are feasible. However, a turbopump design incorporating such a high pressure rise impeller encounters high bearing-rubbing velocities unless shaft speed is reduced. Figure II J-23 shows H_2 turbopump wet weight versus bearing rubbing velocity for a 2, 600 psi pump-discharge-pressure pumping system. The current, proved bearing rubbing velocity limitation of H_2-cooled bearings with properly controlled radial and axial loads is in the range of 1.5- to 1.7-million millimeters multiplied by rpm. In this region of bearing rubbing

II, J, Turbopumps (cont.)

velocity, a single turbopump with two series pump impeller stages, or two series turbopumps, each having a single impeller stage, is clearly superior to one with a single high-pressure impeller having bearings located between the impeller and turbine. Furthermore, the two-stage pump unit or the series turbopump unit offers significantly better pump efficiencies (Figure II J-24). Units with higher pump efficiencies require less turbine flow rate and therefore have lower turbopump equivalent weights.

Although the inert and equivalent weights of a hydrogen turbopump having a single, high-pressure-rise, pump stage can be improved by using shaft bearings located outboard of the pump and turbine rotors, it can be concluded that a single, high-pressure-rise, pump-stage turbopump offers no overall weight advantage over either a dual, series, pump-stage turbopump or a pumping system having dual, series turbopumps.

A high-pressure H_2 turbopump for a staged combustion-cycle engine was designed. This design was made to verify the applicability of the curve of turbopump wet weight versus pump discharge pressure (Figure II J-19) to staged combustion units. Because of the large turbine flow rates of the staged combustion cycle, two, single-stage, parallel-flow turbines are used to give reasonable values of turbine bucket root stress. Single-stage turbines give excellent performance (in the order of 0.70 to 0.80 isentropic efficiency, because of the low turbine pressure ratio). The mating O_2 turbopump for this H_2 turbopump would be very similar to a gas generator cycle turbopump at the same pump discharge pressure. The oxygen turbopump turbine would have a three-stage, series flow turbine, which also has a high isentropic efficiency. Refer to Figures II E-12 through II E-17 for cycle analysis schematics of staged combustion engines.

II, J, Turbopumps (cont.)

One design problem created by high-pressure turbopumps is that of containing the high turbine-inlet pressure in the turbine-inlet nozzle assembly. A turbine inlet nozzle configuration was designed which restrains the high turbine-inlet nozzle pressure in small diameter hoop stress, thus yielding a lightweight design which minimizes turbine static-part deflection under operating conditions of pressure and temperature. This arrangement consists of multiple, large-inlet nozzles welded to the inlet housing to form a single-piece inlet nozzle and turbine stator construction. Exit flow from the nozzles is annular for good performance, and the nozzle throat and exit angles are finally machined after welding to accurately control flow rates and direction. This inlet nozzle configuration may be fed by multiple, individual, cross-fire tube coupled, gas generators, or it may be fed by a single gas generator through a multibifurcated, all-welded feed duct that is somewhat similar to the exhaust duct system of a radial, reciprocating engine.

Another design problem associated with high-pressure and large-diameter turbopumps is that of equalizing radial hydraulic forces upon the pump impeller. Radial hydraulic forces must be minimized for two reasons. First, so that the impeller shaft will not deflect to an extent that would cause interference between rotating and stationary parts, and second, to maintain radial bearings loads within permissible values. Radial hydraulic force is a function of pump diameter, flow rate, and discharge pressure, which means that, for large-thrust or high-pressure engines, additional provisions for balancing these radial forces must be made. One means for balancing the radial forces is to design a pump discharge housing that has multiple, diametrically opposed outlets and to connect these opposed outlets with symmetrical lines that meet at an equidistant point from each outlet. This arrangement provides equal pressures upon opposing sides of the impeller. Figures II J-24 and II J-25 show turbopumps for a 6-million-lb-thrust O_2-H_2 engine that incorporate this feature.

II, J, Turbopumps (cont.)

5. Series Turbine Flow Compared to Parallel Turbine Flow for Various Engine Cycles

For gas generator cycles, heated hydrogen bleed cycles, and chamber bleed cycles, a series flow through the separate turbopump turbines requires less total turbine flow rate than an engine cycle with parallel flow through the separate turbine sets. This is because the gas velocity per stage for series flow is less, thus giving a higher turbine-bucket-to-gas-velocity ratio, which improves efficiency. Reduced turbine flow rate improves engine specific impulse; however, as shown in Figure II J-20, the engine specific impulse improvement is relatively small. Therefore, for gas generator, heated hydrogen bleed, or chamber bleed cycles, the choice of either series or parallel turbine flow cycles will have little effect upon vehicle cost or performance. Although either cycle is workable, the final selection will be influenced by factors of control complexity and component interaction.

In the third fluid cycle, the series-flow turbine cycle is again desirable because it reduces the auxiliary fluid flow rate, thus decreasing boiler and condenser size. However, the choice again will be determine primarily by control and system operation criteria.

In the staged combustion cycles, series flow turbines offer no significant performance advantage because the relatively low pressure-ratio parallel turbine sets are highly efficient. Because of the superior engine-control capability provided by the parallel flow turbines, series flow turbines are not competitive for these cycles.

II, J, Turbopumps (cont.)

6. Single Pumping Systems Compared to Clustered Pumping Systems

Based on the preliminary design work completed in Task 1, a pumping system consisting of single, separate turbopumps feeding either single or multiple thrust chambers is superior to a pumping system consisting of a cluster of multiple turbopumps, in terms of lower cost, better reliability, and fewer requirements for operational support equipment as well as checkout equipment.

Figure V J-1 shows turbopump wet weight for single pumping system in relationship to thrust. Based on this curve, the combined weight of a cluster of small turbopumps is very nearly equal to the weight of a set of single turbopumps. Also, the weight of additional valves (control and suction) and discharge distribution lines must be added to the clustered system. Investigations, which consisted of applying rudimentary scaling factors to existing small turbopumps to obtain large pumping system weights, could have lead to considerable error because it is very difficult to scale weight upward in large steps. Also, it is a faulty assumption that the large machines are necessarily dynamically similar to the small units.

Figure II J-2 shows turbopump production cost for single pumping systems in relation to engine thrust. Again, cost of individual turbopumps for clustered pumping systems can be obtained from the graph by appropriately dividing the total thrust value. In the thrust range of 800,000 to 3,500,000 lb, turbopump production unit cost decreases with increasing size. Although turbopumps within this range are similar and material costs vary directly with weight, which is nearly proportional to thrust level, items such

II, J, Turbopumps (cont.)

as machining, welding, and heat treating of larger parts do not increase directly with weight. This accounts for the decreasing cost trend. Costs of turbopumps per pound of delivered thrust below the 800,000-lb thrust level increase rapidly with decreasing size because of increased complexity, smaller allowable tolerances, and, in some cases, exceedingly small parts sizes. Fabrication of turbopump parts up through the 6-million-lb thrust level is entirely within the capability of existing tooling and process facilities.

In terms of simplicity of controls, propellant lines, and support structure, a single turbopump offers substantially higher reliability than multiple turbopumps because of the smaller number of moving parts and components. One of the arguments for multiple turbopumps is that, should one pump fail, the remaining operating pumps could continue to reliably furnish propellant requirements. It is generally agreed within the rocket industry that pump failures usually are catastrophic. Therefore, if one of a multiple group of pumps fails, it is very likely that the pump housing, the suction line, or the discharge line near the pump housing will be ruptured. Suction and discharge valves must be provided for closing in the event of a failure, but considerable propellant will be spilled before the closure of these valves. This spilled propellant may burn or explode, creating further failures. Furthermore, shrapnel from a catastropic pump failure can damage other parts of the engine, creating additional failures.

From the foregoing reasons, it can be seen that a multiple, redundant pumping system has no basic reliability advantage over a single pumping system if a catastrophic failure should occur. Therefore, the systems should be compared on the probability of catastrophic failure occurring. Possible means of catastrophic failure as well as a comparison of the probability of system failure follow.

II, J, Turbopumps (cont.)

a. Failure caused by pump suction cavitation reducing pump load, followed by turbopump overspeeding to destruction.

Excessive cavitation may be caused by abnormally high pump shaft speed caused by high turbine-inlet temperature, high turbine-inlet pressure, or by a restricted thrust-chamber-valve setting. Generally, the time rate of these perturbations is such that a control feedback circuit can reduce turbine flow rate to correct for the condition, or adequate margins can be applied to the engine nominal uprating point to accommodate any likely disturbances. A single or multiple system would have equal turbopump component reliability in this respect.

Excessive cavitation may also be caused by abnormally high propellant bulk temperatures or by loss of tank pressure. If this occurs, the loss of pump load is so rapid that turbine weight flow rate cannot be adjusted in time and an overspeed destruction would occur. For this type of abnormality, a single system would again have equal reliability with a multiple system because one or all of the turbopumps in a multiple system would have the same tendency to cavitate as would a single turbopump. This type of failure is best avoided by providing adequate margins of pump capability for high propellant temperature.

b. Failure of turbopump part because of fatigue or abnormal operation.

In this respect, a single pumping system is clearly more reliable because it has fewer total numbers of parts and components. It is expected that a single large turbopump in the thrust range of interest will have higher potential reliability than the intercontinental missile turbopumps because the large unit will have substantially fewer parts than the existing

II, J, Turbopumps (cont.)

units. Also, a very significant factor in reliability is the required amount of ground support checkout and maintenance. A single pumping system, because of its fewer functional parts, would offer better reliability in this respect.

Another important reliability factor at the launch site is propellant bleed and drain of the pumping system. Here again, a single pumping system with fewer traps would be simpler to drain and bleed.

7. Pumping System Concepts for Forced-Deflection or Plug Nozzle Engines

The design of engines having forced-deflection or plug nozzle thrust chambers presents an extremely difficult problem in component packaging, propellant distribution line arrangement, and propellant valving arrangement. All of the design efforts prior to and during Task I resulted in engine designs with tangled propellant distribution lines with many exposed flanges and flexible joints. This pointed to a definite need for a different approach to the integration of the pumping system and thrust chambers.

Because, in either a plug nozzle or forced-deflection engine, the multiple thrust chamber injectors are located equidistant from a central point, the desirability of locating the pumping systems in the center of the engine is apparent. In the integrated pumping system, the separate turbopumps are located in tandem with a common center line. There, the hydrogen turbopump is fed from the lower tank and is the upper turbopump with its pump inlet flange on top. The O_2 turbopump is below with its downward-facing pump inlet fed by four suction lines

II, J, Turbopumps (cont.)

reaching from the upper tank. Both turbopumps are encased in a common, integral, all-welded housing that includes all pump discharge distribution lines, heated H_2 feed lines and all the multiple thrust chamber injectors (this unit is designed for a forced-deflection nozzle engine). Bolted flanges provide for the separate removal of either turbopump subassembly from the integrated housing.

8. Turbine Staging and Back Pressure Selection for Various Engine Cycles

In the staged combustion cycle, it is important to select turbine stages and diameters to obtain a high turbine efficiency. This minimizes turbine pressure ratio and pump discharge pressure, thereby keeping pumping system inert weight as low as possible. The relatively low pressure ratios of staged combustion turbines yield a favorably high bucket-to-gas velocity ratio and good efficiencies can be achieved with few stages. In the 3,000-psia-pump-discharge-pressure hydrogen turbopump of a staged combustion cycle engine an isentropic efficiency of 0.80 is achieved with a single, axial-flow, impulse-turbine stage. However, the large turbine flow rate requires parallel stages to provide permissible turbine bucket root stresses. The matching oxygen pump for this staged combustion engine has three series, axial flow, impulse stages to obtain an isentropic efficiency of 0.80.

II, J, Turbopumps (cont.)

Design goals for a gas generator cycle engine do not include high turbine efficiency or minimum turbine weight flow. Appropriate trade-offs must be made considering the effects of turbine inert weight, turbine exhaust thrust, turbine weight flow, tankage weight, and flight duration. Design goal for these trade-offs is to obtain a minimum turbine equivalent weight equal to turbine inert weight, plus the turbine weight flow, multiplied by an exchange ratio. This exchange ratio accounts for flight duration, the equivalent inert weight of turbine propellant consumed, the excess tankage weight for turbine propellant, and the ratio of turbine exhaust effective specific impulse to thrust chamber effective specific impulse. Exchange ratio varies with each change in turbine staging, turbine diameter, or turbine back pressure. Turbine inlet pressure is established by subtracting gas generator line, valve, injectors, and mixing pressure drops from pump discharge pressure. Gas generator mixture ratio is limited to a value at which turbine materials are known to operate satisfactorily.

For any gas generator cycle turbopump, an analysis will determine the best staging, diameter, and back pressure. An example follows:

Figures II J-27 and II J-29 show turbine equivalent weight in relationship to turbine back-pressure for H_2 and O_2 turbopumps in a 6-million-lb-thrust parallel-turbine-flow, gas generator cycle engine with a 180-sec flight-duration booster stage. For both turbopumps, optimum is two stages. The O_2 turbopump shaft speed was fixed by pump specific speed considerations and the hydrogen turbopump shaft speed was fixed by bearing rubbing velocity limits.

II, J, Turbopumps (cont.)

For each turbine, back-pressure, turbine diameter, or bucket pitch line velocity was selected as shown by the typical curves at 100-psia back pressure in Figures II J-28 and II J-30

An over-all vehicle cost comparison for a single-stage versus two-stage turbine for a hydrogen turbopump of a 6-million-lb-thrust O_2-H_2 engine is shown in Figure II J-31. This comparison shows that there is very little difference in the mission cost of a nonrecoverable booster stage whether a single-stage or two-stage turbine is used.

9. Gear-Driven Pumps Compared to Direct-Driven Pumps for Various Engine Cycles

There is no engine cycle wherein there is an application for a gear drive in a hydrogen turbopump because the maximum hydrogen pump speed for a given turbopump closely matches that of the turbine.

In the fuel-rich gas generator, staged combustion cycle, high O_2 turbopump turbine efficiency is achieved at pump shaft speed with a three-stage, moderate-diameter turbine. In the fuel-rich plus oxidizer-rich staged combustion cycle, high O_2 turbopump turbine efficiency is achieved at pump shaft speed with a single-stage turbine. Hence, there is no application for a gear-driven pump in a staged combustion cycle.

In the gas generator cycle, however, a gear drive can be used in the oxygen turbopump. Even if an inducer stage is used, or if pump suction pressure is high, the maximum allowable O_2 pump specific speed limits the pump shaft speed to a value far below the optimum turbine shaft speed.

II, J, Turbopumps (cont.)

To compare the equivalent wet weights of O_2 turbopumps with and without gear drives, weights of rocket engine and turbopump gear drives were obtained. They are plotted in relation to low-speed shaft torque in Figure II J-32.

Referring to Figure II J-3, if main-stage pump net positive suction pressure is 52 psi, the wet weight of the turbopump is 1,900 lb. Pump-shaft speed is 4,700 rpm and pump-shaft torque is 470,000 in.-lb. With no gearbox, the equivalent turbopump wet weight is 4,430 lb (Figure II J-3). Turbine weight flow with no gearbox is 70 lb/sec, the optimum turbine bucket velocity is 500 ft/sec, the back-pressure is 100 psia, and the exchange ratio of turbine weight flow to equivalent inert weight is 36.1 sec. A gearbox could be added to increase the turbine-bucket velocity to 1,400 ft/sec, thereby improving turbine efficiency and lowering turbine weight flow.

As shown by Figure II J-32, it is found that the gearbox weight is 1,180 lb for a unit having 470,000-in.-lb low-shaft-speed torque, and a 3:1 gear ratio. This increases the turbopump wet weight from 1,900 to 3,080 lb. Turbine weight flow is 35 lb/sec but because of the lower turbine exit temperature and gas velocity, the turbine exhaust effective impulse is lower and the exchange ratio of turbine weight flow to equivalent inert weight is increased to 42.1 sec. Thus, the main-stage turbopump equivalent wet weight with a gearbox is 3,200 lb for a main-stage turbopump without a gearbox. Hence, if an inducer stage is used, or if tank pressures are sufficiently high, there is no application for a gearbox in a gas-generator cycle engine.

II, J., Turbopumps (cont.)

10. Axial-Flow Pumps Compared to Centrifugal-Flow Pumps

Axial-flow pumps could be substituted for centrifugal-flow pumps in any of the previously discussed turbopumps. However, because of its multiple stages, an axial-flow pump has some increased cost and weight as compared with a centrifugal-flow pump. At one time there was some uncertainty in the industry as to whether a centrifugal H_2 pump could satisfactorily deliver high pressure, but successful testing by both NASA and Aerojet-General has proved the suitably of centrifugal pumps for H_2 systems.

In view of the fact that centrifugal pumps have been proved and are simple, and the axial-flow pump offers no apparent significant gain, the axial-flow pumps were eliminated from Task I consideration. This viewpoint is on the basis of previously prepared designs which compare axial and centrifugal H_2 pumps for an 800,000-lb-thrust engine.

11. Positive-Displacement Pumps Compared to Centrifugal-Flow Pumps

A large variety of positive-displacement pumping systems may be conceived; however, they offer no advantages in cost, weight, or simplicity. Therefore, the general category of positive displacement systems was eliminated from Task I considerations.

Figure II J-33 shows the specific weight versus flow rate for various air-breathing reciprocating engines. If it is assumed that these engines could be converted to 1,300 psia discharge pressure pumps for the same specific weights (which is an optimistic assumption), then the weight of positive-displacement O_2 and H_2 pumps for a 2-million-lb-thrust engine would be considerably greater than the combined weight of centrifugal-pump turbopumps for the same engine. In addition, positive-displacement pumps would require heavier turbine drives and heavier suction manifolding.

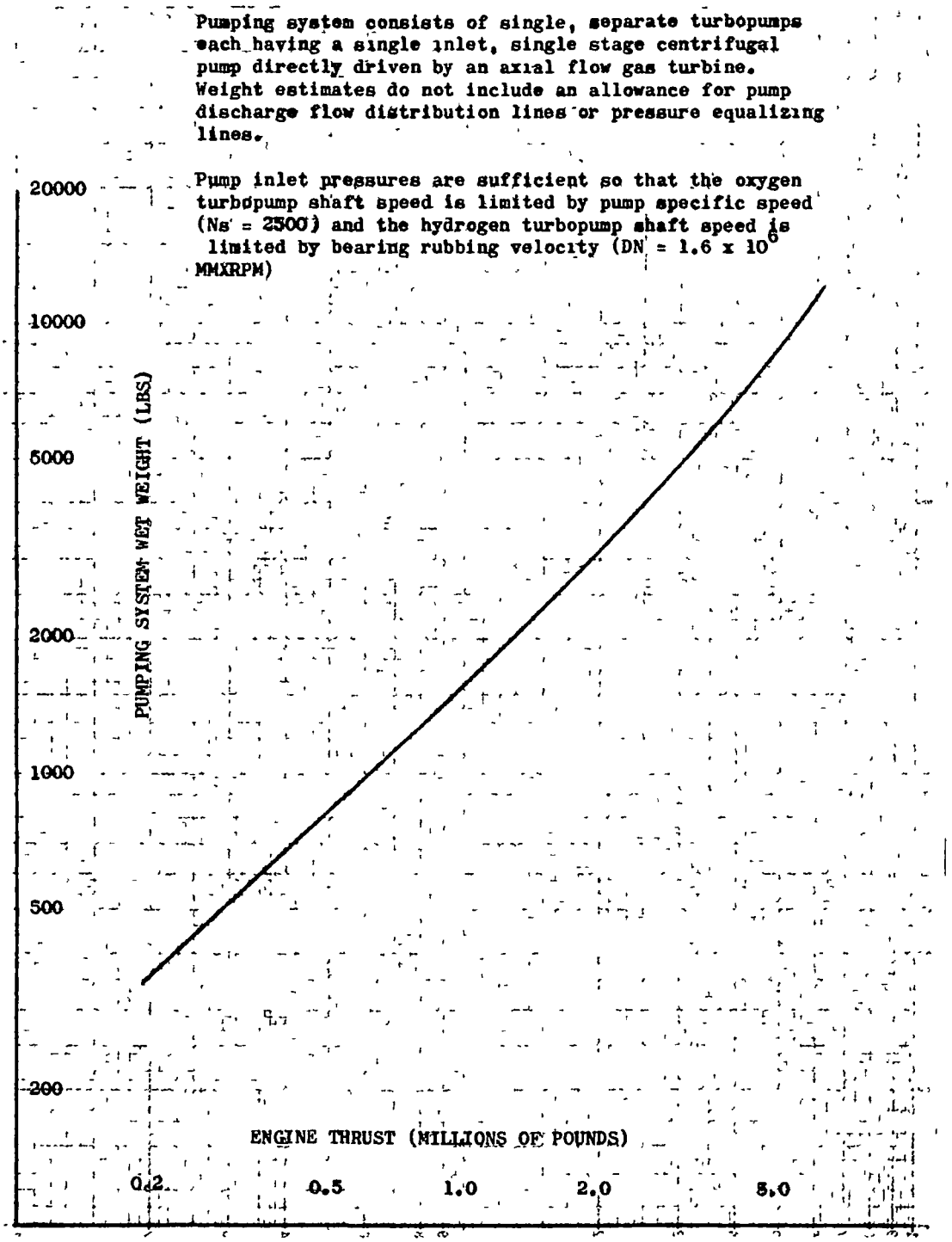

Pumping System Wet Weight Versus Engine Thrust

Figure II J-1

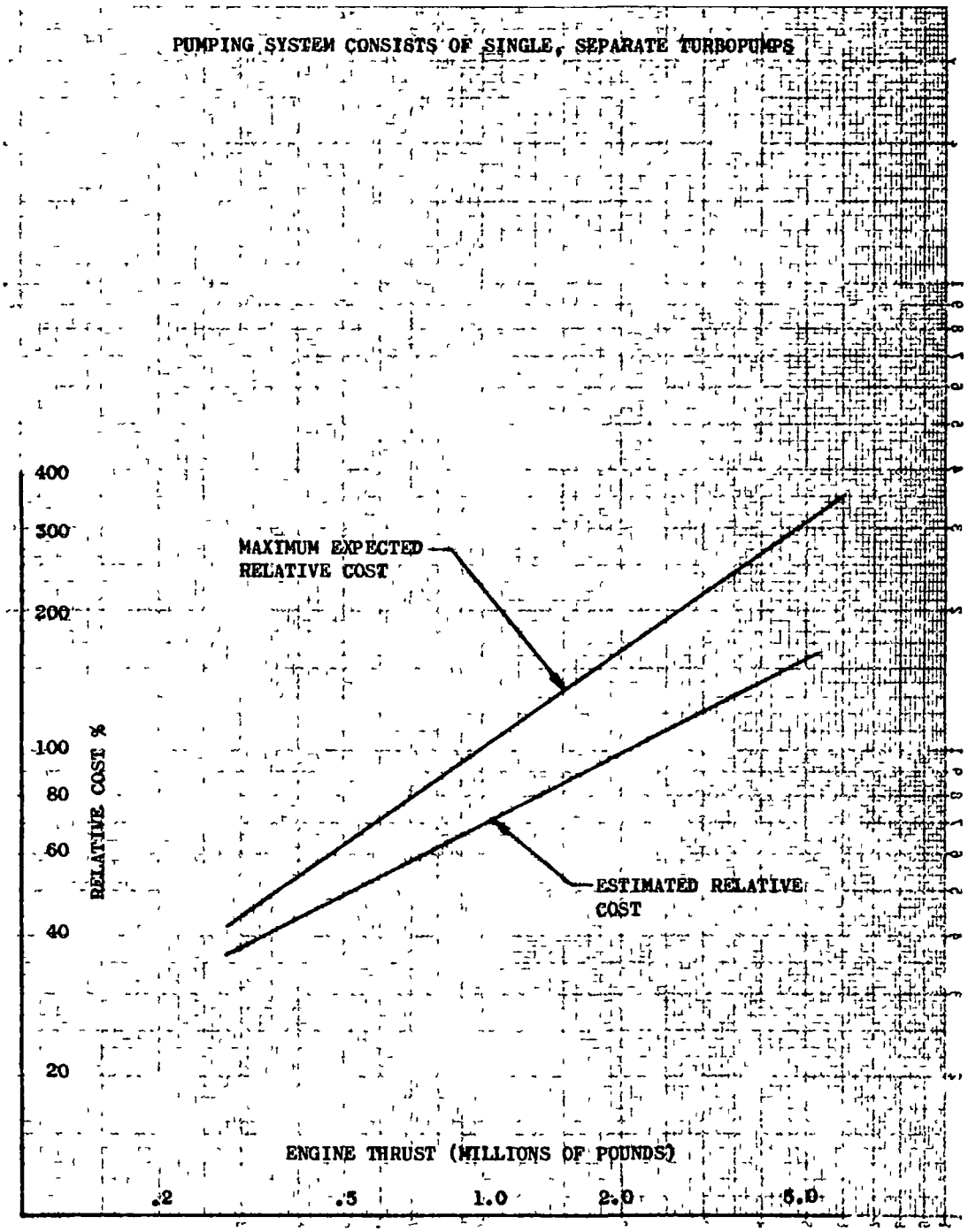

Relative Pumping System Production Cost Versus Engine Thrust

Figure II J-2

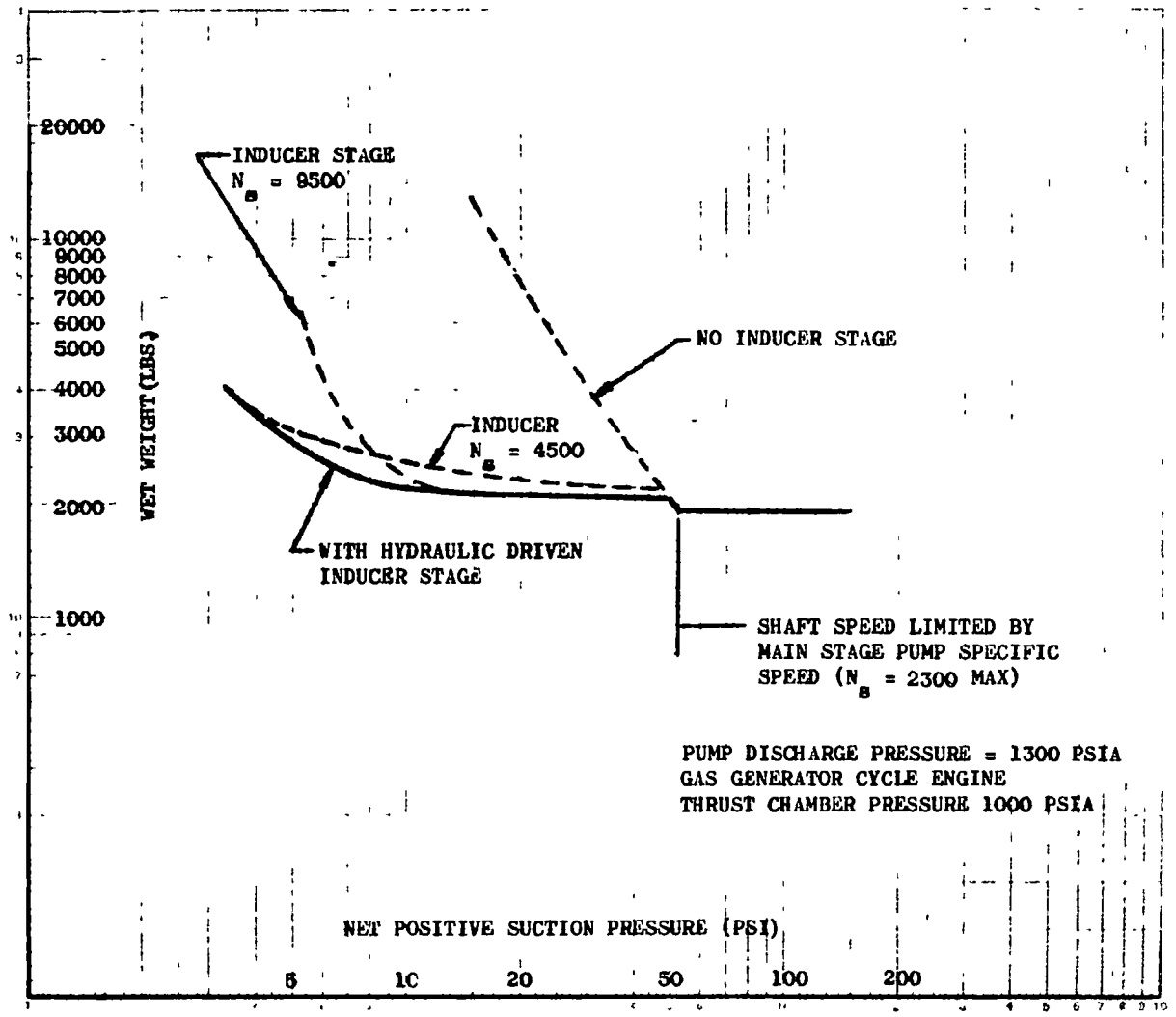

Wet Weight Versus Net Positive Suction Pressure for 2$\overline{m}$-lb-Thrust O_2 Turbopump

Figure II J-3

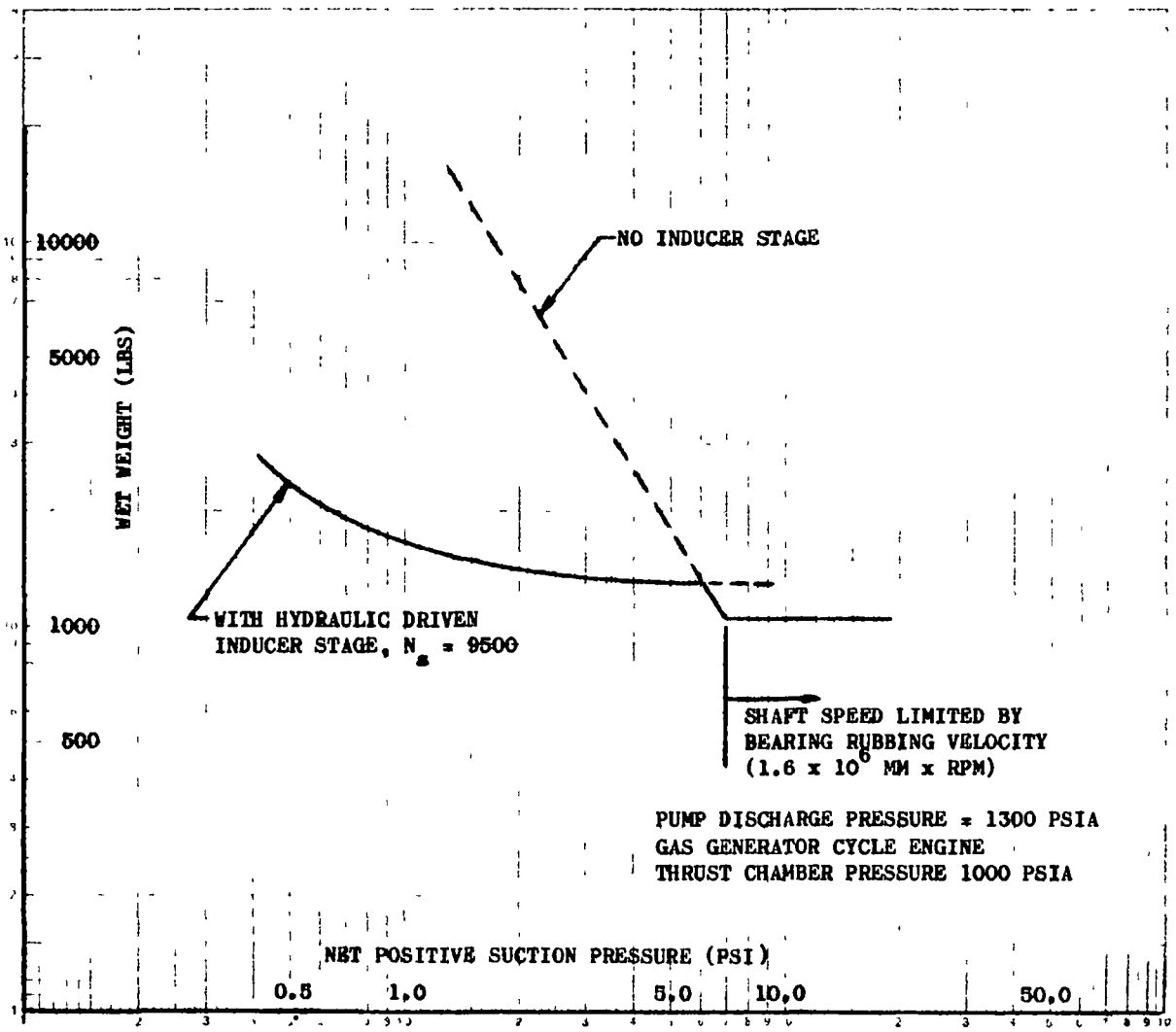

Wet Weight Versus Net Positive Suction Pressure for 2m-lb-Thrust H_2 Turbopump

Figure II J-4

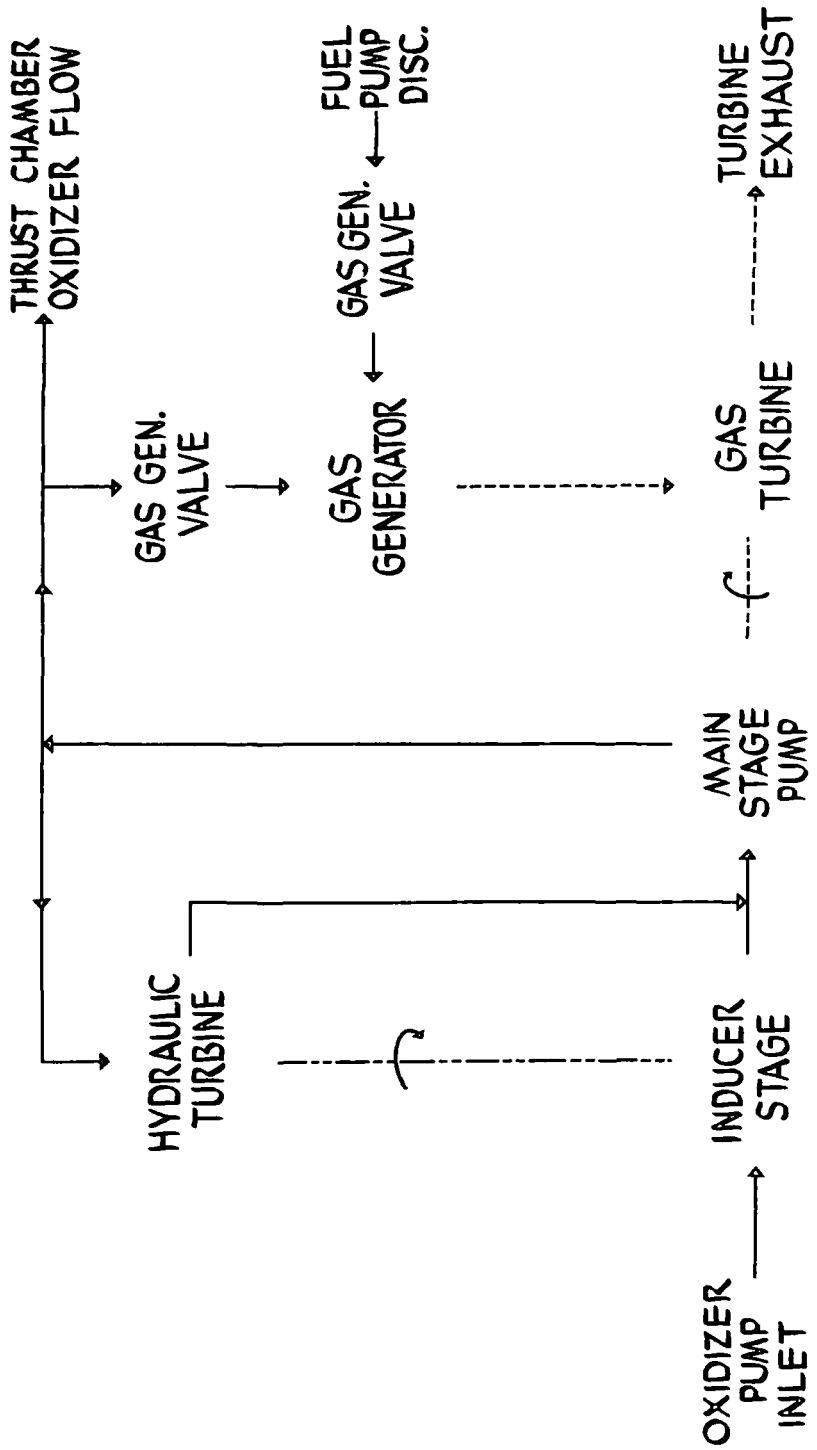

Flow Schematic (Turbopump with Inducer Stage)

Figure II J-5

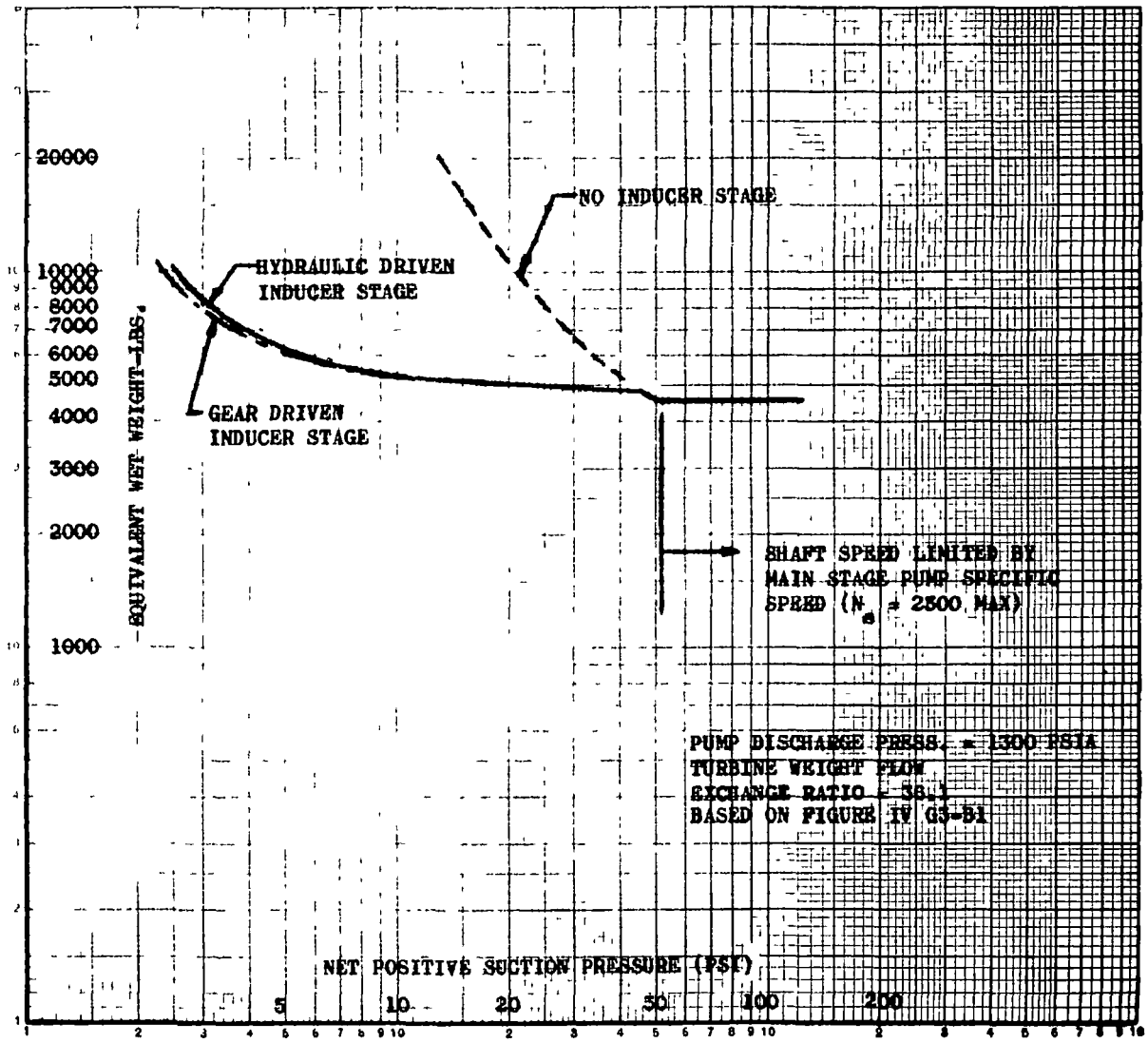

Equivalent Wet Weight Versus Net Positive Suction Pressure
for 2m-lb-Thrust O_2 Turbopump

Figure II J-6

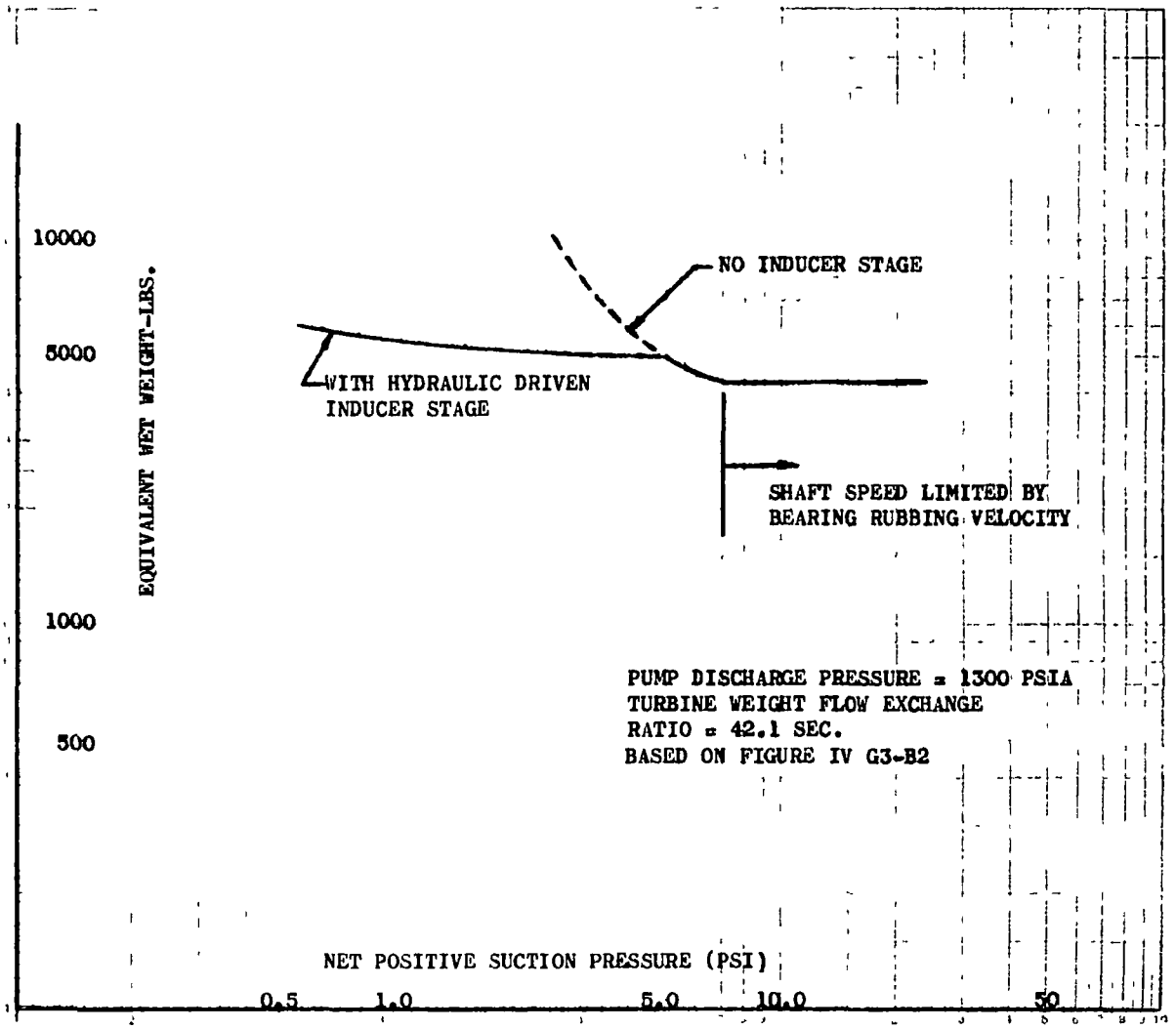

Equivalent Wet Weight Versus Net Positive Suction Pressure for 2m-lb-Thrust H_2 Turbopump

Figure II J-7

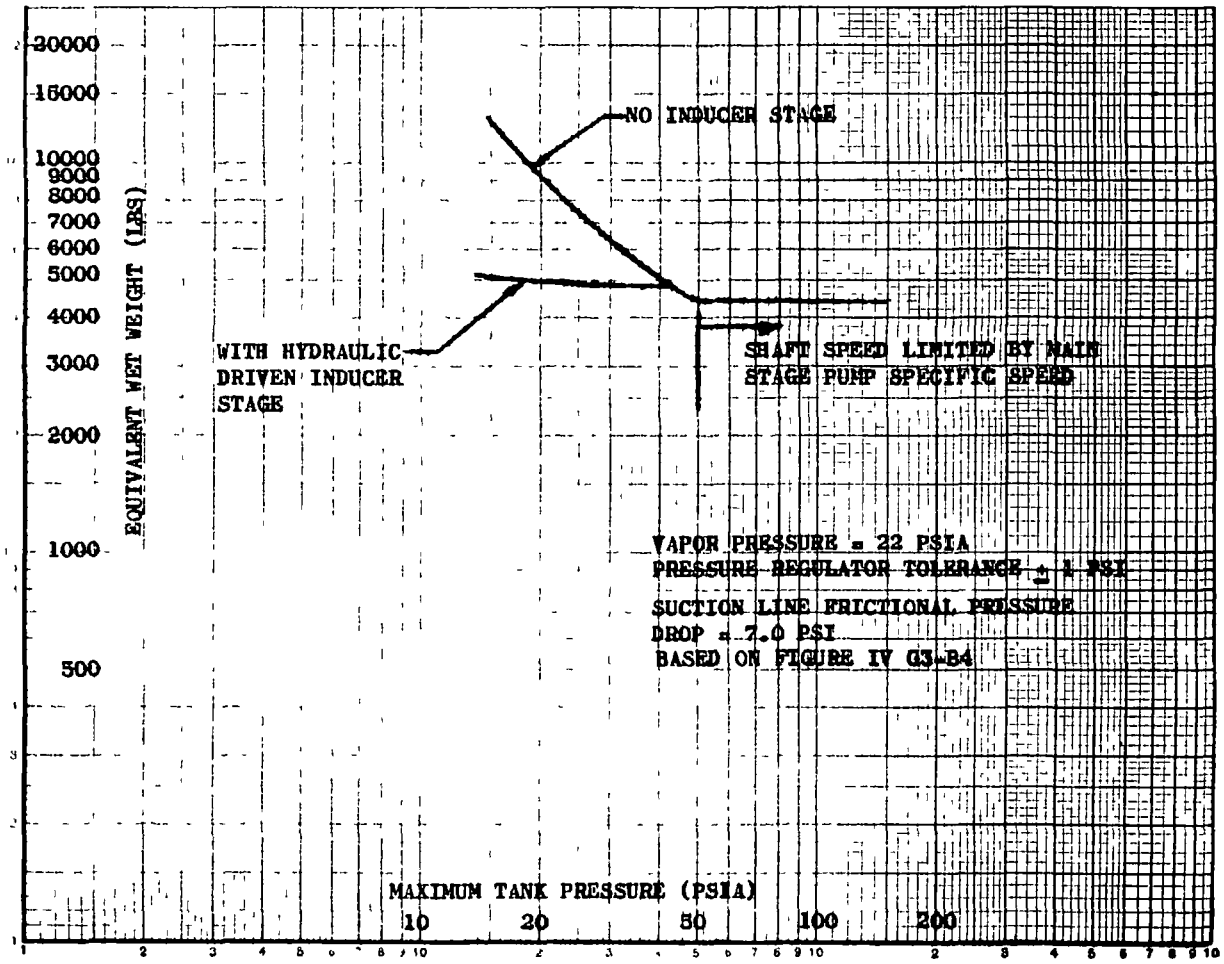

Figure II J-8

Equivalent Wet Weight Versus Maximum Tank Pressure for $2\bar{m}$-lb-Thrust Oxygen Turbopump With O_2 Tank Above Hydrogen Tank

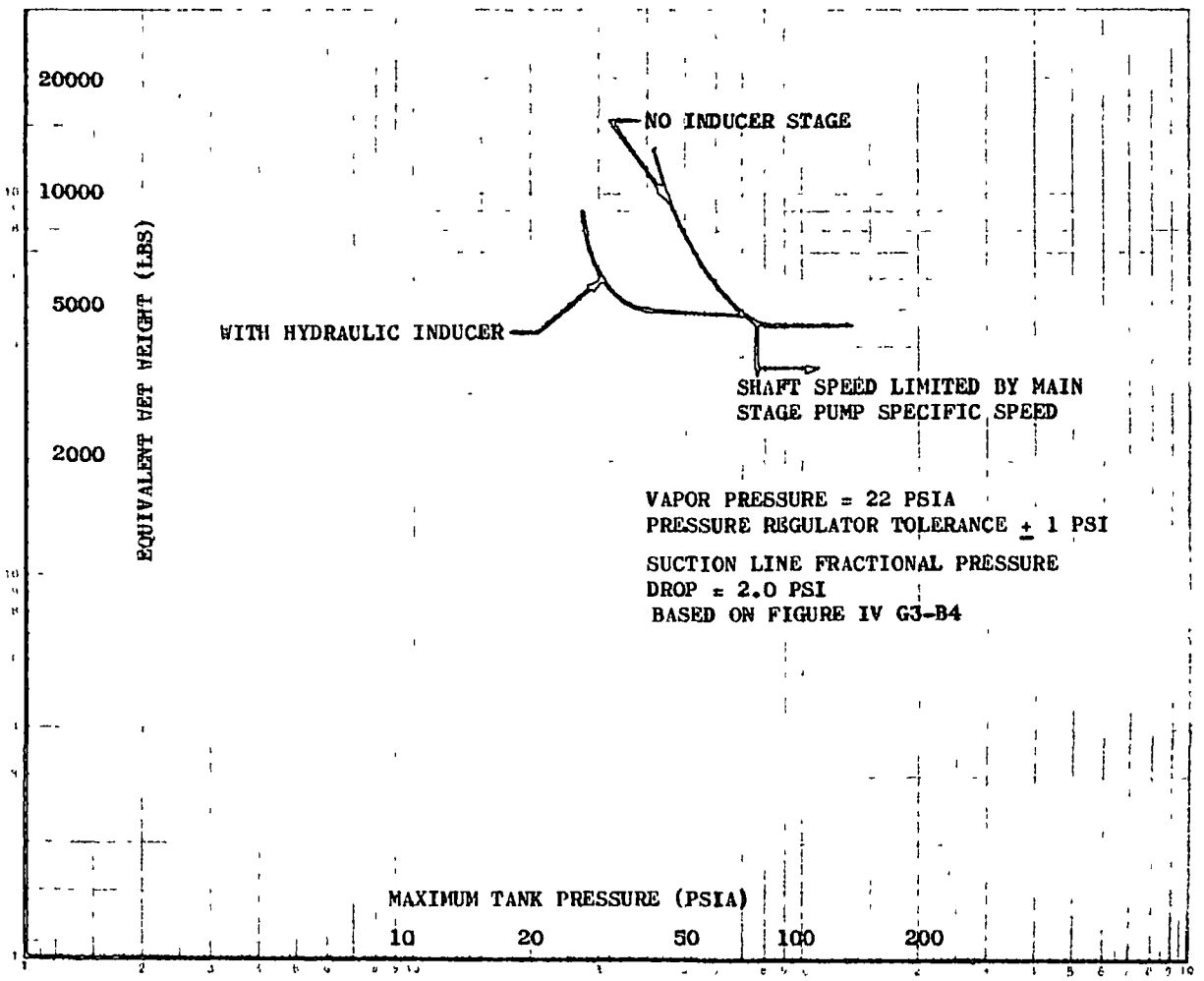

Equivalent Wet Weight Versus Maximum Tank Pressure for 2-$\bar{m}$-lb-Thrust Oxygen Turbopump With O_2 Tank Below Hydrogen Tank

Figure II J-9

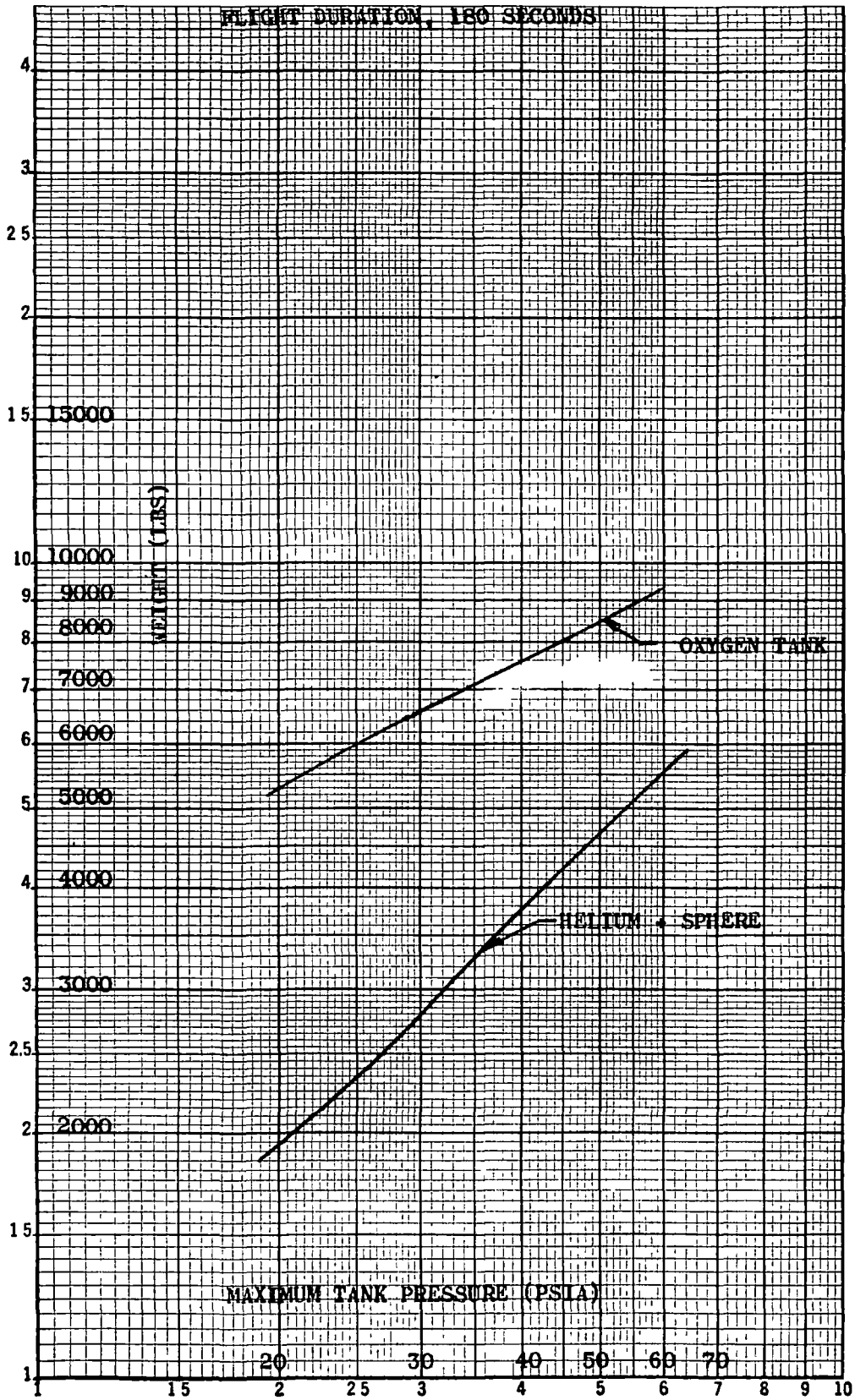

Figure II J-10

Equivalent Wet Weight Versus Maximum Tank Pressure for 2-$\bar{m}$-lb-Thrust H_2 TPA

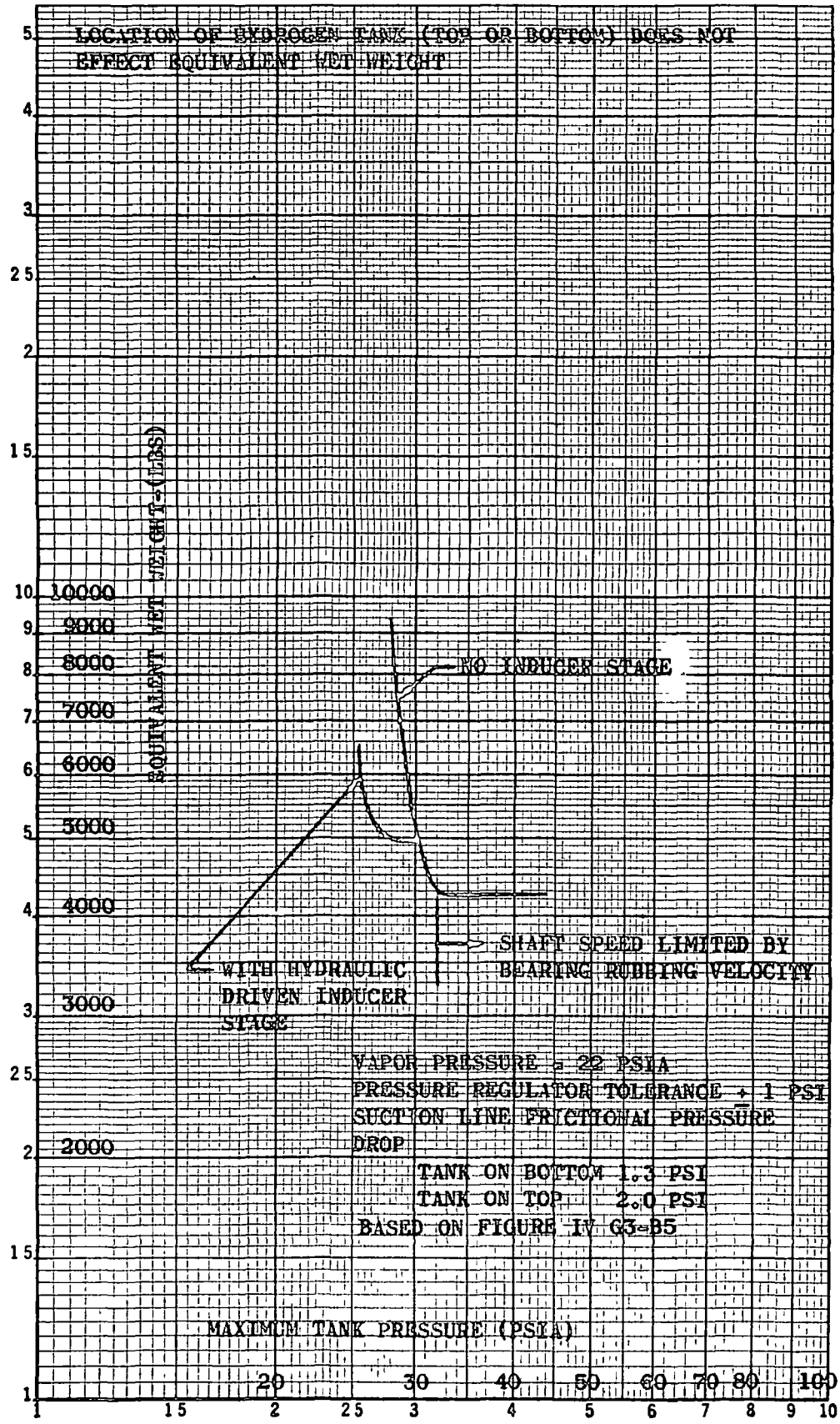

Figure II J-11

Weight of O_2 Tank and Pressurization System Versus Maximum Tank Pressure

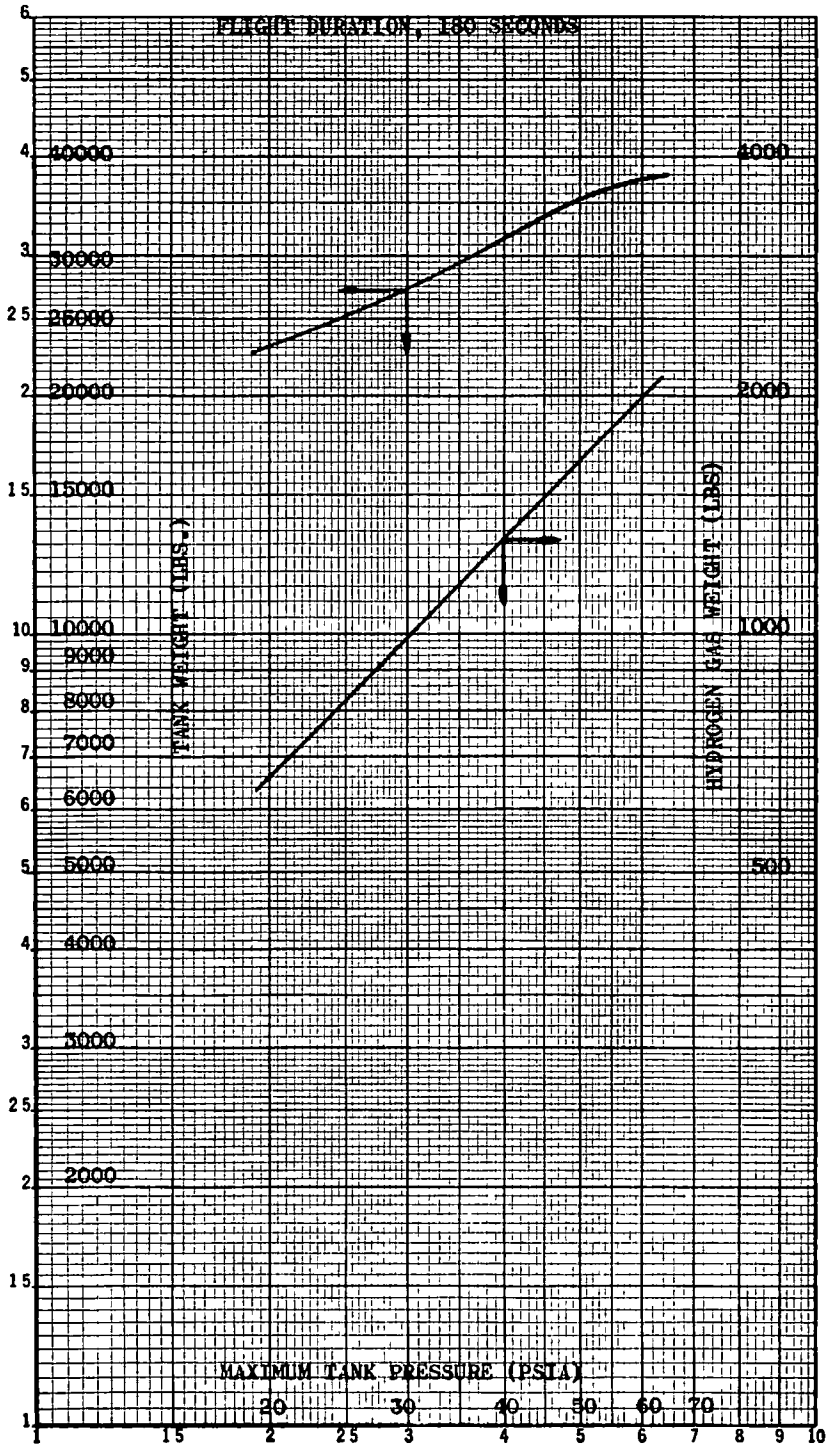

Weight of H_2 Tank and Pressurization System Versus Maximum Tank Pressure

Figure II J-12

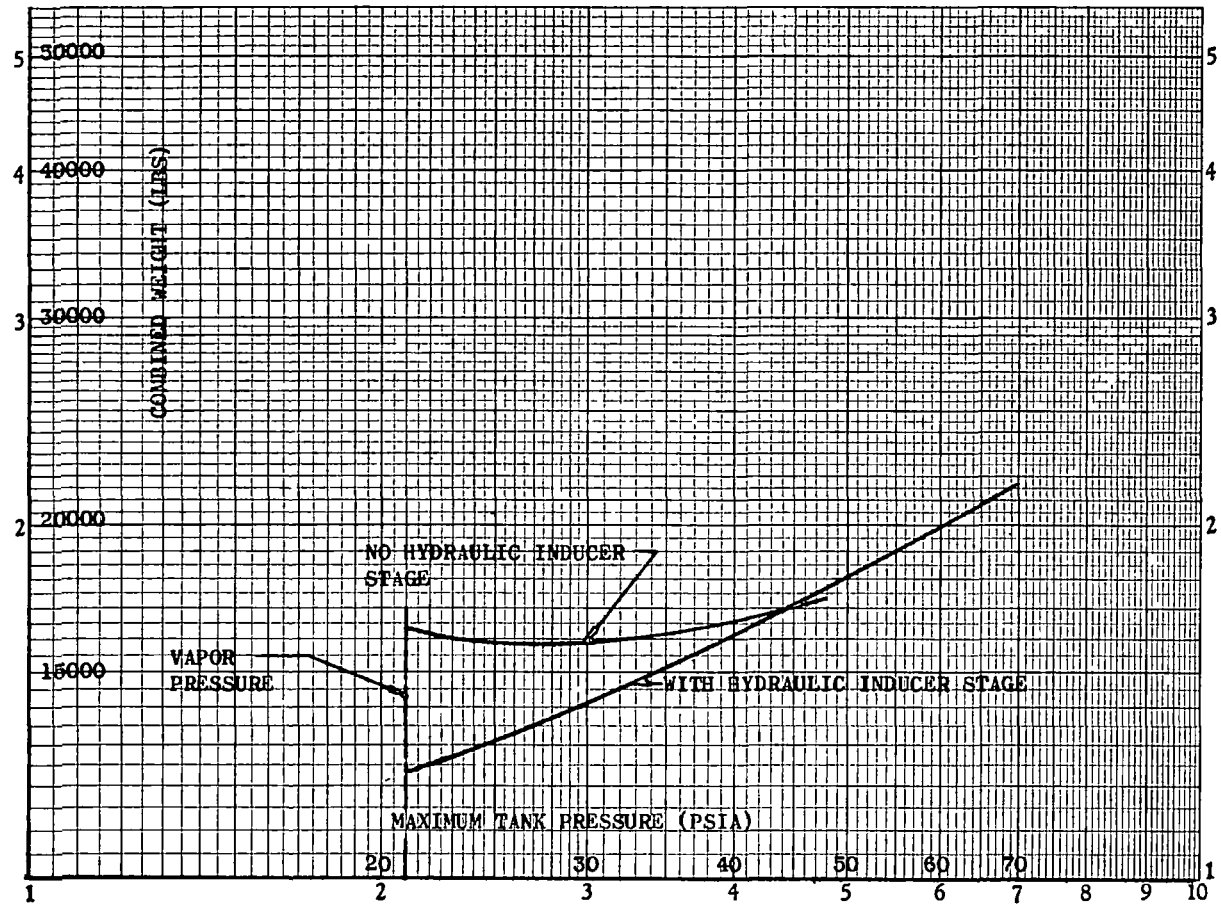

Combined Equivalent Weight Versus Maximum Tank Pressure for 2-$\bar{m}$-lb-Thrust O_2 System With O_2 Tank Above H_2 Tank

Figure II J-13

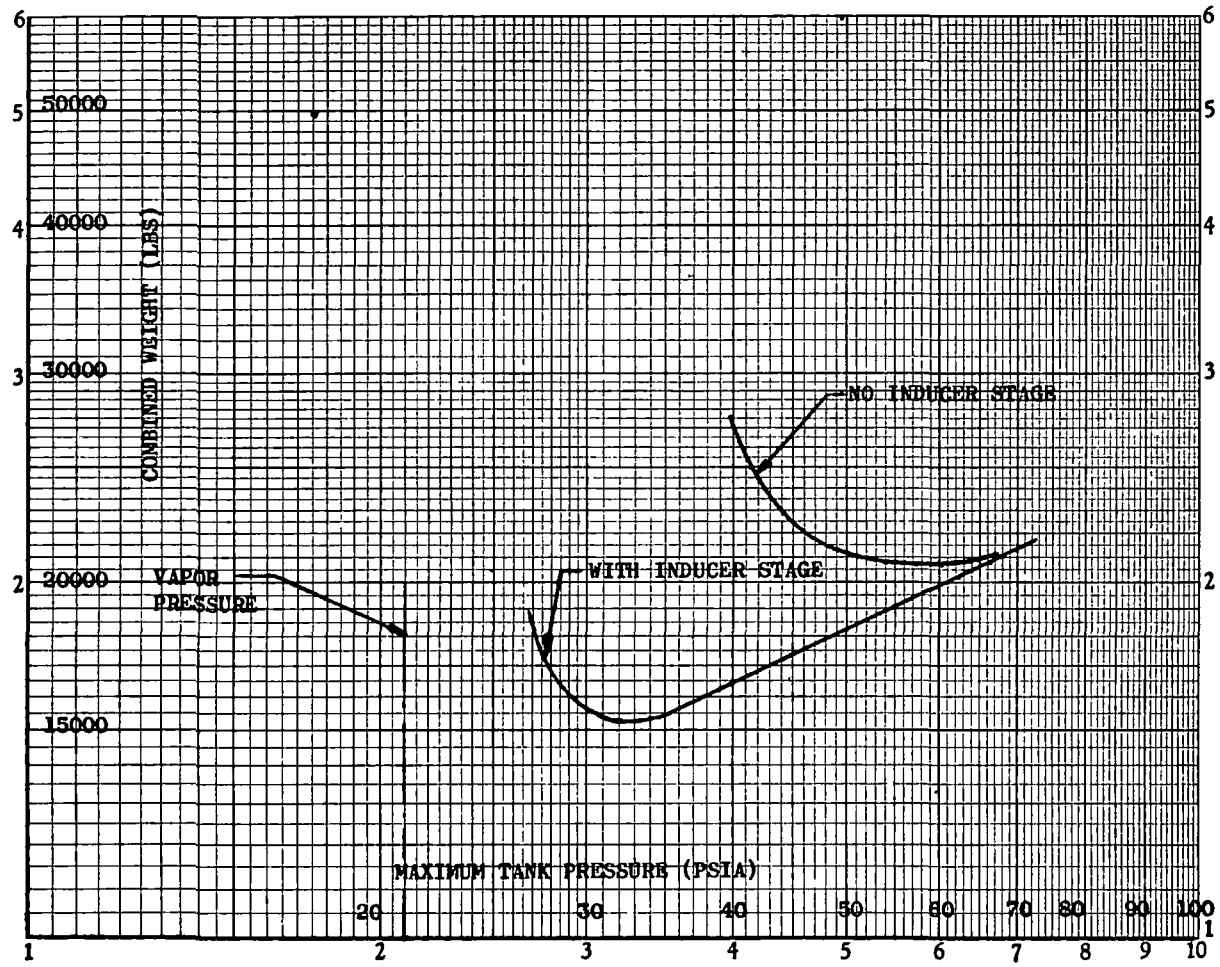

Combined Equivalent Weight Versus Maximum Tank Pressure for 2-$\overline{m}$-lb-Thrust O_2 System With O_2 Tank Below H_2 Tank

Figure II J-14

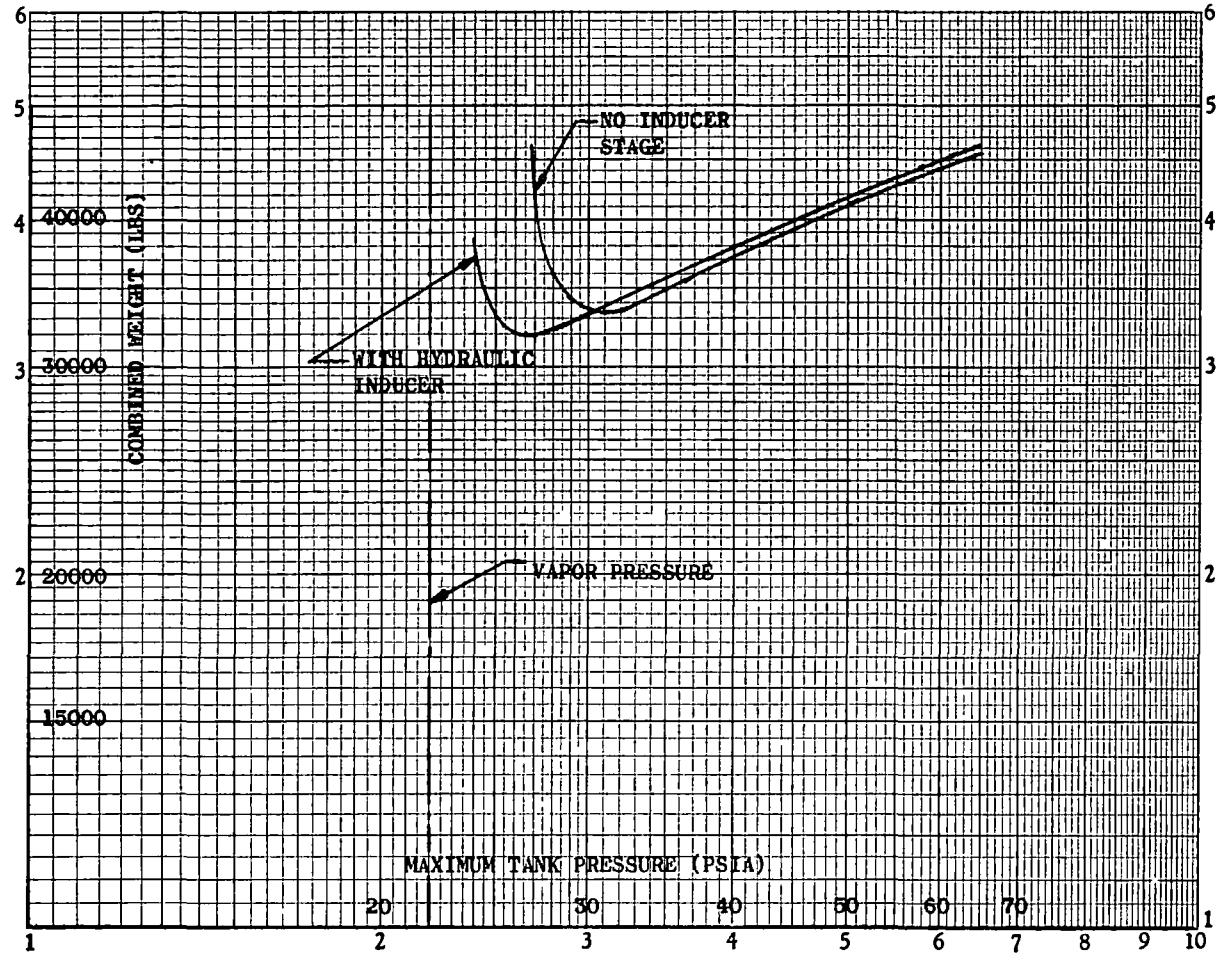

Combined Equivalent Weight Versus Maximum Tank Pressure for 2-$\bar{m}$-lb-Thrust H_2 System With Tank at Either Top or Bottom

Figure II J-15

FIRST STAGE OF TWO-STAGE VEHICLE HAVING THE OXYGEN TANK ABOVE THE HYDROGEN TANK AND HAVING A BURNOUT ACCELERATION OF 4.3 g's

2-MILLION-LB SEA LEVEL THRUST

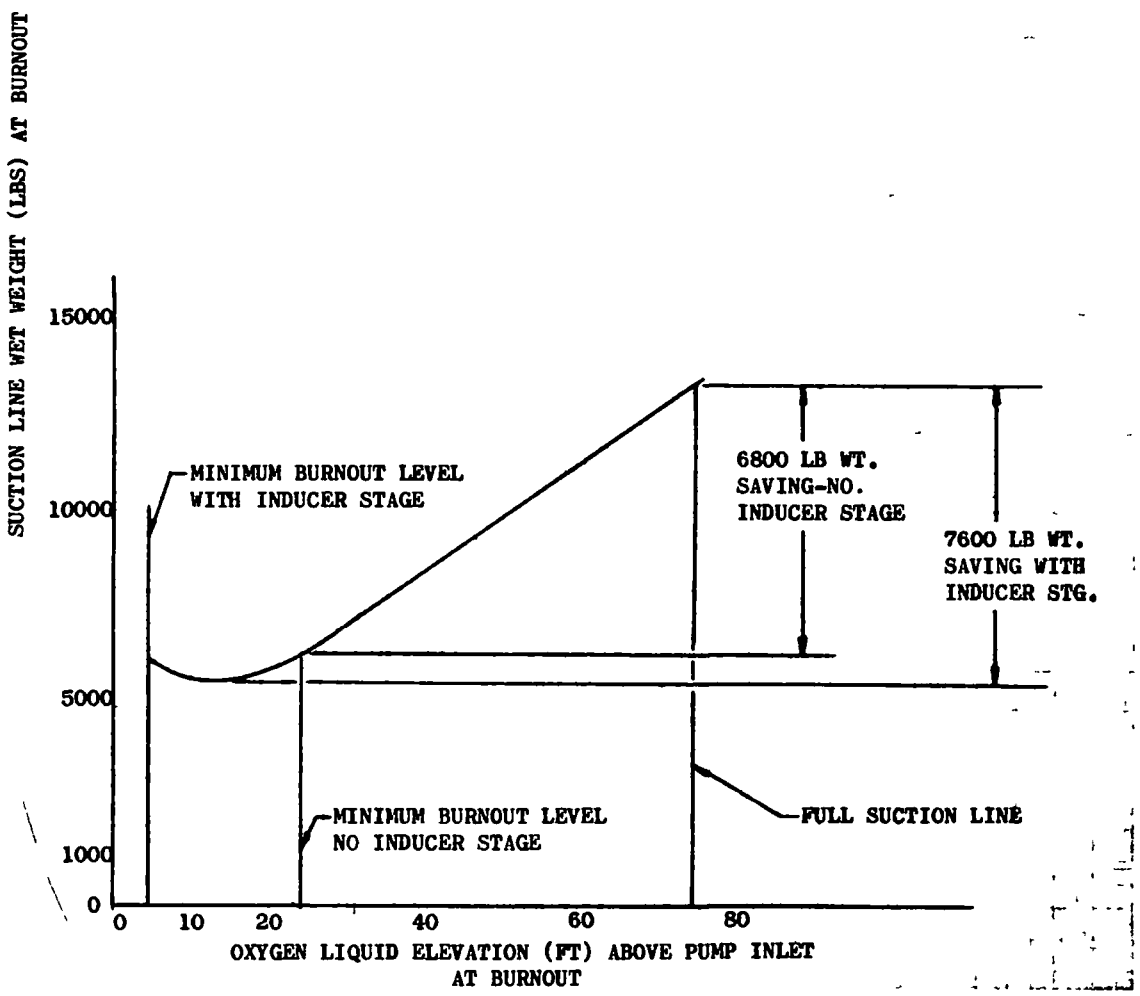

Suction Line Wet Weight at Burnout Versus O_2 Liquid Elevation Above Pump Inlet at Burnout

Figure II J-16

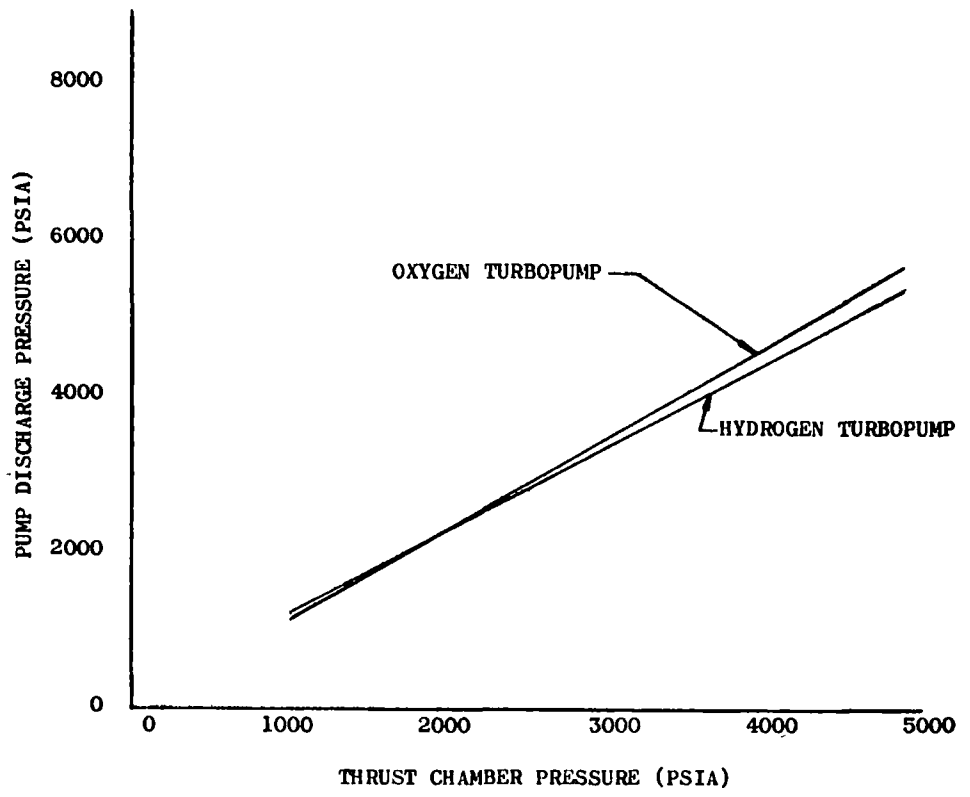

Figure II J-17

Pump Discharge Pressure Versus Thrust Chamber Pressure for Various Engine Cycles

ASSUMPTIONS:

GAS GENERATOR MIXTURE RATIO	1.20
OXYGEN PUMP EFFICIENCY	0.70
HYDROGEN PUMP EFFICIENCY	0.80
TURBINE EFFICIENCY (BOTH TURBOPUMPS)	0.80

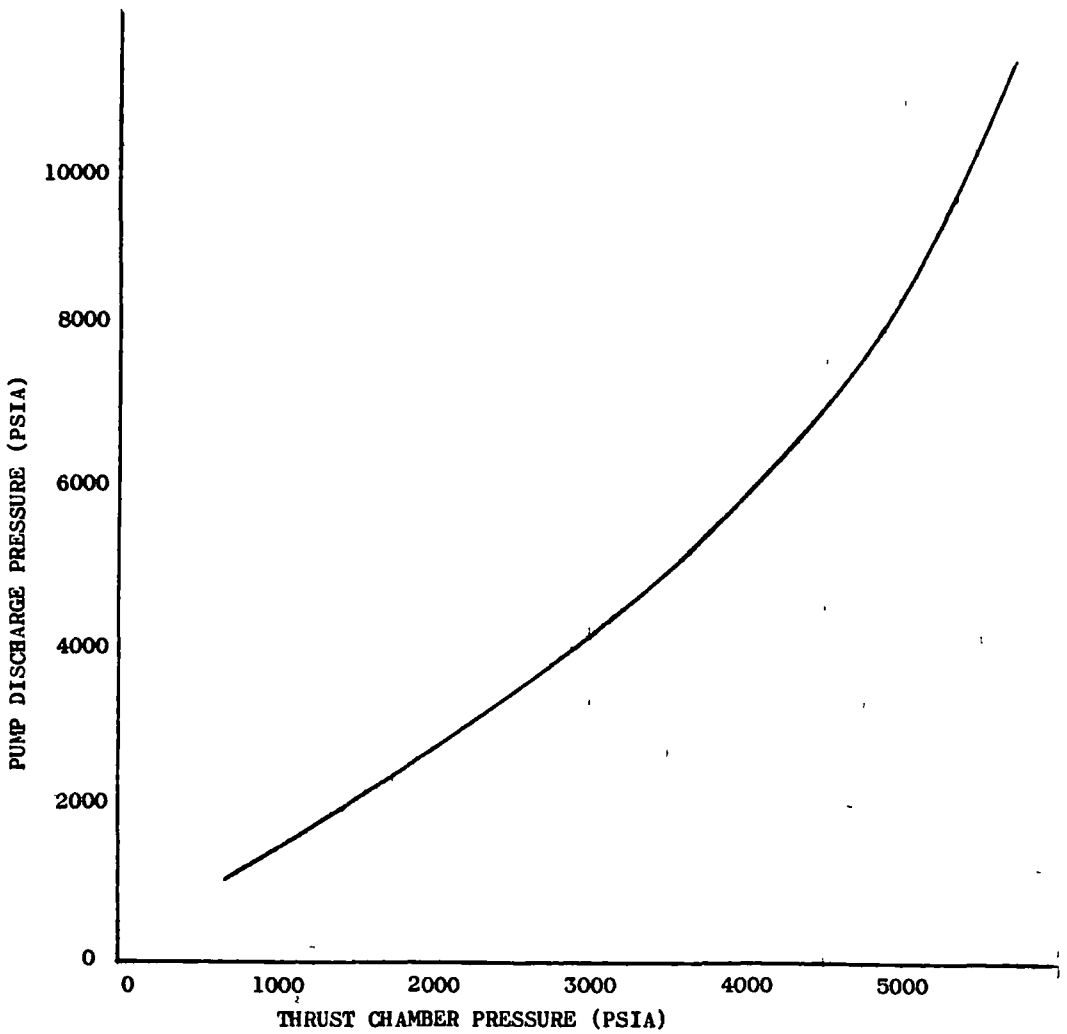

Pump Discharge Pressure Versus Thrust Chamber Pressure for a Staged Combustion Cycle

Figure II J-18

2M LB OXYGEN-HYDROGEN ENGINE
HAVING ANY ONE OF THE FOLLOWING
ENGINE CYCLES:
GAS GENERATOR CYCLE
THIRD FLUID CYCLE
HEATED HYDROGEN BLEED CYCLE
CHAMBER BLEED CYCLE
STAGED COMBUSTION CYCLE
PUMP AUGMENTED, INTERMITTENT DELIVERY FEED CYCLE
... TURBOPUMPS CONSIST OF SINGLE INLET, SINGLE STAGE CENTRIFUGAL PUMPS DIRECTLY DRIVEN BY A TWO STAGE, AXIAL FLOW GAS TURBINE. MAXIMUM PRESSURE RISE PER STAGE: 1300 PSI FOR HYDROGEN; 5000 PSI FOR OXYGEN. PUMP NET POSITIVE SUCTION PRESSURE: 7 PSI FOR HYDROGEN; 52 PSI FOR OXYGEN

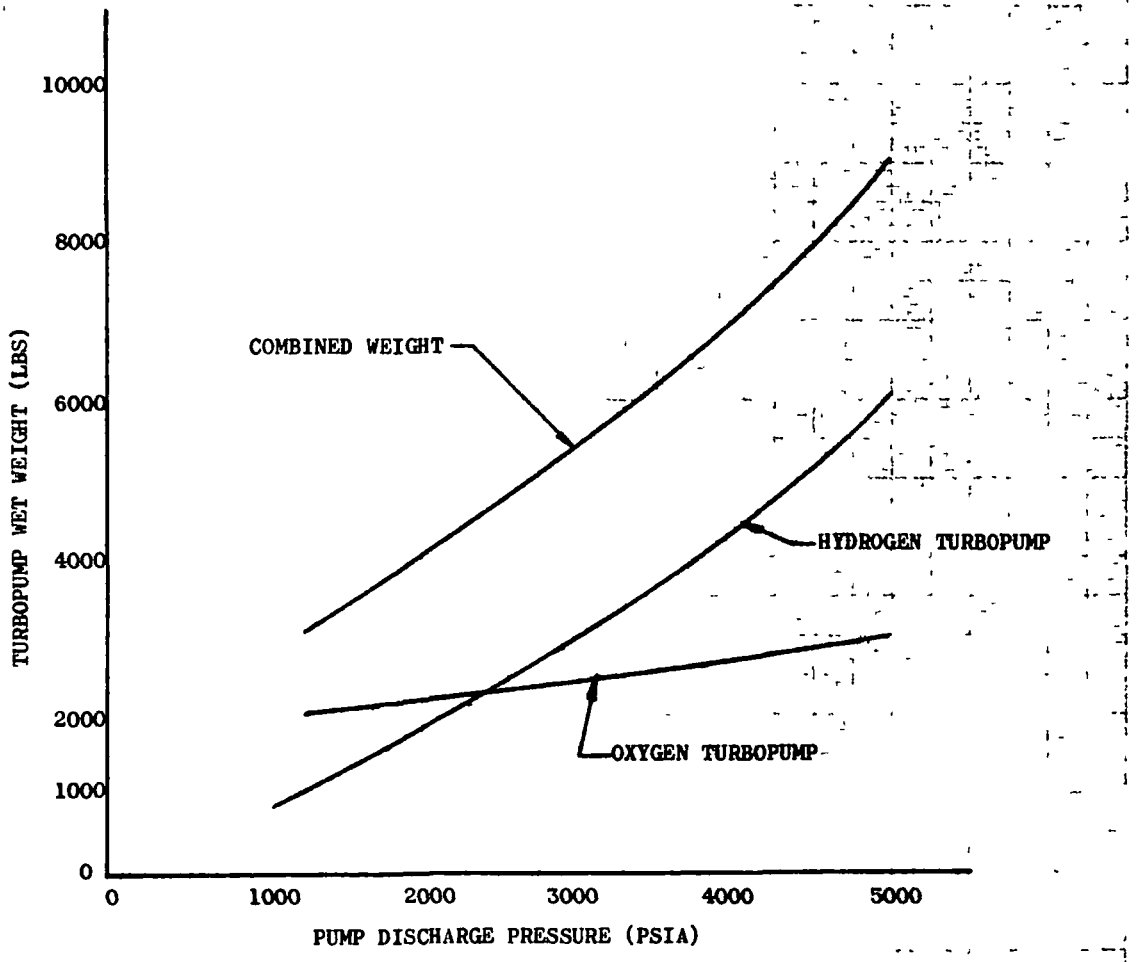

Turbopump Wet Weight Versus Pump Discharge Pressure

Figure II J-19

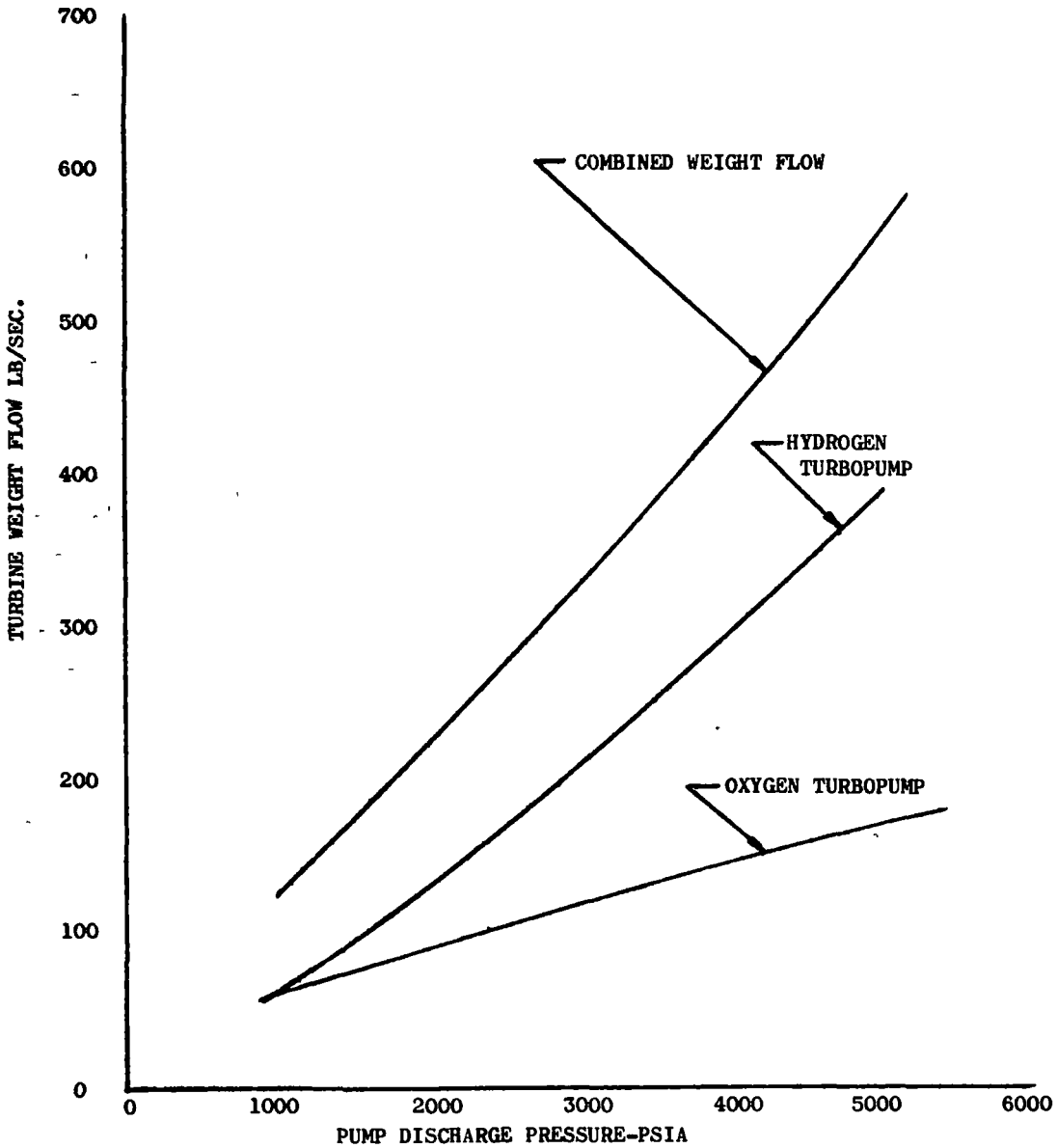

Turbine Weight Flow Versus Pump Discharge Pressure

Figure II J-20

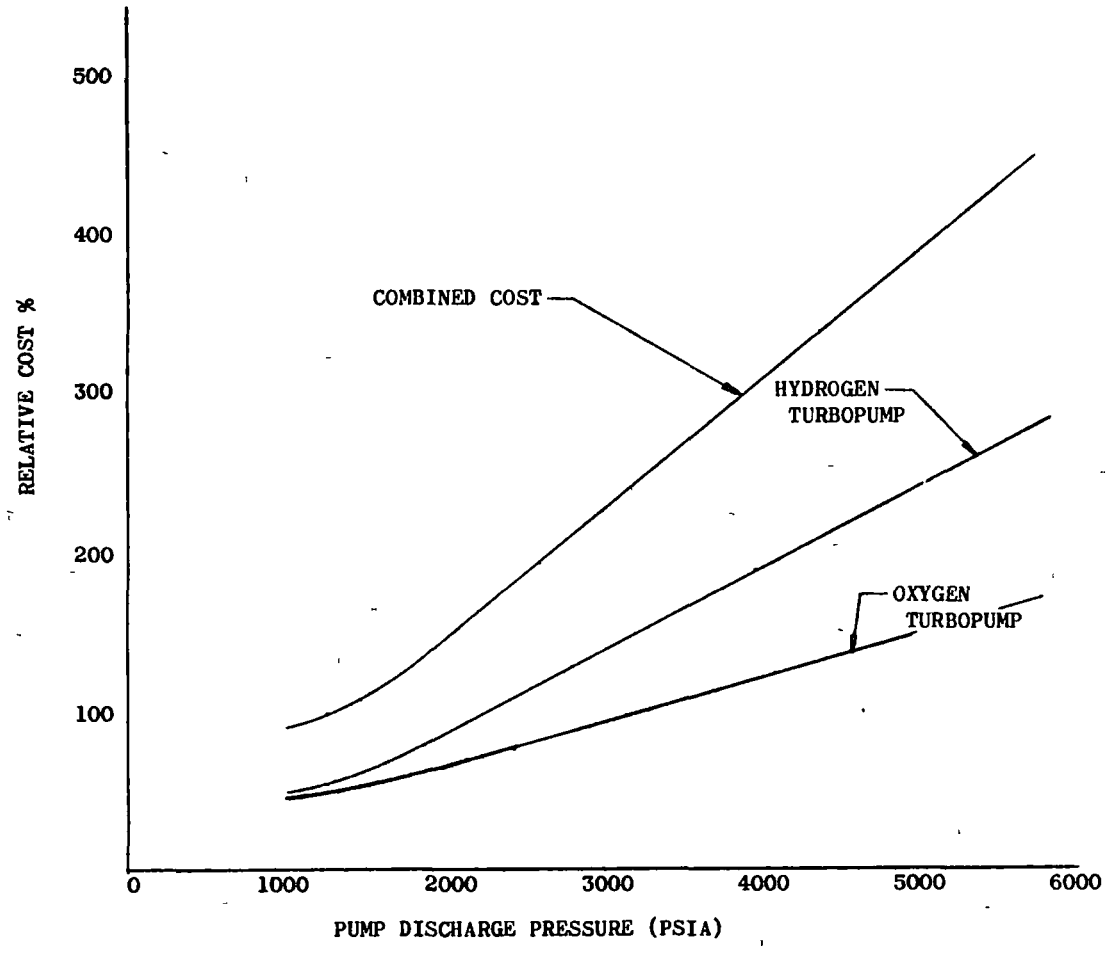

Relative Turbopump Production Unit Cost Versus Pump Discharge Pressure

Figure II J-21

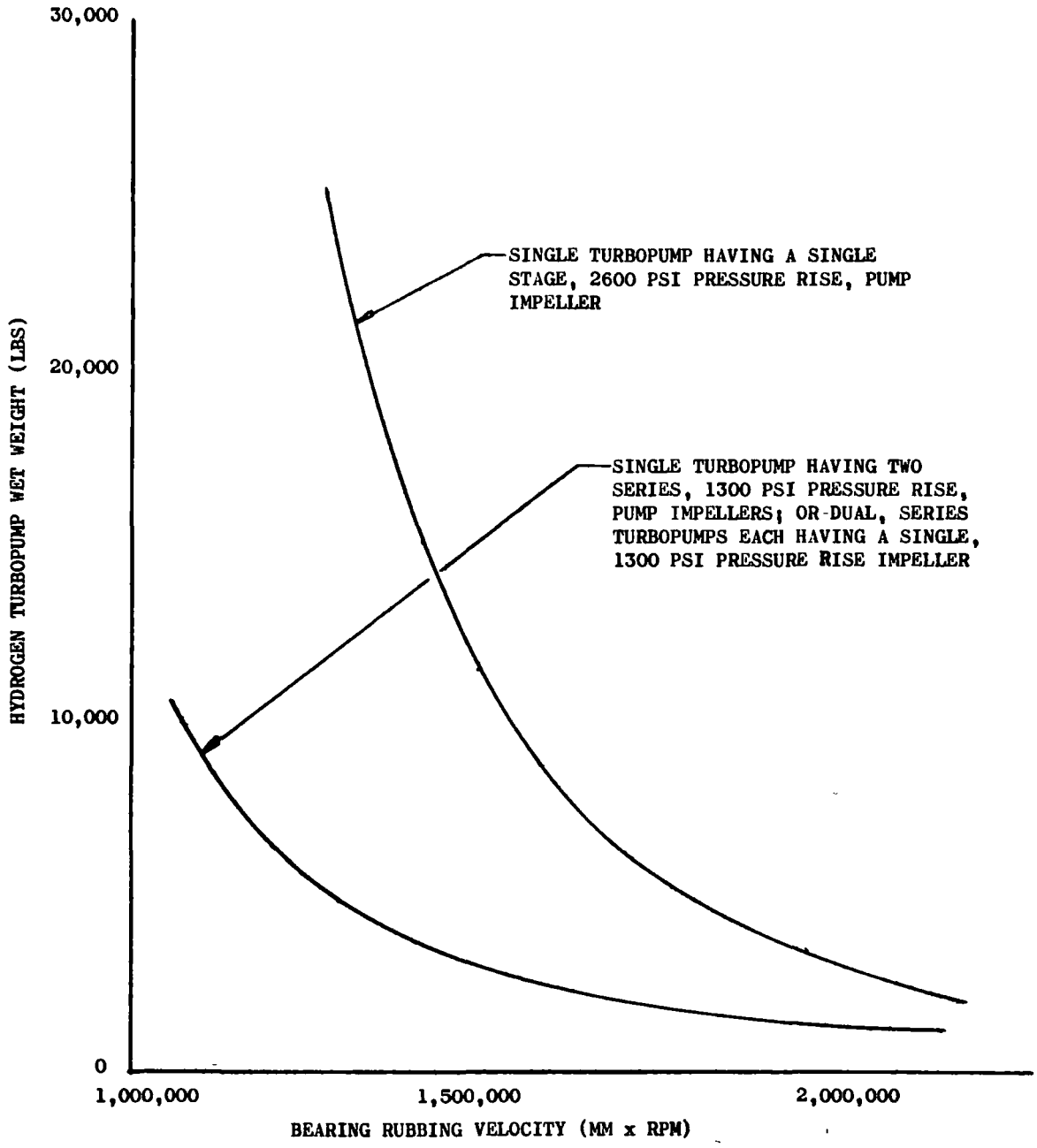

H_2 Turbopump Wet Weight Versus Bearing Rubbing Velocity

Figure II J-22

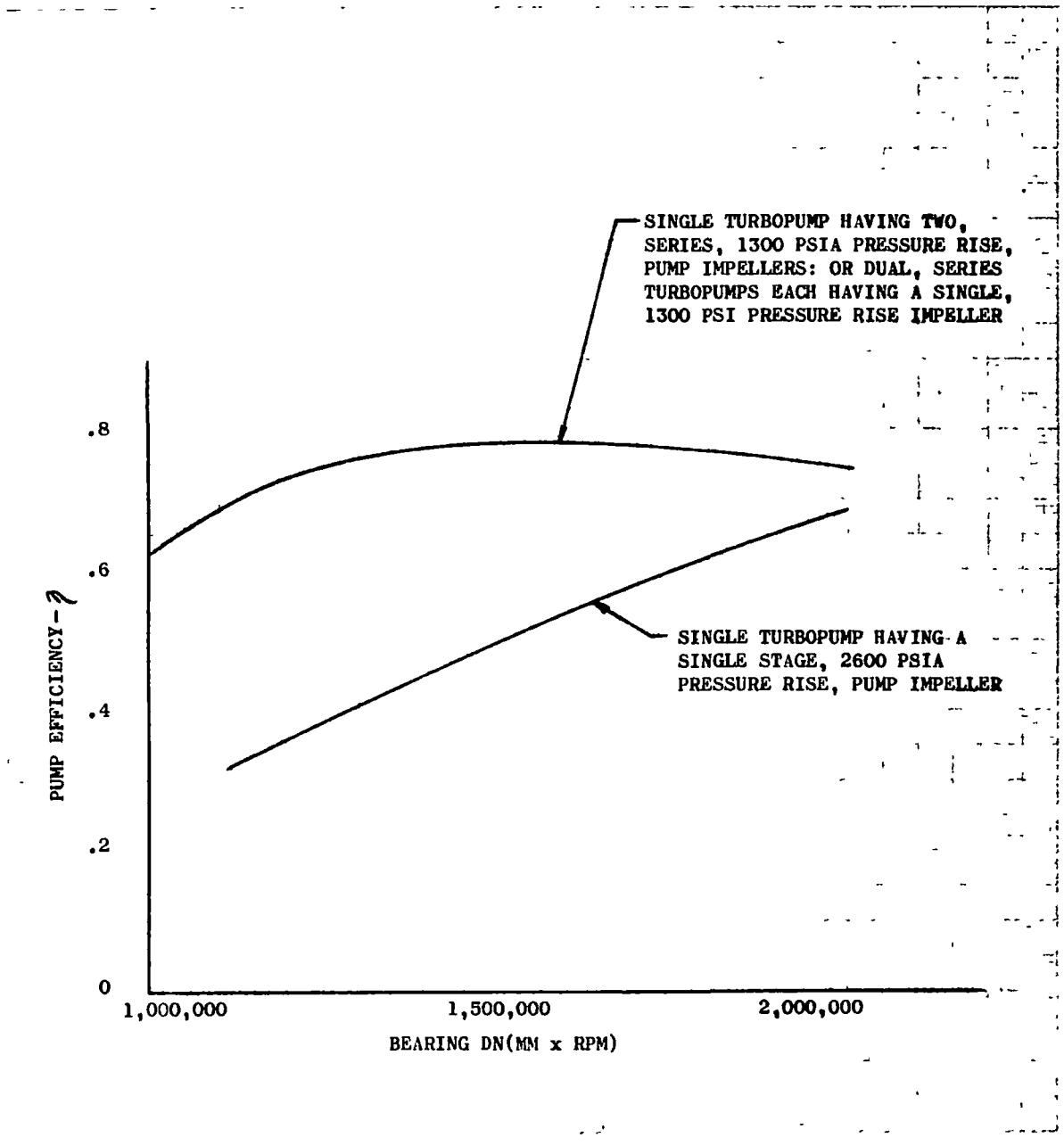

H_2 Pump Efficiency Versus Bearing Rubbing Velocity

Figure II J-23

SINGLE SHAFT TURBOPUMP - SINGLE STAGE, SINGLE INLET CENTRIFUGAL PUMP
ONE STAGE IMPULSE TURBINE - FOUR HYDRAULICALLY BALANCED DISCHARGE OUTLETS
WITH COMMON MANIFOLD

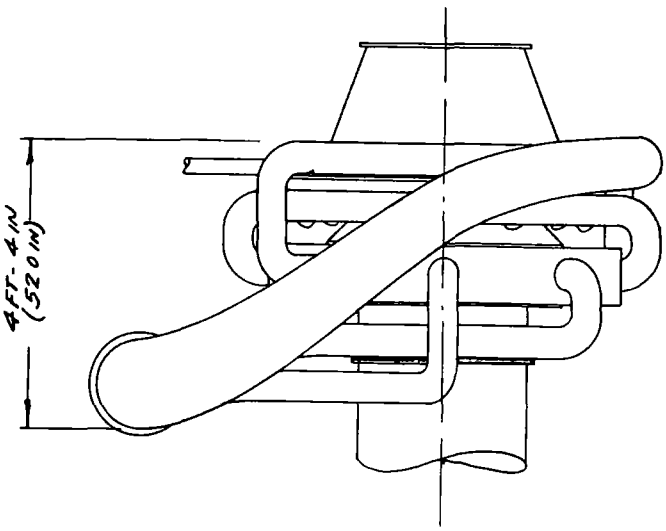

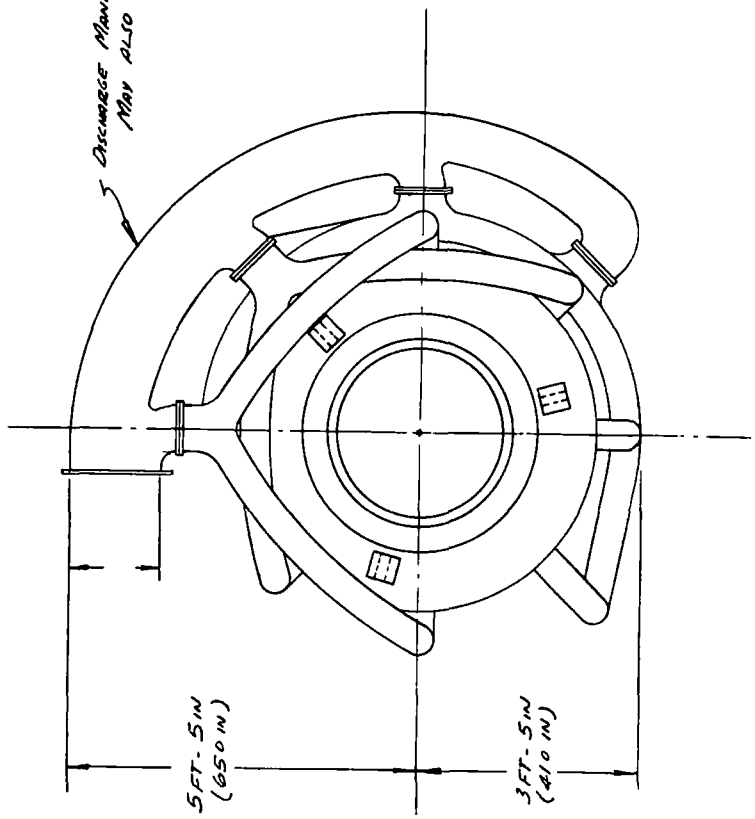

Figure II J-24

H_2 Turbopump With Four Hydraulically Balanced Discharge Outlets

A SINGLE SHAFT, SINGLE STAGE, SINGLE INLET CENTRIFUGAL PUMP WITH INDUCER. FOUR HYDRAULICALLY BALANCED OUTLETS WITH COMMON MANIFOLD TWO STAGE VELOCITY COMPOUNDED TURBINE

SPECIFICATIONS

P_{os}		36.5 PSIA
P_{od}		1300 PSIA
W_{os}		17,475 LB/SEC
T_{os}		-294 °F
N		26800 RPM
N_s	MAIN 2493	IND. 9240
P_{TI}		1000 PSIA
P_{rse}		100 PSIA
W_{sg}		210 LB/SEC
MR 88		1

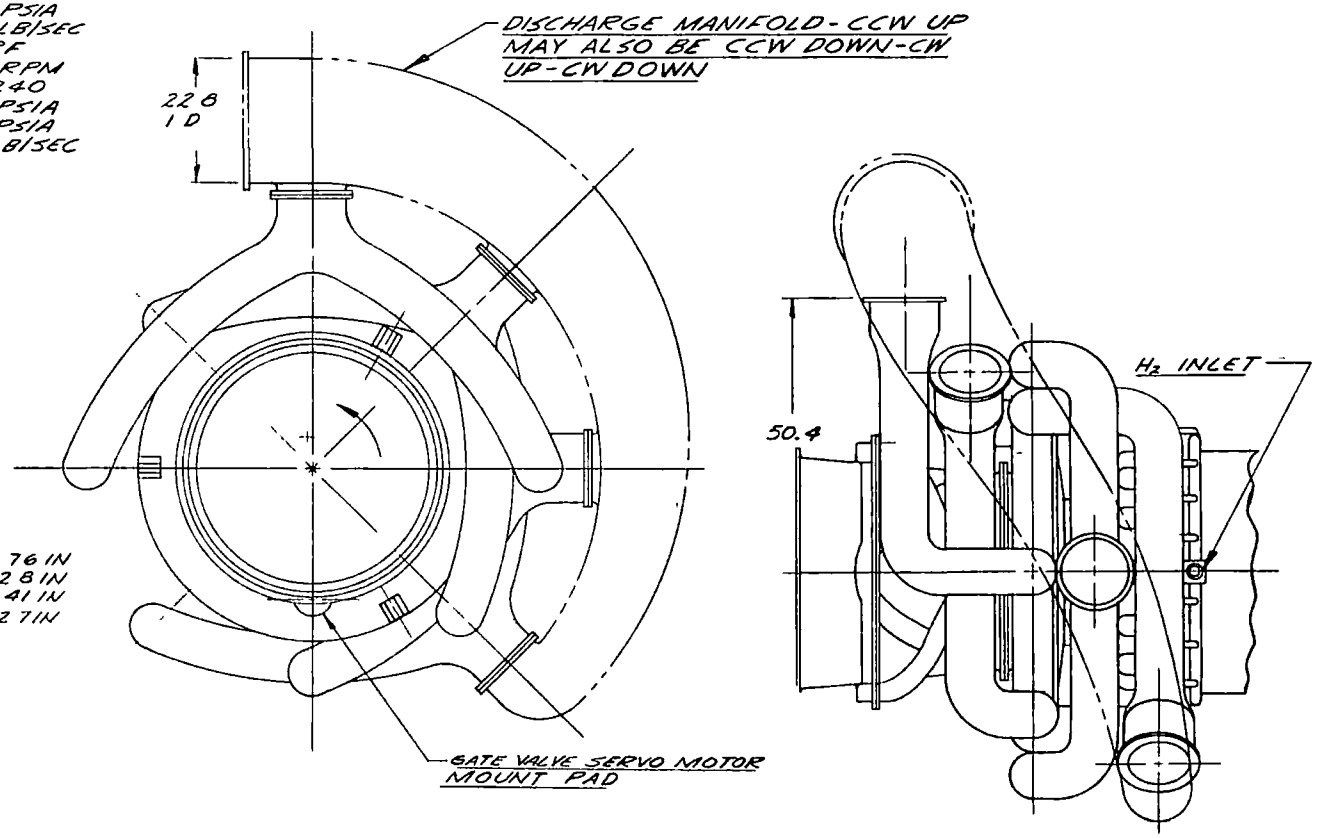

DIMENSION

LENGTH	76 IN
PUMP INLET DIA	42.8 IN
PUMP IMPELLER TIP DIA	41 IN
TURBINE PITCH DIA	42.7 IN

Figure II J-25

O_2 Turbopump With Four Hydraulically Balanced Discharge Outlets

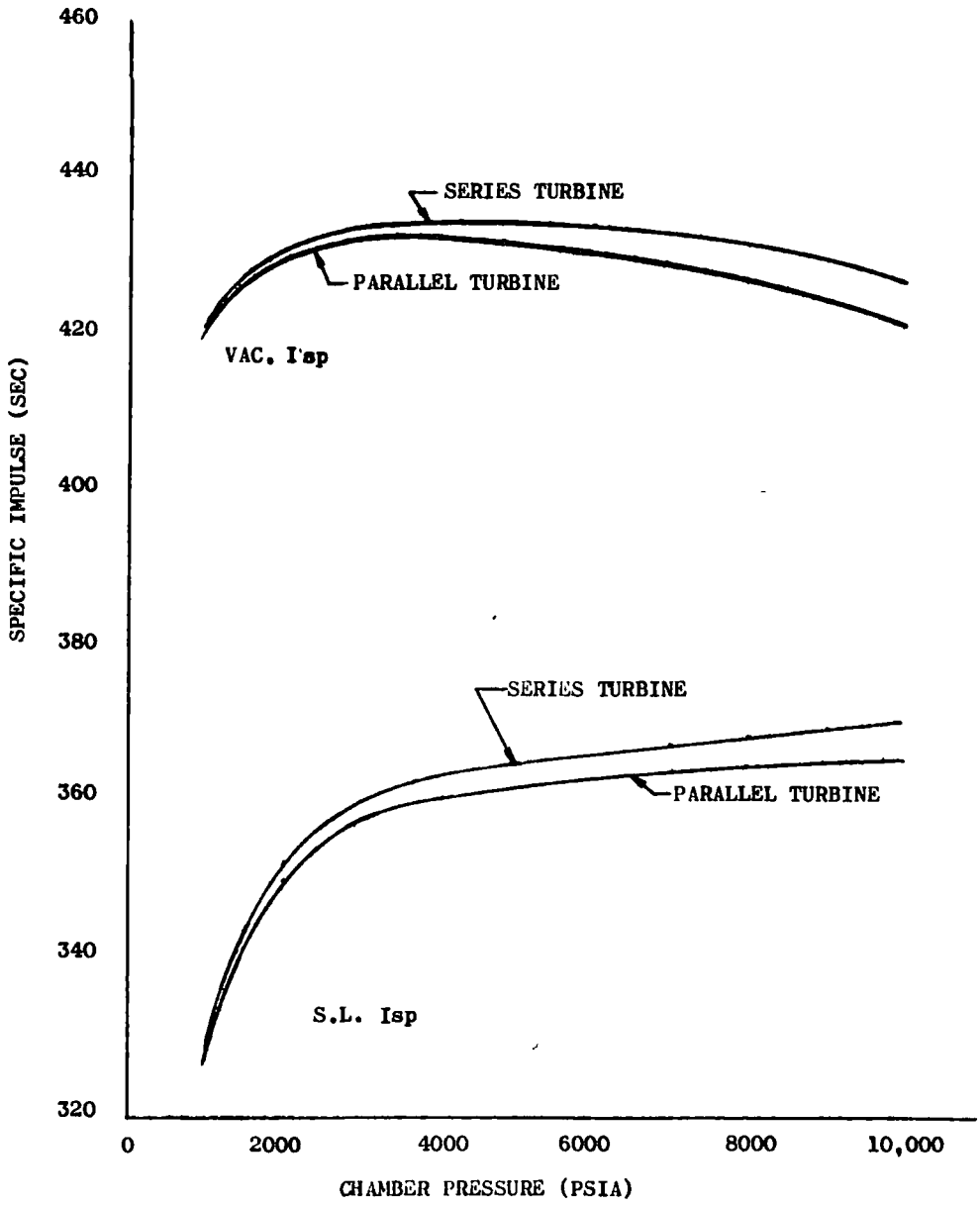

Specific Impulse Versus Chamber Pressure

Figure II J-26

VEHICLE CONDITIONS:
BOOSTER STAGE
180 SECONDS FLIGHT DURATION
TANKAGE FACTOR; 0.4 LB/FT^3

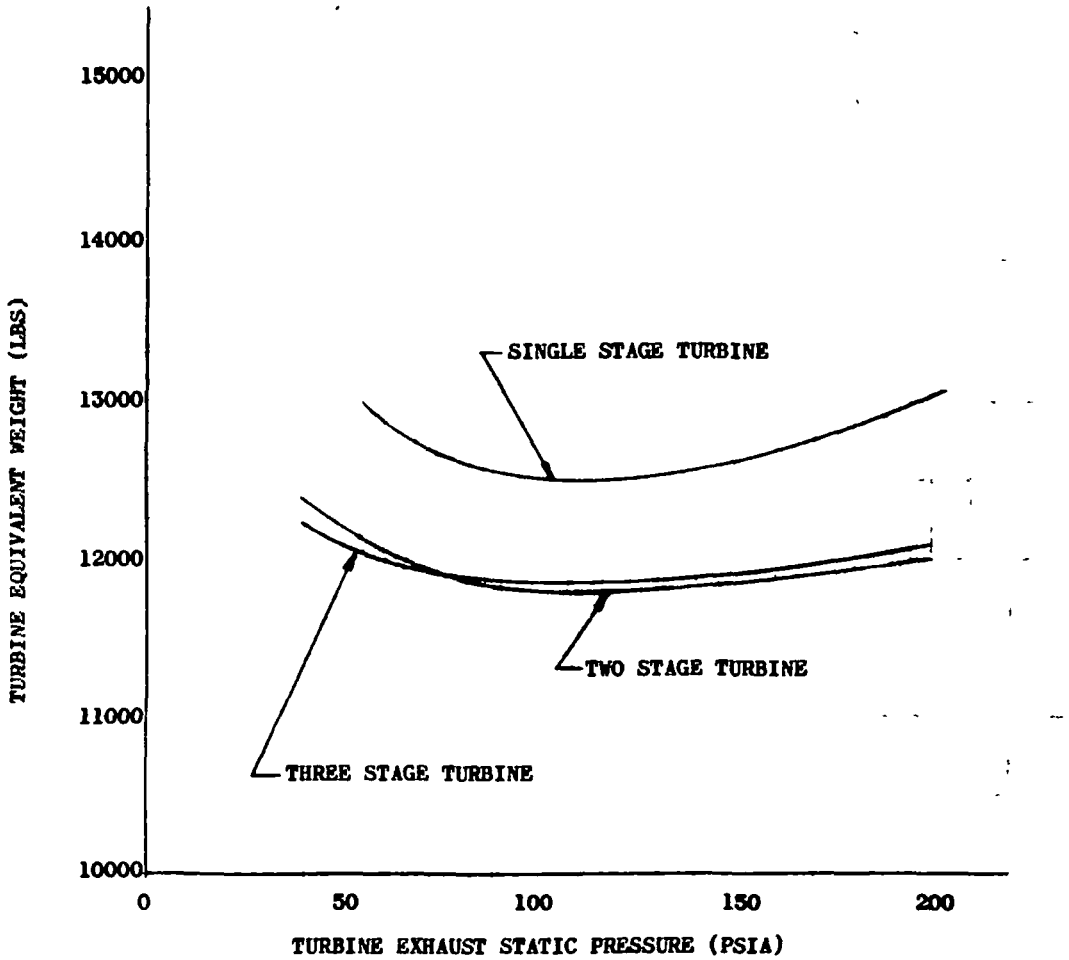

Turbine Equivalent Weight Versus Turbine Exhaust Pressure for H_2 Turbopump

Figure II J-27

VEHICLE CONDITIONS:
BOOSTER STAGE
180 SECONDS FLIGHT DURATION
TANKAGE FACTOR; 0.4 LB/FT^3

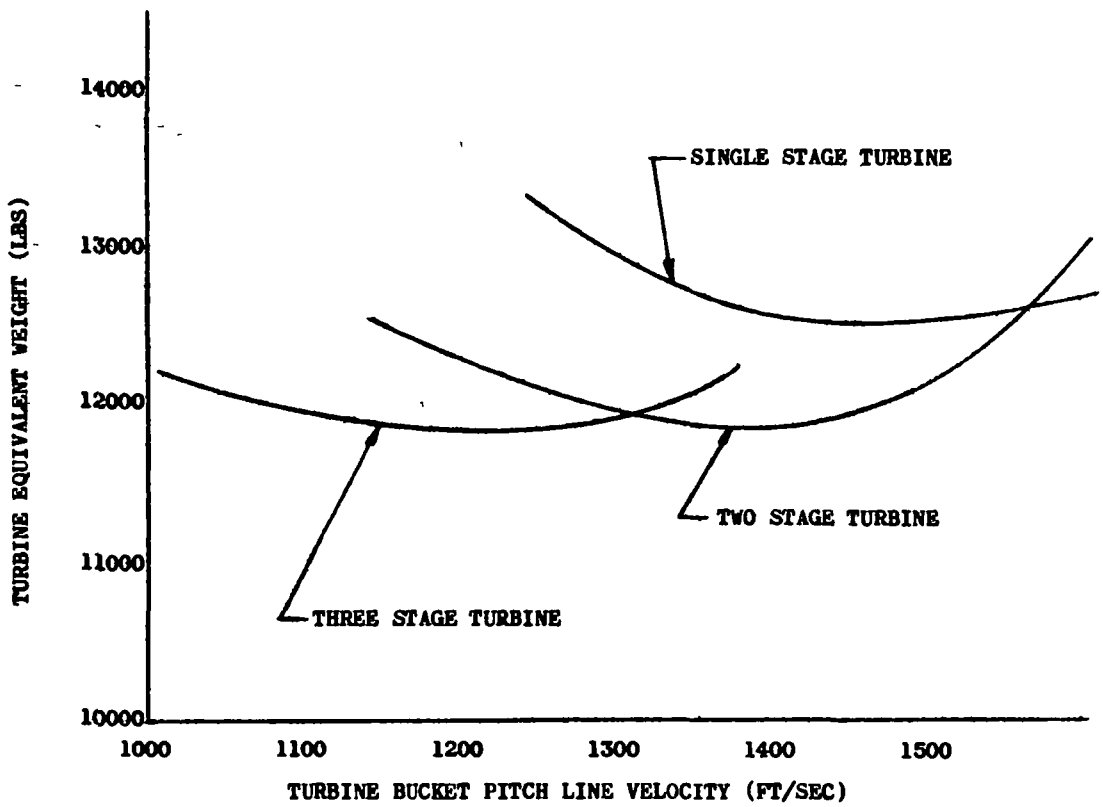

Turbine Equivalent Weight Versus Turbine Bucket Pitch Line Velocity For an H_2 Turbopump

Figure II J-28

VEHICLE CONDITIONS:
BOOSTER STAGE
180 SECONDS FLIGHT DURATION
TANKAGE FACTOR; 0.4 $^{LB}/_{FT^3}$

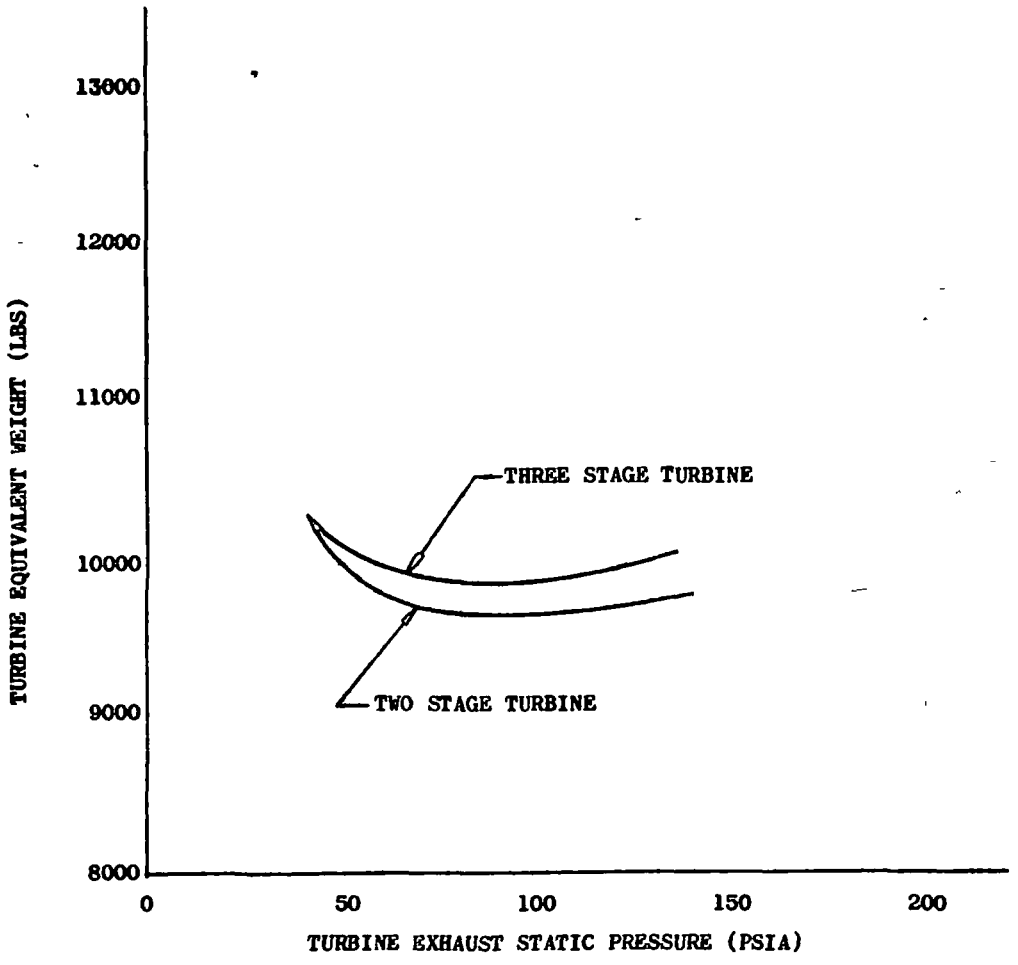

Turbine Equivalent Weight Versus Turbine Exhaust Pressure for an O_2 Turbopump

Figure II J-29

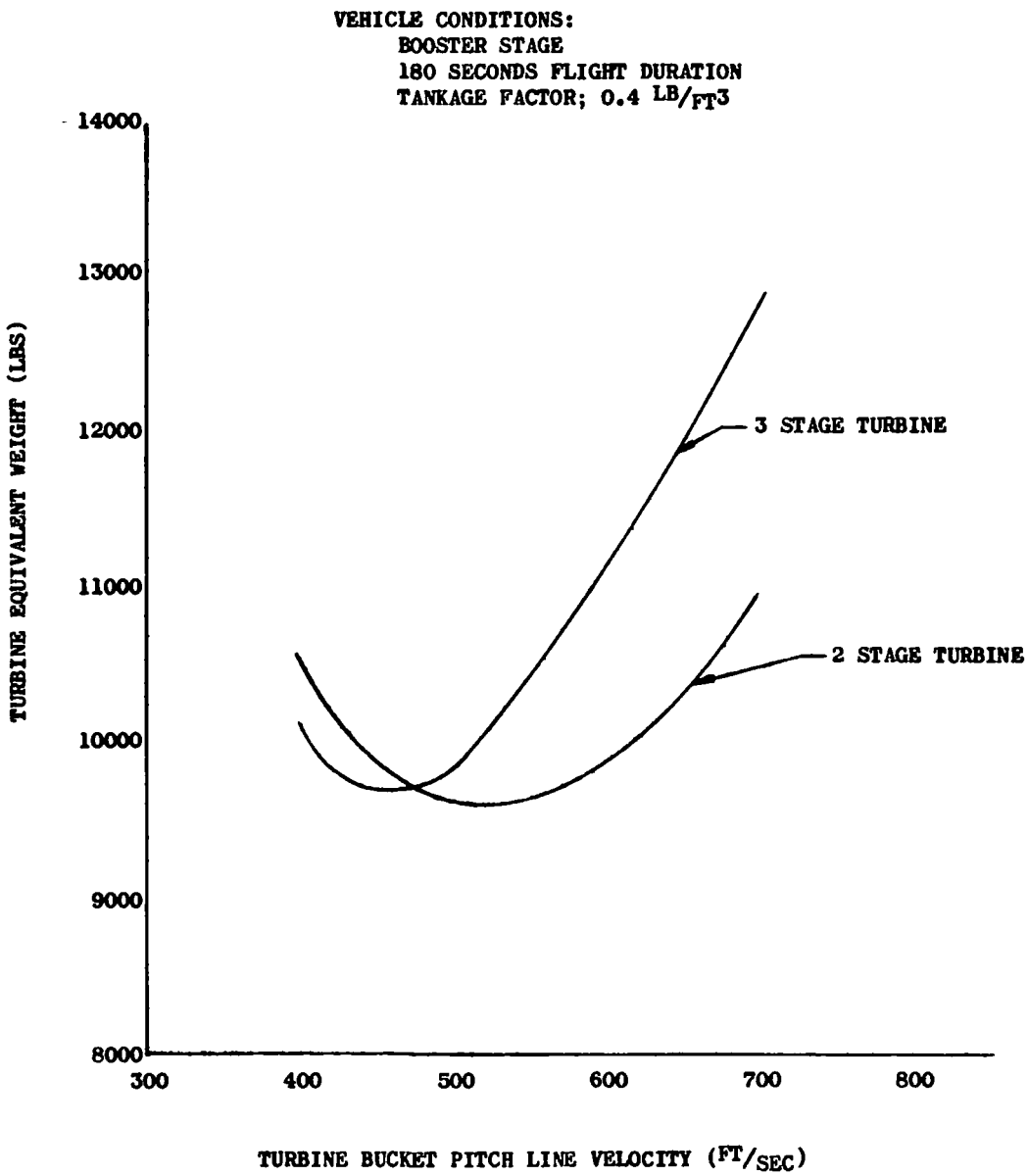

Turbine Equivalent Weight Versus Turbine Bucket Pitch Line Velocity For an O_2 Turbopump

Figure II J-30

VEHICLE CONDITIONS: BOOSTER STAGE, 180 SECONDS FLIGHT DURATION, TANKAGE FACTOR 0.4 LB/FT^3

	Single Stage Turbine	Two Stage Pressure Compounded Turbine
PARAMETER COMPARISON:		
Optimum bucket pitch line velocity (ft/sec)	1400	1400
Optimum turbine static exhaust pressure (psia)	100	100
Turbine equivalent weight (lb)	12,530	11,840
Turbine weight flow rate (lb/sec)	303	234
Additional volume hydrogen tank (ft^3)	1400	0
Additional volume oxygen tank (ft^3)	88	0
Additional weight hydrogen (lb)	6200	0
Additional weight oxygen (lb)	6200	0
Additional payload (lb)	0	173
COST COMPARISON:		
Additional hydrogen propellant cost	$ 805	
Additional oxygen propellant cost	$ 62	
Additional hydrogen tank cost	$ 7000	
Additional oxygen tank cost	$ 440	
Lost payload in terms of cost	$ 8650	
Additional turbopump cost		$ 16,500
TOTAL DIFERENTIAL COST	$ 16,957	$ 16,500

COST ASSUMPTIONS:

Cost of delivery one pound payload, $ 50.00
One pound of booster stage inert weight is equivalent to 0.25 lb payload
Average tank cost per cubic foot, $ 5.00
Hydrogen propellant cost 25¢/lb, oxygen propellant cost 1¢/lb

Overall Cost Comparison--Single-Stage Turbine Versus Two-Stage Turbine for an H_2 Turbopump

Figure II J-31

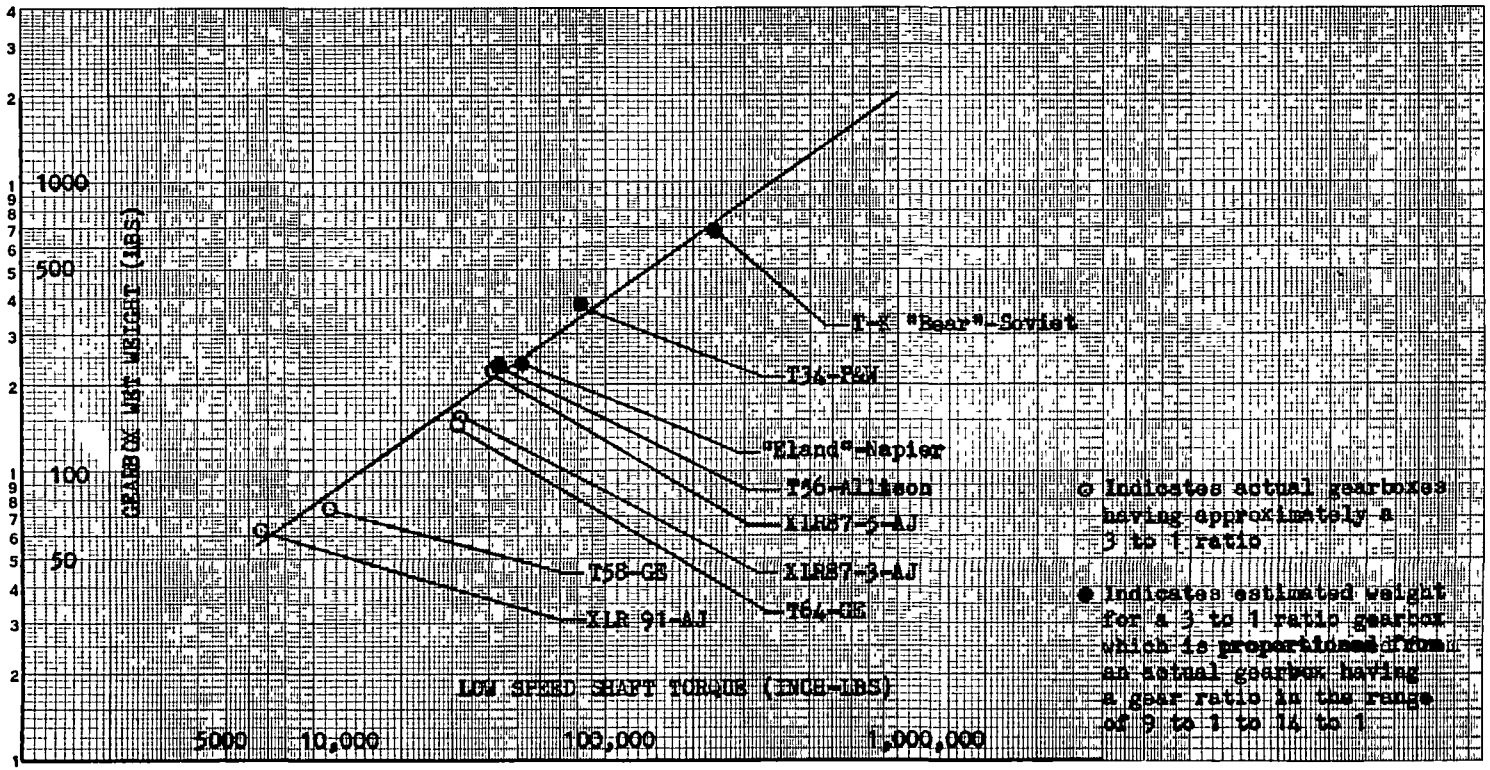

Figure II J-32

Gear Drive Dry Weight Versus Low-Speed Shaft Torque for 3:1 Speed Ratio Gearbox

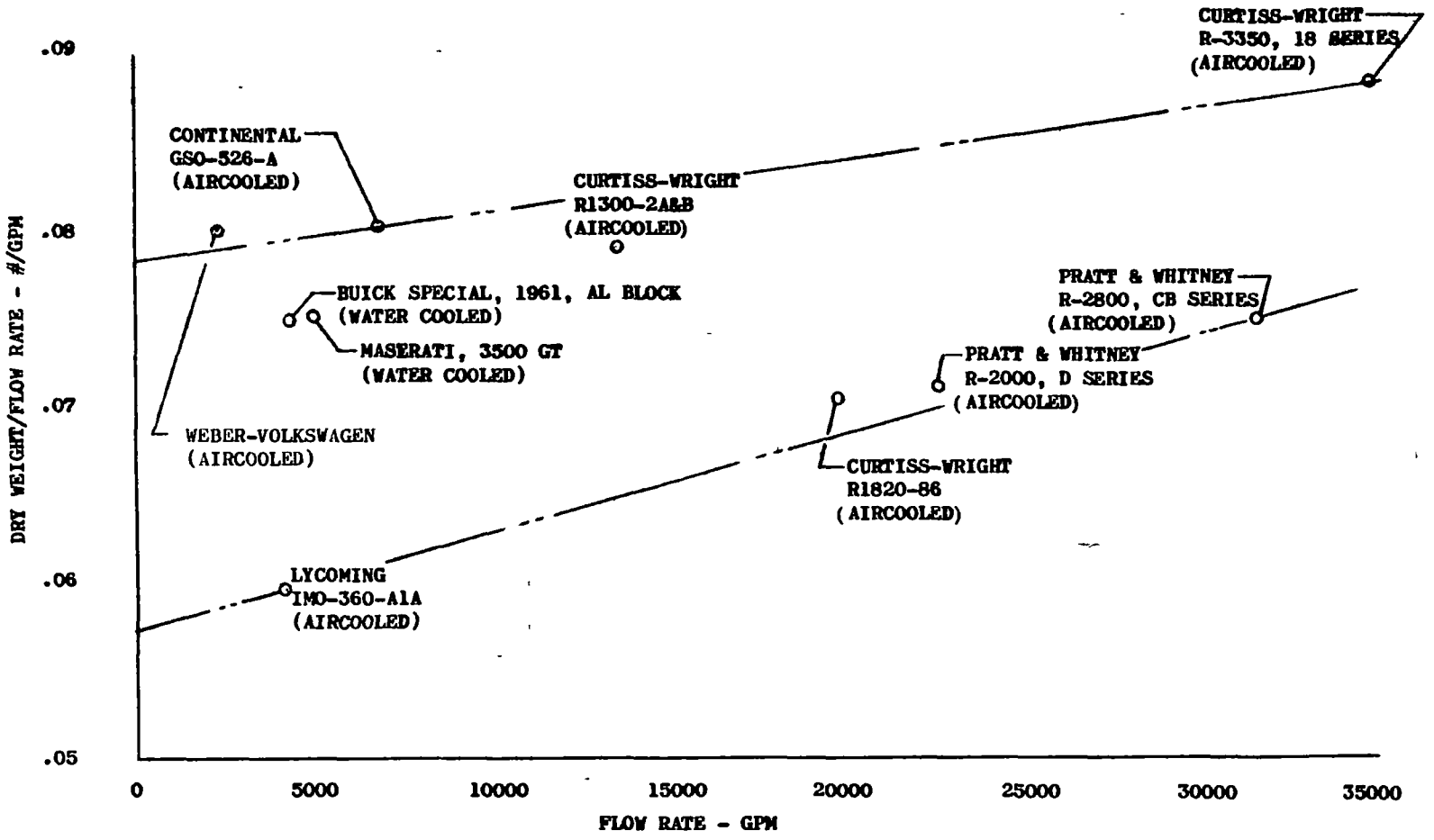

Specific Weight Versus Volumetric Flow Rate
for Flightweight Reciprocating Machinery

Aerojet-General CORPORATION

II, Concepts Considered (cont.)

K. JET PUMPS

Jet pump engine cycles are attractive because they require only a minimum number of moving parts, however, they are not suitable for obtaining reasonably high hydrogen pressures.

The significant cost and reliability gains of single-stage-to-orbit booster stages can be attained only with relatively high-pressure oxygen/hydrogen engines; therefore, jet-pump engines were eliminated from the scope of this investigation. Prior to this investigation, designs of jet pumps for a 500 psia chamber pressure, 6-million-lb thrust, oxygen/hydrocarbon engine were made to compare jet-pump size and weight against turbopump size and weight. Figures II K-1, II K-2 and II K-3 show the jet pump designs and weights.

It is concluded that the best jet-pump arrangement for large engines consists of clustering small jet pumps perpherally around the thrust chamber. The individual jet pumps are shown in Figures II K-2 and II K-3. Grouping the individual jet pumps into a single unit, as shown in Figure II K-1, invokes a heavy weight penalty, as well as creating undesirable propellant flow passages within the jet-pump unit.

It was also found that the wet weights of a 500 psia chamber pressure, oxygen/hydrocarbon engine are approximately equal to the turbopump wet weights at a 1,000 psia chamber pressure, oxygen/hydrocarbon engine. Thus, for an oxygen/hydrocarbon booster-stage engine, the apparent simplicity of jet pumps is considerably offset by the complexity of the jet-pump engine-drive fluid heat exchanger and by the performance degradation resulting from the relatively low chamber pressure.

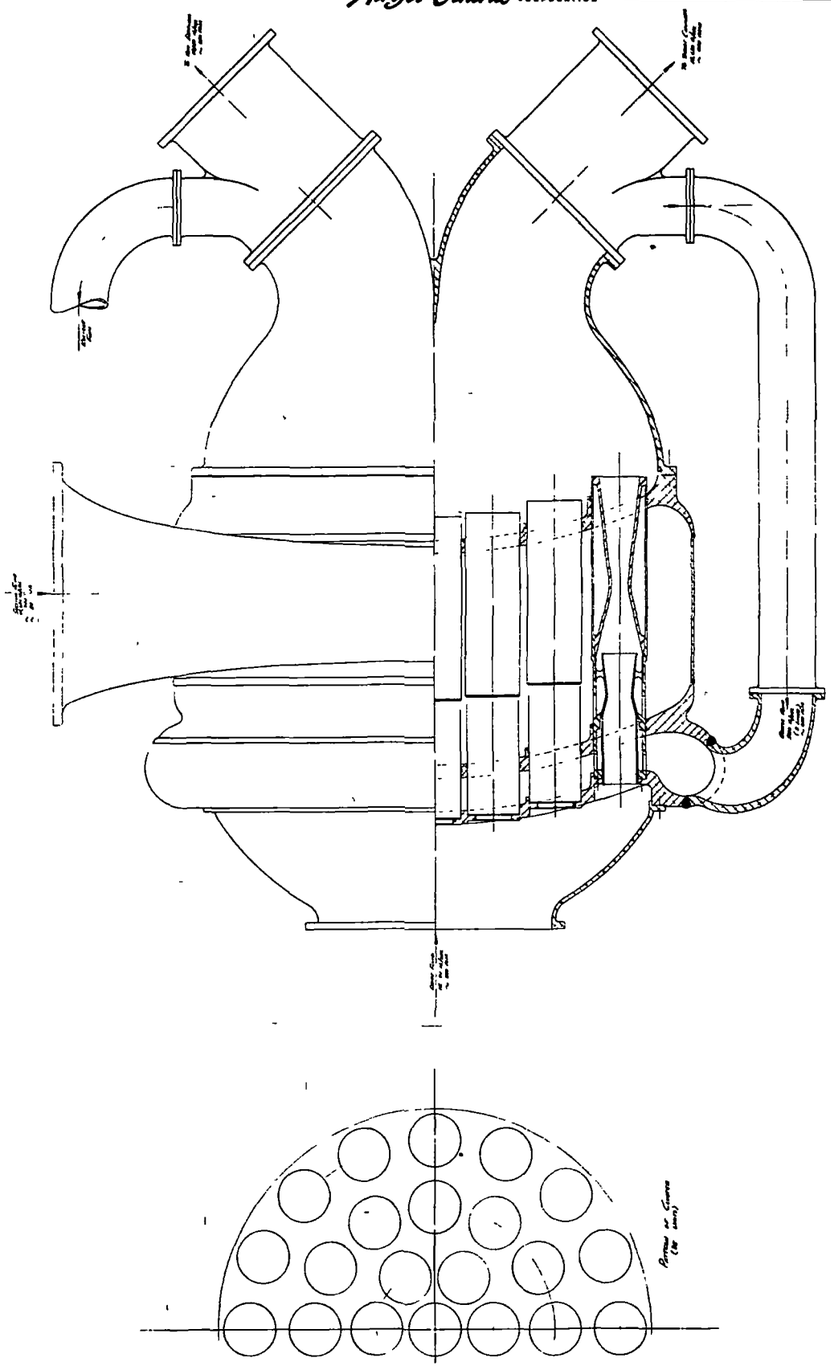

Oxidizer Jet Pump (clustered) for 6-Million-lb-Thrust O_2/Hydrocarbon Booster

Figure II K-1

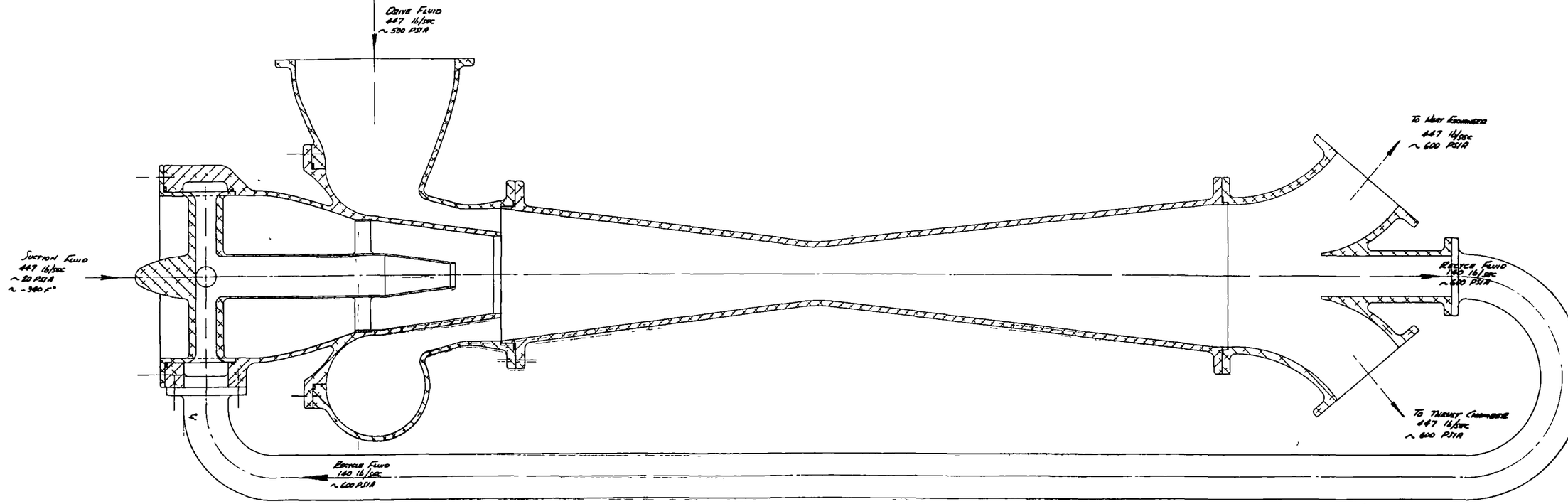

~ Overall Length - 6 FT - 2 IN
~ Overall Dia = 1 FT - 10 IN
~ Dry Weight - 75 lbs
~ Wet Weight = 194 lbs

6 MM O_2 Jet Pump Unit
(35 Req'd)
Scale ½
M. Gurney
2-17-61

Oxidizer Jet Pump for 6-Million-lb-Thrust O_2/Hydrocarbon Booster

Figure II K-2

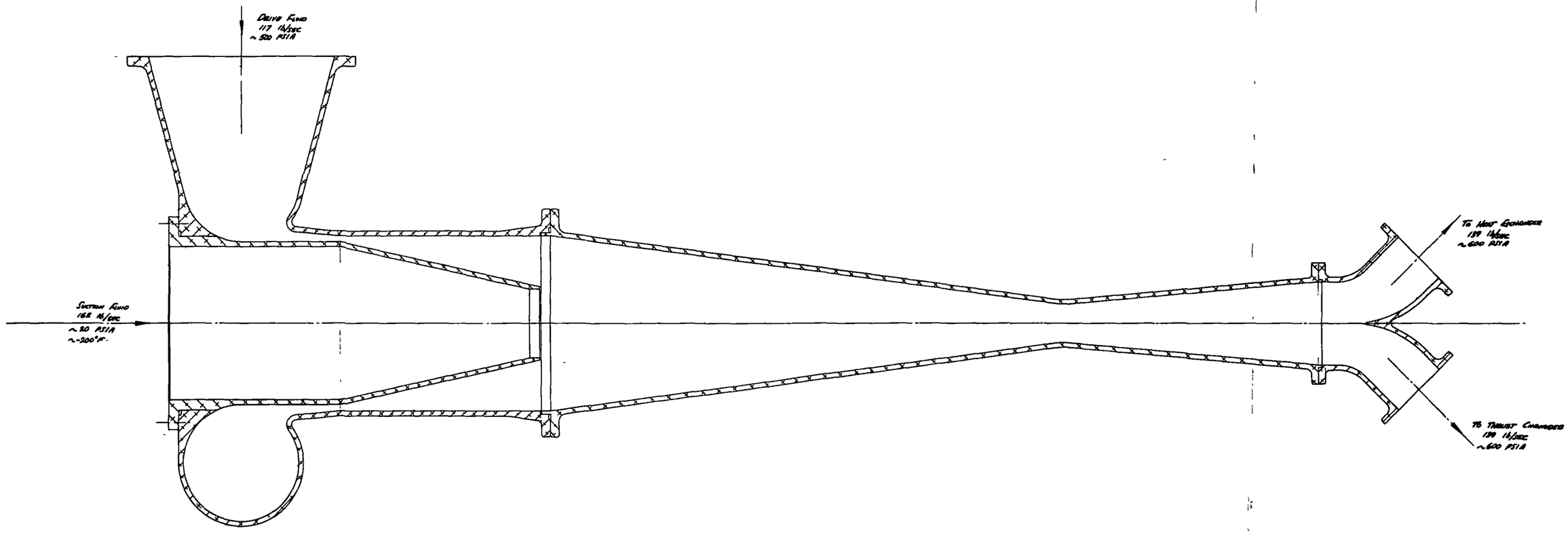

~ OVERALL LENGTH — 6 FT
~ OVERALL DIA — 1 FT
~ DRY WEIGHT — 60 LBS
~ WET WEIGHT — 120 LBS

Fuel Jet Pump for 6-Million-lb-Thrust O_2/Hydrocarbon Booster

Figure II K-3

II, Concepts Considered (cont.)

L. ENGINE CONTROL CONCEPTS

1. Summary

The investigation made of engine controls determined the design and development problems associated with large rocket systems. The major portion of this evaluation was conducted considering components for a 6-million-lb thrust engine, a thrust level high enough to stimulate new ideas. Resulting configurations were then evaluated for use at the 2-million-lb thrust level.

Included in the investigation were valves, actuators, and governors (for turbine speed control). All configurations were evaluated to determine their influence upon weight, cost, and reliability of the total engine system. Conceptual sketches and design layouts were made as required to determine size, weight, and feasibility.

Results of this investigation indicate that there are no insurmountable problems associated with controls and actuation systems for large boosters.

Two new thrust chamber valve designs, with a ring gate concept, were derived. Both offer reduced development cost, a lower actuator power requirement, and higher reliability than current configurations. In one of the designs, a ring type gate is used as a propellant line valve, and in the other the ring gate in the pump housing is used to simultaneously control multiple discharges from the same pump. Valves required for other control functions can be modifications of present configurations because they are no larger than currently available components. A ring gate valve in the pump

II, L, Engine Control Concepts (cont.)

housing is mandatory for certain engines with unique features, such as the forced-deflection nozzle with an integrated pumping system, as discussed in Section II, J.

For actuators requiring high operating power, such as a gimbal actuator, a pneumatic actuation system is recommended. This pneumatic system is the lightest of all systems, operates satisfactorily under low temperature conditions, and can derive its power source from engine gases, thus eliminating any need for an auxiliary power source (alternator or pump). A weight comparison of the various methods for actuating gimbal actuators is shown in Figure II L-1. For low-power controls, the weight penalty associated with the other actuation methods becomes much less significant and for certain engines, the selection of one may be desirable. For engines with liquid oxygen/RP-1 propellants, a hydraulic system is feasible. For liquid oxygen/liquid hydrogen systems, electrically-operated controls offer complete environmental insensitivity, ease of checkout, minimum aerospace ground equipment, and high potential reliability. If the operation of all controls by a single power method is desired, pneumatic operation is recommended.

The cost difference between the various control configurations is insignificant with respect to the overall booster system. Therefore, choice depends upon the technical evaluation.

A governor was evaluated for use as a turbine speed controller. It was found to be a feasible and attractive control method for engines with continuous turbine speed control.

II, L, Engine Control Concepts (cont.)

2. Valves

Valves required for control of the main propellant flow are significantly larger than those needed for all other control functions. With the exception of these valves, it was found that all valves required for engines up to 6-million-lb thrust can be of a currently used configuration (i.e., butterfly, ball, or poppet types).

Main propellant valve configurations were evaluated in detail. Conceptual sketches of some 60 valving methods were generated. From these, seven configurations (Figures II L-2 through II L-8) were selected for a detailed design analysis. These valves, including their weights at the 6-million-lb level, include:

Pump-mounted gate valve	500 lb
Ring gate valve	485 lb
Butterfly valve	590 lb
Gate valve	760 lb
Spring valve	553 lb
Plug valve	740 lb
Ball valve	1,275 lb

The two ring gate valves were found to have several significant advantages, which is why they were selected over the other configurations. Primarily, main seal development -- which is considered the most difficult development problem for all large valves having rocket applications -- is considerable less for this configuration than for the others. Secondly, actuation power requirements are low because the valve gate is balanced. As a third point, its weight is minimum by comparison with the other configurations.

II; L, Engine Control Concepts (cont.)

The pump-mounted ring gate valve is used in engines with integrated pumping systems. Total discharge flow can be controlled by a single valve rather than by synchronous control of several pump discharge valves. Two main problems associated with this valve are the dynamic effects upon the pump impeller during the shutdown transient and binding during actuation. A number of solutions have been proposed and additional design study is planned for Task 2.

Physical, flow, and operating characteristics were determined for the ring gate valve. Figures II L-9 and II L-10 give valve size as a function of weight and K_w, (an admittance factor), respectively. Operating horsepower and torque in relationship to valve size are given in Figures II L-11 and II L-12

Secondary injection, as a method of thrust vector control, presents a new control design problem. There are two methods for controlling secondary injection, each with a completely different concept. One controls liquid as an injectant or as the propellant for a gas generator injector. The other controls hot gas directly. Presently designed valves for cryogenics are usable for liquid control. For gas control, new designs were studied.

In methods for satisfying vector control requirements, turbine exhaust gases are used. They are illustrated in Figures II L-13 and II L-14. The main difference in these methods is the design of the hot-gas valves. Figure II L-15 is a sketch of a throttling butterfly valve for control of the gas injectant. When all the throttling valves are closed, the spring-loaded poppet relief valves allow the hot gas to be ejected through the fixed nozzles. In another method of gas control (Figure II L-14), the jet-pipe principal is used to control the secondary gas flow. When no secondary flow is required, the turbine gas is discharged through reed valves to the nozzles. Either method can be developed and further study was planned for Task 2.

II, L, Engine Control Concepts (cont.)

3. Actuation Systems

An investigation was made into the various methods for actuating engine controls. The four major methods are: electrical, mechanical, hydraulic, and pneumatic. If a homogenous system is desired, the major power requirement determines the method of actuation for all the controls. A gimbal actuator is the highest-powered unit in gimbaled engine systems; consequently, the greater effort was directed toward the design of high-powered actuators to satisfy gimbal actuation requirements. This study was made at the 6-million-lb thrust level so that the actuators could easily be scaled for lower as well as higher thrust systems. Low-power controls (below 20 hp) for large rocket engines are within current technology for electrical, hydraulic, and pneumatic. Mechanical controls are currently in the research and development phase.

a. Electrical

The electrical actuation system consists of a generator or alternator, transmission lines, motor, ball-screw or gear train (or a combination of both), brakes, and low-power level electrical control system (i.e., amplifiers and transducers). For high-powered electrical systems, a weight-power ratio of 1 lb/hp can be optimistically expected. This ratio applies to all components converting or transmitting power individually; an alternator would be 1 lb/hp; a clutch, 1 lb/hp, a motor, 1 lb/hp. If electrical parts only were considered with no allowance for the frame or mount and cooling systems, a weight estimate of 0.3 lb/hp can be made. The values stated for motors and alternators are based upon design information obtained from the Westinghouse Corporation.

II, L, Engine Control Concepts (cont.)

As indicated, a cooling system must be considered for any high-powered electrical equipment. Another major problem is the vacuum operation of high-voltage equipment. A suggested solution for both problems is exemplified by Figure II L-15. This system is usable in an oxygen/hydrogen engine. Pressure in the transmission lines is kept at the same level as pump discharge pressures and losses are held to a minimum by keeping lines at a low temperature. Hydrogen is used as a coolant for the motors By keeping the high voltage equipment under pressure, corona and arcing problems can be eliminated.

A method of electrical control that would satisfy servo operation requirements of a gimbal system is shown in Figure II L-16. The motor is uni-directional and drives two counter-rotating clutches. Each clutch must be capable of transmitting full motor power.

The electrical control system inherently offers the following significant advantages for a control system.

Components will operate at extremely low temperatures without compartment or component conditioning.

II, L, Engine Control Concepts (cont.)

Minimum Aerospace ground equipment is required for engine checkout.

The system has the highest potential degree of reliability and flight readiness.

Components are insensitive to contamination.

Stored energy is not required.

Absence of a working fluid avoids the in-flight fluid or gas leakage problems found in other systems.

The major limitation of electrical systems is high system weight, especially for actuators having large power requirements. For multi-million-lb thrust engines, this weight is considered prohibitive for high-power components (i.e., gimbal actuators). However, for other control functions, the weight penalty is small and the electrical system remains attractive.

b. Mechanical

A mechanical control system provides driving power from a takeoff shaft linked to the engine pump drive system (Figure II L-17). This system is similar to an electrical one in that the prime mover rotates in a single direction and control is obtained by coupling one or the other counter-rotating clutches. Major problems lie in the clutching and speed reduction of the system. To obtain smooth clutching, a hydraulic torque converter or an electro-magnetic clutch is required. The hydraulic fluid transmission would require protection from low-temperature environments. It would also require the same complex controls as a hydraulic system.

II, L, Engine Control Concepts (cont.)

The electro-magnetic clutch weighs as much as a prime mover (motor) to couple the required torque (approximately 1 lb/hp). A new concept in coupling, a spring-clutch under development by the Curtis-Wright Corporation, provides power transmission and is light in weight. The clutch is composed of a power transmission spring that is engaged by a "teaser" spring by rotating it to the point that it will rub on the turning drum. The spring helix is such that rotation in the direction of the turning drum causes the coils to contact the drum and it becomes self-locking by means of friction. This locking "teaser" spring engages the power spring in the same manner. When fully engaged, the input and output shaft are coupled, with the output member turning in the direction of the particular clutch energized. To reverse direction, one torque motor is de-energized and the other energized. Opposite rotation of the first clutch causes it to free-wheel because the output shaft would be attempting to drive the input (i.e., opposite to the self-locking direction of the spring helix).

The major problem involved with direct-acting mechanical coupling is the high peak acceleration of the output member. This problem may eventually be solved by using appropriate torque or shock absorbers.

Other mechanical clutches under development incorporate the epicycloid or planetary system, wherein relative speeds of the planetary drivers control the output speed and direction (General Motors Corporation). Heretofore, friction-drive mechanisms have been shunned in rocket applications, but great promise of simplicity and low weight lie in a mechanical control system. As a system, it would weigh more than the pneumatic but less than either a hydraulic or electrical system.

II, L, Engine Control Concepts (cont.)

c. Hydraulic

Hydraulic controls are probably the most highly-developed method for actuation. A three-stage servo system is needed for high power control. Figure II L-18 is a sketch of such a system. The first and second stage comprise the servo valve. A third stage is used to obtain the high flow required for actuator motion. Investigation was also made to determine the optimum supply pressure for a linear actuator. It was found that at pressures above 3,000 psi, the actuator wall weight together with the fixed shaft and mount weights resulted in an over-all assembly weight increase. Approximately 3,000 psi seems to be an optimum pressure. This is the normal operating pressure for most hydraulic systems. Hydraulic pump design becomes much more difficult at higher pressures because of bearing and sealing problems.

Figure II L-19 is a sketch of a three stage servo actuator. This unit has the capability of producing 750 hp and a dry weight of 335 lbs. The multiple-piston pump required to drive two of these actuators would weigh 1,350 lb, using current designs (see Figure II L-20). Manufacturers of hydraulic pumps have stated that pumps of such capacity are completely feasible.

The main disadvantage with hydraulic systems is in low-temperature operation. For cryogenic propellants, a long hold-fire would freeze the hydraulic system. Insulation or warming systems would be required to ensure proper operation. Sensitivity to contamination is another major problem, and a large-volume system system would have a high degree of contamination. Its major advantage is the advanced state of current technology. Hydraulic systems are well-developed and much of the required hardware is available.

II, L, Engine Control Concepts (cont.)

d. Pneumatic

A pneumatic control system has a gas source, control or servo valve, and a power conversion unit or actuator. The power converter can be a piston actuator or a rotary device, such as a gear motor, turbine, or vane motor. For high response requirements, a rotary actuator must be used. Response of a pneumatic actuator is a function of the gas bulk modulus, pressure, temperature, and trapped volume to be pressurized. Bulk modulus, pressure, and temperature will be the same for any actuator, but the trapped volume is a function of actuator design. Rotary actuators of a variable displacement design -- such as gear and turbine motors -- have the highest response. They also require more gas for operation than a linear or fixed-displacement actuator. Figure II L-21 is a sketch of a typical pneumatic gear motor. Power is obtained from pressure applied across the differential area of the face of the mating teeth. The high speed of this device and other rotary actuators necessitates a speed reducer for most applications.

II, L, Engine Control Concepts (cont.)

A pneumatic control system has many advantages. It is the lightest system of any considered. A dry weight ratio of 0.2 lb/hp is attainable. On-board gas can be used if temperatures can be held within the acceptable range. The system is relatively insensitive to contamination, and it can operate over a wide range of temperatures. Pneumatics are in the research and development phase of study but hardware is available. The use of designs such as the turbine actuator makes such systems merely another application of known working principals.

4. Turbine Speed Controllers

An investigation was made into various methods for controlling turbine speed. The five major methods considered are:

Throttling of the turbine gas supply

Control of the turbine nozzle angle of attack

Controlling production of the gas by regulating the generator propellant flow.

Throttling the turbine exhaust gas

By-passing gas around the turbine

All these control methods require systems that include a speed sensor, amplifier, controller, actuator, control valve, and a feedback loop, Some existing rocket engines have a turbine overspeed shutdown mechanism, but do not have continuous control of turbine speed. In the shutdown systems, an electrical sensor monitors turbine speed and generates a varying voltage, which changes the signal frequency as a function of speed. This signal is fed into the comparator unit that has been preset for a maximum signal frequency. When this frequency is reached, an engine shutdown signal is initiated.

II, L, Engine Control Concepts (cont.)

For continuous control, the comparator output can be amplified to control a servo-valve-controlled actuator to position a control valve. This control valve position is fed back if required for stability. The control valve completes the functional control as required via the particular control method selected.

Another method for controlling the valve is through a governing device. Figure II L-22 is a schematic of a governor satisfying the requirements of a heated-hydrogen cycle system. The centrifugal transducer is set to control at the desired speed. As speed increases, the fly-weights move out, repositioning the servo valve. When the set point is passed, the servo spool applies gas to the closing side of the gear motor which, in turn, drives the control valve through the speed reducer. The valve bypasses hydrogen from the turbine to the exhaust duct, decreasing pump speed.

The set point is adjusted by preloading the spring system in the centrifugal transducer. To change the set point during engine operation, the torque motor or push-pull solenoid provides a force in opposition to, or in addition to, the mechanical spring load (depending upon the desired directional change in set point) and re-establishes the operating datum. This override can be used for propellant utilization, mixture ratio, thrust control, or acceleration control. This governor is usable for any of the control methods.

In an engine system in which a hydraulic supply is available, the governor would use the hydraulic fluid for actuation instead of gas. The transducer is mass-balanced through the setpoint override circuit fulcrum. For engines with high temperature turbine exhaust, insulation and cooling would be needed for the centrifugal transducer.

II, L, Engine Control Concepts (cont.)

A governor for a rocket turbine is completely feasible. Such governors are in industrial use for steam turbines and other gas turbines. The governor shown in the sketch is a redesign of an available piece of hardware. The Woodward Governor Company produces governors for this application and has conducted research and development studies with pneumatics as the control fluid. Units using hydraulic fluid are developed and considered "off-the-shelf" hardware.

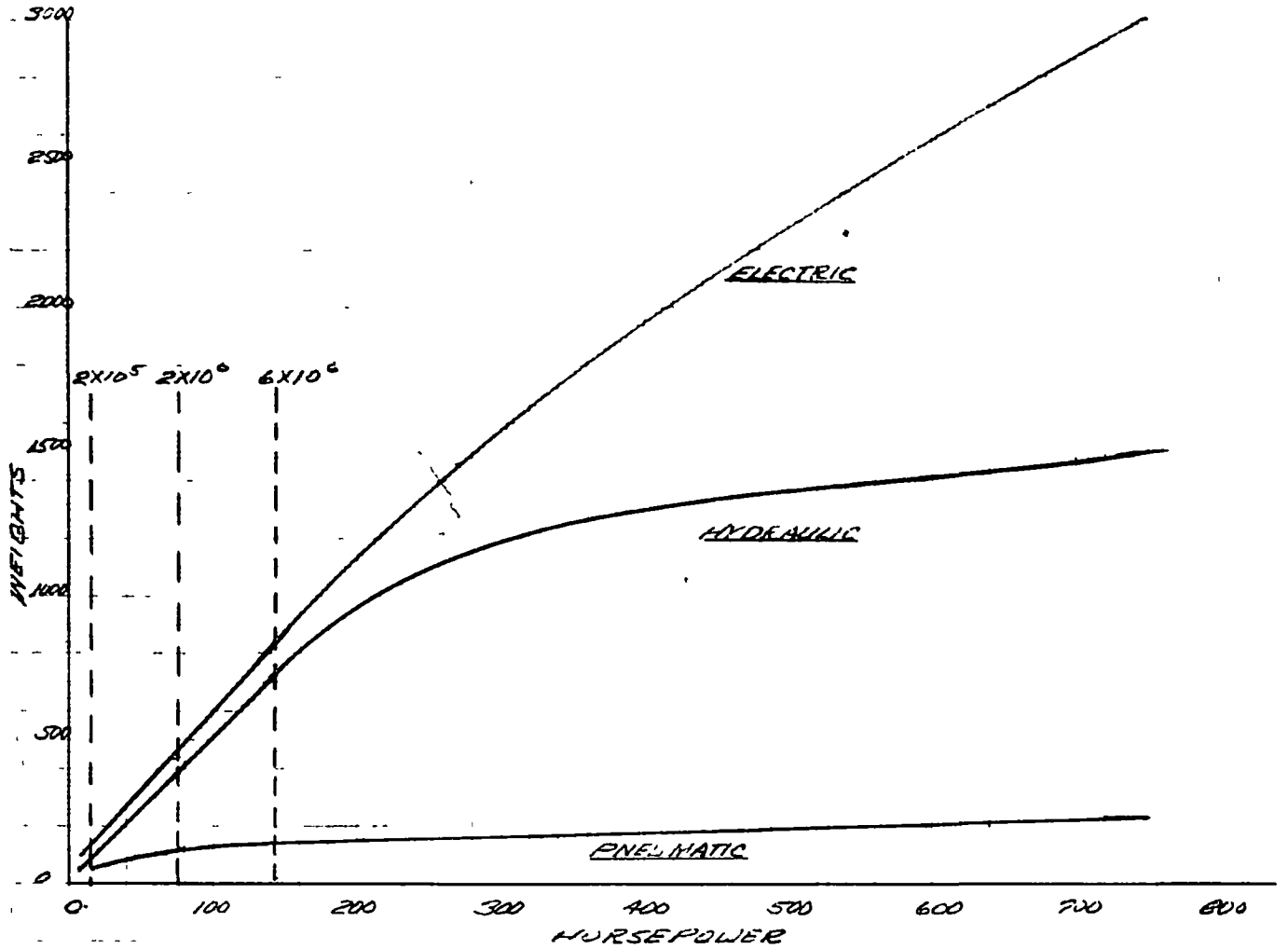

Weight Comparison of Three Types of Gimbal Actuators

Figure II L-1

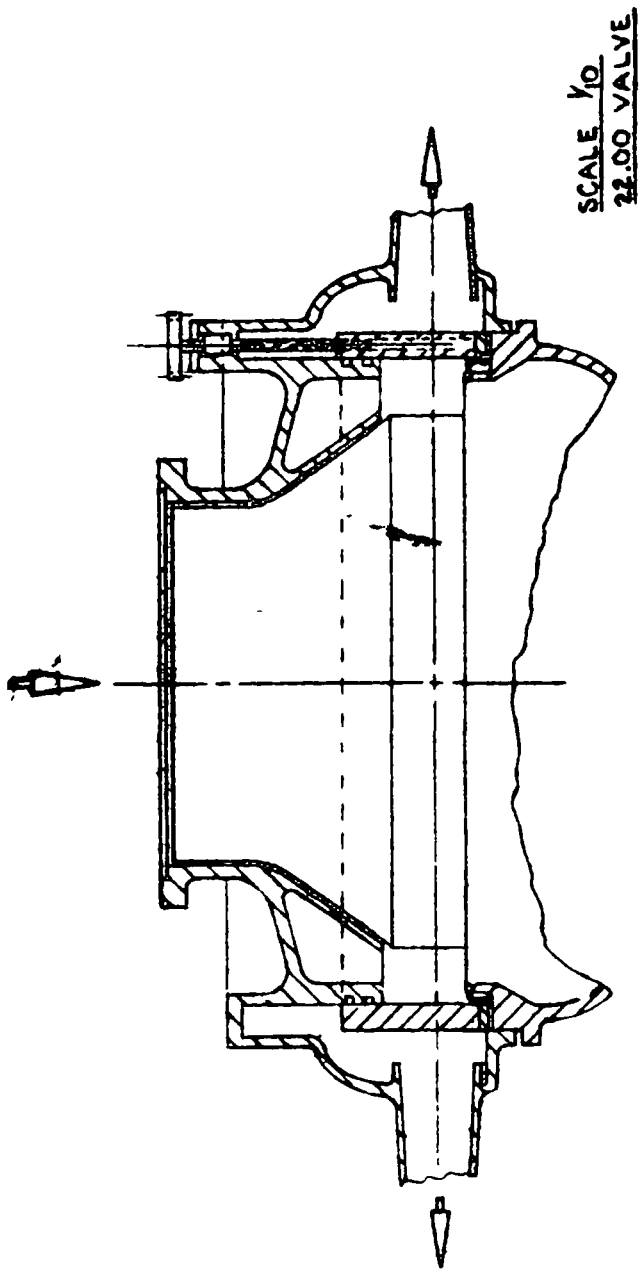

Pump-Mounted Gate Valve

Figure II L-2

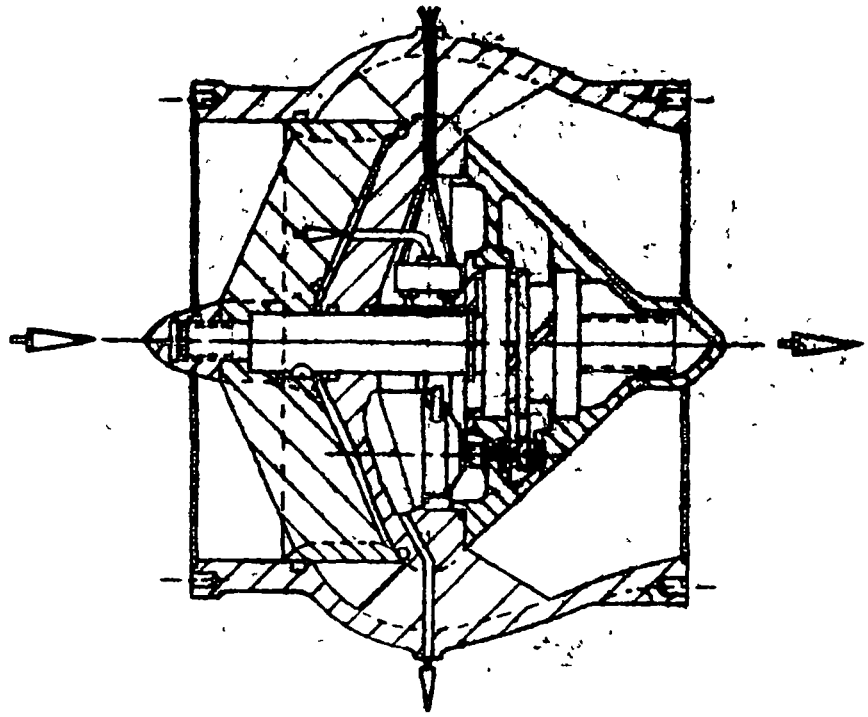

Ring Gate Valve

Figure II L-3

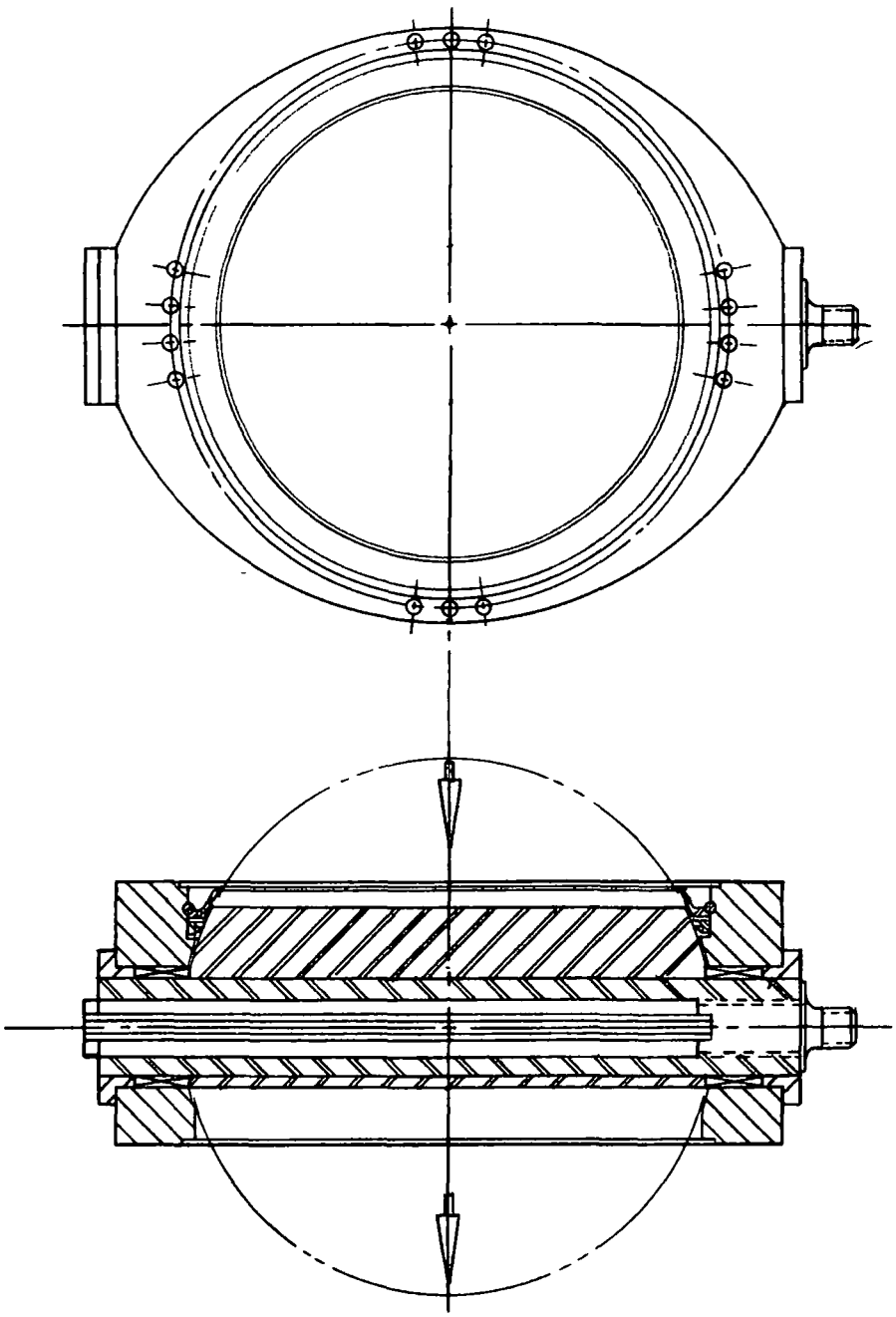

Butterfly Valve

Figure II L-4

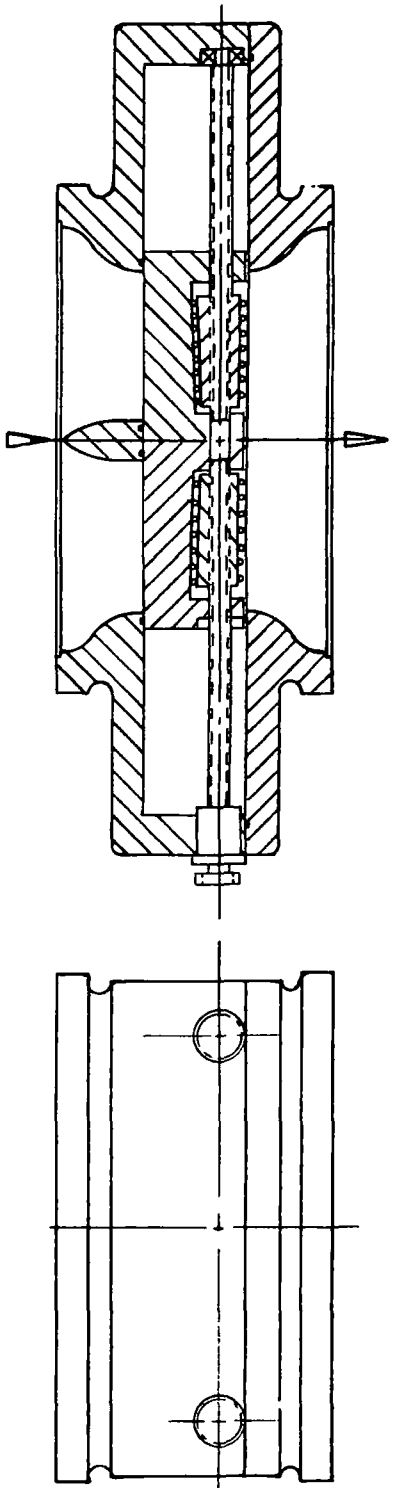

Gate Valve

Figure II L-5

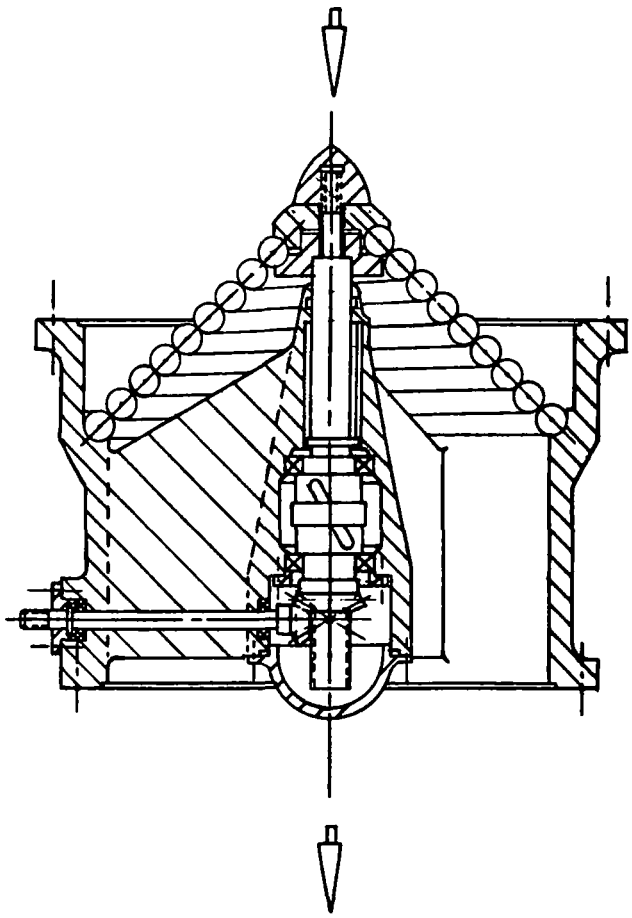

Spring Valve

Figure II L-6

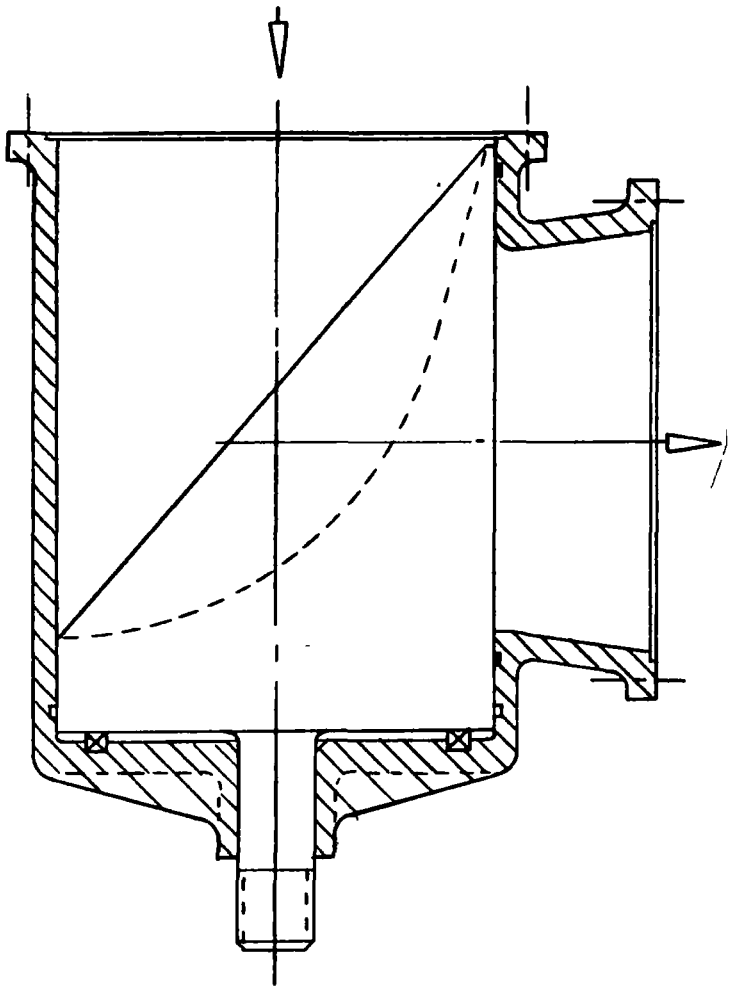

Plug Valve

Figure II L-7

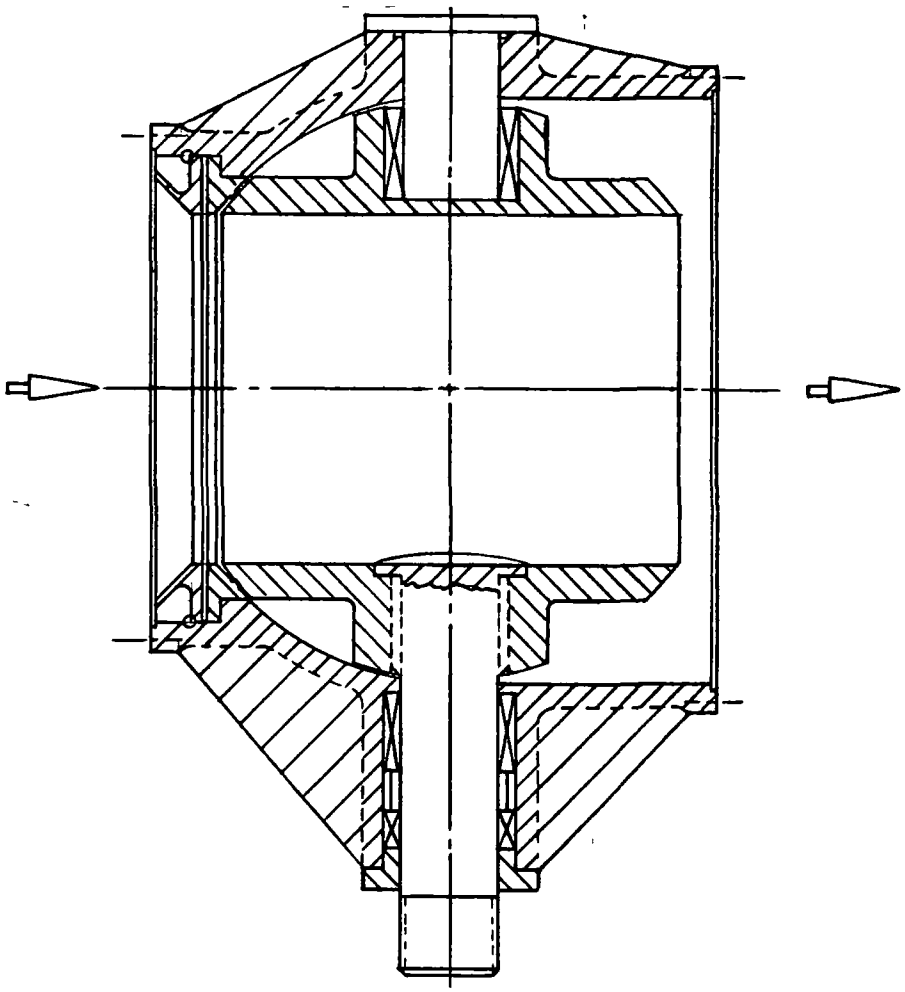

Ball Valve

Figure II L-8

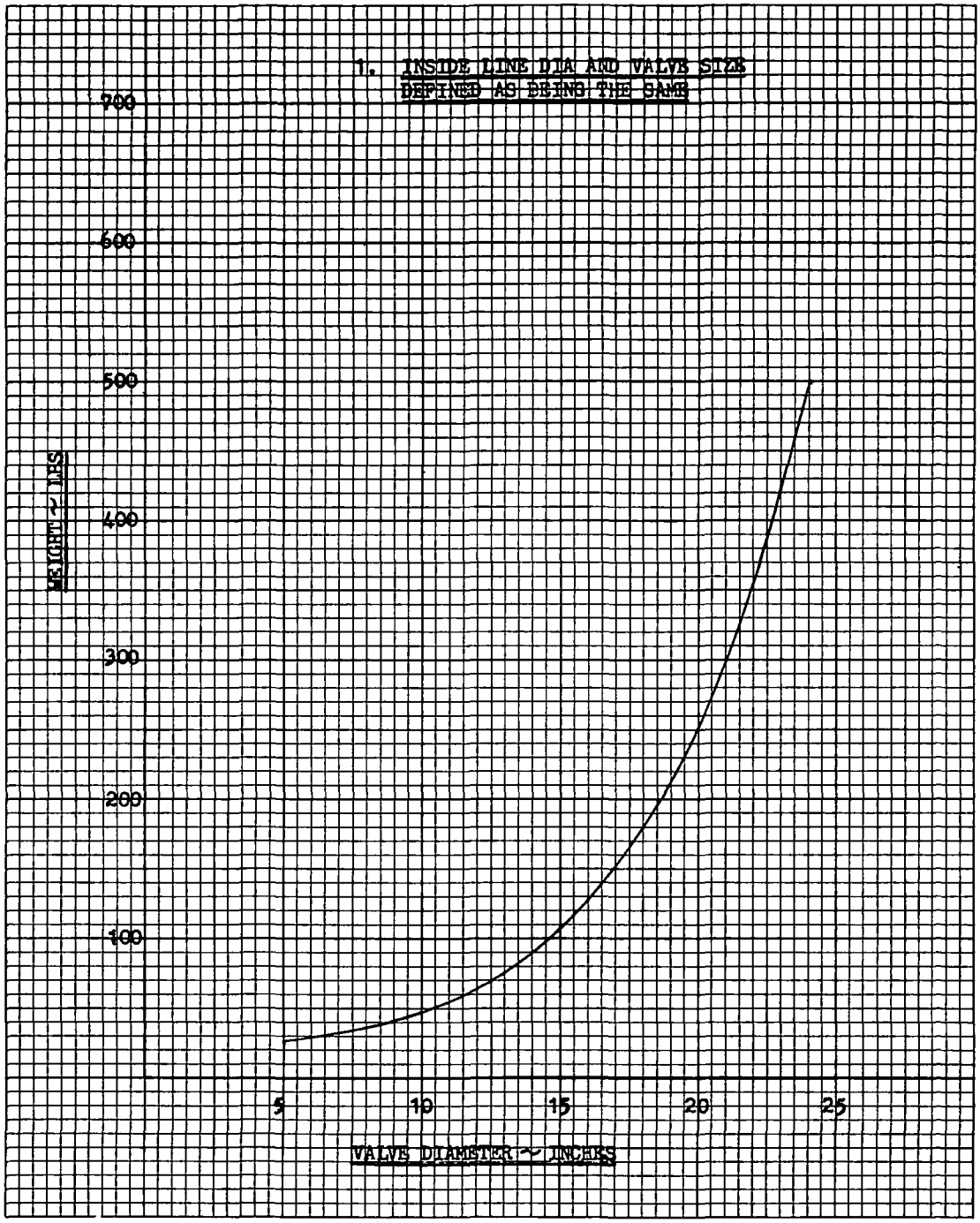

Valve Diameter vs Weight For Ring Gate Valve

Figure II L-9

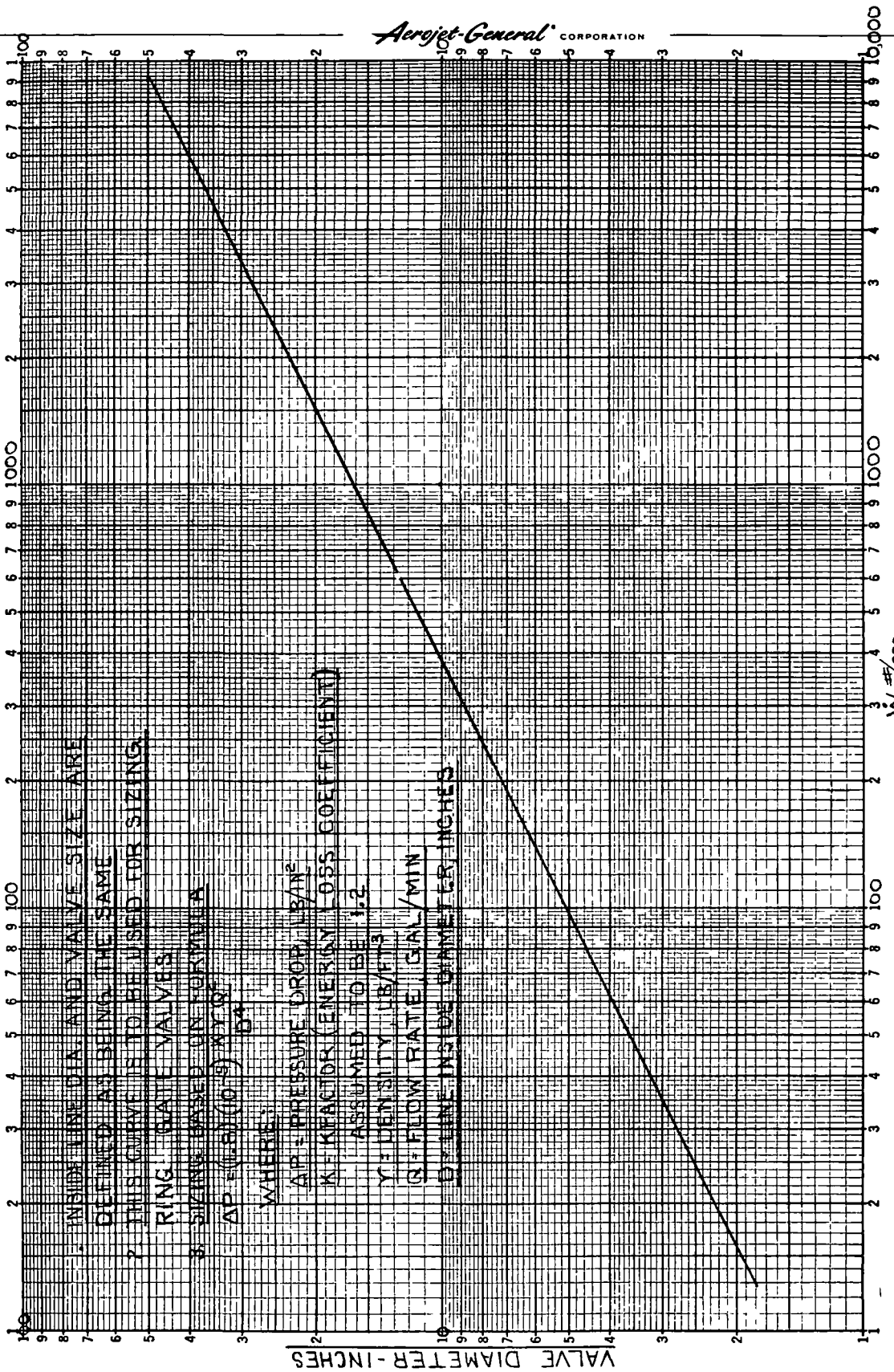

Valve Size vs K_W for Ring Gate Valve

Figure II L-10

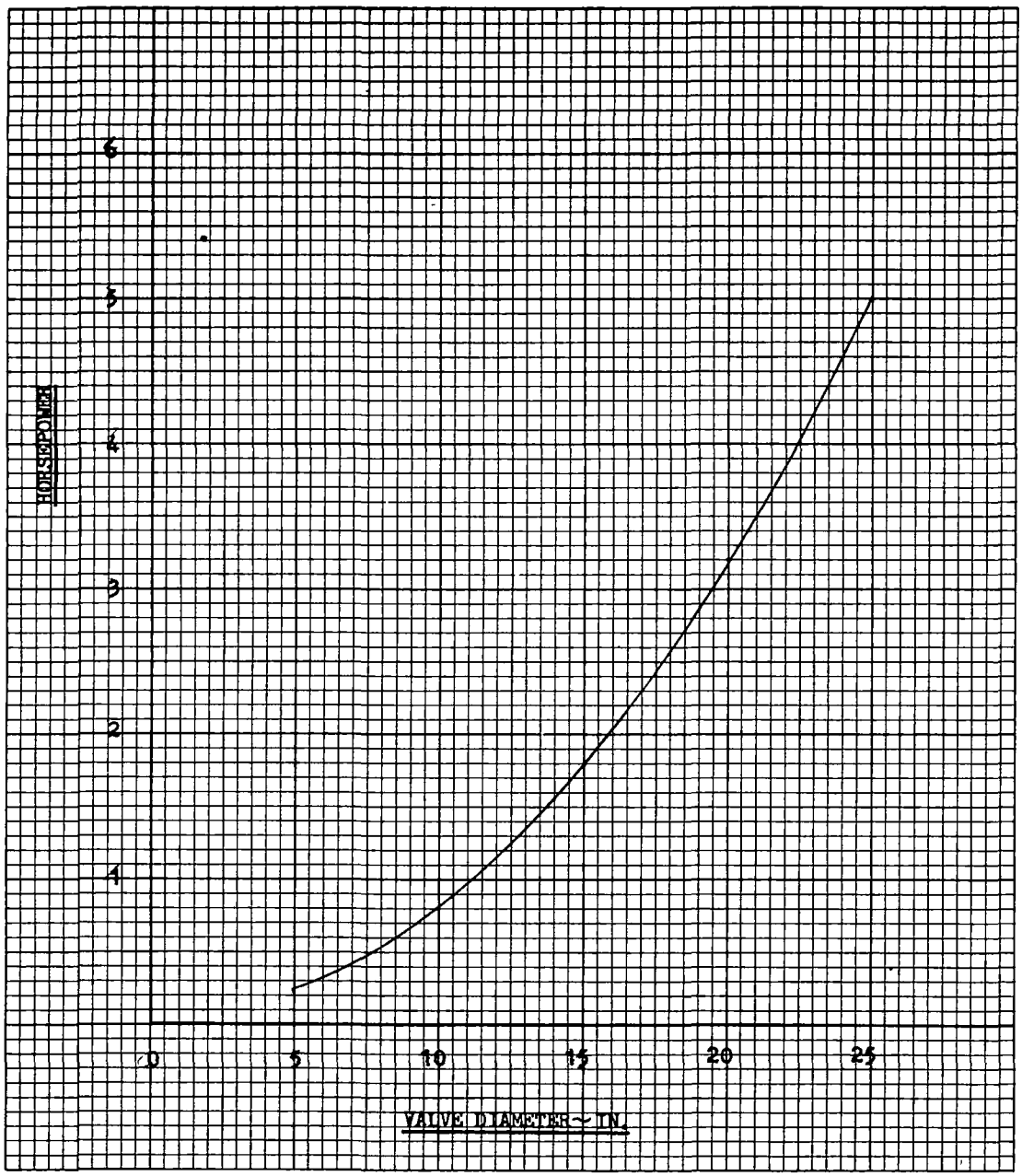

Horse Power vs Diameter for Ring Gate Valve (for a 1.0 sec opening time)

Figure II L-11

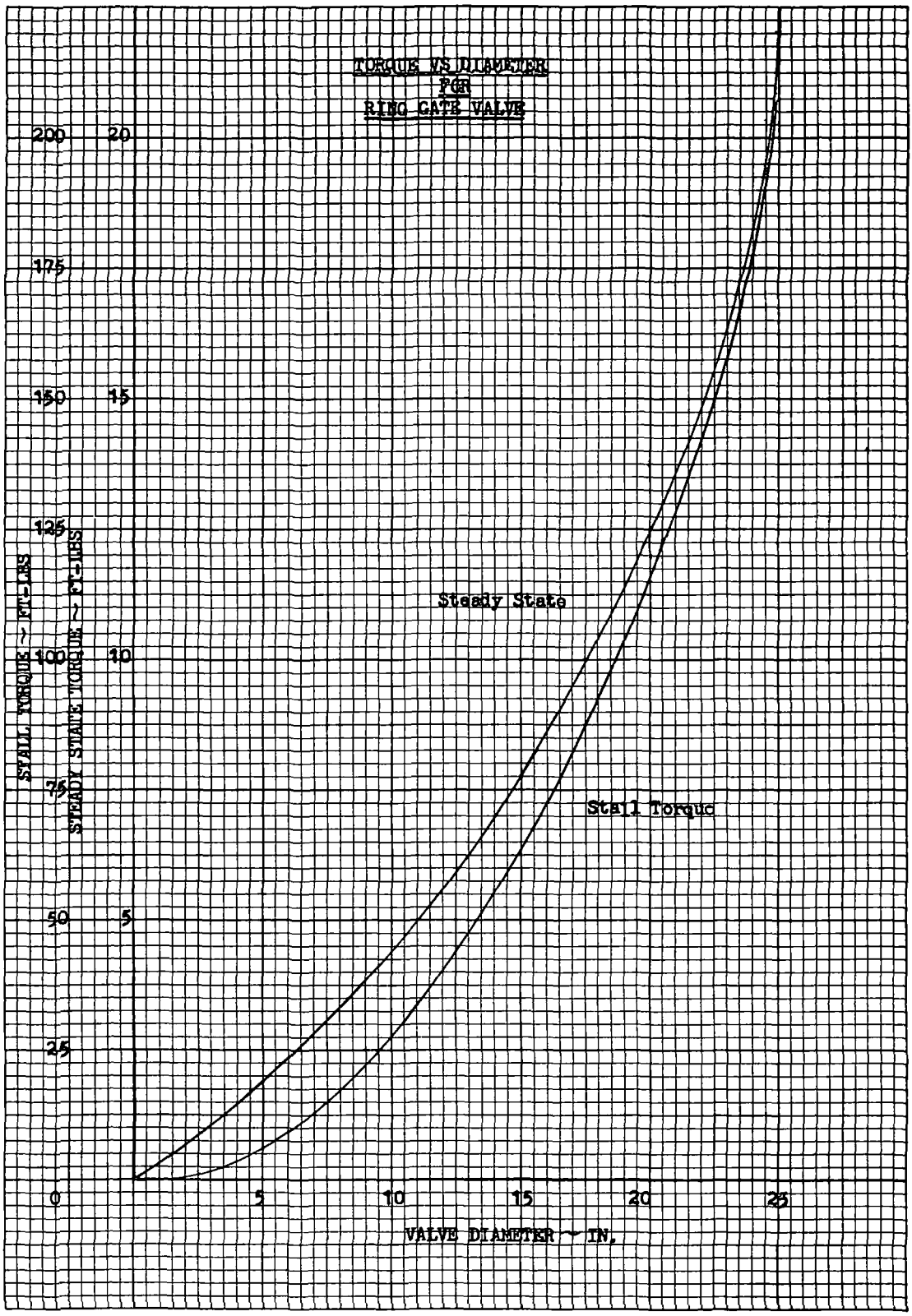

Torque vs Diameter for Ring Gate Valve

Figure II L-12

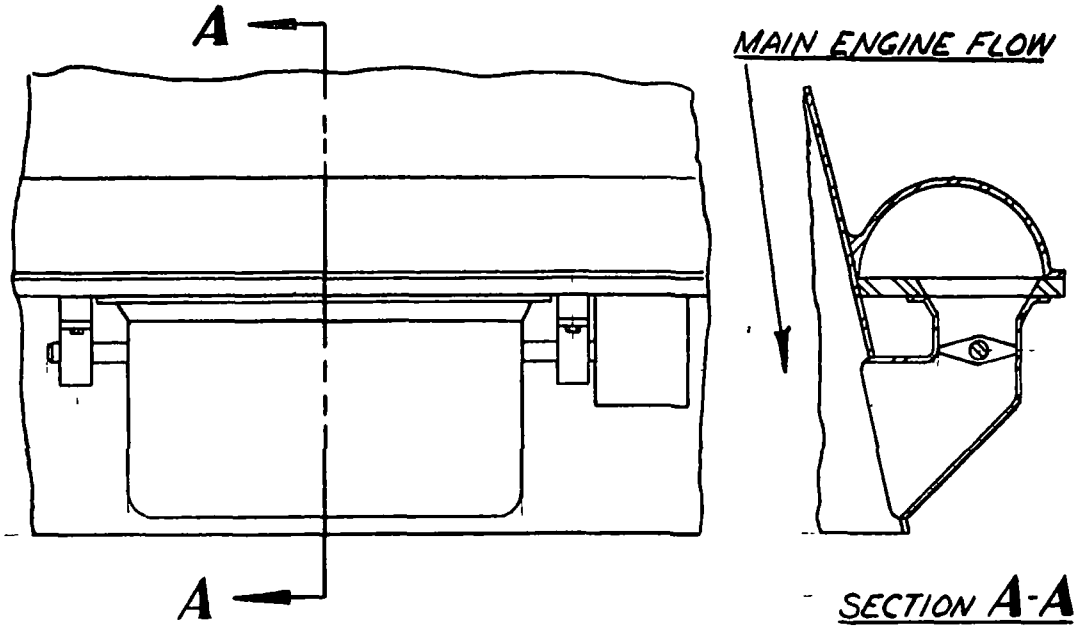

HOT GAS CONTROL FOR SECONDARY
INJECTION BUTTERFLY VALVE PRINCIPAL

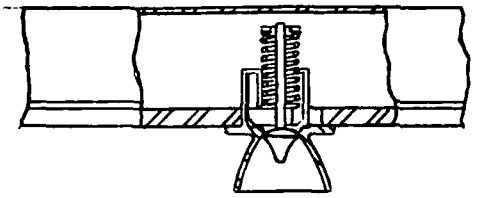

RELIEF VALVE NOZZLE ASSEMBLY

Hot Gas Control for Secondary Injection Butterfly Valve Principle

Figure II L-13

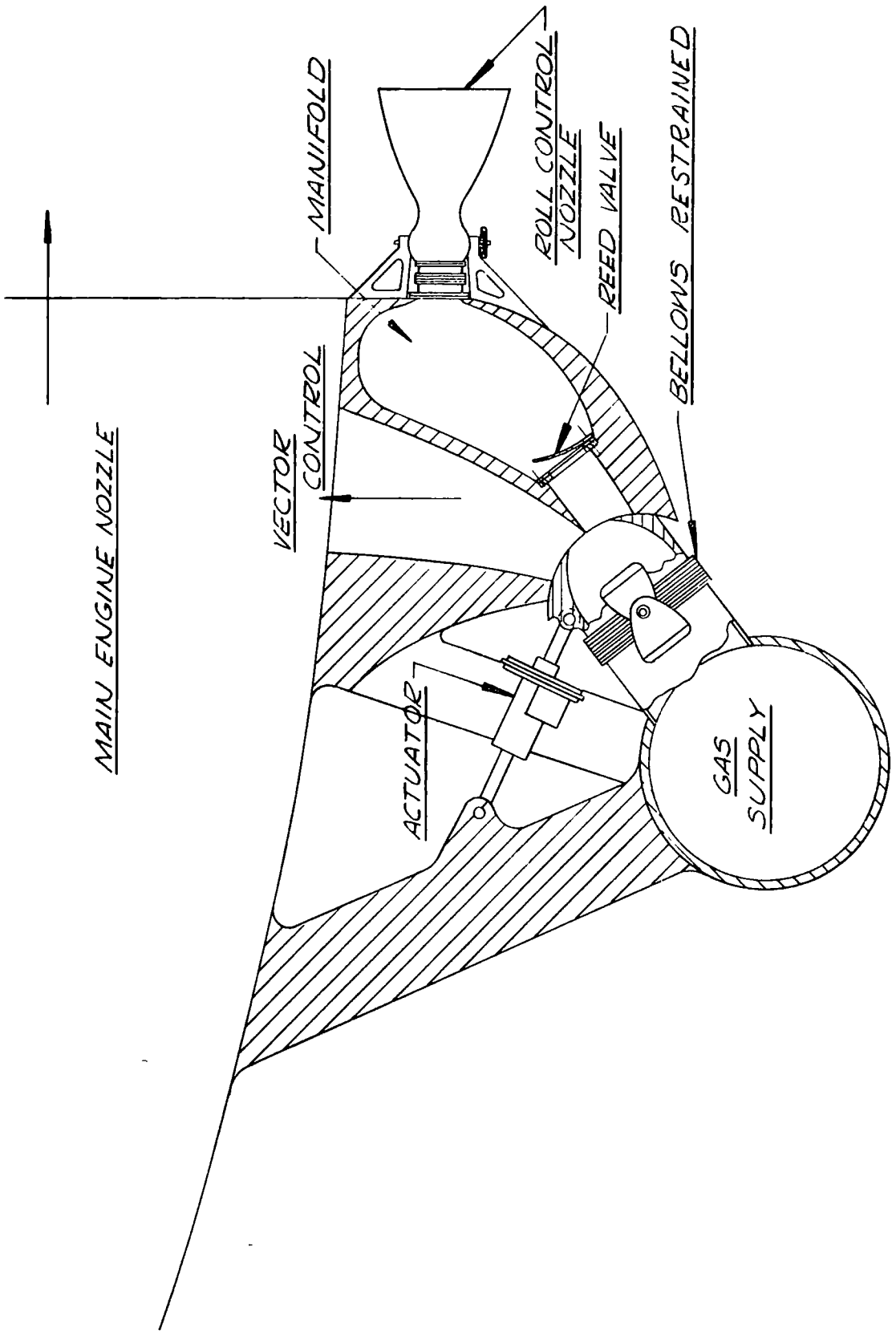

Hot Gas Control for Secondary Injection Jet Pipe Principle

Figure II L-14

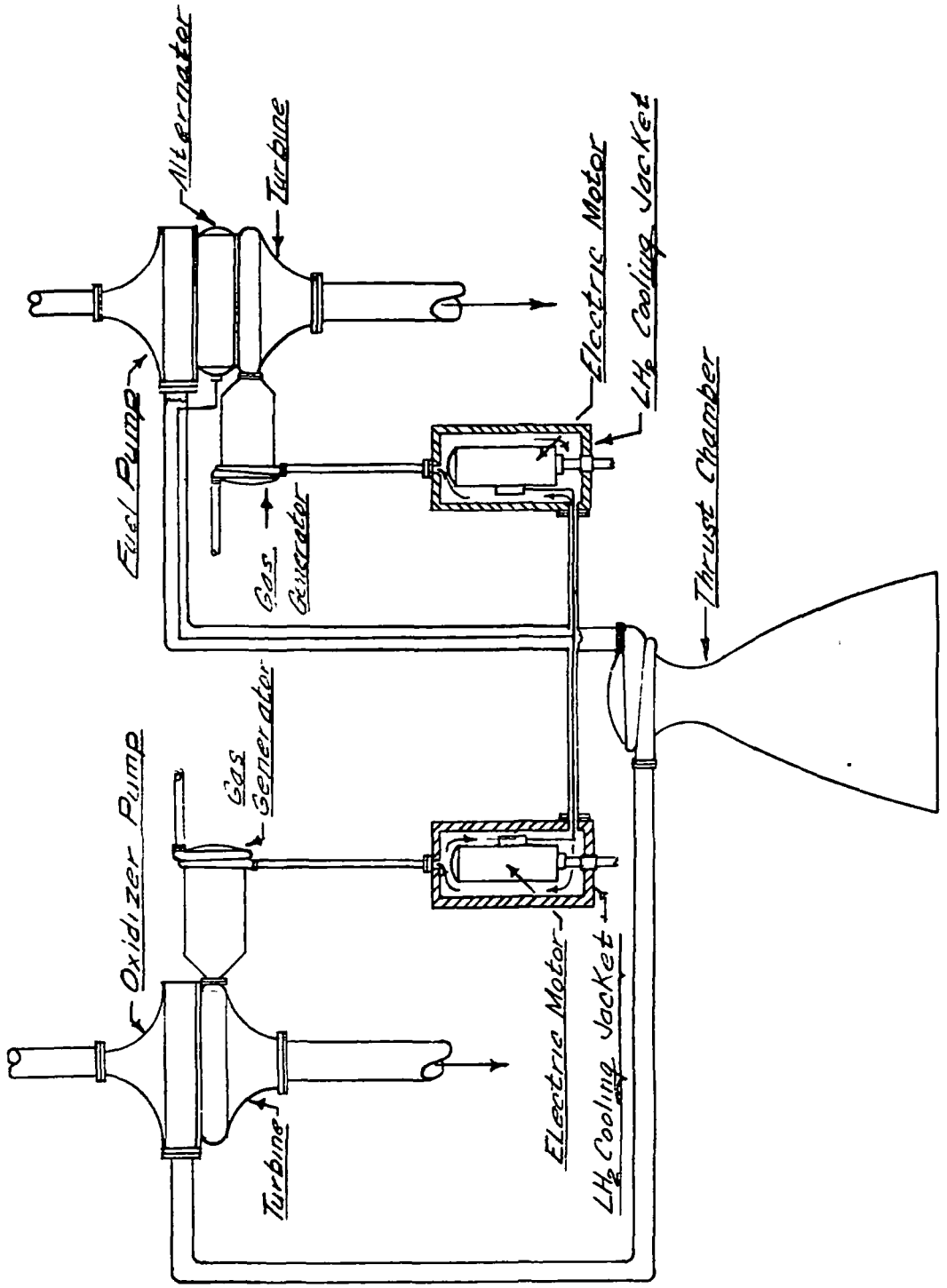

Electric Control LH_2 Cooled and Pressurized

Figure II L-15

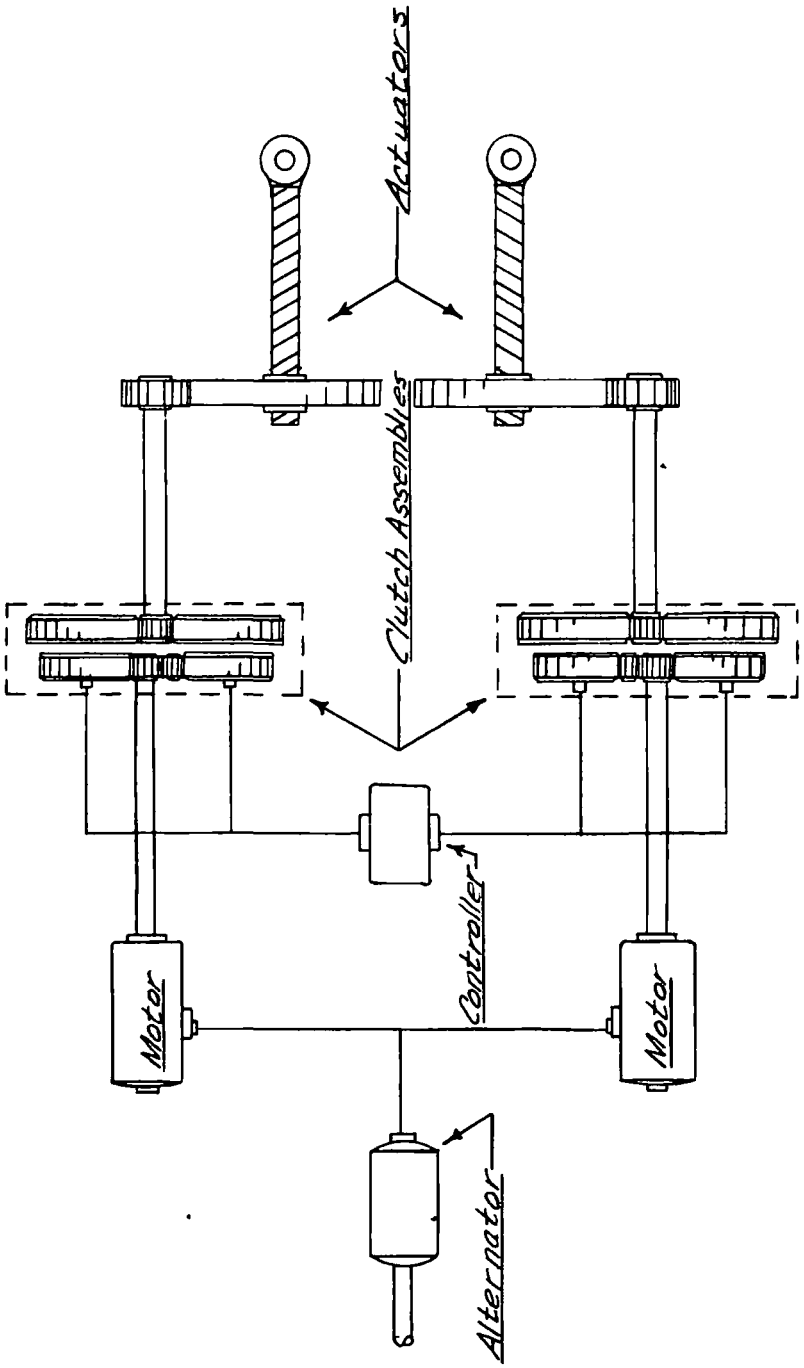

Gimbal Actuation System-Electric

Figure II L-16

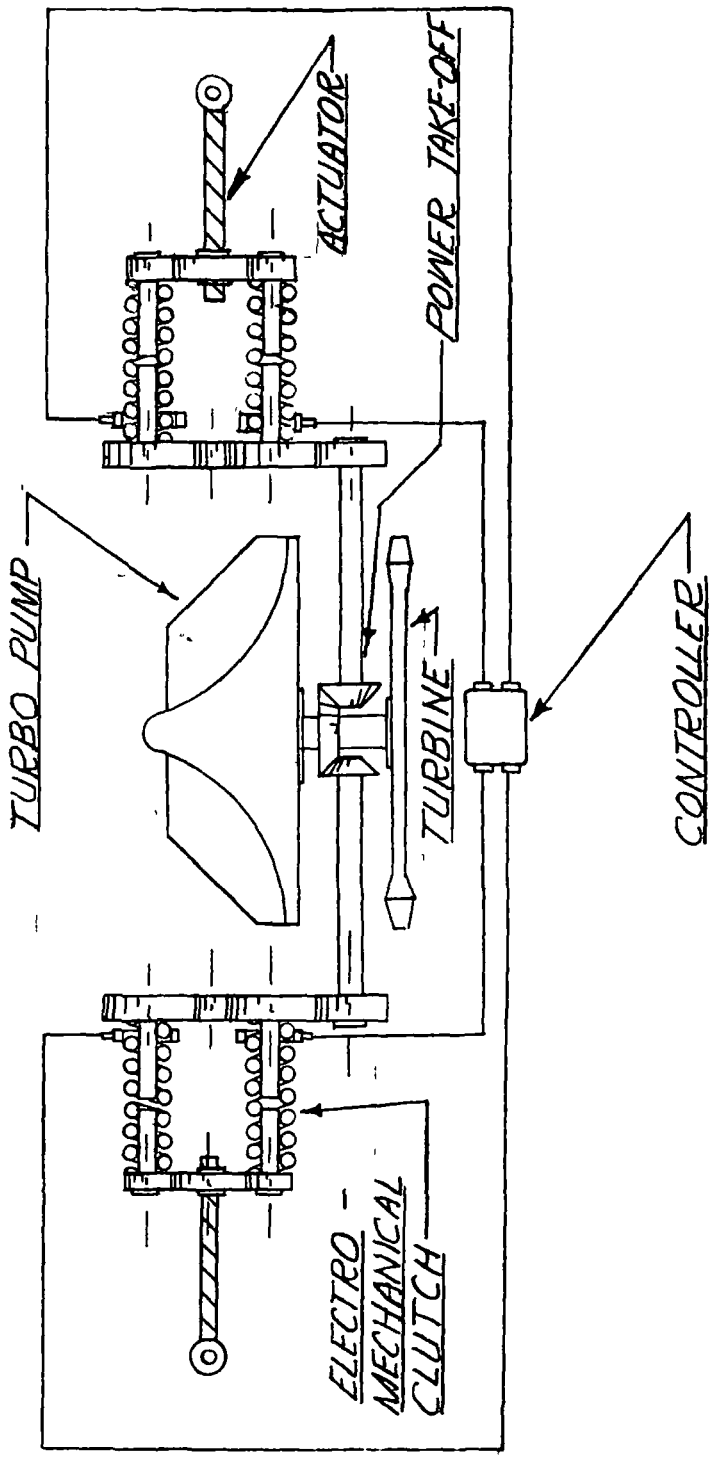

Gimbal Actuation System-Power Take Off, Direct Mechanical Control

Figure II L-17

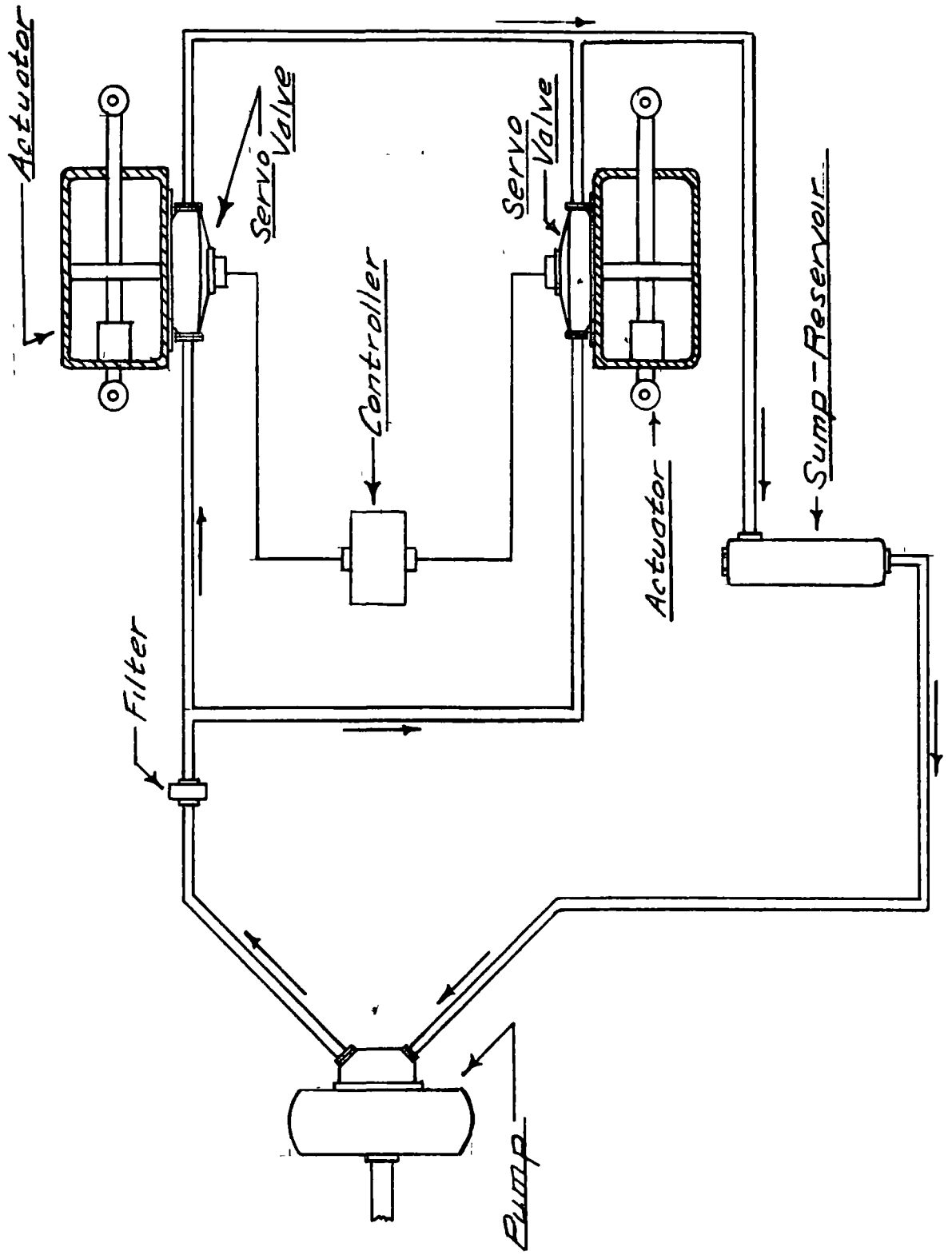

Gimbal Actuation System-Hydraulic

Figure II L-18

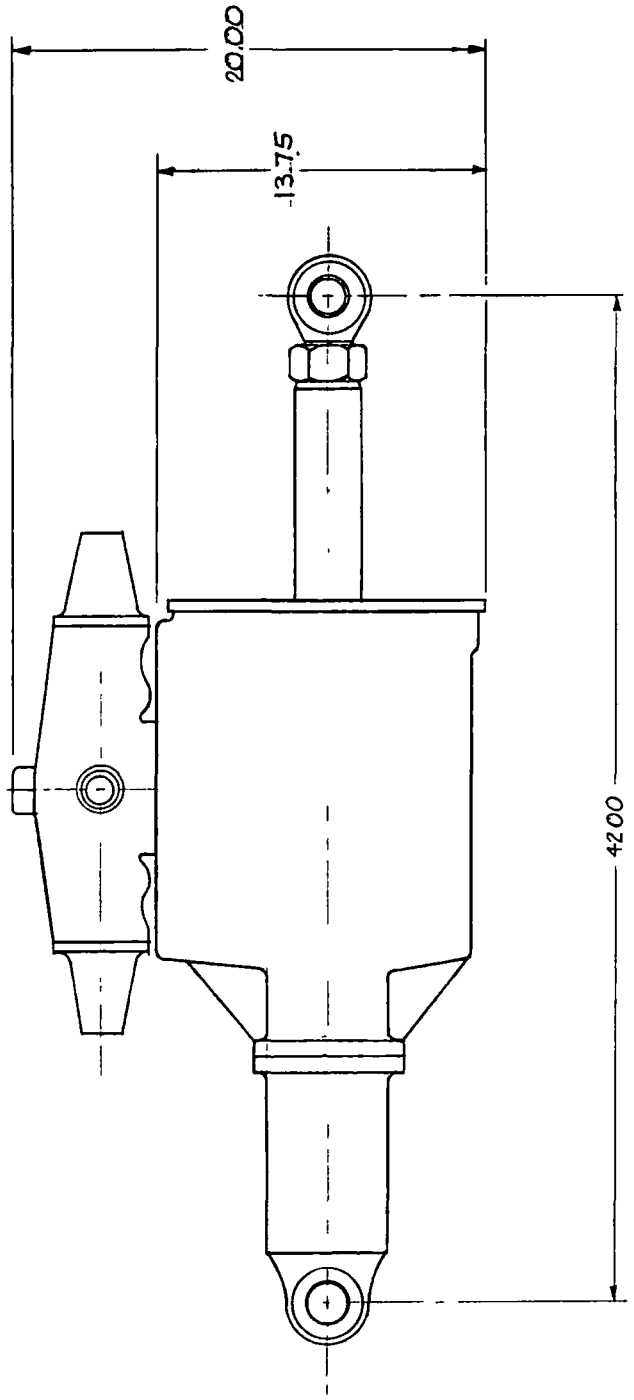

1 SUPPLY PRESSURE 3000 PSI
2 FLUID HYDRAULIC OIL OR EQUIV
3 WEIGHT 33.5 44 LBS
4 STROKE ± 4 IN
5 OVERTRAVEL .060.

Servo Actuator-3 Stage Hydraulic

Figure II L-19

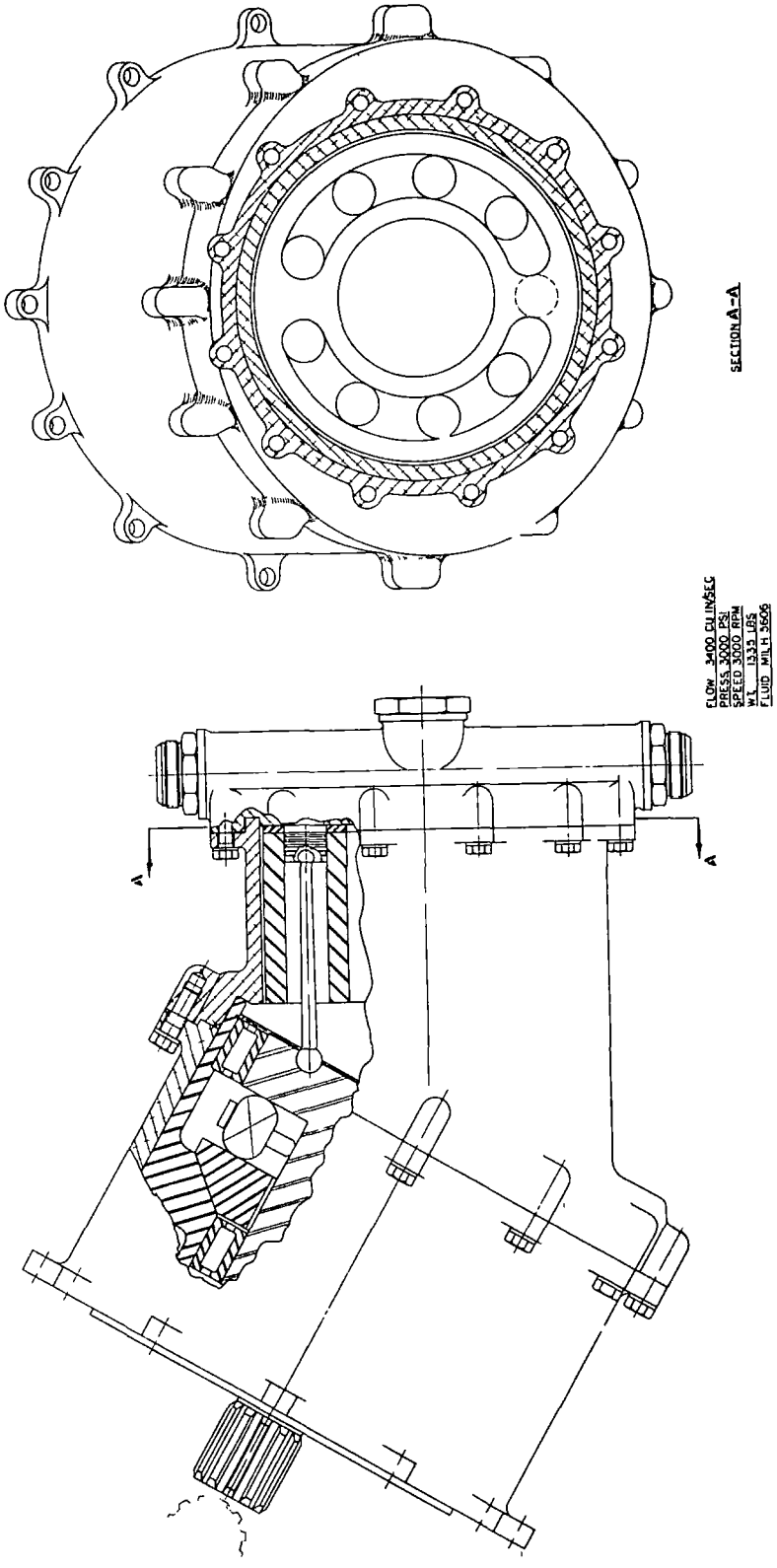

Multiple Piston Hydraulic Pump

Figure II L-20

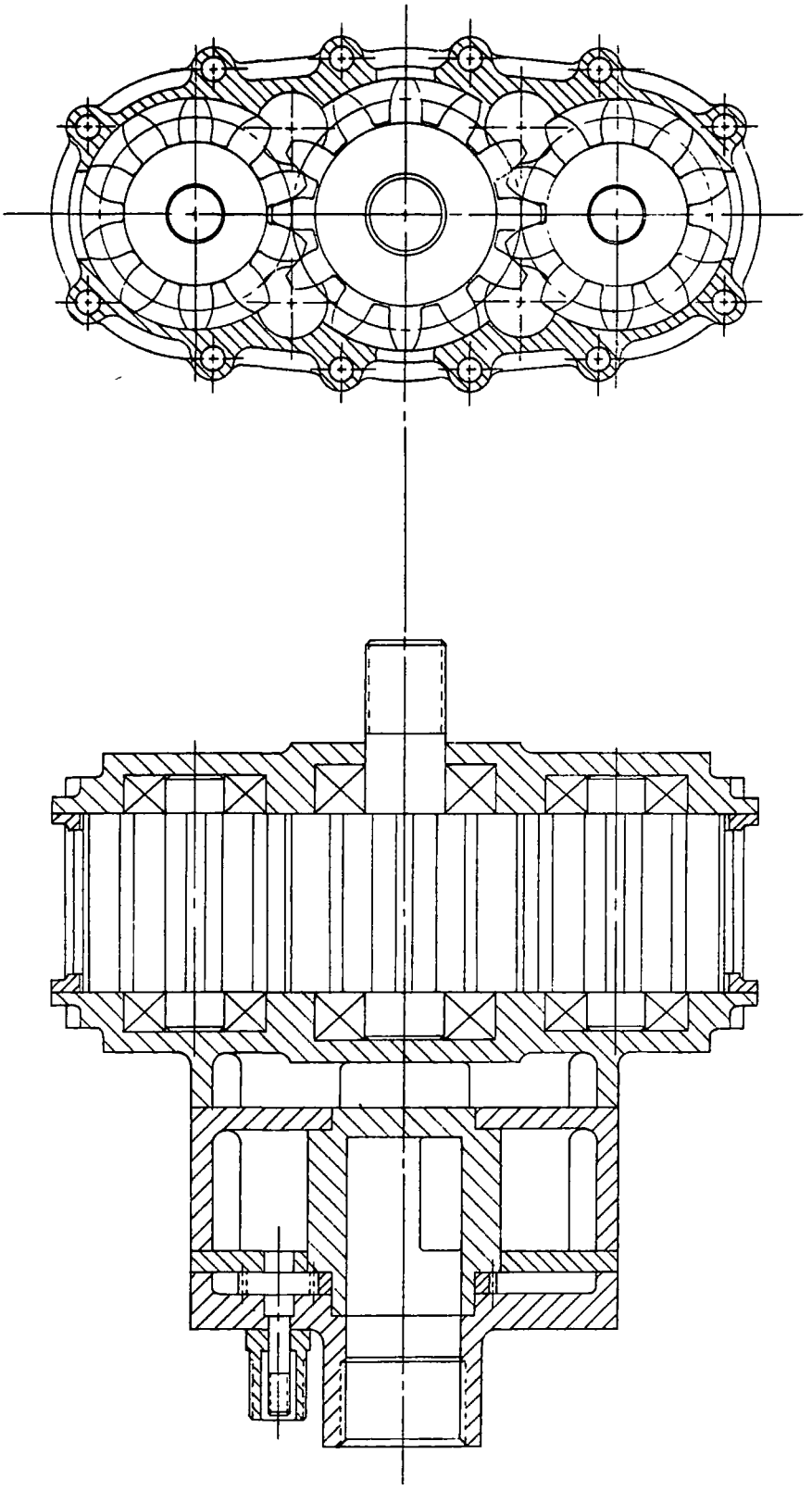

Pneumatic Gear Motor

Figure II L-21

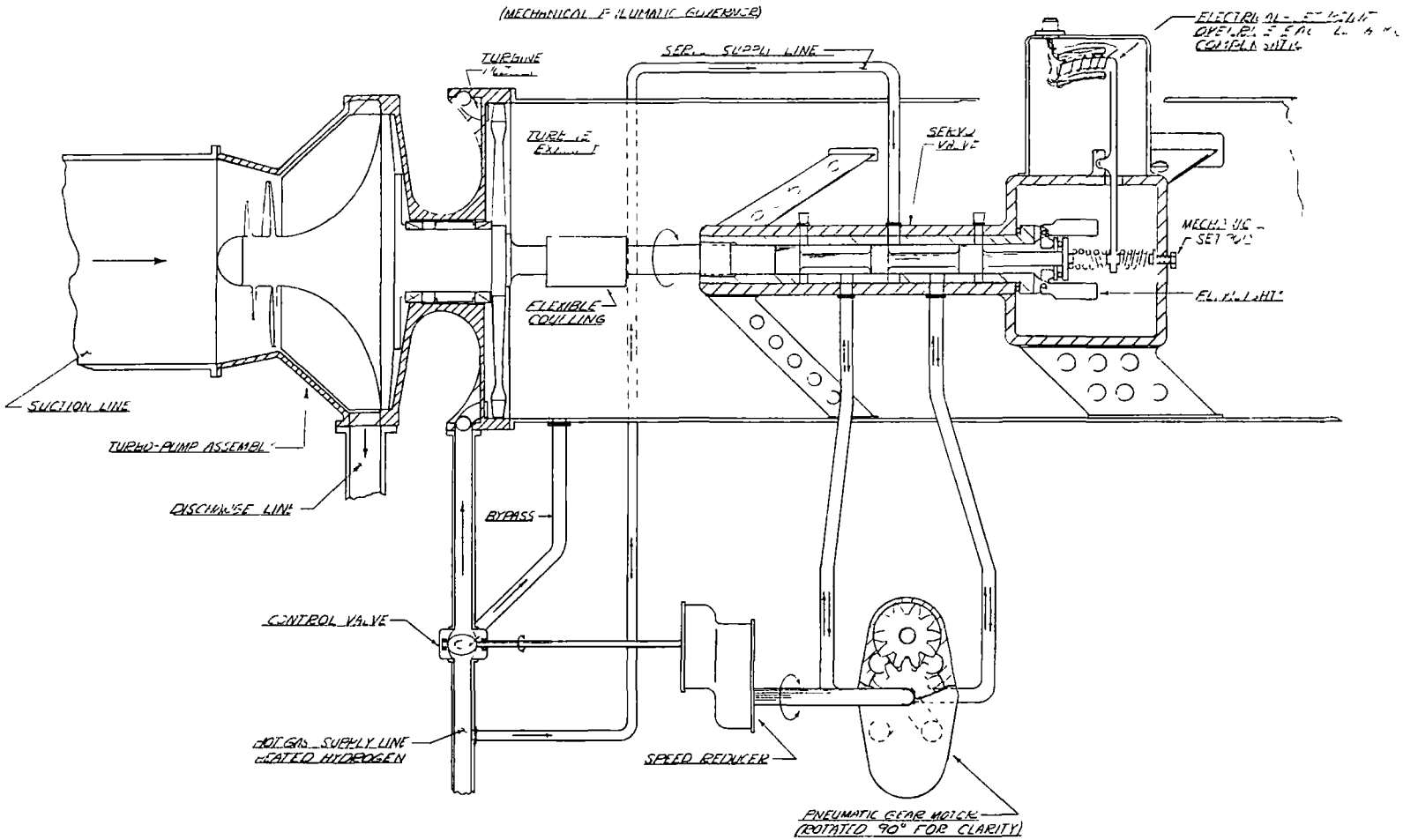

Schematic of Turbine Speed Control for Hydrogen Cycle

Figure II L-22

II, Concepts Considered (cont.)

M. AIRFRAME AND TANKAGE

1. Introduction

The airframe and tankage investigation was made to determine if there is an unconventional booster tankage configuration offering significant advantages over the standard vehicle, and what effect the airframe configuration might have on engine selection.

Initially, many unconventional configurations were considered. The effect of various airframe design criteria upon engine selection was evaluated. Preliminary designs of several configurations were made to establish weight and cost data. Also, different materials were evaluated.

A subcontracted investigation was conducted by the Boeing Airplane Company. Results of this study are reported as Volume 5 of this report. A non-funded airframe study conducted by The Martin Company is presented as Volume 6.

2. Summary

An evaluation of unconventional configurations in the airframe and tankage phase of this investigation revealed that conventional cyclindrical tanks are the best configuration for pump-fed rocket systems. The influence of these tanks upon engine system selection has been shown to be of secondary importance. Any of the more promising engine systems can be adapted to cylindrical tanks by using the proper interface structure.

II, M, Airframe and Tankage (cont.)

Because of the man-rating consideration, it was assumed that aerodynamic neutral stability was required. This is most easily obtained by the use of a conical skirt at the base of the booster stage.

Single tanks have been shown to be superior to clustered tanks from the standpoint of weight and complexity.

3. Design Considerations

Several design considerations were weighed in the airframe analyses. A summary of the considerations used by the Boeing Airplane Company, The Martin Company, and Aerojet-General is presented in the following discussion. Where it has been concluded that a consideration has little influence upon engine system selection, further study was not made. More detailed discussions of the design considerations are presented in Volumes 5 and 6 of this report.

a. Man-Rating Design Criteria

The application of man-rating criteria to large boosters has two effects upon the design approach. First, the design objectives must include a safe margin of aerodynamic stability. Secondly, the material stress factor must be sufficiently high for manned rating.

Neutral aerodynamic stability was assumed to be a requirement. The Boeing Airplane Company work shows that this can best be attained with a conical skirt at the base of the booster.

The Aerojet-General Corporation's comparison of configurations was based upon safety factors of 1.25 for yield and 1.5 for ultimate. These factors have been previously established for use in vehicles

II, M, Airframe and Tankage (cont.)

having manned applications. However, recent projects (Dyna Soar and Saturn S-II Stage) have used a safety factor of 1.4.

The Martin Company data associated with this report used as an ultimate safety factor, 1.25, while the Boeing Airplane Company used 1.4, which is consistent with the Dyna Soar program. The magnitude of the safety factor is relatively unimportant for Task 1 comparison purposes, and the Aerojet-General airframe comparison has been substantiated by both Boeing and The Martin Company efforts.

b. Design Loads

Ground winds, launch, and burnout loads were investigated considering the effects of axial loads, bending moments, and internal pressure. It was assumed that the vehicle must have free-standing capability on the launch pad without tank pressurization and with any combination of propellant tanks filled.

Handling and transportation loads were assumed to be common to all systems and, consequently, were not critical design considerations.

II, M, Airframe and Tankage (cont.)

c. Airframe Dynamics

Topics covered under a thorough airframe dynamics study include: vehicle vibration modes; vehicle pitching and yawing motion, as well as related attitude control requirements; and propellant sloshing--along with their interrelationships. A comprehensive study of the related effects was not within the scope of this study, however, preliminary conclusions have been drawn.

Because some of the engine systems considered in this investigation can provide more thrust-vector angle than others, the attitude control requirement, as it affects engine selection, will be discussed.

Vehicles of conventional configuration are aerodynamically unstable. Present day ICBMs, which are also aerodynamically unstable, are controlled with thrust-vector control angles of 3 to 5°. Conventional configuration vehicles in the 1-6-million-lb-thrust range can also be controlled with 3-5° of thrust-vector angle. Pitching natural frequency in this thrust range is on the order of 0.1 to 0.5 cps.

It has also been concluded from these investigations that a parametric study over a large thrust range does not provide practical information concerning required thrust-vector control. This conclusion has been reached because of the difficulty in scaling the significant parameters from one thrust level to another. These parameters are:

Vehicle configuration, including the number of stages, required fins or wings, and payload configuration;

Propellant selection and tankage arrangement that affect mass, center-of-gravity location, and mass moment of inertia;

II, M, Airframe and Tankage (cont.)

Type or mode of control which, in turn, depends upon allowable angle of attack as well as permissible path deviation.

The man-rating consideration associated with large vehicles requires aerodynamic static stability. This can be accomplished by the addition of fins or conical skirts to the booster stage. Such an addition reduces thrust-vector angle requirements to those necessary for guidance and thrust-vector misalignment. For large booster applications, 1 to 2° is adequate to satisfy these requirements.

Further discussion of vehicle dynamics is contained in The Boeing and The Martin Company reports (Volumes 5 and 6).

d. Aerodynamic Heating and Insulation

Previous investigation has shown that aerodynamic heating of non-recoverable booster has little effect upon structural or configurational design. While insulation will affect detail design, it was assumed to be a problem common to all airframe configurations and was not included in the configuration comparison.

The airframe comparison was with room temperature properties of the materials. Strength increase resulting from use at cryogenic temperatures and strength decrease from aerodynamic heating were neglected with no expected effect upon the conclusions.

II, M, Airframe and Tankage (cont.)

e. Materials

For the configuration evaluation of Section II,N,4, tankage designs using 2014-T4 aluminum, 9%Ni, steel, and A-110-AT titanium were compared. It was concluded that aluminum tanks offered the best compromise between weight and cost.

The weight saving afforded by titanium is not significant enough to offset the increased cost in a single-mission application. However, consideration of booster recovery places less emphasis upon tankage cost and indicates a possible advantageous use of titanium.

The use of high strength-to-weight ratio materials has been considered. Examples of materials presently undergoing research are fiber glass reinforced plastics, beryllium, and molybdenum. It appears that, through improved technology, strength-to-density ratios of 1.5 to 3 million in. may be attained. This compares to an upper limit of approximately 1 million in. for conventional materials. Advantageous use of such materials may be limited when applied to conventional configurations. For example, structurally, the fiber glass reinforced plastic allows a very thin tank wall; however, because of its porosity, a tank liner is necessary and tank insulation is still required. Buckling instability criteria may require greater wall thicknesses, which again leads to the loss of high strength-to-weight ratio advantages.

Such materials may offer new approaches to the recovery aspect of large boosters; however, further research is needed to fully evaluate their potential.

II, M, Airframe and Tankage (cont.)

f. Fabrication and Logistics

As thrust levels increase, the fabrication and transportation of propellant tanks as well as the more standard weight and performance criteria, must be considered in the design. This is a result of the problems associated with the handling of very large objects.

Clustered cylindrical tanks offer a solution to this problem because individual tanks can be kept to diameters within transportation and fabrication limitations. However, it has been concluded that, for tanks in two-million pound thrust range, clustering is not required for land or water transportation or fabrication considerations. It has also been shown in Section II,M,4,b, that clustering of tanks imposes vehicle weight and reliability penalties.

For diameters up to 34 ft tankage can be transported from the Aerojet facility to launch facilities over land and water, with minimum travel over highways. However, in going to tank diameters greater than 34 ft, additional consideration must be given to clustering because transportation limitations could become formidable.

g. Recoverability

Airframe design of an orbital booster vehicle will be affected by recovery considerations. Only if the recovery device (e.g., a parachute) is independent of the airframe design will the recovery considerations be of little significance to the airframe design. When the airframe itself contributes to recovery (e.g., a winged booster with fly-back capability), such considerations may contribute important criteria to the airframe design. Investigation of the latter class of vehicles would be based upon mission requirements and airframes

II, M, Airframe and Tankage (cont.)

with secondary emphasis upon engine selection. A few typical examples are shown in the accompanying the Boeing Airplane Company report.

4. Unconventional Concepts

a. Large Booster Tank Investigation

(1) Many of the unconventional concepts considered were eliminated because they were too heavy or impractical. Several of the better unconventional tankage arrangements were evaluated and compared with the standard vehicle of this study. Unconventional tank arrangements evaluated were toroidal tanks, tandem spheres, clustered spheres, and clustered cylinders. An estimated weight comparison for these configurations made of aluminum is shown in Figure II M-1.

The toroidal tanks, tandem spheres, and clustered spheres were compared on the same basis. Drawings at the 6-million-lb thrust level are shown in Figures II M-2 through II M-4. The estimated weights for these configurations are:

Toroidal tankage (lb)	197,000
Clustered spheres (lb)	227,000
Tandem spheres (lb)	102,000

The tandem spheres obviously offer significant weight savings over the other two configurations. The use of titanium tanks in the weight estimate of the tandem spheres and aluminum in the other two is not expected to affect this conclusion. It is assumed that this conclusion is also applicable at the 2-million-lb level.

II, M, Airframe and Tankage (cont.)

(2) A comparison has been made in Section II M 5 between clustered cylinders and the tandem cylinders of the standard configuration at the 2-million-lb thrust level. The following weight estimates were made: clustered cylinders--39,700 lb; tandem cylinders--31,300 lb.

It is apparent that tandem cylinders (the standard configuration) are superior to clustered cylinders in weight considerations.

(3) The tandem cylinder design was compared with the tandem sphere design at the 2-million-lb thrust level. Figure II M-5 shows a tandem sphere design and associated weight for a 2-million-lb booster with titanium tanks. Including the same components in each design gives the following weights: tandem spheres--36,000 lb; tandem cylinders--32,900 lb.*

These calculations show the tandem spheres with titanium tanks to weigh approximately 10% more than the standard vehicle tankage.

It has been established that no unconventional tank shape is superior to the cylindrical tanks of the standard configuration for pump-fed systems. It has also been shown that several unconventional configurations impose weight penalties. Therefore, the design comparison of various engine-airframe combinations was made with cylindrical tankage.

b. Clustering

Clustering of propellant tanks is often suggested for large booster rockets, however, this investigation has determined that clustering imposes reliability and weight penalties upon the system. The weight estimate in

* This weight corresponds to the standard vehicle tank weights in Table II F-1 minus engine thrust structure and interstage structure weights.

II, M, Airframe and Tankage (cont.)

Figure II M-1 shows that the clustered tankage structure imposes a weight increase of approximately 20% over the standard vehicle. Because of the increased system complexity, a reliability degradation should also be expected.

c. Lighter-Than-Air Structures

The ultimate application of high strength-to-weight ratio materials leads to the idea of lighter-than-air structures. Such structures would not only increase system performance but would greatly aid the recovery aspect of large boosters.

Because all structural materials are much heavier than air, the lighter-than-air structure must be an enclosure from which air is displaced by a vacuum or with a lighter-than-air gas, such as hydrogen. The weight savings of a vacuum over hydrogen amounts to only .0000032 lb/cu in. The vacuum structure would also require more structural stiffeners or additional wall thickness to prevent collapse at atmospheric pressure, therefore, hydrogen gas at a positive pressure slightly above atmospheric would be preferable. For a structure to be buoyant in air, 13.3 cu ft of air must be displaced for each lb of structural weight.

Using the simple right circular cylinder as the basic structure--from which larger structures can be made by various multiples or combinations--the effect of density upon wall thickness, and the effect of wall thickness with various length-to-radius ratios can be seen in Figures II M-6 through II M-8. In each graph, the volume and structural weight of the cylinders are constant, with the structural weight being offset by the displacement of air with hydrogen to give a lighter-than-air structure.

II, M, Airframe and Tankage (cont.)

The following materials were used for this graphical illustration:

Material	Density lb/cu. in.	Modulus of Elasticity (psi)	Approximate Tensile Strength (psi)
Beryllium	0.066	40,000,000	40,000
Aluminum	0.098	9,600,000	25,000
Steel	0.29	30,000,000	150,000
Titanium	0.165	15,500,000	120,000

The first item apparent from these graphs is that the maximum wall thickness permitted for a lighter-than-air right circular cylinder occurs for all the structural materials when the ratio of length to radius is approximately 2. Ratios above and below this would require thinner walls to displace the same volume using the same total structural weight.

The second item apparent from these graphs--when using the optimum ratio of length to radius for a right circular cylinder--is that the maximum wall thickness allowable for steel is 0.0003 in., for aluminum 0.0009 in., and for beryllium 0.0013 in. For titanium (not illustrated) the maximum wall thickness would be approximately 0.0006 in. Conclusions drawn from these graphs would indicate that the strength-to-weight ratio of a structural material is not necessarily the major factor. Rather, it is a combination of density, compressive strength, modulus of elasticity, and tensile strength of the material. The limiting factor is the minimum sheet thickness that can be satisfactorily produced and fabricated to resist bending or buckling loads of larger structures (i.e., propellant tanks).

II, M, Airframe and Tankage (cont.)

From the illustrated data, it becomes apparent that beryllium offers the optimum potential for large lighter-than-air structures because the maximum allowable wall thickness for any designed structure can be 4.5 times that of steel and the ability of beryllium to resist bending or buckling loads is greater than any of the structural materials that could be considered for this application.

To pursue this approach for a realistic application to future structures, the following development work in three basic areas would be required to obtain positive results prior to final design applications:

Methods of manufacturing ultrathin sheets of the structural materials in the range of 0.0002 to 0.0015 in,

Instruments with improved limits of accuracy for measuring tolerances and determining the quality of the material on a microscopic scale;

New or improved equipment, methods, and techniques for joining the ultra-thin wall sheets to provide structural integrity (i.e., ultra-sonic, pressure diffusion, or electron beam welding).

5. Evaluation of Promising Configuration

Preliminary review of various shapes has indicated that, for pump-fed systems, a cylindrical tankage configuration is structurally and economically the most efficient. For pressure-fed systems, with tank pressures of 300 to 500 psia, spherical tanks become the most efficient.

Because pressure-fed systems have been shown unattractive in Section II D of this report, the remaining tankage design was carried out with both

II, M, Airframe and Tankage (cont.)

single and clustered cylindrical tanks. Seven specific configurations were evaluated to establish airframe data for the standard vehicle, the single-stage-to-orbit vehicle, a clustered tankage vehicle, and a liquid-oxygen/RP-1 vehicle. Aluminum, steel, and titanium were each considered for tank design. The optimum material selection, considering cost and weight, was aluminum--as is shown in Tables II M-1 and II M-2. The following is a brief discussion of each design.

a. Standard 2-Million-Lb Cylindrical Tank (Figure II M-9)

This tankage is used for the standard configuration vehicle and is the basis for comparison with the other airframe designs. The material used was 2014-T4 aluminum. For cost estimates, fabrication was assumed to be accomplished with extruded sheet stringer combination panels. Tank wall thickness was reinforced locally to compensate for loss of strength in the welds.

A common head separates the fuel from the oxidizer. The oxidizer was placed above the fuel to obtain a more aerodynamically stable configuration. Insulation is sandwiched between the two tank heads and around the fuel tank only.

The lower fuel tank head is of conical shape and is reinforced by internal stringers. All loading for captive firing is reacted in this portion of the tank. The engine-tankage interface is the only area where the engine configuration has a direct bearing upon the characteristics of the tankage configuration. The Boeing analysis also confirms that this is the area of fundamental difference in tankage for various systems. It is indicated that a 3,000-lb weight variation can occur with various interface structures.

II, M, Airframe and Tankage (cont.)

b. Cylindrical Separate Tanks

All details of this tank are similar to the standard tank, except separate tank heads are used to replace a common head. The intertank structure is aluminum. This configuration resulted in a 13% weight increase over the standard configuration and a 22% direct fabrication cost increase.

c. Standard Configuration, 9% Nickel Steel

This configuration is the same as the standard vehicle, except 9% nickel steel replaces aluminum. Table II M-2 shows a severe weight penalty associated with this material..

d. Standard Configuration, A-110-AT Titanium

Using the standard configuration and titanium as the material, weight and cost data were derived. Table II M-1 shows a factor of 2.75 in direct fabrication costs, and Table IIM-2 shows a slight weight savings.

e. Single-Stage-to-Orbit System (Figure II M-10)

The volume of the tankage was increased over the standard to provide propellants for the longer firing duration of 272 sec as compared to 188 sec for the standard vehicle. The L/D was increased to 4 instead of the standard L/D of 3. An ellipsoidal head was selected for the bottom of the fuel tank because this head configuration appears to be slightly superior to the conical head for use with engines having a forced-deflection nozzle.

II, M, Airframe and Tankage (cont.)

Preliminary weight analysis indicated that this tankage would weigh approximately 34,240 lb--or approximately 10% more than the standard tankage. The direct fabrication costs for this tank were not significantly different than those for the standard tank.

f. Clustered Tanks (Figure II M-11)

This tank configuration was investigated to determine the advantages or penalties resulting from clustering booster modules. The cluster investigated consists of four 500,000-lb tanks of 17.8-ft diameter. This tank diameter is approximately the diameter of second-stage tankage. To simplify the approach, it was assumed that the tankage detail, materials, and engine system details duplicated the standard, however, each booster would operate at the thrust level of 500,000 lb. This would allow an approximate evaluation of the penalties or advantages of engine-out conditions and the integrating structure required for clustering. A weight increase of approximately 20% over the standard configuration results from clustering. The preliminary analysis indicated that penalties associated with engine-out capability can be minimized by providing shear ties between the booster tankage. Direct fabrication costs are increased by a factor of 1.38.

An engineering drawing and an isometric view of the clustered booster concept are shown in Figures II M-12 and II M-13, respectively.

g. Liquid Oxygen/RP-1 Tankage

For weight comparison purposes, the tankage for a liquid oxygen/RP-1 system was designed and is shown in Figure II M-14. The weight of this tankage is also found in Table II M-2.

TABLE II M-1

COMPARISON OF TANKAGE FABRICATION COSTS

Tank Configuration and Description	Comparison, Total Direct Fab. Costs with Standard
2,000K, cyl, common tank heads (standard tank)	1.00
2,000K, cyl, separate tanks	1.22
2,000K, cyl, common tank head (9% N_1 Steel)	1.03
2,000K, cyl, common tank head (A-110-AT- titanium	2.75
2,000K, cyl, common head (single-stage-to-orbit)	1.19
2,000K, cyl, common head (modular booster concept)	1.38

Note: K = lb thrust x 1,000

TABLE II M-2

COMPARISON OF TANKAGE WEIGHTS

Tank Configuration and Description	Interstage Structure Wt (lb)	Fuel Tank Wt (lb)	Fuel Tank Comparison with St'd	Oxidizer Tank Wt (lb)	Oxidizer Tank Comparison with St'd	Total Tankage Weight (lb)
1. 2000K-cyl-common tank heads (standard tank)	-	25,470	1.0	5,875	1.0	31,345
2. 2000K-cyl-separate tanks	3,925	24,420	0.96	7,025	1.195	35,370
3. 2000K-cyl-common tank head (9% N_1 steel)	-	36,505	1.43	7,120	1.21	43,625
4. 2000K-cyl-common tank head (A-110-AT titanium)	-	23,875	0.938	5,285	0.900	29,160
5. 2000K-cyl-common head (single-stage-to-orbit)	-	26,590	1.045	7,650	1.300	34,240
6. 2000K-cyl-common head (modular booster concept)	4,750	28,660	1.125	6,310	1.074	39,720
7. 2000K-cyl-common head (LO_2/RP-1 propellants)	-	14,770	0.580	9,700	1.651	24,470

K = lb thrust x 1,000

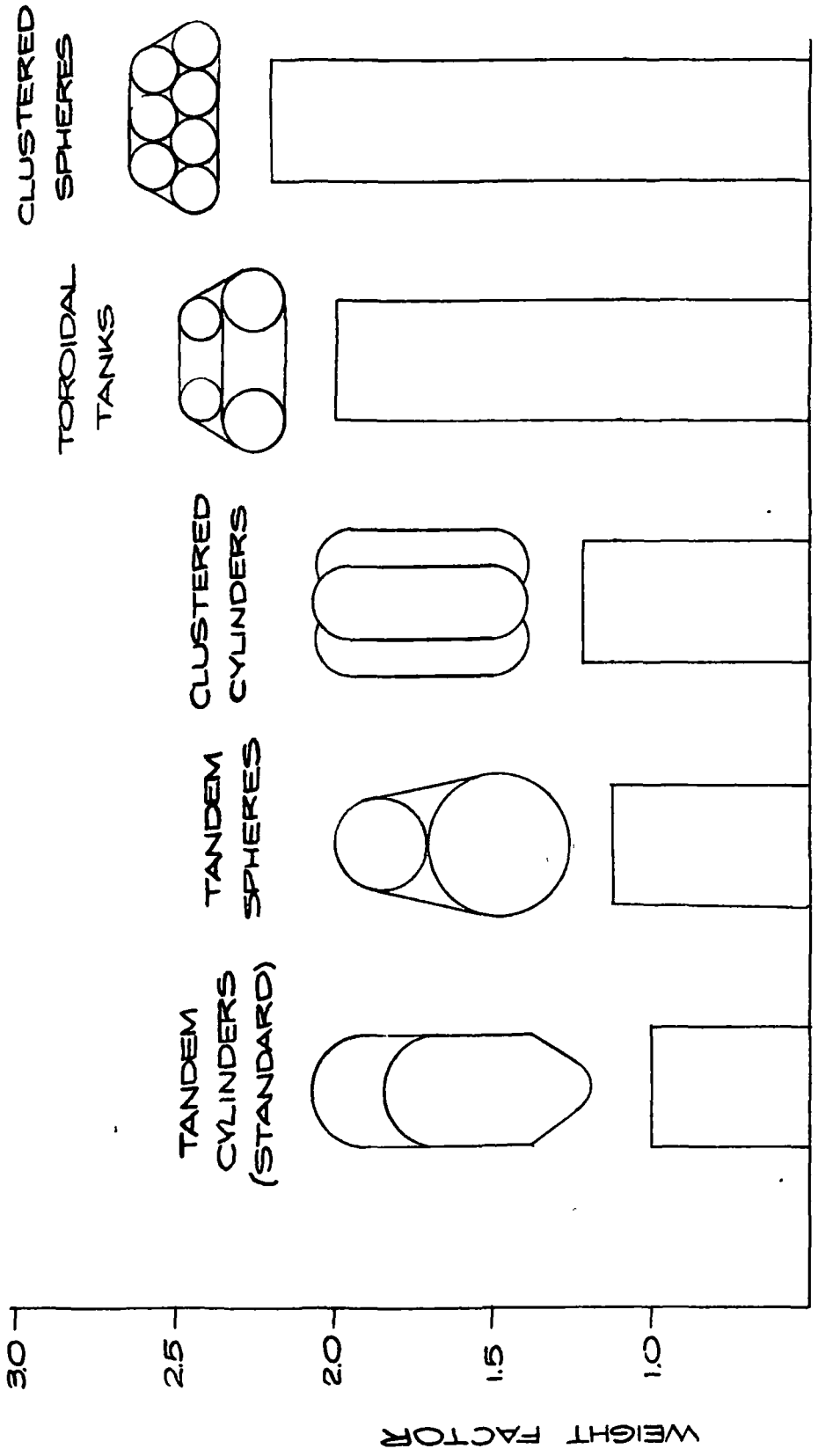

Tankage Weight vs Configuration

Figure II M-1

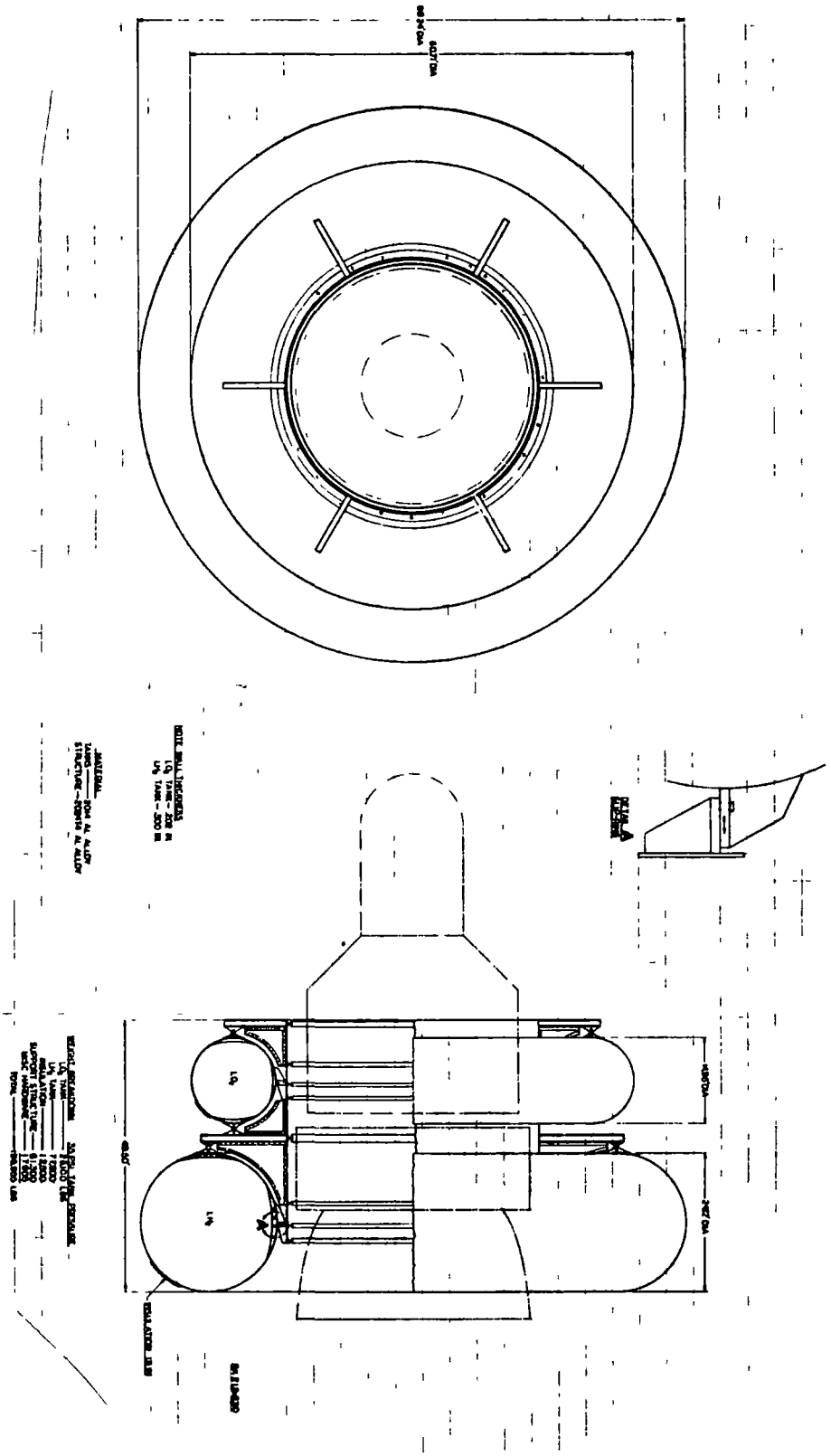

Toroidal Tank Configuration, 6-Million-lb Thrust

Figure II M-2

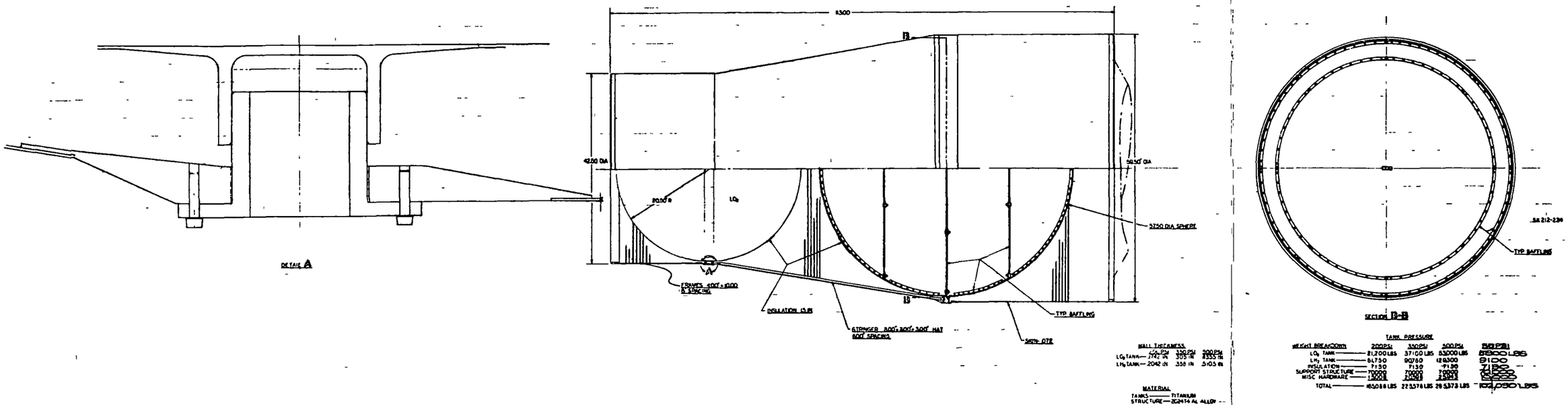

Tandem Sphere Tank Configuration, 6-Million-lb Thrust

Figure II M-3

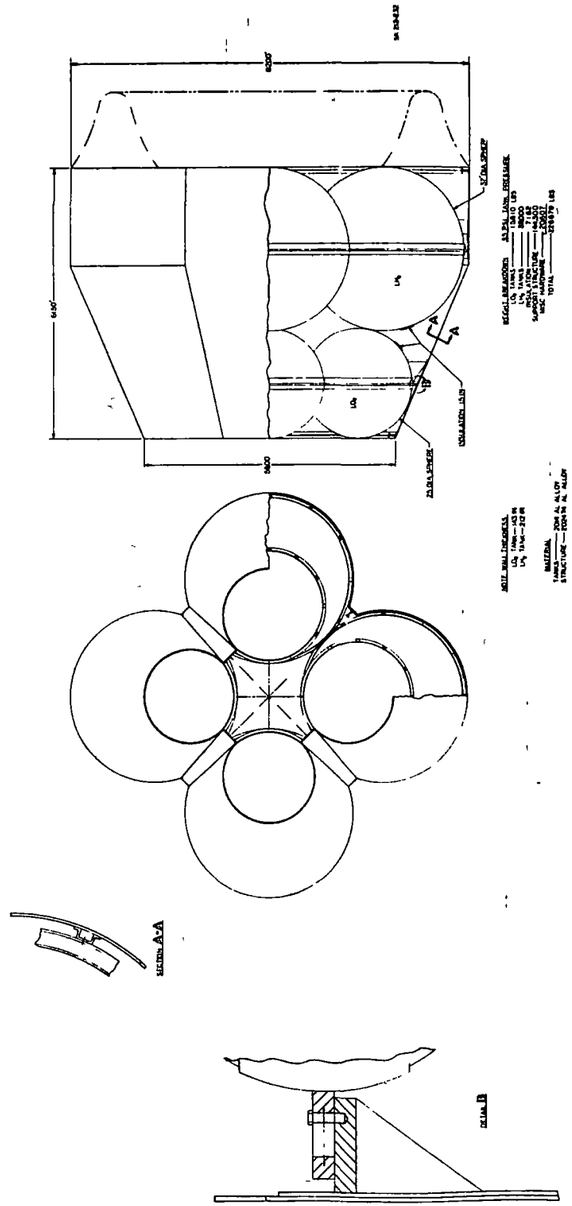

Clustered Sphere Tank Configuration, 6-Million-lb Thrust

Figure II M-4

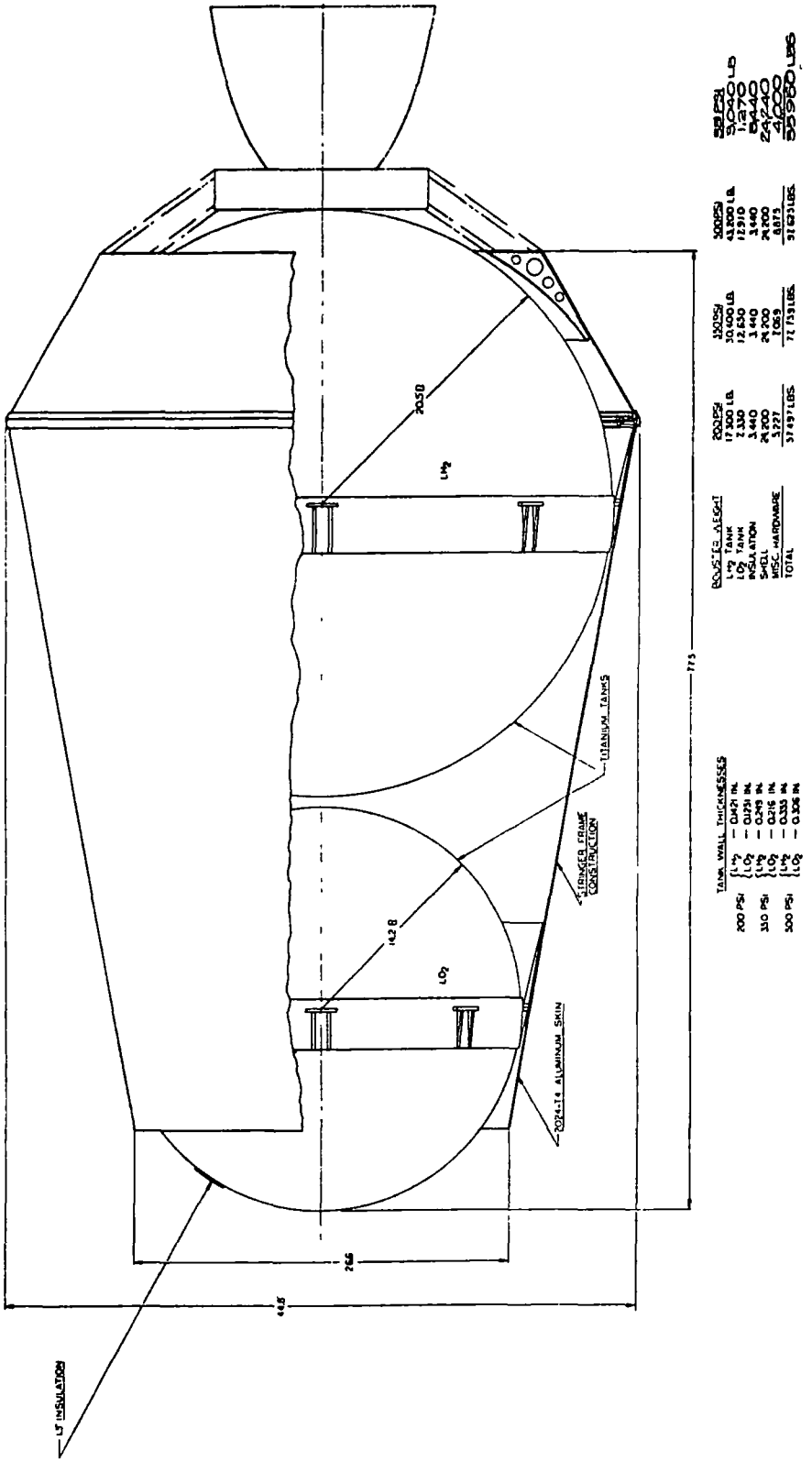

Tandem Sphere Tank Configuration, 2-Million-lb Thrust

Figure II M-5

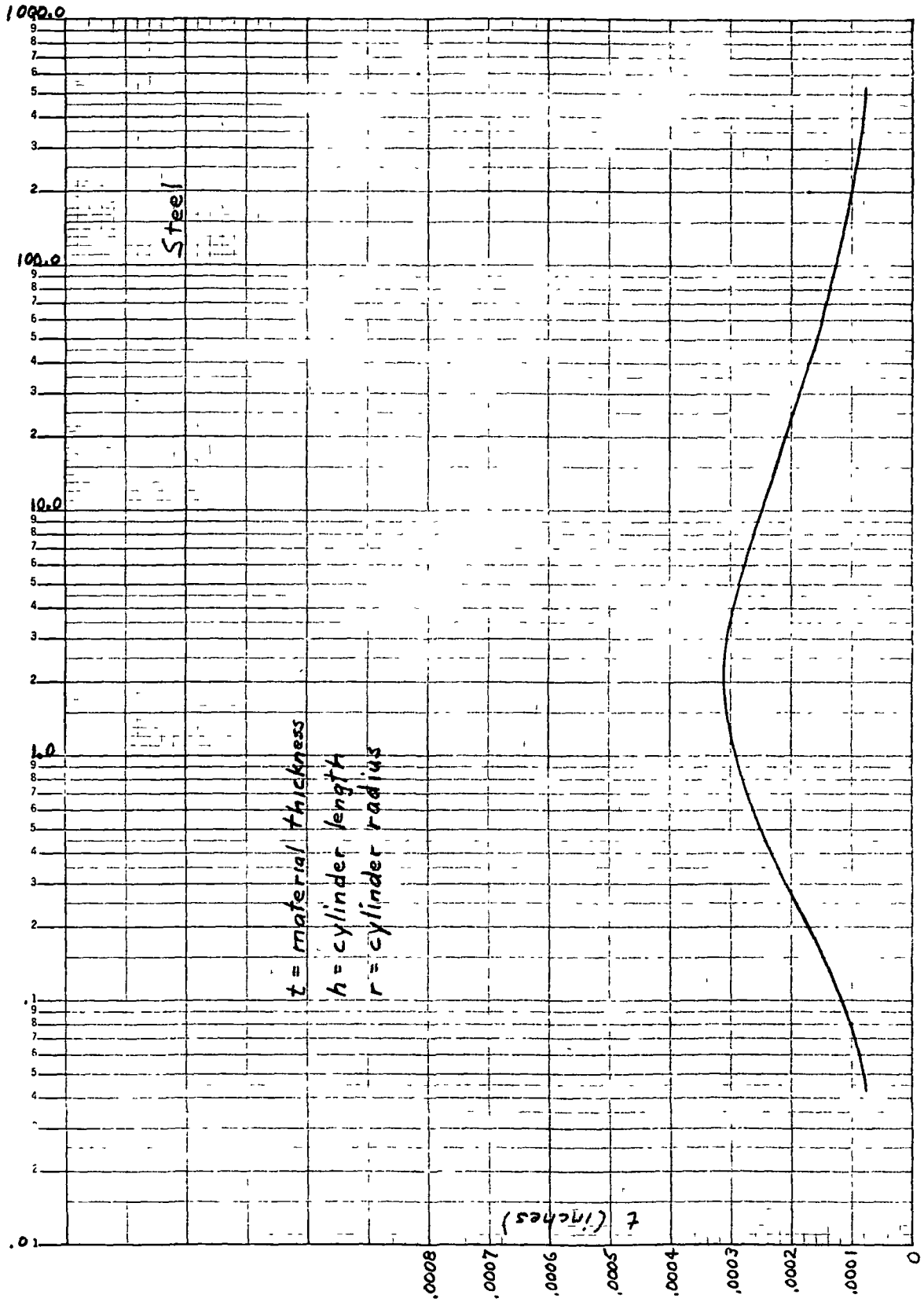

Wall Thickness vs Length-to-Radius Ratio
for Lighter-Than-Air Hydrogen-Filled Steel Cylinder

Figure II M-6

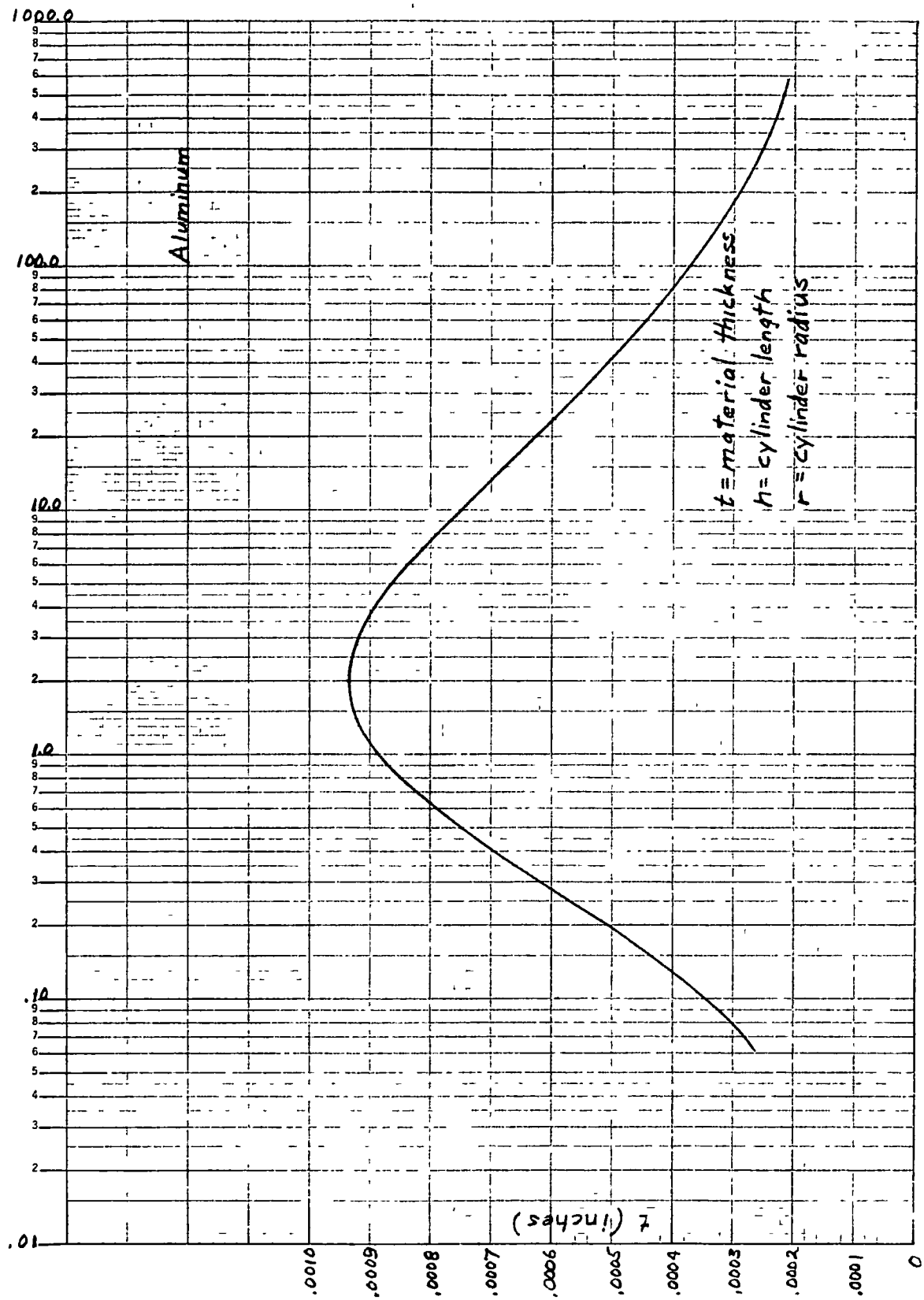

Wall Thickness vs Length-to-Radius Ratio
for Lighter-Than-Air Hydrogen-Filled Aluminum Cylinder

Figure II M-7

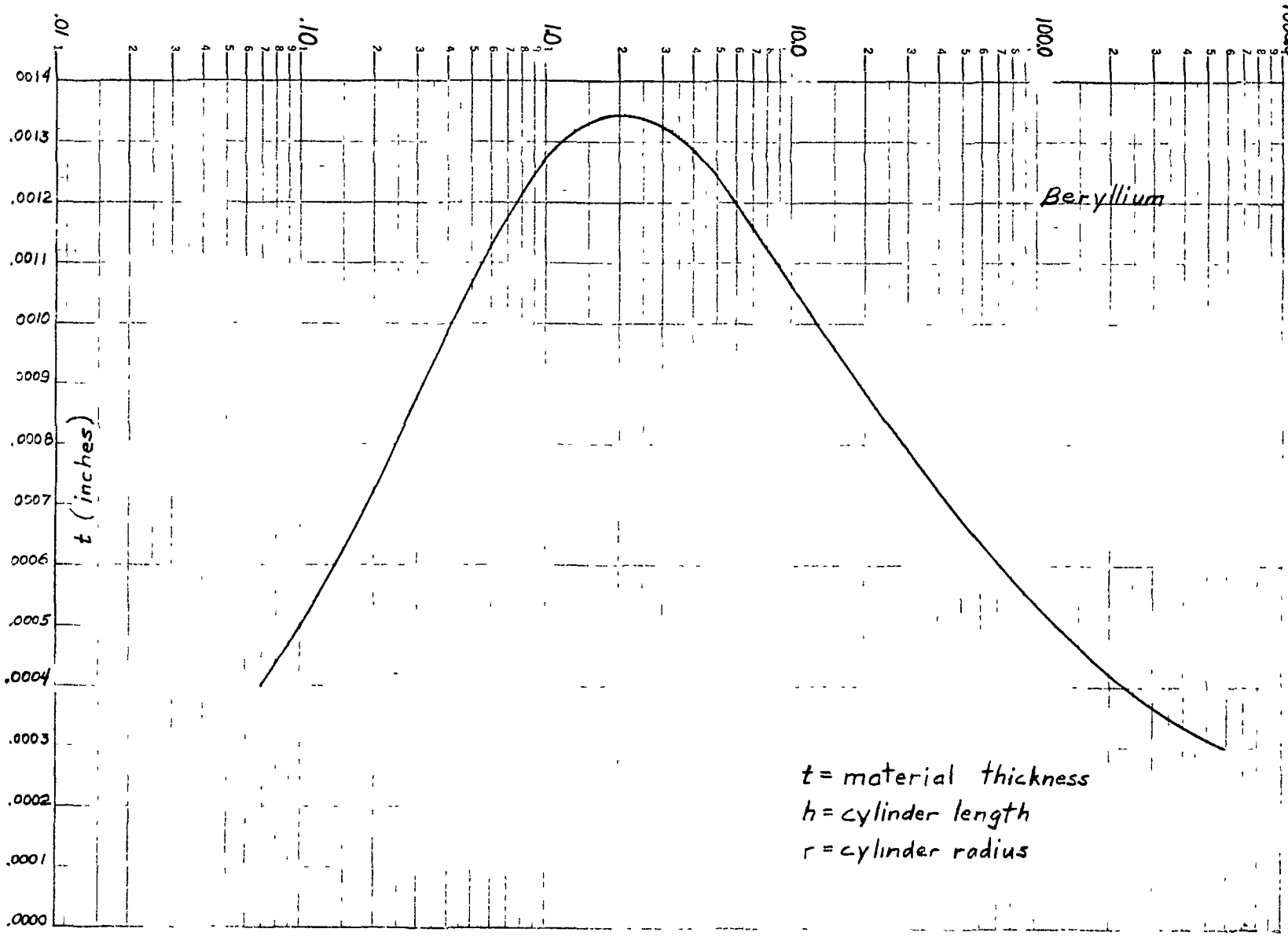

Figure II M-8

Wall Thickness vs Length-to-Radius Ratio for Lighter-Than-Air Hydrogen-Filled Beryllium Cylinder

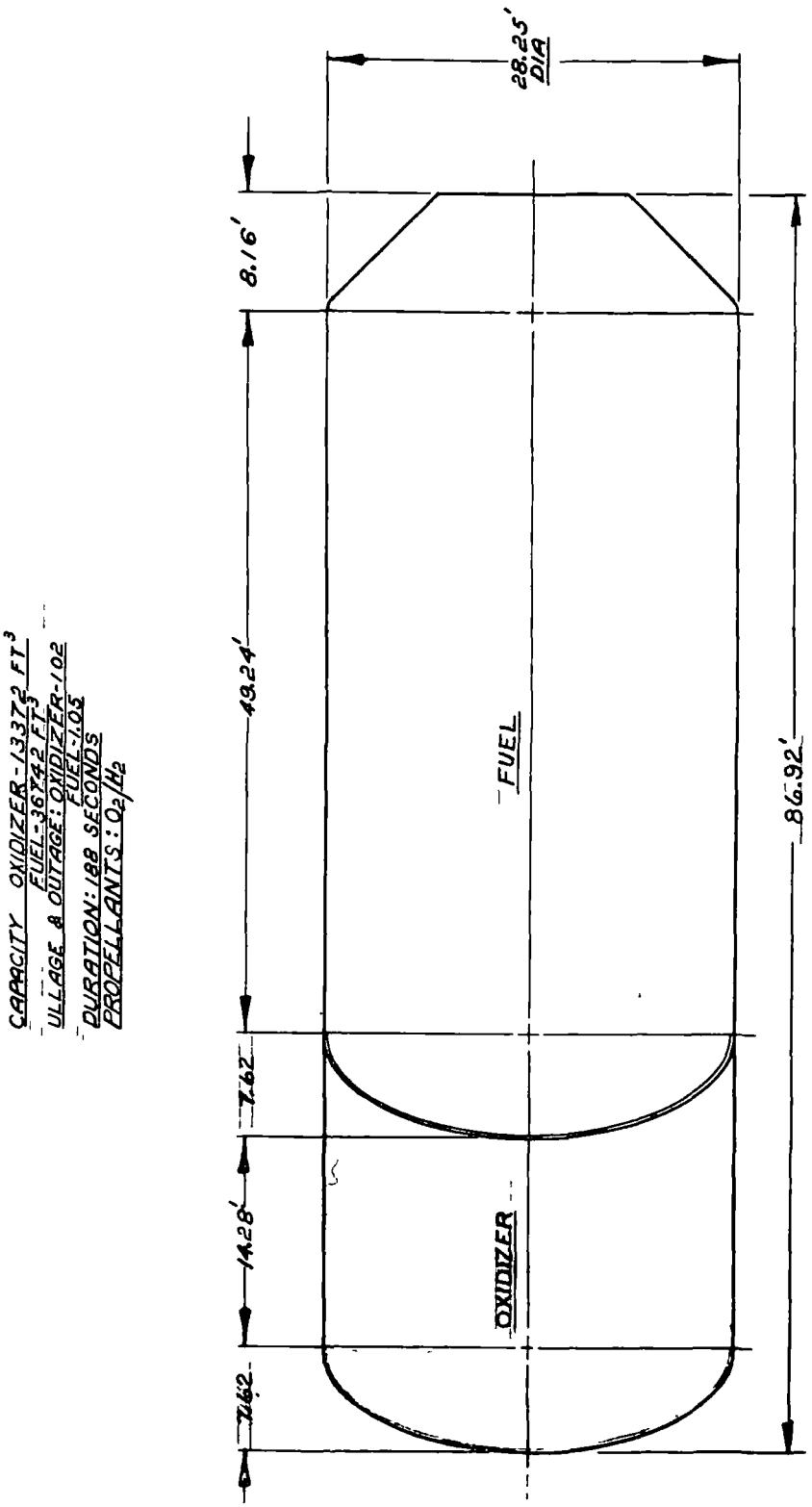

Standard Vehicle Tank Configuration

Figure II M-9

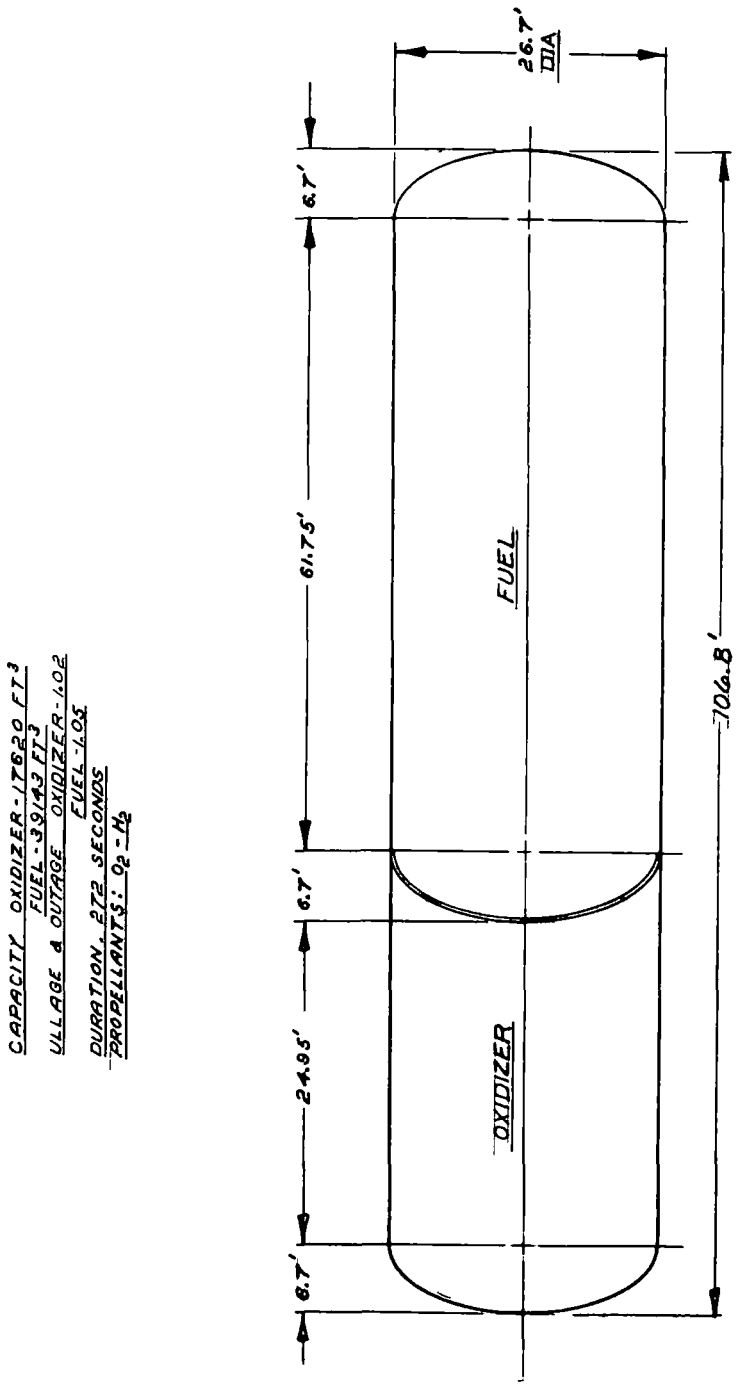

Single-Stage-to-Orbit Tank Configuration

Figure II M-10

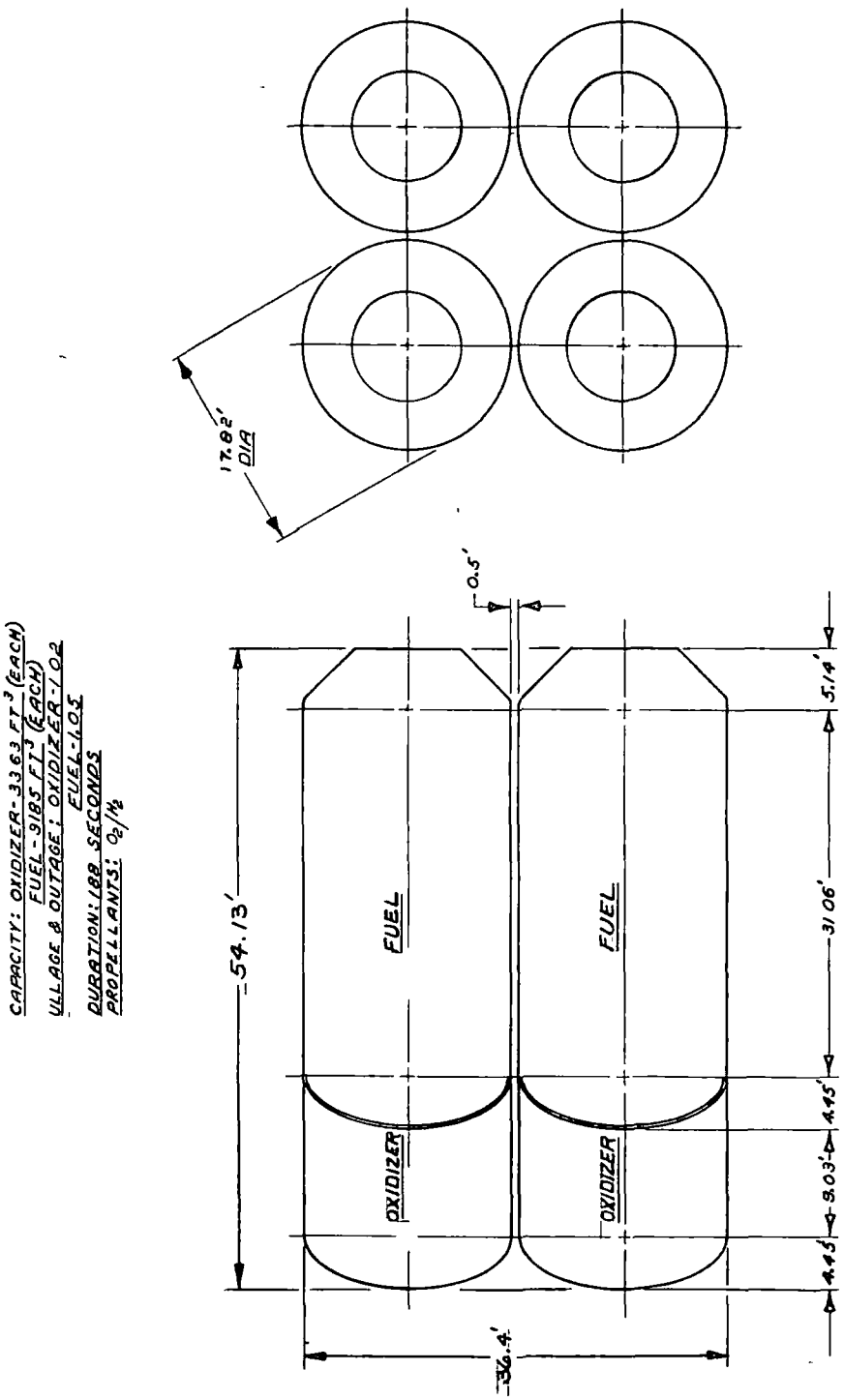

Clustered Cylindrical Tank Configuration

Figure II M-11

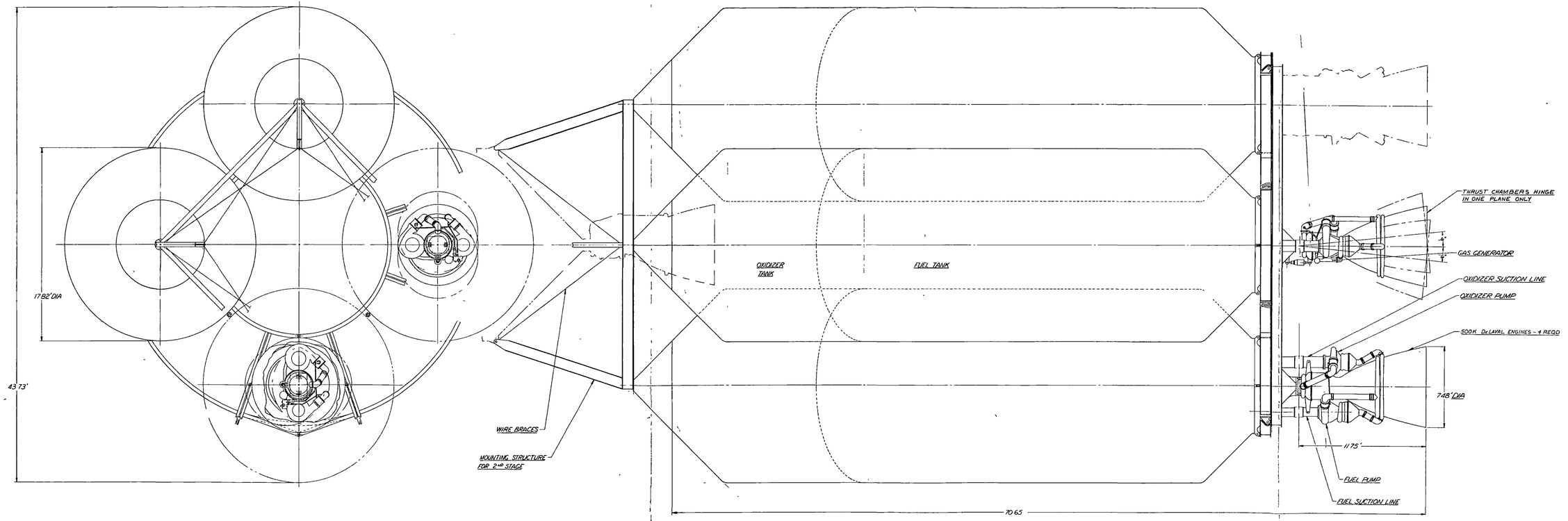

Clustered Booster

Figure II M-12

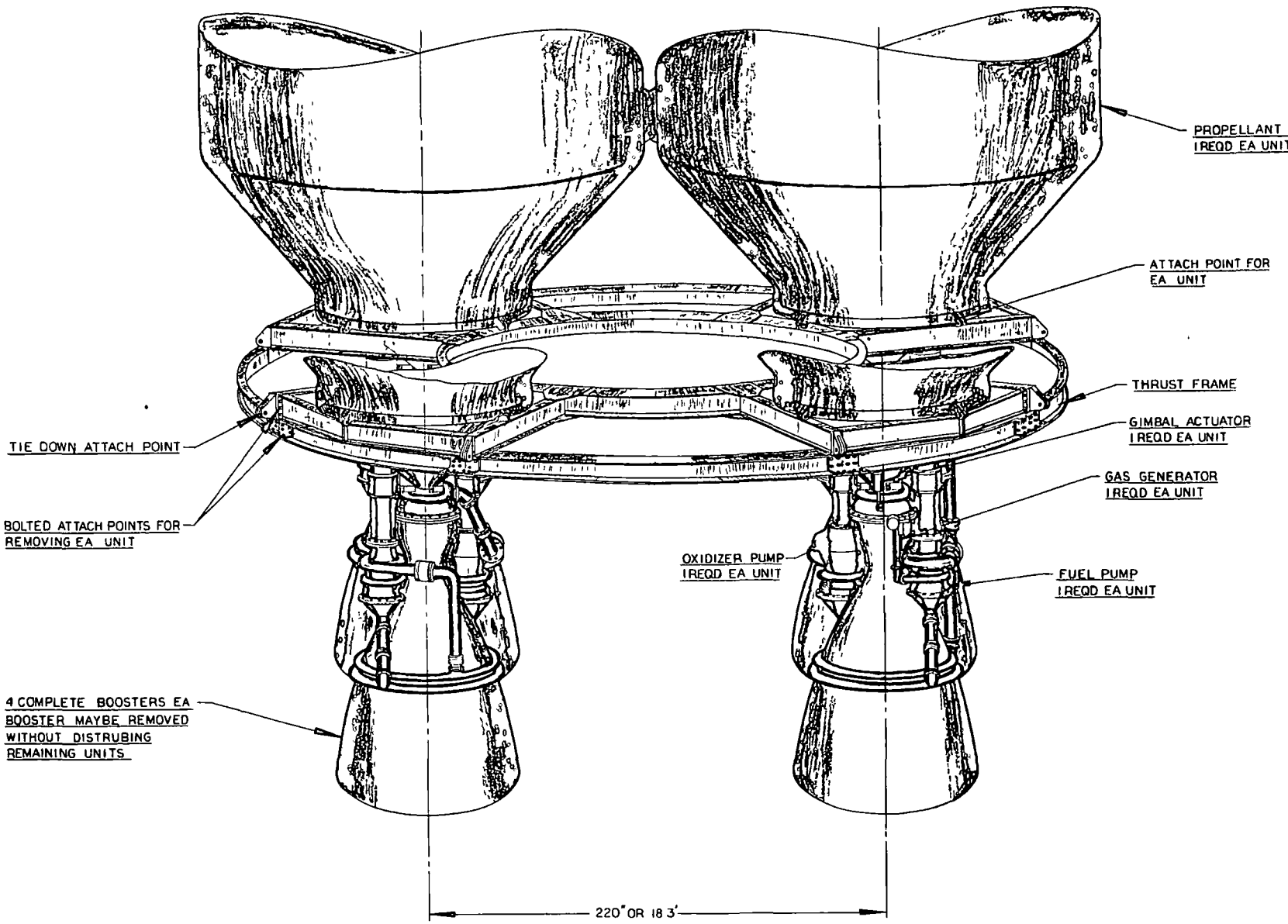

Isometric of Clustered Booster

Figure II M-13

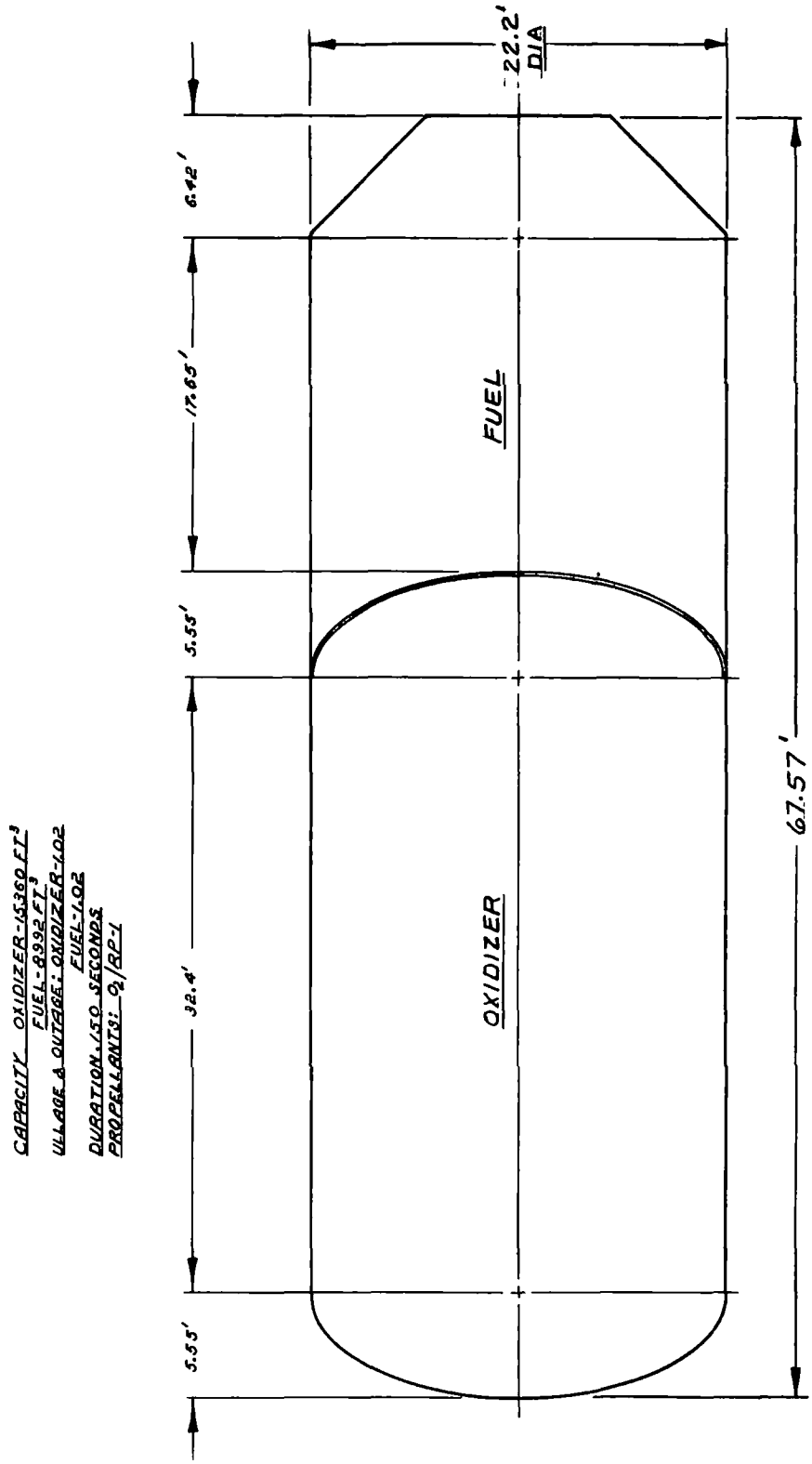

Liquid Oxygen/RP-1 Tankage

Figure II M-14

II, Concepts Considered (cont.)

N. AIR-BREATHERS

1. Conventional Air-Breathers

An airbreathing engine is an engine that depends upon the atmosphere through which it passes for the oxidizing portion of its propellant supply. It is possible to conceive many seemingly different cycles, however, all of these cycles, reduced to basic essentials, follow the flow diagram below.

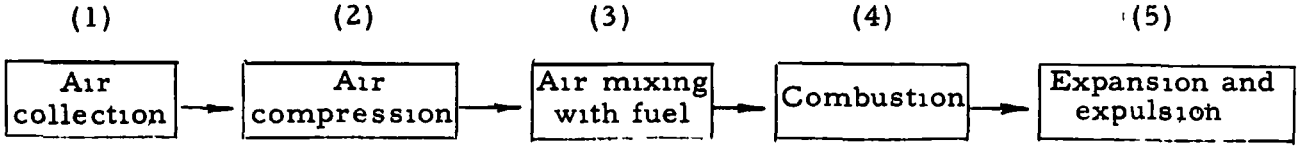

One exception to this is the aerospace plane, in which a heat exchanger is added between the air-compression stage and the mixing. Following its cooling, the air is liquefied and stored for later use in the space portion of the trajectory Because this cycle implies concepts of flight and operations entirely different from ordinary rocket booster flight, it is discussed separately.

Air collection may vary from the simplified air intakes of the reciprocating engine to the complex air inlets of supersonic ramjets. Air intakes influence the overall configuration of the vehicle and must be considered in any weight and design analysis. One of the salient points to be considered in any scheme for using atmospheric air in a rocket booster is that its density--hence the volume available at any constant velocity--decreases rapidly with altitude. To take advantage of air scoops, any vehicle must, of necessity, fly a low trajectory.

Air compression may be accomplished in several ways. Mechanical devices (i.e., compressors, pistons) or a shocking action caused by high flight

II, N, Air-Breathers (cont.)

velocity can be used.

The shocking system used by pure ramjet engines is by far the lightest in weight because it has no moving parts but relies upon the physical geometry of the inlet and the diffuser section to bring the air to rest at a high pressure. However, it has the disadvantage of requiring a high flight speed before becoming operative For this reason, any ramjet system must be supplemented at launch by some other propulsion system, which adds weight. Despite this disadvantage, the shocking system shows the most promise of all airbreathing systems and is detailed later in this discussion.

In conjunction with the air inlet and compression portions of the airbreathing cycle, the sensitivity of this type of engines to variation in angle of attack and air density must be mentioned. Inherently, a rocket designed for boosting payloads to orbit must transverse the denser layers of the atmosphere rapidly, and therefore--to obtain any degree of efficiency--the geometry of the inlet section must be continuously varying.

The final three sections of the cycle--mixing, combustion, and expansion of the gaseous products--must include any turbines or other equipment necessary to power compressors, accessory pumps, or like items. Although many airbreathing concepts appear at first inspection to be simple, experience has proved them quite the opposite. In addition to their complexity they are heavy in relationship to the rocket engine. This weight is made up of expensive machinery that must be carried or recovered, resulting in payload penalties.

Figure II N-1 is a series of sketches of various means for accomplishing each phase of the aforementioned cycle. A number of cycles may be obtained by substituting various components, and in recent years, many types

II, N, Air-Breathers (cont.)

and sub-types of engines have been built that vary the arrangement and number of the basic components in the flow cycle. To mention a few: the turbo-compound reciprocating engine, the turbo-prop, turbojet, turbo-ramjet, the air-turbo rocket, the ram rocket, both solid and liquid fueled, and the turbo-fan engine. It is possible to utilize several of these in combination with the rocket booster in an attempt to increase overall specific impulse.

As previously mentioned, one of more promising is the ramjet engine. This is true because it is one of the simplest and lightest of the air-breathing engines.

Ramjet engines have a higher specific impulse than present-day rocket engines because they obtain oxidizer from the atmosphere through which they travel and are not required to carry it aboard the vehicle to be accelerated. However, ramjet engines have large cross-sectional areas--inferring high drag--and are well known for their sensitivity to fuel mixture, velocity, and angle of attack.

To realistically compare the ramjet-augmented rocket with an all-rocket system, some of the aforementioned parameters must be evaluated and the overall performance, with respect to the mission profile, determined.

It is necessary, when selecting the ground rules for the comparison of the two propulsion systems, to make some determination of the general configurations involved. Figure II N-2 is a sketch of the two vehicles. Identical length-to-diameter ratios were selected, as well as approximately the same volume to be enclosed by each vehicle body. The exit area for both engines was assumed to be the same, resulting in a larger cross-section for Model B.

II, N, Air-Breathers (cont.)

Assuming the proportions shown in Figure II N-2, equal motor exit areas would provide:

$$\frac{\pi d^2}{4} = \frac{\pi}{4} \left(d^2_R - 0.81d^2\right)$$

$$d^2_R = 1.81d^2$$

$$d_R = 1.34d$$

$$\frac{\text{Frontal area Model B}}{\text{Frontal area Model A}} = 1.81$$

The aerodynamic drag coefficient of Model A, $C_{D\ Total}$, is comprised of several component coefficients, which may be determined by wind tunnel tests. Figure II N-3 is a curve of total $C_{D\ Total}$ versus Mach number. In the same curve is shown the contributions made by each of the several components of the total. The term B drag refers to the drag incurred by the open area in front of the combustion chamber. The detailed sources of this information were derived from wind tunnel and free-flight tests. (1), (2), (3), (4), (5)

1. Davis, O.H. and Mitchell, G.A., Performance of a Mach Number 3.0 Design Axisymmetric Double-Cone External-Compression Inlet in the Mach Number Range 1.97 to 0.79. NASA TMX-154, April 1960 (Confidential)
2. Davis, O.H. and Mitchell, G.A., Performance Summary and Analysis of a Mach 3.0 Design Axisymmetric All-External-Compression Double-Cone Inlet from Mach Number 3.0 to 0.8. NASA TMX-149, April 1960 (Confidential)
3. Hoerner, S.F., Fluid Dynamic Drag, Published by the Author, 1958
4. Smanich, N.E., Pressure Drag of Axisymmetric Cowls Having Large Initial Lip Angles at Mach Numbers from 1.90 to 4.90, NASA Memo 1-10-59E, January 1959
5. Silhan, F. V. and Cubbage, J.M., Jr., Drag of Conical and Circular-Arc Boat-Tail After Bodies at Mach Numbers from 0.6 to 1.3. NACA RM L56K22, January 1957 (Confidential)

II, N, Air-Breathers (cont.)

Additive drag represents the partial blockage of air flow into the diffuser and occurs at any velocity except the diffuser design velocity. At supersonic speeds, this results from turning of the flow streamlines by the frontal shockwave At subsonic velocities, loss of thrust is attributable to the fact that only a fraction of the required air is being ingested into the engines intakes because of its low velocity Figure II N-4 is a curve of the drag coefficient of Model B in relationship to Mach number. The mass flow ratio (mass flow at Mach number M to mass flow at design Mach number) is included. The correlation with the additive drag coefficient is direct over the supersonic range, where the spillage phenomena resulting from shockwave deflection, as discussed above, takes place.

Figure II N-5 is the total drag coefficients of models A and B superimposed on the same graph. It should be noted that these curves represent coefficients only, and that the total drag force is also a function of the cross-sectional area of the vehicle and the dynamic pressure. When this is taken into account, the total drag of Model B exceeded that of A by 81%

An approximation of drag, based upon drag per square foot, has been made for an altitude of 35,000 ft and a flight velocity of M 3.0 Under these conditions, this quantity is 780 lb/sq ft.

The ramjet thrust computed in this study is based upon the following simplifying assumptions:

Complete mixing of fuel and air;
Burning is complete and takes at a low subsonic velocity,
Distribution of the reaction heat is complete and uniform;
No losses.

II, N, Air-Breathers (cont.)

The indicated conditions are valid for an ideal ramjet only However, for the purposes of an initial preliminary design study, they are adequate

The thrust, T, of an ideal ramjet is:

$$T = \dot{m}\ (V_2 - V_1) + A_2 (P_2 - P_0)$$

Let $P_2 = P_0$

$$T = \dot{m}\ (V_2 - V_1) \qquad \dot{m} = \frac{\text{slug}}{\text{sec}}\ V = \text{ft/sec}$$

Figure II N-6 illustrates a ramjet flow model

At the engine design point, the ingested air flow is:

$$\frac{m}{A_o} = \rho_o V_1 \text{ slug/sec-ft.}^2$$

In this case, for the design conditions of M 3.0 at 35,000 ft, the engine mass flow becomes (ignoring fuel weight)·

$$\frac{\dot{m}}{A_o} = \rho_o V_1 = 7\ 37 \times 10^{-4} \times 2{,}919 = 2.15\ \frac{\text{slug}}{\text{sec}} - \text{ft}^2 \text{ air}$$

$$2.15 \text{ slugs air} = \frac{2.15}{5} = 0.43\ \frac{\text{slugs}}{\text{sec ft}^2}\ O_2$$

The required hydrogen for the ideal combustion reaction is:

II, N, Air-Breathers (cont.)

$$2\,H_2 + O_2 \rightarrow 2H_2O$$

$$\frac{0.43}{8} = 0\ 0538\ \frac{\text{slugs } H_2}{\text{sec ft}^2} = 1.728\ \text{lb/sec - ft}^2 \text{ of } H_2$$

It can be shown by proper substitutions in the thrust equation that the thrust is also equal to:

$$T = \dot{m}_{V1}\left[\sqrt{\frac{T_3}{T_2}} - 1\right]$$

Where T_2 is the total temperature just before combustion and T_3 is the mixture temperature just after burning

$$T_2 = T_o + \frac{Rv^2}{2Jg_{c_p}} = 394°\ \text{(at 35000 ft)} + 640°\text{R (for Mach 3)}$$

$$= 1034°\text{R}$$

The mixture combustion temperature is a function of the mixture ratio of fuel to oxidizer combustion chamber pressure, and the completeness of fuel-oxidizer mixing. Mixture combustion temperature has been the subject of extensive computer studies at Aerojet-General. Figure II N-7 is a plot of T_3 versus combustion pressure for a stoichiometric mixture ratio of hydrogen and air when the propellants have been preheated to 1,000°R. Because this is very near the stagnation temperature of air at M 3 at 35,000 ft, and because air is the greatest part of the propellant weight, it is safe to use the values in Figure II N-6 for an estimation of thrust.

At 35,000 feet $P_o = 3.46\ \text{lb/in.}^2$

At M = 3.0 $P_2/P_1 = 10.33$ for normal shock wave)

II, N, Air-Breathers (cont.)

$$P_2 = 35.8 \text{ lb/in.}^2$$

$$T_3 = 4725°R$$

The thrust is, therefore,

$$T = 2.15 \times 2919 \times \left(\sqrt{\frac{4725}{1,034}} - 1\right) = (1.14)\ (6260) = \underline{7,150 \text{ lb/ft}^2}$$

The net thrust is:

$$T_N = T - \text{Drag} = 7,150 - .81 \times 780 = 7,150 - 632 = 6,518 \text{ lb/ft}^2$$

This yields a specific impulse of:

$$I_s = \frac{6,518}{1,728} = \underline{3.772 \text{ sec}}$$

This value of thrust is greatly idealized, of course, and applies only to the performance of the engine at its design velocity and altitude. In flight, the engine would actually fly a trajectory that would be continuously changing, both in altitude and velocity. For a more realistic evaluation, the ramjet must be evaluated over such a trajectory.

The 2-million-lb-thrust standard booster was selected as the basic vehicle to be used in such an evaluation. It was assumed that ramjets of 100,000, 200,000, and 400,000-lb maximum thrust were attached, in turn, to the booster, and that it then theoretically flew the trajectory shown in Figure II N-8. Additional payload plus airframe weight that would provide a burnout velocity of 29,900 fps was then computed. Results of this computation are presented as Table II N-1.

II, N, Air-Breathers (cont.)

Ramjet engine weight was estimated at 1 lb for each 15-lb thrust produced by the engine. This figure was selected after reference to literature[6] and an independent analysis by Aerojet-General. Even when it is assumed, as was done here, that the ramjet engine had a variable geometry and was capable of high efficiency during its period of operation, it still appears to be incapable of contributing to performance for a space booster.

In an effort to improve this situation, a new, lower trajectory was selected and again ramjet performance was calculated. In this case, the performance was poorer than in the first case because of the fact that, while ramjet efficiency increased, the specific impulse of the rocket engines suffered from the increased operating time at lower altitude.

What has been shown for the ramjet in this study can be demonstrated for other types of air-breathing engines in general. Though they develop a higher specific impulse, they lose their advantage when performance is computed over trajectory ranging from sea level to vacuum.

2. The Aerospace Plane

A new concept for placing payloads into orbits is that of the aerospace plane, which is a winged vehicle. It owes its unique characteristics to the fact that it has an air-breathing propulsion system that, in addition to having the forementioned basic essentials in its operating cycle, also is capable of liquifying and storing oxygen collected from the atmosphere through which it passes. This is accomplished, at least in theory, by means of light, highly efficient, heat exchangers and air compressors.

---

6 Casamassa and Bent, Jet Aircraft Power Systems, McGraw-Hill, 1957

II, N, Air-Breathers (cont.)

Studies of this concept conducted at Aerojet-General indicate that the device may provide a highly flexible operational capability for moderate payloads (30,000-60,000 lb). In pursuance of this study, Aerojet-General has developed new concepts and approaches to the problem, which should simplify the cycle and offer the lightest and most feasible current means for producing such a cycle. Efforts are underway to develop this system to its optimum.

TABLE II N-1

RAMJET PERFORMANCE EVALUATION

	Case 1	Case 2	Case 3
Maximum ramjet thrust / Rocket engine thrust	0.05	0.10	0.20
Maximum ramjet thrust	100,000 lb	200,000 lb	400,000 lb
Additional payload and airframe, accelerated to 29,900 fps	4,900 lb	12,700 lb	17,700 lb
Estimated weight of ramjet, fairings, and attaching struts	6,600 lb	13,320 lb	26,640 lb
Payload gain or loss	1,760-lb loss	620-lb loss	8,940-lb loss

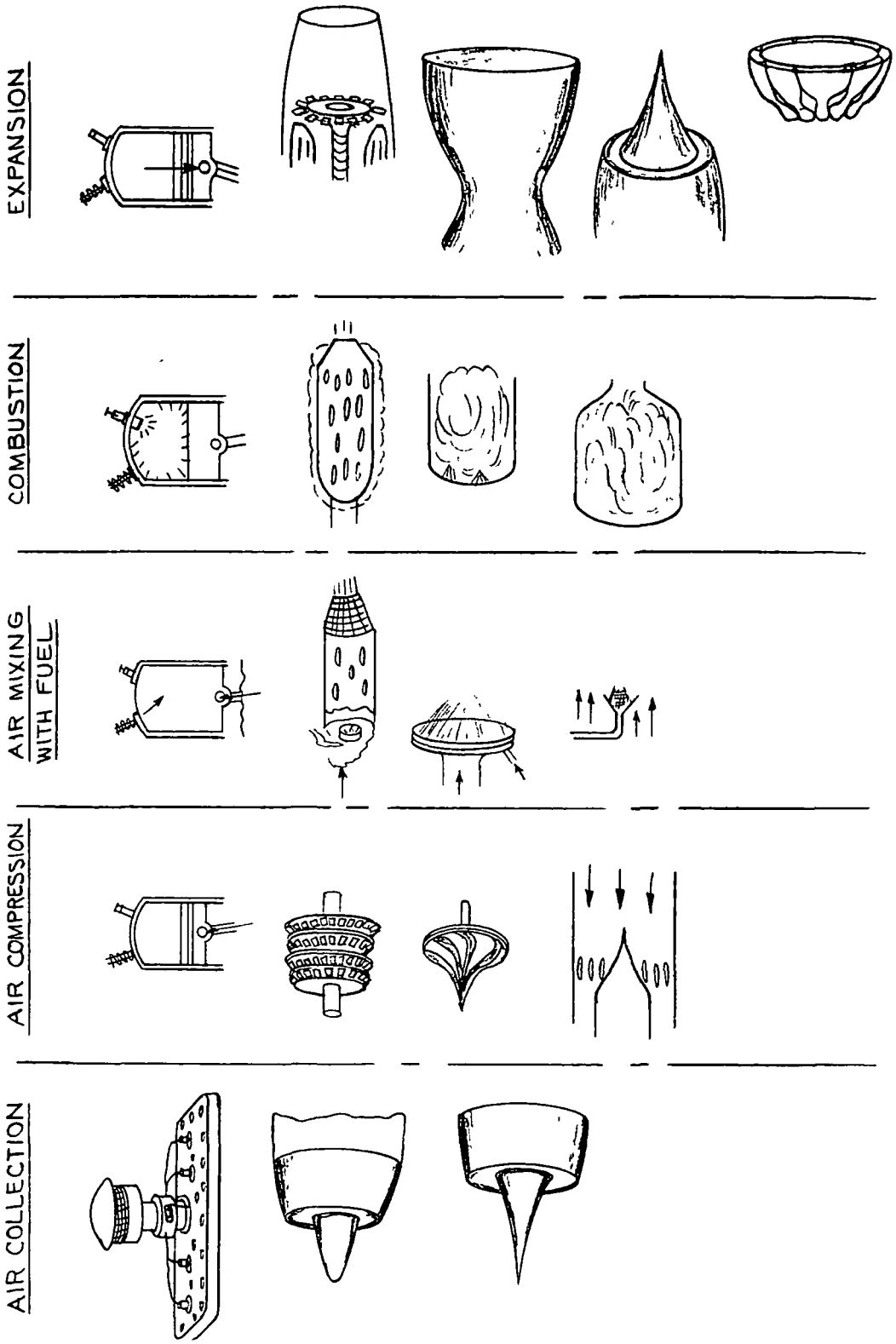
EXPANSION
COMBUSTION
AIR MIXING WITH FUEL
AIR COMPRESSION
AIR COLLECTION

Figure II N-1

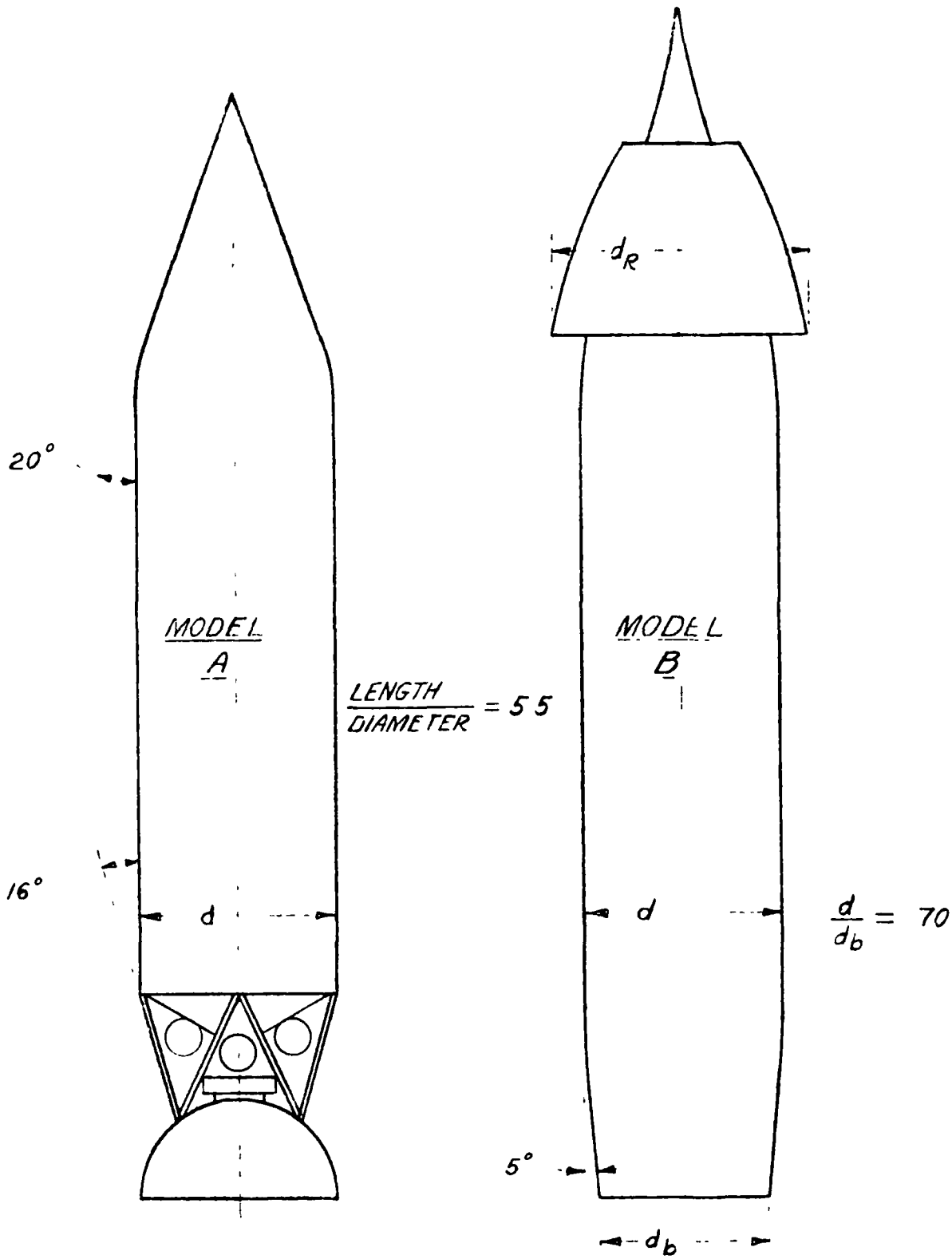

Comparative Models

Figure II N-2

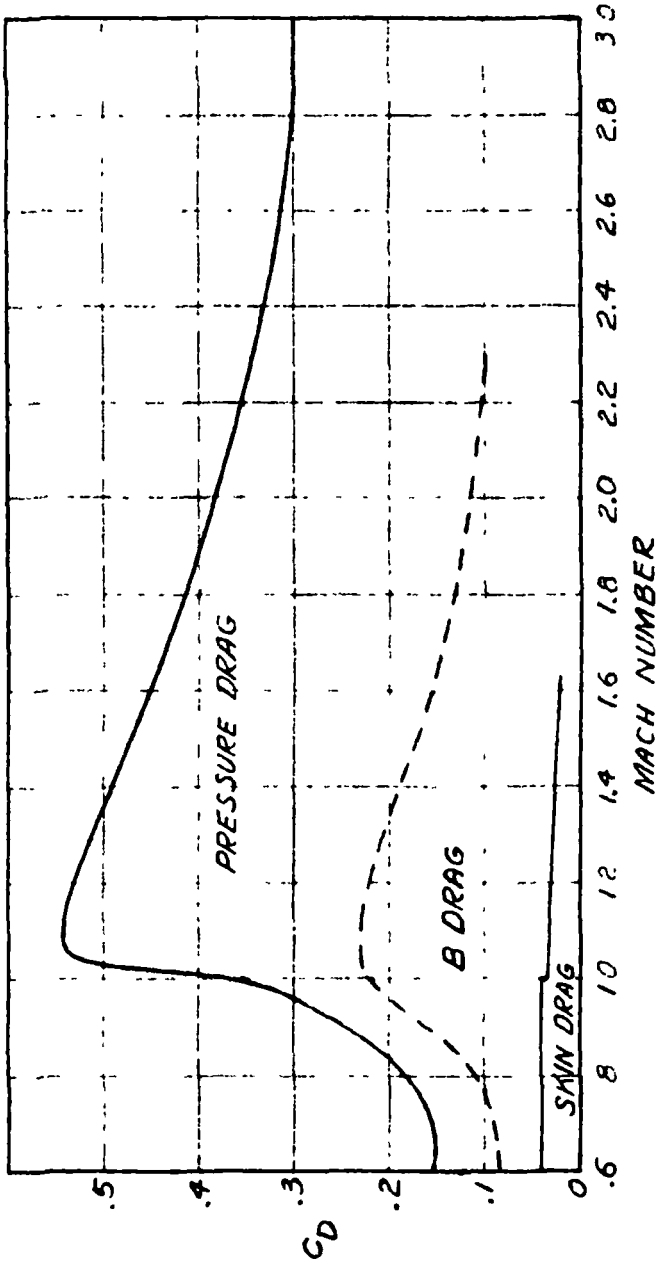

Drag Coefficient for Model A

Figure II N-3

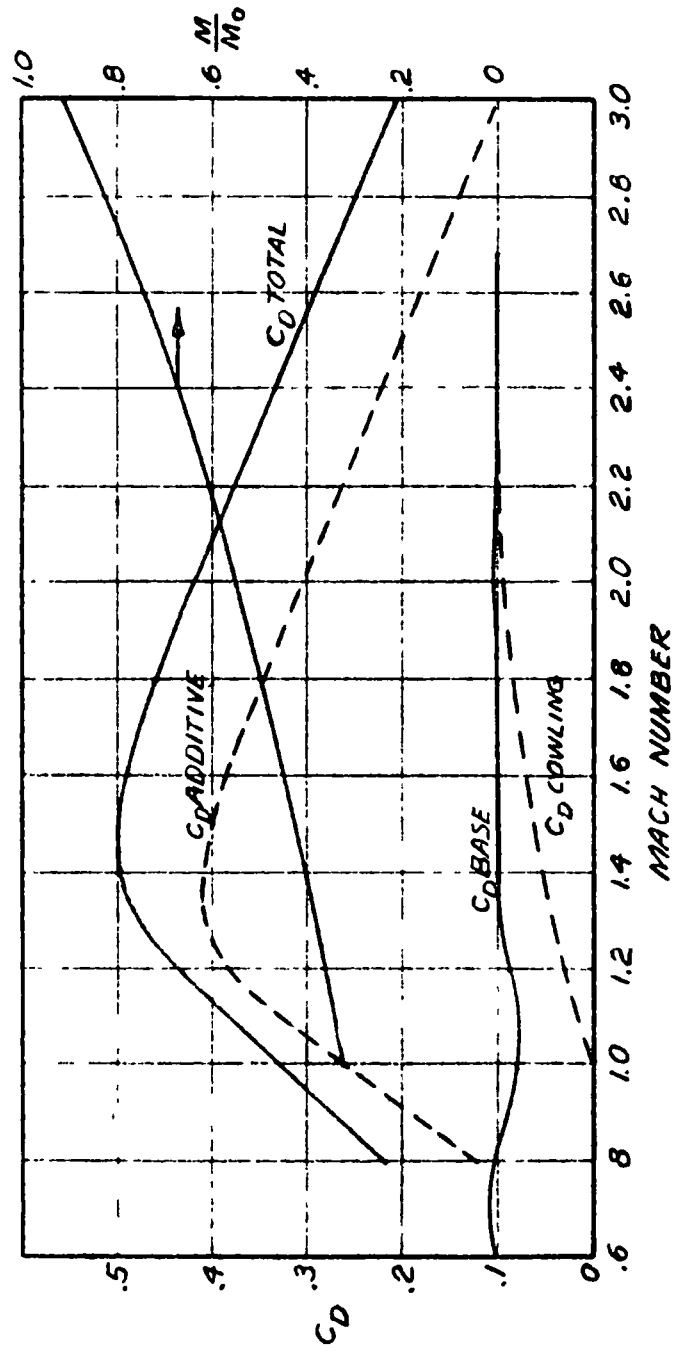

Drag Coefficient for Model B

Figure II N-4

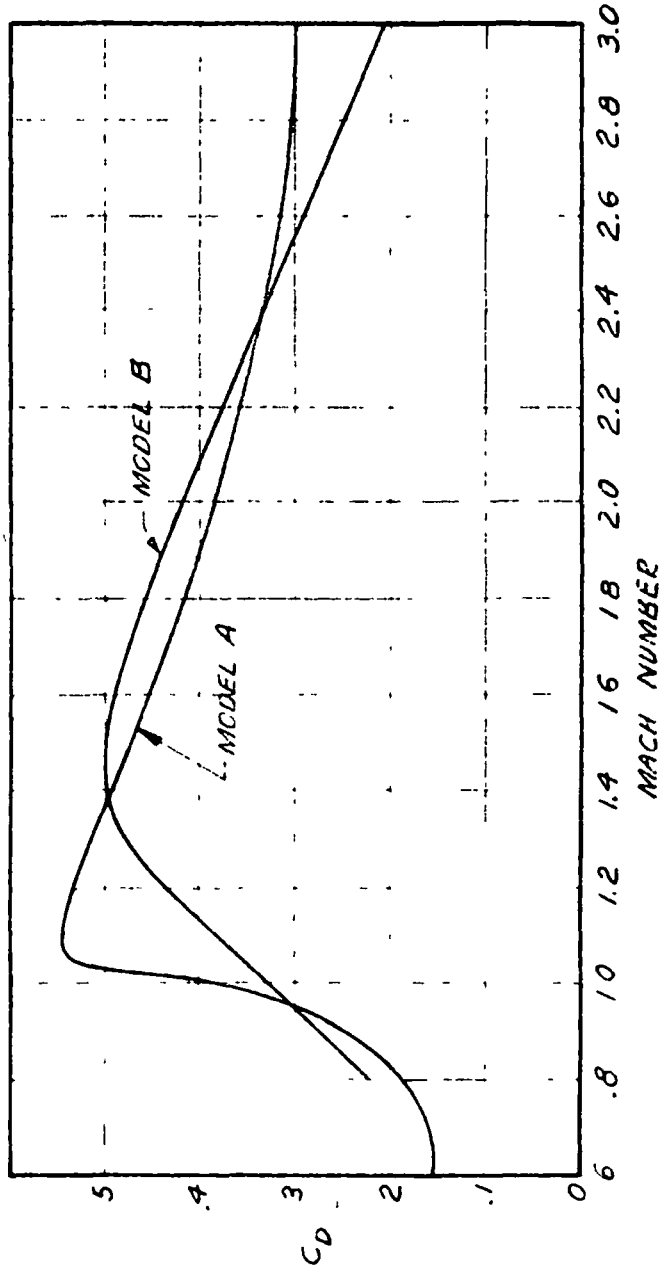

Drag Coefficient for Model A and B

Figure II N-5

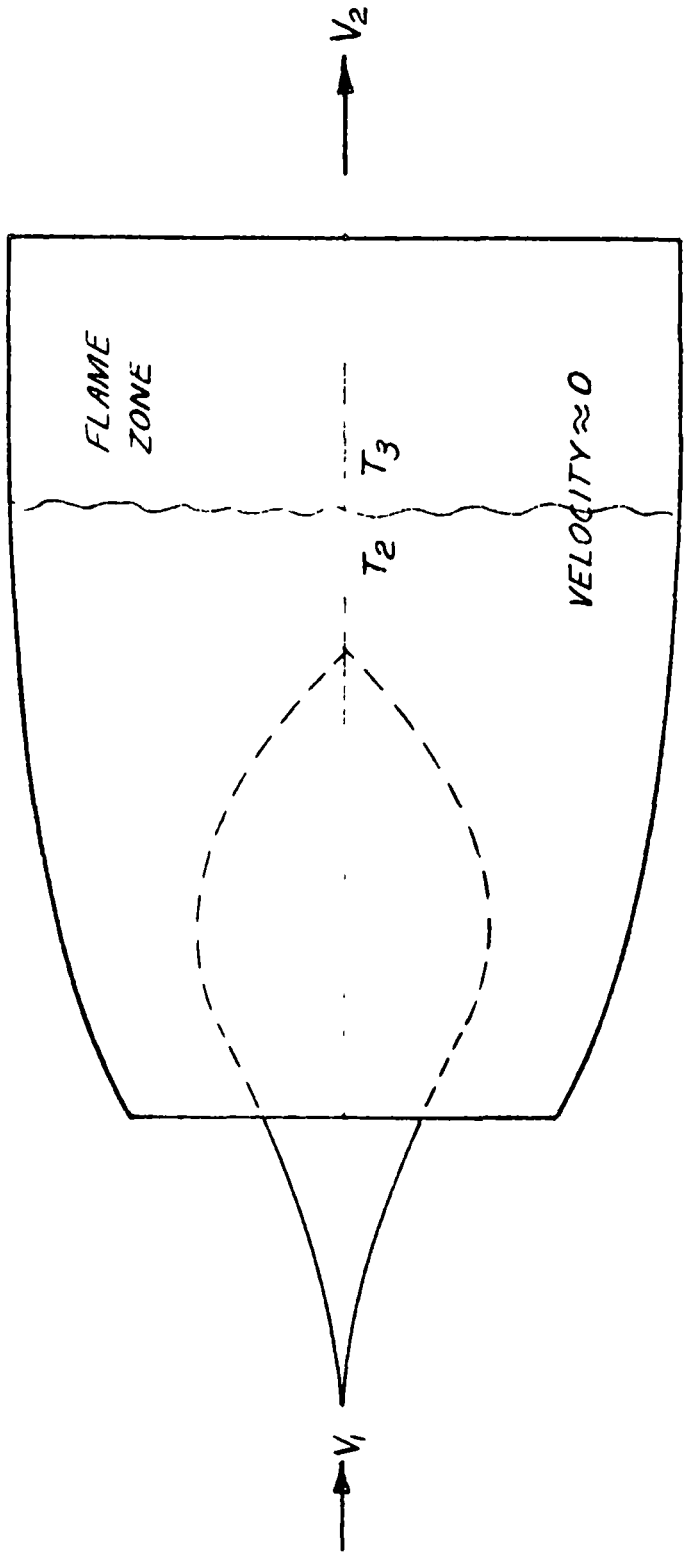

Ramjet Flow Model

Figure II N-6

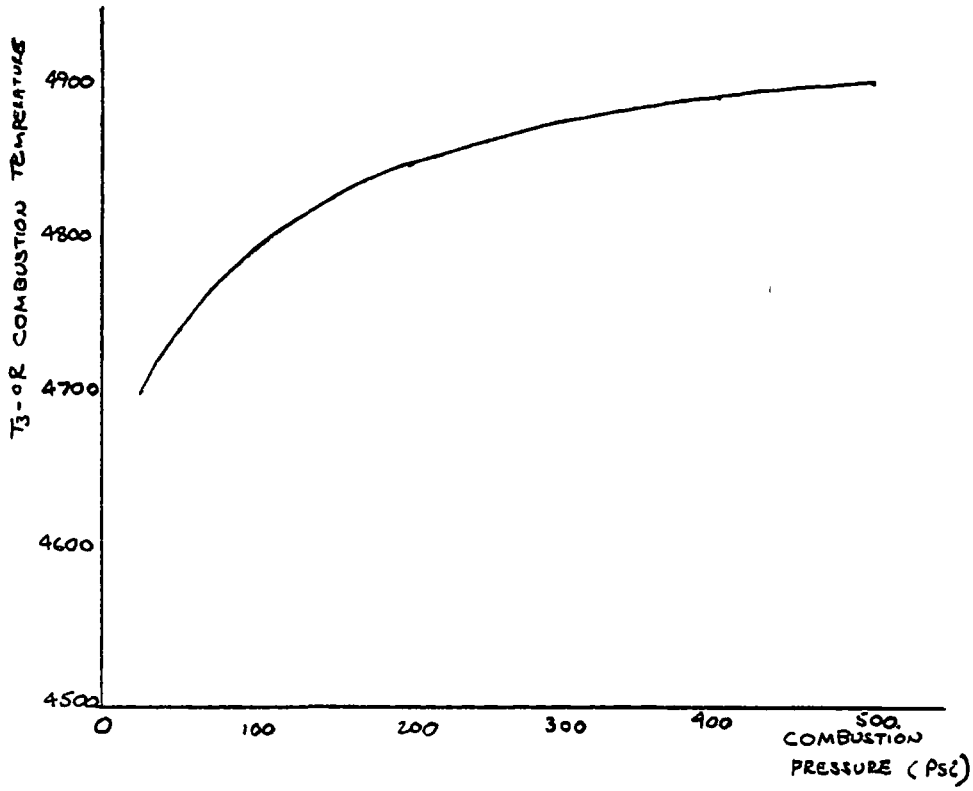

Combustion Temperature vs C_p for H_2-Air at Stoichiometric Mixture Ratio and Preheated to 1,000°R

Figure II N-7

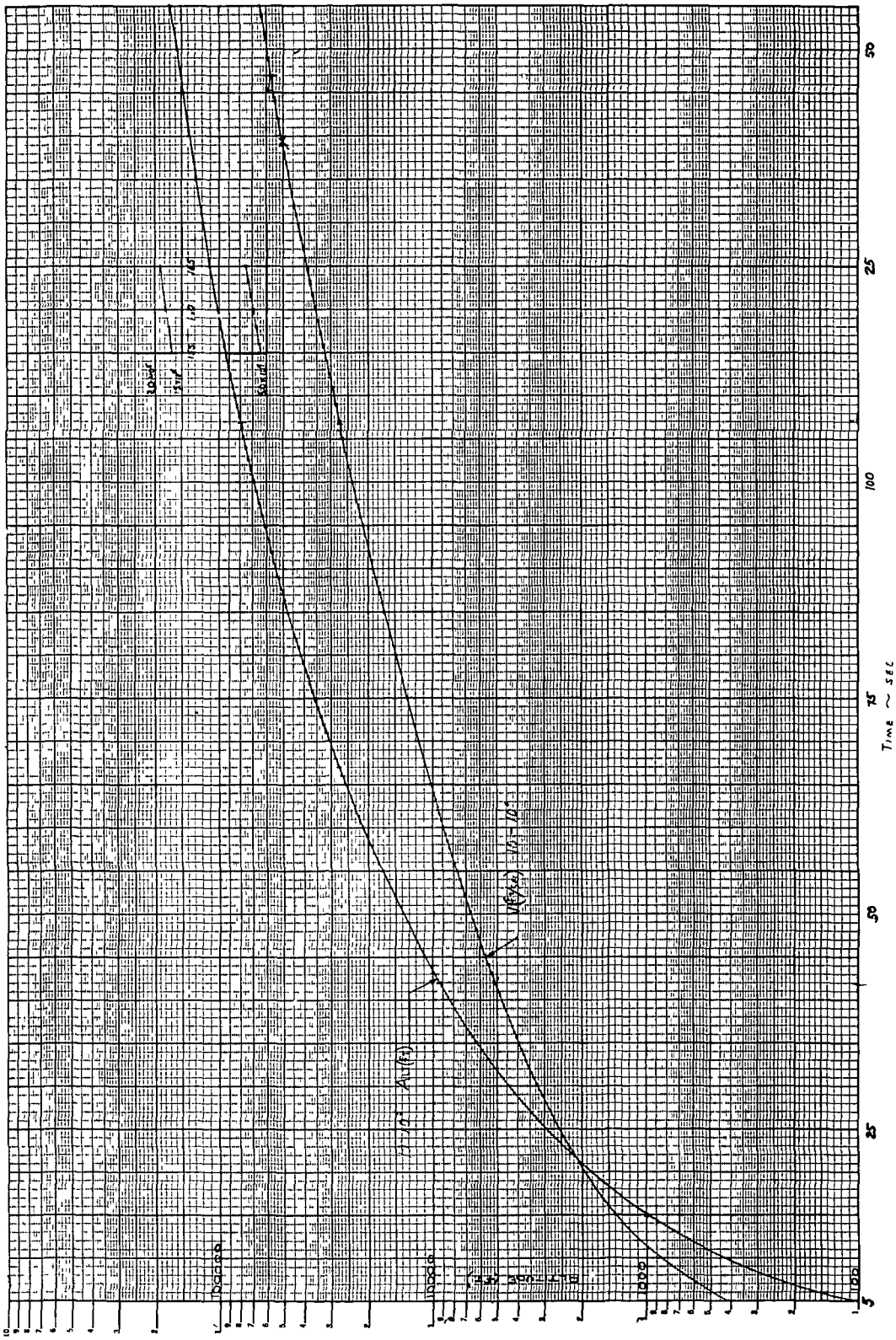

Figure II N-8

TABLE OF CONTENTS

		PAGE NO.
III.	BASES FOR EVALUATION	
A.	DESCRIPTION OF STANDARD VEHICLE	III A-1
B.	MISSIONS, TRAJECTORY, AND VEHICLE ASSUMPTIONS	III B-1
C.	COST AND RELIABILITY	III C-1
D.	VEHICLE DESIGN PROGRAM	III D-1
E	RECOVERY FACTORS	III E-1

TABLE LIST

	TABLE NO.
Engine Characteristics for the Standard Vehicle Booster	III A-1

FIGURE LIST

	FIGURE NO.
Standard Vehicle, 2,000,000-lb-Thrust Booster	III A-1
Standard Booster, 2,000,000-lb-Thrust De Laval Engine	III A-2
Controls Schematic, 2,000,000-lb-Thrust, Standard Vehicle	III A-3
Weight of Oxygen Tank Pressurization System vs Tank Pressure	III A-4
Weight of Hydrogen Tank Pressurization System vs Tank Pressure	III A-5
Rocket Engine Conventional De Laval, 2,000,000-lb-Thrust	III A-6
Trajectory Program Diagram	III B-1
Engine Weight vs Vacuum Thrust	III B-2
Engine Development Cost, Engineering, Test, Fab, and R and D Tooling Cost vs Engine Vacuum Thrust	III D-1
Propellant Costs for Engine Development vs Engine Vacuum Thrust	III D-2
Engine Facilities Cost vs Engine Vacuum Thrust	III D-3
Engine GSE Cost vs Engine Vacuum Thrust	III D-4
Engine Production Tooling Cost vs Engine Vacuum Thrust	III D-5
Stage Development and Postdevelopment Program Costs	III D-6
Engine Production Cost vs Engine Vacuum Thrust	III D-7
Acceptance Testing Cost vs Engine Vacuum Thrust	III D-8
Stage Production Cost vs Propellant Tank Volume (Cumulative Average of 100 Units)	III D-9
Transportation Cost vs Propellant Tank Volume	III D-10
Stage Launch Operation Cost vs Engine Vacuum Thrust	III D-11
Propellant Cost for Operational Stage	III D-12
300 nm Orbit Optimum Second Stage Thrust to Light-Off Mass Ratio with Variations in Payloads	III D-13

III. BASES FOR EVALUATION

A. DESCRIPTION OF STANDARD VEHICLE

1. Vehicle Specifications

A standard vehicle (Figure III A-1) was established and then used as the basis for comparison with all unconventional concepts evaluated during this study.

The standard vehicle is of a two-stage configuration with the propellant combination LOX/LH_2 in both stages. Each stage is powered by a single pump-fed gimbaled deLaval engine. First-stage thrust was fixed at 2,000,000 lb* (sea level) and the vehicle designed for a 300-nm orbit mission. The second stage was established by scaling down the booster configuration. Major vehicle parameters are tabulated as follows:

Parameter	First Stage	Second Stage
Thrust, Sea-Level, lb	2×10^{6}*	--
Thrust, Vacuum, lb	2.39×10^{6}*	579,000
Specific Impulse, Sea-Level, sec	345	--
Specific Impulse, Sea-Level, vac	413	426
Ideal Velocity Increment, ft/sec	15,000	15,000
Payload, lb	--	105,000

2. Booster Description

The booster stage was used for all detailed design work. An engineering layout of the resulting configuration is shown in Figure III A-2. A schematic of the booster system is given in Figure III A-3. Major booster operating characteristics are presented in Table III A-1.

*Not including turbine exhaust.

III, A, Description of Standard Vehicle (cont.)

Propellant tankage for the booster is a cylindrical configuration having an over-all L/D of 3:1. The oxidizer tank is located above the fuel tank, with a common bulkhead separating the two propellants. Positioning the oxidizer tank in this manner reduces the vector control requirements and provides a higher suction pressure to the oxidizer turbopump. It also offers a savings in pump weight. Both top and inner tank closures are elliptically shaped, the bottom closure is conical. Aluminum rib and panel construction is used for both tanks.

Pressurization of the oxidizer tank is provided by helium gas, which is stored under high pressure in the liquid-oxygen tank. It is heated by passing through a heat exchanger (located in the oxidizer turbine exhaust duct) and expanded through a regulator into the oxidizer tank.

The hydrogen tank is pressurized by hydrogen gas tapped from the main hydrogen propellant in the thrust chamber after having passed through the coolant jacket. It is further heated by a heat exchanger (located in the hydrogen turbine exhaust duct) and expanded through a regulator into the hydrogen tank.

Tank pressures for the standard vehicle were established at 4 psi above vapor pressure for the liquid-oxygen and liquid-hydrogen tanks. The 4 psi suppresses boiling and allows for regulator tolerances. Vapor pressures and corresponding tank pressures follow:

III, A, Description of Standard Vehicle (cont.)

	Vapor Pressure (psia)	Tank Pressure (psia)
H_2	22	26
O_2	21	25

For the selected pressures and configuration, the resulting NPSP and corresponding NPSH at the pumps are:

	NPSP (psia)	NPSH (ft)
LH_2 Pump	4.35	143
LO_2 Pump	50.5	103

These conditions correspond to the end-of-the-run pressure for hydrogen and the beginning-of-the-run pressure for oxygen, which represent the lowest pressure conditions.

Effect of other tank pressures upon system weight was investigated, and results are shown in Figures III A-4 and III A-5. The standard vehicle uses pumps without inducers. Some weight saving can be made for the hydrogen side (approximately 2,000 lb) by using an inducer and lowering the tank pressure to 24 psi. Little is to be gained for the oxygen side while maintaining an adequate margin over vapor pressure.

The engine pictured in Figure III A-6 consists of a thrust-chamber, separate oxidizer and fuel turbopumps, a single gas generator, engine controls, propellant lines, and a frame. The thrust chamber and turbopumps are rigidly connected and gimbaled together as a unit. The suction line to each pump incorporates an unrestrained bellows which absorbs all displacements (angular or axial) during gimbaling.

III, A, Description of Standard Vehicle (cont.)

The thrust chamber has a 20:1 area ratio nozzle and is regeneratively cooled with hydrogen. Both turbopumps are the direct-drive type without gears. The separate turbines are driven by gas from a single gas generator, which is fed propellants from the pump outlets. Exhaust gas from each turbine is expelled into the atmosphere through a nozzle at the base of its exhaust duct.

Figure III A-3 is a schematic of the engine control system. This system initiates and terminates the thrust chamber and gas generator propellant flow, ignites the thrust chamber and gas generator, supplies initial starting energy, engine transient control, engine balancing, as well as vector- and roll-control operations.

All engine controls are pneumatically operated. Control components include mechanically linked thrust-chamber valves, mechanically linked gas generator valves, and start cartridge gimbal actuators.

Engine operation is initiated by the ignition of the solid propellant start cartridge. The generated gases start turbopump operation. As the turbopumps accelerate, gas from the start cartridge opens the thrust-chamber and gas-generator valves. The thrust chamber igniter system is energized as the thrust-chamber valves open. These valves open when the fuel pump has accelerated to approximately 30% of rated speed. Gas generator valves open after partial thrust chamber valve opening. The gas generator is ignited by the start cartridge. After ignition takes place in the gas generator and combustion chamber, the engine bootstraps to rated thrust.

During engine steady-state operation, the bipropellant gas generator supplies turbine drive gas for the turbopump assemblies. The fuel

III, A, Description of Standard Vehicle (cont.)

(except gas generator fuel) is directed into the thrust chamber coolant circuit and then through the injector into the combustion chamber. Engine thrust and the gas generator mixture ratio are maintained at the design values by pre-calibrated orifices located in the turbine inlet lines.

Engine shutdown is accomplished by closing the gas-generator valves, which is followed by the closure of the thrust-chamber valves.

3. Propellant Utilization Considerations

In propulsion systems where engine mixture ratio is high and fuel density is low (i.e., LO_2/LH_2 systems), minimization of residual propellant weight by loading extra fuel to ensure oxidizer exhaustion is attractive. An analysis performed for a 6,000,000-lb-thrust engine, similar in configuration to that used as the standard vehicle, indicated that engine tolerance effects may produce a mixture ratio shift of + 1.5 to -1.0%. This analysis is included as Appendix G. When acceleration characteristics during flight are known, tank loading mixture ratio can be accurately adjusted to compensate for mixture-ratio changes resulting from varying suction conditions. Using these results, and an assumed $\pm$ 0.2% tank loading accuracy, the loading of 1.4% extra fuel or 0.21% extra total propellants will ensure oxidizer exhaustion. Increasing the extra loaded propellant to 0.5% still appears attractive and is believed to be very competitive with a propellant utilization system because of simplification in the stage system.

On this basis, it was decided not to incorporate a propellant utilization system into the standard vehicle. If it is later deemed desireable the engine configuration is easily adaptable to either mixture ratio or chamber pressure control.

TABLE III A-1

ENGINE CHARACTERISTICS FOR THE STANDARD VEHICLE BOOSTER

ENGINE	
Vaccum Thrust, lb	2.44×10^6
Sea Level Thrust, lb	2.03×10^6
Vacuum Specific Impplse, sec	412
Sea Level Specific Impulse, sec	345
Oxidizer Flow Rate, lb/sec	5005
Fuel Flow Rate, lb/sec	883
Mixture Ratio, O/F	5.55
Length, ft	18.62
Diameter, ft	15.5
THRUST CHAMBER ASSEMBLY	
Vacuum Thrust, lb	2.40×10^6
Sea Level Thrust, lb	2×10^6
Vacuum Specific Impulse, sec	416
Sea Level Specific Impulse, sec	349
Chamber Pressure, plenum, psia	1000
Chamber Pressure, injector face, psia	1052
Area Ratio, A_e/A_t	20
Mixture Ratio, O/F	6.0
Propellant Flow Rates, lb/sec	5740
Oxidizer	4935
Fuel	805
Characteristic Velocity, C*, ft/sec	7450
Vacuum Thrust Coefficient, C_F	1.78
Sea Level Thrust Coefficient, C_F	1.51

TABLE III A-1 (cont.)

TURBOPUMPS	Oxygen	Hydrogen
Propellant Flow Rate (lb/sec)	5005	883
Pump Discharge Pressure (psia)	1300	1300
Pump Total Suction Pressure (psia)	73	29
Propellant Vapor Pressure (psia)	21	22
Turbine Inlet Total Pressure (psia)	1000	1000
Turbine Exit Static Pressure (psia)	100	100
Turbine Total Flow Rate lb/sec	70	78
Total Exhaust Thrust (lb) sea-level	30,000	
Turbine Exhaust Thrust (lb) Vacuum	40,000	

GAS GENERATOR	
Mixture Ratio	1.0
Flow Rate	148
Chamber Pressure	1000
Gas Temperature	1800

TABLE III A-1 (cont.)

	Oxidizer	Fuel
PRESSURE SCHEDULE (PSIA)		
Propellant System		
Chamber, Plenum	1000	1000
Chamber, Injector Face	1052	1052
△P Injector	120	60
Injector Inlet	1172	1112
△P Coolant Jacket		143
Coolant Jacket Inlet		1255
△P Line and Orifice and Valve	128	45
Pump Discharge	1300	1300
Turbine System		
Turbine Inlet	700	700
△P Orifice and Ducting	150	150
Gas Generator Injector Face	850	850
△P Injector	120	170
Injector Inlet	970	1020
△P GGV	80	100
GGV Inlet	1050	1120
△P Orifice and Line	130	135
GG Propellant Tap-Off	1180	1255

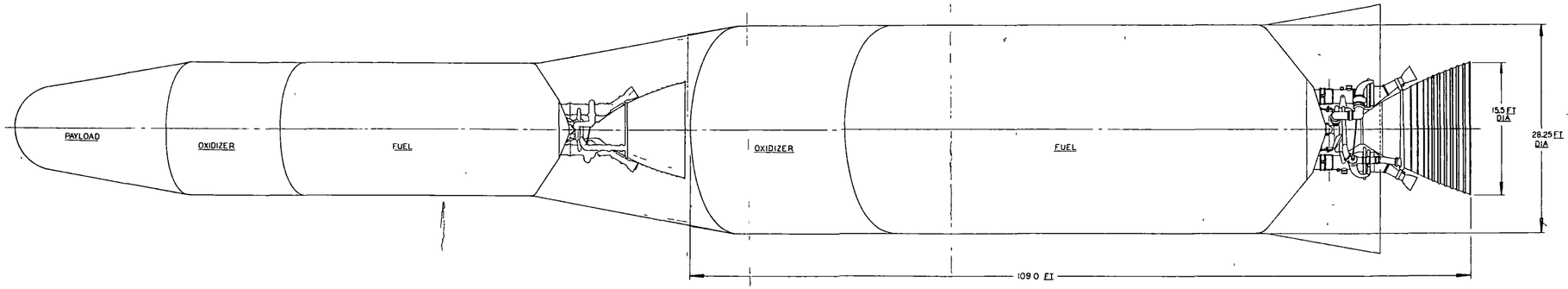

Standard Vehicle, 2,000,000-lb-Thrust Booster

Figure III A-1

TCA		PARAMETER	ENGINE	
SEA LEVEL	VACUUM		SEA LEVEL	VACUUM
670*	824.0*	THRUST	2,000,800*	2,464,000*
349	419	SPECIFIC IMPULSE	345	412
6.0	6.0	MIXTURE RATIO	5.55	5.55
1000	100.0	THRUST CHAMBER PRESS	1000	1000 PSIA
20	20	NOZZLE AREA RATIO	20	20
5745	5719	FLOW RATE LB/SEC	5680	5680
		WET WEIGHT LBS	16401	

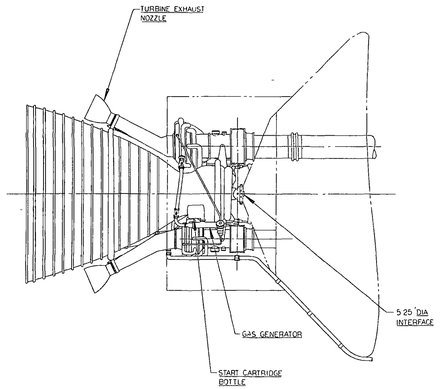

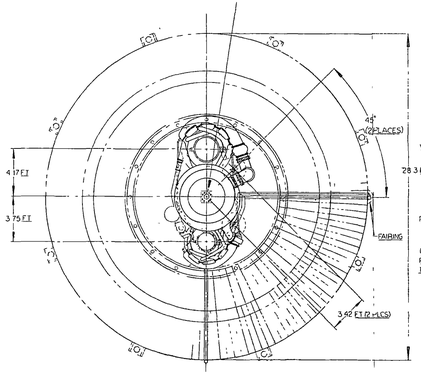

VIEW A-A
(PART OF VIEW OMITTED FOR CLARITY)

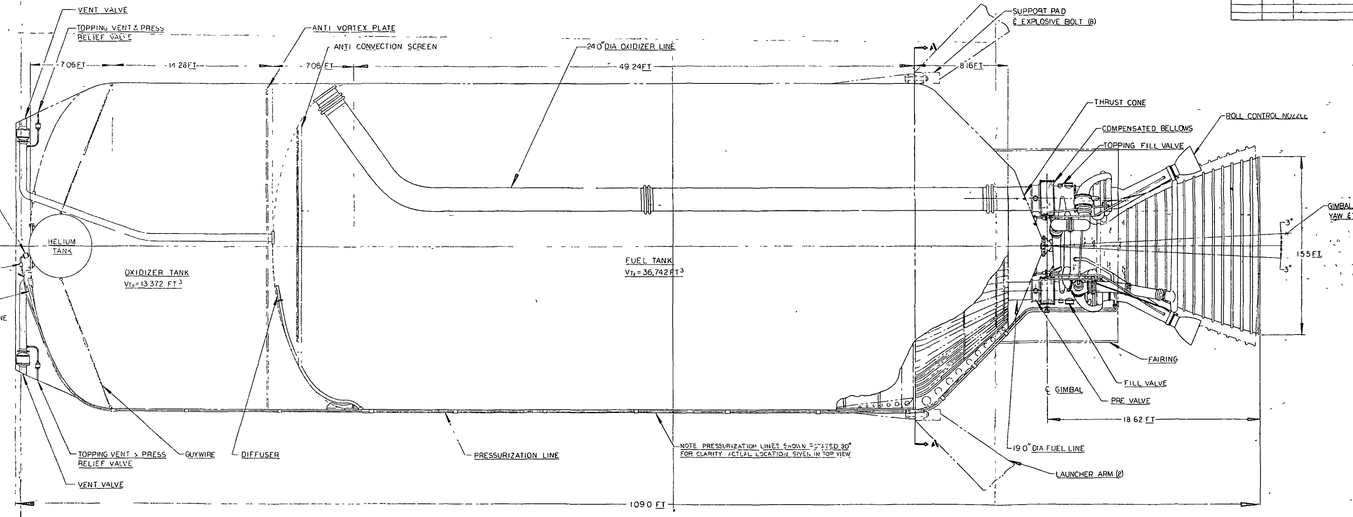

Standard Booster, 2,000,000-lb-Thrust DeLaval Engine

Figure III A-2

23 TOPPING VENT & PRES RELIEF VALVE 100 DIA

24 PRESSURE REGULATOR

25 OXIDIZER TURBINE

26 HELIUM HEAT EXCHANGER FLOW RATE 2.2 LB/SEC

27 HELIUM FILL VALVE

28 THRUST CHAMBER VALVE OXIDIZER FLOW RATE 4420 LB/SEC LINE SIZE 10 IN

29 SAFETY BURST DIAPHRAGM & PRESSURE RELIEF

30 HELIUM TANK VOLUME = 88.6 CU FT WT TANK 1900 LB PRESS (INTIAL) 3000 PSIA

31 SOLID GRAIN START CARTRIDGE

32 PRE VALVE SQUIB OPERATED

22 MAIN VENT VALVE 900 DIA

21 OXIDIZER TANK DIA 28.25 FT. PRESS 63 PSIA MAT'L 2014T6 AL ALLOY WEIGHT 7736 LBS

20 FUEL TANK DIA 28.25 FT PRESS 33 PSIA MAT'L 2014T6 AL ALLOY WEIGHT = 26196 LBS

19 OXIDIZER FILL VALVE CAPACITY = 833 GAL/MIN DIA 4 IN

18 FUEL FILL VALVE CAPACITY 1720 GAL/MIN DIA 4 IN

17 OXIDIZER PUMP FLOW RATE 4989 LB/SEC SUCTION PRESSURE 75 PSIA DISCHARGE PRESSURE 1900PSI

16 FUEL PUMP FLOW RATE 883 LB/SEC SUCTION PRESSURE 29 PSIA DISCHARGE PRESSURE 3000 PSIA

15 FUEL TURBINE

14 GAS GENERATOR IGNITER

13 GAS GENERATOR FLOW RATE 148 LB/SEC MR 60

12 CONTROL VALVES GAS GENERATOR 1% 740 LB/SEC IN VALVE 4% 740 LB/SEC IN VALVE

11 GAS GENERATOR VALVE ACTUATOR

10 GAS GENERATOR BALANCING ORIFICE

9 HYDROGEN HEAT EXCHANGER FLOW RATE 15.2 LB/SEC

8 TCV PNEUMATIC ACTUATOR

7 THRUST CHAMBER VALVE FUEL FLOW RATE 826 LB/SEC LINE SIZE - 13 IN

6

5 TCA IGNITER ASSY

4 ROLL CONTROL ACTUATOR

3 ROLL CONTROL NOZZLE

2 TCA GIMBAL ACTUATOR PNEUMATIC ACTUATOR ELECTRICALLY CONTROLLED

1 THRUST CHAMBER F SL = 15 LBS (1% LEVEL) P/Pc 50 1 W 3740 LB/SEC MR 6.1 Isp 349 SEC (1% LEVEL)

LEGEND

- FUEL LIQUID HYDROGEN
- OXIDIZER LIQUID OXYGEN
- HIGH PRESSURE HOT GAS
- LOW PRESSURE HOT GAS
- FUEL PRESSURIZATION (H2 GAS)

Controls Schematic, 2,000,000-lb-Thrust Standard Vehicle

Figure III A-3

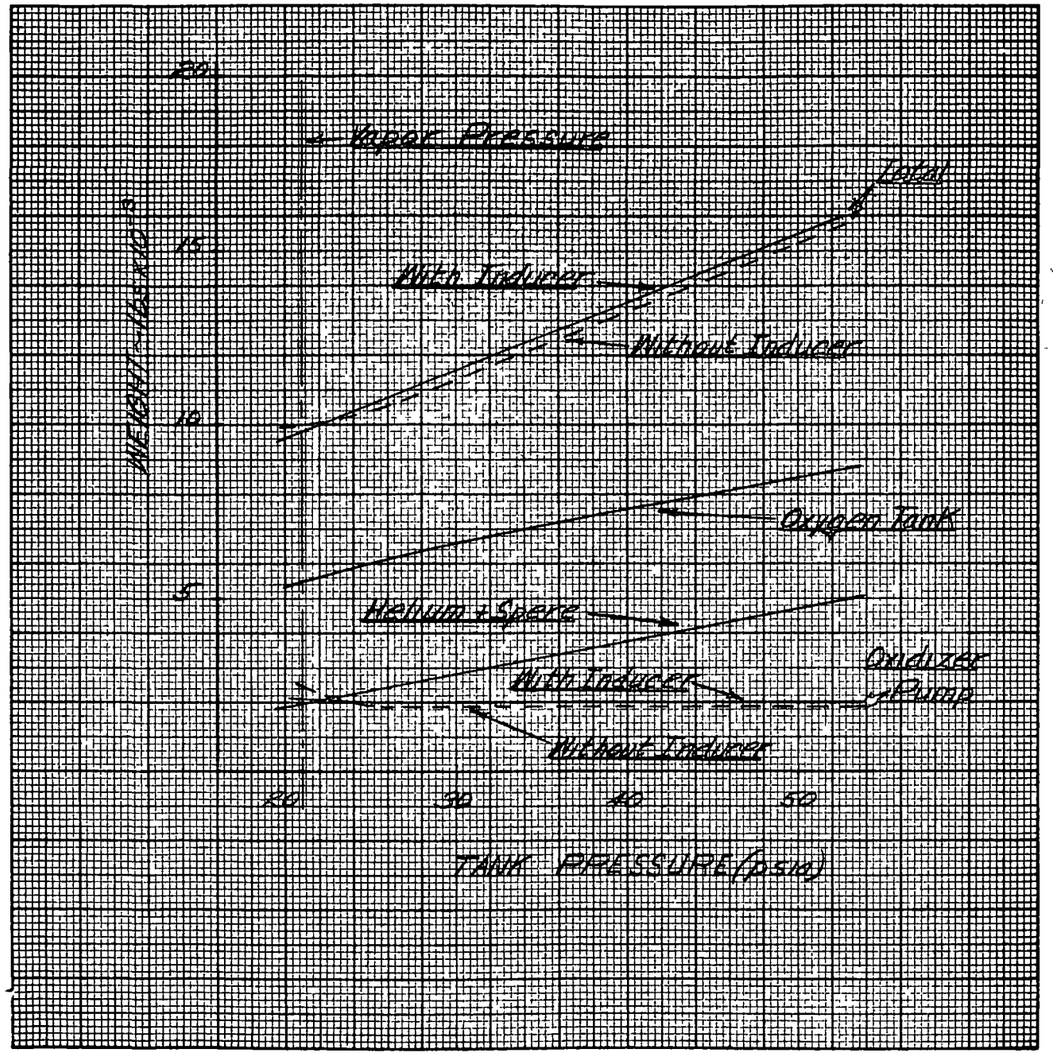

Weight of Oxygen Tank Pressurization System vs Tank Pressure

Figure III A-4

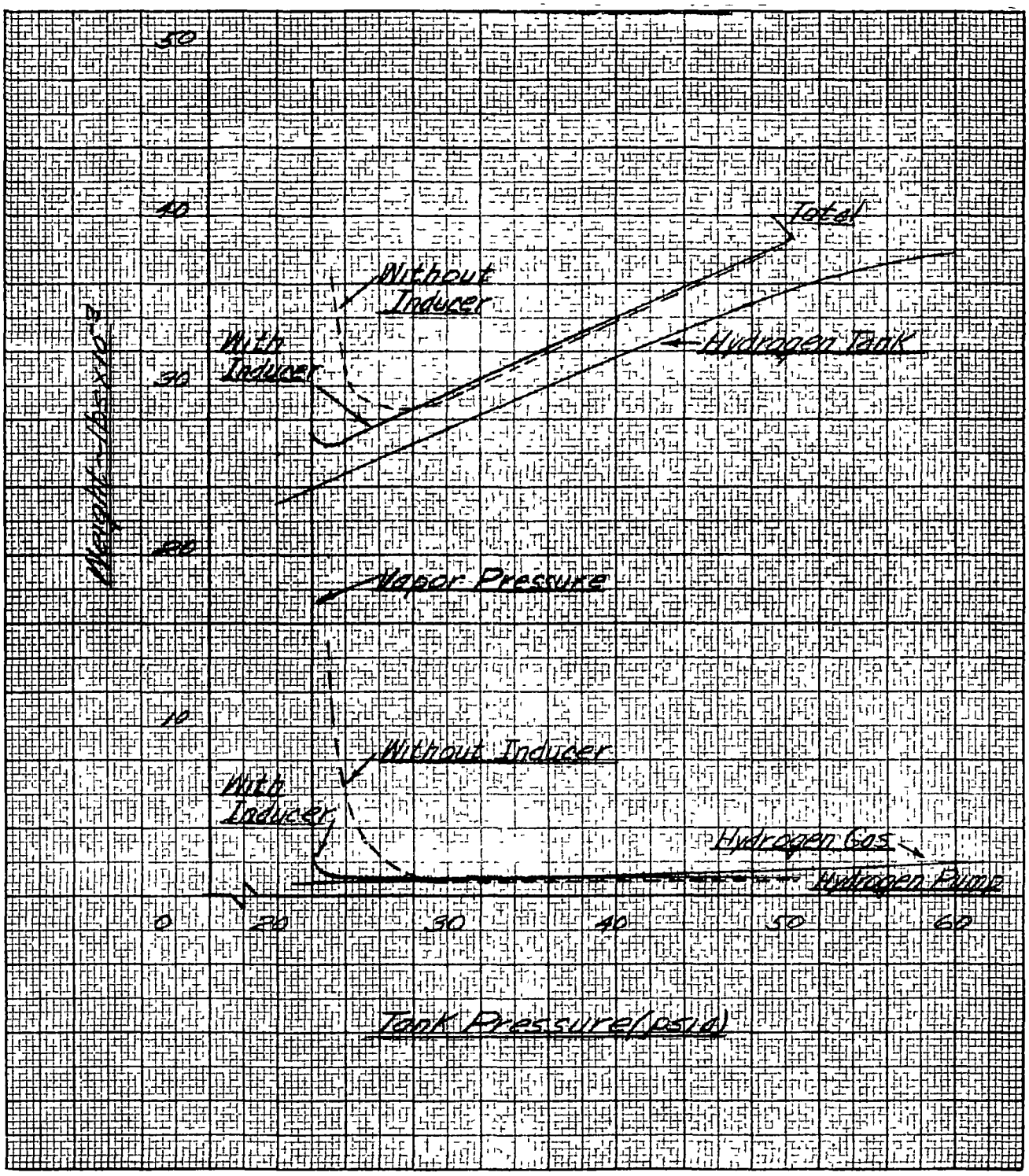

Weight of Hydrogen Tank Pressurization System vs Tank Pressure

Figure III A-5

ROCKET ENGINE CONVENTIONAL DELAVAL 2×10^6 THRUST

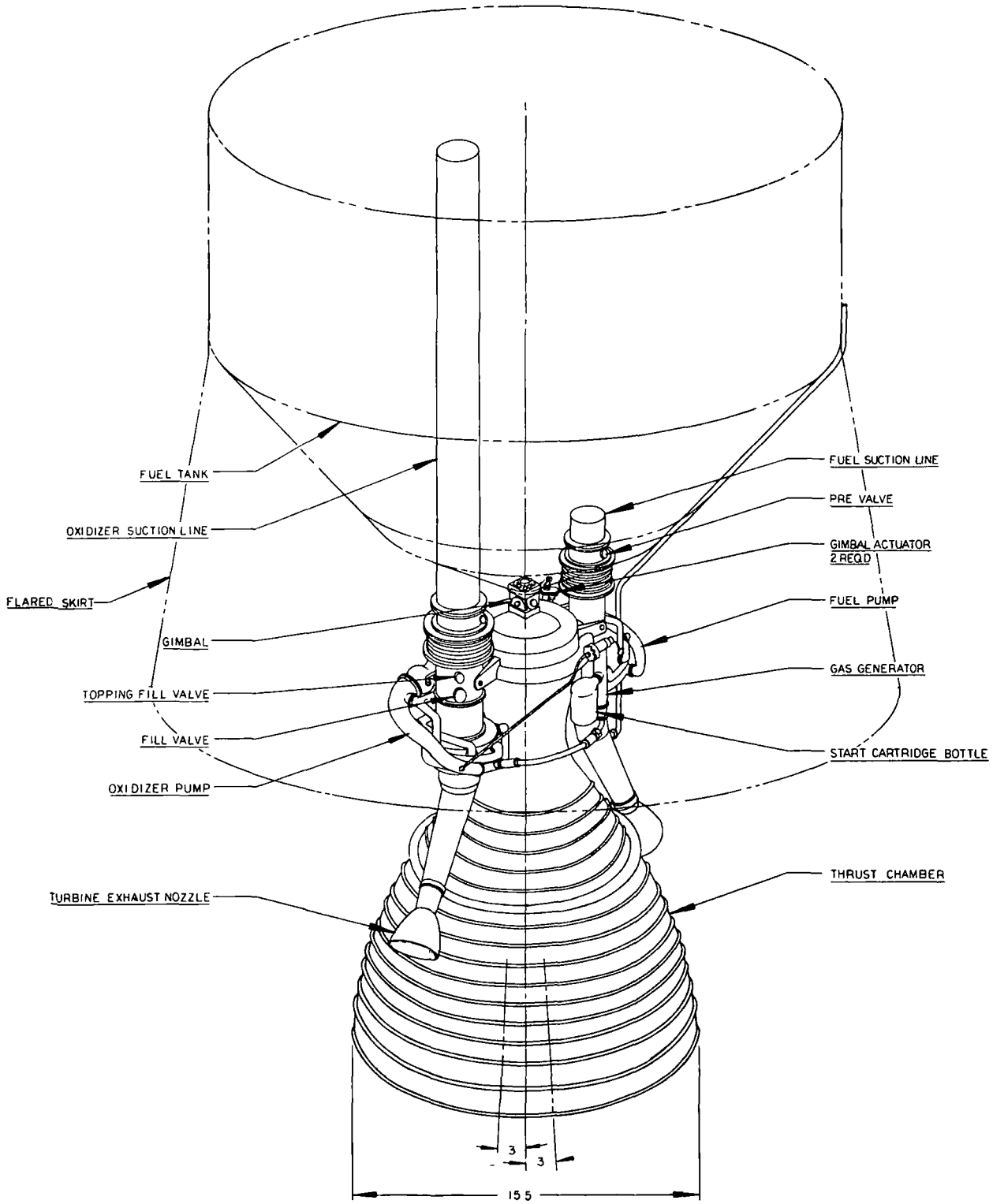

Rocket Engine Conventional DeLaval, 2000,000-lb-Thrust

Figure III A-6

III, Bases for Evaluation (cont.)

B. MISSIONS, TRAJECTORY, AND VEHICLE ASSUMPTIONS

The trajectory and vehicle assumptions used to evaluate the payload capability of the various liquid propellant rocket vehicles are presented in this section.

1. Missions and Trajectory

The performance of boosters is significantly affected by the flight path selected. Once the mission is eatablished, this flight path can be defined within reasonable limits.

Extensive experience in rocket vehicle trajectory analysis over a wide range of vehicle sizes, performance, thrust levels, and a number of stages for many space missions has shown that a realistic booster trajectory analysis can be accomplished simply by using the following vehicle trajectory.

For all space missions, a gravity turn, continuous thrust trajectory to a low altitude circular orbit condition, and subsequent transfer to further missions from this low altitude orbit yields very close to the minimum total required vehicle ideal velocity increment; therefore, maximum vehicle payload. Thus, the specific space mission has little effect upon the first stage flight path. Hence, the low altitude orbit, which generally varies between 50 and 100 nm for most liquid propellant two- and three-stage vehicles, has been used to establish booster flight paths.

An exception to this trajectory is a rescue or intercept mission because the main criterion here is probably minimum time to intercept.

III, B, Missions, Trajectory, and Vehicle Assumptions (cont.)

Missions of this nature will most likely be infrequent and have not been considered in this booster trajectory analysis. Boosters and vehicles designed for the maximum payload flight path could be used to accomplish the intercept mission and the performance penalty accepted for the sake of over-all economy.

Although the booster flight path can be assumed to be independent of the space mission, vehicle staging or weight distribution between stages is not. Besides being dependent upon the mission, vehicle staging is a function of the individual stage engine specific impulses, thrust levels, inert weights, and number of vehicle stages. Because it appears that the most generally used missions for the next generation vehicles will be the 300 nm circular earth orbit and escape missions, these missions have been used to determine optimum vehicle staging and compare vehicles using various booster configurations.

The trajectory calculations which involve the numerical integration of the equations of motion along the vehicle flight path were performed using an IBM-7090 digital computer. The assumptions and equations used in the computer program are discussed in the following paragraphs.

a. Assumptions

(1) Nature of the Earth

(a) The earth is a sphere, of radius $r_e = 2.09029 \times 10^7$ ft rotating about the polar axis with a constant angular velocity $w_e = 7.29211 \times 10^{-5}$ rad/sec.

III, B, Missions, Trajectory, and Vehicle Assumptions (cont.)

(b) Properties of the atmosphere are as given in ARDC Model Atmosphere, AFCRC TN-56-204, December 1956. The atmosphere is stationary with respect to the rotating earth.

(c) The gravitational field of the earth is an inverse square force field. Gravitational acceleration (g_e) at the surface of the earth is 32.17405 ft/sec^2, equivalent numerically to the standard force-mass conversion factor (g_c). Gravitational acceleration (g) is in the direction opposite to the radius vector from the earth's center to the accelerated body, and its magnitude is:

$$g = g_e \left(\frac{r_e}{r}\right)^2 \qquad \text{(Eq 1)}$$

Where r is the distance from the earth's center to the accelerated body.

(2) Coordinate System Used

Nonrotating coordinate system with the origin at the center of the earth.

(3) Pattern of Guidance

(a) Perfect guidance is realized.

(b) The vehicle trajector lies in a plane.

(c) Launch is eastward from a latitude of 28.5° with respect to the equatorial plane, and the deviation of the relative wind velocity from this plane is negligible.

III, B, Missions, Trajectory, and Vehicle Assumptions (cont.)

(d) Staging is instantaneous

(e) The angle pattern develops as follows:

1 Vertical rise with zero angle of attack, until velocity of 280 ft/sec is attained.

2 Step-change in angle of attack (kick angle) and constant vehicle attitude thereafter, until angle of attack returns to zero. The value of the "kick angle" is determined so that the magnitude and direction of the velocity vector necessary for circular orbit are achieved simultaneously.

3 Zero angle of attack thereafter (gravity turn).

(4) Forces and Accelerations Acting Upon the Vehicle

(a) The aerodynamic drag (D) is independent of the angle of attack and is directed opposite to the relative wind velocity vector.

$$D = \frac{\rho_a \, v_{RW}^2}{2g_c} C_{D1} S_1 \qquad \text{(Eq 2)}$$

where, ρ_a is the atmospheric density, v_{RW} is scalar relative wind velocity, C_{D1} is the drag coefficient for the entire vehicle, and S_1 is the cross-sectional area of the first stage, $v_{RW} = v - w_e \, r \cos \lambda$, where λ is the latitude at launch, and r is the distance from the earth's center to the vehicle. Because C_{D2} (after staging) is typically higher than C_{D1} by roughly the ratio of S_1 and S_2, and the

III, B, Missions, Trajectory, and Vehicle Assumptions (cont.)

drag during second-stage operation is small, the drag formula (Eq 2) is used through both first- and second-stage operation until second-stage burnout. The required program input is drag coefficient as a function of Mach number.

(b) The aerodynamic lift is zero.

(c) After burnout of the second stage, the vehicle motion is in a vacuum.

(d) The instantaneous mass (M) of the vehicle in any particular stage of operation is:

$$M = M_o - \dot{w}_E (t - t_o) \qquad \text{(Eq 3)}$$

where M_o is the vehicle mass at start of that stage; $\dot{w}_E$ is the propellant mass flow rate; t is the elapsed time from launch, and t_o is the elapsed time from launch until start of the stage.

(e) The engine thrust (F_E) is in the direction of the longitudinal axis of the vehicle. Its magnitude is determined from

$$F_E = F_E \text{ (vac)} - P_a A_E \qquad \text{(Eq 4)}$$

where F_E (vac) is the thrust in vacuum of the engine ($\dot{w}_E$ assumed constant), P_a is the atmospheric pressure, and A_E is the effective exhaust area of the engine (the actual thrust-chamber exit area plus the projected turbine-exhaust exit area).

III, B, Missions, Trajectory, and Vehicle Assumptions (cont.)

(f) The vector acceleration (a) of the vehicle is

$$\vec{a} = \frac{g_c}{M}(\vec{F}_E + \vec{D}) + g \qquad \text{(Eq 5)}$$

scalar components tangent (subscript t) and normal (subscript n) to the flight

$$a_t = \dot{v} = \frac{g_c}{M}(F_E \cos\alpha - D) - g_e \left(\frac{r_e}{r}\right)^2 \cos\gamma \qquad \text{(Eq 6)}$$

$$a_n = v\dot{\psi} = \frac{g_c}{M} F_E \sin\alpha - g_e \left(\frac{r_e}{r}\right)^2 \sin\gamma \qquad \text{(Eq 7)}$$

The overhead arrow denotes a vector and the overhead dot denotes differentiation with respect to time. See the following list for remaining symbols.

The various angles are shown diagramatically in Figure III B-1 and are positive as shown.

The angles are related:

$$\beta + \gamma + \psi = \frac{\pi}{2} \qquad \text{(Eq 8)}$$

$$\theta - \alpha = \psi \qquad \text{(Eq 9)}$$

Components of velocity tangent and normal to the earth's surface are

$$\dot{r} = v \cos\gamma \qquad \text{(Eq 10)}$$

$$r\dot{\beta} = v \sin\gamma \qquad \text{(Eq 11)}$$

III, B, Missions, Trajectory, and Vehicle Assumptions (cont.)

LIST OF SYMBOLS

Symbol	Meaning	Typical Unit
A_E	Effective exhaust area of engine (the actual thrust-chamber exit area plus the projected turbine-exhaust exit area)	ft^2
a	Vehicle acceleration	ft/sec^2
a_n	Component of vehicle acceleration normal to flight path	ft/sec^2
a_t	Component of vehicle acceleration tangent to flight path	ft/sec^2
C_{D1}	Drag coefficient for the entire vehicle (to be used with first stage, cross-sectional area)	-
D	Aerodynamic drag force	lb_f
F_E	Engine thrust	lb_f
$F_{E(vac)}$	Engine thrust in vacuum	lb_f
g	Gravitational acceleration	ft/sec^2
g_c	Conversion factor in Newton's Law	$\frac{lb_m ft}{lb_f sec^2}$
g_e	Gravitational acceleration at the earth's surface	ft/sec^2
L	Aerodynamic lift force	lb_f
M	Instantaneous mass of vehicle	lb_m
M_o	Vehicle mass at start of a particular stage	lb_m
N_{Ma}	Mach number	-
P_a	Atmospheric pressure	lb_f/ft^2
r	Distance from earth's center to an accelerated body	ft
r_e	Radius of the earth	ft

III, B, Missions, Trajectory, and Vehicle Assumptions (cont.)

LIST OF SYMBOLS (cont.)

Symbol	Meaning	Typical Unit
S_1	Cross-sectional area of the first stage of the vehicle	ft^2
t	Elapsed time from launch	sec
t_o	Elapsed time from launch start of a particular stage	sec
v	Vehicle velocity	ft/sec
$\dot{w}$	Propellant mass flow rate	lb_m/sec
α	Angle of attack, the angle from the instantaneous velocity vector to the longitudinal axis of the vehicle	rad
β	Angle from the vertical at launch to the instantaneous radius vector from earth's center to the vehicle, the "local" vertical	rad
γ	Angle from instantaneous radius vector from earth's center to the vehicle, the local vertical to the instantaneous velocity vector	rad
θ	Angle from the horizontal at launch to the longitudinal axis of the vehicle	rad
ψ'	Angle from the horizontal at launch to the instantaneous velocity vector	rad
w_e	Earth's rotation about the Polar Axis	rad/sec
v_{RW}	Scalar relative wind velocity	ft/sec
	Latitude at launch	-
P_a	Atmospheric density	lb_m/ft^3

III, B, Missions, Trajectory, and Vehicle Assumptions (cont.)

2. Vehicle Assumptions

a. Jettison Weight Parameters

To calculate vehicle payload, it was necessary to determine certain stage jettison weight parameters. A total stage jettison weight, MD, is defined by the following relationship:

$$MD = MT + MOUT + MAF$$

where:
- MD = Total stage jettison weight, lb
- MT = Thrust dependent inert weight, lb
- MOUT = Propellant outage, lb
- MAF = Volume dependent airframe weight, lb

$$MT = (KT)(FV)$$

where:
- FV = Engine vacuum thrust, lb
- KT = Thrust dependent inert weight factor

$$MOUT = (KOUT)(MP)$$

where:
- MP = weight of useable propellant, lb
- KOUT = Propellant outage fraction

$$MAF = (KAF)(VPT)$$

where:
- VPT = Total propellant tank volume, ft^3
- KAF = Propellant tank weight factor (lb of tankage per cu ft of total propellant tank volume), lb/ft^3

$$VPT = (1 + KOUT + KULL)\,VP$$

where:
- VP = Volume of usable propellant, ft^3
- KULL = Ullage fraction

III, B, Missions, Trajectory, and Vehicle Assumptions (cont.)

If the stage jettison weight parameters, KT, KAF, KOUT, and KULL are known, the stage payload can be calculated from the stage burnout weight (stage light-off weight less usable propellant) by using the following relationship:

$$MPL = MBO - MD$$

where:

- MPL = Payload, lb
- MBO = Burnout weight, lb
- MD = Jettison weight, lb

Based on vehicle designs at the two-million-pound thrust level, values for the stage jettison weight parameters were determined. These values are summarized in the following tabulations.

JETTISON WEIGHT FACTORS
Standard O_2/H_2 Vehicle

FACTOR	FIRST STAGE	SECOND STAGE
Thrust dependent inert weight factor, KT	0.0155	0.015
Propellant tank weight factor, KAF	0.62	0.68
Propellant outage factor, KOUT	0.01	0.01
Ullage factor, KULL	0.01	0.01

III, B, Missions, Trajectory, and Vehicle Assumptions (cont.)

JETTISON WEIGHT FACTORS (cont.)

Standard O_2/H_2 Vehicle

FACTOR	FIRST STAGE	SECOND STAGE
	Single-Stage O_2/H_2 Vehicle	
Thrust dependent inert weight factor, KT	0.0143	--
Propellant tank weight factor, KAF	0.623	--
Propellant outage factor, KOUT	0.01	--
Ullage factor, KULL	0.01	--
	Hydrocarbon Vehicle	
Thrust-dependent inert weight factor, KT	0.0147	0.0128
Propellant tank weight, factor, KAF	0.813	0.813
Propellant outage factor, KOUT	0.01	0.01
Ullage factor, KULL	0.01	0.01

III, B, Missions, Trajectory, and Vehicle Assumptions (cont.)

CLUSTERED VEHICLE JETTISON
WEIGHT FACTORS

O_2H_2 PROPELLANT TANK WEIGHT FACTOR, KAF = 0.68		HYDROCARBONS PROPELLANT TANK WEIGHT FACTOR, KAF = 0.813	
Number of Engines Clustered	Thrust Dependent Factor, KT	Number of Engines Clustered	Thrust Dependent Factor, KT
2	0.0159	2	0.0151
3	0.0161	3	0.0153
4	0.0164	4	0.0156
6	0.0167	6	0.0159
8	0.0169	8	0.016

The thrust dependent inert weight parameter includes engine weight and thrust dependent structure weight. For first stages, this factor also includes a weight for an engine skirt, which is lower for single-stage vehicles than for two-stage vehicles because interstage structure is not required. The thrust dependent factor for engine clusters was determined from the single unit thrust dependent weight and Figure III B-2 which shows engine weight as a function of engine vacuum thrust. Figure III B-2 shows that engines become lighter per pound of thrust as the thrust level is increased. No further weight penalties were applied to clustered engine thrust-dependent factors, although it is expected that structural weight penalties would exist to tie the units together.

The thrust dependent factor for O_2/H_2 vehicles is larger than for vehicles using hydrocarbon propellants because of the larger vehicle diameter required for O_2/H_2 propellants. Large vehicle diameter results in bigger thrust carrying members and heavier structure.

III, B, Missions, Trajectory, and Vehicle Assumptions (cont.)

The propellant tank weight factor includes all airframe weights that vary with propellant tank volume. A safety factor of 1.5 was used in calculating the tank weights from the various tank designs. Upper stage O_2/H_2 first stage tank weight factors are higher than O_2/H_2 first stage tank factors largely because of hydrogen tank insulation weight. This insulation weight does not vary directly with propellant tank volume but actually becomes lighter per cubic foot of volume as tank size is increased. It is also mainly because of this that the tank weight factors shown for clustered O_2/H_2 tanks are also larger. Because the structural weight needed to join the tanks has not been included, this tank weight factor for clustered tankage is optimistic.

Tank weight factors for hydrocarbons are larger than for O_2/H_2, mainly because of the larger propellant head caused by the higher density of the fuel.

The tank factor for the single stage O_2/H_2 vehicle is slightly higher than for the booster of a two-stage vehicle because the tank L/D was increased from 3 to 4. Propellant outage factors are shown as 0.01. This factor can be realized if a propellant utilization system is used and if approximately 80% of the propellant normally left in the porpellant suction lines can be utilized. If the propellant in the suction lines is not used before stage shutdown in a system with the oxidizer tank on top, the unused propellant would be approximately 2% of the usable propellant weight. Because this 100% increase in unused propellant appreciably lowers the payload capability of a vehicle, methods for draining the propellant suction lines were investigated and appear to be feasible. Therefore, a propellant outage factor of 0.01 has been used throughout for vehicle payload calculations.

III, B, Missions, Trajectory, and Vehicle Assumptions (cont.)

An ullage factor of 0.01 was also assumed. This assumption may not be reasonable for a hydrogen tank but because the effect of ullage upon total stage jettison mass is extremely small, any error will not appreciably affect the results. For example, increasing the ullage factor from 0.01 to 0.05 will increase the total first stage tank volume of the standard O_2/H_2 vehicle 4%, and the total first-stage airframe weight 4%. However, the effect upon the total first-stage jettison weight is only 1%.

b. Specific Impulse

Specific impulse values used to determine vehicle performance in this report are based upon shifting equilibrium flow. Values of nozzle efficiency, λ, and combustion efficiency, η_c, of 0.97 and 0.98, respectively, were assumed. A thrust chamber mixture ratio of 6:1 was selected for O_2/H_2 propellants. The thrust chamber mixture for hydrocarbons was selected for maximum specific impulse. Area ratios of 20:1 and 16:1, where used for O_2/H_2 vehicles and hydrocarbon vehicles, respectively, are for boosters of the conventional De Laval nozzle configuration. A 40:1 area ratio was assumed for all upper stages. For vehicles using an altitude compensating nozzle operating at optimum expansion at sea level, the area ratio was limited by the vehicle diameter.

$\frac{\vec{M}_g}{g_c}$ Gravitational force vector directed toward center of earth

$\vec{V}$ Velocity vector, tangent to flight path

$\vec{F}$ Thrust vector, in direction of longitudinal axis of vehicle

$\vec{D}$ Aerodynamic drag vector, in negative v direction

$\vec{L}$ Aerodynamic lift vector, perpendicular to D

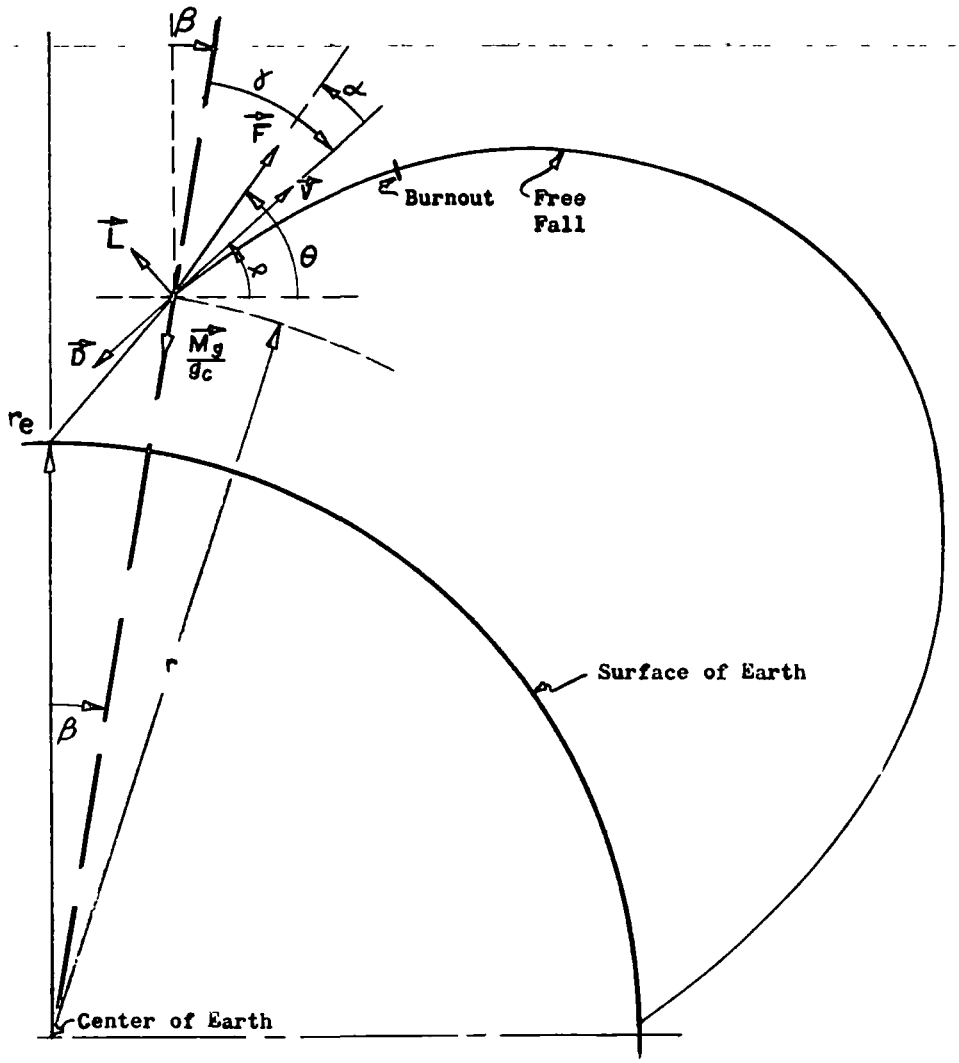

Trajectory Program Diagram

Figure III B-1

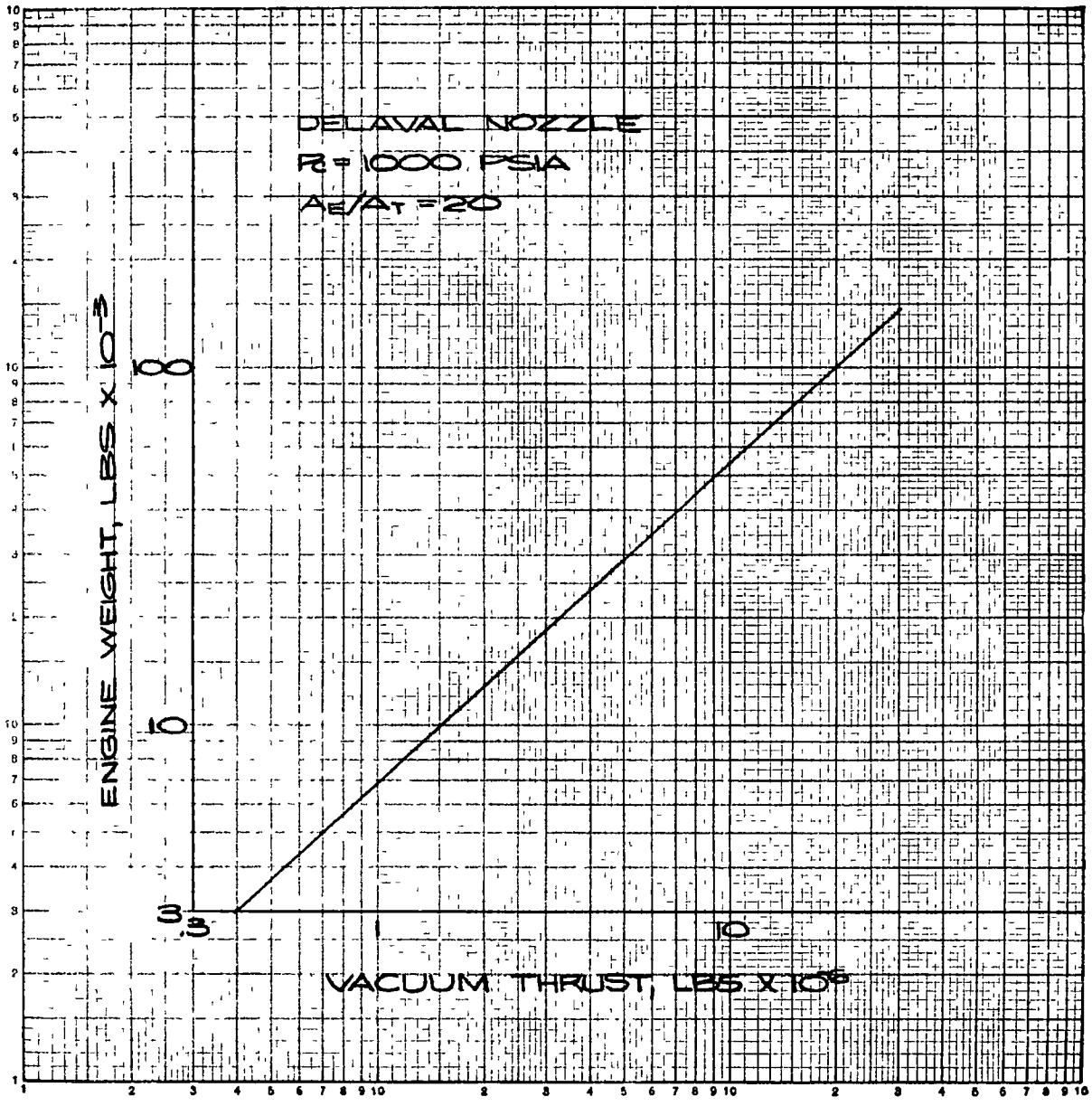

Engine Weight vs Vacuum Thrust

Figure III B-2

III, Bases for Evaluation (cont.)

C. COST AND RELIABILITY

1. General

The objectives of this investigation were to review all concepts suggested for large liquid propellant rockets and determine if one, or more could provide substantially lower costs or higher reliability for space mission payload delivery. It is recognized that neither cost nor reliability can be measured precisely, particularly in preliminary design. Therefore, alternative bases, reflecting trends in cost and reliability, were sought.

In the discussions that follow, the most important objectives for achieving low cost and high reliability are evolved. It is shown that all of the factors contributing to low cost, except low development cost, also contribute to high reliability. It is then shown that most significant contribution a rocket engine can make towards achieving these objectives is high specific impulse and low inert parts weight.

2. Costs

To identify major areas of cost, two airframe manufacturers were approached (The Boeing Airplane Company and The Martin Company). With their aid, costing methods were established. Cost data from the Aerojet-General Corporation Saturn S-II prime contractor proposal were also incorporated. Adequate engine cost data was available at Aerojet-General. These costs were combined to form a cost model, which represents a reasonably accurate picture of rocket vehicle costs (Section III, D).

III, C, Cost and Reliability (cont.)

Examination of this cost model revealed that there was a great deal of fixed cost associated with each stage which had very little dependency upon stage size. This immediately suggested that reducing the number of stages required for a given mission, even if the vehicle size increased somewhat for a particular payload, would cause a significant reduction in rocket vehicle cost-per-pound of payload.

Ultimately, recovery systems will be developed that will permit economical recovery of boosters. Therefore, boosters should be designed, insofar as practicable, so that they can be adapted to these recovery systems with little or no major changes.

Another result shown by the cost model was that engine production costs are quite small as compared with the other vehicle costs involved; therefore, concepts involving methods for reducing engine production costs would not significantly affect program cost. Substantial reduction in development costs would result in important decreases in payload delivery costs. Use of upper stages already developed, where possible, would be advantageous in reducing development costs. Means for significantly reducing development costs through use of current technology must also be considered.

These objectives are tabulated as follows:

a. Minimum number of stages
b. Adaptability to recovery systems
c. Use of developed stages where possible
d. Low development cost for new stages.

III, C, Cost and Reliability (cont.)

3. Reliability

Sources of ultimate unreliability are difficult to assign, however, it was recognized that elimination of major components without serious compromise of other components would improve reliability. This is consistent with the use of a minimum number of stages.

Recoverable vehicle stages that are recovered in a manner that minimizes stage refurbishment have greater reliability than nonrecoverable stages because the reliability of a stage which has completed a flight is greater than the reliability of a stage that has never flown.

Use of upper stages that have already been developed to a high reliability level also can contribute to high mission reliability early in the program

4. Relationship of Objective to Stage Parameters

a Minimum Number of Stages

The single-stage vehicle is the ultimate objective when attempting to reduce the number of stages. Even with O_2/H_2 propellants, the 300 nm orbit mission is a difficult task for a single-stage vehicle. However, reliability is degraded only if the design becomes so marginal that safety factors commensurate with high reliability cannot be used. Inherently high specific impulse and low inert parts weight tend to increase design margin capability so that reliability is not compromised. Small specific impulse increases and inert weight reductions increase single-stage design margin considerably.

III, C, Cost and Reliability (cont.)

b. Adaptability to Recovery System

There are many booster recovery schemes that have been suggested Several of these are discussed in Section III, E, and evaluated when used with the vehicles described in Section II. They have one thing in common All result in weight additions to the booster; however, in all of these methods, the amount of weight added depends upon the inert parts weight without a recovery system. Thus, reducing these booster inert parts weights also reduces the recovery system weight. The benefit from low booster inert weights is thus amplified when recovery is considered. Addition of recovery system weight to the booster also makes high specific impulse more attractive.

c. Use of Developed Stages Where Possible

The possibility of using an existing stage becomes more probable as second-stage size is reduced. The second-stage size can best be reduced if a larger percentage of the mission is accomplished with the first stage. Then, existing second stages can be adapted to larger boosters for larger payload missions. The most important factors in increasing the booster portion of the mission are low inert parts weight and high specific impulse.

d. Conclusions

Evidently, specific impulse increases and inert weight reductions are the most significant contributions that a rocket engine can make towards reducing costs and increasing reliability.

III, C, Cost and Reliability (cont.)

5. Methods of Concept Evaluation

In general, the concepts considered involve both weight and specific impulse changes. To evaluate the combined effects of these changes, vehicle payloads are compared. The effect of specific impulse and inert weight can then be combined so that direct comparisons, on the basis of payload alone, is sufficient to show relative advantages within groups of concepts. This is not always adequate, particularly when comparing single-stage vehicles to two-stage vehicles and O_2/RP-1 with O_2/H_2 propellants because of the differing nature of systems. Consequently, relative costs are shown in these cases. Unreliability, as measured by the number of stages, is used when comparing vehicles with different numbers of stages. A growth potential factor, based on vehicle payload-per-pound of upper stage thrust level is used in cases where upper stage development cost is not included (see Section II., A).

Vehicle payload, as a measure of design margin, should not be interpreted to mean that higher payload always means higher reliability. Design margin actually affects reliability only when close to the design limits. However, as vehicle payload is decreased, the effect of small changes in specific impulse and inert weights upon payload become more pronounced and it becomes of greater necessity to operate near design limits. Therefore, systems of inherently high specific impulse and low inert weight offer greater assurance of not approaching design margins that would adversely affect reliability

III, Bases for Evaluation (cont.)

D. VEHICLE DESIGN PROGRAM

A vehicle design program, incorporating cost factors into the vehicle design selection is described. This program contains a cost and trajectory section which is discussed below.

1. Cost Model

The cost portion of the vehicle design program calculates rocket vehicle costs based upon the cost model described herein.

The cost model contains major areas of propulsion costs as a function of the most important parameters. Costs apply to stages similar to the standard booster (single Laval nozzle engine, tankage, and components). This cost model contains the elements delineated as follows.

Development	Figure
Engine:	
Engineering	
Fabrication	
Testing	III D-1
R and D tooling	
Propellants	III D-2
Test facilities (R and D and production)	III D-3
GSE	III D-4
Production tooling	III D-5

III, D, Vehicle Design Program (cont.)

Development	Figure
Airframe:	
Engineering and project control	
Tooling	
Hardware	III D-6
Test facilities	and III D-7
Stand Operation	
Propellant	
Production	
Engine:	
Fabrication and assembly	III D-8
Acceptance test	III D-9
Airframe:	
Fabrication	
Assembly	
Checkout	III D-10
Test	
Miscellaneous items	
Transportation	III D-11
Launch Support:	
Stage checkout	III D-12
Range time	
Propellants	III D-13

Sources and justification for each of these elements follow as well as rationalization of the parametric variations of these costs.

III , D, Vehicle Design Program (cont.)

a. Engine Development

(1) Engineering, Fabrication, Testing, R and D Tooling (Figure III D-1)

These costs include all engine contractor costs (and fee) through engine qualification for the areas listed. Costs are based upon several engine proposals issued by the Aerojet-General Corporation within the past 18 months. The six-million-pound thrust engine study completed recently by this company verifies the extrapolation of these costs to that thrust level. There is a high degree of confidence at the 10 million-lb thrust level. Thrust chamber development and engine fabrication make up the major thrust dependent development costs. Therefore, for engines using clustered combustors and a single turbopump, the development cost can be expected to be somewhat less than that shown. It is estimated that a 30% development cost savings would result. For clustered engines, the total engine development cost would be increased approximately 30% over that of a single engine of the unit thrust level, whether the engine contractor or the stage contractor integrated the engines to a common structure. This assumption should be applied to clusters of four or more units.

Engine development cost increases by a factor of only two when thrust is increased by a factor of 10. This is rationalized as follows:

If the same type of development program were maintained as thrust level was increased, development hardware and testing costs would increase substantially, but engineering costs would remain constant. However, as hardware and testing costs increase, it becomes economical to

III, D, Vehicle Design Program (cont.)

increase engineering effort to reduce the number of tests and therefore the amount of development hardware required. For each thrust level, an optimum devision of effort exists. This shift of effort for an optimum program results in the development cost increase with thrust level shown in Figure III D-1.

(2) Propellants for Engine Development (Figure III D-2)

Approximate propellant requirements for engine development are shown. These requirements are based upon typical engine test schedules. The reduction in propellant per pound of thrust reflects the assumption that as engines become larger and hardware and testing become more expensive, greater emphasis is placed upon engineering analysis for the solution of problems.

(3) Engine Facilities (Figure III D-3)

The major difference between facilities requirements for O_2/RP-1 and O_2/H_2 is the hydrogen storage. Costs indicated reflect all new facilities. For programs where existing facilities are to be modified, each case must be considered individually. At Aerojet-General, the new facilities required to develop engines to one-million pounds of thrust are insignificant. At higher thrust levels, the curves shown are still somewhat high because existing control rooms can be applied. At some thrust level between three- and ten- million pounds, the Aerojet-General Sacramento facility cannot be used. Then, all new test facilities will have to be relocated. Development test facilities are also adequate for production testing.

III, D, Vehicle Design Program (cont.)

Test facility costs include test stand instrumentation and control rooms. These instrumentation and control room costs do not depend upon thrust level. For a two-million-pound thrust engine, approximately 75% of the costs are for instrumentation and control room. Therefore, test facility costs do not increase very rapidly with thrust level.

(4) Ground Support Equipment (Figure III D-4)

Ground support equipment development includes all transportation trailers, installation fixtures, special tools, ground checkout consoles, ground power supply, and any other special equipment required for engine operations.

Fabrication of a sufficient number of units to support the production engine program is also included. The major variable in ground support equipment costs are transtainers, transportation trailers, and installation fixtures. Other costs, such as special tools and checkout consoles, do not change as the thrust level increases.

(5) Engine Production Tooling (Figure III D-5)

The cost of equipment to initiate engine production is included. Some of the research and development tooling included in engine development cost may be applied to engine production; however, there are additional production machines and fixtures that must be added.

III, D, Vehicle Design Program (cont.)

b. Airframe Development (Figure III D-6)

Costs included in airframe development are the engineering, project control, tooling, hardware expended for qualification of airframe components, establishment of test facilities, test area operation, and propellants. These costs were evolved, based on the program shown in Figure III D-7. Manpower requirements, costs, and schedules were developed from conferences with The Martin Company. Costs shown include only one delivered stage Other stages are charged under production costs. Costs are for a 92-month program. This represents 72 months after first unit delivery.

Development cost appears to have minor dependence upon thrust because major costs are incurred from project management which is unaffected by stage size. The major source of variable cost is actual test stand construction and this cost is a function of thrust level. Because it is a relatively small portion of the total cost (roughly 10% at two-million pounds thrust), the stage development cost changes only slightly with thrust level.

c. Launch Site Cost

Saturn C3 could be launched from the facilities being constructed at AMR, Cape Canaveral, Florida. These facilities appear to be adequate, with only minor modifications, for use with vehicles considered in Task I up to three-million pounds of thrust. Therefore, no cost for establishing the launch site was included in this model.

III, D, Vehicle Design Program (cont.)

d. Engine Production

(1) Fabrication and Assembly (Figure III D-8)

This cost includes: raw materials, fabrication (or outside purchase of components), inspection and quality control of all components; engine assembly, support engineering, overhead, general and administrative, and contractors fees.

Figure III D-7 was prepared by plotting known cumulative average production costs of 100 units for the Titan engines and several recently proposed engines as functions of thrust level. Engine costs at other production quantities were determined using an 85% learning curve. The costs for the standard booster engine as well as a six-million-pound thrust engine estimated prior to the initiation of this study were also used.

Figure III D-7 shows a substantial reduction in engine production cost-per-pound of thrust as thrust is increased. This is attributable to two major factors. Firstly the engine weight-per-pound of thrust decreases somewhat with increasing size. Secondly, there exists a substantial number of fixed costs in production. Costs that remain almost constant as size increases are: inspection, support engineering and quality control

(2) Engine Acceptance Testing (Figure III D-8)

Rocket engine acceptance testing requires: installation of the rocket engine into the test stand, inspection, installation of instrumentation; checkout; hot firing for calibration, installation of required

III, D, Vehicle Design Program (cont.)

orifices for engine balance trim; hot firing for acceptance; postfire inspection; and removal from the test stand. Cost of acceptance testing of major components, such as the thrust chamber assembly and turbopump assembly, are also included. Cost of most of these operations is nearly independent of engine thrust level for a single engine. Those operations depending upon thrust level are engine installation inspection, and installation of instrumentation. The cost of these operations is a relatively minor portion of over-all cost; therefore, acceptance testing cost increases very slightly as thrust level is increased. For clustered engines tested separately, acceptance test cost per engine module can be determined directly from the curve. Clustered engines tested as a unit would offer a small savings (approximately 30%) over testing of the separate modules.

e. Airframe Production

(1) Stage Production Cost (Figure III D-9)

Stage production costs included the following items; stage fabrication, including purchased raw materials and subsystems; detail fabrication; assembly; production checkout; stage acceptance testing; postfire checkout; flight instrumentation; quality control and inspection, flight evaluation; and documentations. These costs were established by reference to the Saturn S-II proposal* and through conferences between Aerojet-General and Martin Company production personnel. In addition, fabrication costs of the cumulative 100 units average were estimated for the airframe of a two-million-pound thrust O_2/H_2 booster, a six-million-pound thrust O_2/H_2 booster, and a two-million-pound

* Aerojet-General Corporation, Proposal AGC-61002, subject: Saturn S-II Stage Prime Contractor, July 1961

III , D, Vehicle Design Program (cont.)

thrust O_2/RP-1 booster. By comparison with these design costs, the costs in Figure III D-9 appear to be conservative. Program airframe production costs were calculated using an 85% learning curve.

Of these costs, only stage fabrication (exclusive of production checkout) shows a significant amount of increase as the size gets bigger. This cost increase is approximately the same as the two-thirds power of propellant tank volume. As a consequence, the stage production cost-per-pound decreases substantially with increasing stage size.

(2) Stage Transportation Cost (Figure III D-10)

Stage transportation costs include all costs involved in transporting a completed stage from the Aerojet-General Liquid Rocket Plant in Sacramento, California to Cape Canaveral, Florida. This involves transportation to the Sacramento River by trailer truck, by barge to San Francisco, and ship to Cape Canaveral via the Panama Canal. A more detailed description of this transportation is available in the Saturn S-II proposal[2].

f. Launch Operations

(1) Launch Support (Figure III D-11)

Launch support includes the stage contractor's personnel required at the launch site. Again, the basis for establishing this cost was the Saturn S-II proposal[3]. Because size has very little effect upon personnel required for this function, stage cost is nearly constant.

2. Ibid.
3. Ibid.

III , D, Vehicle Design Program (cont.)

(2) Launch Operation

It was assumed that the launch operation would be performed by NASA personnel at the Saturn launch facility. Because a staff is continuously assigned to this facility regardless of the type of vehicles being launched, no cost was included, except range time for the actual period of launching. Range time cost was estimated by ascertaining Titan costs, which are approximately $60,000 per hour (eight hours). It was assumed that this time was for approximately 20 equivalent units and that cost is independent of vehicle size. Based on an 85% learning curve, the average cost for 100 units would be $330,000.

g. Propellant Costs for Operational Vehicles (Figure III D-12)

Propellant cost for engine calibration, acceptance, and stage acceptance testing and flight is included. Other assumptions are noted in Figure III D-12.

2. Trajectory

The vehicle design program contains a trajectory section Thus if given a mission ideal velocity increment as well as stage ideal velocity increments, it can provide all of the vehicle parameters required for the program cost phase . If stage ideal velocities are not given, the program will automatically provide values of stage ideal velocity increments resulting in a minimum cost-per-pound of payload. Vehicles up to three stages can be analyzed using this program.

III, D, Vehicle Design Program (cont.)

In the trajectory portion of the computer program, the vehicle size is based upon the input information. The basic trajectory equation used in the program is:

$$\frac{MPL}{MTO} = 1 - KT\left(\frac{FV}{MTO}\right) - \left[1 + KOUT + (1 + KOUT + KULL)\frac{KAF}{RHOB}\right]\left(1 - e^{\frac{VI}{(g)(I_{spv})}}\right)$$

where,

MPL = Stage payload, lb

MTO = Stage light-off weight, lb

KT = Thrust dependent inert weight factor

KV = Engine vacuum thrust, lb

KOUT = Propellant outage fraction

KULL = Propellant ullage fraction

KAF = Propellant tank inert weight factor (lb of tankage per ft^3 of total propellant tank volume), lb/ft^3

RHOB = Propellant bulk density, lb/ft^3

VI = Stage ideal velocity increment, on basis of vacuum specific impulse ft/sec

g = Force mass conversion factor,

$$32.174 \quad \frac{lb_m ft}{lb_f sec^2}$$

ISPV = Vacuum specific impulse, sec

The ideal velocity increment for a particular mission is determined from an IBM - 7090 trajectory program which numerically integrates the equations of motion along the vehicle flight path.

III , D, Vehicle Design Program (cont.)

Detailed weight analyses have been completed for various vehicle configurations. From the results, vehicle inert weight factors were determined and used for performance calculations as well as input to the computer cost program (Section III,B). Inert weight factors are used in determing stage inert weight:

Inert weight = (KT) (FV) + (KAF) (VPT)

Where, VPT = Total propellant tank volume, ft^3

The inert weight factors calculated for O_2/H_2 and $O_2/RP\text{-}1$ tandem staged vehicles are:

	First Stage		Upper Stages	
	O_2/H_2	$O_2/RP\text{-}1$	O_2/H_2	$O_2/RP\text{-}1$
KT	0.0155	0.0147	0.015	0.0128
KAF	0.62	0.813	0.68	0.813

For each stage of the vehicle, the trajectory program prints out oxidizer and fuel total weight, flow rate, and volumes, tank volume, burning time, sea level and vacuum thrust, burnout weight, and propellant mass ratio.

Individual stage thrust to mass ratio or thrust may be input, or the upper stage thrust to light-off mass ratio can be determined from Figure III D-13, which shows the optimum thrust to mass ratio as a function of the stage light-off velocity. This optimum thrust to mass ratio will give the highest vehicle payload-per-pound of first-stage light-off weight and was established through trajectory calculations performed using the IBM-7090 digital computer. The first-stage thrust to light-off mass ratio was assumed to be 1.25:1 in plotting Figure III D-13.

III, D, Vehicle Design Program (cont.)

An important feature of the trajectory program is its ability to determine the staging of a vehicle to provide minimum cost-per-pound of payload. The computer, in conjunction with input, assigns each stage an ideal velocity increment. Then, the size and cost is determined. This procedure is repeated four times, in each instance a different velocity increment split is used. The computer plots the cost-per-pound of payload for each of the five vehicles and selects a stage velocity distribution which results in minimum cost-per-pound of payload. Size and costs are then calculated and printed out for the optimum vehicle. If preferred, stage velocity increments may be input and the optimization routine omitted. Parameters, such as vehicle takeoff weight and stage inert parts weight, are often valuable in determining cost trends. The program can calculate maximum payload/take-off weight ratio and maximum payload/inert weight ratio, as well as associated vehicle costs using a similar optimization routing.

With output from the trajectory portion of the program and basic cost model input, the cost discussed can then be calculated.

3. Cost Investigation Ground Rules

It is noteworthy that all major costs in the described cost model increase less than proportionally with increases in thrust level or size; however, the payload of any particular type of vehicle increases very nearly proportionally as the vehicle is scaled up in size. This means that payload delivery cost per pound will decrease for a given vehicle type as size is increased. There is a further implication. If two different vehicle types are compared at equal take-off weights, the ratio of the resultant cost per pound of payload would be different than if the two vehicle types were compared on the basis of equal payloads. In view of

III , D, Vehicle Design Program (cont.)

this, it is necessary to select a basis for the comparisons. The primary purpose of a rocket vehicle is to deliver a given payload for a given mission; therefore, constant payload was selected as the basis for cost comparisons.

The problem of comparing rocket vehicles over a range of missions is further complicated. If two vehicles have the same payload for one mission, they rarely have the same payload for other missions. Therefore, comparison of these vehicles is only valid at the point where payloads were made equal.

Payloads for the two missions are:

300 nm orbit	122,000 lb
Escape	48,500 lb

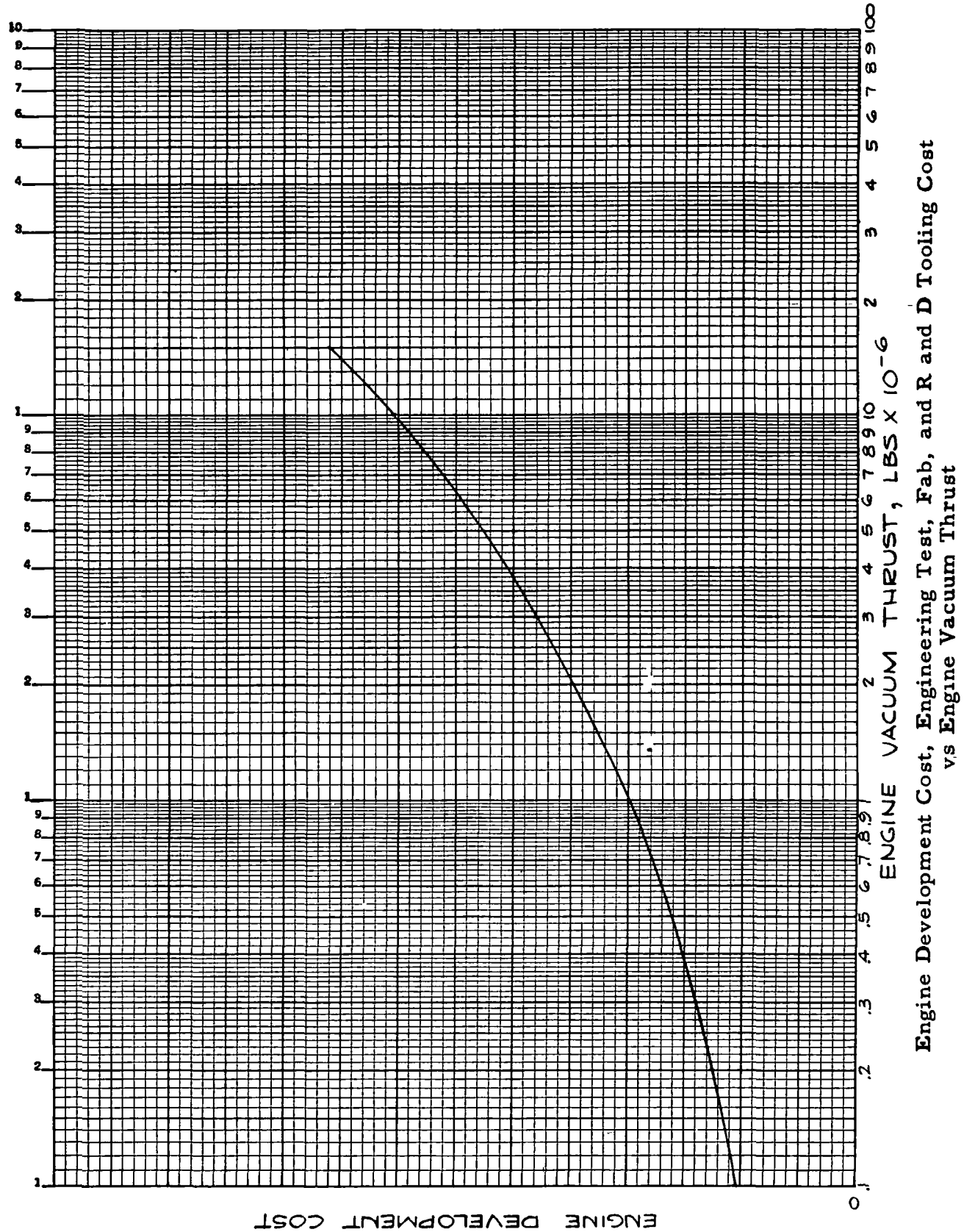

Engine Development Cost, Engineering Test, Fab, and R and D Tooling Cost vs Engine Vacuum Thrust

Figure III D-1

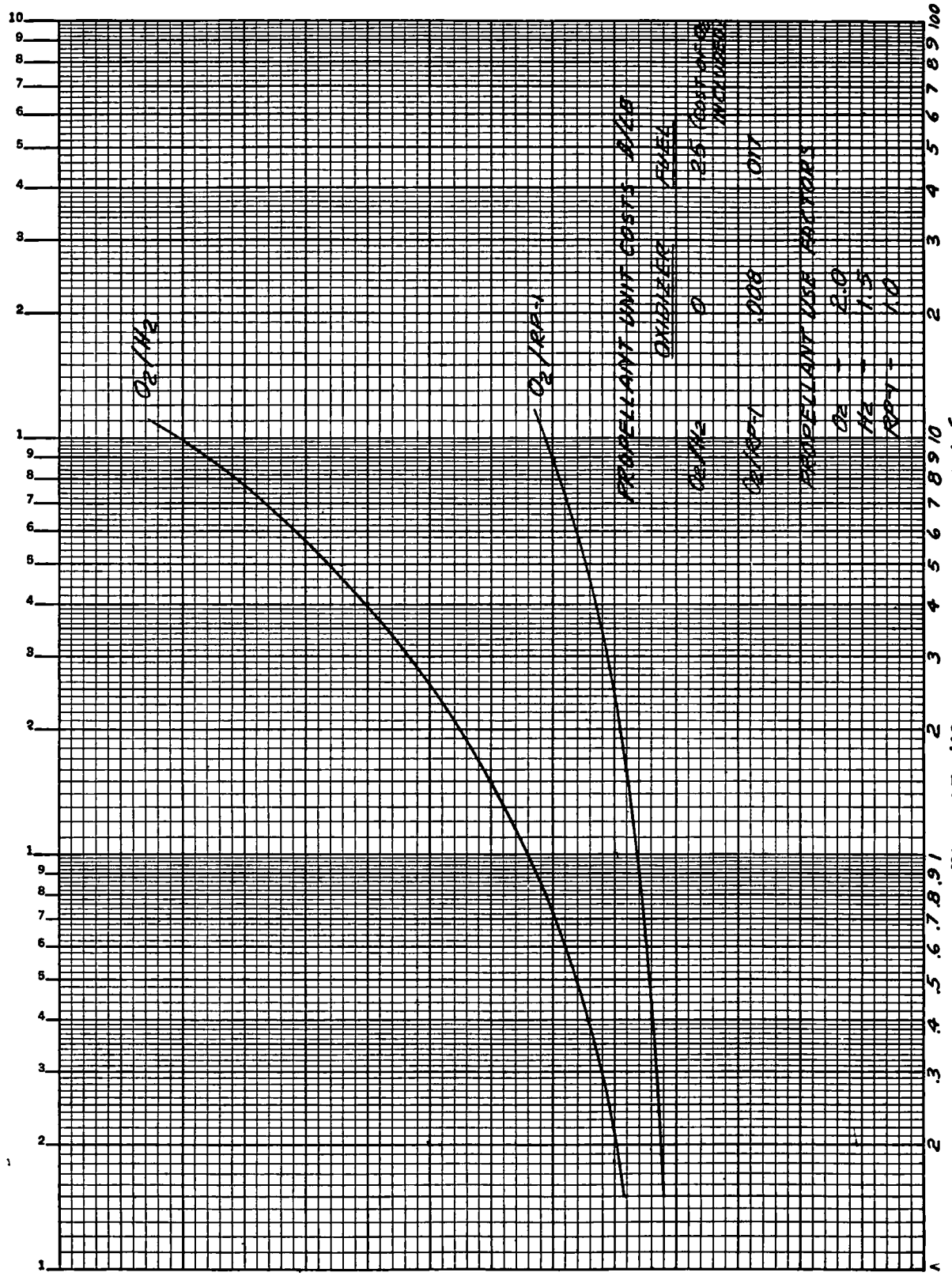

Propellant Costs for Engine Development vs Engine Vacuum Thrust

Figure III D-2

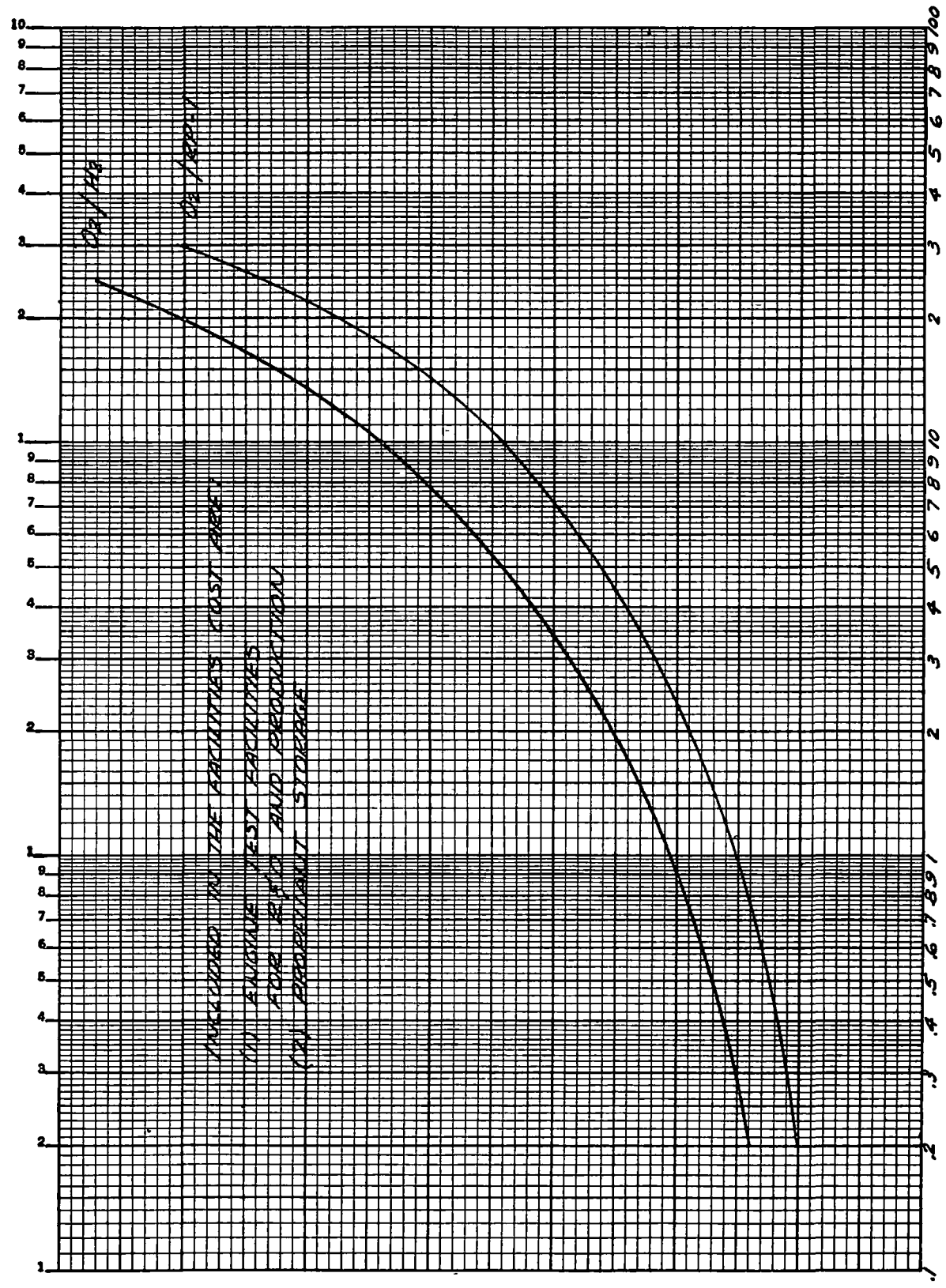

Engine Facilities Cost vs Engine Vacuum Thrust

Figure III D-3

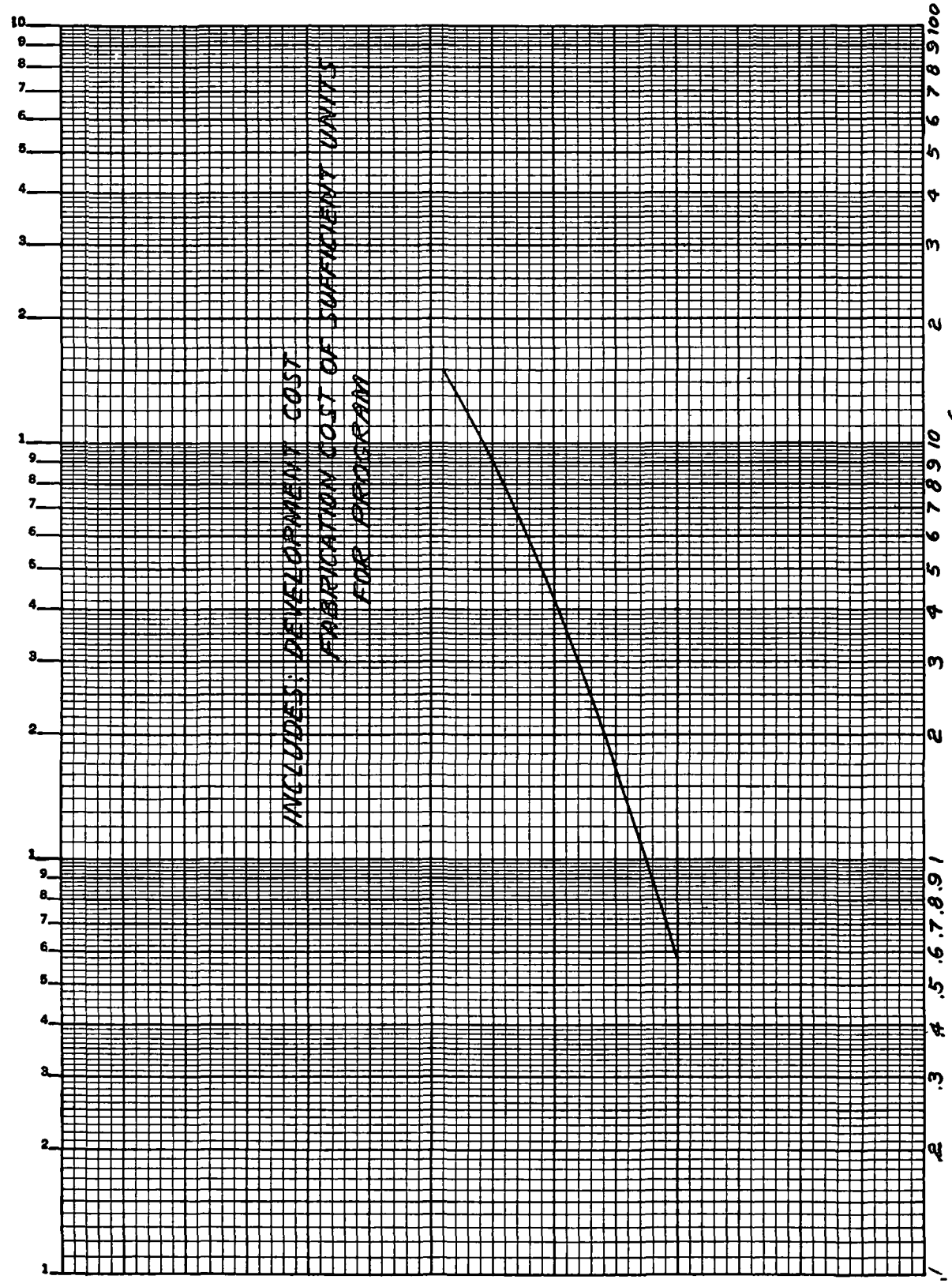

Engine GSE Cost vs Engine Vacuum Thrust

Figure III D-4

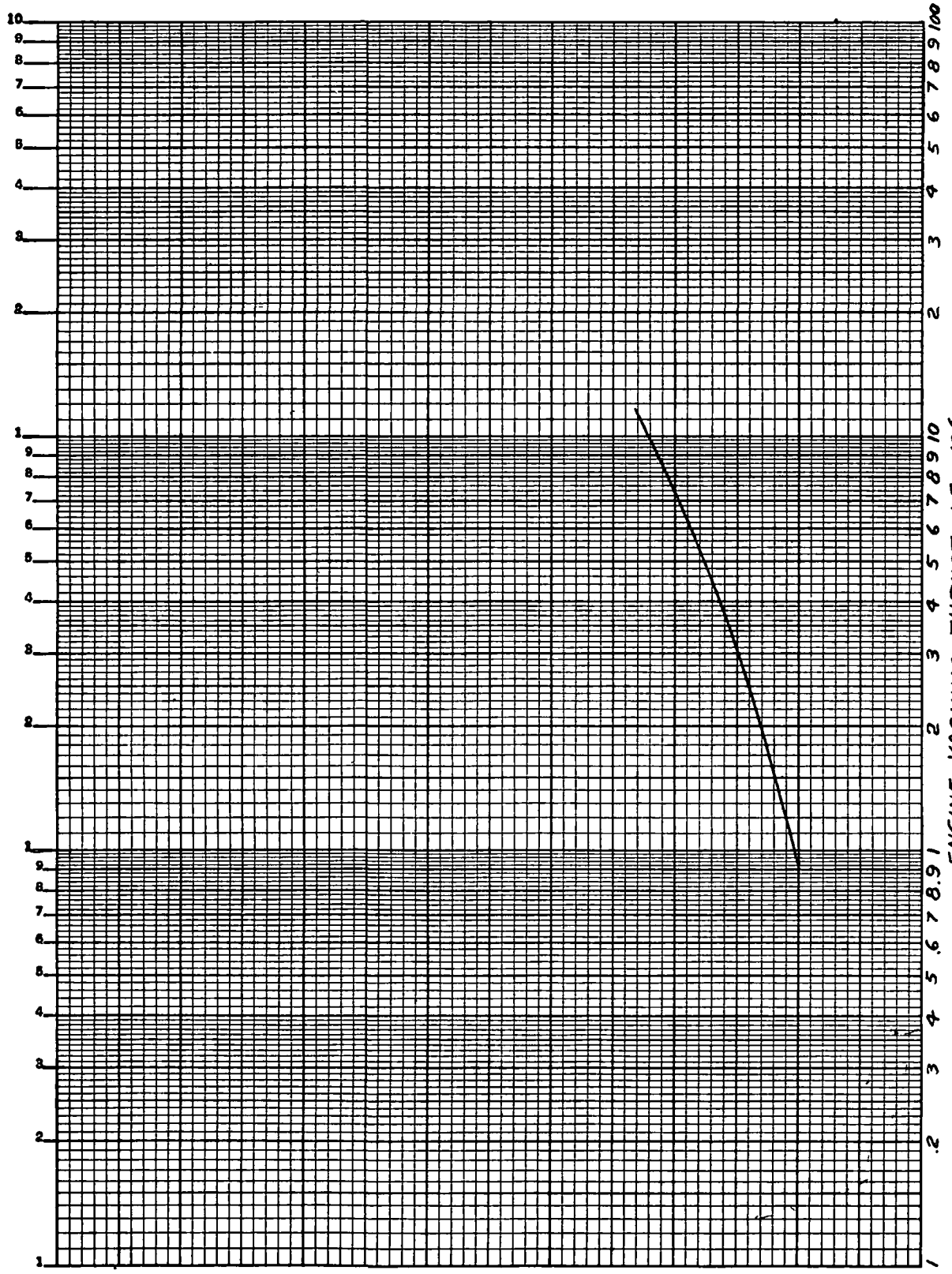

Engine Production Tooling Cost vs Engine Vacuum Thrust

Figure III D-5

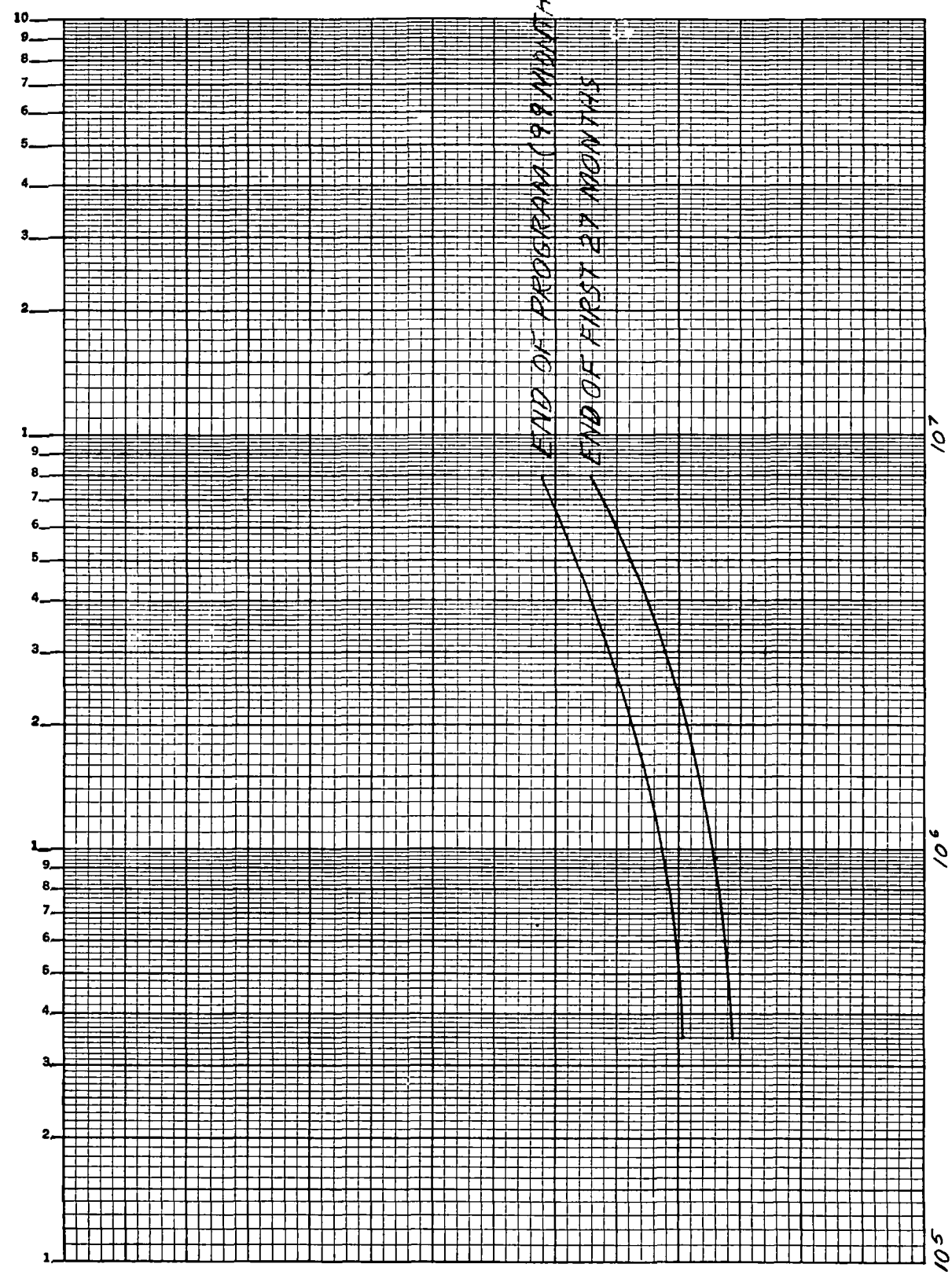

Stage Development and Postdevelopment Program Costs

Figure III D-6

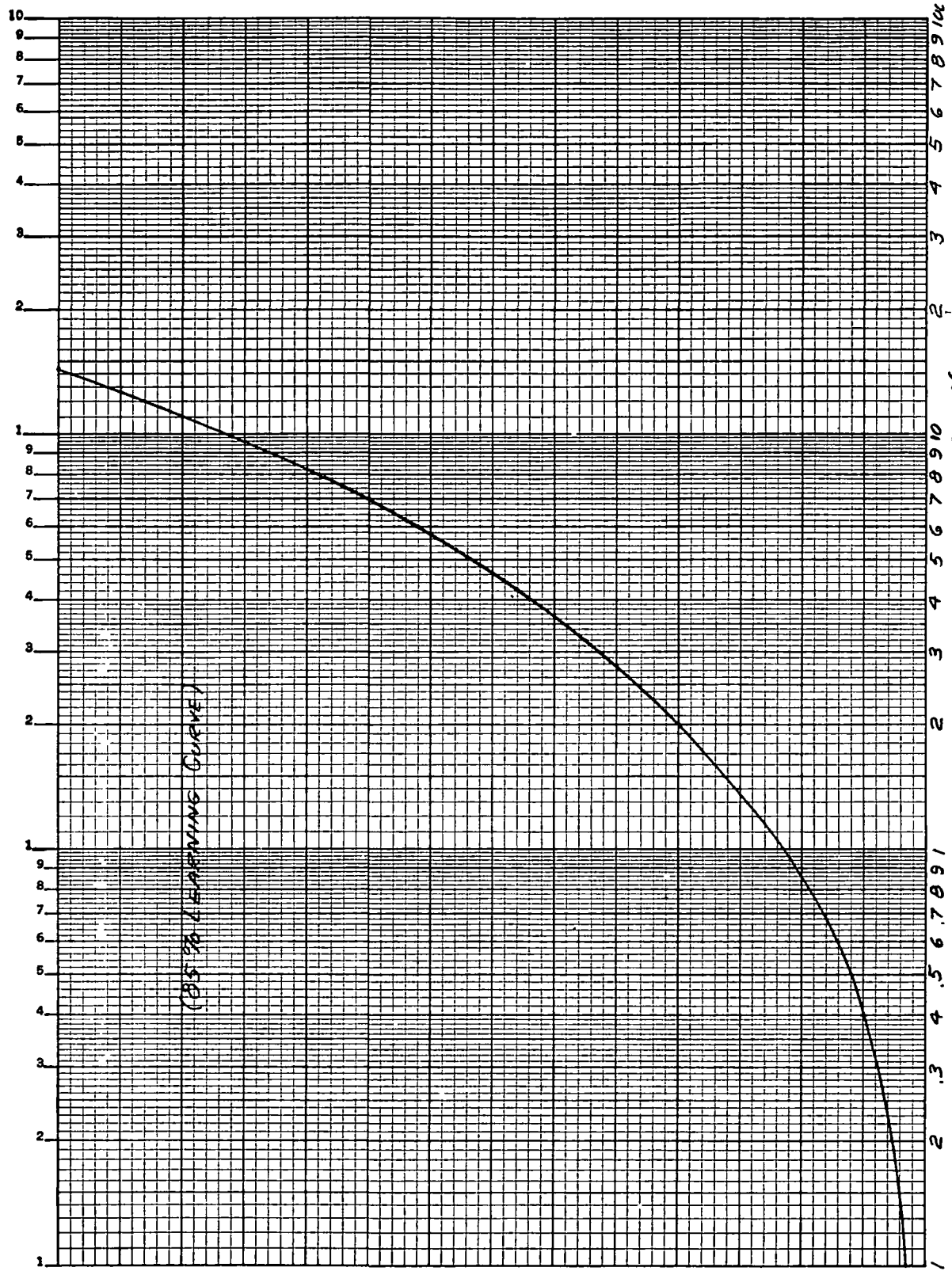

Engine Production Cost vs Engine Vacuum Thrust (Cumulative Average of 100 units)

Figure III D-7

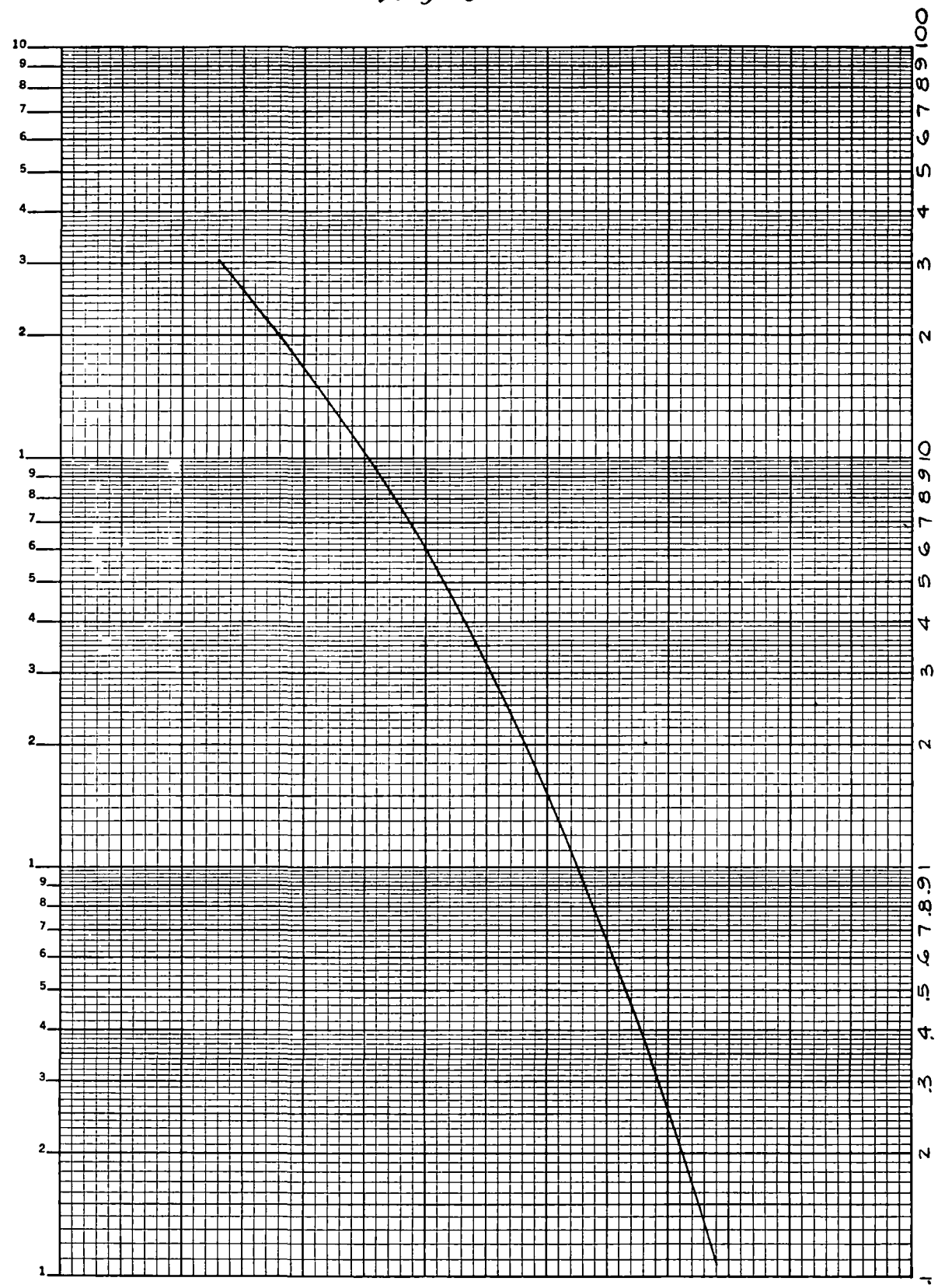

1507

Figure III D-8

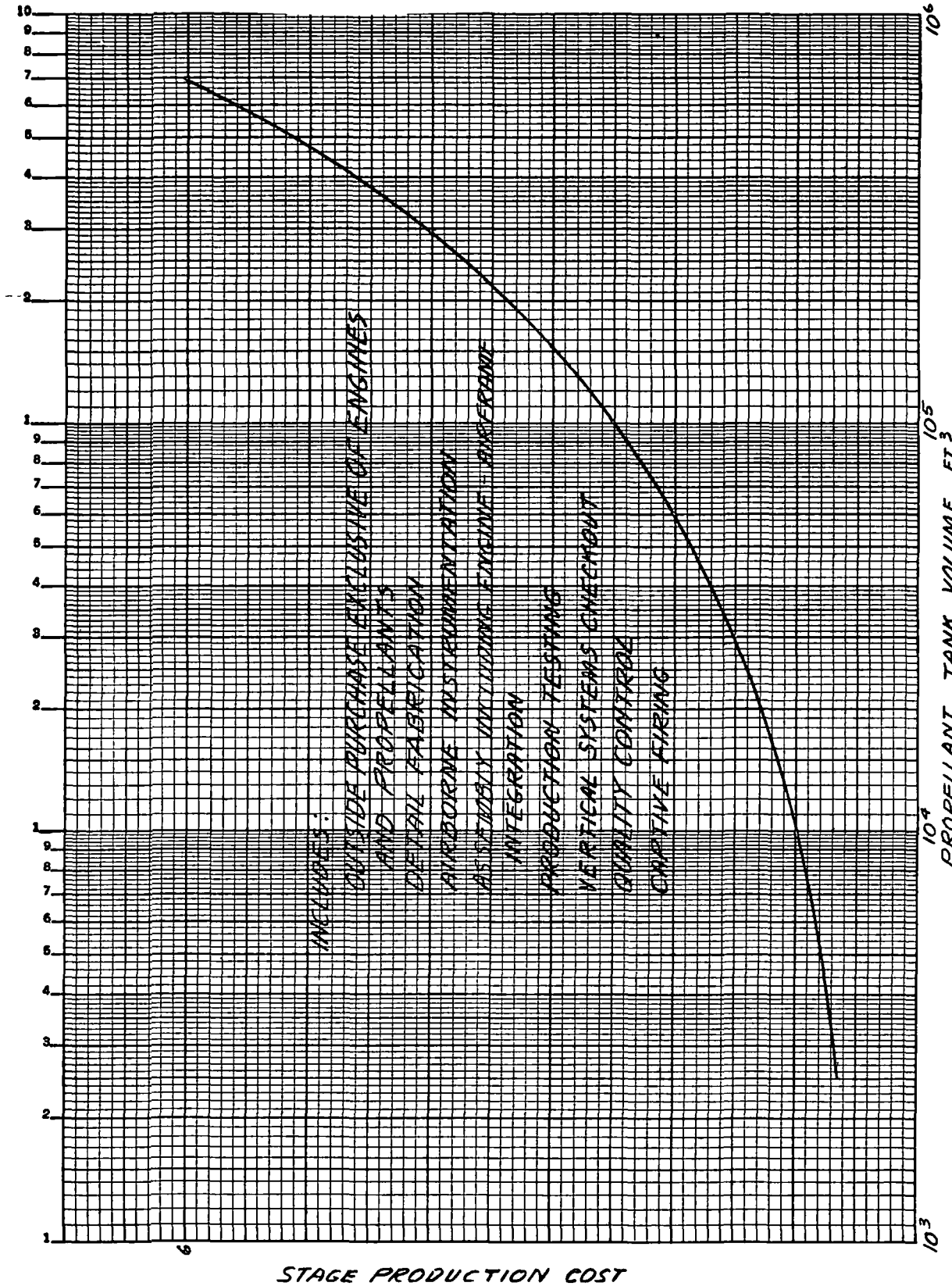

Figure III D-9

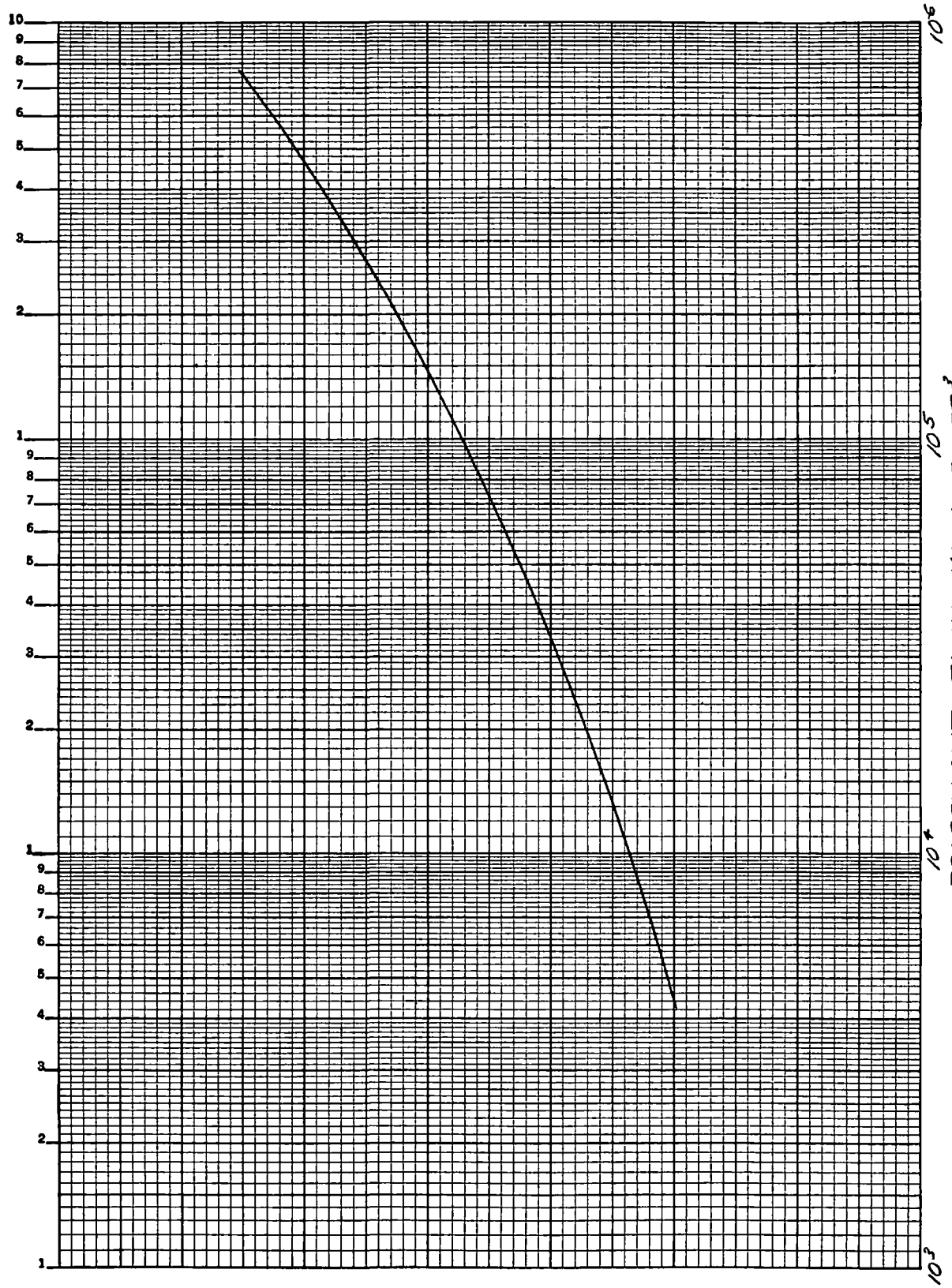

Transportation Cost vs Propellant Tank Volume

Figure III D-10

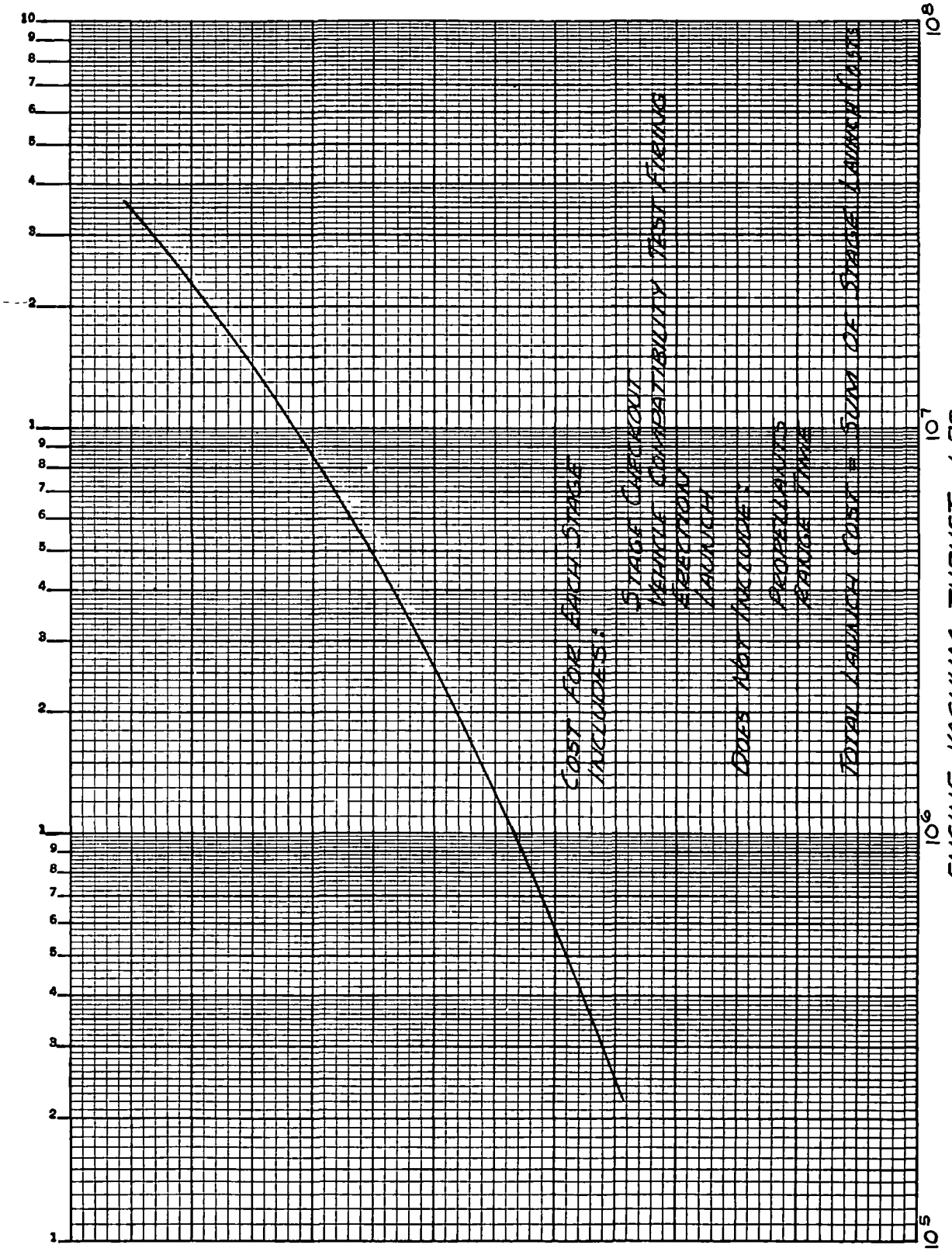

Stage Launch Operation Cost vs Engine Vacuum Thrust

Figure III D-11

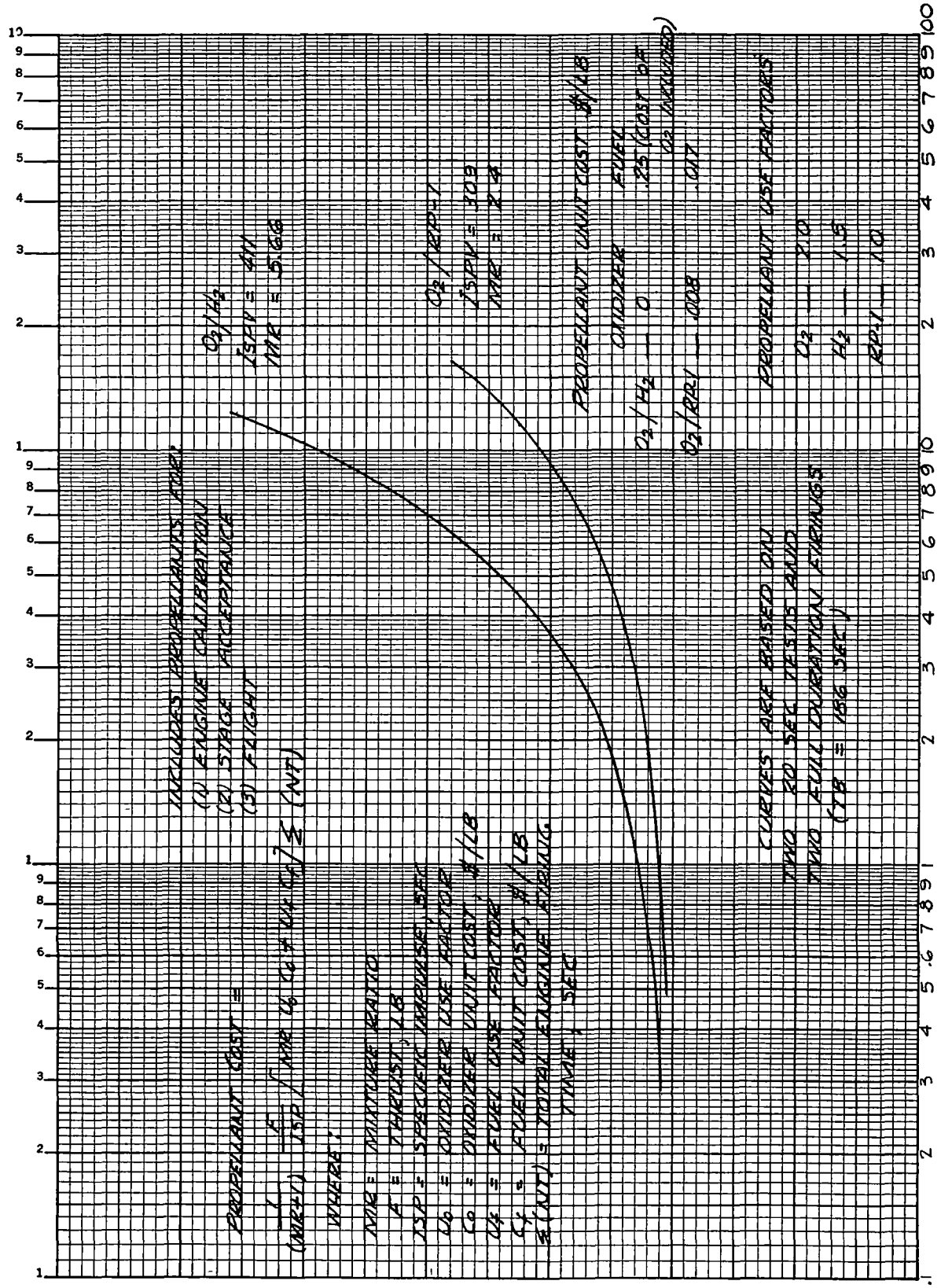

1507

Figure III D-12

Propellant Cost for Operational Stage

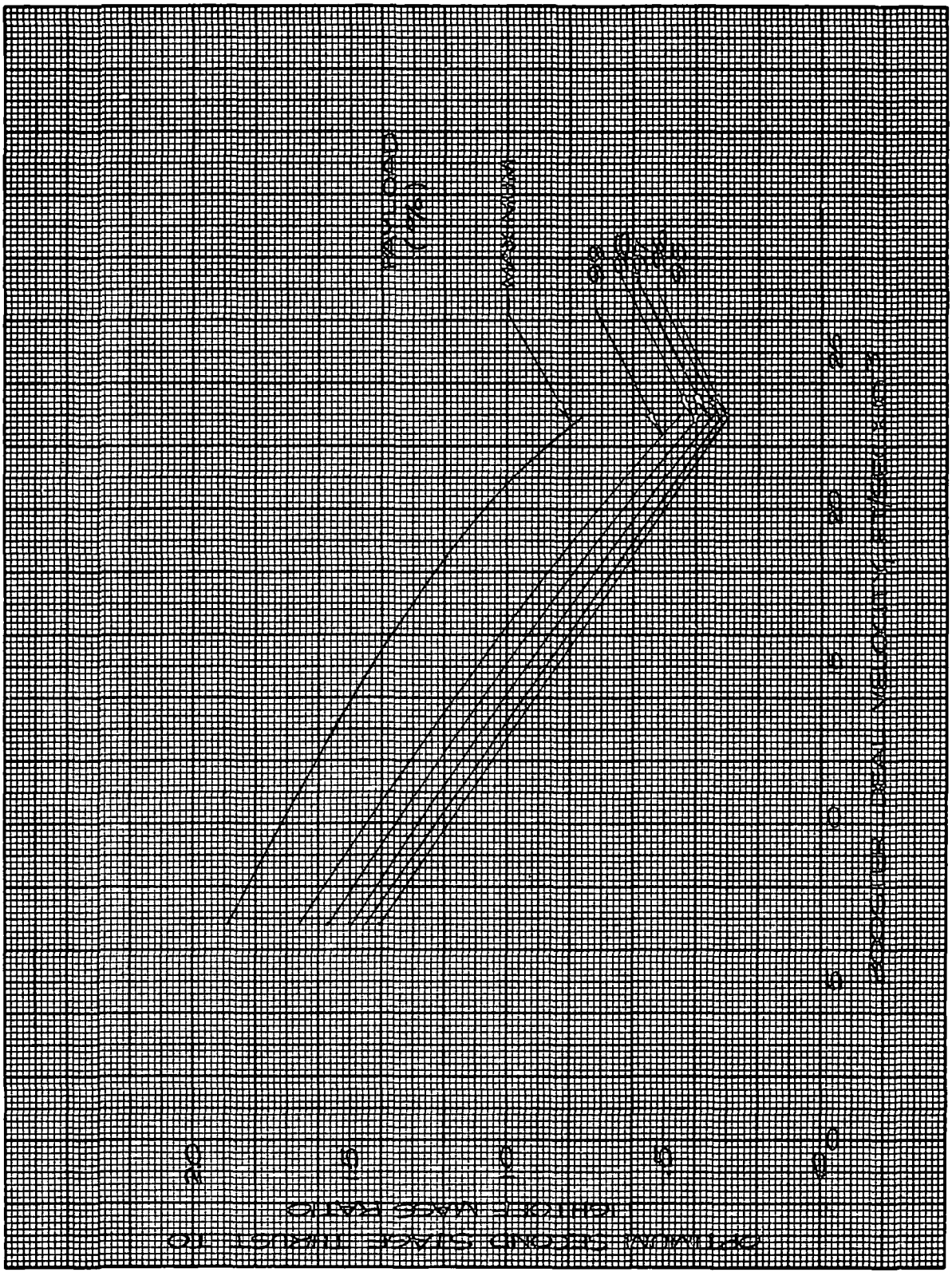

300 NM Orbit Optimum Second Stage Thrust to Light-Off Mass Ratio
With Variations in Payloads

Figure III D-13

III, Bases for Evaluation (cont.)

E. RECOVERY FACTORS

1. General

Three clases of recovery were considered to determine their effects upon the vehicles analyzed. These are:

a. Ballistic recovery of boosters from a low burnout velocity.

b. Winged vehicle recovery from higher burnout velocities.

c. Ballistic recovery from orbit.

To analyze the effect each of these recovery methods has upon the vehicles considered, it was necessary to determine recovery-system weights and limiting conditions (i.e., applicable burnout velocities) for each method. The basis and methods used to establish these parameters are discussed herein.

Recovery system costs are not included in any of the cost comparisons discussed in subsequent sections, but from the relative magnitudes of savings indicated, it is possible to speculate as to the chances for achieving economy by incorporating the recovery devices described.

III, E, Recovery Factors (cont.)

2. Ballistic Recovery of Boosters from Low Burnout Velocity

There are a great many methods that have been investigated for recovering boosters from relatively low burnout velocities. Several of these investigations were conducted by the Aerojet-General Corporation Spacecraft Division[1]. The methods investigated and the weight penalties associated with each system (as a percentage of recovered empty stage weight) are tabulated as follows:

a. Dive brakes, parachute and retrorockets, 10% weight penalty.

b. Parachute and retrorockets, 8% weight penalty.

c. Dive brakes, parachute, and balloon, 13% weight penalty.

d. Parachute and balloon, 11% weight penalty.

e. Dive brakes and air-turborockets, 25% weight penalty.

f. Controlled rotary wings, 10% weight penalty.

Note that none of these methods carried a particularly severe weight penalty. However, the authors of the referenced report are of the opinion that these methods are limited in application to approximately 7,000 ft/sec burnout velocities because of severe heating problems at higher velocities. At these low burnout velocities, small weight addition to the booster have very little effect upon payload or payload delivery costs. Therefore, no weight was added

1. Aerojet-General Corporation, Booster Recovery Study, Spacecraft Division Report No. 1816, July 1960.

III, E, Recovery Factors (cont.)

for recovery of booster from low velocities. As discussed in Section II of this volume, even with this optimistic assumption, low velocity recovery shows no promise of significantly reducing costs because large second stages are required.

3. Winged Recovery

At velocities greater than 7,000 ft/sec, the use of a winged vehicle may make possible adequate control of the re-entry trajectory to avoid the overheating associated with ballistic recovery. This also makes possible a direct return to the launch site through the atmosphere.

A fair degree of confidence exists that booster recovery by this method can be achieved from burnout velocities somewhat in excess of 15,000 ft/sec without more than doubling stage weight. This recovery system weight is based upon the assumptions that rigid wings would be used. The weight includes air-breathing propulsion and propellants for return to the launch site.

The Rogallo Wing, a lightweight flexible-type wing, has been suggested as a possible means for eliminating the rigid wings, thereby saving substantial weight in the system; however, the magnitude of this weight saving is not known. In view of this, stage weights were doubled for boosters recovered from velocities of approximately 15,000 ft/sec.

4. Ballistic Recovery from Orbit

With this method, the booster would be recovered after circling the earth once. The high re-entry velocity would be reduced by means of hypersonic declerator.

III, E, Recovery Factors (cont.)

If properly designed, this device could be used to provide minor trajectory corrections to the vehicle while decending to earth through the atmosphere. This could be accomplished by triming the lines that secure the decelerator to the vehicle. It would be similiar in manner to the way a parachutist controls his landing by spilling wind from the proper side of the parachute. It may be possible that this device could be designed like a Rogallo Wing. Additional maneuverability would then become available.

Immediately prior to landing, it would probably be advisable to jettison the decelerator so that unfavorable winds would not be so likely to interfere with landing. Nullification of residual horizontal and vertical-velocity operation, as well as final landing of the vehicle, would be accomplished by means of variable thrust retro-rockets or perhaps air-breathing engines. These rockets would be ignited just prior to jettisoning the hypersonic decelerator. The vertical landing would permit the use of simple and lightweight tripod-type landing gear. Little information was obtained as to the feasibility of this approach. Investigation of this recovery system resulted in opinions that the required recovery system wieght would be too great to permit delivery of any payload to orbit. However, there is little to substantiate these opinions. Some helpful information was evolved for estimating the weight of the hypersonic decelerator which is the key item to the success of this recovery method[2]. An involved study would be necessary to establish these requirements with any degree of accuracy. Further inquiry into this method is recommended because of its apparent desirability.

A preliminary investigation of high-velocity recovery methods was completed by the Space-General Corporation. Their findings are presented in Appendix C.

---

2. In conferences with the Vidya Corporation, Palo Alto, California

III, E, Recovery Factors (cont.)

Trajectory requirements and recover-system weights were estimated as follows.

a. Trajectory

It was assumed that the booster would accelerate to sufficient velocity to complete one circuit around the earth. Burnout conditions for this were the perigee conditions for an ellipse with a perigee at booster burnout altitude (approximately 40 nm) and a apogee of approximately 300 nm. A small auxiliary rocket would be used to inject the payload into circular orbit.

On the basis of these conditions, the total booster ideal velocity increment was decreased by 450 ft/sec. This is the injection velocity at 300-nm orbit from the described ellipse. The payload degradation for the injection rocket was calculated on the basis that solid rockets of the current technology would be used for this purpose.

b. Injection-Rocket Weight

An expression for the injection rocket weight penalty is derived as follows:

The weight separated from the booster, W_{SEP}, is

$$W_{SEP} = W_{PL} + W_P + 1 \qquad \text{(Eq 1)}$$

W_{PL} = Net payload weight, lb
W_P = Injection rocket propellant weight, lb
W_I = Injection rocket inert weight, lb

III, E, Recovery Factors (cont.)

The inert weight, W_I, is

$$W_I = \left[W_P \right] \left[\frac{1 - \lambda}{\lambda} \right] \qquad \text{(Eq. 2)}$$

λ = Injection rocket propellant mass ratio as defined in the following expression

$$\lambda = \frac{W_P}{W_P + W_I} \qquad \text{(Eq. 3)}$$

Combining Equations 1 and 2 and dividing by the separated weight, W_{SEP}, gives the following expressions.

$$\frac{W_{PL}}{W_{SEP}} = 1 - \left(\frac{W_P}{W_{SEP}} \right) \left(\frac{1}{\lambda} \right) \qquad \text{(Eq. 4)}$$

The ratio of propellant weight to separation weight is

$$\frac{W_P}{W_{SEP}} = 1 - \frac{W_{BO}}{W_{SEP}} \qquad \text{(Eq. 5)}$$

W_{BO} = weight of the net payload and separation rocket after the separation rocket burnout, lb.

The ratio of burnout weight to separation weight can be related to the injection velocity, V_I, and the injection rocket specific impulse, I_{SP}, by the familiar ideal velocity increment expression,

$$\frac{W_{BO}}{W_{SEP}} = - \frac{V_I}{g I_{sp}} \qquad \text{(Eq. 6)}$$

g = Gravitations constant, 32.174 ft/sec^2

III, E, Recovery Factors (cont.)

Combining Equations 4, 5 and 6 yields an expression for the ratio of net payload to separation weight

$$\frac{W_{PL}}{W_{SEP}} = 1 - \frac{1}{\lambda}\left[1 - \rho^{-\left(\frac{V_I}{gI_{sp}}\right)}\right] \qquad \text{(Eq. 7)}$$

Typical solid rocket parameters are;

$$\lambda = 0.89$$
$$I_{sp} = 255$$

The required injection velocity was obtained from the tajectory computer program described in Section II, B and is approximately 450 ft/sec.

Substituting these values in Equation 7 yields;

$$W_{PL} = 0.938\ W_{SEP}$$

c. Hypersonic Decelerator

A weight estimate for this decelerator was obtained[3]. To prevent excessive vehicle structure temperatures, a value of stage weight to drag force $\frac{W}{C_D A}$ of approximately 1.0 is required. Using a vehicle weight of 100,000 lb and a drag coefficient of 0.8, an area of 120,000 sq ft is then required.

3. Ibid.

III, E, Recovery Factors (cont.)

René 41 was suggested as a material that may be suitable for this application. The area density of a drag device fabricated from this material was estimated to be 0.15 lb/sq ft. This would result in a total weight for the decelerator of 0.15 x 120,000 = 18,000 lb per 100,000 lb of total weight to be decelerated (including the decelerator weight). The total weight penalty for the booster alone would then be,

$$\frac{18,000}{100,000 - 18,000} = 0.22$$ lb per lb of weight decelerated, not including the decelerator.

d. Decelerator Trim Winches

The winches and associated equipment used to adjust the drag device for trajectory correction during descent through the atmosphere were assumed to weigh 3% of the stage weight, excluding the decelerator. This amounts to 3,000 lb in the 100,000-lb stage used in the above example. The weight includes cable drums, motors, clutches, and power source (including propellants). Because this device is operated within the atmosphere, an air-breathing prime mover could probably be used. Propellant requirements would then be small.

e. Retro-Rockets

The retro-rockets used during the landing maneuver would probably require a maximum thrust of approximately 1.5 times the vehicle weight at that time. A reasonable weight estimate for liquid propellant rocket engines can be obtained by multiplying the thrust level by 0.01. This is based upon current rocket engines for Titan and Atlas. Retro-rockets would then weigh 0.015 times the stage weight at initiation of the final landing maneuver. Propellants for this maneuver must be included.

III, E, Recovery Factors (cont.)

f. Weight of Propellants for Final Landing Maneuver

The weight of required propellants for the final landing maneuver was estimated by assuming the vehicle must be suspended at zero velocity via the retro-rocket for one minute. Using this criterion, the propellant weight can be estimated from the expression for vertical rocket flight, neglecting drag.

$$V = g\, I_{sp}\, \ln\left(\frac{W_{TO}}{W_{BO}}\right) - g\, t_b \qquad \text{(Eq. 1)}$$

V = velocity increment, ft/sec
g = gravitational constant, 32.174 ft/sec
I_{sp} = specific impulse, lb sec/lb
W_{TO} = vehicle start-burn weight, lb
W_{BO} = vehicle end-burn weight, lb
t_b = burning time/sec.

Because this is a hover operation, velocity increment is zero and the equation becomes

$$I_{sp}\, \ln\left[\frac{W_{TO}}{W_{BO}}\right] = t_b \qquad \text{(Eq. 2)}$$

The weight of propellant, W_P, is

$$W_P = W_{TO} - W_{BO} \qquad \text{(Eq. 3)}$$

III, E, Recovery Factors (cont.)

The expression for the propellant weight can be determined by combining Equations 2 and 3.

$$W_P = W_{BO}^{\frac{t_b}{I_{sp}}} - 1 \qquad \text{(Eq. 4)}$$

W_{BO} is then the weight of the landed stage.

Burning time is assumed to be 60 sec. The value of I_{sp} was calculated on the basis of 95% of theoretical shifting equilibrium at 1,000-psi thrust chamber pressure, mixture ratio of 6:1 and optimum expansion. The I_{sp} was further degraded by 1.5% to account for pumping system losses. This resulted in a value of 358 sec for net landing engine specific impulse.

Using these values, the propellant weight can be calculated:

$$W_P = 0.183\ W_{BO} \qquad \text{(Eq. 5)}$$

Additional tankage and pressurization gas are also required for these propellants. This can be calculated by multiplying the volume of propellants by the volume dependent airframe factor, K_{AF}, discussed in Section III, B.

$$W_T = K_{AF}\ V_{PT} \qquad \text{(Eq. 6)}$$

W_T = Propellant tank weight, lb

V_{PT} = Propellant tank volume ft^3

III, E, Recovery Factors (cont.)

Outage and ullage effects can be ignored in this calculation because they are of second order magnitude in comparison with the other weights involved. Therefore, the additional propellant tank volume necessary for the landing engine propellants can be equated to the volume of propellants consumed.

$$V_{PT} = \frac{W_P}{\rho_B} \qquad \text{(Eq. 7)}$$

ρ_B = Propellant bulk density, lb/ft^3. Combining Equations 6 and 7 yields

$$W_T = \frac{K_{A_F}}{B} \quad W_P \qquad \text{(Eq. 8)}$$

The total weight degradation for landing propellants and tanks, $W_P + T$, is then

$$W_P + T = W_P \quad 1 + \frac{K_{AF}}{\rho_B} \qquad \text{(Eq. 9)}$$

Bulk density of O_2/H_2 at mixture ratio of 6:1 is approximately 22.35. A value of $K_{AF} = 0.623$ is developed in Section II, B. Because the ratio K_{AF}/ρ_B is very much less than 1, only propellant weight for the landing maneuver was included.

g. Landing Gear and Miscellaneous

An additional 5% of landed stage weight was allowed for the landing gear and miscellaneous control equipment not previously accounted for. The landing gear could be a simple tripod without wheels because the landing is accomplished vertically. Equipment that is unaccounted for includes items such as guidance for recovery, maneuver and landing, as well as controls for the terminal landing maneuver.

III, E, Recovery Factors (cont.)

h. Total Weight Penalty

The indicated weights were combined and a total booster weight penalty determined. This was accomplished as follows.

A summary of all weight penalties is shown in the table below. The formulae are based upon the previous discussions.

Decelerator, lb	$W_D = 0.22\ W_S$
Winches, lb	$W_W = 0.03\ W_S$
Retro-Rockets, lb	$W_R = 0.015\ W_S$
Propellants, lb	$W_P = 0.183\ W_{BO}$
Landing Gear and Miscellaneous, lb	$W_L = 0.05\ W_{BO}$
Payload Injection Weight, lb	$W_A = 0.062\ W_{P_L}$
Stage Weight Decelerated, lb (does not include hypersonic decelerator)	W_S
Stage Weight at Landing, lb (does not include hypersonic decelerator)	W_{BO}

These weights are most useful if they are expressed as a function of non-recoverable vehicle jettisoned weight, W_{JN}. Then the recoverable vehicle jettisoned weight can be determined directly if nonrecoverable-vehicle performance is known. All weight, except for the payload injection rocket, can be related to the nonrecoverable vehicle jettison weight. The recoverable vehicle jettisoned weight, W_{JR} is

$$W_{JR} = W_{JN} + W_{RS} \qquad \text{(Eq. 1)}$$

III, E, Recovery Factors (cont.)

where W_{RS} is the weight added for recovery system. W_{RS} is the sum of all items in the preceding table, except the payload injection rocket.

$$W_{RS} = W_D + W_W + W_R + W_P + W_L = 0.22\ W_S + 0.03\ W_S + 0.015\ W_S +$$

$$0.183\ W_{BO} + 0.05\ W_{BO} = 0.265\ W_S + 0.233\ W_{BO} \qquad \text{(Eq. 2)}$$

The non-recoverable vehicle jettison weight and W_S includes all items in W_{RS}, except the hypersonic decelerator

$$W_S = W_{RS} - W_D + W_{JN}$$

$$= W_{RS} - 0.22\ W_S + W_{JN} \qquad \text{(Eq. 3)}$$

$$W_S = \frac{W_{RS} + W_{JN}}{1.22}$$

W_{BO} is the landed stage weight. Included are the non-recoverable stage weight, W_{JN} and all items in W_{RS}, except the hypersonic decelerator and the propellants for landing

$$W_{BO} = W_{RS} - W_D - W_P + W_{JN} = W_S - W_P = W_S - 0.183\ W_{BO}$$

$$W_{BO} = \frac{W_S}{1.183} \qquad \text{(Eq. 4)}$$

III, E, Recovery Factors (cont.)

Substituting Equation 3 for W_S, Equation 4 becomes

$$W_{BO} = \frac{W_{RS} + W_{JN}}{1.44} \qquad \text{(Eq. 5)}$$

Combining Equations 2, 3, and 5 results in the following equation

$$W_{RS} = 0.61\, W_{JN} \qquad \text{(Eq. 6)}$$

In addition, the payload must be reduced by 6.2% to account for the weight of the injection rockets and the booster ideal velocity increment for a 300-nm circular orbit reduced by 450 ft/sec.

"PAGE MISSING FROM AVAILABLE VERSION"

TABLE OF CONTENTS

		PAGE NO.
IV.	BEST UNCONVENTIONAL SYSTEM	IV-1
	A. VEHICLE SPECIFICATIONS	IV-1
	B. VEHICLE CONTROL	IV-2
	C. ENGINE SPECIFICATION	IV-2
	D. REASONS FOR SELECTION	IV-3

FIGURE LIST

	FIGURE NO.
Comparison of Conventional vs Unconventional Configurations, Man-Rated	IV-1
Unique vs Best Conventional	IV-2
Controls Schematic for Staged Combustion in 2,000,000-lb-Thrust Forced-Deflection	IV-3

IV. BEST UNCONVENTIONAL SYSTEM

After analyzing and evaluating the previously described airframe concepts, engine cycles, and engine and component concepts, the most attractive concepts were synthesized to make the best unconventional booster vehicle shown in the frontespiece. In this section the best unconventional vehicle is described, reasons for selecting various concepts are given, and the best unconventional vehicle is compared to the standard vehicle.

A. VEHICLE SPECIFICATIONS

1. Manned Rating

2. Staging: Single stage to 300 nm orbit; two stages for escape.

3. Payload (300 nm Orbit): 105,000 lb, nonrecoverable; 50,000 lb, recoverable.

4. Shape: Cylindrical with flared skirt for aerodynamic stability

5. Propellants: Oxygen; hydrogen

6. Tankage: Tandem, cylindrical tanks; oxygen tank of top; helium pressurized oxygen tank; hydrogen gas pressurized hydrogen tank.

7. Engine: Two-million-lb thrust; staged combustion cycle; forced deflection, altitude compensating, multiple throat, single skirt nozzles; high pressure, multiple combustors; single pumping system.

IV, Best Unconventional System (cont.)

B. VEHICLE CONTROL

1. Thrust Vector: Secondary injection of high pressure turbine exhaust into the main thrust stream

2. Roll: Turbine exhaust supplied nozzles

3. Acceleration: Stepped reductions of thrust effected by changing engine valve positions

4. Propellant Utilization: Modulation of oxygen turbopump gas generator valve; oxygen cutoff sensor in suction line 25 ft above pump inlet.

C. ENGINE SPECIFICATION

1. Cycle: Staged combustion, fuel-rich gas generators; parallel hydrogen flow-through gas generators and thrust-chamber coolant jacket.

2. Thrust Chambers: Eight combustors; mixture ratio of 6:1; chamber pressure of 2,200 psia; ignition by turbine exhaust; hydrogen-cooled chamber walls, air-breathing, altitude area ratio compensating, eight throat, single skirt, forced deflection nozzle; vacuum area ratio of 230:1

3. Feed System: Centrally located turbopumps, gas generators, all distribution lines and valves.

IV, C, Engine Specification (cont.)

4. Hydrogen Turbopump: A single inlet, two-stage, centrifugal-flow pump directly driven by a two-stage, parallel-flow gas turbine; pump discharge pressure of 3,000 psia.

5. Oxygen Turbopump: A main stage turbopump consisting of a single inlet, single stage, centrifugal flow pump directly driven by a three stage, series flow, gas turbine; an integrally packaged, hydraulic driven, low shaft speed inducer pump stage preceeds the main stage turbopump; pump discharge pressure of 3,000 psia

6. Gas Generators: Dual, fuel-rich, annular, side-by-side generators; mixture ratio of 1.2:1; chamber pressure of 2,800 psia; single valve control of each generator; flash-over ports between generators for ignition redundancy.

7. Start Method: Tank-head start with phased gas generator valve control to give matched pump discharge pressures during start transient. After pump discharge pressures attain a prescribed value, oxygen flow is admitted to the main chambers by a controlled opening of the thrust chamber oxygen valve.

8. Shutdown Sequence: Gas generator valves shutoff is followed by a sequenced closing of the oxygen thrust chamber throttling valve and the hydrogen coolant valve.

D. REASONS FOR SELECTION

The most important feature of an earth-to-orbit vehicle is its number of stages. This investigation has concluded that an orbital booster (single stage from earth to orbit) offers tremendous improvements in booster vehicle operational

IV,D, Reasons for Selection (cont.)

simplicity, reliability, and cost. Further, an orbital booster substantially reduces the escape vehicle thrust requirement, which extends the use of currently-developed upper stages to much higher payload capacity. Also, an orbital booster would make possible the recovery of the entire earth-to-orbit booster system using a single recovery device. This gives good recovery economy and precludes the possibility of stages falling in populated areas, thus making eastward launches from the U.S. west coast or interior safe.

Orbital booster development cost is low because there is only a single set of tanks, frames, and engines to develop. Also, as compared to multistage boosters, the orbital booster has no in-flight engine starts, no interstage separation devices, no interstage retro rockets, less flight instrumentation; fewer malfunction detection systems; fewer ordinance systems, and less ground support and checkout equipment.

The orbital booster, with its minimum number of propellant tanks and engines, is easy to maintain in operational readiness. Its simplified checkout requirements reduce operational costs and minimize the number of launch base operating personnel.

Orbital booster reliability is superior because there is no in-flight separation of booster vehicle stages and no in-flight starting of booster vehicle engines. Also, the reduced amount of fill, bleed, vent, malfunction detection, flight instrumentation, and ordnance systems improve operational reliability.

In Section II, oxygen/hydrogen was selected as the best propellant combination for a two-stage-to-escape vehicle with conventional components. The reason for selection was higher reliability, greater growth potential, and a cost improvement. High reliability results from the elimination of stages. Greater

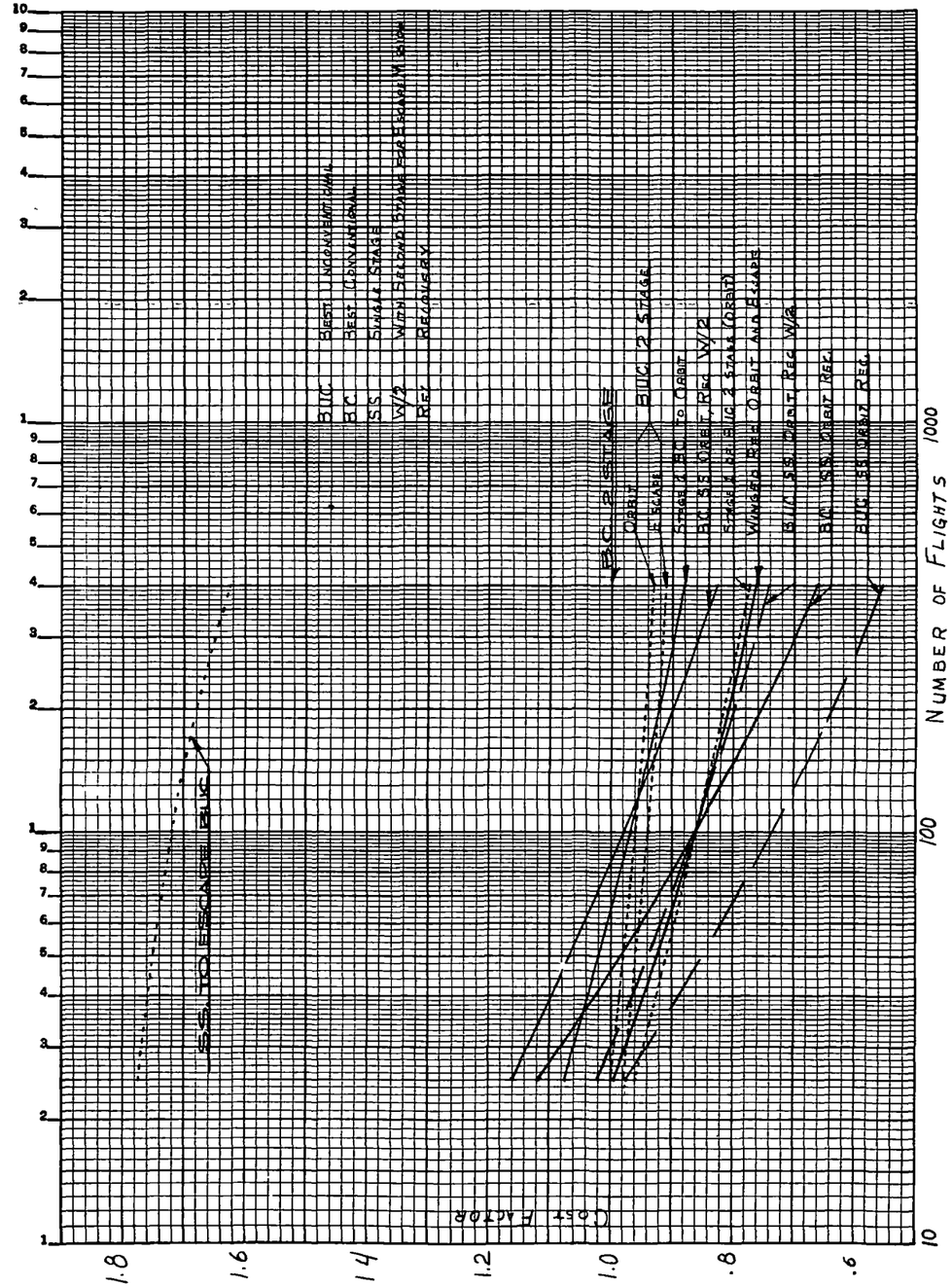

Figure IV-1

Comparison of Conventional vs Unconventional Configurations, Man-Rated

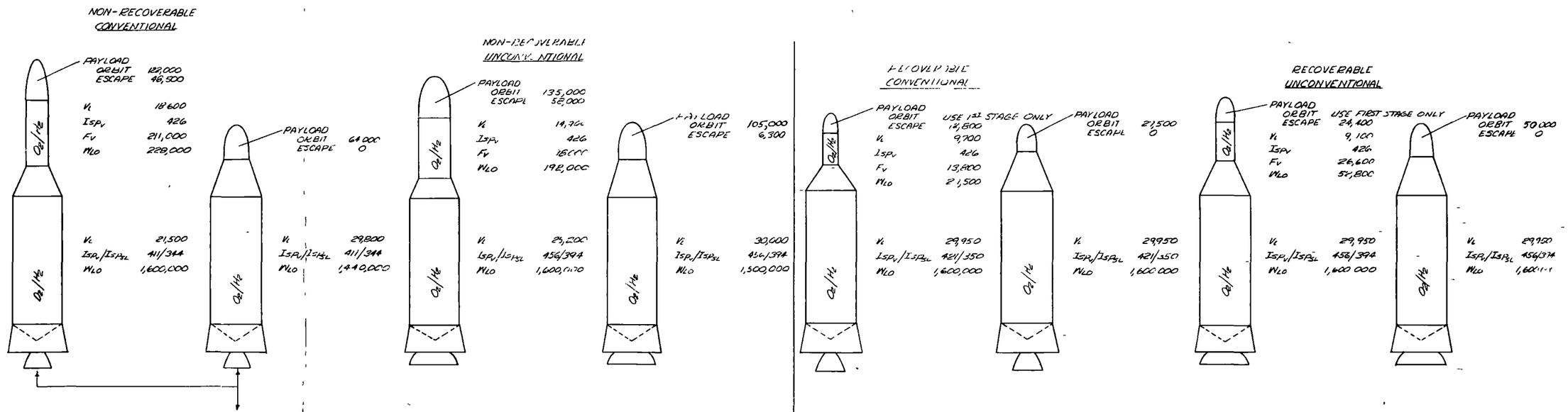

(1) RELATIVE UNRELIABILITY, BOOSTER	15	15	15	15	15	15	15
(2) GROWTH POTENIAL FACTOR PAYLOAD WEIGHT (ESCAPE) 2ND STAGE THRUST LEVEL	23	6	6	93	93	92	92

NOTES PAYLOAD, LIFT OFF WEIGHT, AND THRUST ARE IN LB, IDEAL VELOCITY INCREMENT IN FT/SEC AND IS FOR ESCAPE MISSION, SPECIFIC IMPULSE IN SEC

Unique vs Best Conventional

Figure IV-2

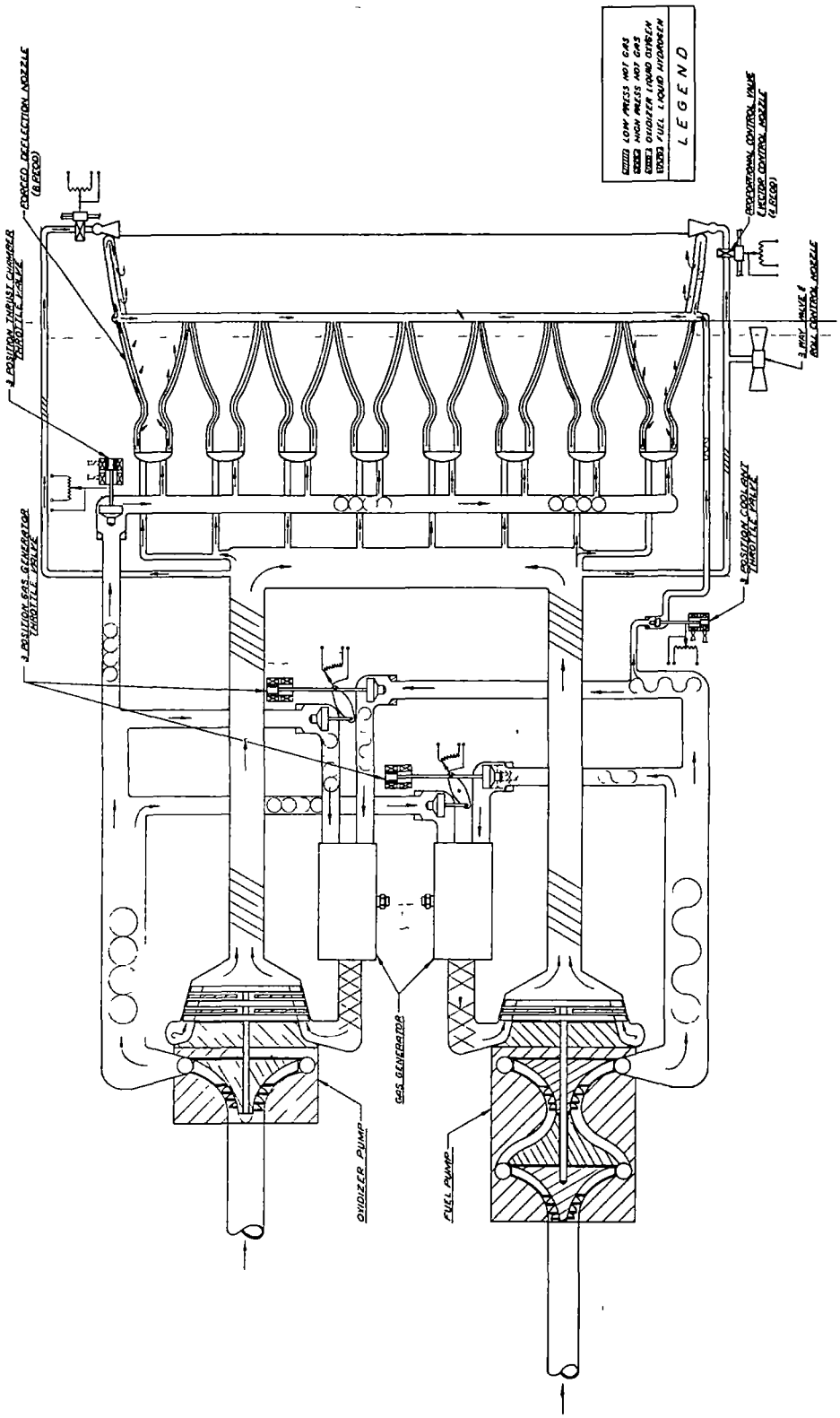

Controls Schematic for Staged Combustion in 2,000,000-lb-Thrust Forced-Deflection

Figure IV-3

"PAGE MISSING FROM AVAILABLE VERSION"

IV, D, Reasons for Selection (cont)

growth potential is available because the escape payload-per-lb of second stage thrust is highest of all conventional systems considered. Also, in Section III, it was concluded that the best potential recovery gains are available from the recovery of a single-stage-to-orbit booster.

The primary differences between the conventional and unconventional vehicles are in the engine cycle and engine configuration. Oxygen/hydrogen propellants are used for both vehicle types. Both conventional and unconventional vehicles have orbital boosters.

Conventional and unconventional concepts are compared for vehicles that have "throw-away" orbital boosters and for vehicles that have recoverable orbital boosters. Two types of vehicles are considered, single-stage-to-orbit and two-stage-to-escape. Figure IV-1 depicts all the vehicles in which conventional and unconventional configurations are compared; thrust, payload growth potential, and reliability factors for each vehicle are also presented. Figure IV-2 shows a relative cost factor with relation to the number of flights for the vehicles. For vehicles having "throw-away" orbital boosters, the unconventional concept gives a 5% cost improvement for a two-stage-to-escape mission and a 10% cost improvement for a single-stage-to-orbit mission. For vehicles with recoverable orbital boosters, the unconventional concept gives a 10% cost improvement for a two-stage-to-escape mission and a 15% improvement for a single-stage-to-orbit mission. These cost benefits become significant amounts of money when the total cost of space-booster programs is considered.

IV, D, Reasons for Selection (cont.)

In addition to cost benefits, the engine configuration of the unconventional system offers the advantages detailed in Section II, E, 3 and II, F, 2 and those discussed as follows.

For the same payload and a recoverable orbital booster, the unconventional vehicle would be approximately half the size of the conventional, which would make shipping and operation easier.

The multiple combustors of the unconventional system engine would require less development than a single large deLaval thrust chamber.

Compared to a configuration consisting of clustered deLaval thrust chamber engines, the unconventional system engine with its single, unitized pumping and feed system gives superior reliability.

The forced-deflection thrust nozzles of the unconventional system give maximum utilization of the vehicle base area. Full use of the exit area becomes more important in large vehicles because engine area requirements increase proportionally to the square of thrust, whereas vehicle diameter increases approximately proportional to the cube of thrust. Also, the forced-deflection nozzles minimize base recirculation of engine exhaust.

As explained in Section II, E, the staged combustion cycle of the unconventional system is superior to the gas generator cycle for high chamber-pressure engines. It gives greater payload and combines thrust vector control, roll control, and the turbine drive gas into a single hot gas system. It also eliminates main combustor igniter requirements. Figure IV-3 is a control schematic of the unconventional vehicle engine system.

IV, D, Reasons for Selection (cont.)

Although categorized as unconventional, this system has no components or subsystems that require basic research prior to development. The Aerojet-General Corporation has started development of the major items for the unconventional systems.

"PAGE MISSING FROM AVAILABLE VERSION"

TABLE OF CONTENTS

PAGE NO.

V. GROUND SUPPORT EQUIPMENT

A. INTRODUCTION V-1

B. DESCRIPTION AND DISCUSSION V-1

C. SUMMARY AND CONCLUSIONS V-6

FIGURE LIST

	FIGURE NO.
GSE Relative Costs	V-1

VI. GROUND SUPPORT EQUIPMENT

A. INTRODUCTION

Ground support equipment complexity is dependent upon the requirements of transportation, service, checkout, control, and system monitoring. Actual design of equipment for a 2,000,000-lb-thrust vehicle is beyond the scope of this investigation; however, an analysis was made to determine the relative cost of ground support equipment for a vehicle stage as well as the effect that the number of stages has upon this cost. This study was divided into four areas of consideration; range, payload, launch area, and stage. Equipment cost in any one area is directly proportional to the number and type of functions to be executed in a particular area. There are certain functions required that are independent of the type or size of the vehicle, and these are usually associated with the range. There are also functions that are stage sensitive, which satisfy the needs of the launch area, stage system, and payload.

B. DESCRIPTION AND DISCUSSION

The following discussion is on the basis of the requirements for a single-stage-to-orbit vehicle system.

1. Range and Communication Complex

The range complex support equipment includes on-site optical infrared and radar tracking system, a segment of the master control, Doppler velocity measurement network, computer and record processing equipment, visual trajectory readout devices, destruct transmitters, associated antenna systems, and telemetry receivers.

V , B, Description and Discussion (cont.)

Certain equipment is necessary to support the communication complex, such as public address systems, communication network (land line), meteorological data network, camera systems, visual and warning systems, sound level measurement network, RF communication network with associated antenna, and various maintenance equipment. The relative cost range of ground support equipment is shown in Figure V-1.

2. Payload

The support equipment associated with the payload is designed to satisfy the requirements for transportation, environmental control and checkout, instrumentation monitoring and checkout, preflight checkout and control, servicing, safety, repair, and maintenance. Because the guidance system is usually located in the payload for a manned system, equipment must be provided to check out, orient, and set the guidance system. The payload system has certain functions which must be connected through appropriate umbilicals so that maximum capabilities of the mission are not influenced by any hold-fire periods. The relative cost of necessary support equipment for the payload in relationship to the over-all system is shown in Figure V-1.

3. Launch Area

The equipment necessary to support the launch area comprises ground instrumentation, integrated vehicle checkout, facilities checkout, master console control, and monitoring for controlled countdown. Launch area costs are presented as a percentage of over-all ground support equipment cost in Figure V-1.

V., B, Description and Discussion (cont.)

The launch-area system consists of the master control console for manual initiation of checkout or countdown, the slave sequencing units (necessary for vehicle checkout, monitor, and control), the ground instrumentation recording equipment, and a computer for analyzing countdown and instrumentation data.

4. Stage

The support equipment required for a rocket vehicle stage must satisfy the requirements necessary to transport, handle, service, check out, monitor, control, and maintain the vehicle system. The cost of providing ground support equipment for a stage system relative to the total ground support equipment cost is shown in Figure V-1.

a. Transportation

The requirements for transportation of large vehicle systems included investigation of normal dimensional limits for air, land, and water transport.

Transportation of large rocket vehicle systems by common carrier via interstate highway systems is practicable for limited distances using special routing. Highway systems are capable of handling large loads with special permission from responsible agencies.

The limit for normal highway transport of large vehicles, considering optimum routing and agency approval, is a vehicle diameter of approximately 40 ft. Length limitations are not considered critical.

V , B, Description and Discussion (cont.)

The equipment required to accomplish transportation by this method would include a trailer designed to the specifications imposed by particular vehicle design. This trailer would be a direct scale-up of existing equipment.

Water transportation of the large vehicle systems under consideration via suitable existing ocean going vessels or river barges is considered practicable and within present vessel limits.

Included among the limitations for this type of transport are extended shipping times and the requirements for comparatively complex environmental protection.

Normal air transportation (airplane) of an entire vehicle is feasible if package diameters do not exceed 12 ft.

Other methods of air transportation for large rocket vehicles (i.e., lighter-than-air and vertical takeoff and landing craft) were considered but found impractical.

Normal rail transportation of large vehicles is limited by a maximum rectangular clearance outline of 10 ft-8 in. by 10 ft-10-1/2 in. Lengths of the vehicles being studied do not fall within the maximum rail transport limitation.

It is considered, in light of the above dimensional limitations, that normal rail transportation of large-diameter vehicles is not feasible.

V1, B, Description and Discussion (cont.)

b. Handling Equipment

The handling equipment includes all slings, fixtures, maintenance stands, and other items of ground support equipment required during transportation, maintenance, and erection of the vehicle for the moving, rotating, or lifting of the stage.

c. Service Systems

This system is composed of the umbilical system, which consists of the interface hardware between the facilities and vehicle; hydraulic/pneumatic system, which provides the control valves necessary for propellant loading, flight control checkout, air conditioning, pressurization system filling, pumping, and tank precooling system; and the hydraulic/pneumatic link from the facilities supply sources to the vehicle for transporting propellants and gases.

d. Checkout, Monitoring, and Control Systems

These systems comprise the equipment required for stage continuity and functional checkout, together with the control and monitoring of the countdown and critical stage parameters. All portable checks for leak testing and component functional checks are included.

e. Maintenance

Maintenance ground support equipment includes cleaning systems, dehydrating systems, tool kits, work platforms, and special tooling.

V , Ground Support Equipment (cont.)

C. SUMMARY AND CONCLUSIONS

An analysis was made of the ground support equipment costs associated with a single-stage-to-orbit vehicle and a multiple-staged vehicle. Figure V-1 shows that total ground support equipment costs are increased by 36.1% when a second stage is added. If a third stage is required, the total ground support equipment would be 1.72 times that required for a single-stage vehicle. These values are not greatly affected by the choice of O_2/H_2 or O_2/RP-1 as propellants because the amount and complexity of ground support equipment basically remains the same.

It can be concluded that ground support equipment for a large booster system constitutes no great problems, and much of the required equipment is current technology. Recommended transportation for this vehicle is by highway trailer to a waterway for boat transportation.

COST OF TOTAL GSE

VEHICLE "A"
ONE-STAGE VEHICLE & PAYLOAD

INCREASE IN GSE COST AS FUNCTION OF ADDED STAGES

INCREASE 36.1%

VEHICLE "B"
TWO-STAGE VEHICLE & PAYLOAD

COST OF GSE FOR ANY VEHICLE = "A" X[100 + .361(N-1)]
WHERE N IS THE NUMBER OF STAGES

Figure V-1

GSE Relative Costs

"PAGE MISSING FROM AVAILABLE VERSION"

TABLE OF CONTENTS

		PAGE NO.
VI.	FACILITIES	
A.	INTRODUCTION	VI-1
B.	RESEARCH AND DEVELOPMENT FACILITIES	VI-2
C.	FINAL FABRICATION ASSEMBLY, PROPELLANT PRODUCTION TEST, AND LAUNCH FACILITIES	VI-5
D.	SAFETY	VI-33
E.	ACOUSTIC ANALYSIS	VI-36

TABLE LIST

	TABLE NO.
Test/Launch Weights, Sizes and Clearances	VI-1
Basic Factors for Propellant Production, Transfer, and Storage	VI-2
Basic Assumptions	VI-3
Design Forces on Test Stands	VI-4
LO_2/LH_2 Propellants; Quantity Distances--Comparison Tabulation	VI-5
LO_2/LH_2 Propellants; Quantity Distances--Comparison Tabulation	VI-6

FIGURE LIST

	FIGURE NO.
Projected Test Cost Trends, De Laval Nozzle Thrust Chamber	VI-1
Projected Test Cost Trends, Pen Nozzle Thrust Chamber, Wedge Segments	VI-2
Projected Test Cost Trends, Turbopump for Booster Engines S-L Thrust as Designated	VI-3
Projected Test Cost Trends, GG for Booster Engine S-L Thrust as Designated	VI-4
Projected Test Cost Trends, Valves and Components for Booster Engine S-E Thrust as Designated	VI-5
Research and Development Facility Cost Trends	VI-6
Over-All Sound Pressure Level vs Distance from Rocket	VI-7
Fabrication and Assembly Test and Launch Site	VI-8
Gorge Test and Launch Area	VI-9
Water Systems Schematic Flow Diagram	VI-10

FIGURE LIST (cont.)

	FIGURE NO.
LN_2, LO_2, and LN_2 Production Schematic Flow Diagram	VI-11
Hydrogen Facilities Schematic Flow Diagram	VI-12
Nitrogen, Oxygen, and Helium Systems Schematic Flow Diagram	VI-13
Test and Launch Facility, Lower Cliff Area	VI-14
Fixed Test and Launch Tower	VI-15
Planetary Rocket Ocean Platform, Above Water	VI-16
Planetary Rocket Ocean Platform, Below Water	VI-17
Projected Acceptance Testing Cost Trends for Systems of 2 to 24 Million-lb Thrust	VI-18
U.S Coastal Gorge Concept	VI-19
U.S Coastal Cliff Concept	VI-20
Remote Island Concept	VI-21
Texas Tower Concept	VI-22
PROP Concept	VI-23

VI. FACILITIES

A. INTRODUCTION

Methods of testing adopted for development of large liquid rocket boosters, within the selected thrust range, are based upon peripheral design requirements operating under intended environments. Environments are created to satisfy planned test objectives and encompass set combinations of environmental conditions.

Size and magnitude of required facilities is determined by booster thrust level. At the three-million-pound-thrust level, existing facilities at the Atlantic Missile Range can be utilized (with some modifications) for launching, but existing research and development component testing facilities have reached their upper capability limits from the conventional engine design aspect; therefore, a facility design approach has been selected that will allow for component testing at existing modified facilities. Complete engine testing is proposed for a facility that may be used for launching, and at the higher thrust ranges, for complete assembly. A combined assembly, engine test, and launch facility is an economical alternative that must be considered at the two-million-pound-thrust level, and which appears to become of greater need as the 24-million-lb-thrust level is approached.

VI,, Facilities (cont.)

B. RESEARCH AND DEVELOPMENT FACILITIES

1. Component Development

The use of existing liquid rocket testing facilities for research and development testing of both conventional and unconventional designs of large boosters is considered feasible when the segmental engine building block design philosophy is adopted. Existing facilities can accommodate up to two-million-pound deLaval engines, or segments of larger engines. These two-million-pound segments form the upper testing limits for many of the segmented concepts of a 24-million lb engine.

An analysis of required component test facilities for a conventional deLaval nozzle, LO_2/LH_2 engines, or segmental combustors was made. It includes testing of engine components or segmental combustors. Location of the modified facilities is within Aerojet-General Corporations Liquid Rocket Plant Test Area.

2. Research and Development Costs

a. Testing Costs

(1) Projected cost trends are presented in Figures VI-1 through VI-5. They are based upon a two-shift day, a five-day week, one-stand operation with the testing rate ranging from an anticipated program minimum of four tests per month to the test stand maximum capability for each thrust level indicated. Although the ultimate booster thrust rating will range between 2- and 24-million lb, testing will be performed at the Liquid Rocket Plant, Sacramento, California using thrust-chamber assembly hardware rated up to a maximum of

VI, B, Research and Development Facilities (cont.)

two-million-pounds thrust and on other components scaled and sized proportionately. Required propellants and pressurants are assumed to be government-furnished and are not included in the cost estimates.

(a) The curves shown in Figures VI-1 are applicable to a booster rated at two-million pounds of thrust for either a single or double thrust-chamber assembly with a deLaval-type nozzle. Costs represent the requirements for testing 60° wedge segments for a one-million-pound thrust thrust chamber assembly, as well as 60° wedge segments for a two-million-pound sea-level thrust thrust-chamber assembly, and for testing a complete one-million-pound thrust thrust-chamber assembly.

(b) The cost trend curves presented in Figure VI-2 represents the costs for a two-million-pound thrust booster composed of eight pen nozzle wedge segments rated at 250,000-lb thrust each, and a 24-million-lb thrust booster composed of 12 nozzle wedge segments rated at two-million-pound thrust each.

(c) Figures VI-3, VI-4 and VI-5 represent the cost trends for turbopump, gas generator, and valve tests, respectively, needed for the large booster engines. Testing costs for each component are presented in three curves representing thrust levels of 500,000, one-million, and two-million pounds. It was assumed that components required for booster engines rated at greater than two-million-pounds sea-level thrust will be scaled to a level between 500,000- and two-million-pounds thrust for all development testing.

VI, B, Research and Development Facilities (cont.)

b. Facility Modification Costs

The estimated research and development facility cost trend for booster thrust levels up to 24-million-lb thrust is shown in Figure VI-6. It will be noted that cost increase at the 24-million-lb thrust level is approximately 23% higher than at the two-million-lb point. This higher cost results mainly from larger turbopump assemblies, valves and gas generators, and not by segmental thrust chamber size, which is set at the two-million-pound level. The lower cost of LO_2/RP-1 component development results from the use of carbon steel piping and tankage for the fuel circuit rather than cryogenically compatible vacuum-insulated pipe and vessels needed for the liquid hydrogen circuit of a LO_2/LH_2 engine.

VI, Facilities (cont.)

C. FINAL FABRICATION ASSEMBLY, PROPELLANT PRODUCTION TEST, AND LAUNCH FACILITIES

While the purpose of this investigation primarily encompassed booster units of a vehicle, it was necessary to consider a complete vehicle for launch facilities. Shipping fully-assembled vehicles to a launching site becomes increasingly difficult as sizes and weights are increased to the magnitude encompassed within the scope of this investigation. From a cost consideration, it appears that beyond the 2,000,000 to 24,000,000-lb-thrust range, final fabrication and testing at the launch site will be competitive or even possibly superior to the conventional methods. The thrust level at which this change of current practice should be instituted can not be precisely defined; however, facilities costs are not appreciably affected by this selection when the smaller sized vehicles are considered. In the case of the larger size vehicles, the unconventional approach will be cheaper. Thus, by using this assumption, reasonable cost trends can be conveniently estimated.

The Atlantic Missile Range will probably be used for vehicles up to 6,000,000 or 8,000,000 lb of thrust. Thus, some savings will be reflected in the 2,000,000 to 8,000,000-lb-thrust range.

Alternatives for LO_2/LH_2(A) and LO_2/RP-1 (B) have been investigated for U.S. Coastal gorge, cliff site, remote island, off-shore, and planetary rocket ocean platform concepts. Alternative A is for vehicles with all stages using LO/LH engines and includes production facilities for LH_2, LO_2, and LN_2. Alternative B is for vehicles with all stages using LO_2/RP-1 engines and propellant delivered to continental U.S. storage or dockside in vendor transport carriers.

VI, C, Final Fabrication Assembly, Propellant Production Test, and Launch Facilities (cont.)

1. Facility Integration

a. Basic Assumptions

An integrated facility for final assembly, test and launch is assumed for final assembly and test of booster units from 2- to 24 million-lb thrust as well as launch of complete vehicles.

Table VI-1 lists the assumed vehicle clearance dimensions, propellant weights, stage weights, gantry span for gorge cuts, and flame deflector sizes.

Table VI-2 lists basic factors for production, storage, pipe line transfer of fuels, oxidizers, and liquid nitrogen for continental U.S. concepts.

Table VI-3 lists factors for storage and transfer of propellants and gases for continental U.S. concepts, supply ships, and storage for concepts outside of the continental U.S.

VII, C, Final Fabrication Assembly, Propellant Production Test, and Launch Facilities (cont.)

Storage capacity for continental U.S. concepts are based upon one launching or engine test per month, including cryogenic holding and cool-down losses. Transfer rates are based upon four hours for cool-down and fill of vehicle tanks. Production capacity is for one launching or engine test per month.

Ship capacity and storage for concepts outside of the continental U.S. are based upon two launchings. Production capacity is for one launching per month, including all losses. Transfer to the vehicle is based upon four hours for cool-down and fill.

Design factors applied to thrust loads for determining equivalent static loads for structure design are outlined in Table VII-4.

Distances assumed for blast and sound pressure levels are outlined in pertinent sections. Table VII-5 gives a tabulation of distances for vehicles with 2-, 6-, 20-, 80-, and 150-million-lb thrust ranges using various assumptions for TNT equivalents for propellant combinations. Figure VII-6, as explained in a later section, gives a range of distances for sound pressure levels for engines with thrusts ranging from 2- to 150-million lb. As the Saturn (1,500,000-lb thrust) tests indicate, weather conditions give a wide band of results. Engine design, stability, and terrain will also affect each testing and launching concept.

VI., C., Final Fabrication Assembly, Propellant Production Test, and Launch Facilities (cont.)

b. Existing Test and Launch Facilities

(1) Alternative A (LO_2/LH_2 Engines)

The alternative A vehicle with a booster unit up to two-million-lb thrust with a LO_2/LH_2 engine could possibly be launched at the Saturn Launch Facility of the Atlantic Missile Range if final booster and total vehicle designs fall within diameters, heights, and weights of an existing or modified gantry. Limited engine testing up to six-million-pounds thrust could be accomplished at Edwards Air Force Base with extensive test stand modification and augmentation of the existing facilities. Each facility would require blast analysis, sound pressure analysis, and propellant and gas storage modified to suit vehicle requirements.

(2) Alternative B (LO_2/RP-1 Engines)

The alternative B vehicle with a booster unit up to 6 or 8 -million-pound-thrust engine using LO_2/RP-1 could also be launched from the Atlantic Missile Range. A six-million-pound engine could be tested at Edward Air Force Base. Support facilities for storage, transfer, instrumentation, and control will vary depending upon upper stage design (LO_2/RP-1, storable propellants, nuclear engines, etc.).

VI, C, Final Fabrication Assembly, Propellant Production Test, and Launch Facilities (cont.)

c. Continental U.S. Coastal Gorge Concept

(1) Alternative A (LO_2/LH_2 Engines)

Figure VI-8 shows one type of facility located in and area that satisfies the requirements of on-site fabrication and assembly, propellant production static test hot firings, and actual launch operations. This facility is shown adapted to an actual mountainous area of the Pacific seaboard spanning a gorge or ravine, and having a navigable waterway below with access to the Pacific Ocean and major shipping lanes.

Near the gorge, but separated from the blast by natural terrain, are level areas suitable for fabrication and assembly shops, warehousing, landing docks, heliports, and integrated liquid hydrogen, liquid nitrogen, liquid oxygen plants.

VI., C, Final Fabrication Assembly, Propellant Production Test, and Launch Facilities (cont.)

(a) Figure VI-9, shows an enlargement of the gorge test and launch area of the complete site shown in Figure VI-8.

Geology of the area, while not ideal, has suitable bearing and shear characteristics when stabilized as shown. The promontory itself is approximately 300 to 400 ft high, thereby allowing for built-in access platforms at stage elevations and sufficient clearance for the 200-ton gantry crane above. (Three 100-ton cranes for lifting 200 tons from horizontal to vertical).

Gorge width is sufficient to allow the vehicle to rise at the launch, but not so wide that thrust take-out structures and umbilical propellant line platforms are excessively complex.

The locks shown accomodate tides, rough water, and provide access to the submerged draft tube, which comprises the jet exhaust system. A rock deflector is required for jet exhaust directional control, and is water-cooled by flow around the outside and top of the draft tube.

Propellant plants, propellant, and water storage are placed at the upper elevation of the plateau which allows for gravity-feed to the launch pad. Advantages of this concept are:

1 Ease of transporting large prefabricated sections and materials

VI, C, Final Fabrication Assembly, Propellant Production Test, and Launch Facilities (cont.)

2 Shops at each stage level

3 Overhead crane access for handling and erection

4 Accommodation of jet exhaust

5 Gravity feed propellant fill

6 Hydrocarbon fuel sources and available power in vicinity

(b) Support Facilities

1 Administration and General Plant Services

For the purposes of this report, the requirements for land, roads, paved areas, railroad, water storage and distribution, power supply and distribution, fire and disaster service, administration, maintenance, and security are grouped under the Administration and General Plant Services (AGPS).

VI., C, Final Fabrication Assembly, Propellant Production Test, and Launch Facilities (cont.)

a Land

The land required for facilities and buffer zones is determine from safety criteria and base concept needs. The investigation is performed in such a manner as to have costs and requirements in units so that they can be easily tabulated for any combination of concepts and alternatives. To delineate the many variables for each specific site, concept, and alternative, cost analysis of each unit necessary to the over-all concept was completed. Areas and costs for land are separated from AGPS in the cost summaries.

b Roads

All roads within the entire area (except for the production plant) are included in each concept and alternative. For a specific site, concept, or alternative, lengths were taken from a plot plan and rates for the area applied. The tabulations within thrust ranges, concepts, and alternatives are assumed to be logical averages only.

c Paved Areas

All paved areas within the entire area (except for the production plant and railroad or truck unloading for storage areas) are included in each concept and alternative.

VII, C, Final Fabrication Assembly, Propellant Production Test, and Launch Facilities (cont.)

d Railroad

The length of railroad required depends upon the location of an existing line. This includes the length of line from the existing vicinity of the general site to the fabrication and assembly buildings and to the production plant. For concepts and alternatives with railroad delivery to storage areas, additional extensions are required. Cost tabulations for other than the six-million-pound thrust level are extrapolations based upon present day experience.

e Water Storage and Distribution

Water storage and distribution under AGPS consists of the supply system, raw water storage, raw water distribution to each area or building, treatment plant, and treated water distribution to each area or building (Figure VII-10). For the six-million-pound thrust level, each of the three principal areas, manufacturing, production, and launch and storage, is assumed to have a separate supply and distribution system consisting of a well capable of supplying 1,000 gpm raw water through an eight-inch line to a one-million-gallon storage tank. From storage, raw water is supplied to the various buildings and subareas within the principal area for process water and fire protection through 14-in. mains capable of distributing 3,000 to 5,000 gpm per subarea. A treatment plant in each area furnishes potable water at the rate of 250 gpm distributed through six-inch mains.

VI, C, Final Fabrication Assembly, Propellant Production Test, and Launch Facilities (cont.)

Available ground water supply and necessary pumps for distribution pressure will vary costs for any particular site and concept.

f Power Supply and Distribution

This is the most costly item under AGPS. Power requirements, propellant production, transfer to storage, and transfer to the vehicle have been analyzed for all thrust ranges. Except for distances for power distribution, cost will vary only slightly for different sites within the U.S. Outside of the U.S., factors of increased construction and material delivery costs will apply. At some locations power plants will be required and costs will range from $200 to $1,000 per kva depending on fuel, water supply, and type of equipment. Variations resulting from finalization of building sizes, equipment, water system, and other demands are considered minor compared to the totals.

A 138 kv line is assumed available in the vicinity of the proposed site, as well as feed lines with the required capacity. A 138 kv to 13.8 kv substation and 13.8 distribution lines are estimated and costs are included in AGPS. It may be possible to have the main substation furnished by the power supply company on a deposit-and-use contract basis. Substations from 13.8 kv to lower voltages and all other power and lighting requirements are included in costs of buildings, plants, areas, and stand. Detailed analyses have also been made for alternative concepts without full propellant production or with storage close to the stand.

VI., C, Final Fabrication Assembly, Propellant Production Test, and Launch Facilities (cont.)

g Fire and Disaster Service

Estimated six-million-pound-thrust-level fire and disaster services include a 15,000 sq ft building to house fire-control rolling-equipment disaster vehicles, and the personnel to operate this equipment. Equipment costs are included.

h Administration

For the six-million-pound thrust level and Administration Building of 10,000 sq ft is estimated. This is for personnel to perform administrative, managerial, and operational functions. For the Base Case, this building is located near the fabrication and assembly building.

i Maintenance

A plant maintenance shop, for the six-million-pound thrust level is assumed to be a 60 x 200 ft building with a five-ton crane. The building will be used to perform plant maintenance functions as well as plant repairs. Mobile equipment will be available.

j Security

Security includes general area gencing, guard facilities, lighting, warning, and traffic control systems not directly applicable to an individual building or area. Cost trends for the six-million-pound-thrust-level vehicles are estimated from plot plan take-offs and scaling factors for other thrust levels.

VI, C, Final Fabrication Assembly, Propellant Production Test, and Launch Facilities (cont.)

2 Propellant Production

Production facilities dependent upon the availability of raw material, water and power, type of material used, process used to manufacture hydrogen gas, process used to manufacture liquid oxygen, liquid nitrogen and liquid hydrogen, degree of automation, and numerous other factors which were determined for the concept selected.

Propellant production facilities for the six-million-pound thrust level were estimated from data obtained for design, construction, and operation of Air Force Plant 74 at West Palm Beach (Figure VI-11).

3 Test/Launch Stand

Costs for the test/launch stand in each case includes all site preparation, foundations, structural steel, umbilical system, gantry and cranes, flame deflector system, on-stand piping and components, static, test fixtures, and on-stand test equipment shops and rooms. The various alternatives compare cost of systems dictated by site requirements and different piping concepts.

4 LH_2 Storage and Transfer to the Test/Launch Stand

Costs trends for storage are separate from transfer to the stand but for comparison to other concepts and alternatives, they are considered together. For pipe line transfer from the propellant production area to the storage area, fill piping within the storage area only is included. A flow schematic is shown in Figure VI-12.

VII., C, Final Fabrication Assembly, Propellant Production Test, and Launch Facilities (cont.)

5 LOX Storage and Transfer to the Test/ Launch Stand

The same comments apply for LOX as for LH_2. Another alternative to consider would be to have the LH_2 storage as close to the stand as possible and separate the LOX from the stand by a distance as required for 15% TNT equivalent of the total propellant on the stand with LH_2 storage empty and purged with nitrogen at the time of testing or firing.

6 RP-1 Storage and Transfer to the Test/ Launch Stand

The same comments apply for RP-1 as for LH_2 and LOX. An economical alternative to consider when using LOX/RP-1 as propellant is to have the LOX as close to the stand as possible and separate the RP-1 storage from the stand as per safety requirements.

7 LN_2 Storage and Transfer

LN_2 is used to obtain GN_2 and to cool-down the LH_2 systems and is assumed to be adjacent to LH_2 and GN_2 areas so that LN_2 and GN_2 transfer lines are included in the LN_2 storage area in all cases. LN_2 and GN_2, being inert, can be located where most convenient and economical.

VI, C, Final Fabrication Assembly, Propellant Production Test, and Launch Facilities (cont.)

8 GH_2 Storage and Transfer to the Test/ Launch Stand

GH_2 storage is kept as close the LH_2 storage as possible. It is, however, even more important for the GH_2 storage to be close to the stand, as flow rates to the stand during a test will be extremely large and at pressures up to 6,000 psig, and available pipe and valves are limited to small sizes for such high pressures. Also, provisions must be made for explosive or fire hazards as outlined elsewhere in this report.

9 GN_2 Storage and Transfer to the Test/ Launch Stand

The same comments apply to GN_2 as do for GH_2, except that, being inert, GN_2 does not have to be given consideration as an explosive hazard. Nitrogen, oxygen, and helium gas flow systems are shown in Figure VI-13.

10 GHe Storage and Transfer to the Test/ Launch Stand

The same comments apply for GHe as for GN_2. In addition, compressor capacity is required to transfer helium from 2,200 psig as received in shipping containers to the 6,000 psia storage vessels. The compressors used in this operation must be oil-free units.

VII, C, Final Fabrication Assembly, Propellant Production Test, and Launch Facilities (cont.)

11 LH_2 Transfer from Production to Storage

When hydrogen is transferred by pipeline from production to ready storage, production plant storage capacity can be reduced to a minimum. Less production capacity is required as losses from production to production storage, to truck or tank car, and to ready storage are reduced. Vacuum-insulated pipe line transfer for LH_2 can be easily justified for on-site production just outside of a 130 db sound radius.

12 LOX Transfer from Production to Storage

Plant and production costs for LOX are not as great as for LH_2; therefore, it is more difficult to justify a vacuum-insulated transfer line. Detailed analysis of total plant, equipment, labor, and time schedules is required to compare pipe line transfer with truck or railroad delivery. These factors would vary for each location, concept, and thrust range.

13 LN_2 Transfer from Production to Storage

The same comments apply for LN_2 as for LOX, and the flow rates are lower. The thrust level at which the pipeline transfer could be justified would be greater for LN_2 than for LOX.

VI, C, Final Fabrication Assembly, Propellant Production Test, and Launch Facilities (cont.)

14 Fabrication and Assembly Plant

Components and subassemblies that are small and light enough to be transported by rail or truck are assumed to be fabricated and tested at other facilities and delivered to this final fabrication and assembly building. These are further fabricated, tested, and assembled into units of 200-tons maximum weight. For the six-million-pound thrust and greater units, the 200-ton assemblies and parts would be loaded onto barges or ships for transport to the stand. For the two-million-pound thrust level, sizes, and weights are assumed to be within limits of on-site overload transport.

15 Fabrication and Assembly Breakwater

The fabrication and assembly building per the Base Case plot plan is assumed to be located in an unprotected area of the U.S. West Coast and a breakwater is required to protect the loading operation. Availability of materials will affect costs for this item and are determined more accurately by the concept selected. Materials removed for a gorge-type concept can be used for this breakwater.

16 Test/Launch Breakwater

The test/launch stand plot plan is assumed to be located in an unprotected area of the U.S. West Coast and the breakwater is required to protect the unloading operation from the sea transport unit to the stand. Materials removed for a gorge-type concept can also be used for this breakwater. Other sites and concepts requiring material to be brought in from a distance are more costly.

VII. C, Final Fabrication Assembly, Propellant Production Test, and Launch Facilities (cont.)

17 Test/Launch Locks

For more stability during lifting operations into the stand, locks are desirable. In some areas, tides are great enough to require locks and pumps to provide clearance over draft tubes or deflector plates without excessive depths of construction; and for all areas, locks are essential to construction and maintenance of these draft tubes and deflector plates.

18 Control Building, Tunnel, and Cable

The control building cost at the six-million-pound thrust level is based on a dome construction, heavily reinforced and partially below grade. The dome structure is covered by a thick layer of sand which, in turn, is covered by a dense concrete applied pneumatically. The building is to be designed structurally for an overpressure of 1,500 psi and located approximately 1,000 ft from the stand with a 14- by 10-ft tunnel connection to a 20- x 40-ft terminal room at the test/launch stand.

The building will be approximately 125 ft in diameter and will have a maximum inside height of approximately 26 ft. Two floors of equipment and working area are assumed. This control building will be equipped with a recirculating air-conditioning system which includes humidity control and air purifying as well as oxygen replenishment equipment. This, along with a system of gas-tight doors, will be required for blast protection and will serve to protect personnel from the effects of a possible malfunction of a vehicle containing toxic propellants.

VI, C, Final Fabrication Assembly, Propellant Production Test, and Launch Facilities (cont.)

The instrumentation and service tunnel between the control building and the terminal room at the launch stand will be located below finish grade. The tunnel, however, will not be designed to resist high overpressures. Costs for this section include equipment for complete automatic operation during missile fill periods, instrumentation cable, terminals, and cable supports.

The structural design criteria for this control building is based upon the control building design for the Titan stands at Cape Canaveral. This design was based on a fully-loaded missile impacting and exploding at a distance of 50 ft from the structure.

If two-million-pounds of high explosive energy propellant (TNT equivalent) exploded, the expected overpressure at 1,000 ft would be 11.8 psi. The likelihood of portions of a manfunctioned or destroyed missile exploding near the control room, with any appreciable percentage in stoichiometric mixture at ignition temperatures, is very small. This design of the control building, on the basis of the above criteria, should thus serve for the full range of thrusts contemplated in this investigation.

19 Control Systems

Control systems include consoles, panels and equipment, conduit wiring and tubing in the control building, and interconnection to the stand for control of propellant systems only.

VI. C, Final Fabrication Assembly, Propellant Production Test, and Launch Facilities (cont.)

(2) Alternative B (LOX/RP-1 Engines)

Alternative B facilities are similar to Alternative A, except that production and pipe line transfer of LH_2, LOX, and LN_2 are extracted and storage and transfer of propellants to the stand have been modified to suit LOX/RP-1 engine requirements. The electrical power and distribution of AFPS have also been reduced to reflect these changes. LOX and LH_2 in Alternative B are assumed to be delivered to the site in vendor-owned-and-operated trucks, and RP-1 by pipeline. In both alternatives, GHe is assumed to be delivered by existing trucks or railroad cars.

Maximum effort was expended on Alternative A of the Continental U.S. Coastal Gorge Concept at the six-million-pound thrust level. Design and cost analysis as well as scaling factors for other concepts are based upon values derived for this basic facility. Any combination of stages can be analyzed in a similar manner by reference to pertinent plots various alternatives.

d. Continental U.S. Coastal Cliff Concept

(1) Alternative A (LOX/LH_2 Engines)

(a) Test and Launch Facility

This type facility, shown in Figure VI-14 would be situated at a cliffside of a suitable geological formation, the upper elevation of which would form a level area for propellant plants, propellant and water storage, fabrication, and other support functions.

VI. C, Final Fabrication Assembly, Propellant Production Test, and Launch Facilities (cont.)

Vehicle sections and segments are brought to the engine test and launch pad on tracks from the fabrication and assembly shops situated outside of the effective blast/pressure wave radii.

The sections are then assembled within a fixed U-shaped tower equipped with folding platforms that can be moved for proper vehicle clearance at the launch. At the six-million-pound thrust level, the fixed-tower concept with provisions for accommodating the jet exhaust at lift-off is considered the economical trade-off, rather than a movable gantry-type service tower.

A water film-cooled deflector plate accommodates the jet exhaust, assuming gravity feed from water storage at an upper elevation within the site vicinity. An adaption of the submerged-plate concept could be integrated into the design.

Advantages of this concept are:

1. Proximity to fabrication and assembly shops
2. Elimination of movable gantry service tower
3. Less site preparation

This concept could also be used at a beach area with a concrete structure and ramp extending from the shore.

VI, C, Final Fabrication Assembly, Propellant Production Test, and Launch Facilities (cont.)

(b) Support Facilities

The base coastal gorge analysis costs for support facilities were used for this concept because the main difference between the two is in the test/launch area only.

(2) Alternative B (LOX/RP-1 Engines)

Alternative B facilities are similar to Alternative A, except for those costs effected by the LOX/RP-1 propellant selection.

e. Remote Island Concept

(1) Alternative A (LOX/LH_2 Engines)

Basic costs were scaled by a factor of 2.2 to cover the remote island increased cost of construction and equipment. The island concept consists of final fabrication and assembly, engine test, and launch. At the two-million-pound thrust level, transport from the fabrication and assembly by land to the test stand is assumed, as well as a coastal cliff engine test and launch stand. Storage capacity is adequate for two engine tests or launchings (one per month) to allow for ship delivery of LH_2, LOX, LN_2 and GHe.

Propellant and LN_2 production facilities are assumed to be a continental U.S. coastal site and approximately 50% greater in cost to allow for transport losses and production plant power in AGPS. Ship capacities are equivalent to island storage plus transport and transfer losses, and nominal transfer capacities aboard for transfer from ship to island storage.

VI, C, Final Fabrication Assembly, Propellant Production Test, and Launch Facilities (cont.)

(2) Alternative B (LOX/RP-1 Engines)

Propellant and LN_2 production is assumed to be available and delivered to existing docks by vendor-owned-and-operated equipment. Island storage, ship, power, and other factors for LOX/RP-1 engines, instead of LOX/LH_2 engines, have been considered in cost analysis.

f. Texas Tower Concept

(1) Alternative A (LOX/LH_2 Engines)

(a) Test and Launch Facility

The fixed concept or Texas Tower could be adapted as an on-shore or off-shore facility. Figure VI-15 shows the tower situated off-shore with a vehicle being assembled within it. Access platforms and overhead deflector plate or draft tube is used for jet exhaust directional control. It is placed at a sufficient depth so that augmented-pressure film-cooling is not required.

Vehicle sections/segments are brought to the facility by ship or barge and raised into the tower by the overhead cranes. Personnel and material access to the tower is provided by ship or causeway, while instrumentation and communication wiring would be routed by causeway or submarine cable to a shore-based or underwater control blockhouse.

VI., C, Final Fabrication Assembly, Propellant Production Test, and Launch Facilities (cont.)

Advantages of this concept are:

1. Wide range of coastal site selections
2. Minimum tidal land acquisition costs
3. Ease of transporting large prefabricated sections and materials
4. Overhead crane handling
5. Blast and sound level protection by remote location

(b) Support Facilities

Cost summaries for the Texas Tower concept assumes construction in 80 ft of water and continental U.S. based production as for a remote island. Transport ships must have docking facilities at the Texas Tower and transfer capacities for four-hour cool-down and fill of the vehicle. Topping tanks and pumping systems must be sufficient on the tower to allow the ship to move off to a safe distance. Breakwater, locks, and docks are not shown in Figure VI-15, but are required.

Base headquarters are assumed to be available on the Continental U.S.

VI, C, Final Fabrication Assembly, Propellant Production Test, and Launch Facilities (cont.)

(2) Alternative B (LOX/RP-1 Engines)

Propellant and LN_2 production is assumed to be available and delivered to existing docks by vendor-owned-and-operated equipment. Differential factors for RP-1 instead of LH_2 have been incorporated into capacities and cost data.

g. Planetary Rocket Ocean Platform Concept (PROP)

(1) Alternative A (LOX/LH_2 Engines)

The PROP concept is a novel, sea-based system meeting all qualifications for assembling, testing, and launching very large vehicles. The PROP is especially applicable to nuclear-powered systems because of the isolation inherent in ocean locations and the possibilities offered for nuclear shielding by unlimited quantities of sea water; however, the PROP should prove equally effective for extremely large chemical boosters.

An artist's concept of the PROP is shown in Figures VI-16 and VI-17. For purposes of general scale, the space vehicle shown is approximately 40 ft in diameter and 300 ft long. The superstructure

VI, C, Final Fabrication Assembly, Propellant Production Test, and Launch Facilities (cont.)

is well above the reach of extremely high seas and is supported by an underwater buoyant chamber well below the wave forces of such seas. Supply ships are shown in the proper proportion. The deck crane carries a cocoon to insulate the vehicle, if necessary, prior to launch. The submarine is used to evacuate personnel through an air lock in case of a nuclear incident or after a nuclear launching. There is no intent to imply by the illustration that there is any specific size, functional capacity, or mode of operation for the PROP. The general concept can be varied in many ways to conform with specific mission requirements. In the PROP concept, it is envisioned to construct big vehicles inside a long central tube, always working at the floor level inside the superstructure. The vehicle under construction is positioned by a hydraulic ram, or other device, so that the working level at the top is maintained level with the superstructure floor. Also, the ram positions the vehicle, or its stages, above the superstructure deck for static testing. Finally, the ram positions the vehicle for launching

A structure such as the PROP, with its buoyant and mechanical capabilities, is a unique approach to the difficult problem of preparing, constructing, testing, and launching big space vehicles. In this concept, complete immunity to weather-generated forces of hurricane intensity is envisioned.

VI, C, Final Fabrication Assembly, Propellant Production Test, and Launch Facilities (cont.)

As a PROP can be located remotely from the continental U. S., island base costing is included in cost summaries and curves for this concept.

Continental U. S. propellant and LN_2 production and GHe supply for the remote island concept is assumed; however, support ships must have incorporated in them high-transfer-rate systems for propellant handling, as well as pumps, vaporizer, and compressors for GH_2, GN_2, and GHe handling.

All land-based facilities and equipment costs for fabrication, final assembly, engine test, and launch are included in the PROP cost summaries.

(2) Alternative B (LOX/RP-1 Engines)

Alternative B facilities are similar to Alternative A, except that propellant and LN_2 production is assumed to be available and delivered to existing docks by vendor-owned and-operated equipment. Ship storage and transfer factors for LOX/RP-1 engines instead of LOX/LH_2 engines have been considered in the cost analysis.

VI., C, Final Fabrication Assembly, Propellant Production Test, and Launch Facilities (cont.)

2. Fabrication and Assembly, Production, Engine Test, and Launch Facility Costs

a. Production Acceptance Testing

(1) The unit cost trends for acceptance testing a complete system, shown in Figure VI-18, are based upon a two-shift day, 40-hour work week and the requirements to operate a test stand and control room only employing such personnel as: supervisors, engineers, technicians, engineering aides, data reductionists, and clerks. No consideration has been made for the additional requirements associated with plant security, maintenance, plant engineering, shop support, traffic, and other allied functions.

(2) These cost trends were based upon the following assumptions or limitations:

(a) The maximum testing rate is one system per stand, every three months, therefore, over a six-year period a production of 25 units would require 1 test stand, 100 units 4 test stands, and 400 units 16 test stands.

(b) The system will be supplied for testing in an assembled or semiassembled condition and the start installation will not encompass detailed build-up of the system.

(c) Transportation of units from the fabrication and assembly area to test stand are not included.

VI, C, Final Fabrication Assembly, Propellant Production Test, and Launch Facilities (cont.)

(d) Complete data analysis and evaluation will be handled by an engineering project group.

(e) Propellants and pressurant gases required for the program are assumed to be G.F.P.

b. Facility Cost Trends

The costs of manufacturing, fabricating, and assembly facilities includes the costs of installed machine tools and production tooling. In each type of facility concept presented, it is assumed that the use of existing machine tools of applicable size and capacity, owned or in use by Aerojet-General, will be utilized. Cost trends for each facility concept discussed is presented as follows:

(1) Continental U.S. coastal gorge (Figure VI-18)
(2) Continental U.S. coastal cliff (Figure VI-19)
(3) Remote island (Figure VI-20)
(4) Planetary rocket ocean platform concept (Figure VI-21)
(5) Planetary rocket ocean platform concept (Figure VI-22)

VII, Facilities (cont.)

D. SAFETY

1. Quantity Distances and Blast Pressures

Department of Defense Directive - 4145.17, December 7, 1956, Quantity-Distance Standards for Manufacturing, Handling, and Storage of Mass-Detonating Explosives and Ammunition which references DOD Directive 5154.5 Armed Services Explosives Safety Board, November 21, 1953, amended December 23, 1954 is the accepted standard of all armed services and adapted by most other agencies and industries. Air Force Regulation 86-6, Installation Planning and Development, Quantity Distance Standards for Storage of Mass-Detonating Military Explosives, 3 May 1957 has quantity distance tables identical to the DOD directive.

Air Force TO 11C-1-6, General Safety Procedures for Chemical Guided Missile Propellants, 12 December 1956 recommends reasonable and adequate safety standards for handling, storage, transportation, and use of highly reactive chemicals. Eleven groups of liquids, gases, and solids are tabulated. Increasing group numbers indicates an increase in hazard. Letter O signifies oxidizer; letter C signifies combustible; and letter P signifies poison.

In letter dated 28 September 1960 from Headquarters Air Force Flight Test Center, Air Research and Development Command, United States Air Force; Hollis L. Miller, Jr.; Major, USAF; Chief, Operations Branch, Directorate of Rocket Propulsion; Edwards Air Force Base, California, states: "All quantity-distances for: explosive hazards to inhabited buildings, explosive hazards within a technical area, and toxic hazards within a technical area, will be based on TNT equivalents. These TNT equivalents will be based on 25 percent of the weight of propellants in ready storage and 15 percent of weights of propellants in operation run tanks. The TNT equivalent tables will be based upon AFR 86-6. Separations are required for incompatible propellants only."

VI, D, Safety (cont.)

A letter dated 15 November 1960 from D. A. Armstrong, Director of Chemistry, Aerojet-General Corporation Chemical Division, indicates that a TNT equivalent of 5% for liquid propellants may be adopted by the Inspector General's Office of the Air Force. It is, however, assumed that TNT equivalents only apply when fuels and oxidizers are in close proximity, not separated by fire hazard distances from each other.

Liquid oxygen is now classed as Group 1-0 in TO 11C-1-6C with no limitations in amounts stored other than that required to limit fire hazard. Liquid hydrogen is classed as Group 7-C in TO 11C-1-6 with a maximum limit of 100,000 lb requiring an inhabited building distance of 1,800 ft, passenger railroad and public highway distance of 1,200 ft and unbarricaded separations of other Group 7 storage or operating buildings of 400 ft. WADC Technical Report No. 59-386, July 1959, Storage, Transfer and Servicing Equipment for Liquid Hydrogen, voids this section of TO 11C-1-6 and defines hydrogen storage as a fire hazard only. It recommends dike or gravel filled excavation to contain a spill and separation based on a radiant flame from a rising cloud of vapor as for Group 1-C of TO 11C-1-6. RP-1 Kerosene, etc., is classed as Group 1-C in TO 11C-1-6 with no limitations other than necessary precautions against fire hazards.

As the weights of propellants for vehicles in this study are beyond the limits of existing tables, Aerojet-General has prepared extrapolation of existing quantity-distance tables. To use these tables it is necessary to determine the TNT equivalent of the fuel or oxidizer in question. Tabulations of distances have been made with the 100% TNT equivalent using DOD 4145.17 and dividing the distance obtained by 2, as permitted. Tabulations have also been made of separation distances based on 5, 10 and 15% of vehicle propellant weights using AFR 86-6; 15 and 25% of storage weights; and equivalents used for Saturn

VII, D, Safety (cont.)

test and launchings at Cape Canaveral. The Cape Canaveral equivalents are 40% of H_2 under 500,000 lb and 60% over, plus 10% of O_2 under 500,000 lb and 20% over to obtain a TNT equivalent.

It is possible at the Gorge Concept location to comply with all regulations by extrapolation of tables in AFR 86-6--with the 15% TNT equivalent or one-half distance calculations of DOD 4145.17--without space and cost penalties.

During assembly, checkout, and possible fabrication operations in the stand it is logical to keep fuel and oxidizer combinations out of the test/launch stand. Fuel (hydrogen or hydrocarbon) storage could be located close to the stand with only a fire hazard potential. Oxygen or other oxidizer storage should be separated from the fuel storage at a distance to protect the oxidizer area from damage due to a fuel fire, engine malfunction, or sound pressure during engine firings. Structural designs must be based upon the possible over-pressures anticipated for the distances selected because of either explosive malfunctions or high sound pressure levels.

A quantity-distance comparison table is presented as Table VI-7.

VI, Facilities (cont.)

E. ACOUSTIC ANALYSIS

1. Introduction

Ultra-high thrust rocket engines proposed for the future will generate acoustic power and sound levels that could have a detrimental effect on exposed or unprotected equipment, and would be injurious to unprotected personnel exposed to sound levels above 140 db. The purpose of this analysis was to predict the maximum expected sound pressure levels resulting from the firing of rocket engines in the thrust range of 2 to 150-million lb.

2. Discussion

Data presented here reflects ths study and evaluation of varied information.*

The Acoustical Analysis in AGC Report 1675 is based upon sound measurements from a rocket engine of 10,000 lb thrust taken at a distance of 50 nozzle diameters from the sound source. Hemispherical propagation of sound from the rocket engine was assumed in order to relate sound pressure level (SPL) in decibels to the engine thrust. Curves presented reflect only the attenuation effects caused by divergence of the sound waves, viscosity, heat conduction and molecular absorption. Attenuation effects resulting from wind velocity, temperature gradients and terrain must be determined by measurements conducted under local conditions. The data from this report indicates that a maximum of 0.8% of the total jet-stream power can be converted to sound.

* (1) Aerojet-General Corp., Feasibility Study for Multiple Thrust Rating Launch Complex, Report No. 1675, October 1959.

(2) Aerojet-General Corp., Sound Level Measurements, Technical Memorandum No. 129, Revision A

(3) Marshal Space Flight Center - Supplied information about measurements of sound levels obtained during the static firings of the Saturn S-I Stage.

VII, E, Acoustic Analysis (cont.)

The conclusions of Technical Memorandum No. 129 was based upon measurements of near- and far-field sound pressure levels resulting from static test firing of 80,000- and 300,000-lb thrust rocket engines. The acoustic power level of the rocket engine was computed from the sound pressure level (SPL) measurements assuming the sound source to be spherical. Curves and data resulting from the measurements reflect the sound attenuation effects due to local conditions of atmosphere, terrain and deflector plate configuration as well as attenuation due to divergence, viscosity, heat conduction and molecular absorption, and indicated an acoustical power conversion factor of from 0.2 to 0.4% of the jet stream power. This is shown in Figure VII-23.

A curve, shows a plot of over-all sound pressure level in decibels in relationship to distance from the rocket engine in feet for predicted maximum sound levels to be expected from firing rocket engines of thrust ranges to 150-million lb on basis of AGC Report No. 1675. A plot of measurements obtained from static firing of the Saturn S-I Stage 1,500,000 lb of thrust at Huntsville indicates the variations in sound pressure level which can be expected because of varying atmospheric conditions.

It is interesting to note that actual sound measurements from the test firings of the Saturn S-I Stage form an irregular envelope which fluctuates between the values predicted in Technical Memorandum No. 129 and the values predicted in Report No. 1675, which emphasized the variations in sound level intensity that may be experienced at a given distance from the sound source due to various atmospheric conditions.

VI,, E, Acoustic Analysis (cont.)

It is known that other factors may also affect the a oustical power conversion factor such as engine design, after burning of exhaust gases, weight of exhaust gases, surrounding terrain features and shape of deflector plate. High sound sources from jet-streams can be attenuated by firing into water pools or by water injection techniques. Where existing test facilities are so located that the level of sound produced during test firings becomes objectionable to inhabited areas, these methods of sound reduction should be used where applicable or possible. However, to provide ground rules for costing and siting purposes, minimum radius distances of sound intensity are realted to contemplated propulsion system thrust levels based upon the conservative data predicted from AGC Report 1675.

3. Recommendations

It is recommended that test or launch facilities be located based upon the following separation distances·

Thrust (10^6 lb)	100 db Inhabited Area Radius (ft)	130 db Unprotected Operating Personnel Radius (ft)	120 db Public Roads and Highways Radius (ft)
2	90,000	4,700	12,500
6	140,000	7,400	20,000
10	180,000	9,300	25,000
20	240,000	12,000	33,000
80	440,000	23,000	61,000
150	640,000	32,000	85,000

TABLE VI-1

TEST/LAUNCH WEIGHTS, SIZES AND CLEARANCES

VEHICLE WEIGHTS

THRUST $\times 10^6$ #	EMPTY $\times 1000$#	LIFT-OFF $\times 1000$#
2	225	1,610
6	680	4,839
24	2700	19,350

1ST STAGE WTS WITH LO_2/LH_2 ENGINE

THRUST $\times 10^6$#	LO_2 $\times 1000$#	LH_2 $\times 1000$#	EMPTY $\times 1000$#
2	945	165	130
6	2,840	504	390
24	11,380	2,020	1,560

2ND STAGE WTS WITH LO_2/LH_2 ENGINE

THRUST $\times 10^6$#	LO_2 $\times 1000$#	LH_2 $\times 1000$#	EMPTY $\times 1000$#
2	235	40	65
6	697	118	190
24	2,790	472	761

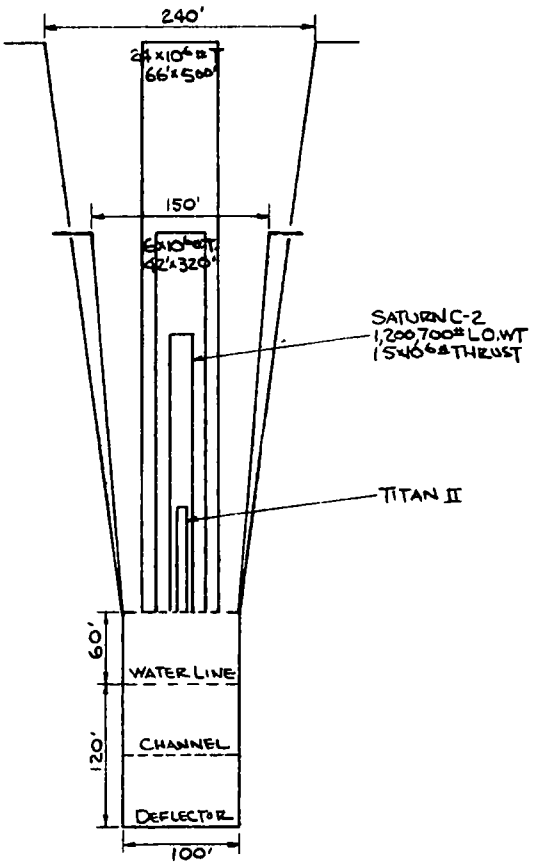

1ST STAGE WTS WITH $LO_2/RP\text{-}1$ ENGINE

THRUST $\times 10^6$#	LO_2 $\times 1000$#	RP-1 $\times 1000$#	EMPTY $\times 1000$#
2	743	247	145
6	2,231	902	435
24	8,920	3,615	1,740

2ND STAGE WTS WITH $LO_2/RP\text{-}1$ ENGINE

THRUST $\times 10^6$#	LO_2 $\times 1000$#	RP-1 $\times 1000$#	EMPTY $\times 1000$#
2	296	99	50
6	740	286	145
24	2,960	1,145	582

PAYLOAD WT

THRUST $\times 10^6$#	PAYLOAD 1000#
2	35
6	100
24	402

Table VI-1

TABLE VI-2

BASIC FACTORS FOR PROPELLANT PRODUCTION, TRANSFER, AND STORAGE

Thrust Range (lb)	Launch Use (lb)	Storage Capacity for Pipe Transfer Concept (lb)	Production Plant Storage for Truck or Rail Transfer (lb)	Production Capacity for Pipe Transfer Concept (tons/day)	Production Capacity for Truck or Rail Transfer (tons/day)	gpm Pipe Line	Transfer 150 lb ASA Pipe (in.)
			LH_2				
2 x 10^6	205,000	312,000	32,000	10	12	25	1
6 x 10^6	622,000	935,000	65,000	25	28	60	1-1/2
24 x 10^6	2,485,000	3,730,000	316,000	102	114	240	3
			LO_2 (WITH LO_2 - LH_2 ENGINES)				
2 x 10^6	1,180,000	2,360,000	158,000	55	56	8	1
6 x 10^6	3,537,000	6,980,000	475,000	160	163	25	1-1/2
24 x 10^6	14,200,000	28,000,000	2,370,000	642	651	96	3
			LH_2				
2 x 10^6	Per Criteria	328,000	16,000	10	10	2	1
6 x 10^6	Eq to Stor.	1,010,000	50,000	25	26	5	1
24 x 10^6	given at 6 x 10^6 Range	4,040,000	200,000	102	104	24	1-1/2
			RP-1				
2 x 10^6	Same as	346,000	N.A.	10.4	Same as	7	1
6 x 10^6	Storage	1,188,000		22.6	Pipe Trans.	15	1-1/2
24 x 10^6		4,760,000		93		57	1 1/2
			LO_2 (WITH LO_2 - RP-1 ENGINES)				
2 x 10^6	1,039,000	2,078,000	140,000	47.5	48.5	7	1
6 x 10^6	2,971,000	5,942,000	398,000	136	138	20	1-1/2
24 x 10^6	11,900,000	23,800,000	1,590,000	547	555	79	3

TABLE VI-3

BASIC ASSUMPTIONS

		Alternative A, LO_2/LH_2 Vehicle			Alternative B, LO_2/RP-1 Vehicle		
		2×10^6	6×10^6	24×10^6	2×10^6	6×10^6	24×10^6
VEHICLE CAPACITY	LH_2 GAL	347,000	1,058,000	4,410,000			
	LO_2 GAL	124,000	370,000	1,490,000	109,000	311,000	1,256,000
	RP-1 GAL				346,000	1,188,000	4,760,000
					51,000	176,000	706,000
PROPELLANT &	LH_2 GAL	529,000	1,585,000	6,320,000			
GAS STORAGE	LO_2 GAL	248,000	740,000	2,980,000	218,000	622,000	2,512,000
CONTINENTAL U.S.	LN_2 GAL	49,000	150,000	600,000	49,000	150,000	600,000
CONCEPTS	RP-1 GAL				51,000	176,000	706,000
	GH_2 SCF	150,000	450,000	1,800,000	150,000	450,000	1,800,000
	GN_2 SCF	150,000	450,000	1,800,000	150,000	450,000	1,800,000
	GH_2 SCF	150,000	450,000	1,800,000			
PROPELLANT &	LH_2 GAL	1,058,000	3,170,000	12,640,000			
GAS STORAGE - ALL	LO_2 GAL	496,000	1,480,000	5,960,000	436,000	1,244,000	5,024,000
OTHER CONCEPTS AND	LN_2 GAL	98,000	300,000	1,200,000	98,000	300,000	1,200,000
SHIP TRANSPORT	RP-1 GAL				102,000	352,000	1,412,000
	GH_2 SCF	300,000	900,000	3,600,000	300,000	450,000	3,600,000
	GH_2 SCF	300,000	900,000	3,600,000	300,000	450,000	3,600,000
	GH_2 SCF	300,000	900,000	3,600,000			

TABLE VI-4

DESIGN FORCES ON TEST STANDS

FORCE	DIRECT SUPPORTING MEMBER	REMOTE MEMBERS	FLAME DEFLECTORS	FOUNDATION	PLATFORMS AND STAIRWAYS
A. THRUST = T	1.0T	1-0T	1-0T	1-0T	
1. Thrust Over Shoot (Including sudden loading)	0-5T 1.7T				
B. DEAD LOADS					
1. Tanks and Equipment = W	1.0W	1.0W		1.0W	1.0W
2. Propellants = W_2	1.0W_2	1.0W_2		1.0W_2	
C. LIVE LOADS * = P	1.0P Not app.with thrust	1.0P Not applied with thrust			100#/ft.^{2} or 2000# Concentrated on 2 sq. ft.
D. STRESS REVERSAL **	-5T + W + W_2			1.5 + W + W_2	
E WIND *** 1. Tanks	ALL AFFECTED MEMBERS 20#/ft.^{2} of projected area below 50' high 30#/ft.^{2} of projected area 50' to 100' high				
2. Structure	45#/ft.^{2} on projected area of one side of a 4 sided open structure below 50 ft.high. 60#/ft.^{2} on projected area of a 4 sided open structure 50' to 100' high.				
F. SEISMIC	.1 of Tital Weight of T and propellant and structure applied horizontal @ the center of gravity of the assembly.				

* The total design thrust is computed using a triangular impulse and the worst expected time rise or time decay and period of structure factor.

** Stress reversal is computed using a triangular impulse assuming a thrust rise of 50% followed by thrust decay to zero.

*** Wind loads are affected by location aspect ratio of the structure and height; forces shown are for West Coast on normal run tanks and structures.

NOTES: (1) Do not combine seismic or wind loads with thrust loads. (2) Vibration effects must be evaluated separately. (3) Design allowable stresses are not to exceed 80% of yield.

TABLE VI-5

LO_2/LH_2 PROPELLANTS; QUANTITY DISTANCES-- COMPARISON TABULATION

THRUST RANGE (TOTAL PROP.VEH)	DOD 4145.17 Class 9/2	AFR 86-6 5% Veh. Pd. (TNT Eq.)	AFR 86-6 10% Veh. Pd. (TNT Eq.)	AFR 86-6* 15% Veh.Pd. (TNT Eq.)	AFR 86-6 15% ST Pd. (TNT Eq.)	AFR 86-6 25% STE Pd. (TNT Eq.)	AFR 86-6 SATURN CANAV.STD. (TNT Eq)
INTRALINE DISTANCES - 18 x W-1/3 - W - TNT Equivalent							
2×10^6 pd. (1,385,000#)	1,000 ft	720 ft (69,250#)	930 ft (138,600#)	*1,066 ft (207,750#)	1,331 ft (404,100#)	1,580 ft (673,400#)	1,230 ft (318,000#)
6×10^6 pd. (4,159,000#)	1,450 ft	1,070 ft (207,950#)	1,340 ft (415,900#)	*1,538 ft (623,850#)	1,912 ft (1,197,600#)	2,270 ft (1,995,200#)	1,850 ft (1,080,600#)
20×10^6 pd. (13,879,000#)	2,155 ft	1,595 ft (693,950#)	2,000 ft (1,387,900#)	*2,298 ft (2,081,850#)	2,857 ft (3,999,750#)	3,385 ft (6,670,000#)	2,760 ft (3,605,000#)
80×10^6 pd. (55,490,000#)	3,435 ft	2,530 ft (2,774,500#)	3,185 ft (5,549,000#)	*3,648 ft (8,323,500#)	4,531 ft (15,945,450#)	5,370 ft (26,400,000#)	4,380 ft (14,414,000#)
150×10^6 pd. (103,950,000#)	4,225 ft	3,120 ft (5,150,000#)	3,920 ft (10,300,000#)	*4,497 ft (15,450,000#)	5,588 ft (29,920,000#)	6,620 ft (49,849,500#)	5,400 ft (27,010,000#)
INHABITED DISTANCES - 68 x W-1/3							
2×10^6 pd *(207,750# TNT)	3,775 ft	2,775 ft	3,520 ft	* 4,027 ft	5,028 ft	5,960 ft	4,630 ft
6×10^6 pd *(623,850#)	5,450 ft	4,030 ft	5,070 ft	* 5,810 ft	7,221 ft	8,560 ft	7,000 ft
20×10^6 pd *(2,081,850#)	8,150 ft	6,020 ft	7,550 ft	* 8,683 ft	10,794 ft	12,820 ft	10,420 ft
80×10^6 pd. *(8,323,500#)	13,000 ft	9,560 ft	12,020 ft	*13,781 ft	17,115 ft	20,250 ft	16,550 ft
150×10^6 pd. *(15,450,000#)	16,000 ft	11,750 ft	14,800 ft	*16,988 ft	21,110 ft	25,000 ft	20,400 ft

NOTE: (*) Indicates Base Case Situation

TABLE VI-5 (cont.)

THRUST RANGE (TOTAL PROP. VEH)	DOD 4145.17	AFR 86-6 5% Veh.Pd. (TNT Eq.)	AFR 86-6 10% Veh.Pd. (TNT Eq.)	AFR 86-6* 15% Veh. Pd. (TNT Eq.)	AFR 86-6 15% ST Pd. (TNT Eq.)	AFR 86-6 25% STE Pd. (TNT Eq.)	AFR 86-6 SATURN CANAV.STD. (TNT Eq.)
		PASSENGER RAILROAD AND HIGHWAY DIST. -.6 x 68 x W-1/3					
2×10^6	2,270 ft.	1,670 ft	2,115 ft.	* 2,420 ft	3,020 ft	3,580 ft	2,780 ft
6×10^6	3,270 ft.	2,420 ft	3,045 ft	* 3,480 ft	4,330 ft	5,140 ft	4,200 ft
20×10^6	4,900 ft	3,615 ft	4,530 ft	* 5,210 ft	6,460 ft	7,700 ft	6,250 ft
80×10^6	7,800 ft	5,740 ft	7,220 ft	* 8,270 ft	10,280 ft	12,150 ft	9,940 ft
150×10^6	9,600 ft	7,050 ft	8,870 ft	* 11,200 ft	12,650 ft	15,000 ft	12,250 ft

NOTE: (*) Indicates Base Case Situation

TABLE VI-6

LO_2/LH_2 PROPELLANTS; QUANTITY DISTANCES-- COMPARISON TABULATION

THRUST RANGE (TOTAL PROP.VEH)	DOD 4145.17 Class 9/2	AFR 86-6 5% Veh. Pd. (TNT Eq.)	AFR 86-6 10% Veh. Pd. (TNT Eq.)	AFR 86-6* 15% Veh.Pd. (TNT Eq.)	AFR 86-6 15% ST Pd. (TNT Eq.)	AFR 86-6 25% STE Pd. (TNT Eq.)	AFR 86-6 SATURN CANAV.STD. (TNT Eq)
INTRALINE DISTANCES - 18 x W-1/3 - W - TNT Equivalent							
2×10^6 pd. (1,385,000#)	1,000 ft	720 ft (69,250#)	930 ft (138,600#)	*1,066 ft (207,750#)	1,331 ft (404,100#)	1,580 ft (673,400#)	1,230 ft (318,000#)
6×10^6 pd. (4,159,000#)	1,450 ft	1,070 ft (207,950#)	1,340 ft (415,900#)	*1,538 ft (623,850#)	1,912 ft (1,197,600#)	2,270 ft (1,995,200#)	1,850 ft (1,080,600#)
20×10^6 pd. (13,879,000#)	2,155 ft	1,595 ft (693,950#)	2,000 ft (1,387,900#)	*2,298 ft (2,081,850#)	2,857 ft (3,999,750#)	3,385 ft (6,670,000#)	2,760 ft (3,605,000#)
80×10^6 pd. (55,490,000#)	3,435 ft	2,530 ft (2,774,500#)	3,185 ft (5,549,000#)	*3,648 ft (8,323,500#)	4,531 ft (15,945,450#)	5,370 ft (26,400,000#)	4,380 ft (14,414,000#)
150×10^6 pd. (103,950,000#)	4,225 ft	3,120 ft (5,150,000#)	3,920 ft (10,300,000#)	*4,497 ft (15,450,000#)	5,588 ft (29,920,000#)	6,620 ft (49,849,500#)	5,400 ft (27,010,000#)
INHABITED DISTANCES - 68 x W-1/3							
2×10^6 pd *(207,750# TNT)	3,775 ft	2,775 ft	3,520 ft	* 4,027 ft	5,028 ft	5,960 ft	4,630 ft
6×10^6 pd *(623,850#)	5,450 ft	4,030 ft	5,070 ft	* 5,810 ft	7,221 ft	8,560 ft	7,000 ft
20×10^6 pd *(2,081,850#)	8,150 ft	6,020 ft	7,550 ft	* 8,683 ft	10,794 ft	12,820 ft	10,420 ft
80×10^6 pd. *(8,323,500#)	13,000 ft	9,560 ft	12,020 ft	*13,781 ft	17,115 ft	20,250 ft	16,550 ft
150×10^6 pd. *(15,450,000#)	16,000 ft	11,750 ft	14,800 ft	*16,988 ft	21,110 ft	25,000 ft	20,400 ft

NOTE: (*) Indicates Base Case Situation

TABLE VI-6 (cont.)

THRUST RANGE (TOTAL PROP. VEH)	DOD 4145.17	AFR 86-6 5% Veh.Pd. (TNT Eq.)	AFR 86-6 10% Veh.Pd. (TNT Eq.)	AFR 86-6* 15% Veh. Pd. (TNT Eq.)	AFR 86-6 15% ST Pd. (TNT Eq.)	AFR 86-6 25% STE Pd. (TNT Eq.)	AFR 86-6 SATURN CANAV.STD. (TNT Eq.)
			PASSENGER RAILROAD AND HIGHWAY DIST. = .6 x 68 x W-1/3				
2×10^6	2,270 ft.	1,670 ft	2,115 ft.	* 2,420 ft	3,020 ft	3,580 ft	2,780 ft
6×10^6	3,270 ft.	2,420 ft	3,045 ft	* 3,480 ft	4,330 ft	5,140 ft	4,200 ft
20×10^6	4,900 ft	3,615 ft	4,530 ft	* 5,210 ft	6,460 ft	7,700 ft	6,250 ft
80×10^6	7,800 ft	5,740 ft	7,220 ft	* 8,270 ft	10,280 ft	12,150 ft	9,940 ft
150×10^6	9,600 ft	7,050 ft	8,870 ft	* 11,200 ft	12,650 ft	15,000 ft	12,250 ft

NOTE: (*) Indicates Base Case Situation

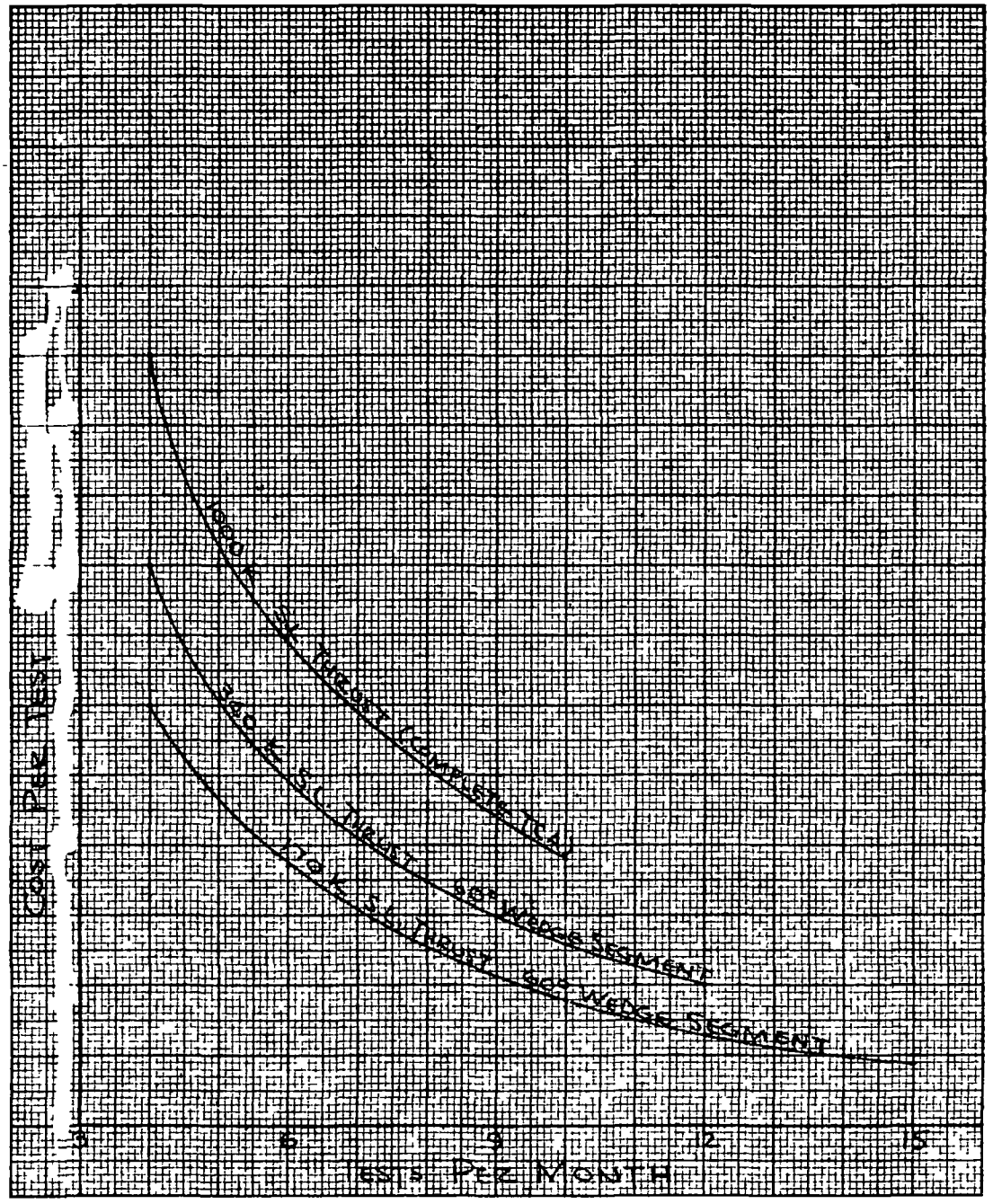

Projected Test Cost Trends, DeLaval Nozzle Thrust Chamber

Figure VI-1

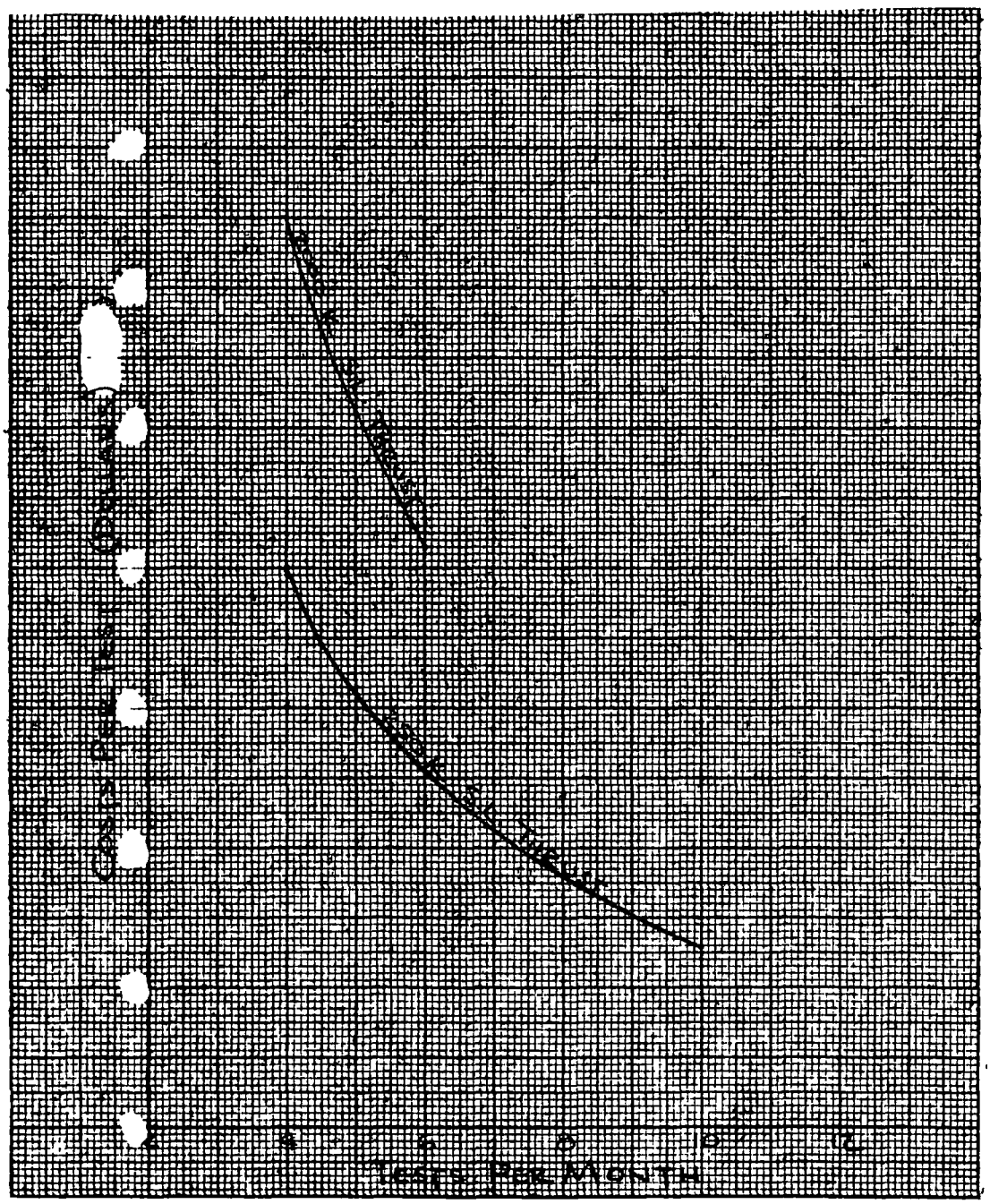

Projected Test Cost Trends, Pen Nozzle Thrust Chamber, Wedge Segments

Figure VI-2

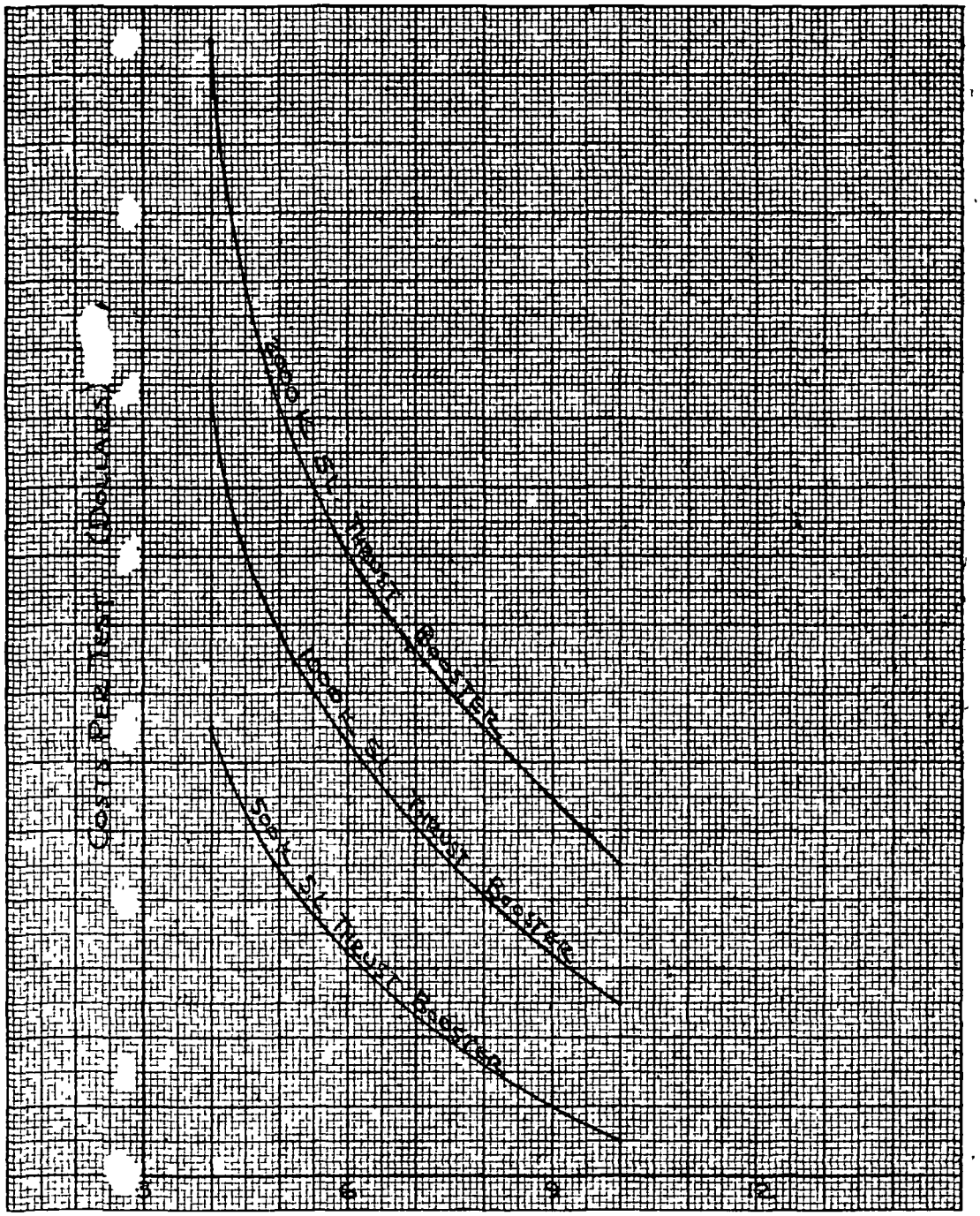

Projected Test Cost Trends, Turbopump for Booster Engines
S-L Thrust as Designated

Figure VI-3

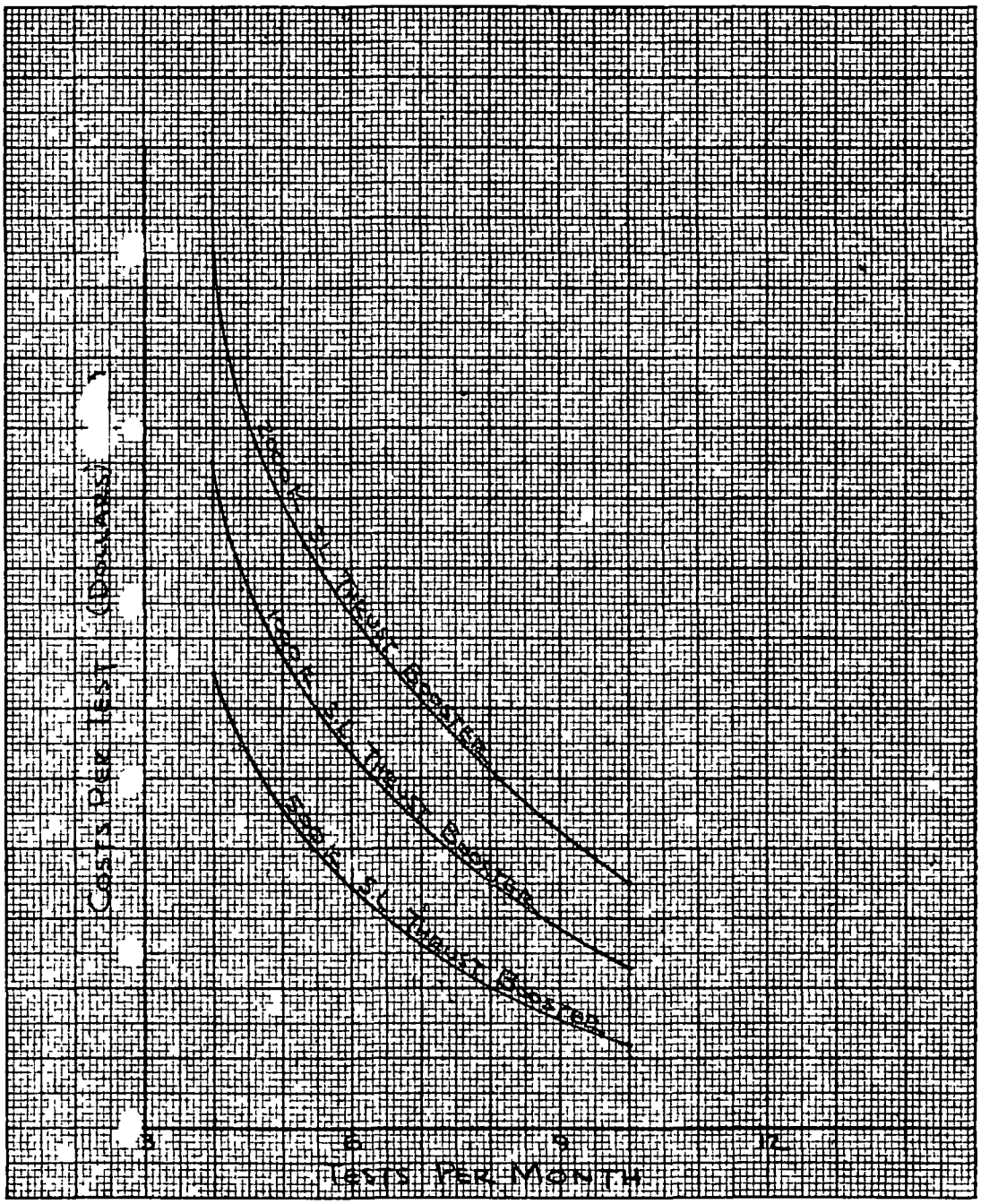

Projected Test Cost Trends, GG for Booster Engine
S-L Thrust as Designated

Figure VI-4

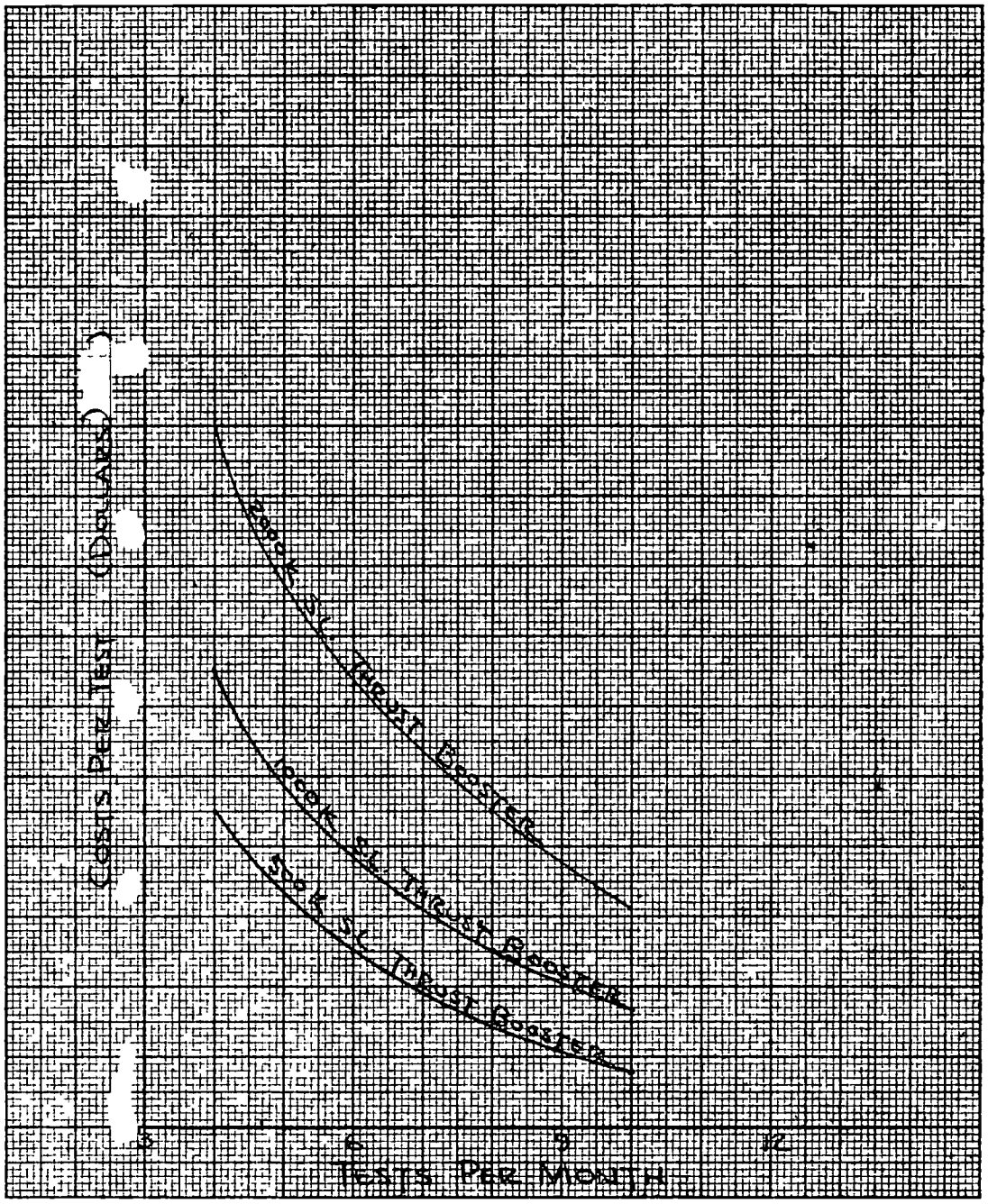

Projected Test Cost Trends, Valves and Components for Booster Engine S-L Thrust as Designated

Figure VI-5

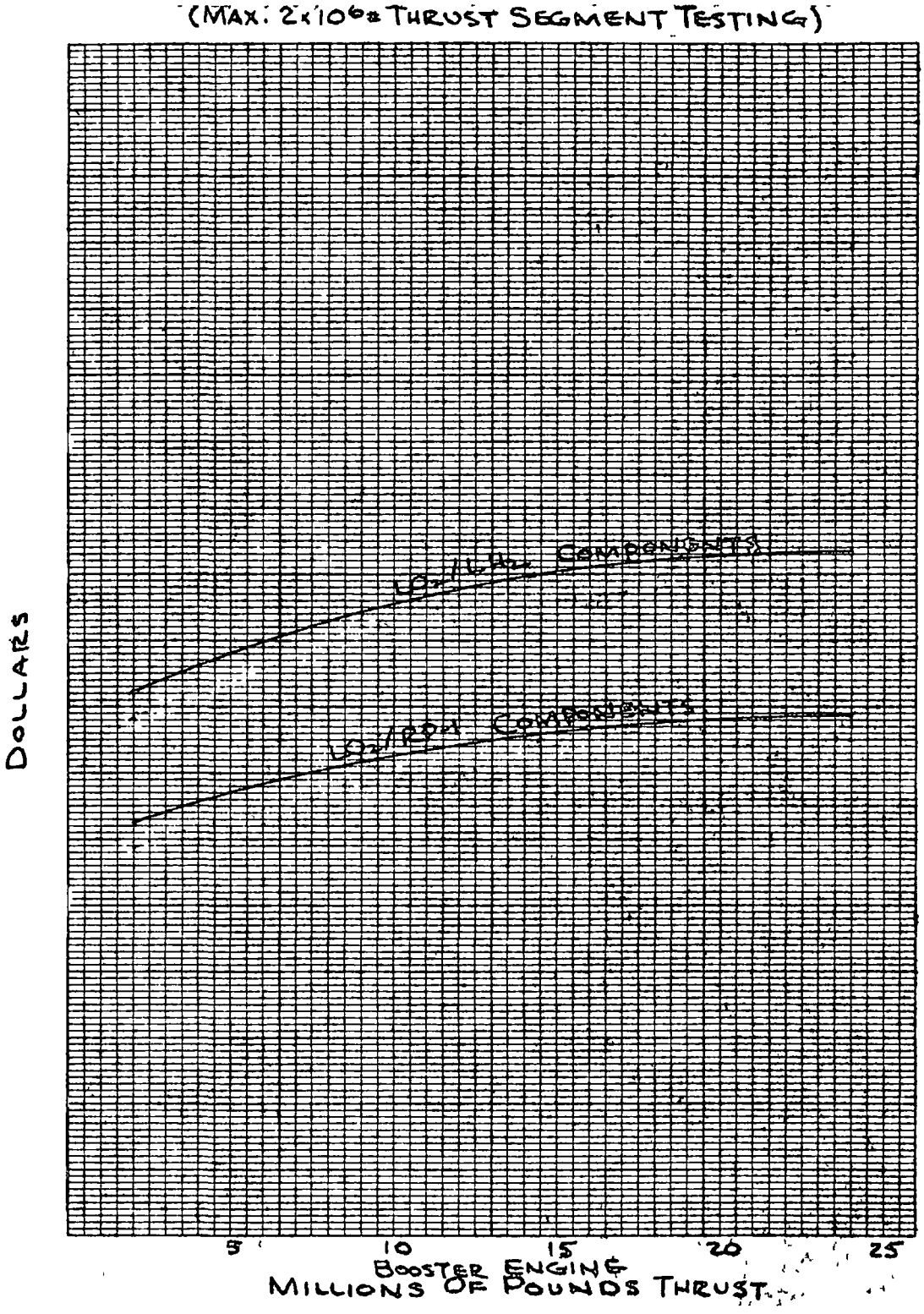

Research and Development Facility Cost Trends

Figure VI-6

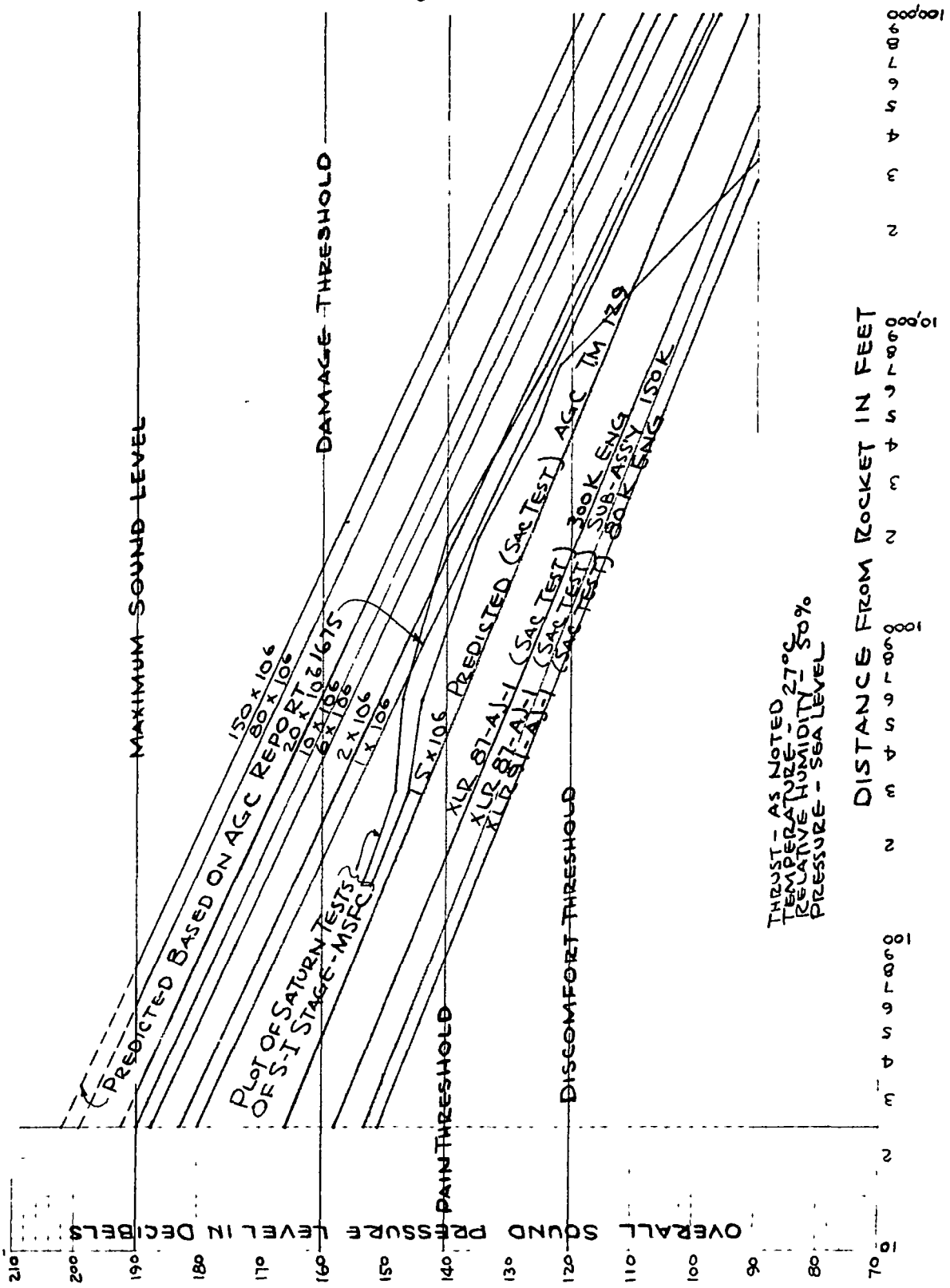

Over-All Sound Pressure Level vs Distance from Rocket

Figure VI-7

Fabrication and Assembly Test and Launch Site

Figure VI-8

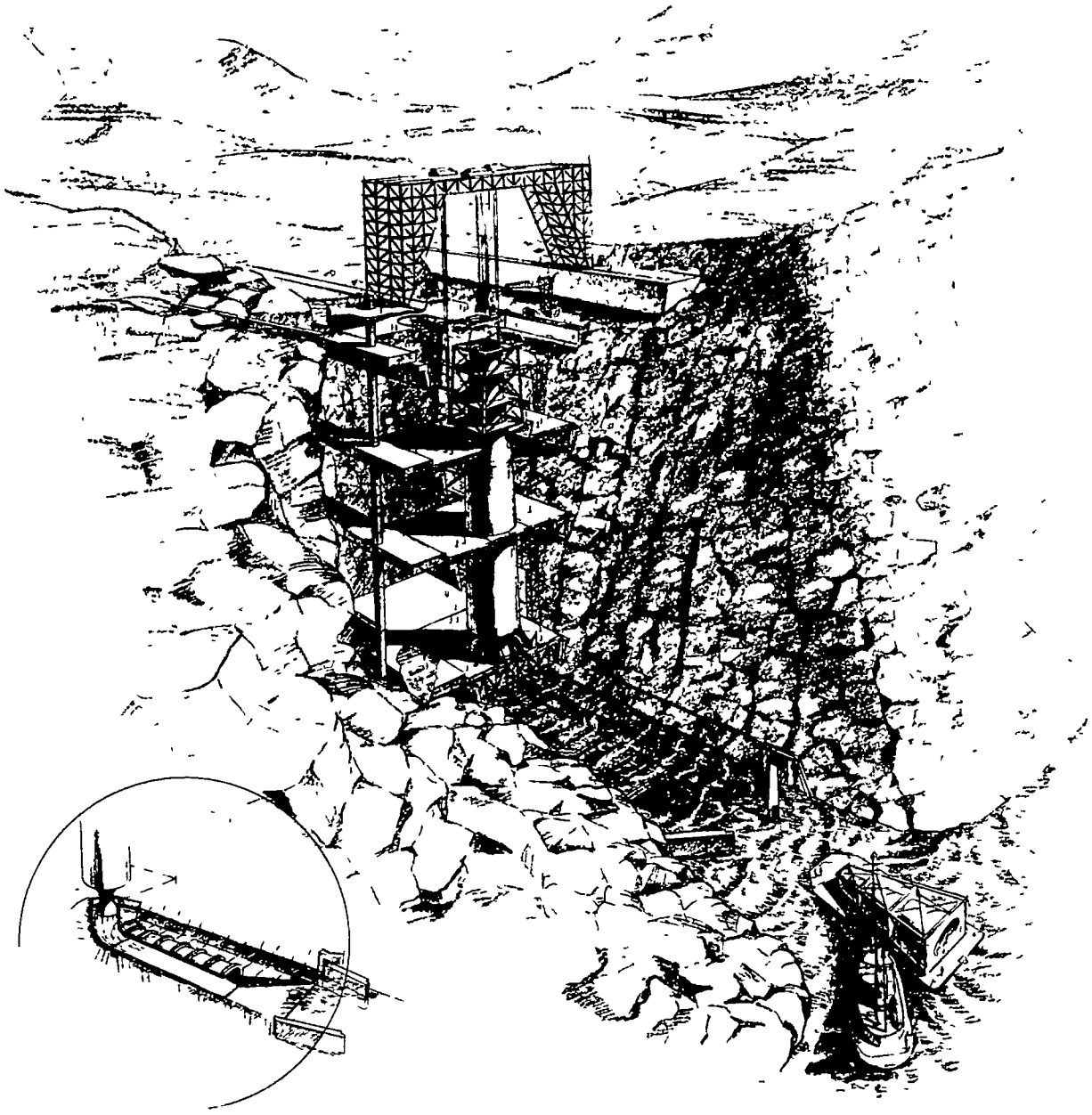

Gorge Test and Launch Area

Figure VI-9

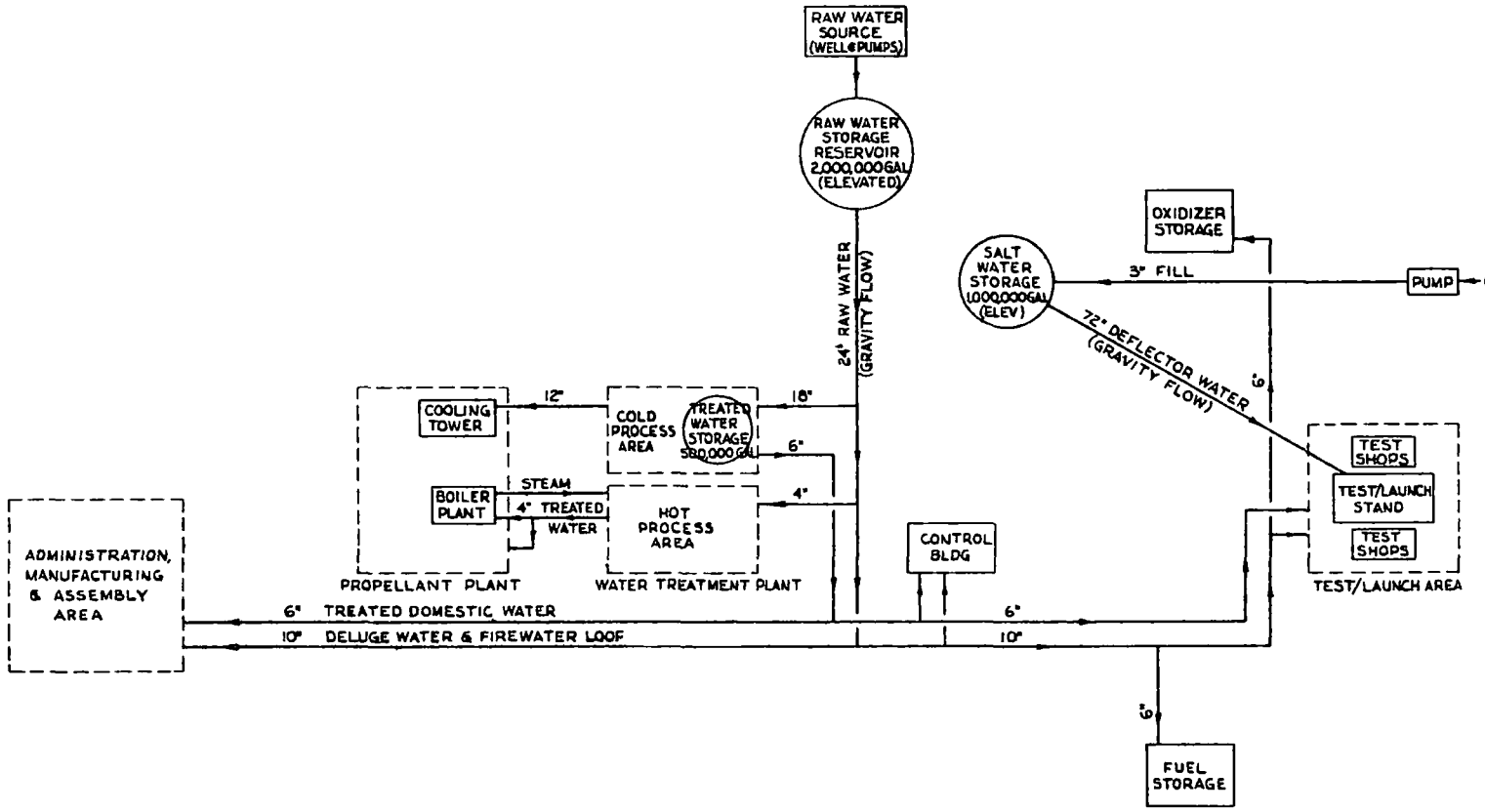

NOTE – SCHEMATIC LAYOUT BASED ON RT SAL AREA LOCATION

Water Systems Schematic Flow Diagram

Figure VI-10

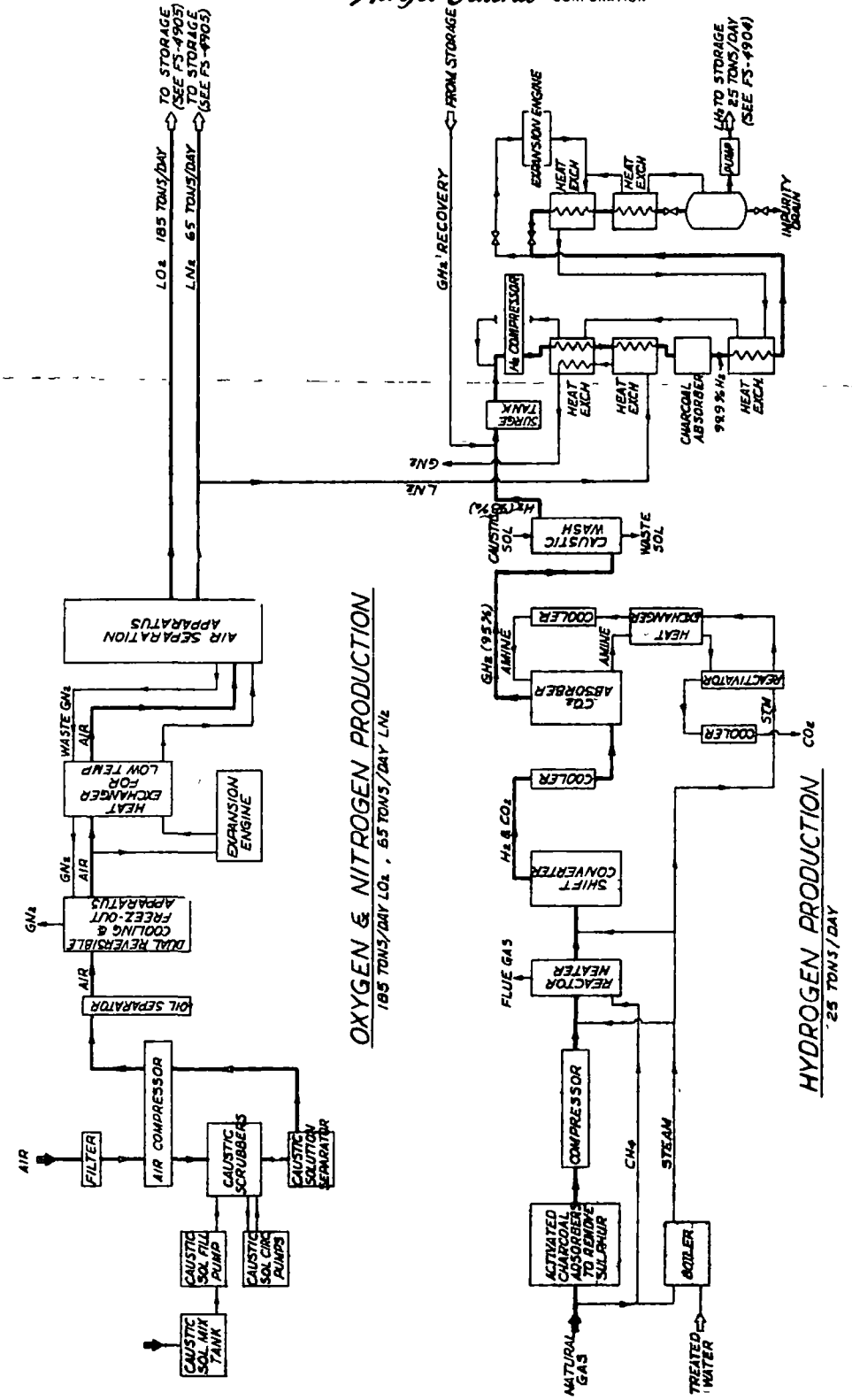

LH_2, LO_2, and LN_2 Production Schematic Flow Diagram

Figure VI-11

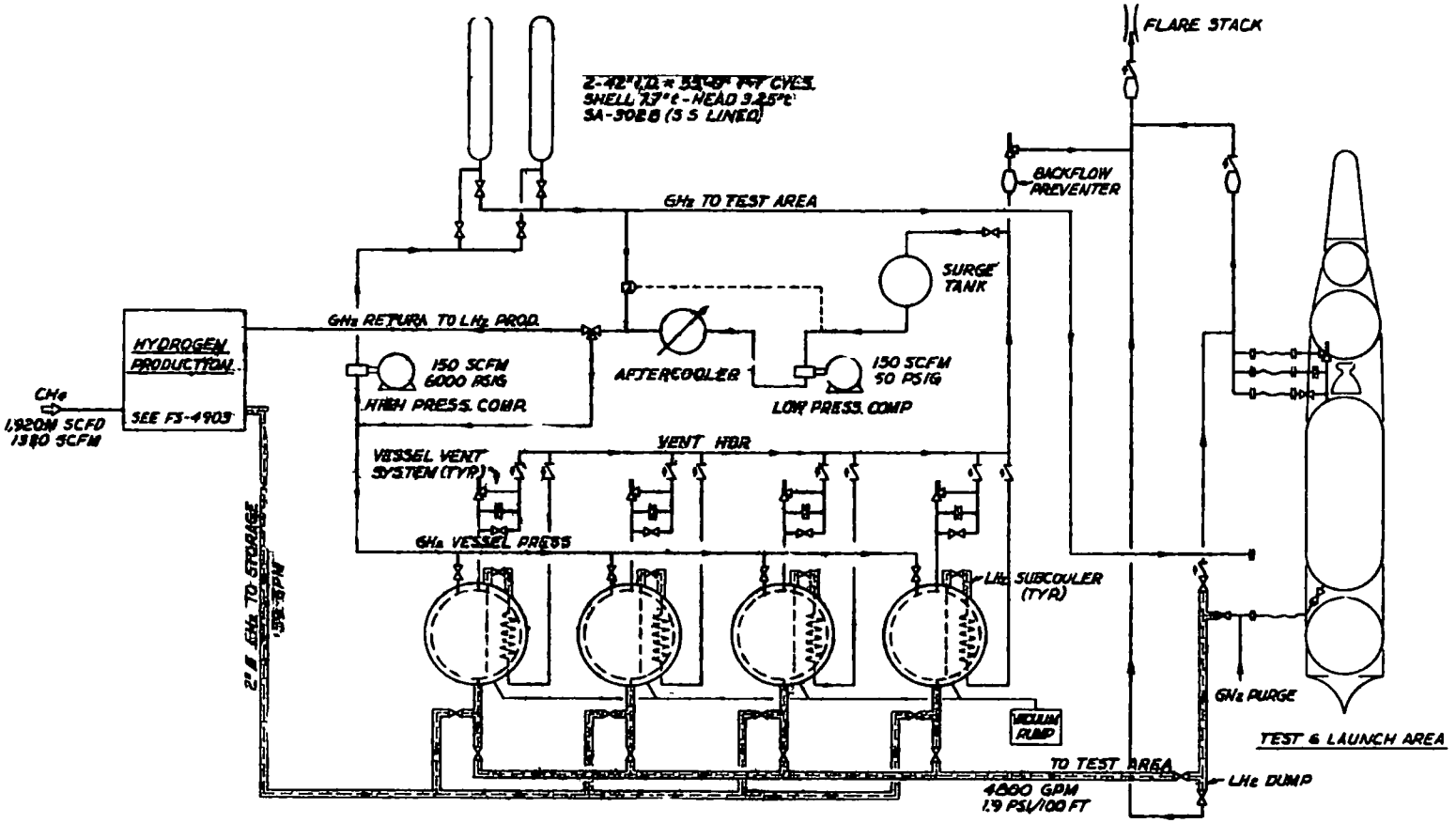

Figure VI-12

Hydrogen Facilities Schematic Flow Diagram

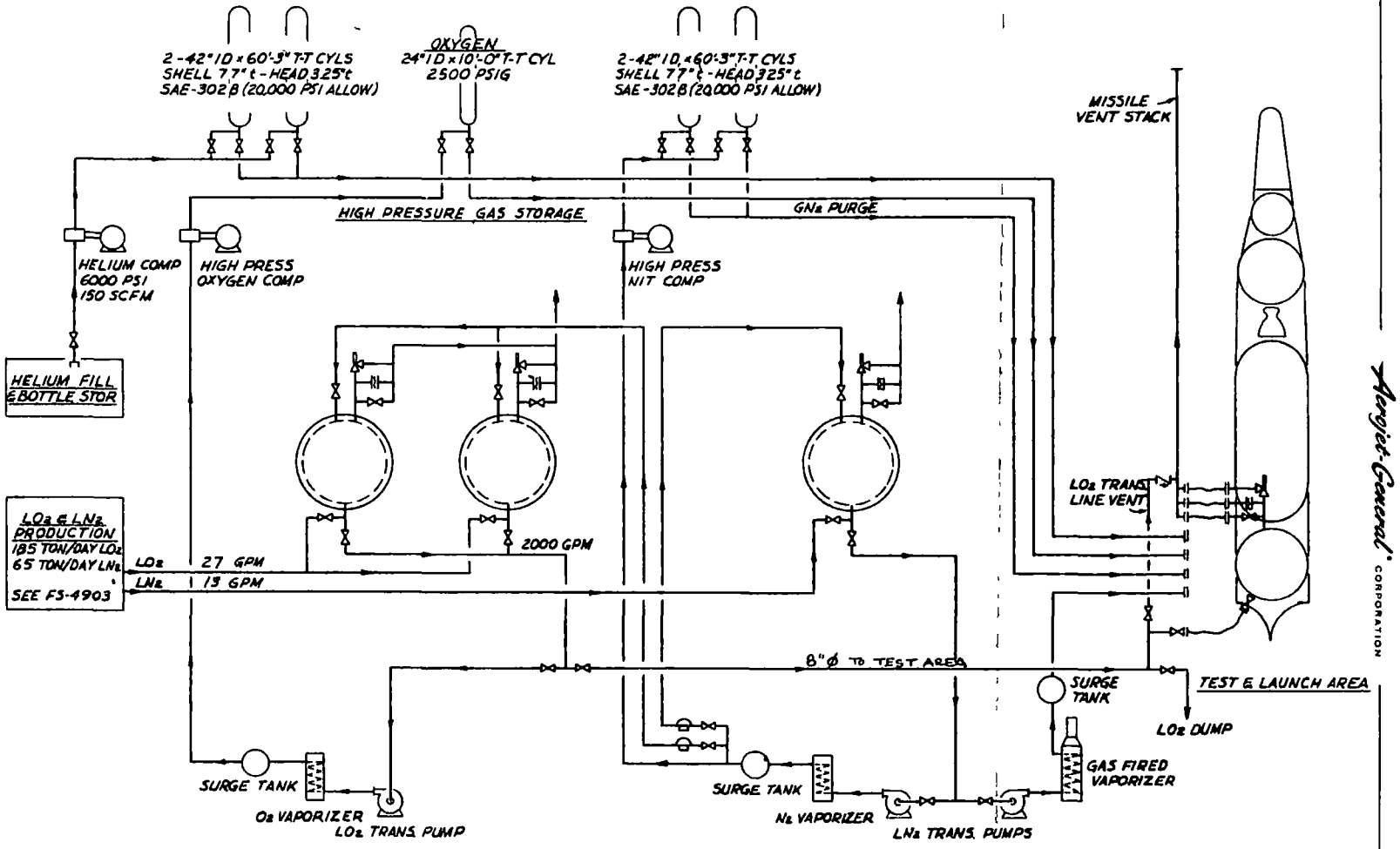

Figure VI-13

Nitrogen, Oxygen, and Helium Systems Schematic Flow Diagram

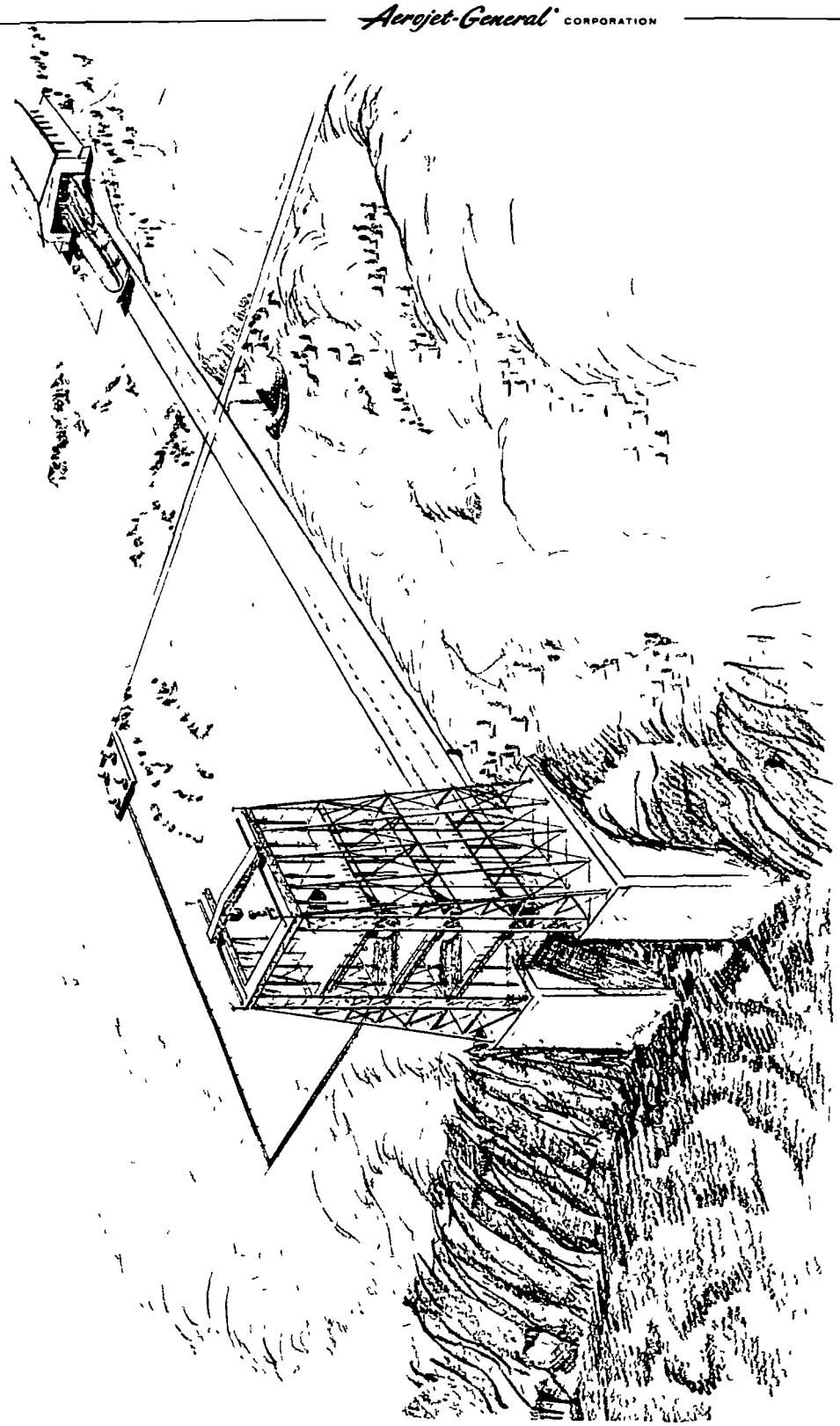

Test and Launch Facility, Lower Cliff Area

Figure VI-14

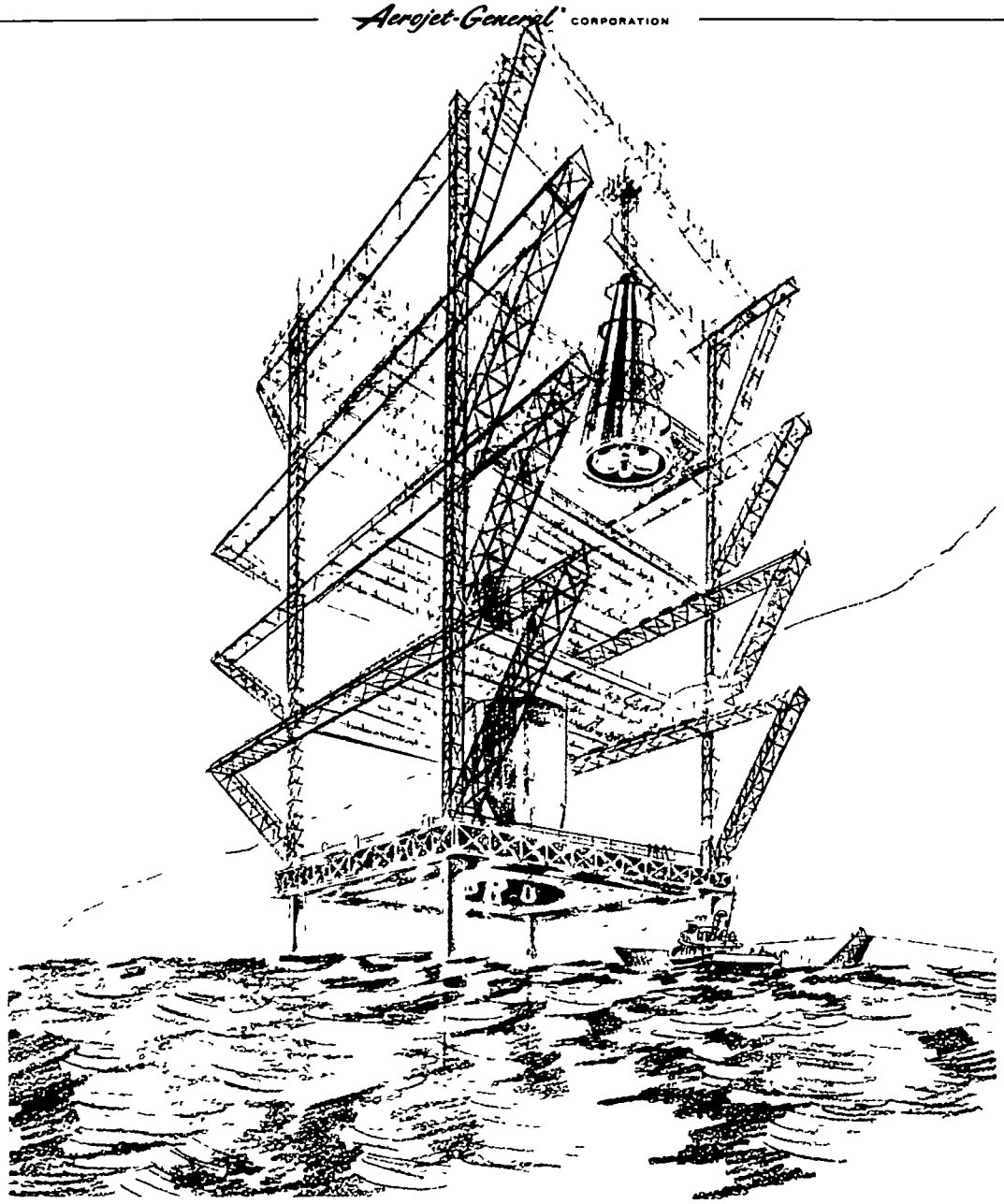

Fixed Test and Launch Tower

Figure VI-15

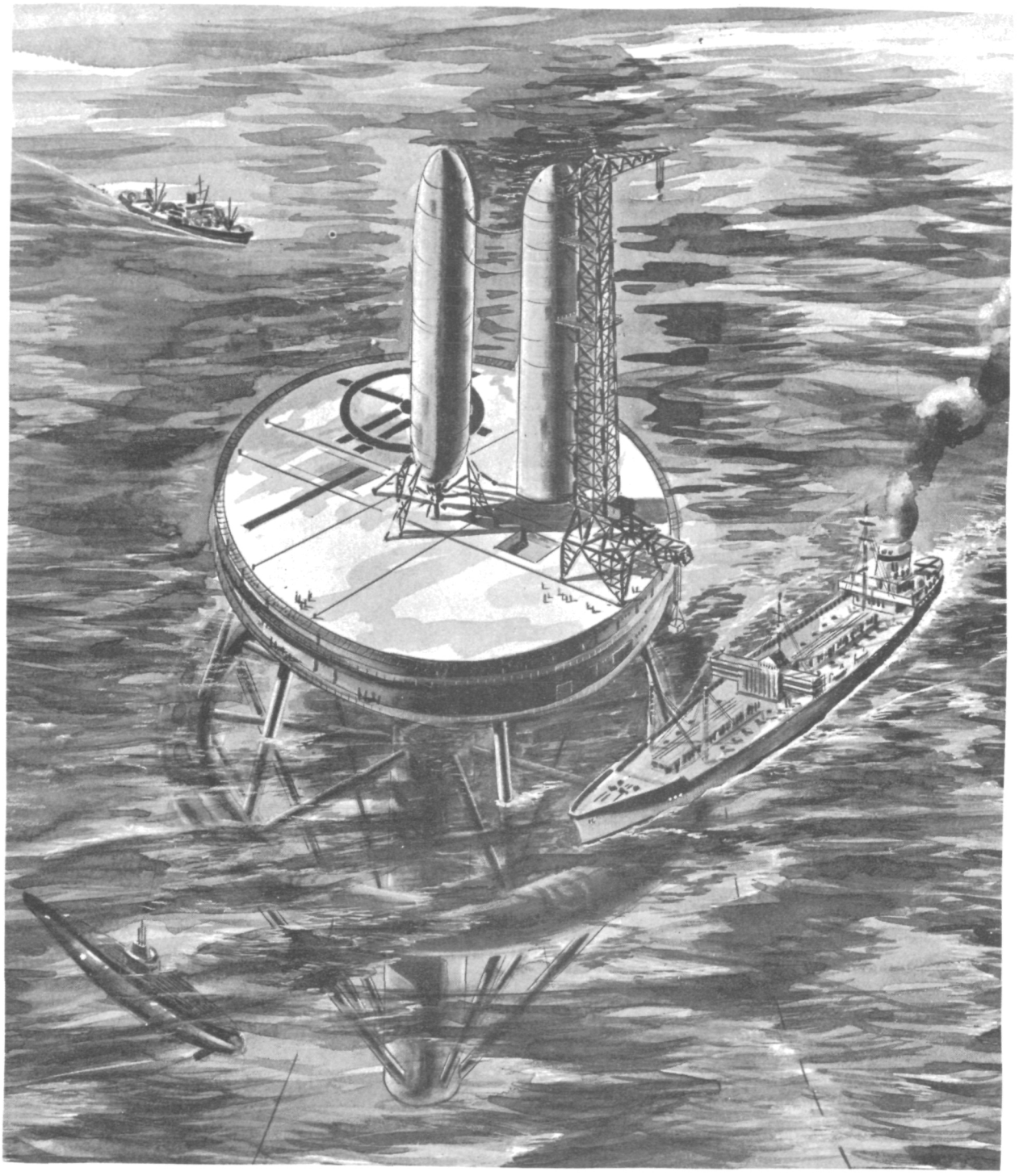

Planetary Rocket Ocean Platform, Above Water

Figure VI-16

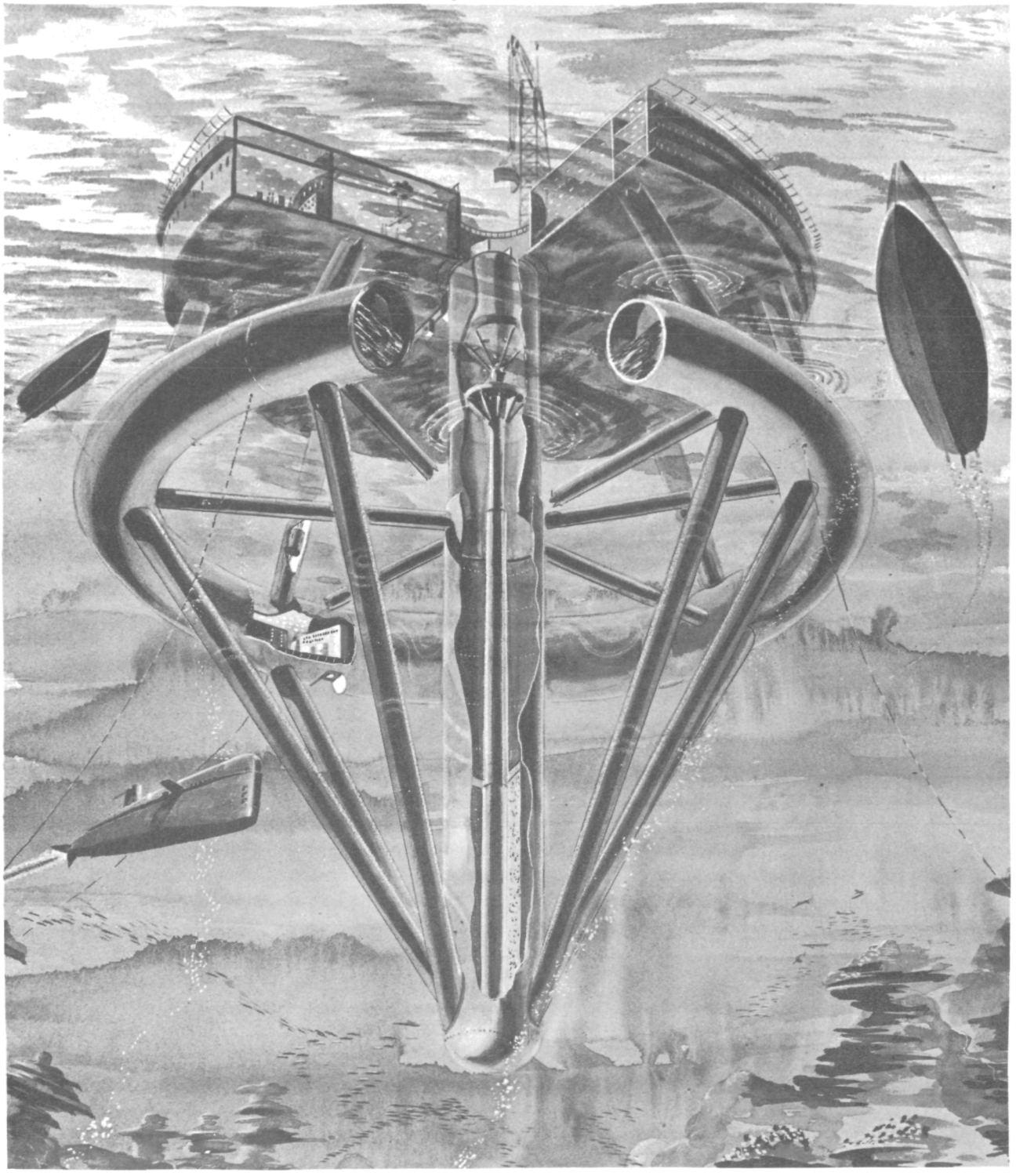

Planetary Rocket Ocean Platform, Below Water

Figure VI-17

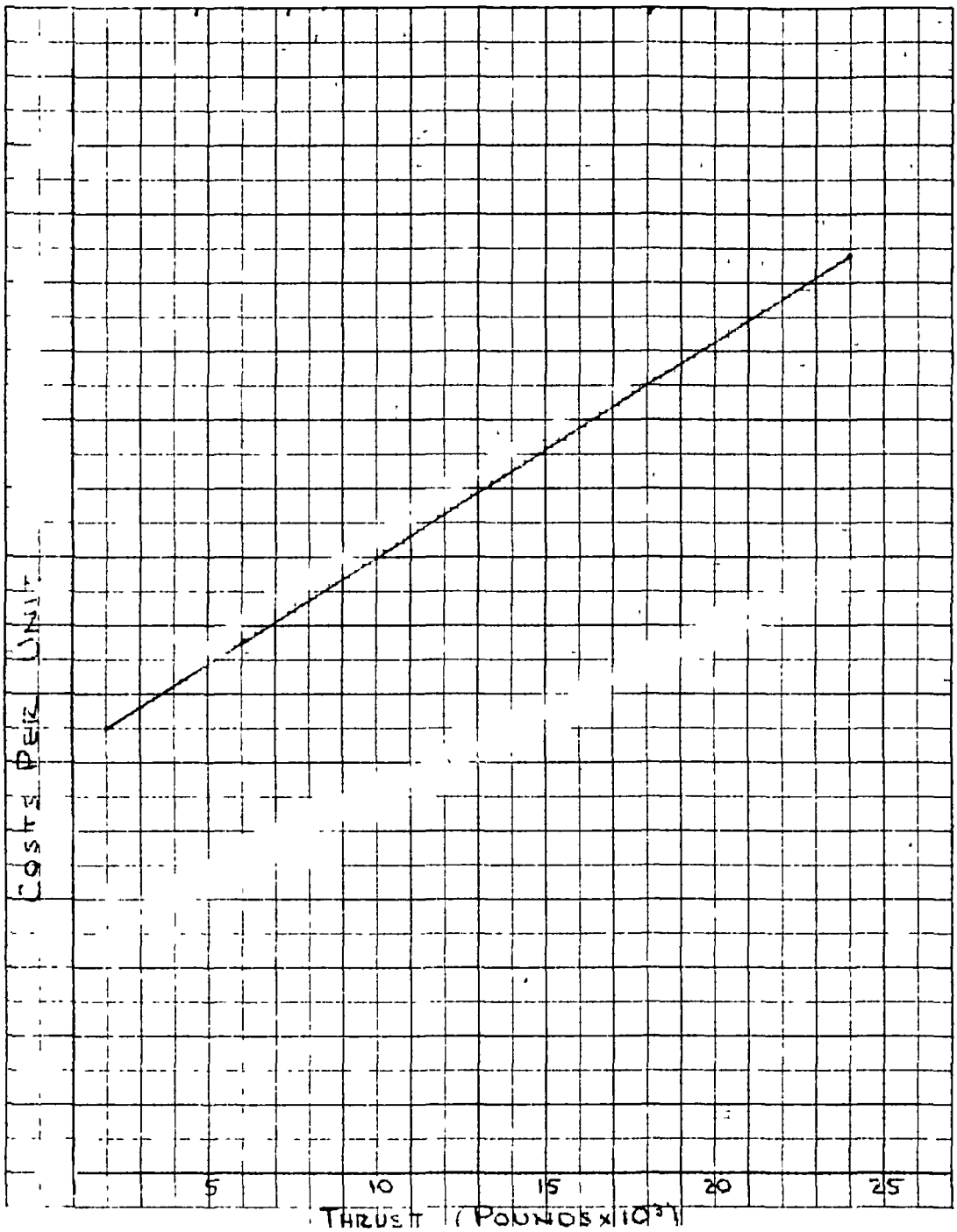

Projected Acceptance Testing Cost Trends
for Systems of 2 to 24-Million-lb Thrust

Figure VI-18

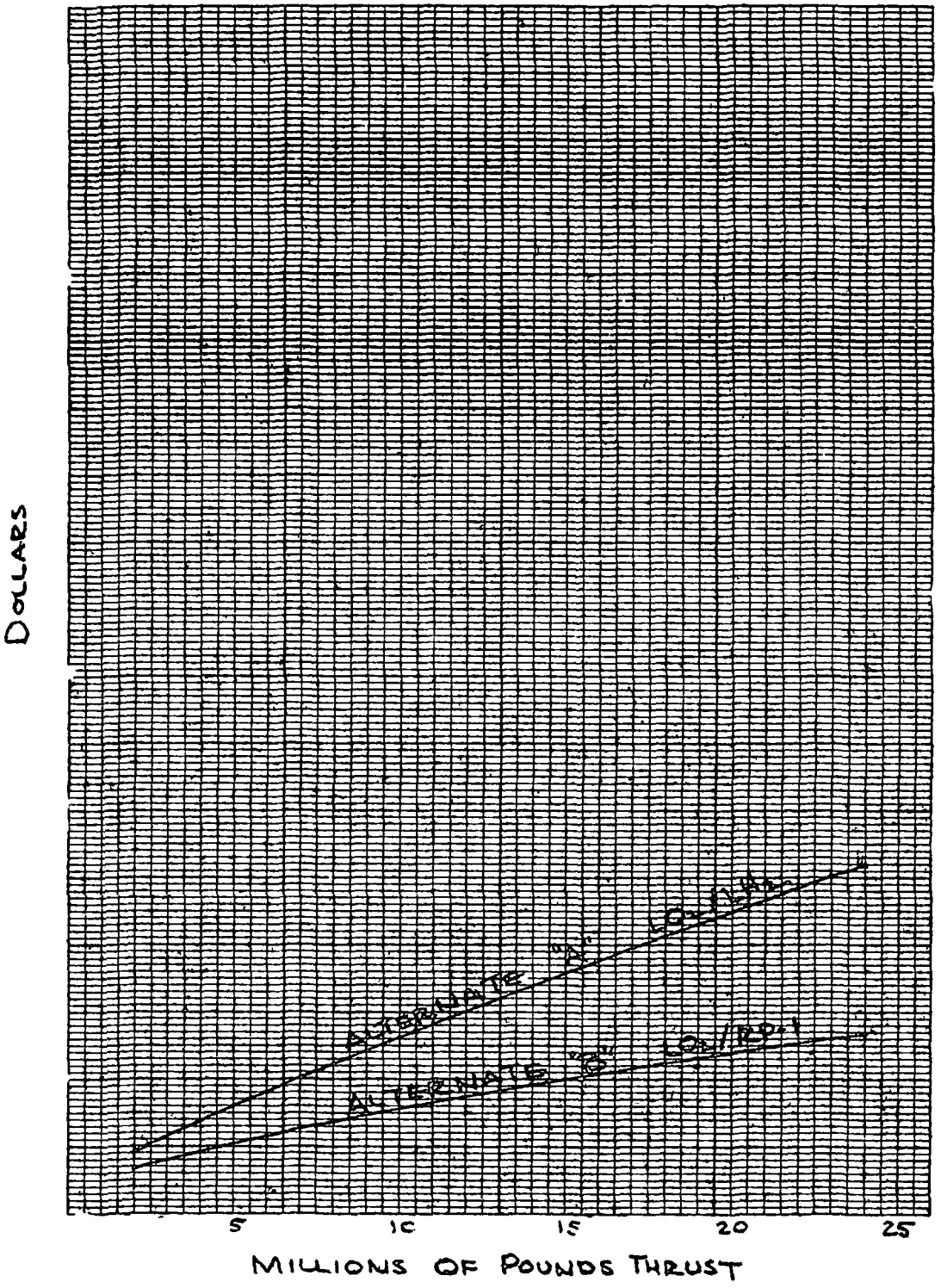

U.S. Coastal Gorge Concept

Figure VI-19

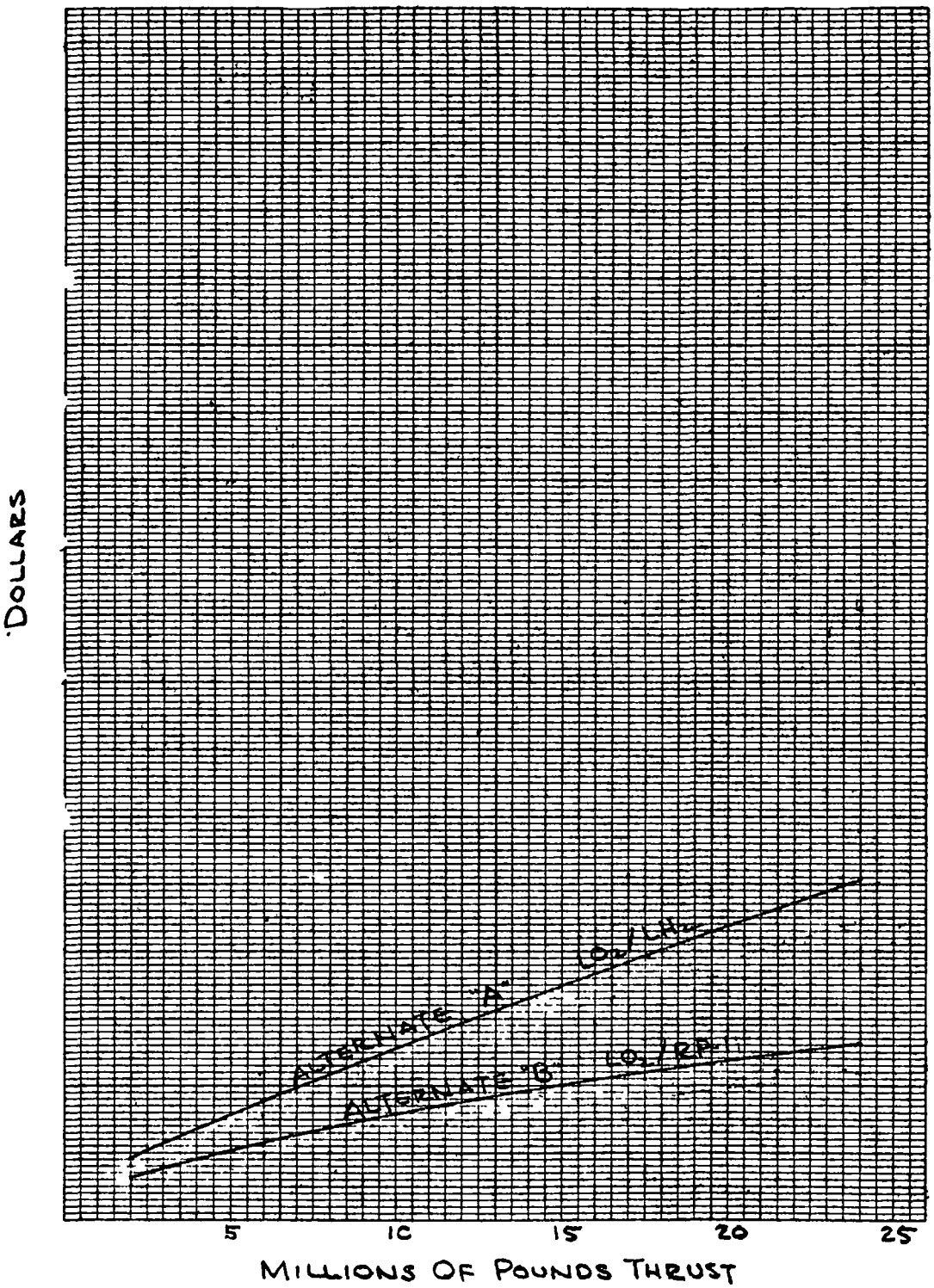

U.S. Coastal Cliff Concept

Figure VI-20

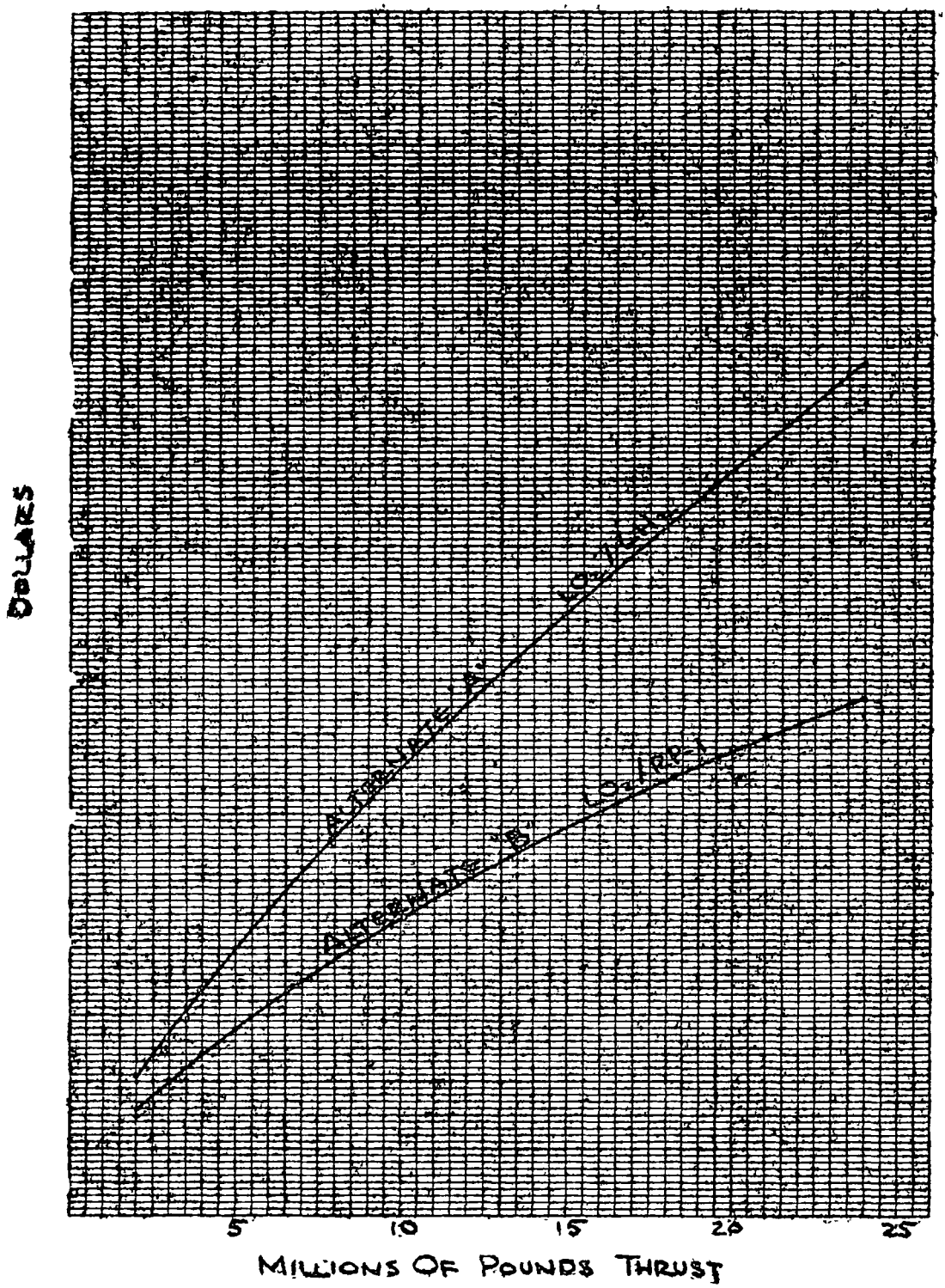

Remote Island Concept

Figure VI-21

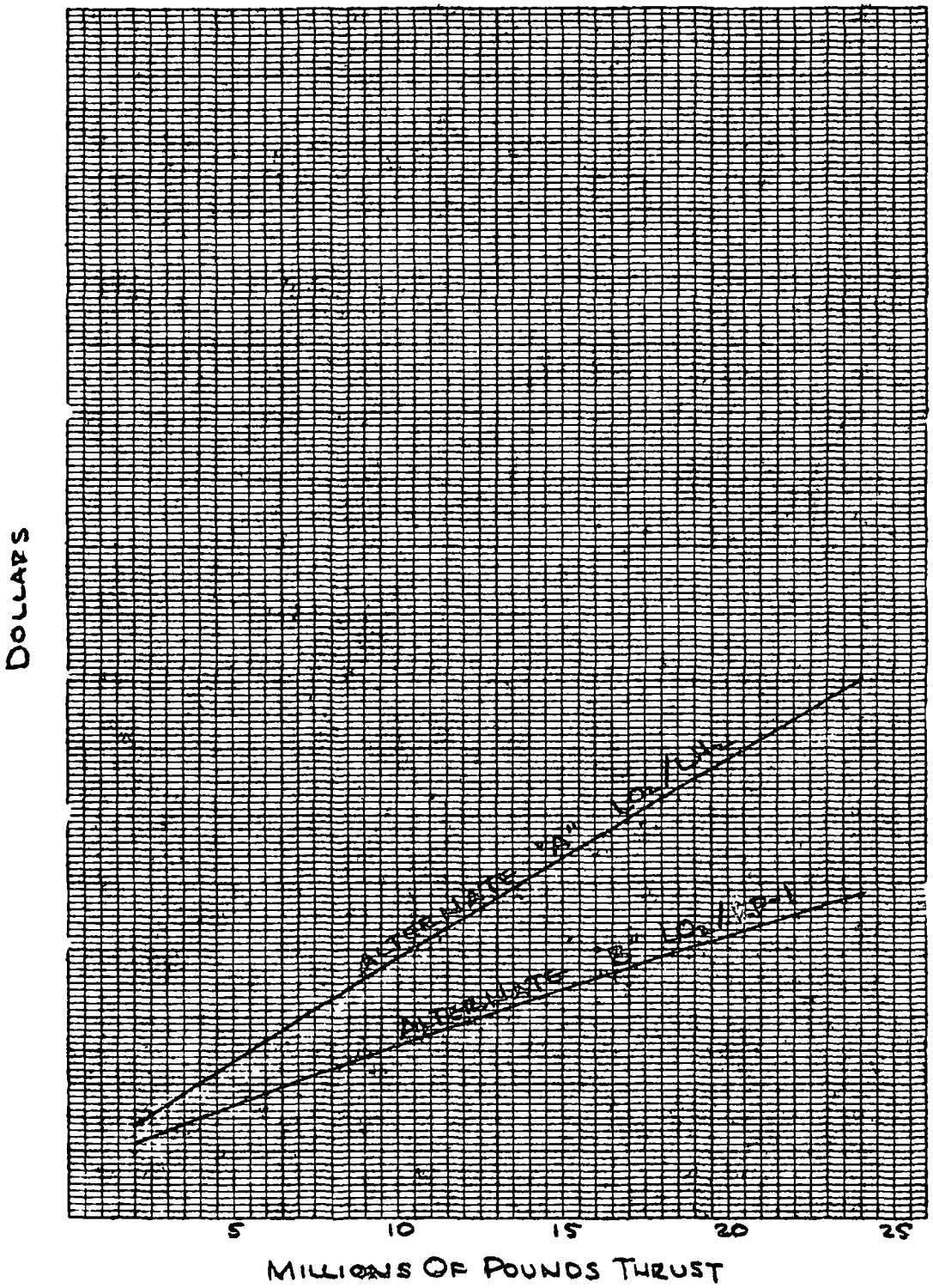

Texas Tower Concept

Figure VI-22

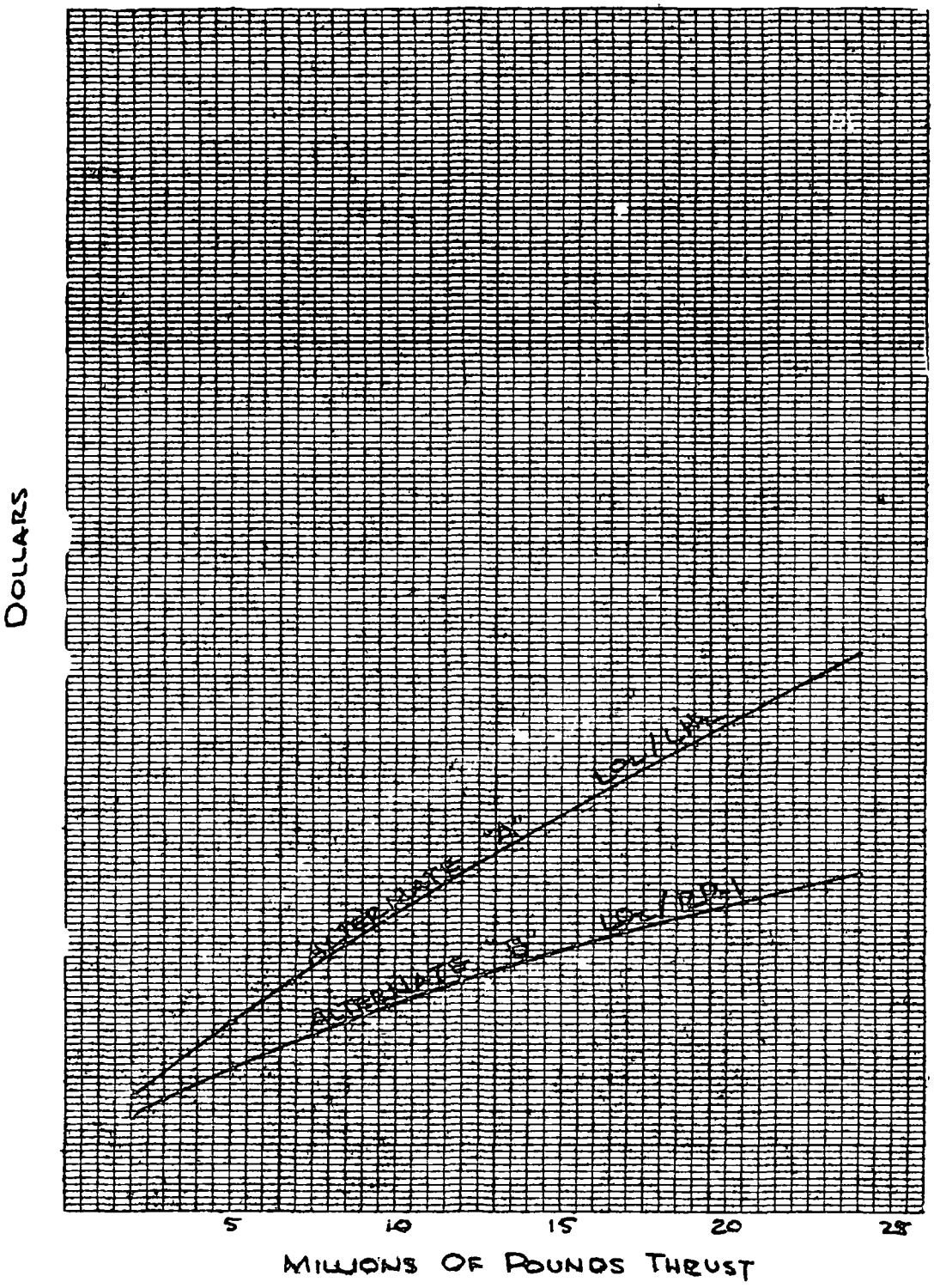

PROP Concept

Figure VI-23

CONFIDENTIAL

CONFIDENTIAL